

UC Berkeley

UC Berkeley Electronic Theses and Dissertations

Title

Gold(I)-Catalyzed Nucleophilic Additions

Permalink

<https://escholarship.org/uc/item/56p145c9>

Author

LaLonde, Rebecca Lyn K. C.

Publication Date

2010

Peer reviewed|Thesis/dissertation

Gold(I)-Catalyzed Nucleophilic Additions

By

Rebecca Lyn K. C. LaLonde

A dissertation submitted in partial satisfaction

of the requirements for the degree of

Doctor of Philosophy

in

Chemistry

in the

Graduate Division

of the

University of California, Berkeley

Committee in charge:

Professor F. Dean Toste, Chair

Professor Kurt P. Vollhardt

Professor Sharon E. Fleming

Spring 2010

Gold(I)-Catalyzed Nucleophilic Additions

© 2010

By Rebecca Lyn K. C. LaLonde

Abstract

Gold(I)-Catalyzed Nucleophilic Additions

By

Rebecca Lyn K. C. LaLonde

Doctor of Philosophy in Chemistry

Professor F. Dean Toste, Chair

The addition of nitrogen, oxygen, and carbon nucleophiles to carbon-carbon unsaturated bonds is an atom economical method of generating structural complexity from simple starting materials. As soft Lewis acids with high oxidation potentials, gold(I)-complexes are attractive catalysts for these types of transformations. Although many reactions catalyzed by gold(I) have now been reported, we identified two conspicuous deficiencies: few of enantioselective methods and a lack of nucleophilic additions to alkenes. This dissertation will describe advances on both fronts. First, we will discuss the discovery and characterization of chiral phosphinegold(I)-bis-*p*-nitrobenzoate complexes which catalyze the asymmetric hydroamination of allenes. Second, the isolation of proposed alkene hydroamination intermediates will be reported.

Chapter 1. A brief perspective on the current resurgence of homogeneous gold(I)-catalysis will be presented, with an emphasis on the development of enantioselective reactions.

Chapter 2. The metal catalyzed asymmetric hydroamination of allenes has been an unsolved problem in synthetic chemistry for many years. In this chapter, we describe our efforts to apply chiral biarylphosphinegold(I) complexes to this transformation. Over the course of this work, we characterized a polymeric mono-cationic complex (*R*)-[BINAP(Au₂Cl)]BF₄, and uncovered a dramatic counterion effect. This discovery led to the utilization of phosphinegold(I)-bis-*p*-nitrobenzoate complexes for the asymmetric hydroamination of allenes. The catalysts were applied to the enantioselective formation of vinyl pyrrolidines and piperidines in 70-99% enantiomeric excess. The structure of a bis-*p*-nitrobenzoategold(I) complex, (*R*)-ClMeOBiPHEP(AuOPNB)₂, was verified by X-ray crystallography.

Chapter 3. Chiral ligands and counterions were employed in the gold(I)-catalyzed enantioselective intramolecular additions of hydrazines and hydroxylamines to allenes. Chiral phosphinegold(I)-bis-*p*-nitrobenzoate complexes are versatile catalysts for the enantioselective hydroamination of allenes. The addition of oxygen nucleophiles, however, required the use of chiral anions. These complementary methods allow access to chiral vinyl isoxolidines, tetrahydrooxazines, and differentially protected pyrazolidines.

Chapter 4. This chapter will describe the first direct experimental evidence for the elementary step of gold-promoted nucleophilic addition to an alkene. Alkylgold(I) complexes were formed from the gold(I)-promoted intramolecular addition of various amine nucleophiles to alkenes. Deuterium-labeling studies and X-ray crystal structures provided support for a mechanism involving *anti*-addition of the nucleophile to a gold-activated alkene. This mechanism was verified by DFT analysis. Ligand studies indicated that the rate of aminoauration was drastically increased by use of electron-poor arylphosphines, which were also shown to be favored in ligand exchange experiments. Attempts at protodeauration led only to recovery of the starting olefins, though the gold could be removed under reducing conditions to provide the purported hydroamination products. The reactivity of alkylgold complexes with zinc and palladium are described. An unexpected oxidation to gold(III) was also uncovered.

Chapter 5. Investigations into the gold(I)-catalyzed addition of carbon nucleophiles to allenes will be discussed. One such reaction, a gold(I)-catalyzed *5-endo-trig* reaction, worked with a variety of carbon nucleophiles, including silyl enol ethers, β -ketoesters and dinitriles. This transformation opens access to a variety of substituted cyclopentenes. These carbocycles are complementary to the products available through the Conia-ene and *5-endo-dig* methodology. In addition, we demonstrate the transfer of chirality from an allene precursor, producing a quaternary stereocenter with a vicinal tertiary center. We also report a gold(I)-catalyzed *5-endo/exo-trig* cyclization of substrates which contain two-carbon linkers between the pendant nucleophile and allene. Investigations into the mechanism of this cyclization are included, as well as attempts to isolate a proposed allylgold(I) intermediate.

Chapter 6. A synopsis of our results will be presented, with a perspective on the evolving field of gold(I)-catalysis.

Gold(I)-Catalyzed Nucleophilic Additions

Table of Contents

Chapter 1. *A Perspective on the Renaissance of Gold(I)-Catalysis*

An Introduction to Modern Gold(I)-Catalysis.....	1
References.....	6

Chapter 2. *Gold(I)-Catalyzed Enantioselective Hydroamination of Allenes*

Introduction.....	8
Results.....	15
<i>Initial Optimization</i>	15
<i>Development and Characterization of p-Nitrobenzoate Catalysts</i>	18
<i>Final Optimization</i>	23
<i>Substrate Scope</i>	24
Conclusion.....	30
Experimental.....	31
References.....	47
Appendix 2A.....	50
Appendix 2B.....	71
Appendix 2C.....	91

Chapter 3. Gold(I)-Catalyzed Enantioselective Synthesis of Pyrazolidines,

Isoxazolidines, and Tetrahydrooxazines

Introduction.....	122
Results.....	128
<i>Initial Optimization</i>	128
<i>Reaction Scope: Hydroamination</i>	132
<i>Reaction Scope: Hydroalkoxylation</i>	134
<i>Substrate Functionalization</i>	135
Conclusion.....	136
Experimental.....	137
References.....	155
Appendix 3A.....	158

Chapter 4. Intramolecular Aminoauration of Unactivated Alkenes

Introduction.....	194
<i>Gold Alkene Activation</i>	195
Results.....	202
<i>Synthesis and Isolation of Alkylgold Complexes</i>	202
<i>Mechanism of Aminoauration</i>	209
<i>Protonation of Alkylgold Complexes</i>	214
<i>Transmetallation of Alkylgold Complexes</i>	215
<i>Oxidation of Alkylgold Complexes</i>	218
Conclusion.....	218

Experimental.....	219
References.....	238
Appendix 4A.....	242
Appendix 4B.....	257
Appendix 4C.....	271

Chapter 5. *Gold(I)-Catalyzed Addition of Carbon Nucleophiles to Allenes*

Introduction.....	288
Results.....	293
<i>Gold(I)-Catalyzed 5-Endo-trig Cyclization.....</i>	293
<i>Gold(I)-Catalyzed 5-Endo/exo-trig Cyclization.....</i>	296
<i>Proposed Mechanism and Allylgold(I) Species.....</i>	301
Conclusion.....	305
Experimental.....	306
References.....	314
Appendix 5A.....	316

Chapter 6. *Synopsis and Future Directions*

The Evolving Field of Gold(I)-Catalysis.....	324
References.....	328

Acknowledgements

First and foremost, I am indebted to my advisor, Professor Dean Toste, for his endless ideas and advice. I'm not sure I can ever express my gratitude for the second chance to earn this degree. I also owe thanks to Dr. Janet Gunzner, for encouraging me to give this whole graduate school thing another try.

At its heart, research is a collaborative effort. I have had the privilege of working with many extraordinary individuals over the years. Although there have been too many colleagues to name, I would especially like to thank the following people (in alphabetical order): Skip Brenzovich, Melanie Chiu, Britt Corkey, David Gorin, Olivia Hung, Eun-Joo Kang, Kristine Nolin, Nate Shapiro, Benjamin Sherry, Jane Wang, Iain Watson, and Cole Witham. I am also thankful for the many staff members in the department of chemistry who somehow make this place work. Our research depends on the support of people like Drs. Rudi Nunlist, Chris Canlas, Fred Hollander, and Antionio dePasquale.

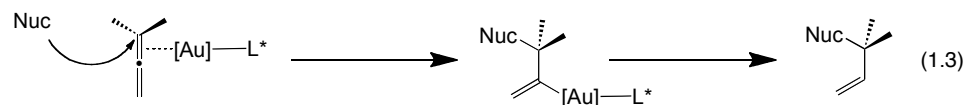
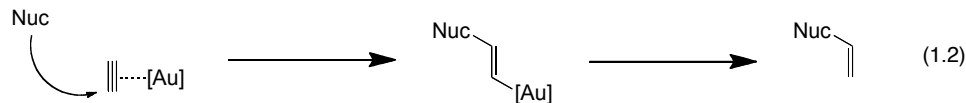
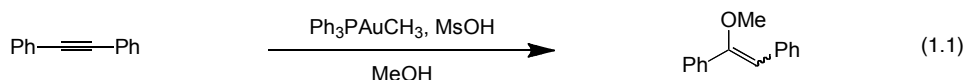
Completing graduate school would not have been possible without my family and friends supporting me along the way. My parents have always been enthusiastic about my education, even when they didn't understand just what exactly I was doing. Kim Malesky probably saved my sanity over these five years by always being ready to join me on a camping or backpacking excursion. And last, but not least, I would especially like to thank Daniel Gray for his unending love, support, and encouragement.

Chapter 1

A Perspective on the Renaissance of Gold(I)-Catalysis

An Introduction to Modern Gold(I)-Catalysis

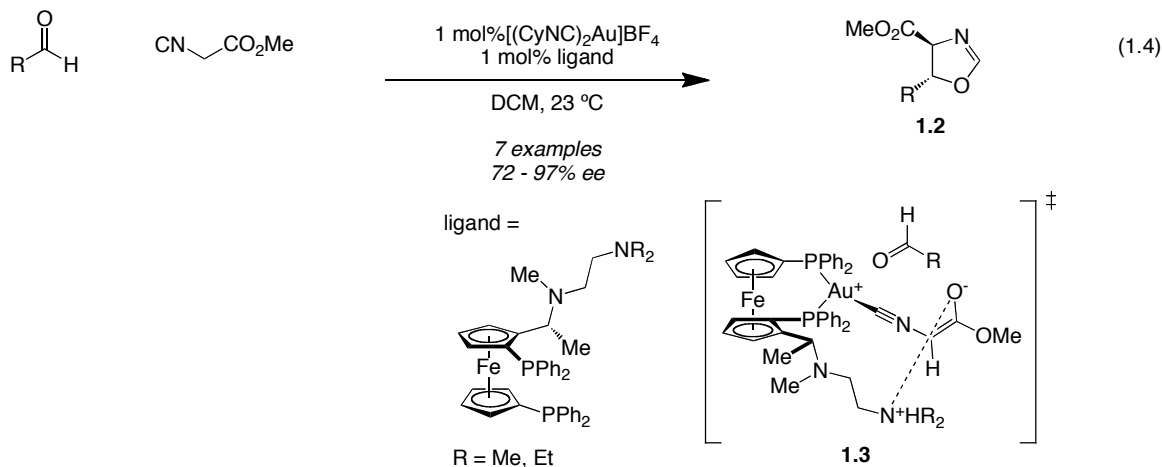
Since Wöhler discovered the synthesis of urea in 1828,¹ the field of organic chemistry has expanded exponentially to encompass an uncounted number of reactions within multiple sub-disciplines. And yet the need for new chemical transformations continues to escalate. Modern chemists are challenged with creating tools to solve global problems: pharmaceuticals, needed for the treatment of medical conditions such as malaria, HIV, and cancer; agrochemicals, which assist in the production of food for the world's population; the degradation of biomass to create biofuels, to name a few. And if those objectives were not lofty enough, the new reactions we create must be environmentally sustainable, broadly applicable to a variety of compounds, and also precise and predictable in their outcome. In 1995 review, Barry Trost coined the term 'atom economy', to embody these ideals.² In the purest sense, an atom economical reaction is comprised of a simple addition in which two starting materials are combined with no waste or extraneous reagents. Of course, due to various issues with selectivity and outright reactivity, relying solely on the ideal atom economical reaction is not possible. The use of homogeneous catalysts enables new bond formation with little waste and the potential of catalyst recycling.



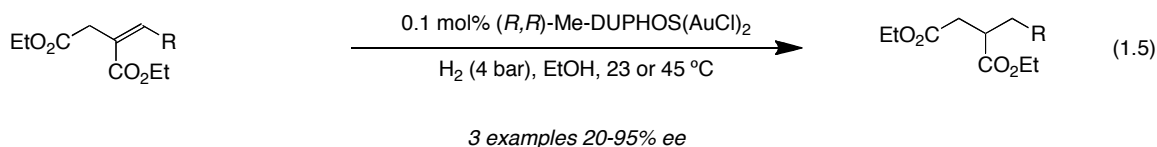
It was in this milieu, that Teles reported a gold(I)-catalyzed hydration of alkynes in 1998 (eq 1.1).³ For reasons that remain unclear, prior to this paper, gold had been underutilized as a catalyst. Hailed as a mild and efficient method of installing C-O bonds, this article marked the beginning of a rising tide of gold chemistry. Some of the key advantages to employing gold as a catalyst rapidly became clear. First, as a soft Lewis acid, gold is often tolerant to functional groups that would otherwise be detrimental. Second, gold-catalyzed reactions are typically performed under ambient conditions, without precautions against oxygen or moisture. Third, the high oxidation potential between gold(I) and gold(III) allows access to mechanisms outside of the oxidative addition/reductive elimination cycles found in traditional transition metal catalysis.

Although the specific mechanism of the Teles hydration has been debated, the addition of nucleophiles to gold-activated alkynes quickly became a dominant paradigm in the field (eq 1.2).⁴ Replacing alkynes with allene electrophiles presents two interesting possibilities for enantioselective reactions (eq 1.3). First, an axially chiral allene could be used for a chirality

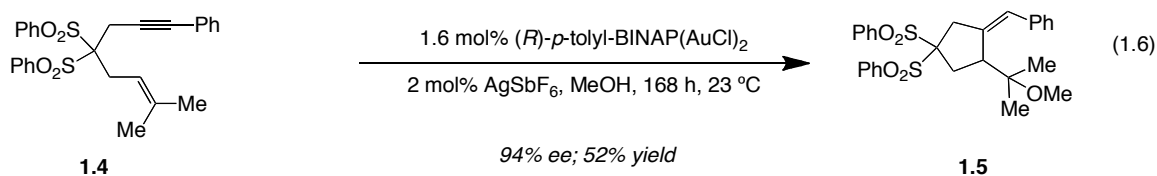
transfer reaction.⁵ The second approach would involve a chiral phosphinegold(I)-catalyst which would render the addition enantioselective. Although the second option offered an attractive opportunity, prior to 2005, very little was known about enantioselective gold(I)-catalysis. In fact, only four enantioselective transformations were known.



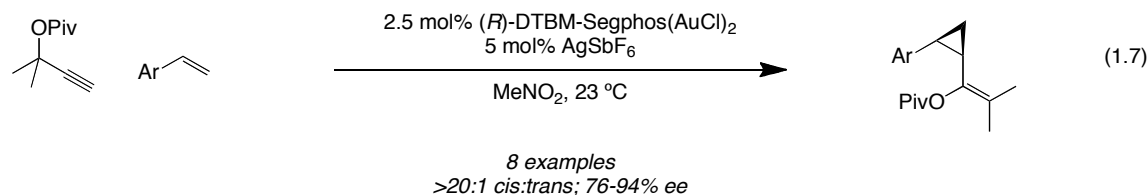
Even those familiar with gold chemistry may have been surprised to find that the first enantioselective gold(I)-catalyzed reaction was reported in 1986 (eq 1.4).⁶ In that year, Hayashi and co-workers described a gold-catalyzed aldol reaction which produced chiral oxazolines. A variety of alkyl and aryl aldehydes were reacted with methyl isocyanoacetate to yield the desired heterocycles with good diastereoselectivity for the *trans* isomer, and 97% ee. The amino side-chain on the ferrocenyl ligand was found to be crucial to the generation of enantioenriched products. For example, when the side chain was extended by one carbon or was absent, the oxazolines were isolated with 0-26% ee. A highly organized transition state (**1.3**) was proposed, in which the side-chain coordinates the enolate. For mysterious reasons, this transformation remained the sole enantioselective gold(I)-catalyzed reaction until 2005.



In 2005, the Corma group reported the enantioselective hydroamination of three electron-deficient alkenes catalyzed by (*R,R*)-Me-DUPHOS(AuCl)₂.⁷ The observed enantioselectivity was highly dependent on the alkene substituent. For example, when R = H, the product was obtained with only 20% ee. A larger substituent, phenyl, resulted in a higher ee (80%). Although the paper did not include a crystal structure of the gold complex, the authors did describe a model for the conformation. They proposed an aurophillic contact which caused a severe deviation from gold(I)'s preferred linear geometry.



In the same year, Echavarren reported his groups efforts towards an enantioselective gold(I)-catalyzed cycloisomerization.⁸ A single substrate cycloisomerized with ee higher than 50%. This starting material possessed an internal alkyne (**1.4**), which appeared to be crucial for enantioselectivity. For example, **1.4** cycloisomerized to **1.5** with the highest ee (94%), but in low yield (52%). Substrates without alkyne substitution produced the desired products with better yield, but less than 50% ee. Unfortunately, despite testing a variety of gold(I)-complexes, the authors did not find a general catalyst system.



Our group's first contribution to the field of enantioselective gold(I)-catalysis was also reported in 2005.⁹ In this transformation, a cyclopropanation of styrene derivatives, the authors initially found that modifying the racemic phosphinegold(I)-complex had a strong effect on the product's *cis/trans* ratio. This effect extrapolated to chiral biarylphosphinegold-catalysts, increasing the d.r. to >20:1. Furthermore, (*R*)-DTBM-Segphos(AuCl)₂ was identified as the optimal catalyst. The highly sterically hindered ligand was key to high enantioselectivities.

The reactions described above (eq 1.4-1.7) represented significant advances in gold chemistry. But these transformations (an aldol, hydrogenation, cycloisomerization, and cyclopropanation) all occur via disparate mechanisms. Moreover, the most common gold(I) mechanistic paradigm, that of nucleophilic addition to C-C unsaturated bonds was conspicuously absent! Chapter 2 will describe our efforts to remedy this deficiency. We initially theorized that chiral biarylphosphinegold(I)-complexes alone would catalyze an enantioselective hydroamination of allenes. However, the key to high enantioselectivities lay with an unlikely source, the counterion. The discussion in chapter 3 will expand on this counterion effect and illustrate the use of chiral counterions. When used alone, and conjunction with chiral phosphinegold(I) complexes, chiral counterions provide a flexible manifold for the enantioselective addition of hydroxylamine and hydrazine nucleophiles.

Although the proclivity of gold to activate allenes (and alkynes) for nucleophilic attack has been widely accepted, the parallel reactivity with alkenes¹⁰ has been subjected to intense scrutiny. Two underlying issues were key to this debate. First, similar (and in some cases identical) reactivity has been reported to be Brønsted acid catalyzed.¹¹ Second, while there was evidence for the complexation of alkenes by gold(I),¹² there was no experimental confirmation for the elementary step of nucleophilic addition. In chapter 4 we report the first such evidence, including the crystal structures of two alkylgold(I)-complexes.

Finally, finding new reactions to form carbon-carbon bonds, and specifically sterically hindered quaternary centers, is an ongoing challenge. In chapter 5 we report two such reactions, gold(I)-catalyzed *5-endo-trig* and *5-endo/exo-trig* carbocyclizations of allenes. In addition, we show that chiral allenes cyclize with complete chirality transfer in the *5-endo-trig* reaction. This method is a mild and efficient way to synthesize carbocycles with sterically demanding quaternary centers.

References

- ¹ Wöhler, F. *Ann. der Phys.* **1828**, 88, 253.
- ² Trost, B. M. *Angew. Chem., Int. Ed. Engl.* **1995**, 34, 259.
- ³ Teles, J. H.; Brode, S.; Chabanas, M. *Angew. Chem., Int. Ed. Engl.* **1998**, 37, 1415.
- ⁴ (a) Dyker, G. *Angew. Chem., Int. Ed. Engl.* **2000**, 39, 4237. (b) Hashmi, A. S. K. *Gold Bull.* **2003**, 36, 3. (c) Hashmi, A. S. K. *Gold Bull.* **2004**, 37, 51.
- ⁵ For examples of chirality transfer, see: (d) Shi, X.; Gorin, D. J.; Toste F. D. *J. Am. Chem. Soc.* **2005**, 127, 5802. (e) Fehr, C.; Galindo, J. *Angew. Chem., Int. Ed. Engl.* **2006**, 45, 2901. (f) Sherry, B. D.; Maus, L.; Laforteza, B. N.; Toste, F. D. *J. Am. Chem. Soc.* **2006**, 128, 8132. (g) Dubé, P.; Toste, F. D. *J. Am. Chem. Soc.* **2006**, 128, 12062.
- ⁶ (a) Hayashi, T.; Sawamura, M.; Ito, Y. *J. Am. Chem. Soc.* **1986**, 108, 6405. (b) Hayashi, T.; Sawamura, M.; Ito, Y. *Tetrahedron* **1992**, 48, 1999.
- ⁷ González-Arellano, C.; Corma, A.; Iglesias, M.; Sánchez, F. *Chem. Commun.* **2005**, 3451.
- ⁸ Muñoz, M. P.; Adrio, J.; Carretero, J. C.; Echavarren, A. M. *Organometallics* **2005**, 24, 1293.
- ⁹ Johansson, M. J.; Gorin, D. J.; Staben, S. T.; Toste, F. D. *J. Am. Chem. Soc.* **2005**, 127, 18002.
- ¹⁰ For a review, see: Widenhoefer, R. A.; Han, X. *Eur. J. Org. Chem.* **2006**, 4555.
- ¹¹ For a recent review of the Brønsted acid vs. metal-catalyzed debate, see: Taylor, J. G.; Adrio, L. A.; Hii, K. K. *Dalton Trans.* **2010**, 39, 1171.
- ¹² For a gold(I)-alkene complex, see: Shapiro, N. D.; Toste, F. D. *Proc. Natl. Acad. Sci. USA* **2008**, 105, 2779.

Chapter 2

Gold(I)-Catalyzed Enantioselective Hydroamination of Allenes

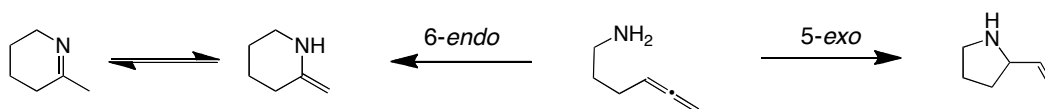
A portion of this work has been published (LaLonde, R. L.; Sherry, B. D.; Kang, E. J.; Toste, F. D. “Gold(I)-Catalyzed Enantioselective Intramolecular Hydroamination of Allenes” *J. Am. Chem. Soc.* **2007**, *129*, 2452-2453), but has been described here in greater detail.¹

¹ Dr. Benjamin Sherry initiated this work, and shared the responsibility of testing the unsubstituted substrates with Dr. Eun Joo Kang. In addition to testing the substituted substrates, I performed the catalyst identification and isolation studies. The X-ray crystal structures were solved by Dr. Fred Hollander.

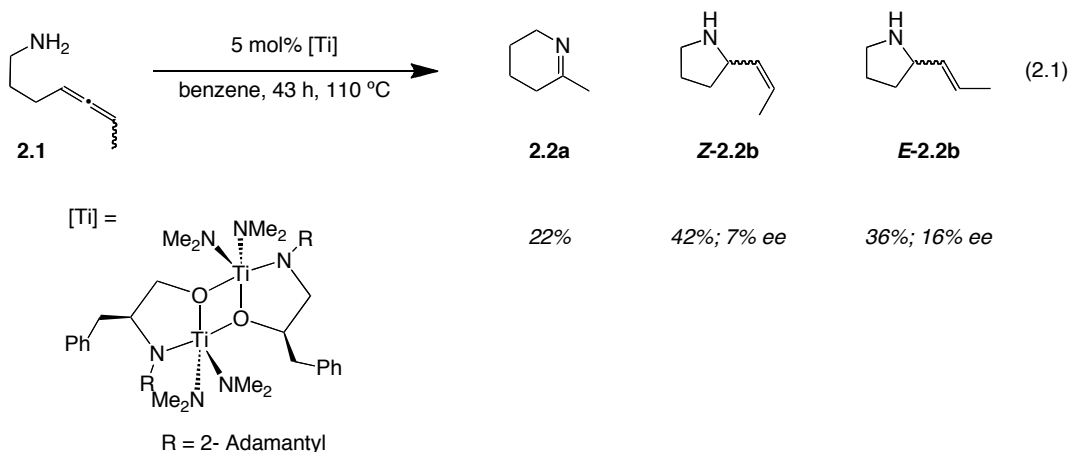
Introduction

The catalytic hydroamination of C-C multiple bonds is an efficient, redox-neutral atom economical method of installing nitrogen. Thus, the areas of metal-catalyzed addition of nitrogen to alkynes,^{1, 2} allenes,³ and alkenes^{4, 5} have received a great deal of attention in the literature. Despite the popularity of this area of research, as of 2007, the asymmetric hydroamination of allenes remained a continuing goal in transition metal catalysis. While at this time, a handful of substrate controlled diastereoselective reactions had been reported, no successful ligand controlled enantioselective methods existed. This chapter will focus specifically on the progress made towards transforming the intramolecular hydroamination of allenes into a stereoselective process.

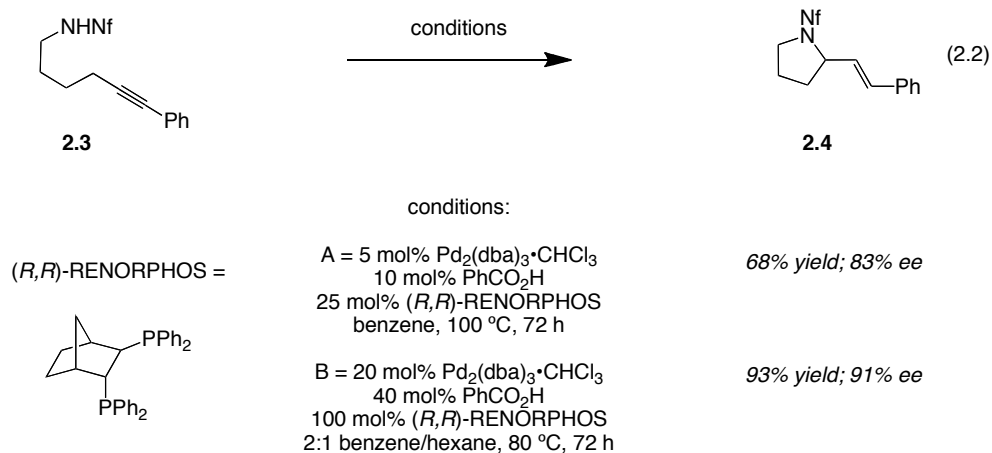
Scheme 2.1. Two Possible Hydroamination Reaction Pathways.



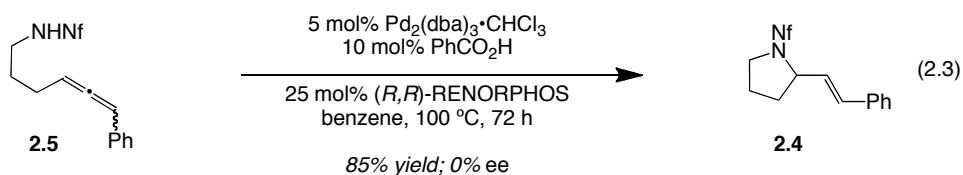
Intramolecular hydroamination of allenes generally proceeds via two reaction pathways (Scheme 2.1), 5-*exo* or 6-*endo*. Many examples of this type of reactivity can be found in early metals, such as titanium and zirconium,⁶ lanthanides,⁷ and late metals such as palladium,⁸ silver,⁹ mercury,¹⁰ and gold.^{3b} While the racemic reactions catalyzed by these metals will not be discussed in depth, it is important to note that each class of metal catalyzed hydroamination gives a different product distribution, each of which is exquisitely sensitive to ligand modifications. For example, titanium amide catalysts usually produce almost exclusively 6-*endo* products,^{6a} whereas employing titanium aminoalcohol^{6d} complexes favors the formation of 5-*exo* products. Zirconium and lanthanide catalysts produce mixtures that can be tuned by adjusting the ligand structure or the substitution pattern of the allene.⁶ In contrast, late metals, like mercury, silver, palladium and gold, tend to produce allyl amine products exclusively.



Due to the extreme sensitivity of the early metal systems to ligand and substrate modifications, it is not surprising that the problem of enantioselectivity remained unaddressed until 2004. In that year, Johnson and co-workers reported a hydroamination of aminoallenes catalyzed by chiral titanium aminoalcohol complexes (eq 2.1).^{6d} Although the authors studied a large number of chiral aminoalcohol based ligands, none of them produced the desired product with enantioselectivities greater than 16%. Their best results are summarized in eq 2.1. One can see that this system suffered from a number of problems: poor regioselectivity (4:1), poor diastereoselectivity (nearly 1:1), and negligible enantioselectivity (16%, favoring the minor diastereomer). These challenges might have been addressed individually, but taken together, they presented a daunting array of issues!

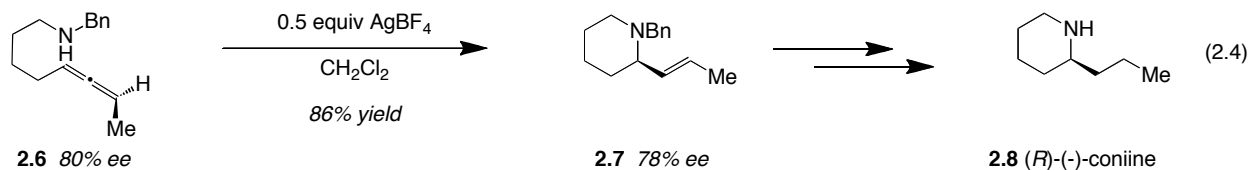


To the best of our knowledge, at the time of our research, Johnson's work constituted the only intramolecular hydroamination of aminoallenes with any (albeit poor) enantioselectivity.¹¹ It is important to mention that in the same year, Yamamoto reported a palladium catalyzed asymmetric synthesis of vinyl pyrrolidines (eq 2.2).¹² The enantioselectivities of this transformation ranged from 47-83% for substrates with various aryl substituents on the terminal alkyne. Interestingly, the observed enantioselectivities increased with higher palladium quantities and stoichiometric use of (*R,R*)-RENORPHOS. For example, the enantiomeric excess of vinyl pyrrolidine **2.4** was improved to 91% ee under the stoichiometric conditions.



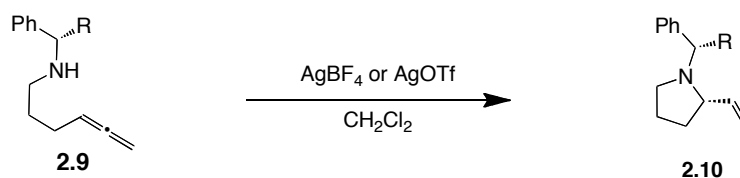
Since the starting materials were alkynes, this transformation cannot be strictly classified as a hydroamination of aminoallenes. However, the authors proposed a catalytic cycle in which the pendant alkyne was isomerized to an allene. The allene was subsequently cyclized to the observed product. But the proposed mechanism was not consistent with the result shown in eq 2.3. When a proposed intermediate **2.5**, was subjected to identical conditions, the reaction

proceeds, but with no enantioselectivity. This inconsistency could be explained by invoking a stereoselective formation of allene **2.5**, followed by a stereospecific hydroamination. Unfortunately, the authors did not test enantiomerically enriched allene **2.5** under the reaction conditions.



As demonstrated by Yamamoto's work, late metals provided an attractive alternative to the early metal hydroamination systems. They not only offered better regioselectivity (generally exclusive formation of the allylamine products), but also are much easier to handle, and provide better functional group compatibility. Another late metal example, the silver nitrate catalyzed hydroamination of amino allenes was reported over forty years ago by Claesson and co-workers.¹³ A few years later, in 1986, Gallagher showed that this transformation could be achieved in a stereospecific manner (eq 2.4).¹⁴ Enantiomerically enriched allene **2.6** was cyclized upon treatment with 0.5 equivalents of silver tetrafluoroborate with good yield and nearly complete chirality transfer. Chiral piperidine **2.7** was used in the synthesis of (*R*)-(-)-coniine, a potent, neurotoxic alkaloid found in hemlock.¹⁵

Table 2.1. Silver-Mediated Diastereoselective Hydroamination of Allenes.

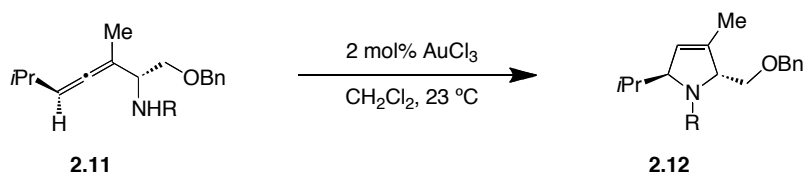


entry	2.9	R =	equiv Ag	% de	% yield
1	2.9a	-CH ₃	0.46	33	87
2	2.9b	-CH ₂ OH	0.15	60	90
3	2.9c	-CONHMe	0.5	81	90
4	2.9d	-CH ₂ NHMe	0.45	78	63
5	2.9e	-CH ₂ SPh	1	96	90
6	2.9f	-CH ₂ S(O)Ph	0.98	99	90

In addition to demonstrating chirality transfer, Gallagher also used a variety of chiral auxiliaries in a silver-mediated diastereoselective hydroamination (Table 2.1).¹⁶ As shown in Table 2.1, the more coordinating groups produced the product with higher de. For example, the methyl substituted substrate cyclized with only 33% de (entry 1), whereas the sulfoxide

substitution (entry 6) yielded the desired pyrrolidine with near perfect de. On the basis of these results, the authors proposed a chair-like transition state organized by silver bridging between the chiral auxiliary and the pendant allene. Although these results were quite promising, this system was found to be extraordinarily sensitive to the amount of silver. In some cases, small amounts, as low as 15 mol%, were beneficial (entry 2); in others, stoichiometric amounts were necessary (entries 5 and 6). In addition, despite being a good demonstration of substrate controlled selectivity, the leap to ligand controlled systems was not forthcoming.

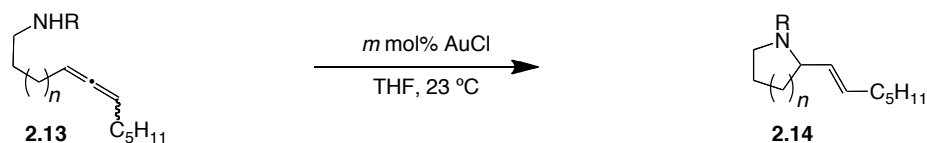
Table 2.2. Gold(III)-Catalyzed Diastereoselective Hydroamination of α -Aminoallenes.



entry	2.11	R =	time	% yield	% dr
1	2.11a	H	5 days	74	>99:1
2	2.11b	Ms	30 min	77	94:6
3	2.11c	Ts	30 min	93	96:4
4	2.11d	Ac	30 min	80	70:30
5	2.11e	Boc	30 min	69	46:54

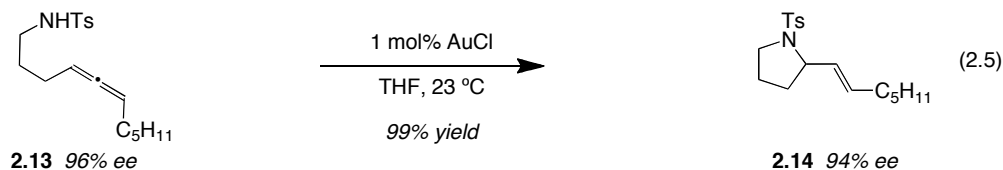
Six years after the Teles hydration¹⁷ marked the beginning of the resurgence of homogeneous gold catalysis, Krause and coworkers reported a diastereoselective gold(III)-catalyzed hydroamination of allenes (Table 2.2).¹⁸ The authors found that despite its propensity to decompose to metallic gold, gold(III) chloride was an effective catalyst for the cycloisomerization of α -aminoallenes. Interestingly, it was found that the protecting group had a strong influence on the diastereoselectivity of the transformation. For example, the unprotected amine **2.11a** and sulfonamides **2.11b** and **2.11c** cyclized with high diastereoselectivity, but acetamide **2.11d** and carbamate **2.11e** were obtained with little to no selectivity.

Table 2.3. Racemic Gold(I)-Catalyzed Hydroamination of Allenes.



entry	<i>m</i> mol%	<i>n</i> =	R =	time (h)	% yield
1	1	1	Ts	3	99
2	1	1	CO ₂ Et	3	97
3	1	1	Cbz	3	99
4	5	1	Bn	24	76
5	5	2	Ts	24	53
6	5	2	Cbz	24	80

Yamamoto and coworkers later extended this methodology to the formation of pyrrolidines and piperidines (Table 2.3).¹⁹ While the authors found that both gold(III) chloride and gold(I) chloride catalyzed the desired reaction with equal efficiency (1 mol%), they preferred the use of gold(I) for its stability. This transformation was applied to a variety of protected amines, including tosylamines, carbamates and benzyl amines. Piperidine formation required extended reaction times as well as higher catalyst loadings (entries 5 and 6). A single example of chirality transfer was also included in this report (eq 2.5). Upon treatment with 1 mol% gold(I) chloride, enantioenriched allene **2.13** cyclized to form tosylpyrrolidine **2.14** with almost complete chirality transfer. This was especially interesting in light of an earlier report of a gold(I)-catalyst racemizing allenes.²⁰



The scope of gold(I)-catalyzed *exo*-hydrofunctionalization of allenes was expanded by Widenhoefer to include a variety of homo-allenic amines, alcohols and carbon nucleophiles (Table 2.4).²¹ This hydroamination protocol was applied to mono- (entries 1-4), as well as di- and tri-substituted allenes with equal success. For example, 3,3-disubstituted allene **2.19** was cyclized to form a sterically challenging tetrasubstituted carbon in excellent yield (97%, entry 5). Also, 1,3-disubstituted allenes were cyclized to form both pyrrolidines and piperidines with near perfect diastereoselectivity (entries 6, 7, and 10). The diastereoselectivity observed for substrates with backbone substitution (entries 4 and 10) was substantially lower (4:1 and 7:1,

respectively). This report by Widenhoefer was important not only due to its broad substrate scope, but also because it demonstrated the high catalytic activity of a gold complex with a sterically demanding *o*-biphenylphosphine ligand. In fact, in the case of alkene hydroamination, the authors found that “employment of the sterically hindered *o*-biphenyl ligand was crucial for high activity.”²¹

Table 2.4. Gold(I)-Catalyzed Hydroamination of N-Allenyl Carbamates.^a

entry	substrate	product	% yield (d.r.)
1 2			94 88
	2.15 R = Boc 2.16 R = Fmoc	2.25 2.26	
3			80 (16:1)
	2.17	2.27	
4			90 (4:1)
	2.18	2.28	
5			97
	2.19	2.29	
6 7			92 (>50:1) 98 (>50:1)
	2.20 R = Me 2.21 R = <i>n</i> -Pr	2.30 2.31	
8			96
	2.22	2.32	
9			92 (7:1)
	2.23	2.33	
10			96 (>50:1) ^b
	2.24	2.34	

^a 5 mol% [P(*t*-Bu)₂(*o*-biphenyl)]AuCl, 5 mol% AgOTf, dioxane, 25 °C, 5 – 180 min. ^b 22 h.

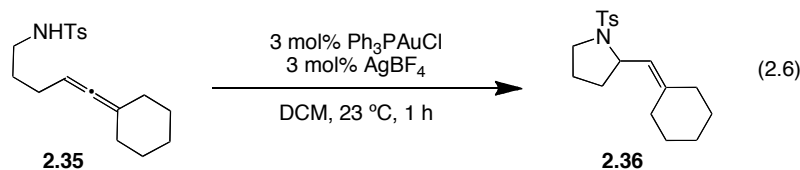
At the time of our research, we had that ligands could exert a strong effect on both diastereoselectivity and enantioselectivity in a gold(I)-catalyzed cyclopropanation.^{37, 22} On the basis of these observations, we hypothesized that chiral phosphinegold(I) complexes could be attractive catalysts for the intramolecular hydroamination of allenes due to their inherent chemoselectivity for activation of C-C multiple bonds. However, the preferred linear geometry of gold(I) complexes places the chiral phosphine ligand distant from the reactive center, rendering enantioselective catalysis challenging. An examination of the crystal structure of (*R*)-

BINAP(AuCl)₂²³ reveals that the P-Au bond was found to be 2.23 Å. In addition, the bond distance between cationic gold and the carbons in a C=C bond can be estimated at 2.2-2.3 Å.²⁴ As a consequence of these measurements, a nucleophile adding *trans*²⁵ across a carbon double bond must be over 4 Å away from the chiral information contained in the ligand!

Results

Initial Optimization

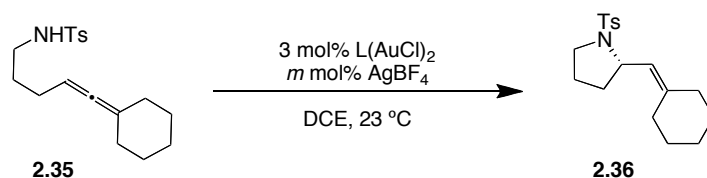
Before embarking on our study of enantioselective hydroamination, it was necessary to establish conditions for the analogous racemic reaction. To this end, a colleague in the Toste group, Dr. Benjamin Sherry, found that upon treatment with a mixture of 3 mol% triphenylphosphine gold chloride and 3 mol% silver tetrafluoroborate, tosylamine **2.35** cyclized to form racemic pyrrolidine **2.36** in excellent yield and minimal reaction time (eq 2.6). These conditions were used throughout the course of this research to generate standard racemic samples.



We began our screen of chiral dinuclear gold(I)-phosphine complexes with the BINAP family of ligands. We were pleased to find that when treated with a mixture of (*R*)-BINAP(AuCl)₂ (**2.37**) and silver tetrafluoroborate, tosylamine **2.35** was transformed efficiently to pyrrolidine **2.36** in 81% yield and 22% ee (Table 2.5, entry 1). Prior work by Dr. David Gorin had shown that adding steric bulk to the aryl phosphine ligands can result in increased enantioselectivity.³⁷ Thus, we found that the use of (*R*)-3,5-xylyl-BINAP as a ligand increased the observed ee to 51% (entry 2). At this point in time a post-doctoral scholar, Dr. Eun Joo Kang, joined our team of researchers. As a reasonable first step, she set about trying to replicate this promising result. We were shocked to find that she was unable to duplicate the enantioselectivities under ostensibly identical reaction conditions.

The irreproducibility of these results prompted a frantic examination of our methodology and standard operating procedures. We were running these reactions on a small (0.1 mmol) scale to maximize screening efficiency and minimize waste. As a consequence, we were weighing approximately 1 mg of silver tetrafluoroborate per reaction. Our standard operating procedure also included storing the hygroscopic silver salt in the glove box. The confluence of a number of factors, the small quantity of salt, static ridden nature of the glove box, inherent accuracy of the balance, and natural human error contributed to a large margin of error in the amount of silver salt actually used. This hypothesis was easily verified by scaling the reactions to determine the optimal amount of silver.

Table 2.5. Initial Ligand Optimization and Salt Effect.

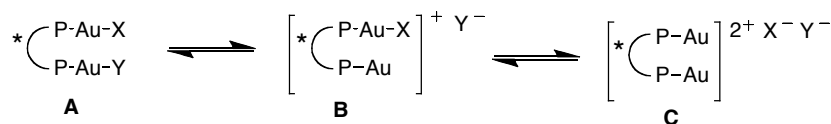


entry	L	m mol%	% ee	% yield
1	(<i>R</i>)-BINAP	3	22	97
2	(<i>R</i>)-3,5-xylyl-BINAP	3	51	81
3	(<i>R</i>)-3,5-xylyl-BINAP	6	1	82

Based on the assumption that a single equivalent of silver salt would abstract an equimolar amount of chloride ions, tosylamine **2.35** was treated with mixtures of pre-catalyst (*R*)-3,5-xylyl-BINAP(AuCl)₂ (**2.38**) and AgBF₄. A species believed to be of type **C** (X = Y = BF₄, Scheme 2.2), generated by the treatment of precatalyst **2.38** with two equivalents of AgBF₄, catalyzed the formation of **2.36** with no stereoselectivity (Table 2.5, entry 3). In contrast, reaction of **2.35** with an *in situ* generated monocationic catalyst of type **B** (X = Cl, Y = BF₄) produced **2.36** in good yield with moderate enantioselectivity (entry 2). This remarkable increase in enantioselectivity¹⁰ led us to hypothesize that the remaining coordinated counterion was crucial for stereoiduction.

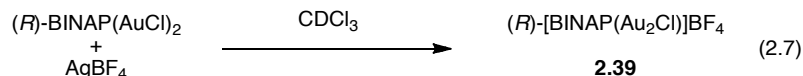
Encouraged by these results, we next attempted to demonstrate substrate scope with the optimized conditions. After a massive screening effort, most of the optimized enantioselectivities were poor to moderate. Because we were not successful at expanding the scope of our optimized reaction, we began to realize that it was necessary to re-examine our assumptions. It is crucial to note that the structure of the *in situ* generated catalysts was unknown. Before proceeding, it was imperative to experimentally verify the nature of the catalysts.

Scheme 2.2. Dinuclear Gold(I)-Phosphine Complexes.



Due to the propensity of cationic gold species to decompose into gold nanoparticles, we attempted to examine the monocationic catalyst mixture (eq 2.7) by NMR. Not surprisingly, the room temperature ¹H NMR spectra displayed a complex mixture of signals. The ³¹P NMR spectra, however, showed a single broad peak at 27.9 ppm. This led us to hypothesize that the catalyst was a single, yet fluxional species. Because heating decomposes the cationic gold species, we embarked on a series of low temperature NMR experiments to freeze out the

structural variations. At -50 °C the ^{31}P NMR resolved into two sharp peaks at 28.8 and 22.0 ppm with a 2.6:1 ratio. This was initially perplexing, because we believed that a catalyst of type **B** ($\text{X} = \text{Cl}$, $\text{Y} = \text{BF}_4$) should appear as one of two possible ^{31}P NMR spectra. First, the two phosphines as represented in Scheme 2.2, are chemically inequivalent and would appear as two distinct signals with a 1:1 ratio. Alternatively, if the coordinated counterion (X) symmetrically bridges between the two gold atoms, a single signal should appear in the ^{31}P NMR spectra. Fortunately, upon slow evaporation, we were able to obtain an x-ray quality crystal from this sample (Figure 2.1).



The crystal structure of **2.39** revealed that the monocationic gold complexes are aligned in polymeric chains linked by bridging chloride anions (Figure 2.1). The structure showed a typical linear, two coordinate geometry around gold with a P-Au-Cl bond angle of 176°. The bond distance between P-Au (2.25 Å) was comparable to the distance observed in the parent BINAP(AuCl)₂ complex (2.27 Å). The Au-Cl bond distances were equal (2.33 Å), indicating a true bridging chloride. These values were also similar to the distances found in the parent BINAP(AuCl)₂ complex (2.32 Å).

Furthermore, the polymeric crystal structure of **2.39** exposed the source of the unexpected integral ratio of phosphine signals in the ^{31}P NMR. If **2.39** existed as a trimer in solution, four of the phosphines would be chlorine bridged, resulting in a 2:1 integral ratio between the two phosphine signals. On the other hand, if **2.39** was a tetramer in solution, a 3:1 integral ration should be observed. Therefore, it is reasonable to hypothesize that the experimentally determined integral ratio of 2.6:1 resulted from a mixture of trimers and tetramers in solution.

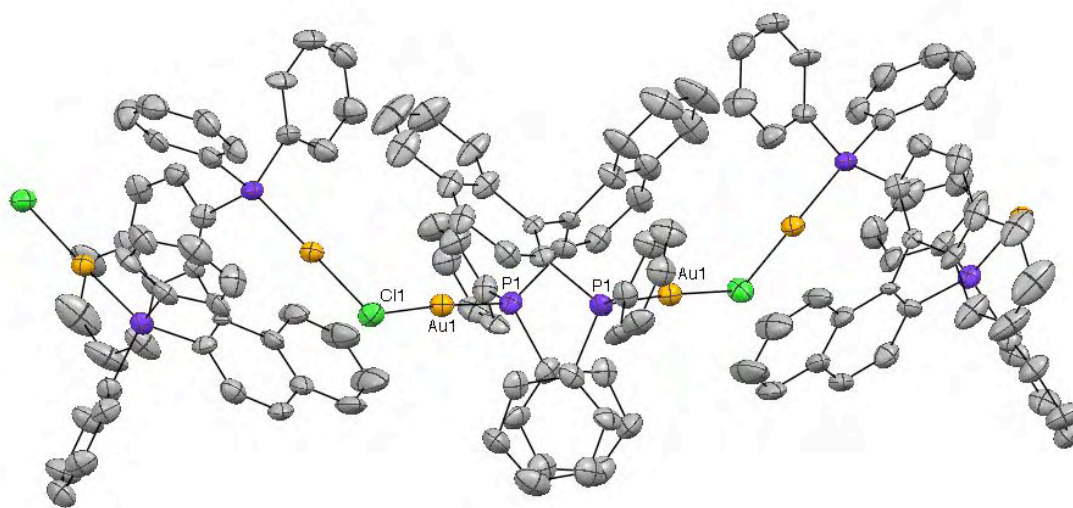


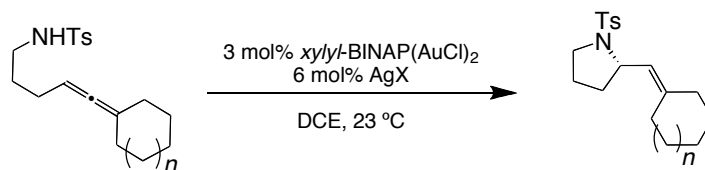
Figure 2.1. ORTEP of (R) -[BINAP(Au₂Cl)]BF₄ (**2.39**). Thermal ellipsoids shown at 50% probability. Hydrogens, tetrafluoroborate counterions and solvent molecules omitted for clarity.

Having experimentally verified the structure of monocationic catalyst **2.39**, we hypothesized that changing either the coordinated or non-coordinated counterions could affect the enantioselectivity of the product. Efforts at modifying the non-coordinating counterion were unsuccessful. For example, a mixture of 3 mol% (R) -3,5-xylyl-BINAP(AuCl)₂ and 3 mol% AgOTs produced **2.36** in 80% and 30% ee. We theorized that the chloride counterion was crucial for the transmission of stereochemical information. As evidence, no enantioinduction was observed when the chloride counterion was absent (Table 2.5, entry 3). Consequently, replacing chloride with a larger coordinated counterion could amplify enantioselectivity. Employing coordinating anions, however, necessitates a complex of type **A** to be in equilibrium with catalytically active species **B**. To ensure that appreciable amounts of active catalyst are present in solution, an ideal counterion must be electronically as well as sterically modifiable. We envisioned that a type **A** carboxylate complex ($X = Y = \text{RCO}_2$) could satisfy these requirements.

*Development and Characterization of *p*-Nitrobenzoate Catalysts*

We began our counterion screen with the simplest type of carboxylate: acetate. Unfortunately a mixture of 3 mol% (R) -3,5-xylyl-BINAP(AuCl)₂ and 6 mol% AgOAc failed to catalyze the formation of **2.36** (Table 2.6, entry 1). As discussed above, we expected that the electronic properties of the coordinating counterions would have to be modified to generate appreciable amounts of active catalyst in solution. This effect was demonstrated by adding electron-withdrawing groups to the acetate counterion. By utilizing silver trifluoroacetate as a co-catalyst with (R) -3,5-xylyl-BINAP(AuCl)₂, **2.38** was transformed to the desired pyrrolidine **2.36** with moderate enantioselectivity (entry 2). Having verified our ability to tune the electronic characteristics of the counterions, we turned to adjusting the steric size of the counterions.

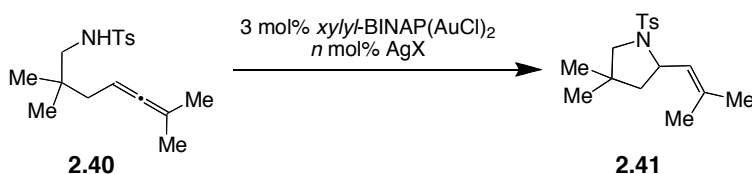
Table 2.6. Counterion Effects on Enantioselectivity.



entry	X	n =	time (h)	% ee	% yield
1	OAc	2	16	-	n.r.
2	OTFA	2	16	86	57
3	OBz	1	24	27	98
4	OPNB	1	24	76	98
5	ODNB	1	24	82	95

We were pleased to find a dramatic amplification of enantiomeric excess when benzoate counterions²⁶ were employed. Treating tosylamine **2.35** with precatalyst **2.38** and two equivalents of silver benzoate provided **2.36** with excellent (98%) ee, but the reaction was low yielding even after extended reaction times (Table 2.6, entry 3). Again, we hypothesized that the poor conversion was due to low equilibrium concentrations of the catalytically active cationic species.²⁷ Therefore, an electron-withdrawing group was added to the benzoate in the hopes of improving conversion. The use of silver *p*-nitrobenzoate (AgOPNB) increased the yield of **2.36** to 76% with no loss of enantioselectivity (entry 4). Silver 3,5-dinitrobenzoate (AgODNB) further enhanced the yield of the reaction to 82%, but eroded stereoselection to 95% ee (entry 5). Presumably this could be explained by the formation of small equilibrium concentrations of dicationic catalyst (type C).

Table 2.7. Optimization of 4,4-Substituted Pyrrolidines.



entry	<i>n</i> mol%	AgX	solvent	temp (°C)	% ee	% conv
1	6	AgOBz	DCM	23	94	23
2	6	AgOPNB	DCM	23	88	19
3	6	AgOPNB	DCE	23	89	24
4	6	AgOPNB	MeNO ₂	23	90	19
5	6	AgOPNB	MeNO ₂	50	90	95

We next screened the benzoate counterions against a tosylamine with backbone substitution (**2.40**). As expected, the use of silver benzoate as co-catalyst yielded disappointingly small amounts of the desired product, but with good ee (Table 2.7, entry 1). We were surprised to find that the use of silver *p*-nitrobenzoate did not improve the conversion (19%, entry 2), and led to a slight decrease in ee (89%). Next, in the hope that increasing the polarity of the solvent would improve conversion the reaction was screened in dichloroethane and nitromethane (entries 3 and 4). Although at room temperature these solvents gave similar results, gentle heating (50 °C) in nitromethane increased conversion to near quantitative without degrading the enantioselectivity (90%, entry 5).

Again, we thought it would be prudent to investigate the nature of the *in situ* generated catalyst. As such, we examined the mixture generated from **2.38** and 2 equivalents of silver *p*-nitrobenzoate using ³¹P NMR. Although we expected that (*R*)-3,5-xylyl-BINAP(AuOPNB)₂ (**2.42**) would be formed quantitatively, instead a mixture of (*R*)-3,5-xylyl-BINAP(Au₂ClOPNB):**2.42**:**2.38** was observed (Figure 2.2). The ³¹P NMR showed four signals (22.4, 21.9, 17.7, 17.1 ppm). The assignment of these peaks to a 1:0.34:2.75 mixture of (*R*)-3,5-xylyl-BINAP(Au₂ClOPNB):**2.42**:**2.38** was supported by independent preparation and characterization of complexes **2.42** (³¹P NMR, 17.7 ppm) and **2.38** (³¹P NMR, 21.9 ppm). Because the bulk of the *in situ* generated catalyst mixture was an inactive complex,²⁸ we believed the reaction would be improved by using purified **2.42** as the precatalyst.

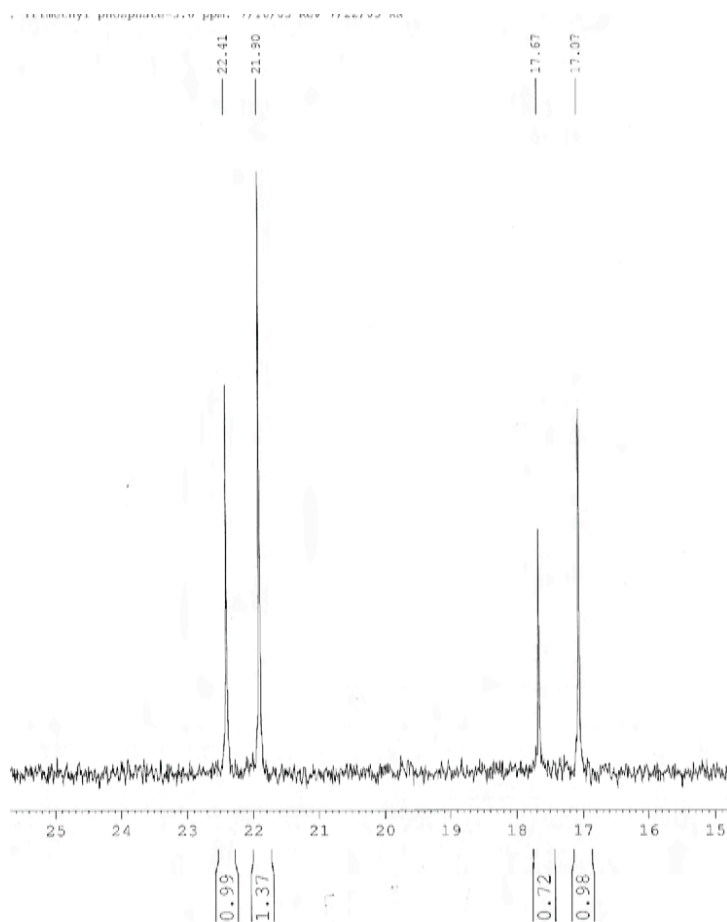


Figure 2.2. ^{31}P NMR of *In Situ* Generated (*R*)-3,5-xylyl-BINAP(AuOPNB) $_2$ (**2.42**).

Since silver *p*-nitrobenzoate is sparingly soluble in halogenated solvents, we attempted sonicating the heterogeneous reaction mixture to further increase the conversion to **2.42**. Sonication increased the ratio of (*R*)-3,5-xylyl-BINAP(Au $_2$ ClOPNB):**2.42**:**2.38** to 1:1:0.25. Gratifyingly, the combination of sonication and 3 equivalents of silver salt produced a quantitative yield of **2.42**. Utilizing **2.42**, an isolable, bench-stable complex, not only streamlined reaction setup, but also increased the yield of **2.36** to 88% with a reduced reaction time (15 vs. 24 h), while maintaining enantioselectivity (Table 2.8, entry 3).

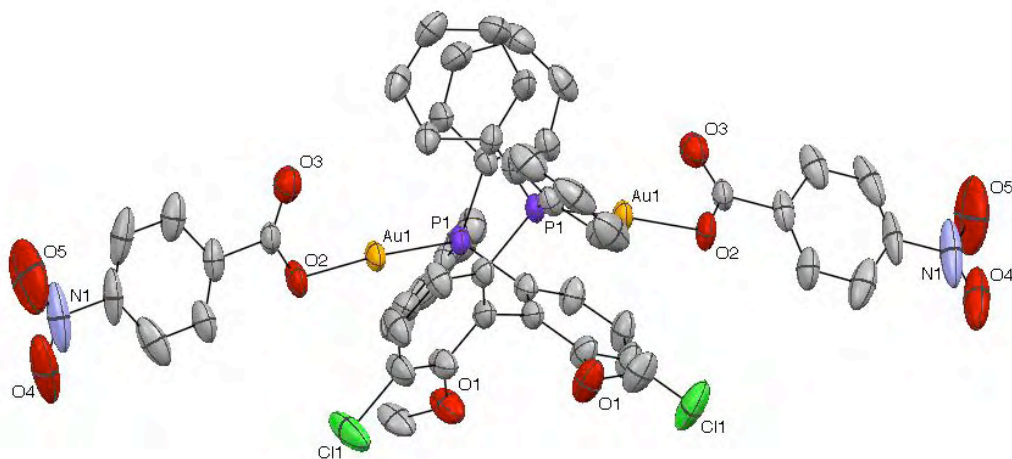
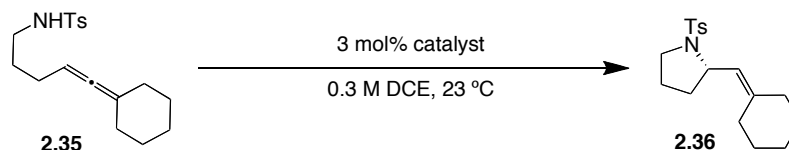


Figure 2.3. ORTEP of (*R*)-C1MeOBiPHEP(AuOPNB)₂ (**2.43**). Thermal ellipsoids shown at 50% probability. Hydrogens and solvent molecules omitted for clarity.

In addition to the usual characterization methods (NMR, HRMS, EA), we were able to confirm the structure of the gold(I)-bis-*p*-nitrobenzoate catalysts with an x-ray crystal structure of (*R*)-C1MeOBiPHEP(AuOPNB)₂ (**2.43**) (Figure 2.3).²⁹ The structure conforms to the typical linear, two coordinate geometry with a P-Au-O2 bond angle of 174°. The Au-O2 bond length (2.05 Å) is slightly shorter than a typical gold chloride complex (2.3 Å). Finally, the P-Au bond length was found to be 2.21 Å.

Final Optimization

Table 2.8. Ligand Optimization for Compound **2.36**.



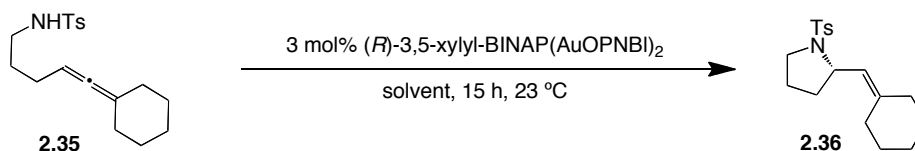
entry	catalyst	time (h)	% yield ^a	% ee ^b
1	(<i>R</i>)-BINAP(AuOPNB) ₂ (R-2.44)	15	82	93
2	(<i>S</i>)-BINAP(AuOPNB) ₂ (S-2.44)	15	86	-94
3	(<i>R</i>)-3,5-xylyl-BINAP(AuOPNB) ₂ (2.42)	17	88	98
4	(<i>R</i>)-Segphos(AuOPNB) ₂ (2.45)	24	57	83
5	(<i>R</i>)-Synphos(AuOPNB) ₂ (2.46)	24	47	92
6	(<i>R</i>)-ClMeOBiPHEP(AuOPNB) ₂ (2.43)	15	85	97

^aIsolated yield after column chromatography. ^bDetermined by HPLC.

A variety of gold chloride complexes were amenable to the preparation of bis-*p*-nitrobenzoate complexes (Table 2.8). Although the use of (*R*)-3,5-xylyl-BINAP(AuOPNB)₂ yielded the highest enantioselectivity (98%, entry 3), all of these complexes (**2.42-2.46**) were found to catalyze the hydroamination with good enantioselectivity (Table 2.8, entries 1-6).

The use of (*R*)-3,5-xylyl-BINAP(AuOPNB)₂ as a catalyst produced **2.36** with similar yields and enantiomeric excess in halogenated solvents (Table 2.9). For example, the use of DCM (95%, 98% ee; entry 1) produced a nearly identical outcome to that obtained with DCE (88%, 98% ee; entry 2). A polar, non-coordinating solvent, nitromethane, also delivered excellent results (94%, 98% ee; entry 3). However, polar, coordinating solvents such as acetonitrile (entry 6) and tetrahydrofuran (entry 5) drastically reduced the observed yield (48 and 16%, respectively), while the ee remained unchanged. Employing a non-polar solvent, benzene (entry 4), also resulted in lower yields of **2.36** (27%) and slightly lower enantioselectivity (94%).

Table 2.9. Solvent Optimization for Compound **2.36**.



entry	solvent	% yield ^a	% ee ^b
1	DCM	95	98
2	DCE	88	98
3	MeNO ₂	94	98
4	benzene	27	94
5	THF	16	98
6	MeCN	48	98

^a Isolated yield after column chromatography. ^b Determined by HPLC.

Substrate Scope

The substrate scope was examined utilizing the optimized reaction conditions (Table 2.10).³⁰ The allene terminus was found to be particularly amenable to substitution. Both cyclic and linear alkanes were well tolerated (entries 1-5) yielding the corresponding pyrrolidines in good yield and excellent enantiomeric excess. For example, both dimethyl (**2.47**, entry 1) and diethyl substituted allenes (**2.48**, entry 2) cyclized with near perfect enantioselectivity (99%) and good yield (98 and 90% respectively). In similar fashion, cyclohexyl (**2.35**, entry 4) and cycloheptyl (**2.50**, entry 5) substituted allenes produced the desired products with excellent enantioselectivity (98%). Interestingly, when the reaction conditions were applied to the analogous cyclopentyl substituted allene (**2.49**, entry 3), the desired pyrrolidine **2.55** was obtained with reduced enantiomeric excess (83%). This decrease in ee could be rationalized by the involvement of the terminal allene substituents in the transition state. In addition, substrates with subtle electronic perturbations (entries 6 and 7) required extended reaction times and slightly elevated temperatures.

Table 2.10. Scope of Allene Substitution in the Gold(I)-Catalyzed Hydroamination of Allenes.^a

entry	substrate	time (h)	product	% yield ^b	% ee ^c
1		15		2.53	98 99
2		17		2.54	90 ^d 99
3		15		2.55	75 83
4		17		2.36	88 98
5		15		2.56	88 98
6		25		2.57	80 98
7		25		2.58	79 ^e 98

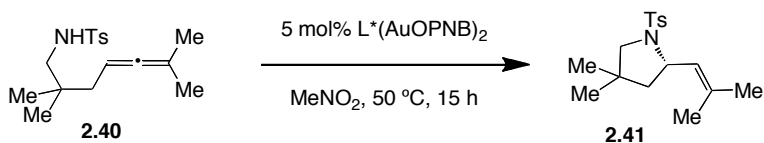
^a Reaction Conditions: 3 mol% (*R*)-3,5-xylyl-BINAP(AuOPNB)₂ (**2.42**), 0.3 M in DCE, 23 °C.

^b Isolated yield after column chromatography. ^c Determined by HPLC. ^d 5 mol% catalyst. ^e 50 °C.

The reaction could also be extended to substrates containing substitution in the tether (Table 2.11). However, even with the isolated catalyst **2.42**, these substrates required that the reaction be carried out in nitromethane at 50 °C with 5 mol% catalyst in order to achieve complete conversion (*vide supra*). For example, gold(I)-catalyzed cyclization of tosylamine **2.40** in nitromethane at 50 °C gave dimethyl substituted pyrrolidine **2.41** in 94% yield and 93% ee (entry 2). While (*R*)-3,5-xylyl-BINAP(AuOPNB)₂ (**2.42**) proved the most general catalyst for the enantioselective synthesis of pyrrolidines, we were curious to see if modifying the ligand would

improve the enantioselectivity. (*R*)-ClMeOBiPHEP(AuOPNB)₂ (**2.43**) was equally competent at catalyzing the cyclization of **2.40** yielding the product **2.41** with 93% ee (entry 5). Further screening of (*S*)-BINAP(AuOPNB)₂ (*S*-**2.44**), (*R*)-Segphos(AuOPNB)₂ (**2.45**), and (*R*)-Synphos(AuOPNB)₂ (**2.46**) did not result in additional improvement of ee (entries 1, 3, and 4, respectively).

Table 2.11. Ligand Optimization for Compound **2.41**.^a

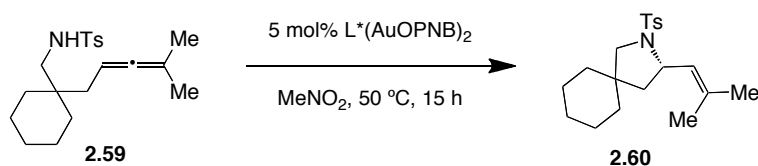


entry	ligand	% yield ^b	% ee ^c
1	(<i>S</i>)-BINAP	90	-90
2	(<i>R</i>)-3,5-xylyl-BINAP	94	93
3	(<i>R</i>)-Segphos	87	82
4	(<i>R</i>)-Synphos	86	88
5	(<i>R</i>)-ClMeOBiPHEP	85	93

^a Reaction Conditions: 5 mol% L*(AuOPNB)₂, 0.3 M in MeNO₂, 50 °C. ^b Isolated yield after column chromatography. ^c Determined by HPLC.

Modifying the 4,4-dimethyl substitution to cyclohexyl resulted in a sharp drop in enantioselectivity (Table 2.12). For instance, both (*R*)-3,5-xylyl-BINAP(AuOPNB)₂ (**2.42**) and (*R*)-ClMeOBiPHEP(AuOPNB)₂ (**2.43**) catalyzed the formation of **2.60** with an enantioselectivity of 70%. The other ligands screened (BINAP, Segphos, Synphos) failed to improve upon this modest result (entries 1, 3, and 4).

Table 2.12. Ligand Optimization for Compound **2.60**.^a

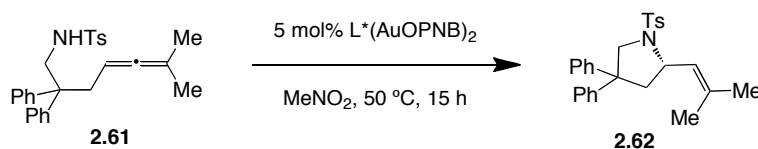


entry	ligand	% yield ^b	% ee ^c
1	(<i>S</i>)-BINAP	92	-60
2	(<i>R</i>)-3,5-xylyl-BINAP	98	70
3	(<i>R</i>)-Segphos	99	69
4	(<i>R</i>)-Synphos	81	69
5	(<i>R</i>)-ClMeOBiPHEP	85	70

^a Reaction Conditions: 5 mol% L*(AuOPNB)₂, 0.3 M in MeNO₂, 50 °C, ^b Isolated yield after column chromatography. ^c Determined by HPLC.

The ee obtained for the cyclization of **2.61** to **2.62**, was distressingly low (53%) when (*R*)-3,5-xylyl-BINAP(AuOPNB)₂ was employed as the catalyst (Table 2.13, entry 2). Fortunately, the enantioselectivity improved to 88% by replacing **2.42** with (*R*)-SEGPHOS(AuOPNB)₂ (**2.45**) as the catalyst (entry 3). Other catalysts, such as (*S*)-BINAP(AuOPNB)₂, (*R*)-Synphos(AuOPNB)₂, and (*R*)-ClMeOBiPHEP(AuOPNB)₂ also catalyzed the formation of **2.62** with moderate ee (80-81%).

Table 2.13. Ligand Optimization for Compound **2.62**.^a

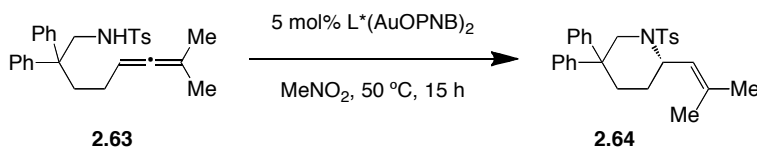


entry	ligand	% yield ^b	% ee ^c
1	(<i>S</i>)-BINAP	92	-80
2	(<i>R</i>)-3,5-xylyl-BINAP	98	53
3	(<i>R</i>)-Segphos	99	88
4	(<i>R</i>)-Synphos	81	82
5	(<i>R</i>)-ClMeOBiPHEP	85	81

^a Reaction Conditions: 5 mol% L*(AuOPNB)₂, 0.3 M in MeNO₂, 50 °C. ^b Isolated yield after column chromatography. ^c Determined by HPLC.

While a wide variety of complexes, including (*R*)-3,5-xylyl-BINAP(AuOPNB)₂, catalyzed the formation of chiral piperidines (Table 2.14), the optimal enantioselectivity was obtained by simply switching the catalyst to (*R*)-ClMeOBIPHEP(AuOPNB)₂ (**2.43**). For example, reaction of **2.63** catalyzed by 5 mol% **2.43** afforded piperidine **2.64** in 98% conversion and 88% ee.

Table 2.14. Ligand Optimization for Piperidine Formation. ^a



entry	ligand	% conv ^b	% ee ^c
1	(<i>S</i>)-BINAP	80	75
2	(<i>S</i>)- <i>p</i> -tolyl-BINAP	65	80
3	(<i>R</i>)-3,5-xylyl-BINAP	50	40
4	(<i>S</i>)-BINAPO	25	16
5	(<i>R</i>)-Segphos	42	85
6	(<i>R</i>)-Difluorophos	98	82
7	(<i>R</i>)-ClMeOBiPHEP	98	88

^a Reaction Conditions: 5 mol% L*(AuOPNB)₂, 0.3 M in MeNO₂, 50 °C, 15 h. ^b Determined by ¹H NMR. ^c Determined by HPLC.

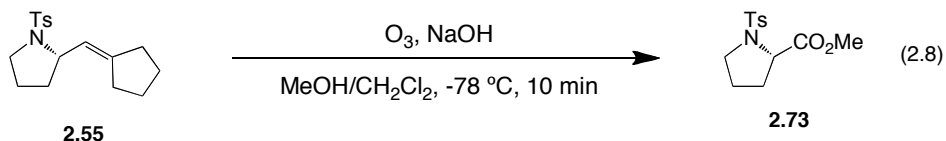
Applying the optimized reaction conditions to a series of substrates revealed some interesting trends (Table 2.15).³¹ In addition to elevated temperature (50 °C) and increased catalyst loading (5 mol%), the majority of piperidines (entries 2-4) also required extended reaction times to achieve reasonable conversion. Also, unsubstituted piperidines (entries 1 and 2) were obtained with lower enantioselectivities than the corresponding 4,4-dialkylsubstituted substrates (entries 3 and 5), which were isolated with excellent ee. This was in contrast to the 4,4-disubstituted pyrrolidines, which generally were formed with lower ee than their unsubstituted counterparts (*vide supra*).

Table 2.15. Scope of Piperidine Formation in the Gold(I)-Catalyzed Hydroamination of Allenes.^a

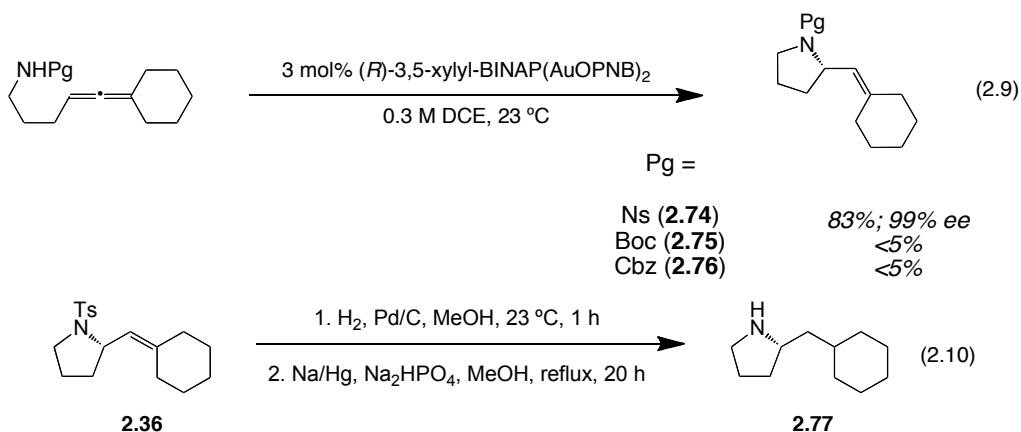
entry	substrate	time (h)	product	% yield ^b	% ee ^c	
1		15		2.69	88	81
2		24		2.70	41	74
3		24		2.71	70	98
4		24		2.64	70	88
5		17		2.72	66	97

^a Reaction Conditions: 5 mol% (*R*)-ClMeOBiPHEP(AuOPNB)₂, 0.3 M in MeNO₂, 50 °C. ^b Isolated yield after column chromatography. ^c Determined by HPLC.

Although the pyrrolidine and piperidine products formed by this methodology are simple, the vinyl group provides a functional handle for further modification. Despite the steric bulk of a trisubstituted alkene, the vinyl group of **2.55** was easily ozonolytically cleaved to yield *N*-*p*-toluenesulfonyl-L-(–)-proline methyl ester **2.73** (eq 2.8).³² Gratifyingly, the basic conditions did not affect the stereochemistry of the product. The absolute stereochemistry of **2.73** was determined by comparison to the literature values.³³ The stereochemistry of the remaining products were determined by analogy to **2.73**.



Finally, modifying the sulfonyl protecting group to the easily cleaved *o*-nosyl group³⁴ proved successful (eq 2.9), but carbamate derivatives failed to react. It was also imperative to establish a deprotection procedure, especially because toluenesulfonyl protecting groups often are considered difficult to remove. However, tosylpyrrolidine **2.36** underwent smooth deprotection under reductive conditions (eq 2.10).³⁵ No racemization was observed in the product.³⁶



Conclusion

In summary, we have uncovered a remarkable counterion effect on the enantioselectivity of gold-catalyzed intramolecular hydroamination of allenes. This discovery resulted in the development of phosphinegold(I)-*bis-p*-nitrobenzoate complexes as catalysts for enantioselective formation of vinyl-substituted pyrrolidines and piperidines. Application of our chiral gold(I)-*p*-nitrobenzoate complexes to the enantioselective addition of hydrazines and hydroxylamines will be discussed in chapter 3.

Experimental

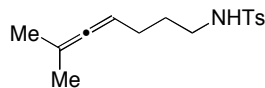
General Information

Unless otherwise noted all commercial materials were used without further purification. 1,2-dichloroethane (DCE) and nitromethane (MeNO₂) utilized in gold(I)-catalyzed reactions was used as received from Aldrich Chemical Company. Gold(I)-catalyzed reactions were conducted in two dram vials equipped with a magnetic stir bar, fitted with a threaded cap, and protected from ambient light. All other reactions were conducted in flame-dried glassware under an inert (N₂) atmosphere with magnetic stirring and dried solvent. Solvents were dried by passage through an activated alumina column under nitrogen. Silver *p*-nitrobenzoate was prepared according to the method of Rubottom.²⁶ Chiral gold(I) chloride complexes were prepared according to a procedure previously described by our group.³⁷ Substrates **2.40**, **2.59**, **2.61**, **2.67**, **2.63**, and **2.68** were prepared according to the methods of Widenhoefer.^{21a} Bis(homoallylic)sulfonamides were prepared according to the methods of Bäckvall.³⁸ Thin-layer chromatography (TLC) analysis of reaction mixtures was performed using Merck silica gel 60 F₂₅₄ TLC plates, and visualized by a combination of UV and permanganate or anisaldehyde staining. Flash column chromatography was carried out on Merck 60 silica gel (32-63 μm). ¹H and ¹³C NMR spectra were recorded with Bruker DRX-500, AVB-400, AVQ-400, and AV-300 spectrometers and referenced to CDCl₃ unless otherwise noted. IR spectra were recorded with a ThermoNicolete Avatar 370 FTIR spectrometer as thin films on a ZnSe plate. Enantiomeric excess was determined on a Shimadzu VP Series Chiral HPLC. Mass spectral and analytical data were obtained via the Micro-Mass/Analytical Facility operated by the College of Chemistry, University of California, Berkeley.

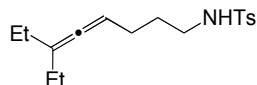
General Procedure for Au(I)-Catalyzed Hydroamination

To a solution of tosylamine (1 equiv) in DCE or MeNO₂ (0.30 M) was added the appropriate gold(I) complex. The resulting homogeneous mixture was protected from ambient light and left to stir at the indicated temperature (23° or 50° C). Upon completion, as judged by TLC analysis of the reaction mixture, the solution was loaded directly onto a silica gel column. Purification by flash column chromatography afforded the desired cyclized product.

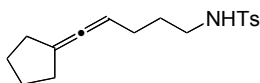
Characterization Data



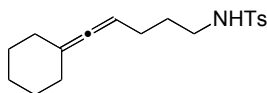
Tosylamine 2.47. The crude mixture was purified by flash column chromatography (8:1 hexanes:EtOAc) to afford **2.47** as a clear oil: TLC $R_f = 0.47$ (3:1 hexanes:EtOAc); $^1\text{H NMR}$ (400 MHz, CDCl_3) δ 7.75 (d, 2H, $J = 8.0$ Hz), 7.29 (d, 2H, $J = 8.0$ Hz), 4.85-4.82 (m, 2H), 2.95 (q, 2H, $J = 6.8$ Hz), 2.41 (s, 3H), 1.91 (q, 2H, $J = 6.8$ Hz), 1.60 (s, 3H), 1.60 (s, 3H), 1.57-1.51 (m, 2H) ppm; $^{13}\text{C NMR}$ (100 MHz, CDCl_3) δ 201.7, 143.2, 137.0, 129.6, 127.0, 95.7, 87.4, 42.6, 28.6, 26.0, 21.4, 20.5 ppm; IR (thin film) ν 3281, 2932, 1323, 1156 cm^{-1} ; HRMS (FAB) calcd. for $[\text{C}_{15}\text{H}_{22}\text{NO}_2\text{S}]^+$: m/z 280.1371, found 280.1370; Anal calcd. for $\text{C}_{15}\text{H}_{21}\text{NO}_2\text{S}$: C, 64.48; H, 7.58; N, 5.01; found: C, 64.47; H, 7.75; N, 4.91.



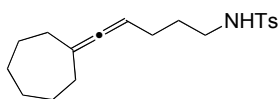
Tosylamine 2.48. The crude mixture was purified by flash column chromatography (10:1 hexanes:EtOAc) to afford **2.48** as a clear oil: TLC $R_f = 0.50$ (3:1 hexanes:EtOAc); $^1\text{H NMR}$ (400 MHz, CDCl_3) δ 7.74 (d, 2H, $J = 8.4$ Hz), 7.28 (d, 2H, $J = 8.0$ Hz), 5.07-5.02 (m, 1H), 4.95 (t, 1H, $J = 6.2$ Hz), 2.95 (q, 2H, $J = 6.9$ Hz), 2.40 (s, 3H), 1.93 (q, 2H, $J = 6.9$ Hz), 1.87 (q, 2H, $J = 7.2$ Hz), 1.86 (q, 2H, $J = 7.2$ Hz), 1.53 (quint, 2H, $J = 7.2$ Hz), 0.90 (t, 6H, $J = 7.4$ Hz) ppm; $^{13}\text{C NMR}$ (100 MHz, CDCl_3) δ 200.0, 143.2, 136.9, 129.6, 127.0, 108.6, 91.5, 42.7, 28.9, 26.4, 25.5, 21.4, 12.3 ppm; IR (thin film) ν 3275, 2965, 1323, 1157, 814 cm^{-1} ; HRMS (FAB) calcd. for $[\text{C}_{17}\text{H}_{26}\text{NO}_2\text{S}]^+$: m/z 308.1684, found 308.1688; Anal calcd. for $\text{C}_{17}\text{H}_{25}\text{NO}_2\text{S}$: C, 66.41; H, 8.20; N, 4.56; found: C, 66.45; H, 8.39; N, 4.68.



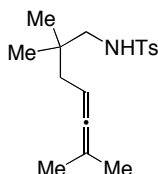
Tosylamine 2.49. The crude mixture was purified by flash column chromatography (12:1 hexanes:EtOAc) to afford **2.49** as a yellow oil: TLC $R_f = 0.40$ (3:1 hexanes:EtOAc); $^1\text{H NMR}$ (400 MHz, CDCl_3) δ 7.74 (d, 2H, $J = 8.4$ Hz), 7.30 (d, 2H, $J = 8.0$ Hz), 5.01-4.93 (m, 1H), 4.48 (t, 1H, $J = 6.0$ Hz), 2.97 (q, 2H, $J = 6.8$ Hz), 2.42 (s, 3H), 2.28-2.24 (m, 4H), 1.94 (q, 2H, $J = 6.8$ Hz), 1.66-1.61 (m, 4H), 1.55 (quintet, 2H, $J = 6.8$ Hz) ppm; $^{13}\text{C NMR}$ (100 MHz, CDCl_3) δ 197.1, 143.3, 137.1, 129.7, 127.1, 104.5, 90.0, 42.7, 31.2, 28.7, 27.0, 26.3, 21.5 ppm; IR (thin film) ν 3277, 1322, 1156 cm^{-1} ; HRMS (FAB) calcd. for $[\text{C}_{17}\text{H}_{24}\text{NO}_2\text{S}]^+$: m/z 306.1528, found 306.1532.



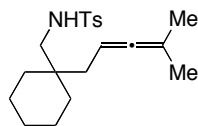
Tosylamine 2.35. The crude mixture was purified by flash column chromatography (12:1 hexanes:EtOAc) to afford **2.35** as a colorless oil: TLC $R_f = 0.41$ (3:1 hexanes:EtOAc); ^1H NMR (400 MHz, CDCl_3) δ 7.74 (d, 2H, $J = 8.4$ Hz), 7.30 (d, 2H, $J = 8.0$ Hz), 4.89-4.85 (m, 1H), 4.47 (t, 1H, $J = 6.4$ Hz), 2.97 (q, 2H, $J = 6.4$ Hz), 2.42 (s, 3H), 2.02-2.00 (m, 4H), 1.93 (q, 2H, $J = 6.4$ Hz), 1.61-1.43 (m, 8H) ppm; ^{13}C NMR (100 MHz, CDCl_3) δ 198.4, 143.3, 137.0, 129.7, 127.1, 103.3, 87.3, 42.6, 31.6, 28.6, 27.5, 26.2, 26.1, 21.5 ppm; IR (thin film) ν 3278, 1444, 1322, 1156 cm^{-1} ; Anal calcd. for $\text{C}_{18}\text{H}_{25}\text{NO}_2\text{S}$: C, 67.67; H, 7.89; N, 4.38; S, 10.04; found: C, 67.74; H, 8.09; N, 4.42; S, 10.20.



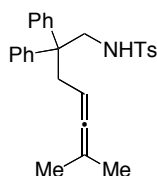
Tosylamine 2.50. The crude mixture was purified by flash column chromatography (16:1 hexanes:EtOAc) to afford **2.50** as a colorless oil: TLC $R_f = 0.47$ (3:1 hexanes:EtOAc); ^1H NMR (400 MHz, CDCl_3) δ 7.74 (d, 2H, $J = 8.4$ Hz), 7.30 (d, 2H, $J = 8.4$ Hz), 4.88-4.83 (m, 1H), 4.48 (t, 1H, $J = 6.0$ Hz), 2.98 (q, 2H, $J = 6.4$ Hz), 2.42 (s, 3H), 2.16-2.13 (m, 4H), 1.92 (q, 2H, $J = 6.8$ Hz), 1.60-1.50 (m, 10H) ppm; ^{13}C NMR (100 MHz, CDCl_3) δ 201.8, 143.3, 137.0, 129.7, 127.1, 105.2, 87.1, 42.7, 32.6, 29.4, 28.7, 28.5, 26.2, 21.6 ppm; IR (thin film) ν 3276, 1440, 1323, 1156 cm^{-1} ; HRMS (FAB) calcd. for $[\text{C}_{19}\text{H}_{28}\text{NO}_2\text{S}]^+$: m/z 334.1841, found 334.1841; Anal calcd. for $\text{C}_{19}\text{H}_{27}\text{NO}_2\text{S}$: C, 68.43; H, 8.16; N, 4.20; S, 9.62; found: C, 68.20; H, 8.33; N, 4.21; S, 9.83.



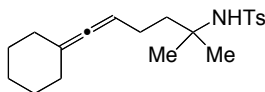
Tosylamine 2.40. The crude mixture was purified by flash column chromatography (5-15% EtOAc:hexanes) to afford **2.40** as a white solid: TLC $R_f = 0.35$ (20% EtOAc:hexanes); ^1H NMR (400 MHz, CDCl_3) δ 7.73 (d, 2H, $J = 7.7$ Hz), 7.29 (d, 2H, $J = 7.7$ Hz), 4.81 (m, 1H), 4.60 (bt, 1H, $J = 7.1$ Hz), 2.71 (d, 2H, $J = 7.1$ Hz), 2.42 (s, 3H), 1.83 (d, 2H, $J = 8.1$ Hz), 1.61 (s, 3H), 1.60 (s, 3H), 0.86 (s, 6H) ppm; ^{13}C NMR (100 MHz, CDCl_3) δ 203.3, 143.3, 137.2, 129.7, 127.1, 94.2, 84.2, 52.5, 39.8, 34.5, 24.8, 21.5, 20.5 ppm; IR (thin film) ν 3283, 2969, 2933, 1315, 1152 cm^{-1} ; HRMS (EI) calcd. for $[\text{C}_{17}\text{H}_{25}\text{NO}_2\text{S}]^+$: m/z 307.1606, found 307.1601.



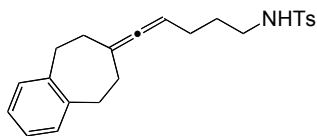
Tosylamine 2.59. The crude mixture was purified by flash column chromatography (5-15% EtOAc:hexanes) to afford **2.59** as a white solid: TLC $R_f = 0.42$ (20% EtOAc:hexanes); $^1\text{H NMR}$ (400 MHz, CDCl_3) δ 7.78 (d, 2H, $J = 8.4$ Hz), 7.34 (d, 2H, $J = 8.4$ Hz), 4.84 (m, 1H), 4.49 (bt, 1H, $J = 7.0$ Hz), 2.85 (d, 2H, $J = 7.0$ Hz), 2.46 (s, 3H), 1.95 (d, 2H, $J = 8.0$ Hz), 1.65 (s, 3H), 1.64 (s, 3H), 1.52-1.28 (m, 10H) ppm; $^{13}\text{C NMR}$ (100 MHz, CDCl_3) δ 203.0, 143.2, 137.2, 129.7, 127.1, 94.4, 83.8, 49.3, 36.7, 36.3, 33.2, 26.1, 21.5, 21.3, 20.5 ppm; IR (thin film) ν 3288, 2931, 2851, 1316, 1152 cm^{-1} ; HRMS (EI) calcd. for $[\text{C}_{20}\text{H}_{29}\text{NO}_2\text{S}]^+$: m/z 347.1919, found 347.1912.



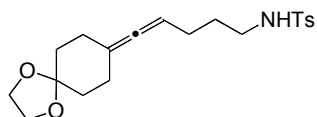
Tosylamine 2.61. The crude mixture was purified by flash column chromatography (5-15% EtOAc:hexanes) to afford **2.61** as a white solid: TLC $R_f = 0.33$ (20% EtOAc:hexanes); $^1\text{H NMR}$ (400 MHz, CDCl_3) δ 7.61 (d, 2H, $J = 8.1$ Hz), 7.32-7.21 (m, 8H), 7.11 (d, 4H, $J = 7.1$ Hz), 4.55 (m, 1H), 3.93 (bt, 1H, $J = 6.5$ Hz), 3.62 (d, 2H, $J = 6.5$ Hz), 2.86 (d, 2H, $J = 7.5$ Hz), 2.46 (s, 3H), 1.56 (s, 3H), 1.55 (s, 3H) ppm; $^{13}\text{C NMR}$ (100 MHz, CDCl_3) δ 203.8, 144.4, 143.4, 136.3, 129.7, 128.4, 127.9, 127.1, 126.7, 94.7, 83.5, 50.0, 49.9, 38.1, 21.6, 20.3 ppm; IR (thin film) ν 3294, 2978, 2934, 1322, 1160 cm^{-1} ; LRMS (FAB) m/z 432 ($\text{M}+1$) $^+$; HRMS (FAB) calcd. for $[\text{C}_{28}\text{H}_{29}\text{NO}_2\text{S}]^+$: m/z 432.1997, found 432.1992.



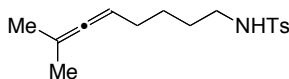
Tosylamine 2.79. The crude mixture was purified by flash column chromatography (12:1 hexanes:EtOAc) to afford **2.79** as a clear oil: TLC $R_f = 0.52$ (3:1 hexanes:EtOAc); $^1\text{H NMR}$ (300 MHz, CDCl_3) δ 7.75 (d, 2H, $J = 8.4$ Hz), 7.27 (d, 2H, $J = 7.8$ Hz), 4.93-4.88 (m, 1H), 4.41 (s, 1H), 2.41 (s, 3H), 2.15-2.03 (m, 4H), 1.95-1.88 (m, 2H), 1.60-1.51 (m, 8H), 1.18 (s, 6H) ppm; $^{13}\text{C NMR}$ (100 MHz, CDCl_3) δ 198.0, 142.7, 140.5, 129.4, 126.9, 103.3, 88.2, 57.0, 42.2, 31.7, 27.6, 27.5, 26.1, 23.9, 21.5 ppm; IR (thin film) ν 3272, 2926, 2853, 1321, 1151, 663, 551 cm^{-1} ; HRMS (FAB) calcd. for $[\text{C}_{20}\text{H}_{30}\text{NO}_2\text{S}]^+$: m/z 348.1997, found 348.1994.



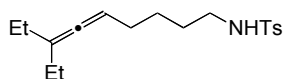
Tosylamine 2.51. The crude mixture was purified by flash column chromatography (9:1-6:1 hexanes:EtOAc) to afford **2.51** as a colorless syrup: TLC $R_f = 0.34$ (3:1 hexanes:EtOAc); ^1H NMR (400 MHz, CDCl_3) δ 7.76 (d, 2H, $J = 8.4$ Hz), 7.30 (d, 2H, $J = 8.0$ Hz), 7.13 (s, 4H), 4.94-4.91 (m, 1H), 4.70 (t, 1H, $J = 6.4$ Hz), 2.98 (q, 2H, $J = 6.8$ Hz), 2.88-2.76 (m, 4H), 2.42 (s, 3H), 2.26-2.18 (m, 4H), 1.96 (q, 2H, $J = 6.4$ Hz), 1.56 (quintet, 2H, $J = 7.2$ Hz) ppm; ^{13}C NMR (100 MHz, CDCl_3) δ 200.8, 143.4, 142.4, 137.0, 129.7, 129.2, 127.1, 126.3, 106.3, 87.0, 42.7, 36.2, 33.6, 28.6, 26.1, 21.6 ppm; IR (thin film) ν 3274, 1491, 1323, 1156, 1093 cm^{-1} ; HRMS (FAB) calcd. for $[\text{C}_{23}\text{H}_{28}\text{NO}_2\text{S}]^+$: m/z 382.1841, found 382.1838.



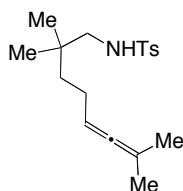
Tosylamine 2.52. The crude mixture was purified by flash column chromatography (3:1 hexanes:EtOAc) to afford **2.52** as a colorless oil: TLC $R_f = 0.43$ (1:1 hexanes:EtOAc); ^1H NMR (500 MHz, CDCl_3) δ 7.73 (d, 2H, $J = 8.0$ Hz), 7.30 (d, 2H, $J = 8.0$ Hz), 4.93-4.90 (m, 1H), 4.49 (t, 1H, $J = 6.0$ Hz), 3.95 (s, 4H), 2.96 (q, 2H, $J = 7.0$ Hz), 2.42 (s, 3H), 2.19 (td, 4H, $J = 6.0, 1.5$ Hz), 1.94 (q, 2H, $J = 6.5$ Hz), 1.73-1.65 (m, 4H), 1.55 (quintet, 2H, $J = 7.0$ Hz) ppm; ^{13}C NMR (125 MHz, CDCl_3) δ 198.5, 143.3, 136.9, 129.6, 127.0, 108.2, 100.7, 87.9, 64.3, 42.5, 35.3, 28.6, 28.5, 26.0, 21.5 ppm; IR (thin film) ν 3278, 1437, 1325, 1156, 1073 cm^{-1} ; HRMS (FAB) calcd. for $[\text{C}_{20}\text{H}_{28}\text{NO}_4\text{S}]^+$: m/z 378.1739, found 378.1738.



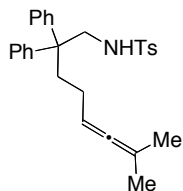
Tosylamine 2.65. The crude mixture was purified by flash column chromatography (12:1 hexanes:EtOAc) to afford **2.65** as a clear oil: TLC $R_f = 0.57$ (3:1 hexanes:EtOAc); ^1H NMR (400 MHz, CDCl_3) δ 7.75 (d, 2H, $J = 8.4$ Hz), 7.29 (d, 2H, $J = 8.4$ Hz), 4.87-4.81 (m, 2H), 2.91 (q, 2H, $J = 6.8$ Hz), 2.41 (s, 3H), 1.86 (q, 2H, $J = 6.8$ Hz), 1.63 (s, 3H), 1.62 (s, 3H), 1.51-1.42 (m, 2H), 1.38-1.29 (m, 2H) ppm; ^{13}C NMR (100 MHz, CDCl_3) δ 201.6, 143.2, 136.9, 129.6, 127.0, 95.1, 88.0, 43.0, 28.8, 28.5, 25.9, 21.4, 20.6 ppm; IR (thin film) ν 3281, 2972, 1322, 1154 cm^{-1} ; HRMS (FAB) calcd. for $[\text{C}_{16}\text{H}_{24}\text{NO}_2\text{S}]^+$: m/z 294.1528, found 294.1533; Anal calcd. for $\text{C}_{16}\text{H}_{23}\text{NO}_2\text{S}$: C, 65.49; H, 7.90; N, 4.77; found: C, 65.61; H, 8.23; N, 4.76.



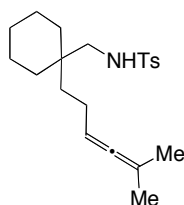
Tosylamine 2.66. The crude mixture was purified by flash column chromatography (12:1 hexanes:EtOAc) to afford **2.66** as a clear oil: TLC $R_f = 0.60$ (3:1 hexanes:EtOAc); $^1\text{H NMR}$ (400 MHz, CDCl_3) δ 7.74 (d, 2H, $J = 8.0$ Hz), 7.31 (d, 2H, $J = 8.0$ Hz), 5.10-5.03 (m, 1H), 4.34 (t, 1H, $J = 5.8$ Hz), 2.94 (q, 2H, $J = 6.8$ Hz), 2.43 (s, 3H), 1.95-1.88 (m, 6H), 1.54-1.47 (m, 2H), 1.39-1.32 (m, 2H), 0.95 (t, 6H, $J = 7.4$ Hz) ppm; $^{13}\text{C NMR}$ (100 MHz, CDCl_3) δ 200.0, 143.3, 136.9, 129.6, 127.1, 108.2, 92.2, 43.1, 29.0, 28.9, 26.2, 25.6, 21.5, 12.3 ppm; IR (thin film) ν 3281, 2966, 1324, 1157 cm^{-1} ; HRMS (FAB) calcd. for $[\text{C}_{18}\text{H}_{28}\text{NO}_2\text{S}]^+$: m/z 322.1841, found 322.1832.



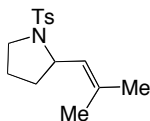
Tosylamine 2.67. The crude mixture was purified by flash column chromatography (5- 15% hexanes:EtOAc) to afford Tosylamine **2.67** as a white solid: TLC $R_f = 0.41$ (20% EtOAc:hexanes); $^1\text{H NMR}$ (400 MHz, CDCl_3) δ 7.78 (d, 2H, $J = 8.0$ Hz), 7.35 (d, 2H, $J = 8.0$ Hz), 4.92 (m, 1H), 4.39 (bt, 1H, $J = 7.1$ Hz), 2.73 (d, 2H, $J = 7.1$ Hz), 2.47 (s, 3H), 1.85 (m, 2H), 1.71 (s, 6H), 1.70 (s, 2H), 0.89 (s, 6H) ppm; $^{13}\text{C NMR}$ (100 MHz, CDCl_3) δ 201.4, 143.3, 137.0, 129.7, 127.1, 95.4, 88.9, 53.0, 38.9, 33.8, 24.9, 23.8, 21.6, 20.8 ppm; IR (thin film) ν 3286, 2962, 1325, 1159, 662 cm^{-1} ; HRMS (EI) calcd. for $[\text{C}_{18}\text{H}_{27}\text{NO}_2\text{S}]^+$: m/z 321.1762, found 321.1762.



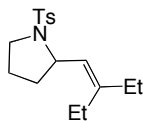
Tosylamine 2.63. The crude mixture was purified by flash column chromatography (5- 15% EtOAc:hexanes) to afford Tosylamine **2.63** as a white solid: TLC $R_f = 0.37$ (20% EtOAc:hexanes); $^1\text{H NMR}$ (400 MHz, CDCl_3) δ 7.63 (d, 2H, $J = 8.4$ Hz), 7.35-7.21 (m, 8H), 7.10 (d, 4H, $J = 7.3$ Hz), 4.84 (m, 1H), 3.91 (bt, 1H, $J = 6.3$ Hz), 3.59 (d, 2H, $J = 6.3$ Hz), 2.46 (s, 3H), 2.23 (m, 2H), 1.71 (s, 3H), 1.70 (s, 3H), 1.61 (m, 2H) ppm; $^{13}\text{C NMR}$ (100 MHz, CDCl_3) δ 201.4, 144.8, 143.5, 136.3, 129.7, 128.5, 127.8, 127.2, 126.7, 95.6, 88.5, 49.7, 49.6, 36.4, 23.9, 21.6, 20.8 ppm; IR (thin film) ν 3286, 2931, 1328, 1161, 909, 730 cm^{-1} ; LRMS (FAB) m/z 445 (M) $^+$; HRMS (FAB) calcd. for $[\text{C}_{29}\text{H}_{31}\text{NO}_2\text{S}]^+$: m/z 446.2154, found 446.2151.



Tosylamine 2.68. The crude mixture was purified by flash column chromatography (5-15% EtOAc:hexanes) to afford Tosylamine **2.68** as a white solid: TLC $R_f = 0.44$ (20% EtOAc:hexanes); $^1\text{H NMR}$ (400 MHz, CDCl_3) δ 7.79 (d, 2H, $J = 8.2$ Hz), 7.35 (d, 2H, $J = 8.2$ Hz), 4.90 (m, 1H), 4.52 (bs, 1H), 2.79 (d, 2H, $J = 6.8$ Hz), 2.47 (s, 3H), 1.77 (m, 2H), 1.71 (s, 3H), 1.70 (s, 3H), 1.49-1.33 (m, 8H), 1.28 (m, 4H) ppm; $^{13}\text{C NMR}$ (100 MHz, CDCl_3) δ 201.4, 143.3, 136.9, 129.7, 127.1, 95.5, 88.9, 48.9, 35.8, 34.9, 33.5, 26.1, 22.8, 21.6, 21.3, 20.8 ppm; IR (thin film) ν 3284, 2927, 2855, 1159, 730 cm^{-1} ; HRMS (EI) calcd. for $[\text{C}_{21}\text{H}_{31}\text{NO}_2\text{S}]^+$: m/z 361.2075, found 361.2082.

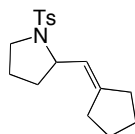


Tosylpyrrolidine 2.53. The crude mixture was purified by flash column chromatography (12:1 hexanes:EtOAc) to afford the desired pyrrolidine **2.53** as a white solid (49 mg, 98% yield): TLC $R_f = 0.54$ (3:1 hexanes:EtOAc); $^1\text{H NMR}$ (400 MHz, CDCl_3) δ 7.67 (d, 2H, $J = 8.0$ Hz), 7.27 (d, 2H, $J = 8.0$ Hz), 5.04 (d, 1H, $J = 9.2$ Hz), 4.36-4.30 (m, 1H), 3.41-3.31 (m, 2H), 2.41 (s, 3H), 1.89-1.77 (m, 2H), 1.69 (s, 3H), 1.67-1.59 (m, 1H), 1.64 (s, 3H), 1.57-1.49 (m, 1H) ppm; $^{13}\text{C NMR}$ (100 MHz, CDCl_3) δ 142.9, 136.0, 132.9, 129.3, 127.4, 125.8, 58.0, 48.5, 33.5, 25.7, 24.2, 21.4, 18.0 ppm; IR (thin film) ν 2956, 1336, 1155, 662 cm^{-1} ; HRMS (EI $^+$) calcd. for $[\text{C}_{15}\text{H}_{21}\text{NO}_2\text{S}]^+$: m/z 279.1293, found 279.1293; $[\alpha]_D -70.4$ ($c = 0.80$, CHCl_3); HPLC Chiralpak AD-H column (95:5 hexanes:isopropanol, 1 mL/min) t_R 11.0 min (minor), 13.7 min (major): 99% ee.

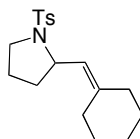


Tosylpyrrolidine 2.54. The crude mixture was purified by flash column chromatography (15:1 hexanes:EtOAc) to afford the desired pyrrolidine **2.54** as a white solid (45 mg, 90% yield): TLC $R_f = 0.60$ (3:1 hexanes:EtOAc); $^1\text{H NMR}$ (400 MHz, CDCl_3) δ 7.68 (d, 2H, $J = 8.4$ Hz), 7.26 (d, 2H, $J = 8.0$ Hz), 4.96 (d, 1H, $J = 8.8$ Hz), 4.44-4.38 (m, 1H), 3.42-3.36 (m, 2H), 2.41 (s, 3H), 2.26-2.17 (m, 1H), 2.05-1.81 (m, 5H), 1.68-1.61 (m, 1H), 1.59-1.53 (m, 1H), 1.00 (t, 3H, $J = 7.6$ Hz), 0.89 (t, 3H, $J = 7.4$ Hz) ppm; $^{13}\text{C NMR}$ (100 MHz, CDCl_3) δ 143.7, 142.8, 136.3, 129.3, 127.4, 123.7, 57.6, 48.4, 34.1, 28.7, 24.3, 23.5, 21.4, 13.3, 12.2 ppm; IR (thin film) ν 2965, 1336, 1150, 665 cm^{-1} ; HRMS (EI $^+$) calcd. for $[\text{C}_{17}\text{H}_{25}\text{NO}_2\text{S}]^+$: m/z 307.1606, found 307.1606;

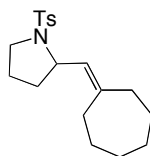
$[\alpha]_D -48.9$ ($c = 1.12$, CHCl_3); HPLC Chiralpak AD-H column (98:2 hexanes:isopropanol, 1 mL/min) t_R 13.6 min (minor), 14.1 min (major): 99% ee.



Tosylpyrrolidine 2.55. The crude mixture was purified by flash column chromatography (15:1 hexanes:EtOAc) to afford the desired pyrrolidine **2.55** as a colorless oil (37 mg, 74% yield): TLC $R_f = 0.54$ (3:1 hexanes:EtOAc); $^1\text{H NMR}$ (400 MHz, CDCl_3) δ 7.67 (d, 2H, $J = 8.4$ Hz), 7.26 (d, 2H, $J = 8.0$ Hz), 5.13-5.10 (m, 1H), 4.27-4.22 (m, 1H), 3.40-3.13 (m, 2H), 2.50-2.40 (m, 1H), 2.40 (s, 3H), 2.19-2.14 (m, 3H), 1.89-1.77 (m, 2H), 1.74-1.50 (m, 6H) ppm; $^{13}\text{C NMR}$ (100 MHz, CDCl_3) δ 144.8, 142.9, 136.2, 129.3, 127.5, 121.0, 59.6, 48.4, 33.7, 33.2, 28.6, 26.4, 26.0, 24.2, 21.5 ppm; IR (thin film) ν 1336, 1153, 820 cm^{-1} ; HRMS (EI^+) calcd. for $[\text{C}_{17}\text{H}_{23}\text{NO}_2\text{S}]^+$: m/z 305.1449, found 305.1447; $[\alpha]_D = -39$ ($c = 1.0$, CHCl_3); HPLC Chiralcel OJ-H column (95:5 hexanes:isopropanol, 1 mL/min) t_R 12.8 min (minor), 15.6 min (major): 82% ee.

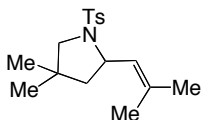


Tosylpyrrolidine 2.36. The crude mixture was purified by flash column chromatography (12:1 hexanes:EtOAc) to afford the desired pyrrolidine **2.36** as a colorless oil (44 mg, 88% yield): TLC $R_f = 0.43$ (3:1 hexanes:EtOAc); $^1\text{H NMR}$ (400 MHz, CDCl_3) δ 7.68 (d, 2H, $J = 8.4$ Hz), 7.26 (d, 2H, $J = 8.0$ Hz), 4.99 (d, 1H, $J = 9.2$ Hz), 4.39-4.34 (m, 1H), 3.40-3.30 (m, 2H), 2.40 (s, 3H), 2.26-2.20 (m, 1H), 2.15-2.09 (m, 1H), 2.01-1.96 (m, 2H), 1.85-1.78 (m, 2H), 1.65-1.43 (m, 8H) ppm; $^{13}\text{C NMR}$ (100 MHz, CDCl_3) δ 143.0, 140.7, 136.0, 129.4, 127.5, 122.7, 57.2, 48.6, 36.9, 34.0, 29.1, 28.2, 27.5, 26.7, 24.2, 21.5 ppm; IR (thin film) ν 1342, 1156, 1092, 814 cm^{-1} ; HRMS (EI^+) calcd. for $[\text{C}_{18}\text{H}_{25}\text{NO}_2\text{S}]^+$: m/z 319.1606, found 319.1601; $[\alpha]_D = -54$ ($c = 1.0$, CHCl_3); HPLC Chiralpak AD-H column (95:5 hexanes:isopropanol, 1 mL/min) t_R 10.8 min (minor), 13.4 min (major): 98% ee.

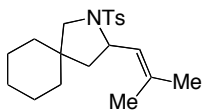


Tosylpyrrolidine 2.56. The crude mixture was purified by flash column chromatography (15:1 hexanes:EtOAc) to afford the desired pyrrolidine **2.56** as a colorless oil (44 mg, 88% yield): TLC $R_f = 0.66$ (3:1 hexanes:EtOAc); $^1\text{H NMR}$ (400 MHz, CDCl_3) δ 7.68 (d, 2H, $J = 8.4$ Hz), 7.27 (d, 2H, $J = 8.0$ Hz), 5.06 (d, 1H, $J = 9.2$ Hz), 4.37-4.32 (m, 1H), 3.40-3.33 (m, 2H), 2.40 (s, 3H),

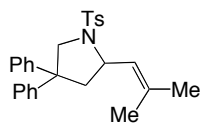
2.32-2.29 (m, 2H), 2.15-2.05 (m, 2H), 1.91-1.79 (m, 2H), 1.70-1.41 (m, 10H) ppm; ^{13}C NMR (100 MHz, CDCl_3) δ 142.9, 142.1, 136.1, 129.4, 127.5, 126.2, 57.6, 48.5, 37.6, 33.7, 30.0, 29.7, 29.1, 28.9, 27.1, 24.3, 21.5 ppm; IR (thin film) ν 2922, 1343, 1334, 1152, 1090, 816 cm^{-1} ; HRMS (EI $^+$) calcd. for $[\text{C}_{19}\text{H}_{27}\text{NO}_2\text{S}]^+$: m/z 333.1762, found 333.1760; $[\alpha]_{\text{D}} = -64$ ($c = 1.0$, CHCl_3); HPLC Chiralpak AD-H column (95:5 hexanes:isopropanol, 1 mL/min) t_{R} 10.7 min (minor), 11.6 min (major): 98% ee.



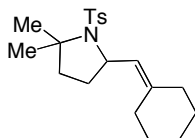
Tosylpyrrolidine 2.41. The crude mixture was purified by flash column chromatography (5-7.5% EtOAc/hexanes) to afford the desired pyrrolidine **2.41** as a white solid (94 mg, 94%): TLC $R_f = 0.32$ (20% EtOAc:hexanes); ^1H NMR (400 MHz, CDCl_3) δ 7.71 (d, 2H, $J = 8.6$ Hz), 7.32 (d, 2H, $J = 8.6$ Hz), 5.06 (m, 1H), 4.05 (q, 1H, $J = 8.7$ Hz), 3.27 (d, 1H, $J = 9.6$ Hz), 3.16 (d, 1H, $J = 9.6$ Hz), 2.46 (s, 3H), 1.80 (dd, 1H, $J = 12.5, 7.2$ Hz), 1.72 (s, 3H), 1.67 (s, 3H), 1.46 (dd, 1H, $J = 12.5, 8.7$ Hz), 1.09 (s, 3H), 0.84 (s, 3H) ppm; ^{13}C NMR (100 MHz, CDCl_3) δ 142.8, 136.7, 132.8, 129.2, 127.5, 126.6, 60.9, 57.8, 47.9, 37.4, 26.5, 26.1, 25.7, 21.5, 17.9 ppm; IR (thin film) ν 2959, 2871, 1338, 1157, 1092, 731, 664 cm^{-1} ; HRMS (EI) calcd. $[\text{C}_{17}\text{H}_{25}\text{NO}_2\text{S}]^+$: m/z 307.1606, found 307.1601; $[\alpha]_{\text{D}} = -36$ ($c = 2.0$; CHCl_3); HPLC Chiralpak AD-H column (98:2 Hex:EtOH; 1 mL/min) t_{R} 8.9 min (minor), 11.6 min (major): 93% ee.



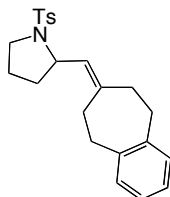
Tosylpyrrolidine 2.60. The crude mixture was purified by flash column chromatography (5-7.5% EtOAc/hexanes) to afford the desired pyrrolidine **2.60** as a white solid (99 mg, 99%): TLC $R_f = 0.38$ (20% EtOAc:hexanes); ^1H NMR (400 MHz, CDCl_3) δ 7.71 (d, 2H, $J = 8.1$ Hz), 7.32 (d, 2H, $J = 8.1$ Hz), 5.07 (d, 1H, $J = 8.9$ Hz), 4.30 (q, 1H, $J = 8.9$ Hz), 3.40 (d, 1H, $J = 10.3$ Hz), 3.15 (d, 1H, $J = 10.3$ Hz), 2.46 (s, 3H), 1.88 (dd, 1H, $J = 12.6, 7.2$ Hz), 1.71 (s, 3H), 1.68 (s, 3H), 1.51-1.29 (m, 9H), 1.10 (m, 2H) ppm; ^{13}C NMR (100 MHz, CDCl_3) δ 142.9, 136.3, 132.6, 129.2, 127.5, 126.7, 58.5, 57.0, 45.9, 41.2, 36.6, 34.6, 25.9, 25.7, 23.7, 22.9, 21.5, 18.0 ppm; IR (thin film) ν 2925, 2856, 1343, 1161, 664 cm^{-1} ; HRMS (EI) calcd. for $[\text{C}_{20}\text{H}_{29}\text{NO}_2\text{S}]^+$: m/z 347.1919, found 347.1913; $[\alpha]_{\text{D}} = -34$ ($c = 2.0$; CHCl_3); HPLC Chiralpak AD-H column (98:2 Hex:EtOH; 1 mL/min) t_{R} 10.7 min (minor), 14.6 min (major): 70% ee.



Tosylpyrrolidine 2.62. The crude mixture was purified by flash column chromatography (5-7.5% EtOAc/hexanes) to afford the desired pyrrolidine **2.62** as a clear oil (99 mg, 99%): TLC R_f = 0.34 (20% EtOAc:hexanes); ^1H NMR (400 MHz, CDCl_3) δ 7.64 (d, 2H, J = 8.3 Hz), 7.34-7.17 (m, 12H), 4.83 (d, 1H, J = 9.4 Hz), 4.46 (m, 2H), 3.92 (d, 1H, J = 10.3 Hz), 2.79 (dd, 1H, J = 12.7, 6.7 Hz), 2.44 (s, 3H), 2.37 (dd, 1H, J = 12.7, 8.4 Hz), 1.69 (s, 3H), 1.63 (s, 3H) ppm; ^{13}C NMR (100 MHz, CDCl_3) δ 145.6, 144.8, 142.7, 137.5, 134.5, 129.2, 128.6, 128.5, 127.2, 126.7, 126.6, 126.5, 126.4, 125.3, 57.8, 57.0, 52.6, 45.8, 25.7, 21.5, 18.1 ppm; IR (thin film) ν 3058, 2926, 1338, 1156, 700 cm^{-1} ; HRMS (EI) calcd. for $[\text{C}_{27}\text{H}_{29}\text{NO}_2\text{S}]^+$: m/z 431.1919, found 431.1916; $[\alpha]_D = -29$ (c = 2.0; CHCl_3); HPLC Regis Technologies Whelk-O 1 column (98:2 Hex:EtOH; 1 mL/min) t_R 24.1 min (minor), 28.0 min (major): 87% ee.

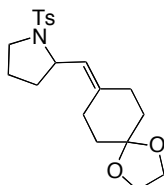


Tosylpyrrolidine 2.78. The crude mixture was purified by flash column chromatography (17:1 hexanes:EtOAc) to afford the desired pyrrolidine **2.78** as a clear oil (19 mg, 76% yield): TLC R_f = 0.57 (3:1 hexanes:EtOAc); ^1H NMR (400 MHz, CDCl_3) δ 7.71 (d, 2H, J = 8.0 Hz), 7.20 (d, 2H, J = 8.0 Hz), 4.86 (d, 1H, J = 9.6 Hz), 4.65 (td, 1H, J = 8.6, 2.0 Hz), 2.39 (s, 3H), 2.14-2.07 (m, 3H), 1.95-1.79 (m, 3H), 1.74-1.68 (m, 1H), 1.59-1.53 (m, 1H), 1.56 (s, 3H), 1.52-1.39 (m, 6H), 1.50 (s, 3H) ppm; ^{13}C NMR (100 MHz, CDCl_3) δ 142.1, 140.3, 139.8, 128.8, 127.7, 123.8, 66.1, 58.5, 41.3, 36.7, 31.2, 29.7, 28.7, 27.9, 27.3, 26.6, 21.4 ppm; IR (thin film) ν 2925, 2853, 1334, 1152, 671, 552 cm^{-1} ; HRMS (FAB) calcd. for $[\text{C}_{20}\text{H}_{29}\text{NO}_2\text{S}]^+$: m/z 347.1919, found 347.1911; $[\alpha]_D +43$ (c = 0.82, CHCl_3); HPLC Chiralpak AD-H column (97:3 hexanes:isopropanol, 1 mL/min) t_R 10.3 min (major), 11.8 min (minor): 96% ee.

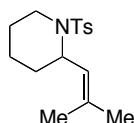


Tosylpyrrolidine 2.57. The crude mixture was purified by flash column chromatography (12:1 hexanes:EtOAc) to afford the desired pyrrolidine **2.57** as a colorless oil (43 mg, 87% yield):

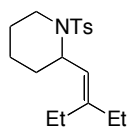
TLC $R_f = 0.50$ (3:1 hexanes:EtOAc); $^1\text{H NMR}$ (400 MHz, CDCl_3) δ 7.17 (d, 2H, $J = 8.4$ Hz), 7.29 (d, 2H, $J = 8.0$ Hz), 7.16-7.13 (m, 4H), 5.15 (d, 1H, $J = 8.8$ Hz), 4.49-4.44 (m, 1H), 3.46-3.37 (m, 2H), 2.93 (ddd, 1H, $J = 14.0, 8.8, 2.0$ Hz), 2.86-2.80 (m, 1H), 2.75-2.69 (m, 2H), 2.46-2.33 (m, 2H), 2.42 (s, 3H), 2.25-2.16 (m, 2H), 1.94-1.84 (m, 2H), 1.69-1.57 (m, 2H) ppm; $^{13}\text{C NMR}$ (100 MHz, CDCl_3) δ 143.1, 142.7, 142.5, 136.1, 129.5, 129.1 (2), 127.5, 126.3, 126.2, 125.9, 57.2, 48.7, 39.1, 36.2, 35.3, 34.1, 30.6, 24.3, 21.6 ppm; IR (thin film) ν 2929, 1336, 1152, 815 cm^{-1} ; HRMS (EI $^+$) calcd. for $[\text{C}_{23}\text{H}_{27}\text{NO}_2\text{S}]^+$: m/z 381.1762, found 381.1764; $[\alpha]_D = -70$ ($c = 1.0$, CHCl_3); HPLC Chiralpak AD-H column (95:5 hexanes:isopropanol, 1 mL/min) t_R 15.2 min (minor), 17.0 min (major): 98% ee.



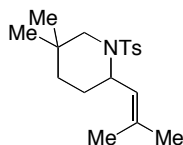
Tosylpyrrolidine 2.58. The crude mixture was purified by flash column chromatography (3:1 hexanes:EtOAc) to afford the desired pyrrolidine **2.58** as a colorless oil (44 mg, 88% yield): TLC $R_f = 0.47$ (1:1 hexanes:EtOAc); $^1\text{H NMR}$ (400 MHz, CDCl_3) δ 7.67 (d, 2H, $J = 8.4$ Hz), 7.27 (d, 2H, $J = 8.0$ Hz), 5.07 (d, 1H, $J = 9.2$ Hz), 4.37-4.32 (m, 1H), 3.99-3.94 (m, 4H), 3.42-3.33 (m, 2H), 2.45-2.38 (m, 1H), 2.40 (s, 3H), 2.28-2.21 (m, 1H), 2.16 (t, 2H, $J = 6.4$ Hz), 1.91-1.52 (m, 8H) ppm; $^{13}\text{C NMR}$ (100 MHz, CDCl_3) δ 143.0, 138.0, 136.1, 129.4, 127.5, 124.1, 108.7, 64.3, 57.3, 48.6, 35.8, 35.1, 33.9, 33.4, 25.5, 24.3, 21.5 ppm; IR (thin film) ν 2925, 1493, 1334, 1151, 1082 cm^{-1} ; HRMS (EI) calcd. for $[\text{C}_{20}\text{H}_{27}\text{NO}_4\text{S}]^+$: m/z 377.1661, found 377.1660; $[\alpha]_D = -55$ ($c = 1.0$, CHCl_3); HPLC Chiralpak AD-H column (93:7 hexanes:isopropanol, 1 mL/min) t_R 21.2 min (major), 24.0 min (minor): 98% ee.



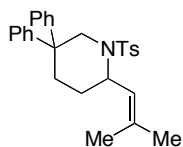
Tosylpiperidine 2.69. The crude mixture was purified by flash column chromatography (15:1 hexanes:EtOAc) to afford the desired piperidine **2.69** as a white solid (35.0 mg, 88% yield): TLC $R_f = 0.65$ (3:1 hexanes:EtOAc); $^1\text{H NMR}$ (400 MHz, CDCl_3) δ 7.57 (d, 2H, $J = 8.4$ Hz), 7.21 (d, 2H, $J = 8.4$ Hz), 5.07 (d, 1H, $J = 9.2$ Hz), 4.77-4.74 (m, 1H), 3.67 (d, 1H, $J = 13.2$ Hz), 2.86 (td, 1H, $J = 12.1, 3.1$ Hz), 2.39 (s, 3H), 1.80-1.71 (m, 1H), 1.68-1.57 (m, 1H), 1.64 (s, 3H), 1.56-1.41 (m, 4H), 1.49 (s, 3H) ppm; $^{13}\text{C NMR}$ (100 MHz, CDCl_3) δ 142.6, 137.0, 133.9, 128.9, 127.5, 119.8, 51.4, 41.7, 31.4, 25.7, 25.3, 21.4, 19.0, 17.9 ppm; IR (thin film) ν 2938, 1338, 1157, 658 cm^{-1} ; HRMS (EI $^+$) calcd. for $[\text{C}_{16}\text{H}_{23}\text{NO}_2\text{S}]^+$: m/z 293.1450, found 293.1448; $[\alpha]_D = -70$ ($c = 1.0$, CHCl_3); HPLC Chiralpak AD-H column (97:3 hexanes:isopropanol, 1 mL/min) t_R 11.3 min (major), 12.6 min (minor): 81% ee.



Tosylpiperidine 2.70. The crude mixture was purified by flash column chromatography (17:1 hexanes:EtOAc) to afford the desired piperidine **2.70** as a yellow oil (16.2 mg, 41% yield): TLC R_f = 0.68 (3:1 hexanes:EtOAc); ^1H NMR (500 MHz, CDCl_3) δ 7.58 (d, 2H, J = 8.5 Hz), 7.20 (d, 2H, J = 8.0 Hz), 5.03 (d, 1H, J = 9.5 Hz), 4.85-4.81 (m, 1H), 3.71 (d, 1H, J = 12.0 Hz), 2.90 (td, 1H, J = 12.2, 3.0 Hz), 2.39 (s, 3H), 2.23-2.15 (m, 1H), 1.99-1.92 (m, 1H), 1.91-1.86 (m, 1H), 1.84-1.77 (m, 2H), 1.69-1.66 (m, 1H), 1.62-1.41 (m, 4H), 0.99 (t, 3H, J = 7.5 Hz), 0.74 (t, 3H, J = 7.5 Hz) ppm; ^{13}C NMR (125 MHz, CDCl_3) δ 144.6, 142.6, 137.1, 129.0, 127.5, 117.4, 50.9, 41.6, 32.3, 28.8, 25.4, 23.6, 21.4, 19.0, 13.0, 11.9 ppm; IR (thin film) ν 2936, 1338, 1156, 657 cm^{-1} ; HRMS (EI $^+$) calcd. for $[\text{C}_{18}\text{H}_{27}\text{NO}_2\text{S}]^+$: m/z 321.1763, found 321.1759; $[\alpha]_D$ -41 (c = 0.51, CHCl_3); HPLC Chiralpak AD-H column (97:3 hexanes:isopropanol, 1 mL/min) t_R 9.3 min (major), 10.8 min (minor): 74% ee.

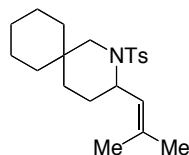


Tosylpiperidine 2.71. The crude mixture was purified by flash column chromatography (5-7.5% EtOAc:hexanes) to afford the desired piperidine **2.71** as a white solid (70 mg, 70% yield): TLC R_f = 0.44 (20% EtOAc:hexanes); ^1H NMR (400 MHz, CDCl_3) δ 7.58 (d, 2H, J = 8.3 Hz), 7.24 (d, 2H, J = 8.3 Hz), 5.06 (d, 1H, J = 9.3 Hz), 4.77 (bs, 1H), 3.26 (d, 1H, J = 11.8 Hz), 2.64 (d, 1H, J = 11.8 Hz), 2.43 (s, 3H), 2.06 (m, 1H), 1.66 (s, 3H), 1.50 (s, 3H), 1.46-1.22 (m, 3H), 1.09 (s, 3H), 0.96 (s, 3H) ppm; ^{13}C NMR (100 MHz, CDCl_3) δ 142.6, 137.1, 133.8, 128.9, 127.5, 119.3, 52.2, 50.9, 32.7, 30.6, 28.9, 28.0, 25.7, 23.6, 21.5, 18.0 ppm; IR (thin film) ν 2905, 1336, 1157, 663 cm^{-1} ; LRMS (EI) m/z 321 (M) $^+$; HRMS (EI) calcd. for $[\text{C}_{18}\text{H}_{27}\text{NO}_2\text{S}]^+$: m/z 321.1762, found 321.1758; $[\alpha]_D$ = +71 (c = 1.0; CHCl_3); HPLC Chiralpak AD-H column (98:2 Hex:EtOH; 1 mL/min) t_R 8.6 min (minor), 10.5 min (major): 98% ee.



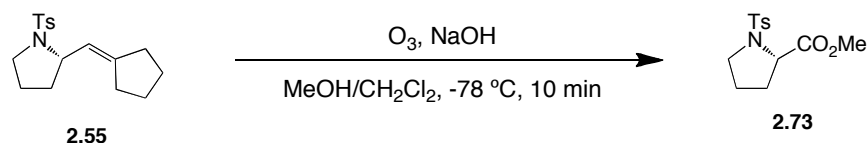
Tosylpiperidine 2.64. The crude mixture was purified by flash column chromatography (5-7.5% EtOAc:hexanes) to afford the desired piperidine **2.64** as a colorless oil (70 mg, 70% yield): TLC R_f = 0.42 (20% EtOAc:hexanes); ^1H NMR (400 MHz, CDCl_3) δ 7.59 (m, 4H), 7.40-7.20 (m, 10H), 4.96 (d, 1H, J = 9.3 Hz), 4.77 (m, 1H), 4.61 (d, 1H, J = 12.9 Hz), 3.02 (d, 1H, J = 12.9 Hz), 2.42 (s, 3H), 2.37 (m, 2H), 1.82 (m, 1H), 1.69 (s, 3H), 1.52 (m, 1H), 1.47 (s, 3H) ppm; ^{13}C

NMR (100 MHz, CDCl₃) δ 147.5, 144.4, 142.9, 136.2, 134.0, 128.9, 128.5, 128.4, 128.3, 127.9, 126.8, 126.5, 125.9, 119.4, 51.3, 49.8, 46.1, 29.7, 27.9, 25.7, 21.5, 17.9 ppm; IR (thin film) ν 2951, 1339, 1157, 730, 664 cm⁻¹; HRMS (EI) calcd. for [C₂₈H₃₁NO₂S]⁺: *m/z* 445.2075, found 445.2078; [α]_D = -146 (c = 1.0; CHCl₃); HPLC Regis Technologies Whelk-O 1 column (97:3 Hex:EtOH; 1 mL/min) t_R 12.6 min (minor), 17.8 min (major): 88% ee.



Tosylpiperidine 2.72. The crude mixture was purified by flash column chromatography (5-7.5% EtOAc:hexanes) to afford the desired piperidine **2.72** as a white solid (33 mg, 66% yield): TLC R_f = 0.5 (20% EtOAc:hexanes); ¹H NMR (400 MHz, CDCl₃) δ 7.60 (d, 2H, *J* = 8.3 Hz), 7.25 (d, 2H, *J* = 8.3 Hz), 5.10 (d, 1H, *J* = 9.4 Hz), 4.77 (m, 1H), 3.59 (d, 1H, *J* = 12.4 Hz), 2.56 (d, 1H, *J* = 12.4 Hz), 2.43 (s, 3H), 2.06 (m, 1H), 1.74 (m, 1H), 1.65 (s, 3H), 1.50 (s, 3H), 1.48-1.21 (m, 12H) ppm; ¹³C NMR (100 MHz, CDCl₃) δ 142.5, 137.2, 133.7, 128.9, 127.4, 119.5, 51.5, 49.6, 38.0, 32.9, 31.2, 30.9, 27.1, 26.6, 25.7, 21.5, 21.4 (2), 18.1 ppm; IR (thin film) ν 2927, 2853, 1338, 1155, 753, 662 cm⁻¹; HRMS (EI) calcd. for [C₂₁H₃₁NO₂S]⁺: *m/z* 361.2075, found 361.2076; [α]_D = +37 (c = 1.0; CHCl₃); HPLC Chiralpak AD-H column (97:3 Hex:EtOH; 1 mL/min) t_R 8.8 min (minor), 16.6 min (major): 97% ee.

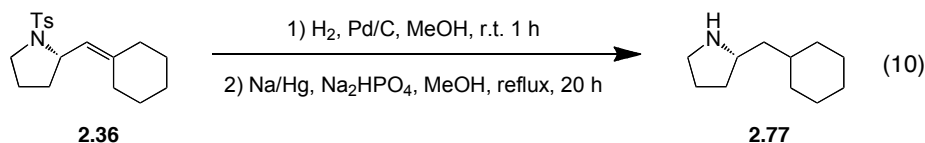
Determination of Absolute Stereochemistry



To a solution of pyrrolidine **2.55** (72.6 mg, 0.238 mmol) in CH₂Cl₂ (2.4 mL) was added a solution of NaOH in MeOH (0.61 mL, 1.53 mmol, 2.5M). The resulting mixture was cooled to -78 °C and O₃ was bubbled through continuously. After approximately 10 min the initially pale yellow solution took on the characteristic blue color of ozone and a yellow precipitate was observed. The reaction mixture was diluted with H₂O (2 mL) and Et₂O (2 mL) and warmed to rt. The aqueous layer was extracted with Et₂O (3x, 5 mL), the combined organic extracts were washed with brine (10 mL), dried over MgSO₄, filtered, and concentrated. The crude oil was purified by flash column chromatography (3:1 hexanes:EtOAc) to afford N-tosylproline methyl ester **2.73** as a white solid (60.0 mg, 89% yield): TLC R_f = 0.15 (3:1 hexanes:EtOAc) ¹H NMR (400 MHz, CDCl₃) δ 7.74 (d, 2H, *J* = 8.4 Hz), 7.30 (d, 2H, *J* = 8.0 Hz), 4.28 (dd, 1H, *J* = 8.0, 4.4 Hz) 3.70 (s, 3H), 3.52-3.45 (m, 1H), 3.32-3.26 (m, 1H), 2.42 (s, 3H), 2.04-1.89 (m, 3H), 1.78-1.68 (m, 1H) ppm; ¹³C NMR (100 MHz, CDCl₃) δ 172.6, 143.6, 135.2, 129.7, 127.5, 60.4, 52.4,

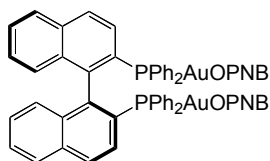
48.4, 30.9, 24.7, 21.6 ppm; IR (thin film) ν 2954, 1739, 1341, 1155 cm^{-1} ; $[\alpha]_{\text{D}} = -73.3$ ($c = 1.0$, CHCl_3) (lit. -93.3 ($c = 1.5$, CHCl_3);⁵ HPLC Chiralpak AS column (90:10 hexanes:isopropanol, 1 mL/min) t_{R} 26.6 min (minor), 32.5 min (major): 82% ee. Spectral data are consistent with previously published literature values.³³

Tosyl Deprotection



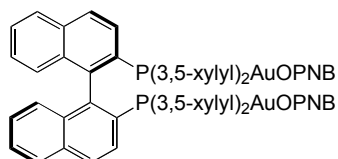
The tosylpyrrolidine **2.36** (100 mg, 0.31 mmol) dissolved in MeOH (4 mL) was treated with Pd/C (67 mg, 0.03 mmol, 5% w/w) and was stirred under H_2 (atm). After 1 h, the solution was filtered through a celite pad and resulting filtrate was concentrated. Purification by flash chromatography (10:1 hexanes:EtOAc) gave the hydrogenated tosylpyrrolidine as a white solid (97 mg, 98%). To a solution of the hydrogenated tosylpyrrolidine (40 mg, 0.12 mmol) in MeOH (5 mL) was added Na_2HPO_4 (195 mg, 0.72 mmol) and Na/Hg amalgam (1.6 g, 5.2 mmol, 8%). The mixture was refluxed for 20 h. Aqueous solution of NH_4OH (38%) was added, and the mixture was extracted with DCM (20 mL), dried over Na_2SO_4 and concentrated to give the desired pyrrolidine **2.77** as a colorless oil (18 mg, 91%): TLC $R_f = 0.30$ (5:1 DCM:MeOH); ^1H NMR (400 MHz, CDCl_3) δ 3.07-2.97 (m, 2H), 2.80 (dt, 1H, $J = 10.4, 7.6$ Hz), 1.90-1.82 (m, 2H), 1.76-1.61 (m, 6H), 1.40-0.99 (m, 7H), 0.93-0.83 (m, 2H) ppm; ^{13}C NMR (100 MHz, CDCl_3) δ 56.7, 46.5, 44.3, 35.8, 33.9, 33.4, 32.3, 26.6, 26.3, 26.3, 25.4 ppm; IR (thin film) ν 2920, 2850, 1447, 1403, 593 cm^{-1} ; HRMS (EI^+) calcd. for $[\text{C}_{11}\text{H}_{22}\text{N}]^+$: m/z 168.1752, found 168.1757; $[\alpha]_{\text{D}} -13$ ($c = 0.92$; CHCl_3).

Representative Procedures for the Preparation of Phosphinegold(I)-bis-*p*-nitrobenzoate Complexes

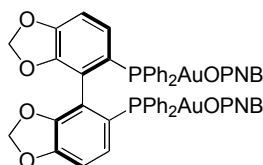


(S)-BINAP(AuOPNB)₂ S-2.44. A suspension of (S)-BINAP(AuCl)₂ (80 mg, 0.074 mmol) and AgOPNB (59 mg, 0.22 mmol, 3 equiv) in chloroform (1.5 mL) was sonicated for 5 min. The resulting off-white dispersion was filtered thru a plug of celite (0.5 x 2 cm), washed with chloroform (3 x 2 mL), and concentrated to approximately 1 mL. A white solid formed upon dropwise addition of hexanes. The remaining solvent was removed *in vacuo* to afford **6** as an analytically pure white solid (100 mg; 98% yield): ^1H NMR (400 MHz, CDCl_3) δ 8.23 (d, 4H, $J = 8.4$ Hz), 8.03 (m, 6H), 7.87 (d, 2H, $J = 7.0$ Hz), 7.77 (m, 4H), 7.58 (t, 2H, $J = 9.3$ Hz), 7.39

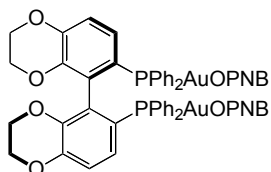
(m, 10H), 7.25 (m, 8H), 6.73 (t, 2H, $J = 7.6$ Hz), 6.58 (d, 2H, $J = 8.5$ Hz) ppm; ^{31}P NMR (160 MHz, CDCl_3) δ 18.9 ppm; Anal calcd. for $\text{C}_{58}\text{H}_{40}\text{Au}_2\text{N}_2\text{O}_8\text{P}_2$: C, 51.65; H, 2.99; N, 2.08; found: C, 51.38; H, 3.19; N, 1.87.



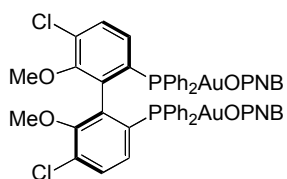
(R)-xylyl-BINAP(AuOPNB)₂ 2.42 was obtained as an off-white solid (100 mg, 92% yield): ^1H NMR (400 MHz, CDCl_3) δ 8.27 (d, 4H, $J = 8.1$ Hz), 8.10 (d, 4H, $J = 8.1$ Hz), 8.04 (d, 2H, $J = 8.8$ Hz), 7.87 (d, 2H, $J = 8.1$ Hz), 7.62 (d, 2H, $J = 8.8$ Hz), 7.55 (t, 2H, $J = 6.8$ Hz), 7.36 (d, 4H, $J = 14.1$ Hz), 7.15 (t, 2H, $J = 7.3$ Hz), 7.05-6.90 (m, 6H), 6.85 (d, 4H, $J = 14.1$ Hz), 2.24 (s, 12H), 2.23 (s, 12H) ppm; ^{31}P NMR (160 MHz, CDCl_3) δ 17.7 ppm; Anal calcd. for $\text{C}_{66}\text{H}_{56}\text{Au}_2\text{N}_2\text{O}_8\text{P}_2$: C, 54.26; H, 3.86; N, 1.92; found: C, 54.57; H, 4.20; N, 1.83.



(R)-SEGPPOS(AuOPNB)₂ 2.45 was obtained as an off-white solid (60 mg, 97% yield): ^1H NMR (400 MHz, CDCl_3) δ 8.24 (d, 4H, $J = 8.8$ Hz), 8.14 (d, 4H, $J = 8.8$ Hz), 7.78 (dd, 4H, $J = 12.9, 7.0$ Hz), 7.70 (dd, 4H, $J = 12.9, 7.3$ Hz), 7.60 (m, 2H), 7.52 (m, 4H), 7.42 (m, 2H), 7.32 (m, 4H), 6.85 (m, 4H), 5.59 (s, 2H), 4.54 (s, 2H) ppm; ^{31}P NMR (160 MHz, CDCl_3) δ 20.7 ppm; Anal calcd. for $\text{C}_{52}\text{H}_{36}\text{Au}_2\text{N}_2\text{O}_{12}\text{P}_2$: C, 46.72; H, 2.71; N, 2.10; found: C, 46.52; H, 2.98; N, 2.02.



(R)-SYNPPOS(AuOPNB)₂ 2.46 was obtained as an off-white solid (100 mg, 99% yield): ^1H NMR (400 MHz, CDCl_3) δ 8.14 (d, 4H, $J = 8.2$ Hz), 7.89 (d, 4H, $J = 8.2$ Hz), 7.68 (m, 4H), 7.60 (m, 4H), 7.52 (m, 6H), 7.37 (m, 6H), 6.87 (m, 4H), 3.98 (m, 2H), 3.68 (m, 2H), 3.56 (m, 2H), 2.96 (m, 2H) ppm; ^{31}P NMR (160 MHz, CDCl_3) δ 17.1 ppm; Anal calcd. for $\text{C}_{54}\text{H}_{42}\text{Au}_2\text{N}_2\text{O}_{12}\text{P}_2$: C, 47.45; H, 3.10; N, 2.05; found: C, 47.60; H, 3.27; N, 1.94.



(R)-ClMeOBIPHEP(AuOPNB)₂ 2.43 was obtained as an off-white solid (210 mg, 93% yield): ¹H NMR (400 MHz, CDCl₃) δ 8.27 (d, 4H, *J* = 8.9 Hz), 8.18 (d, 4H, *J* = 8.9 Hz), 7.63 (dd, 4H, *J* = 13.4, 7.1 Hz), 7.54-7.32 (m, 18H), 7.13 (dd, 2H, *J* = 10.3, 8.3 Hz), 3.69 (s, 6H) ppm; ³¹P NMR (160 MHz, CDCl₃) δ 17.3 ppm; Anal calcd. for C₅₂H₃₈Au₂Cl₂N₂O₁₀P₂: C, 45.33; H, 2.78; N, 2.03; found: C, 45.66; H, 2.79; N, 1.97.

References

- ¹ For selected reviews of alkyne and alkene hydroamination, see: (a) Müller, T. E.; Beller, M. *Chem. Rev.* **1998**, *98*, 675. (b) Nobis, M.; Driessen-Hölscher, B. *Angew. Chem., Int. Ed.* **2001**, *40*, 3983. (c) Bytschkov, I.; Doye, S. *Eur. J. Org. Chem.* **2003**, 935. (d) Pohlki, F.; Doye, S. *Chem. Soc. Rev.* **2003**, *32*, 104. (e) Severin, S.; Doye, S. *Chem. Soc. Rev.* **2007**, *36*, 1407. (f) Alonso, F.; Beletskaya, I. P.; Yus, M. *Chem. Rev.* **2004**, *104*, 3079. (g) Nakamura, I.; Yamamoto, Y. *Chem. Rev.* **2004**, *104*, 2127. (h) Roesky, P. W.; Müller, T. E. *Angew. Chem., Int. Ed.* **2003**, *42*, 2708.
- ² For examples of gold-catalyzed hydroamination of alkynes, see: (a) Mizushima, E.; Hayashi, T.; Tanaka, M. *Org. Lett.* **2003**, *5*, 3349. (b) Gorin, D. J.; Davis, N. R.; Toste, F. D. *J. Am. Chem. Soc.* **2005**, *127*, 11260. (c) Kadzimirsz, D.; Hildebrandt, D.; Merz, K.; Dyker, G. *Chem. Commun.* **2006**, 661. (d) Kang, J.-E.; Kim, H.-B.; Lee, J.-W.; Shin, S. *Org. Lett.* **2006**, *8*, 3537. (e) Hashmi, A. S. K.; Rudolph, M.; Schymura, S.; Visus, J.; Frey, W. *Eur. J. Org. Chem.* **2006**, 4905.
- ³ For a recent reviews of allene hydroamination, see: (a) Bates, R. W.; Satcharoen, V., *Chem. Soc. Rev.* **2002**, *31*, 12-21. For a recent review of gold catalyzed hydroamination, see: (b) Widenhoefer, R. A.; Han, X. *Eur. J. Org. Chem.* **2006**, 4555.
- ⁴ For reviews of enantioselective alkene hydroamination, see: (a) Hultsch, K. C. *Org. Biomol. Chem.* **2005**, *3*, 1819. (b) Hultsch, K. C. *Adv. Synth. Catal.* **2005**, *347*, 367.
- ⁵ For examples of gold-catalyzed hydroamination of alkenes, see: (a) Zhang, J.; Yang, C.-G.; He, C. *J. Am. Chem. Soc.* **2006**, *128*, 1798. (b) Han, X.; Widenhoefer, R. A. *Angew. Chem., Int. Ed. Engl.* **2006**, *45*, 1747. (c) Liu, X.-Y.; Li, C.-H.; Che, C.-M. *Org. Lett.* **2006**, *8*, 2707. (d) Bender, C. F.; Widenhoefer, R. A. *Chem. Commun.* **2006**, 4143. (e) Bender, C. F.; Widenhoefer, R. A. *Org. Lett.* **2006**, *8*, 5303. For related Bronsted acid-catalyzed hydroamination, see: (f) Rosenfeld, D. C.; Shekhar, S.; Takeymiya, A.; Utsunomiya, M.; Hartwig, J. F. *Org. Lett.* **2006**, *8*, 4043. (g) Li, Z.; Zhang, J.; Brouwer, C.; Yang, C. G.; Reich, N. W.; He, C. *Org. Lett.* **2006**, *8*, 4175.
- ⁶ (a) Johnson, J. S.; Bergman, R. G. *J. Am. Chem. Soc.* **2001**, *123*, 2923-2924. (b) Ackerman, L.; Bergman, R. G. *Org. Lett.* **2002**, *4*, 1475-1478. (c) Ackerman, L.; Bergman, R. G.; Loy, R. N. *J. Am. Chem. Soc.* **2003**, *125*, 11956-11963. (d) Hoover, J. M.; Peterson, J. R.; Pikul, J. H.; Johnson, A. R. *Organometallics* **2004**, *23*, 4614.
- ⁷ (a) Arredondo, V. M.; McDonald, F. E.; Marks, T. J. *J. Am. Chem. Soc.* **1998**, *120*, 4871-4872. (b) Arredondo, V. M.; McDonald, F. E.; Marks, T. J. *Organometallics* **1999**, *18*, 1949-1960. (c) Arredondo, V. M.; Tian, S.; McDonald, F. E.; Marks, T. J. *J. Am. Chem. Soc.* **1999**, *121*, 3633-3639.
- ⁸ For a review of palladium mediated additions to allenes, see: Yamamoto, Y.; Radhakrishnan, U. *Chem. Soc. Rev.* **1999**, *28*, 199-207.

-
- ⁹ For a recent review of silver mediated reactions, see: Alvarez-Corral, M.; Munoz-Dorado, M.; Rodriguez-Garcia, I. *Chem. Rev.* **2008**, *108*, 3174-3198.
- ¹⁰ Arseniyadis, S.; Gore, J. *Tetrahedron Lett.* **1983**, *24*(37), 3997-4000.
- ¹¹ After submission of this work a Au(I)-catalyzed asymmetric hydroalkoxylation of allenes was reported, see: Zhang, Z.; Widenhoefer, R.A. *Angew. Chem., Int. Ed. Engl.* **2007**, *46*, 283.
- ¹² Lutete, L. M.; Kadota, I.; Yamamoto, Y. *J. Am. Chem. Soc.* **2004**, *128*, 1622-1623.
- ¹³ Claesson, A.; Sahlberg, C.; Luthman, K. *Acta. Chem. Scand. B* **1979**, *33*, 309-310.
- ¹⁴ Lathbury, D.; Gallagher, T. *J. Chem. Soc., Chem. Commun.* **1986**, 114-115.
- ¹⁵ (a) Hemlock's poisonous attributes were most famously described by Plato, see: Plato, *Phaedo*, translated by Gallop, D., Oxford University Press, Inc: New York, 1993. (b) For a recent comparison of the relative toxicities of Coniine enantiomers, see: Lee, S. T.; Green, B. T.; Welch, K. D.; Pfister, J. A.; Panter, K. E. *Chem. Res. Toxicol.* **2008**, *21*, 2061-2064.
- ¹⁶ (a) Kinsman, R.; Lathbury, D.; Vernon, P; Gallagher, T. *J. Chem. Soc., Chem. Commun.* **1987**, 243-244. (b) Fox, D. N. A.; Gallagher, T. *Tetrahedron* **1990**, *46*, 4697-4710. (c) Davies, I. W.; Gallagher, T.; Lamont, R. B.; Scopes, D. I. C. *J. Chem. Soc., Chem. Commun.* **1992**, 335-337.
- ¹⁷ Teles, J. H.; Brode, S.; Chabanas, M. *Angew. Chem., Int. Ed. Engl.* **1998**, *37*(10), 1415-1418.
- ¹⁸ (a) Krause, N.; Morita, N. *Org. Lett.* **2004**, *6*, 4121-4123. (b) Morita, N.; Krause, N. *Eur. J. Org. Chem.* **2006**, 4634-4641.
- ¹⁹ (a) Patil, N. T.; Lutet, L. M.; Nishina, N.; Yamamoto, Y. *Tetrahedron Lett.* **2006**, *47*, 4749-4751. For an intermolecular hydroamination, see: (b) Nishina, N.; Yamamoto, Y. *Angew. Chem., Int. Ed. Engl.* **2006**, *45*, 3314-3317.
- ²⁰ Sherry, B.D.; Toste, F. D. *J. Am. Chem. Soc.* **2004**, *126*, 15978.
- ²¹ (a) Zhang, Z.; Liu, C.; Kinder, R. E.; Han, X.; Qian, H.; Widenhoefer, R. A. *J. Am. Chem. Soc.* **2006**, *128*, 9066. For an intermolecular hydroamination with aryl amines, see: (b) Duncan, A.; Widenhoefer, R. A. *Syn. Lett.* **2010**, 419.
- ²² For an extensive review of ligand effects in gold catalasys, see Gorin, D. J.; Sherry, B. D.; Toste, F. D. *Chem. Rev.* **2008**, *108*, 3351.
- ²³ Corkey, B. K., unpublished results.
- ²⁴ (a) Shapiro, N. D.; Toste, F. D. *Proc. Nat. Acad. Sci.* **2008**, *105*(8), 2779. (b) Dias, H. V. R.; Wu, J. *Angew. Chem., Int. Ed. Engl.* **2007**, *46*, 7814.
- ²⁵ Kennedy-Smith, J. J.; Staben, S. T.; Toste, F. D. *J. Am. Chem. Soc.* **2004**, *126*, 4526.

-
- ²⁶ For a procedure to prepare silver benzoates, see: Rubottom, G. M.; Mott, R. C.; Henrik D.; Juve, J. *J. Org. Chem.* **1981**, *46*, 2717.
- ²⁷ Biarylphosphine Ag(I) complexes have been previously employed as Lewis acid catalysts, see: (a) Wadamoto, M.; Yamamoto, H. *J. Am. Chem. Soc.* **2005**, *127*, 14556. However, no conversion was observed for the reaction of **2.35** with 5 mol% (*R*)-3,5-xlylyl-BINAP and 10 mol% AgOPNB.
- ²⁸ Phosphinegold(I)-chloride complexes alone do not catalyze this reaction.
- ²⁹ Biarylphosphine gold *bis-p*-nitrobenzoate complexes have not been previously characterized. For the analogous triphenylphosphine gold carboxylate complexes, see: (a) Roembke, P.; Schmidbaur, H.; Cronje, S.; Raubenheimer, H. *J. Mol. Cat. A: Chem.* **2004**, *212*, 35. (b) Low, P. M. N.; Zhang, Z.-Y.; Mak, T. C. W.; Hor, T. S. A. *J. Organomet. Chem.* **1997**, *539*, 45. (c) Fackler, J. P.; Khan, M. N. I.; King, C.; Staples, R. J.; Winpenney, R. E. P. *Organometallics* **1991**, *10*, 2178.
- ³⁰ Dr. Benjamin Sherry and Dr. Eun-Joo Kang explored the pyrrolidine substrate scope.
- ³¹ The piperidine substrates were prepared in collaboration with Dr. Eun-Joo Kang.
- ³² Dr. Benjamin Sherry performed the ozonolytic cleavage.
- ³³ Fujita, Y.; Gottlieb, A.; Peterkofsky, B.; Udenfriend, S.; Witkop, B. *J. Am. Chem. Soc.* **1964**, *86*, 4709.
- ³⁴ Fukuyama, T.; Jow, C.-K.; Cheung, M. *Tetrahedron Lett.* **1995**, *36*, 6373.
- ³⁵ Shono, T.; Matsumura, Y.; Tsubata, K.; Uchida, K.; Kanazawa, T.; Tsuda, K. *J. Org. Chem.* **1984**, *49*, 3711.
- ³⁶ Dr. Eun-Joo Kang carried out the deprotection procedure.
- ³⁷ Johansson, M. J.; Gorin, D. J.; Staben, S. T.; Toste, F. D., *J. Am. Chem. Soc.* **2005**, *127*, 18002.
- ³⁸ Jonasson, C.; Horvath, A.; Bäckvall, J. E. *J. Am. Chem. Soc.* **2000**, *122*, 9600.

Appendix 2A

Data acquisition details for X-ray crystal structure of (*R*)-BINAP(Au₂Cl)BF₄ **2.39**

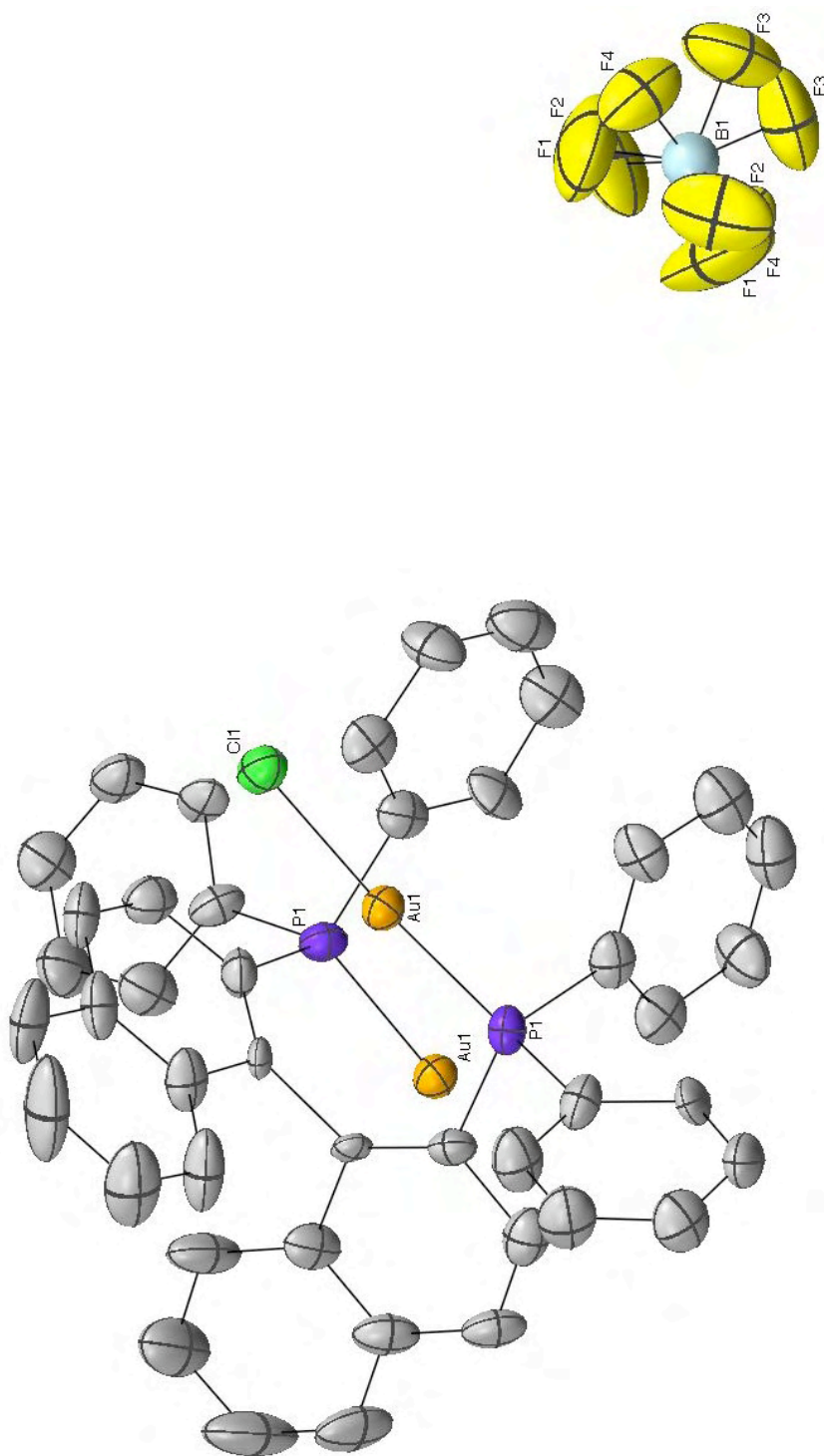


Figure A2.1. ORTEP of (R)-BINAP(Au₂Cl)BF₄ **2.39**. Thermal ellipsoids shown at 50% probability. Hydrogens and solvent molecules omitted for clarity.

Introduction

The crystal structure consists of chloride bridged molecules of the ligand coordinated to gold atoms to form infinite linear chains along the c-axis of the hexagonal unit cell. The chloride and the center of the 2-fold axis of the ligand lie on crystallographic two-fold axes of the space group R32, as does the BF_4 counter-ion and one of the two chloroform molecules of solvation. The other chloroform and the acetonitrile of solvation lie on the three-fold axis, and the acetonitrile is further disordered by an intersecting two-fold axis. It was necessary to apply constraints to the occupancies of the chloroform chlorine atoms and to constrain the thermal parameters of the acetonitrile.

We observed a lot of thermal motion in the model, undoubtedly indicative of the disorder observed in the solvent molecules. As a result of this, the bond distances and angles in the molecule are not all that well determined. The structure is, however, more than enough to determine the overall form of the molecule and to confirm the stereochemistry in the ligand.

Experimental

Data Collection

A fragment of a colorless rod-like crystal of $C_{46.33} H_{35.33} Au_2 B Cl_6 F_4 N_{0.33} P_2$ having approximate dimensions of 0.35 x 0.05 x 0.03 mm was mounted on a Kapton loop using Paratone N hydrocarbon oil. All measurements were made on a Bruker SMART 1000 CCD¹ area detector with graphite monochromated $MoK\alpha$ radiation.

Cell constants and an orientation matrix, obtained from a least-squares refinement using the measured positions of 5550 centered reflections with $I > 10\sigma(I)$ in the range $3.24 < \theta < 26.0^\circ$ corresponded to a R-centered Hexagonal cell with dimensions:

$$\begin{array}{ll} a = 22.057(6) \text{ \AA} & \alpha = 90^\circ \\ b = 22.057(6) \text{ \AA} & \beta = 90^\circ \\ c = 25.443(7) \text{ \AA} & \gamma = 120^\circ \\ V = 10719(5) \text{ \AA}^3 & \end{array}$$

For $Z = 9$ and F.W. = 1352.13, the calculated density is 1.885 g/cm^3 .

Analysis of the systematic absences allowed the space group to be uniquely determined to be:

R 3 2

The data were collected at a temperature of 108(2) K. Frames corresponding to an arbitrary hemisphere of data were collected using ω scans of 0.3° counted for a total of 10 seconds per frame.

Data Reduction

Data were integrated by the program SAINT² to a maximum θ value of 26.78° . The data were corrected for Lorentz and polarization effects. Data were analyzed for agreement and possible absorption using XPREP.³ An empirical absorption correction based on comparison of redundant and equivalent reflections was applied using SADABS.⁴ ($T_{\max} = 0.38$, $T_{\min} = 0.24$). Of the 17233 reflections that were collected, 4696 were unique ($R_{\text{int}} = 0.0627$); equivalent reflections were merged. No decay correction was applied.

Structure Solution and Refinement

The structure was solved by direct methods⁵ and expanded using Fourier techniques.⁶ Some non-hydrogen atoms were refined anisotropically, while the rest were refined isotropically. Hydrogen atoms were included but not refined. The final cycle of full-matrix least-squares refinement⁷ was based on 4696 reflections (all data) and 299 variable parameters and converged (largest parameter shift was 0.001 times its esd) with conventional unweighted and weighted agreement factors of:

$$R_1 = \sum ||F_o| - |F_c|| / \sum |F_o| = 0.0418 \text{ for } 3204 \text{ data with } I > 2\sigma(I)$$

$$wR_2 = [(\sum w (|F_o|^2 - |F_c|^2)^2 / \sum w |F_o|^2)]^{1/2} = 0.0848$$

The standard deviation of an observation of unit weight⁸ was 1.003. The weighting scheme was based on counting statistics and included a factor ($q = 0.05$) to downweight the intense reflections. The maximum and minimum peaks on the final difference Fourier map corresponded to 1.830 and -1.106 e-/Å³, respectively.

Neutral atom scattering factors were taken from Cromer and Waber.⁹ Anomalous dispersion effects were included in F_{calc} ;¹⁰ the values for $\Delta f'$ and $\Delta f''$ were those of Creagh and McAuley.¹¹ The values for the mass attenuation coefficients are those of Creagh and Hubbel.¹² All calculations were performed using the SHELXTL¹³ crystallographic software package of Bruker Analytical X-ray Systems Inc.

Crystal Data

Empirical Formula	$C_{46.33}H_{35.33}Au_2B C_{16}F_4N_{0.33}P_2$
Formula Weight	1352.13
Crystal Color, Habit	colorless, rod
Crystal Dimensions	0.35 x 0.05 x 0.03 mm
Crystal System	Hexagonal
Lattice Type	R-centered
Lattice Parameters	$a = 22.057(6) \text{ \AA}$ $b = 22.057(6) \text{ \AA}$ $c = 25.443(7) \text{ \AA}$ $\alpha = 90^\circ$ $\beta = 90^\circ$ $\gamma = 120^\circ$ $V = 10719(5) \text{ \AA}^3$
Space Group	R 3 2
Z value	9
D_{calc}	1.885 g/cm ³
F000	5820
$\mu(\text{MoK})$	6.61 cm ⁻¹

Intensity Measurements

Diffractometer	Bruker SMART 1000 CCD
Radiation	MoK($\lambda = 0.71073 \text{ \AA}$) graphite monochromated
Detector Position	60.00 mm
Exposure Time	10 seconds per frame.

Scan Type	ω (0.3 degrees per frame)
θ_{\max}	26.78°
No. of Reflections Measured	Total: 17233 Unique: 4696 ($R_{\text{int}} = 0.0627$)
Corrections	Lorentz-polarization Absorption ($T_{\max} = 0.38$, $T_{\min} = 0.24$)

Structure Solution and Refinement

Structure Solution	direct (SHELXS-97 (Sheldrick, 2008))
Refinement	Full-matrix least-squares
Function Minimized	$\Sigma w(F_o ^2 - F_c ^2)^2$
Least Squares Weighting scheme	$w = 1/[\sigma^2(F_o^2) + (qP)^2 + 0.000P]$ where $P = [F_o^2 + 2F_c^2]/3$
q-factor	0.05
Anomalous Dispersion	All non-hydrogen atoms
No. Observations ($I > 2.00\sigma(I)$)	3204
No. Variables	299
Reflection/Parameter Ratio	10.7
Residuals: R; wR_2 ; R_{all}	0.0418; 0.0848; 0.0832
Goodness of Fit Indicator	1.003
Max Shift/Error in Final Cycle	0.001
Maximum peak in Final Diff. Map	1.830 e ⁻ /Å ³
Minimum peak in Final Diff. Map	-1.106 e ⁻ /Å ³

Table 2A.1. Atomic coordinates and $U_{\text{iso}}/U_{\text{eq}}$ and occupancy

atom	x	y	z	U_{eq}^a	Occupancy
Au1	0.2892(1)	0.3318(1)	-0.2753(1)	0.031(1)	1
Cl1	0.3333	0.4262(2)	-0.3333	0.039(1)	1
P1	0.2402(1)	0.2432(1)	-0.2181(1)	0.030(1)	1
C1	0.2961(5)	0.2421(5)	-0.1649(4)	0.033(3)	1
C2	0.2704(6)	0.1782(5)	-0.1380(4)	0.041(3)	1
C3	0.3080(6)	0.1715(6)	-0.0974(4)	0.042(3)	1
C4	0.3733(7)	0.2288(6)	-0.0825(4)	0.042(3)	1
C5	0.4115(8)	0.2219(7)	-0.0406(5)	0.062(4)	1
C6	0.4743(10)	0.2770(9)	-0.0273(6)	0.093(6)	1
C7	0.5017(8)	0.3400(7)	-0.0553(6)	0.075(5)	1
C8	0.4652(7)	0.3491(7)	-0.0949(5)	0.058(4)	1
C9	0.3993(6)	0.2917(6)	-0.1105(4)	0.039(3)	1
C10	0.3561(4)	0.2970(4)	-0.1530(3)	0.021(2)	1
C11	0.1627(6)	0.2388(5)	-0.1871(4)	0.036(3)	1
C12	0.1447(6)	0.2149(6)	-0.1359(4)	0.041(3)	1
C13	0.0835(6)	0.2121(6)	-0.1148(5)	0.052(4)	1
C14	0.0458(7)	0.2307(6)	-0.1452(5)	0.060(4)	1
C15	0.0640(6)	0.2532(6)	-0.1963(5)	0.054(3)	1
C16	0.1238(6)	0.2594(6)	-0.2167(4)	0.041(3)	1
C17	0.2114(6)	0.1589(5)	-0.2498(4)	0.038(3)	1
C18	0.1444(5)	0.1054(5)	-0.2474(4)	0.039(3)	1
C19	0.1266(6)	0.0415(6)	-0.2719(5)	0.047(3)	1
C20	0.1767(6)	0.0325(7)	-0.2970(5)	0.049(3)	1
C21	0.2437(7)	0.0881(6)	-0.3002(5)	0.057(4)	1
C22	0.2611(7)	0.1506(6)	-0.2763(4)	0.050(3)	1
B1	-0.0433(11)	0.3333	-0.6667	0.053(5)	1
F1	-0.040(2)	0.2771(17)	-0.6650(13)	0.150(14)	0.50
F2	0.0038(13)	0.3859(17)	-0.6348(10)	0.110(10)	0.50

F3	-0.1104(9)	0.3125(12)	-0.6515(10)	0.108(9)	0.50
F4	-0.0262(12)	0.3641(9)	-0.7168(6)	0.084(6)	0.50
C23	0.0000	0.0000	0.0771(13)	0.102(10)	1
Cl2A	0.0000	0.0000	0.1487(8)	0.063(14)	0.37(7)
Cl2B	-0.040(2)	-0.0260(18)	0.1453(9)	0.083(8)	0.21(2)
Cl3	0.0525(4)	0.0905(4)	0.0640(3)	0.106(2)	0.67
C24	0.018(3)	0.241(2)	-0.4767(16)	0.123(15)	0.50
Cl4	-0.0720(6)	0.2178(6)	-0.4617(4)	0.135(3)	0.608(9)
Cl5	0.0067(8)	0.2774(8)	-0.5372(5)	0.135(3)	0.484(10)
Cl6	0.0235(8)	0.1751(8)	-0.4698(6)	0.135(3)	0.409(9)
N1	0.0000	0.0000	-0.432(3)	0.194(18)	0.50
C25	0.0000	0.0000	-0.476(3)	0.194(18)	0.50
C26	0.0000	0.0000	-0.533(3)	0.194(18)	0.50
H2A	0.2267	0.1392	-0.1478	0.049	1
H3A	0.2900	0.1282	-0.0794	0.051	1
H5A	0.3933	0.1789	-0.0220	0.074	1
H6A	0.5001	0.2731	0.0011	0.112	1
H7A	0.5468	0.3775	-0.0465	0.090	1
H8A	0.4836	0.3932	-0.1119	0.069	1
H12A	0.1719	0.2009	-0.1158	0.050	1
H13A	0.0696	0.1973	-0.0796	0.063	1
H14A	0.0049	0.2282	-0.1308	0.071	1
H15A	0.0350	0.2642	-0.2171	0.064	1
H16A	0.1386	0.2778	-0.2510	0.050	1
H18A	0.1098	0.1110	-0.2294	0.047	1
H19A	0.0795	0.0041	-0.2710	0.057	1
H20A	0.1651	-0.0114	-0.3120	0.059	1
H21A	0.2783	0.0834	-0.3190	0.068	1
H22A	0.3079	0.1884	-0.2781	0.060	1

^aU_{eq} is defined as one third of the orthogonalized U_{ij} tensor

Table 2A.2. Anisotropic Displacement Parameters

atom	U11	U22	U33	U12	U13	U23
Au1	0.030(1)	0.027(1)	0.035(1)	-0.002(1)	-0.001(1)	0.013(1)
C11	0.042(2)	0.034(1)	0.043(2)	0.003(1)	0.006(2)	0.021(1)
P1	0.024(1)	0.026(1)	0.033(2)	-0.001(1)	0.001(1)	0.007(1)
C1	0.036(7)	0.029(6)	0.040(6)	0.002(5)	-0.002(5)	0.022(5)
C2	0.040(7)	0.033(6)	0.042(6)	-0.005(5)	0.005(6)	0.013(6)
C3	0.065(8)	0.034(7)	0.042(7)	-0.004(6)	-0.007(6)	0.036(7)
C4	0.064(9)	0.040(8)	0.040(6)	-0.011(6)	-0.012(6)	0.039(8)
C5	0.096(11)	0.033(8)	0.069(8)	-0.016(7)	-0.030(9)	0.042(7)
C6	0.127(15)	0.072(12)	0.115(13)	-0.030(11)	-0.069(12)	0.076(11)
C7	0.074(10)	0.046(9)	0.106(13)	-0.031(8)	-0.051(9)	0.031(8)
C8	0.080(9)	0.042(8)	0.069(9)	-0.020(7)	-0.041(8)	0.043(8)
C9	0.048(7)	0.030(6)	0.043(7)	-0.019(5)	-0.021(6)	0.023(6)
C10	0.026(5)	0.014(5)	0.026(5)	-0.002(4)	-0.002(3)	0.014(5)
C11	0.035(7)	0.030(6)	0.039(7)	-0.013(5)	0.001(5)	0.012(5)
C12	0.045(7)	0.034(6)	0.037(7)	-0.018(5)	-0.011(5)	0.015(6)
C13	0.043(7)	0.071(10)	0.044(7)	0.004(6)	0.012(6)	0.030(7)
C14	0.040(8)	0.052(9)	0.073(10)	-0.019(7)	0.005(7)	0.013(6)
C15	0.052(8)	0.057(8)	0.049(8)	-0.021(6)	-0.009(6)	0.025(7)
C16	0.039(6)	0.049(8)	0.042(6)	-0.019(6)	0.001(5)	0.026(6)
C17	0.034(7)	0.027(6)	0.037(6)	0.001(5)	0.002(5)	0.005(5)
C18	0.019(6)	0.031(6)	0.057(8)	0.002(6)	-0.013(5)	0.005(5)
C19	0.030(7)	0.031(6)	0.067(8)	0.002(6)	-0.009(6)	0.005(5)
C20	0.051(8)	0.045(8)	0.050(7)	-0.015(6)	-0.007(6)	0.021(7)
C21	0.053(10)	0.042(7)	0.077(9)	-0.015(6)	0.005(7)	0.025(7)
C22	0.041(8)	0.041(6)	0.061(7)	-0.019(5)	-0.002(7)	0.015(7)
F1	0.23(4)	0.11(2)	0.16(3)	0.06(3)	0.05(3)	0.12(2)
F2	0.064(16)	0.16(3)	0.074(15)	-0.036(18)	-0.040(14)	0.031(17)
F3	0.048(11)	0.12(3)	0.13(3)	-0.038(16)	0.006(12)	0.023(12)
F4	0.129(16)	0.057(11)	0.045(10)	-0.006(8)	-0.029(10)	0.031(11)

C13	0.083(5)	0.100(5)	0.123(6)	0.004(5)	-0.013(4)	0.035(4)
-----	----------	----------	----------	----------	-----------	----------

The general temperature factor expression:

$$\exp(-2\pi^2(a^2U_{11}h^2 + b^2U_{22}k^2 + c^2U_{33}l^2 + 2a*b*U_{12}hk + 2a*c*U_{13}hl + 2b*c*U_{23}kl))$$

Table 2A.3. Bond Lengths (Å)

atom	atom	distance	atom	atom	distance
Au1	P1	2.235(3)	Au1	Cl1	2.332(2)
Cl1	Au1#1	2.331(2)	P1	C17	1.824(11)
P1	C1	1.839(10)	P1	C11	1.839(11)
C1	C10	1.306(12)	C1	C2	1.407(13)
C2	C3	1.376(14)	C2	H2A	0.95
C3	C4	1.412(17)	C3	H3A	0.95
C4	C9	1.401(15)	C4	C5	1.415(15)
C5	C6	1.35(2)	C5	H5A	0.95
C6	C7	1.40(2)	C6	H6A	0.95
C7	C8	1.364(16)	C7	H7A	0.95
C8	C9	1.426(15)	C8	H8A	0.95
C9	C10	1.485(13)	C10	C10#2	1.553(16)
C11	C16	1.379(15)	C11	C12	1.386(14)
C12	C13	1.425(15)	C12	H12A	0.95
C13	C14	1.340(16)	C13	H13A	0.95
C14	C15	1.380(17)	C14	H14A	0.95
C15	C16	1.357(15)	C15	H15A	0.95
C16	H16A	0.95	C17	C18	1.355(14)
C17	C22	1.375(17)	C18	C19	1.405(15)
C18	H18A	0.95	C19	C20	1.374(16)
C19	H19A	0.95	C20	C21	1.372(16)
C20	H20A	0.95	C21	C22	1.374(14)
C21	H21A	0.95	C22	H22A	0.95
B1	F1	1.28(3)	B1	F1#3	1.28(3)
B1	F3#3	1.37(3)	B1	F3	1.37(3)
B1	F2#3	1.37(2)	B1	F2	1.37(2)
B1	F4	1.406(16)	B1	F4#3	1.406(16)
F1	F2#3	0.89(3)	F1	F4#3	1.48(3)

F2	F1#3	0.89(3)	F2	F4#3	1.71(3)
F3	F3#3	1.11(4)	F3	F4#3	1.58(3)
F4	F1#3	1.48(3)	F4	F3#3	1.58(3)
F4	F2#3	1.71(3)	C23	C13#4	1.768(10)
C23	C13	1.768(10)	C23	C13#5	1.768(10)
C23	C12A	1.82(4)	C23	C12B#5	1.90(4)
C23	C12B#4	1.90(4)	C23	C12B	1.90(4)
C12A	C12B	0.78(4)	C12A	C12B#5	0.78(4)
C12A	C12B#4	0.78(4)	C12B	C12B#5	1.35(8)
C12B	C12B#4	1.35(8)	C12B	C13#4	2.30(3)
C13	C12B#5	2.30(3)	C24	C15#6	1.09(5)
C24	C24#6	1.37(8)	C24	C16	1.53(5)
C24	C15	1.81(4)	C24	C14	1.82(5)
C24	C14#6	1.94(5)	C24	C16#6	2.19(4)
C14	C15#6	1.325(15)	C14	C24#6	1.94(5)
C15	C24#6	1.09(5)	C15	C14#6	1.325(15)
C15	C15#6	1.91(3)	C16	C16#6	1.78(3)
C16	C24#6	2.19(4)	N1	C25	1.142(9)
C25	C26	1.440(9)			

Table 2A.4. Bond Angles (°)

atom	atom	atom	angle	atom	atom	atom	angle
P1	Au1	Cl1	175.49(9)	Au1	Cl1	Au1#1	93.68(12)
C17	P1	C1	101.9(5)	C17	P1	C11	107.2(5)
C1	P1	C11	107.2(5)	C17	P1	Au1	111.9(3)
C1	P1	Au1	117.1(3)	C11	P1	Au1	110.8(4)
C10	C1	C2	122.0(9)	C10	C1	P1	122.2(8)
C2	C1	P1	115.8(8)	C3	C2	C1	120.6(10)
C3	C2	H2A	119.7	C1	C2	H2A	119.7
C2	C3	C4	120.3(10)	C2	C3	H3A	119.8
C4	C3	H3A	119.8	C9	C4	C3	118.7(10)
C9	C4	C5	121.2(12)	C3	C4	C5	120.1(11)
C6	C5	C4	119.3(13)	C6	C5	H5A	120.3
C4	C5	H5A	120.3	C5	C6	C7	120.3(13)
C5	C6	H6A	119.9	C7	C6	H6A	119.9
C8	C7	C6	121.9(14)	C8	C7	H7A	119.1
C6	C7	H7A	119.1	C7	C8	C9	119.3(12)
C7	C8	H8A	120.4	C9	C8	H8A	120.4
C4	C9	C8	118.0(10)	C4	C9	C10	119.1(10)
C8	C9	C10	122.9(10)	C1	C10	C9	119.3(9)
C1	C10	C10#2	127.9(8)	C9	C10	C10#2	112.7(7)
C16	C11	C12	122.1(11)	C16	C11	P1	117.7(8)
C12	C11	P1	120.3(9)	C11	C12	C13	117.1(11)
C11	C12	H12A	121.4	C13	C12	H12A	121.4
C14	C13	C12	119.2(12)	C14	C13	H13A	120.4
C12	C13	H13A	120.4	C13	C14	C15	122.7(13)
C13	C14	H14A	118.6	C15	C14	H14A	118.6
C16	C15	C14	119.3(13)	C16	C15	H15A	120.3
C14	C15	H15A	120.3	C15	C16	C11	119.4(11)
C15	C16	H16A	120.3	C11	C16	H16A	120.3

C18	C17	C22	120.0(10)	C18	C17	P1	122.7(9)
C22	C17	P1	117.3(8)	C17	C18	C19	119.4(11)
C17	C18	H18A	120.3	C19	C18	H18A	120.3
C20	C19	C18	120.5(10)	C20	C19	H19A	119.7
C18	C19	H19A	119.7	C21	C20	C19	118.9(11)
C21	C20	H20A	120.5	C19	C20	H20A	120.5
C20	C21	C22	120.5(13)	C20	C21	H21A	119.8
C22	C21	H21A	119.8	C21	C22	C17	120.6(12)
C21	C22	H22A	119.7	C17	C22	H22A	119.7
F1	B1	F1#3	115(4)	F1	B1	F3#3	138(3)
F1#3	B1	F3#3	104(2)	F1	B1	F3	104(2)
F1#3	B1	F3	138(3)	F3#3	B1	F3	48(2)
F1	B1	F2#3	38.9(14)	F1#3	B1	F2#3	114(2)
F3#3	B1	F2#3	110.7(19)	F3	B1	F2#3	105(2)
F1	B1	F2	114(2)	F1#3	B1	F2	38.9(14)
F3#3	B1	F2	105(2)	F3	B1	F2	110.7(19)
F2#3	B1	F2	141(3)	F1	B1	F4	111.5(18)
F1#3	B1	F4	66.7(16)	F3#3	B1	F4	69.3(13)
F3	B1	F4	114(2)	F2#3	B1	F4	76.1(14)
F2	B1	F4	102.8(15)	F1	B1	F4#3	66.6(16)
F1#3	B1	F4#3	111.5(18)	F3#3	B1	F4#3	114(2)
F3	B1	F4#3	69.3(13)	F2#3	B1	F4#3	102.8(15)
F2	B1	F4#3	76.1(14)	F4	B1	F4#3	177(3)
F2#3	F1	B1	76(3)	F2#3	F1	F4#3	132(4)
B1	F1	F4#3	60.8(15)	F1#3	F2	B1	65(3)
F1#3	F2	F4#3	114(4)	B1	F2	F4#3	52.9(11)
F3#3	F3	B1	66.0(10)	F3#3	F3	F4#3	118.6(15)
B1	F3	F4#3	56.5(9)	B1	F4	F1#3	52.5(12)
B1	F4	F3#3	54.2(13)	F1#3	F4	F3#3	85.9(18)
B1	F4	F2#3	51.0(10)	F1#3	F4	F2#3	88.3(16)
F3#3	F4	F2#3	86.3(14)	C13#4	C23	C13	116.5(7)
C13#4	C23	C13#5	116.5(7)	C13	C23	C13#5	116.5(7)

CI3#4	C23	CI2A	100.9(11)	CI3	C23	CI2A	100.9(11)
CI3#5	C23	CI2A	100.9(11)	CI3#4	C23	CI2B#5	106.1(13)
CI3	C23	CI2B#5	77.5(15)	CI3#5	C23	CI2B#5	117.2(16)
CI2A	C23	CI2B#5	24.2(13)	CI3#4	C23	CI2B#4	117.2(16)
CI3	C23	CI2B#4	106.1(13)	CI3#5	C23	CI2B#4	77.5(15)
CI2A	C23	CI2B#4	24.2(13)	CI2B#5	C23	CI2B#4	42(2)
CI3#4	C23	CI2B	77.5(15)	CI3	C23	CI2B	117.2(16)
CI3#5	C23	CI2B	106.1(13)	CI2A	C23	CI2B	24.2(14)
CI2B#5	C23	CI2B	42(2)	CI2B#4	C23	CI2B	42(2)
CI2B	CI2A	CI2B#5	118.8(10)	CI2B	CI2A	CI2B#4	118.8(10)
CI2B#5	CI2A	CI2B#4	118.8(10)	CI2B	CI2A	C23	84(3)
CI2B#5	CI2A	C23	84(3)	CI2B#4	CI2A	C23	84(3)
CI2A	CI2B	CI2B#5	30.6(5)	CI2A	CI2B	CI2B#4	30.6(5)
CI2B#5	CI2B	CI2B#4	60.000(5)	CI2A	CI2B	C23	72(3)
CI2B#5	CI2B	C23	69.2(11)	CI2B#4	CI2B	C23	69.2(11)
CI2A	CI2B	CI3#4	119(3)	CI2B#5	CI2B	CI3#4	104.0(14)
CI2B#4	CI2B	CI3#4	115.8(9)	C23	CI2B	CI3#4	48.7(7)
C23	CI3	CI2B#5	53.8(15)	CI5#6	C24	C24#6	94(3)
CI5#6	C24	CI6	146(4)	C24#6	C24	CI6	97.7(16)
CI5#6	C24	CI5	78(3)	C24#6	C24	CI5	37(2)
CI6	C24	CI5	128(3)	CI5#6	C24	CI4	46(2)
C24#6	C24	CI4	73(4)	CI6	C24	CI4	108(3)
CI5	C24	CI4	86(2)	CI5#6	C24	CI4#6	106(3)
C24#6	C24	CI4#6	64(4)	CI6	C24	CI4#6	107(3)
CI5	C24	CI4#6	41.3(10)	CI4	C24	CI4#6	128(3)
CI5#6	C24	CI6#6	129(3)	C24#6	C24	CI6#6	44.0(12)
CI6	C24	CI6#6	53.7(17)	CI5	C24	CI6#6	77.4(14)
CI4	C24	CI6#6	88.4(17)	CI4#6	C24	CI6#6	82.0(17)
CI5#6	CI4	C24	36.6(15)	CI5#6	CI4	C24#6	64.1(14)
C24	CI4	C24#6	42(2)	C24#6	CI5	CI4#6	97(3)
C24#6	CI5	C24	49(3)	CI4#6	CI5	C24	74.6(16)

C24#6	C15	C15#6	68(2)	C14#6	C15	C15#6	98.4(11)
C24	C15	C15#6	34.1(17)	C24	C16	C16#6	82.3(16)
C24	C16	C24#6	38(2)	C16#6	C16	C24#6	44.0(12)
N1	C25	C26	180.000(12)				

Table 2A.5. Torsion Angles(^o).

atom	atom	atom	atom	angle	atom	atom	atom	atom	angle
P1	Au1	Cl1	Au1#1	-149.0(9)	Cl1	Au1	P1	C17	118.9(10)
Cl1	Au1	P1	C1	-124.1(10)	Cl1	Au1	P1	C11	-0.6(11)
C17	P1	C1	C10	137.7(9)	C11	P1	C1	C10	-109.9(9)
Au1	P1	C1	C10	15.3(10)	C17	P1	C1	C2	-42.0(9)
C11	P1	C1	C2	70.4(8)	Au1	P1	C1	C2	-164.4(7)
C10	C1	C2	C3	0.4(16)	P1	C1	C2	C3	-179.9(8)
C1	C2	C3	C4	-0.4(16)	C2	C3	C4	C9	-1.3(16)
C2	C3	C4	C5	179.6(10)	C9	C4	C5	C6	0.1(18)
C3	C4	C5	C6	179.2(12)	C4	C5	C6	C7	-1(2)
C5	C6	C7	C8	3(2)	C6	C7	C8	C9	-4(2)
C3	C4	C9	C8	179.9(11)	C5	C4	C9	C8	-1.0(17)
C3	C4	C9	C10	2.8(16)	C5	C4	C9	C10	-178.1(10)
C7	C8	C9	C4	2.8(19)	C7	C8	C9	C10	179.8(11)
C2	C1	C10	C9	1.2(15)	P1	C1	C10	C9	-178.5(7)
C2	C1	C10	C10#2	177.5(9)	P1	C1	C10	C10#2	-2.2(14)
C4	C9	C10	C1	-2.9(15)	C8	C9	C10	C1	-179.8(11)
C4	C9	C10	C10#2	-179.7(9)	C8	C9	C10	C10#2	3.4(15)
C17	P1	C11	C16	-90.1(9)	C1	P1	C11	C16	161.2(8)
Au1	P1	C11	C16	32.2(9)	C17	P1	C11	C12	89.4(9)
C1	P1	C11	C12	-19.3(10)	Au1	P1	C11	C12	-148.3(7)
C16	C11	C12	C13	0.2(15)	P1	C11	C12	C13	-179.2(8)
C11	C12	C13	C14	1.6(16)	C12	C13	C14	C15	-0.6(19)
C13	C14	C15	C16	-2.4(19)	C14	C15	C16	C11	4.3(17)
C12	C11	C16	C15	-3.2(16)	P1	C11	C16	C15	176.3(8)
C1	P1	C17	C18	110.8(10)	C11	P1	C17	C18	-1.7(11)
Au1	P1	C17	C18	-123.3(9)	C1	P1	C17	C22	-68.4(10)
C11	P1	C17	C22	179.2(9)	Au1	P1	C17	C22	57.5(10)
C22	C17	C18	C19	0.6(17)	P1	C17	C18	C19	-178.6(8)
C17	C18	C19	C20	1.4(17)	C18	C19	C20	C21	-3.3(18)

C19	C20	C21	C22	3(2)	C20	C21	C22	C17	-1(2)
C18	C17	C22	C21	-0.6(18)	P1	C17	C22	C21	178.6(10)

The ADC (atom designator code) specifies the position of an atom in a crystal. The 5-digit number shown in the table is a composite of three one-digit numbers and one two-digit number: TA (first digit) + TB (second digit) + TC (third digit) + SN (last two digits). TA, TB and TC are the crystal lattice translation digits along cell edges a, b and c. A translation digit of 5 indicates the origin unit cell. If TA = 4, this indicates a translation of one unit cell length along the a-axis in the negative direction. Each translation digit can range in value from 1 to 9 and thus +4 lattice translations from the origin (TA=5, TB=5, TC=5) can be represented.

The SN, or symmetry operator number, refers to the number of the symmetry operator used to generate the coordinates of the target atom. A list of symmetry operators relevant to this structure are given below.

For a given intermolecular contact, the first atom (origin atom) is located in the origin unit cell and its position can be generated using the identity operator (SN=1). Thus, the ADC for an origin atom is always 55501. The position of the second atom (target atom) can be generated using the ADC and the coordinates of the atom in the parameter table. For example, an ADC of 47502 refers to the target atom moved through symmetry operator two, then translated -1 cell translations along the a axis, +2 cell translations along the b axis, and 0 cell translations along the c axis.

An ADC of 1 indicates an intermolecular contact between two fragments (eg. cation and anion) that reside in the same asymmetric unit.

Table 2A.6. Symmetry Operators

x, y, z	$y+2/3, x+1/3, -z+1/3$
$-y, x-y, z$	$x-y+2/3, -y+1/3, -z+1/3$
$-x+y, -x, z$	$-x+2/3,$
$y, x, -z$	$-x+y+1/3, -z+1/3$
$x-y, -y, -z$	$x+1/3, y+2/3, z+2/3$
$-x, -x+y, -z$	$-y+1/3, x-y+2/3, z+2/3$
$x+2/3, y+1/3, z+1/3$	$-x+y+1/3, -x+2/3, z+2/3$
$-y+2/3, x-y+1/3, z+1/3$	$y+1/3, x+2/3, -z+2/3$
$-x+y+2/3,$	$x-y+1/3, -y+2/3, -z+2/3$
$-x+1/3, z+1/3$	$-x+1/3, -x+y+2/3, -z+2/3$

References

- ¹ SMART: Area-Detector Software Package, Bruker Analytical X-ray Systems, Inc.: Madison, WI, (1995-99).
- ² SAINT: SAX Area-Detector Integration Program, V7.06; Siemens Industrial Automation, Inc.: Madison, WI, (2005).
- ³ XPREP: (v 6.12) Part of the SHELXTL Crystal Structure Determination Package, Bruker AXS Inc.: Madison, WI, (1995).
- ⁴ SADABS: (v2.10) Siemens Area Detector ABSorption correction program, George Sheldrick, (2005).
- ⁵ XS: Program for the Solution of X-ray Crystal Structures, Part of the SHELXTL Crystal Structure Determination Package, Bruker Analytical X-ray Systems Inc.: Madison, WI, (1995-99).
- ⁶ XL: Program for the Refinement of X-ray Crystal Structures, Part of the SHELXTL Crystal Structure Determination Package, Bruker Analytical X-ray Systems Inc.: Madison, WI, (1995-99).
- ⁷ Least-Squares:
Function minimized: $\sum w (|F_o|^2 - |F_c|^2)^2$
- ⁸ Standard deviation of an observation of unit weight:
$$[\sum w (|F_o|^2 - |F_c|^2)^2 / (N_o - N_v)]^{1/2}$$
where: N_o = number of observations
 N_v = number of variables
- ⁹ Cromer, D. T. & Waber, J. T.; "International Tables for X-ray Crystallography", Vol. IV, The Kynoch Press, Birmingham, England, Table 2.2 A (1974).
- ¹⁰ Ibers, J. A. & Hamilton, W. C.; *Acta Crystallogr.*, 17, 781 (1964).
- ¹¹ Creagh, D. C. & McAuley, W. J. ; "International Tables for Crystallography", Vol C, (A.J.C. Wilson, ed.), Kluwer Academic Publishers, Boston, Table 4.2.6.8, pages 219-222 (1992).
- ¹² Creagh, D. C. & Hubbell, J.H.; "International Tables for Crystallography", Vol C, (A.J.C. Wilson, ed.), Kluwer Academic Publishers, Boston, Table 4.2.4.3, pages 200-206 (1992).
- ¹³ XP: Molecular Graphics program. Part of the SHELXTL Structure Determination Package. Bruker Analytical X-ray Systems Inc.: Madison, WI, (1995-99).

Appendix 2B

Data acquisition details for X-ray crystal structure of *(R)*-ClMeOBiPHEP(AuOPNB)₂ **2.43**

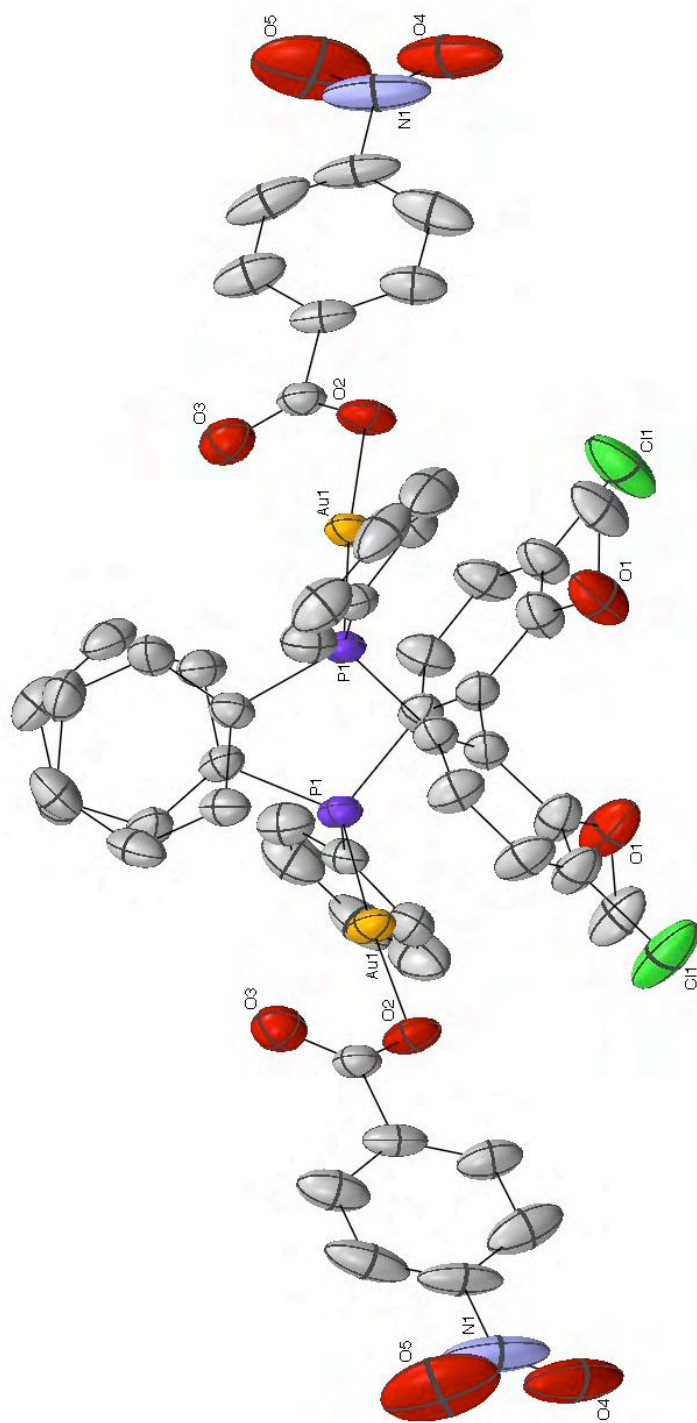


Figure 2B.1. ORTEP of (*R*)-ClMeOBiPHEP(AuOPNB)₂ **2.43**. Thermal ellipsoids shown at 50% probability. Hydrogens and solvent molecules omitted for clarity.

Introduction

This is a chemically simple, crystallographically complex, structure. The molecule of interest was found to be as expected, and the chirality of the molecule and enantiomorph of the space group were confirmed by refinement of the Flack parameter. The methoxy methyl group is disordered over two positions in an approximate 60:40 ratio. The nitrobenzoate ligand is loosely coordinated by the gold and shows increasingly large thermal motion as the distance to the gold atom increases. As a result, distances and angles in the nitrobenzoate are not particularly accurate.

The molecule crystallizes in the chiral space group $P6(5)22$ with one half molecule in the asymmetric unit. A crystallographic two-fold axis bisects the bond (C6-C6') between the two halves of the chiral ligand. The packing of the molecules leaves large channels centered on the 6(5) axis at (0,0) (see Figures). There is diffuse electron density filling this cavity. The electron density was modeled as partially occupied carbon atoms refined with a fixed Uiso of 0.15 (arbitrarily chosen as an appropriate Uiso for solvent in a structure of this quality) and refined positional and occupancy factors. This model gives two interlocked spiral chains of carbon atoms running up adding up to approximately 3 carbon atoms per asymmetric unit, approximately 36 carbons in the unit cell. Attempts to refine the common Uiso "thermal" parameter led to small decreases of the residuals and to very large values of both Uiso and the occupancy factors of the model carbon atoms.

Since the compound was crystallized from hexane, I postulate that this electron density is disordered hexane, with approximately 6 molecules of hexane in the unit cell, one molecule of hexane per molecule of the compound of interest. The formula is reported on that basis, and of course no hydrogen atoms were included for the solvent. Other possibilities exist – it could be Paratone N (long chain hydrocarbon oil that we use for mounting crystals) that has diffused in (the particular crystal sample soaked in Paratone for a month or so), or it could be air molecules (less likely because of the ease with which they could leave, yielding an open channel which could then collapse).

While the spiral form of the solvent electron density is aesthetic, it is not worth discussing because it is demanded by the symmetry operations of the space group running through and along the c-axis. (There is a 6(5) axis and numerous intersecting two-fold axes.) The contents of the cavity are not ordered in the cell in any commensurate way, but rather occupy the cavity ad libitum. What is of note is the fact that the model carbons are not at all unusually close to the molecule of interest, and the two chains are well separated from each other, which lends credence to the hypothesis that they represent something real. It is probable that any editor will want an explanation of the disorder, which is the reason for this lengthy discussion.

Experimental

Data Collection

A fragment of a colorless block-like crystal of $C_{58} H_{51} Au_2 Cl_2 N_2 O_{10} P_2$ having approximate dimensions of 0.38 x 0.36 x 0.33 mm was mounted on a nylon loop using Paratone N hydrocarbon oil. All measurements were made on a Bruker SMART 1000 CCD¹ area detector with graphite monochromated MoK α radiation.²

Cell constants and an orientation matrix, obtained from a least-squares refinement using the measured positions of 9918 centered reflections with $I > 10\sigma(I)$ in the range $2.75 < \theta < 26.1^\circ$ corresponded to a primitive hexagonal cell with dimensions:

$$\begin{aligned} a &= 24.925(2) \text{ \AA} & \alpha &= 90^\circ \\ b &= 24.925(2) \text{ \AA} & \beta &= 90^\circ \\ c &= 15.631(1) \text{ \AA} & \gamma &= 120^\circ \\ V &= 8409.4(11) \text{ \AA}^3 \end{aligned}$$

For $Z = 6$ and F.W. = 1462.78, the calculated density is 1.733 g/cm³.

Analysis of the systematic absences allowed the space group to be uniquely determined to be:

$$P 6(5) 2 2$$

The data were collected at a temperature of 133(2) K. Frames corresponding to an arbitrary hemisphere of data were collected using ω scans of 0.3° counted for a total of 20 seconds per frame.

Data Reduction

Data were integrated by the program SAINT¹ to a maximum θ value of 26.36° . The data were corrected for Lorentz and polarization effects. Data were analyzed for agreement and possible absorption using XPREP³. An empirical absorption correction based on comparison of redundant and equivalent reflections was applied using SADABS.⁴ ($T_{\max} = 0.2669$, $T_{\min} = 0.2349$). Of the 76285 reflections that were collected, 5718 were unique ($R_{\text{int}} = 0.0358$); equivalent reflections were merged. No decay correction was applied.

Structure Solution and Refinement

The structure was solved by direct methods⁵ and expanded using Fourier techniques.⁶ Non-hydrogen atoms were refined anisotropically except for those that were disordered. Hydrogen atoms were included in calculated idealized positions but not refined. The final cycle of full-matrix least-squares refinement⁷ was based on 5718 reflections (all data) and 349 variable parameters and converged (largest parameter shift was 0.008 times its esd) with conventional unweighted and weighted agreement factors of:

$$R_1 = \sum ||F_o| - |F_c|| / \sum |F_o| = 0.0302 \text{ for } 5124 \text{ data with } I > 2\sigma(I)$$

$$wR_2 = [(\sum w (|F_o|^2 - |F_c|^2)^2 / \sum w |F_o|^2)]^{1/2} = 0.0763$$

The standard deviation of an observation of unit weight⁸ was 1.246. The weighting scheme was based on counting statistics and included a factor ($q = 0.05$) to downweight the intense reflections. The maximum and minimum peaks on the final difference Fourier map corresponded to 1.024 and $-0.369 \text{ e}^-/\text{\AA}^3$, respectively.

Neutral atom scattering factors were taken from Cromer and Waber.⁹ Anomalous dispersion effects were included in F_{calc} ;¹⁰ the values for $\Delta f'$ and $\Delta f''$ were those of Creagh and McAuley.¹¹ The values for the mass attenuation coefficients are those of Creagh and Hubbel.¹² All calculations were performed using the SHELXTL¹³ crystallographic software package of Bruker Analytical X-ray Systems Inc.

Crystal Data

Empirical Formula	$C_{58} H_{51} Au_2 Cl_2 N_2 O_{10} P_2$
Formula Weight	1462.78
Crystal Color, Habit	colorless, block
Crystal Dimensions	0.38 x 0.36 x 0.33 mm
Crystal System	Hexagonal
Lattice Type	primitive
Lattice Parameters	$a = 24.925(2) \text{ \AA}$ $b = 24.925(2) \text{ \AA}$ $c = 15.631(1) \text{ \AA}$ $\alpha = 90^\circ$ $\beta = 90^\circ$ $\gamma = 120^\circ$ $V = 8409.4(11) \text{ \AA}^3$
Space Group	P 65 2 2
Z value	6
D_{calc}	1.733 g/cm ³
F000	4290
μ (MoK)	5.44 cm ⁻¹

Intensity Measurements

Diffractometer	Bruker SMART 1000 CCD
Radiation	MoK($\lambda = 0.71073 \text{ \AA}$) graphite monochromated
Detector Position	60.00 mm
Exposure Time	20 seconds per frame.

Scan Type	ω (0.3 degrees per frame)
θ max	26.36°
No. of Reflections Measured	Total: 76285 Unique: 5718 ($R_{\text{int}} = 0.0358$)
Corrections	Lorentz-polarization Absorption ($T_{\text{max}} = 0.2669$, $T_{\text{min}} = 0.2349$)

Structure Solution and Refinement

Structure Solution	direct (SHELXS-97 (Sheldrick, 2008))
Refinement	Full-matrix least-squares
Function Minimized	$\Sigma w(F_o ^2 - F_c ^2)^2$
Least Squares Weighting scheme	$w = 1/[\sigma^2(F_o^2) + (qP)^2 + 0.000P]$ where $P = [F_o^2 + 2F_c^2]/3$
q-factor	0.05
Anomalous Dispersion	All non-hydrogen atoms
No. Observations ($I > 2.00\sigma(I)$)	5124
No. Variables	349
Reflection/Parameter Ratio	14.7
Residuals: R; wR_2 ; R_{all}	0.0302; 0.0763; 0.0401
Goodness of Fit Indicator	1.247
Max Shift/Error in Final Cycle	0.008
Maximum peak in Final Diff. Map	1.024 e-/Å ³
Minimum peak in Final Diff. Map	-0.369 e-/Å ³

Table 2B.1. Atomic coordinates and $U_{\text{iso}}/U_{\text{eq}}$ and occupancy

atom	x	y	z	U_{eq}^a	Occupancy
Au1	0.4383(1)	0.2595(1)	0.0878(1)	0.042(1)	1
Cl1	0.2511(1)	0.1679(1)	-0.3264(1)	0.096(1)	1
P1	0.4505(1)	0.3081(1)	-0.0354(1)	0.035(1)	1
O1	0.2769(3)	0.1065(2)	-0.1799(3)	0.071(2)	1
O2	0.4191(2)	0.2152(2)	0.2039(2)	0.053(1)	1
O3	0.5092(2)	0.2163(2)	0.2047(3)	0.058(1)	1
O4	0.3381(5)	0.0495(3)	0.5781(4)	0.128(4)	1
O5	0.4281(6)	0.0606(6)	0.5880(5)	0.171(5)	1
N1	0.3879(7)	0.0681(4)	0.5510(4)	0.113(4)	1
C1	0.3933(3)	0.2643(3)	-0.1176(3)	0.038(1)	1
C2	0.3850(3)	0.2970(3)	-0.1837(4)	0.048(1)	1
C3	0.3425(3)	0.2676(3)	-0.2473(4)	0.056(2)	1
C4	0.3061(3)	0.2054(3)	-0.2463(4)	0.053(2)	1
C5	0.3133(3)	0.1701(3)	-0.1830(4)	0.049(2)	1
C6	0.3578(3)	0.1998(3)	-0.1182(3)	0.039(1)	1
C7	0.2741(6)	0.0689(4)	-0.2499(8)	0.061(4)	0.587(15)
C7B	0.2219(12)	0.0789(12)	-0.1486(17)	0.103(8)	0.413(15)
C8	0.4448(3)	0.3774(3)	-0.0190(3)	0.039(1)	1
C9	0.4034(3)	0.3749(4)	0.0421(4)	0.054(2)	1
C10	0.3960(4)	0.4274(5)	0.0523(5)	0.074(2)	1
C11	0.4310(4)	0.4807(4)	0.0051(5)	0.072(2)	1
C12	0.4732(4)	0.4823(3)	-0.0518(5)	0.066(2)	1
C13	0.4799(3)	0.4303(3)	-0.0651(4)	0.056(2)	1
C14	0.5266(2)	0.3366(2)	-0.0843(4)	0.039(1)	1
C15	0.5773(3)	0.3657(4)	-0.0300(4)	0.054(2)	1
C16	0.6365(3)	0.3927(3)	-0.0610(5)	0.060(2)	1
C17	0.6460(3)	0.3893(3)	-0.1483(5)	0.058(2)	1
C18	0.5957(3)	0.3604(3)	-0.2029(4)	0.056(2)	1

C19	0.5356(3)	0.3337(3)	-0.1715(4)	0.045(1)	1
C20	0.4587(3)	0.2028(3)	0.2359(3)	0.043(1)	1
C21	0.4391(3)	0.1681(3)	0.3200(3)	0.050(2)	1
C22	0.4838(4)	0.1665(3)	0.3712(4)	0.066(2)	1
C23	0.4666(6)	0.1343(4)	0.4474(5)	0.082(3)	1
C24	0.4062(6)	0.1028(4)	0.4702(4)	0.076(3)	1
C25	0.3597(5)	0.1028(3)	0.4192(5)	0.076(2)	1
C26	0.3778(4)	0.1364(3)	0.3440(4)	0.059(2)	1
C101	0.1652(10)	0.0307(10)	0.5073(17)	0.15	0.70(3)
C102	0.201(2)	0.081(2)	0.390(3)	0.15	0.37(3)
C103	0.1659(16)	0.0239(17)	0.424(3)	0.15	0.47(3)
C104	0.156(3)	0.0781(13)	0.4167	0.15	0.51(4)
C111	-0.0711(18)	-0.079(2)	0.372(2)	0.15	0.42(3)
C112	-0.0544(17)	-0.027(2)	0.380(2)	0.15	0.41(3)
C113	-0.1129(19)	-0.0734(19)	0.465(3)	0.15	0.41(3)
H2A	0.4097	0.3409	-0.1846	0.057	1
H3A	0.3386	0.2911	-0.2922	0.068	1
H7A	0.2737	0.0317	-0.2283	0.092	0.587(15)
H7B	0.3104	0.0922	-0.2866	0.092	0.587(15)
H7C	0.2363	0.0567	-0.283	0.092	0.587(15)
H7BA	0.2096	0.1096	-0.1345	0.154	0.413(15)
H7BB	0.2211	0.0565	-0.0967	0.154	0.413(15)
H7BC	0.193	0.0496	-0.1908	0.154	0.413(15)
H9A	0.3805	0.3389	0.0763	0.065	1
H10A	0.3665	0.4259	0.0922	0.089	1
H11A	0.4257	0.5156	0.0122	0.087	1
H12A	0.4985	0.5192	-0.0829	0.08	1
H13A	0.5088	0.4319	-0.1061	0.067	1
H15A	0.5708	0.3669	0.0297	0.065	1
H16A	0.6709	0.4137	-0.0234	0.072	1
H17A	0.6869	0.4067	-0.1703	0.07	1
H18A	0.6023	0.3588	-0.2625	0.067	1

H19A	0.5012	0.3138	-0.2091	0.054	1
H22A	0.526	0.1875	0.3539	0.079	1
H23A	0.4972	0.1342	0.4837	0.098	1
H25A	0.3174	0.0804	0.4358	0.091	1
H26A	0.3475	0.1377	0.3084	0.071	1

^aU_{eq} is defined as one third of the orthogonalized U_{ij} tensor

Table 2B.2. Anisotropic Displacement Parameters

atom	U11	U22	U33	U12	U13	U23
Au1	0.052(1)	0.060(1)	0.020(1)	0.008(1)	0.003(1)	0.033(1)
Cl1	0.105(2)	0.071(1)	0.070(1)	0.014(1)	-0.053(1)	0.013(1)
P1	0.044(1)	0.046(1)	0.020(1)	0.002(1)	0.000(1)	0.025(1)
O1	0.080(4)	0.042(3)	0.056(3)	0.018(2)	-0.022(3)	0.005(2)
O2	0.075(3)	0.070(3)	0.022(2)	0.014(2)	0.009(2)	0.042(3)
O3	0.068(3)	0.060(3)	0.041(2)	0.008(2)	-0.005(2)	0.029(2)
O4	0.228(10)	0.064(4)	0.039(3)	0.011(3)	0.028(5)	0.032(5)
O5	0.308(15)	0.216(11)	0.063(4)	0.073(6)	0.033(6)	0.186(11)
N1	0.251(13)	0.078(5)	0.025(3)	0.010(3)	0.010(6)	0.093(7)
C1	0.043(3)	0.045(3)	0.028(2)	0.011(2)	0.001(2)	0.025(3)
C2	0.071(4)	0.039(3)	0.038(3)	0.003(2)	-0.011(3)	0.031(3)
C3	0.081(4)	0.047(3)	0.034(3)	0.007(3)	-0.016(3)	0.027(3)
C4	0.058(4)	0.056(3)	0.037(3)	0.007(3)	-0.017(3)	0.022(3)
C5	0.049(3)	0.047(3)	0.040(3)	0.014(3)	-0.009(2)	0.016(3)
C6	0.041(3)	0.048(3)	0.027(2)	0.011(2)	0.001(2)	0.021(3)
C7	0.073(8)	0.027(5)	0.066(7)	-0.001(5)	-0.028(6)	0.012(5)
C8	0.048(3)	0.048(3)	0.029(2)	-0.009(2)	-0.007(2)	0.030(3)
C9	0.046(4)	0.073(4)	0.041(3)	-0.006(3)	-0.006(3)	0.028(3)
C10	0.079(5)	0.099(7)	0.071(5)	-0.043(5)	-0.019(4)	0.064(5)
C11	0.081(5)	0.073(5)	0.083(5)	-0.045(5)	-0.042(5)	0.053(5)
C12	0.085(5)	0.052(4)	0.069(5)	-0.016(3)	-0.025(4)	0.038(4)
C13	0.072(4)	0.066(4)	0.042(3)	-0.005(3)	0.000(3)	0.044(4)
C14	0.046(3)	0.046(3)	0.026(2)	0.005(2)	0.005(2)	0.025(2)
C15	0.048(4)	0.084(5)	0.028(3)	0.014(3)	0.004(2)	0.031(3)
C16	0.041(3)	0.075(5)	0.054(4)	0.004(3)	-0.008(3)	0.023(3)
C17	0.055(4)	0.066(4)	0.060(4)	0.011(3)	0.023(3)	0.035(3)
C18	0.073(4)	0.047(3)	0.041(3)	-0.005(3)	0.020(3)	0.025(3)
C19	0.057(4)	0.041(3)	0.030(3)	-0.002(2)	0.004(2)	0.019(3)
C20	0.053(3)	0.052(3)	0.021(2)	0.001(2)	-0.001(2)	0.025(3)

C21	0.092(5)	0.039(3)	0.022(2)	-0.003(2)	-0.003(3)	0.036(3)
C22	0.114(6)	0.048(4)	0.037(3)	-0.001(3)	-0.019(4)	0.041(4)
C23	0.153(9)	0.046(4)	0.038(4)	-0.005(3)	-0.039(5)	0.044(5)
C24	0.160(9)	0.050(4)	0.019(3)	0.005(3)	-0.005(4)	0.053(6)
C25	0.131(7)	0.050(4)	0.054(4)	0.022(3)	0.043(5)	0.051(4)
C26	0.095(5)	0.060(4)	0.029(3)	0.013(3)	0.012(3)	0.044(4)

The general temperature factor expression:

$$\exp(-2\Pi^2(a*2U_{11}h^2 + b*2U_{22}k^2 + c*2U_{33}l^2 + 2a*b*U_{12}hk + 2a*c*U_{13}hl + 2b*c*U_{23}kl))$$

Table 2B.3. Bond Lengths (Å)

atom	atom	distance	atom	atom	distance
Au1	O2	2.054(4)	Au1	P1	2.2139(13)
C11	C4	1.742(6)	P1	C8	1.822(6)
P1	C1	1.822(6)	P1	C14	1.827(5)
O1	C7B	1.28(3)	O1	C5	1.377(7)
O1	C7	1.420(13)	O2	C20	1.273(7)
O3	C20	1.230(7)	O4	N1	1.167(15)
O5	N1	1.248(15)	N1	C24	1.468(9)
C1	C2	1.392(7)	C1	C6	1.396(8)
C2	C3	1.368(8)	C2	H2A	0.95
C3	C4	1.351(9)	C3	H3A	0.95
C4	C5	1.394(8)	C5	C6	1.408(8)
C6	C6#1	1.507(10)	C7	H7A	0.98
C7	H7B	0.98	C7	H7C	0.98
C7B	H7BA	0.98	C7B	H7BB	0.98
C7B	H7BC	0.98	C8	C13	1.367(9)
C8	C9	1.384(8)	C9	C10	1.418(11)
C9	H9A	0.95	C10	C11	1.383(13)
C10	H10A	0.95	C11	C12	1.362(12)
C11	H11A	0.95	C12	C13	1.402(10)
C12	H12A	0.95	C13	H13A	0.95
C14	C15	1.388(8)	C14	C19	1.390(8)
C15	C16	1.369(9)	C15	H15A	0.95
C16	C17	1.395(10)	C16	H16A	0.95
C17	C18	1.384(11)	C17	H17A	0.95
C18	C19	1.389(9)	C18	H18A	0.95
C19	H19A	0.95	C20	C21	1.514(7)
C21	C26	1.375(10)	C21	C22	1.389(10)
C22	C23	1.379(10)	C22	H22A	0.95
C23	C24	1.353(14)	C23	H23A	0.95
C24	C25	1.406(13)	C25	C26	1.382(9)

C25	H25A	0.95	C26	H26A	0.95
C101	C103	1.32(4)	C101	C101#2	1.34(4)
C101	C103#2	1.60(4)	C101	C104	1.93(3)
C102	C104	1.16(5)	C102	C102#3	1.27(8)
C102	C103	1.35(5)	C103	C104	1.49(4)
C103	C101#2	1.60(4)	C104	C102#3	1.16(5)
C104	C103#3	1.49(4)	C104	C101#3	1.93(3)
C111	C112	1.17(6)	C111	C111#4	1.26(7)
C111	C112#4	1.64(5)	C111	C112#3	1.71(6)
C111	C113#3	1.76(6)	C111	C113#5	1.82(6)
C111	C113	1.84(6)	C112	C112#3	1.15(8)
C112	C113#3	1.34(5)	C112	C111#4	1.64(5)
C112	C111#3	1.71(6)	C112	C112#4	1.88(8)
C112	C113	1.88(5)	C113	C112#3	1.34(5)
C113	C113#3	1.73(8)	C113	C111#3	1.76(6)
C113	C111#6	1.82(6)			

Table 2B.4. Bond Angles (°)

atom	atom	atom	angle	atom	atom	atom	angle
O2	Au1	P1	174.23(13)	C8	P1	C1	104.9(2)
C8	P1	C14	104.5(3)	C1	P1	C14	106.8(3)
C8	P1	Au1	110.01(18)	C1	P1	Au1	115.61(18)
C14	P1	Au1	114.10(18)	C7B	O1	C5	122.9(13)
C7B	O1	C7	104.6(13)	C5	O1	C7	121.3(6)
C20	O2	Au1	118.6(4)	O4	N1	O5	123.1(8)
O4	N1	C24	120.1(12)	O5	N1	C24	116.8(12)
C2	C1	C6	118.4(5)	C2	C1	P1	118.2(4)
C6	C1	P1	123.4(4)	C3	C2	C1	121.9(6)
C3	C2	H2A	119.1	C1	C2	H2A	119.1
C4	C3	C2	120.1(5)	C4	C3	H3A	119.9
C2	C3	H3A	119.9	C3	C4	C5	120.6(5)
C3	C4	Cl1	120.3(5)	C5	C4	Cl1	119.1(5)
O1	C5	C4	122.1(5)	O1	C5	C6	118.2(5)
C4	C5	C6	119.7(5)	C1	C6	C5	119.3(5)
C1	C6	C6#1	124.9(5)	C5	C6	C6#1	115.4(5)
O1	C7	H7A	109.5	O1	C7	H7B	109.5
O1	C7	H7C	109.5	O1	C7B	H7BA	109.5
O1	C7B	H7BB	109.5	H7BA	C7B	H7BB	109.5
O1	C7B	H7BC	109.5	H7BA	C7B	H7BC	109.5
H7BB	C7B	H7BC	109.5	C13	C8	C9	120.7(6)
C13	C8	P1	121.6(4)	C9	C8	P1	117.7(5)
C8	C9	C10	118.2(7)	C8	C9	H9A	120.9
C10	C9	H9A	120.9	C11	C10	C9	121.0(7)
C11	C10	H10A	119.5	C9	C10	H10A	119.5
C12	C11	C10	118.9(7)	C12	C11	H11A	120.5
C10	C11	H11A	120.5	C11	C12	C13	121.1(8)
C11	C12	H12A	119.4	C13	C12	H12A	119.4

C8	C13	C12	119.8(7)	C8	C13	H13A	120.1
C12	C13	H13A	120.1	C15	C14	C19	120.0(5)
C15	C14	P1	116.3(4)	C19	C14	P1	123.6(4)
C16	C15	C14	121.1(6)	C16	C15	H15A	119.5
C14	C15	H15A	119.5	C15	C16	C17	119.3(6)
C15	C16	H16A	120.3	C17	C16	H16A	120.3
C18	C17	C16	119.9(6)	C18	C17	H17A	120.1
C16	C17	H17A	120.1	C17	C18	C19	120.7(6)
C17	C18	H18A	119.6	C19	C18	H18A	119.6
C18	C19	C14	119.0(6)	C18	C19	H19A	120.5
C14	C19	H19A	120.5	O3	C20	O2	126.1(5)
O3	C20	C21	119.6(6)	O2	C20	C21	114.3(5)
C26	C21	C22	120.3(6)	C26	C21	C20	120.8(6)
C22	C21	C20	118.8(7)	C23	C22	C21	119.6(9)
C23	C22	H22A	120.2	C21	C22	H22A	120.2
C24	C23	C22	119.8(8)	C24	C23	H23A	120.1
C22	C23	H23A	120.1	C23	C24	C25	121.9(6)
C23	C24	N1	119.7(10)	C25	C24	N1	118.4(10)
C26	C25	C24	117.7(8)	C26	C25	H25A	121.2
C24	C25	H25A	121.2	C21	C26	C25	120.7(7)
C21	C26	H26A	119.6	C25	C26	H26A	119.6

Table 2A.5. Torsion Angles(^o).

atom	atom	atom	atom	angle	atom	atom	atom	atom	angle
O2	Au1	P1	C8	48.6(14)	O2	Au1	P1	C1	-70.0(14)
O2	Au1	P1	C14	165.6(14)	P1	Au1	O2	C20	-171.8(11)
C8	P1	C1	C2	37.5(5)	C14	P1	C1	C2	-73.0(5)
Au1	P1	C1	C2	158.8(4)	C8	P1	C1	C6	-143.5(5)
C14	P1	C1	C6	106.0(5)	Au1	P1	C1	C6	-22.1(5)
C6	C1	C2	C3	1.6(10)	P1	C1	C2	C3	-179.3(6)
C1	C2	C3	C4	1.3(11)	C2	C3	C4	C5	-3.0(11)
C2	C3	C4	C11	179.1(6)	C7B	O1	C5	C4	-80.3(16)
C7	O1	C5	C4	57.8(10)	C7B	O1	C5	C6	97.9(16)
C7	O1	C5	C6	-124.0(8)	C3	C4	C5	O1	179.8(7)
C11	C4	C5	O1	-2.2(10)	C3	C4	C5	C6	1.7(11)
C11	C4	C5	C6	179.6(5)	C2	C1	C6	C5	-2.9(9)
P1	C1	C6	C5	178.1(5)	C2	C1	C6	C6#1	-175.4(6)
P1	C1	C6	C6#1	5.6(8)	O1	C5	C6	C1	-176.9(6)
C4	C5	C6	C1	1.3(9)	O1	C5	C6	C6#1	-3.7(9)
C4	C5	C6	C6#1	174.5(6)	C1	P1	C8	C13	-90.2(5)
C14	P1	C8	C13	21.9(5)	Au1	P1	C8	C13	144.8(5)
C1	P1	C8	C9	89.7(5)	C14	P1	C8	C9	-158.1(5)
Au1	P1	C8	C9	-35.3(5)	C13	C8	C9	C10	3.3(9)
P1	C8	C9	C10	-176.6(5)	C8	C9	C10	C11	-2.7(10)
C9	C10	C11	C12	-0.1(11)	C10	C11	C12	C13	2.3(11)
C9	C8	C13	C12	-1.2(10)	P1	C8	C13	C12	178.7(5)
C11	C12	C13	C8	-1.6(11)	C8	P1	C14	C15	75.9(5)
C1	P1	C14	C15	-173.2(5)	Au1	P1	C14	C15	-44.2(5)
C8	P1	C14	C19	-100.0(5)	C1	P1	C14	C19	10.8(6)
Au1	P1	C14	C19	139.8(4)	C19	C14	C15	C16	1.0(10)
P1	C14	C15	C16	-175.1(6)	C14	C15	C16	C17	-1.9(11)
C15	C16	C17	C18	2.0(11)	C16	C17	C18	C19	-1.2(11)
C17	C18	C19	C14	0.2(10)	C15	C14	C19	C18	-0.1(9)
P1	C14	C19	C18	175.7(5)	Au1	O2	C20	O3	1.9(8)

Au1	O2	C20	C21	-177.9(4)	O3	C20	C21	C26	-160.4(6)
O2	C20	C21	C26	19.4(8)	O3	C20	C21	C22	16.9(8)
O2	C20	C21	C22	-163.3(6)	C26	C21	C22	C23	-1.7(10)
C20	C21	C22	C23	-179.0(6)	C21	C22	C23	C24	2.2(11)
C22	C23	C24	C25	-1.3(12)	C22	C23	C24	N1	179.4(7)
O4	N1	C24	C23	167.3(9)	O5	N1	C24	C23	-11.8(12)
O4	N1	C24	C25	-12.0(12)	O5	N1	C24	C25	168.9(9)
C23	C24	C25	C26	-0.2(11)	N1	C24	C25	C26	179.1(6)
C22	C21	C26	C25	0.2(10)	C20	C21	C26	C25	177.4(6)
C24	C25	C26	C21	0.7(10)					

The ADC (atom designator code) specifies the position of an atom in a crystal. The 5-digit number shown in the table is a composite of three one-digit numbers and one two-digit number: TA (first digit) + TB (second digit) + TC (third digit) + SN (last two digits). TA, TB and TC are the crystal lattice translation digits along cell edges a, b and c. A translation digit of 5 indicates the origin unit cell. If TA = 4, this indicates a translation of one unit cell length along the a-axis in the negative direction. Each translation digit can range in value from 1 to 9 and thus +4 lattice translations from the origin (TA=5, TB=5, TC=5) can be represented.

The SN, or symmetry operator number, refers to the number of the symmetry operator used to generate the coordinates of the target atom. A list of symmetry operators relevant to this structure are given below.

For a given intermolecular contact, the first atom (origin atom) is located in the origin unit cell and its position can be generated using the identity operator (SN=1). Thus, the ADC for an origin atom is always 55501. The position of the second atom (target atom) can be generated using the ADC and the coordinates of the atom in the parameter table. For example, an ADC of 47502 refers to the target atom moved through symmetry operator two, then translated -1 cell translations along the a axis, +2 cell translations along the b axis, and 0 cell translations along the c axis.

An ADC of 1 indicates an intermolecular contact between two fragments (eg. cation and anion) that reside in the same asymmetric unit.

Table 2B.6. Symmetry Operators

x, y, z	$-y, x-y, z+2/3$
$-x+y, -x, z+1/3$	$-x, -y, z+1/2$
$y, -x+y, z+1/6$	$x-y, x, z+5/6$
$y, x, -z+2/3$	$x-y, -y, -z$
$-x, -x+y, -z+1/3$	$-y, -x, -z+1/6$
$-x+y, y, -z+1/2$	$x, x-y, -z+5/6$

References

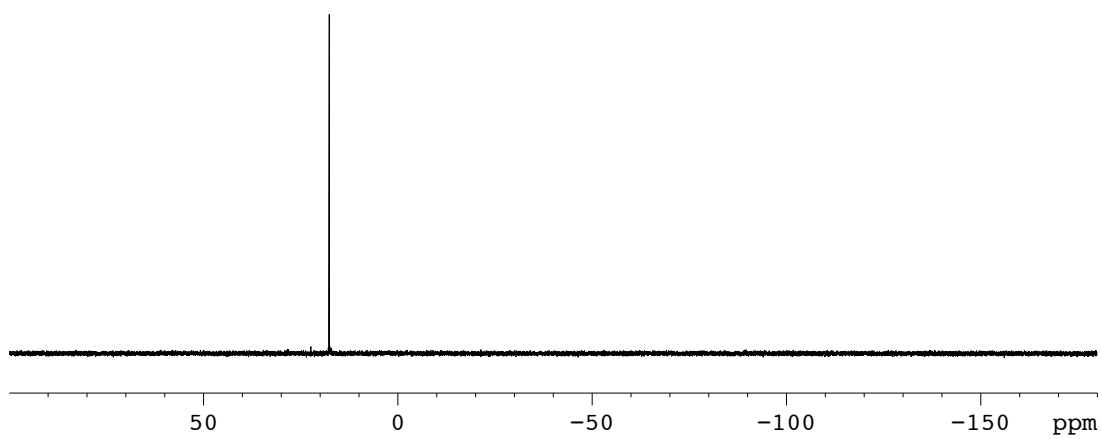
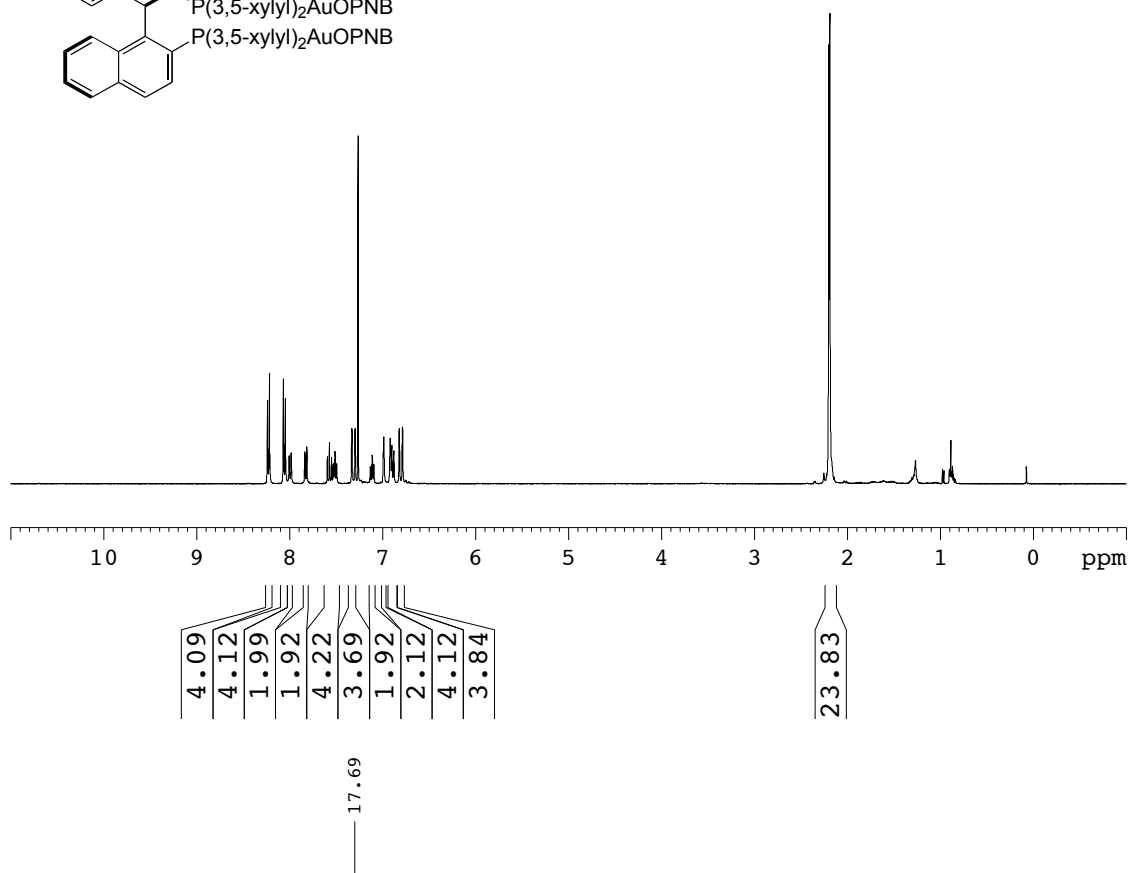
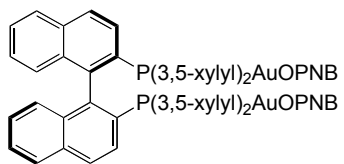
- ¹ SAINT: SAX Area-Detector Integration Program, V7.06; Siemens Industrial Automation, Inc.: Madison, WI, (2005).
- ² The Advanced Light Source is supported by Director, Office of Science, Office of Basic Energy Sciences, of the U.S. Department of Energy under Contract No. DE-AC02-05CH11231.
- ³ XPREP:(v 6.12) Part of the SHELXTL Crystal Structure Determination Package, Bruker AXS Inc.: Madison, WI, (1995).
- ⁴ SADABS: (v2008-1) Siemens Area Detector ABSorption correction program, George Sheldrick, (2008).
- ⁵ XS: Program for the Solution of X-ray Crystal Structures, Part of the SHELXTL Crystal Structure Determination Package, Bruker Analytical X-ray Systems Inc.: Madison, WI, (1995-99).
- ⁶ XL: Program for the Refinement of X-ray Crystal Structures, Part of the SHELXTL Crystal Structure Determination Package, Bruker Analytical X-ray Systems Inc.: Madison, WI, (1995-99).
- ⁷ Least-Squares:
Function minimized: $\sum w (|F_o|^2 - |F_c|^2)^2$
- ⁸ Standard deviation of an observation of unit weight:
 $[\sum w (|F_o|^2 - |F_c|^2)^2 / (N_o - N_v)]^{1/2}$
where: N_o = number of observations
 N_v = number of variables
- ⁹ Cromer, D. T. & Waber, J. T.; "International Tables for X-ray Crystallography", Vol. IV, The Kynoch Press, Birmingham, England, Table 2.2 A (1974).
- ¹⁰ Ibers, J. A. & Hamilton, W. C.; *Acta Crystallogr.*, 17, 781 (1964).
- ¹¹ Creagh, D. C. & McAuley, W.J. ; "International Tables for Crystallography", Vol C, (A.J.C. Wilson, ed.), Kluwer Academic Publishers, Boston, Table 4.2.6.8, pages 219-222 (1992).
- ¹² Creagh, D. C. & Hubbell, J.H.; "International Tables for Crystallography", Vol C, (A.J.C. Wilson, ed.), Kluwer Academic Publishers, Boston, Table 4.2.4.3, pages 200-206 (1992).
- ¹³ XP: Molecular Graphics program. Part of the SHELXTL Structure Determination Package. Bruker Analytical X-ray Systems Inc.: Madison, WI, (1995-99).

Appendix 2C

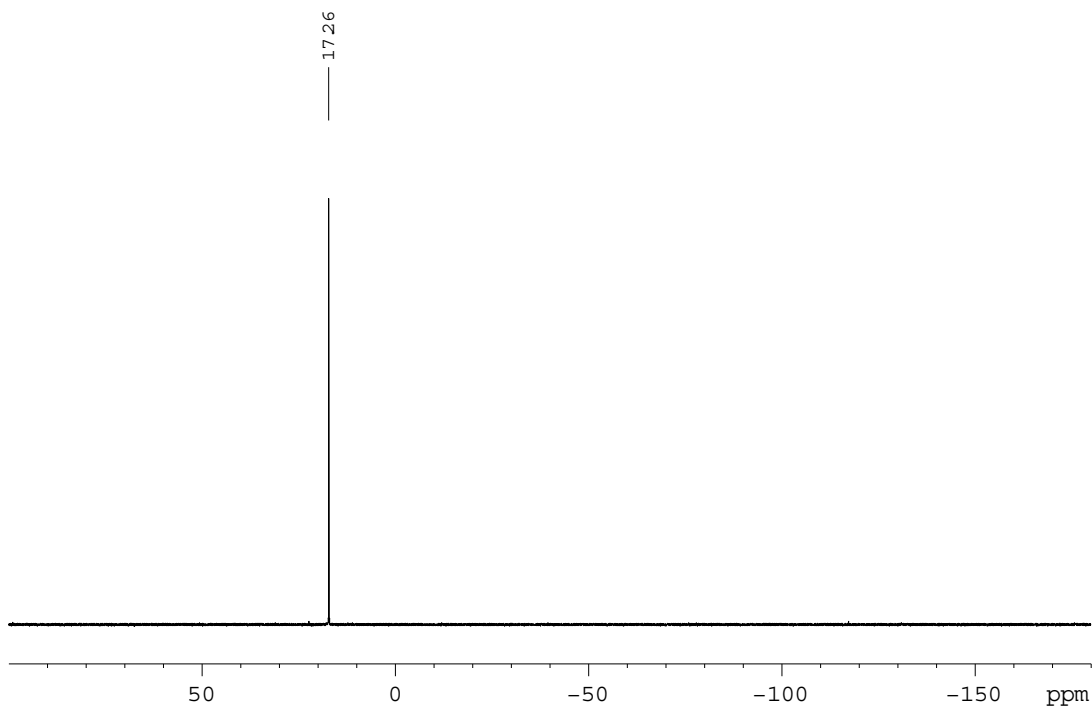
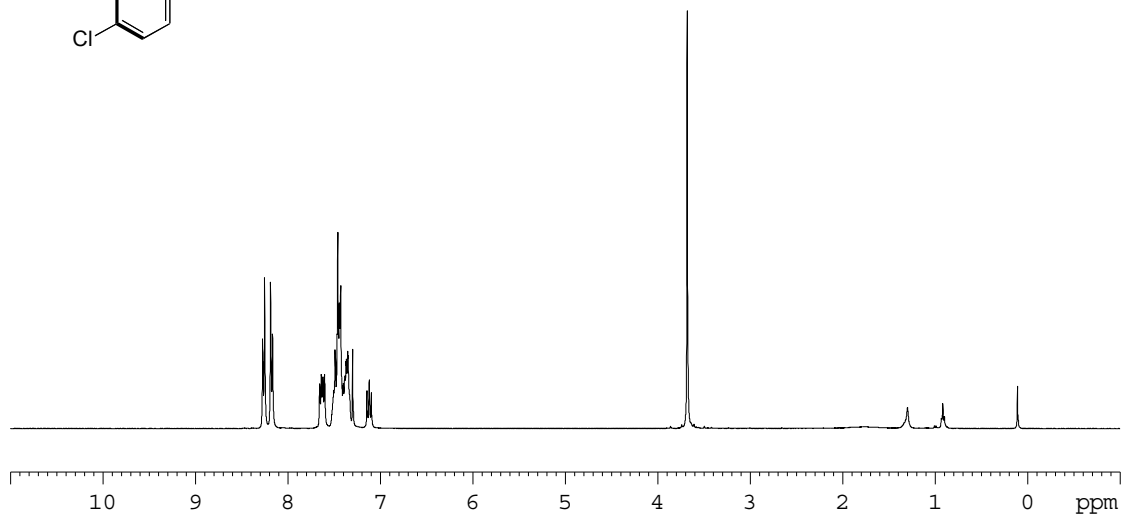
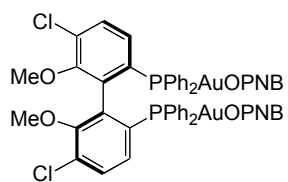
Copies of ^1H and ^{31}P NMR characterization data are included for compounds **2.42-2.46**.
Copies of ^1H and ^{13}C NMR characterization data are included for compounds **2.40, 2.41, 2.59-2.64, 2.67, 2.68, 2.71, 2.72**.

Copies of HPLC chromatographs are included for compounds **2.41, 2.41, 2.62, 2.64, 2.71, 2.72**.

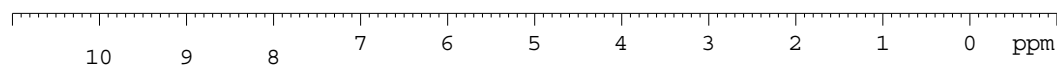
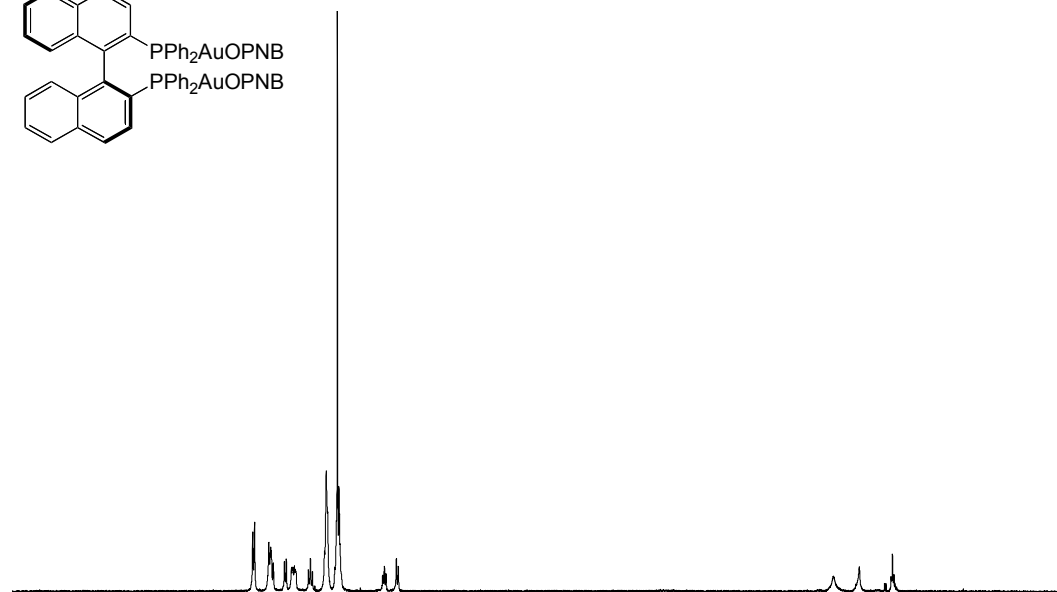
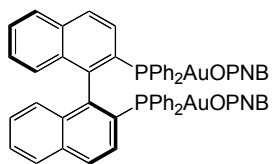
2.42 (*R*)-3,5-xylyl-BINAP(AuOPNB)₂



2.43 (*R*)-ClMeOBiPHEP(AuOPNB)₂

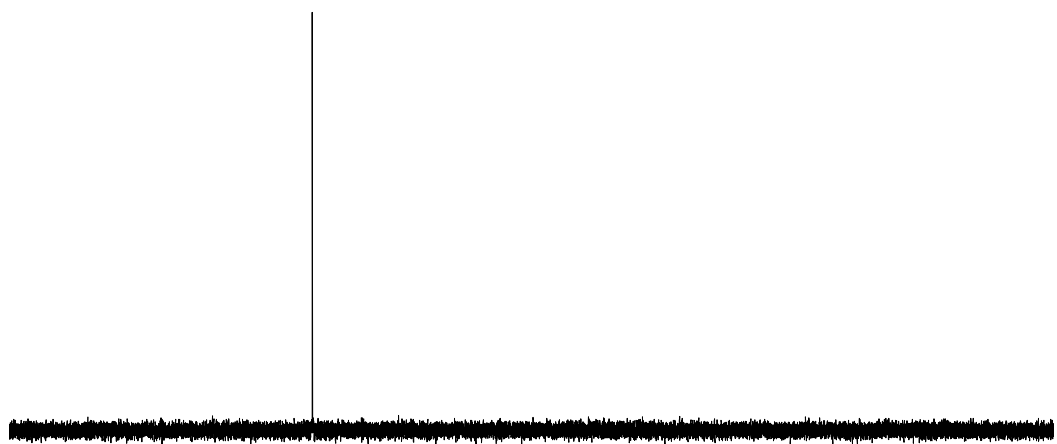


2.44 (*S*)-BINAP(AuOPNB)₂



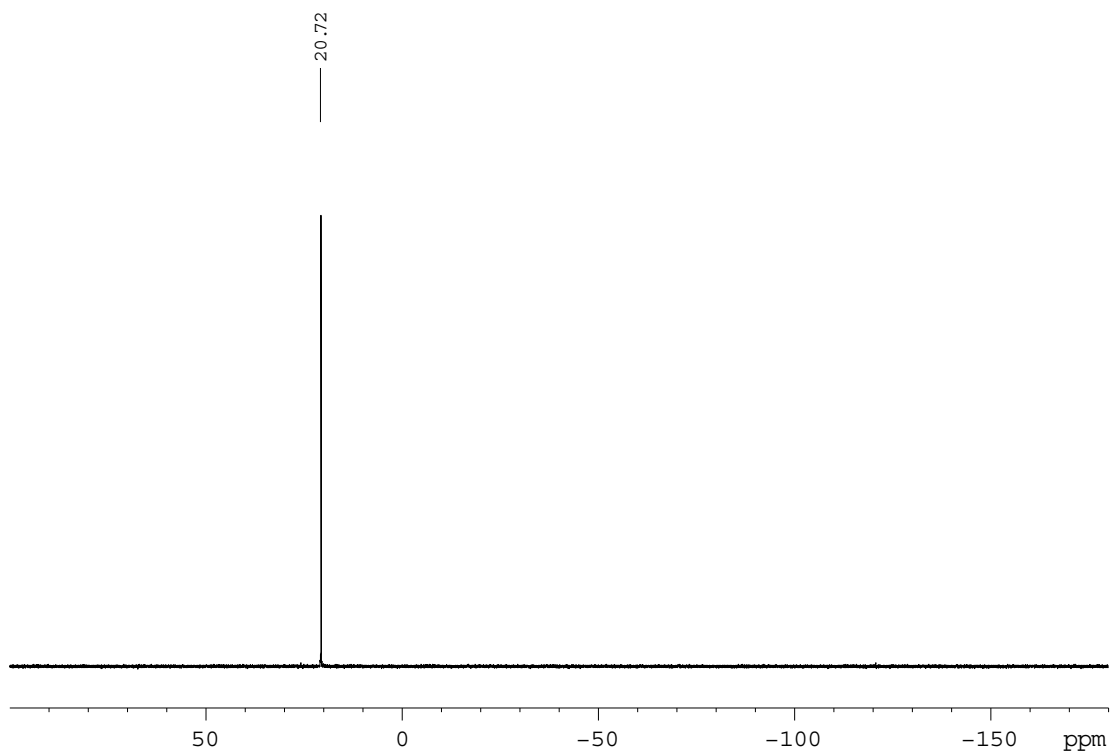
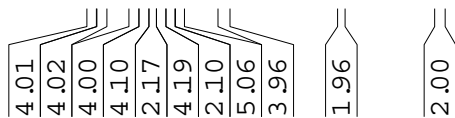
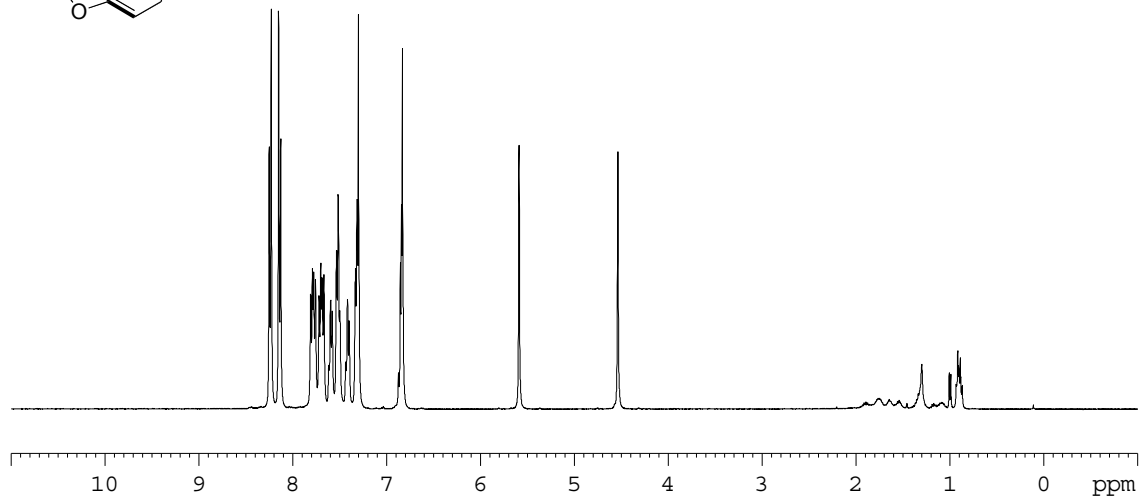
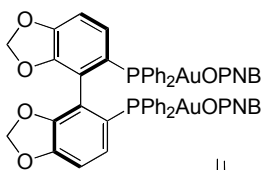
2.04
2.82
1.01
1.88
1.10
4.53
7.35
0.97
0.97

18.87

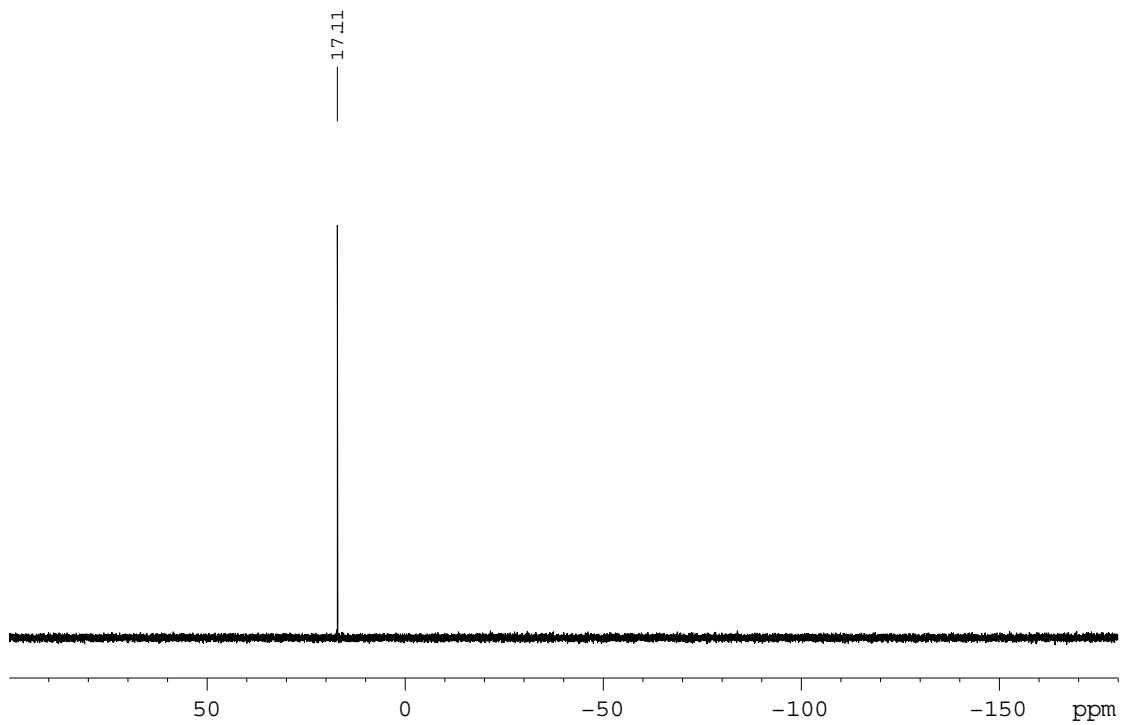
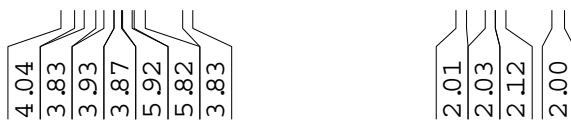
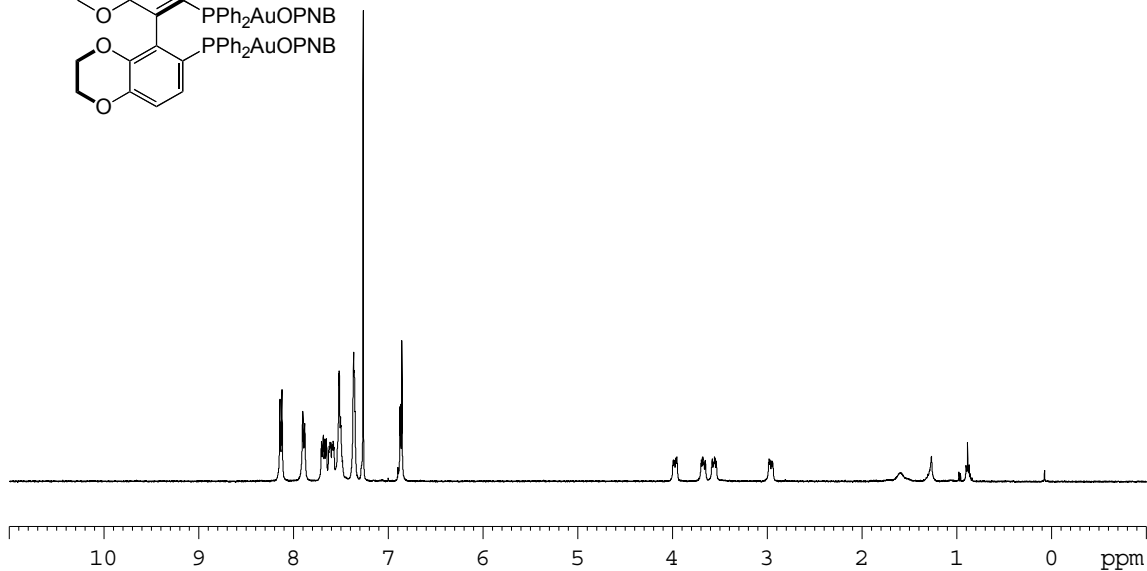
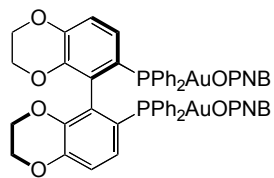


50 0 -50 -100 -150 ppm

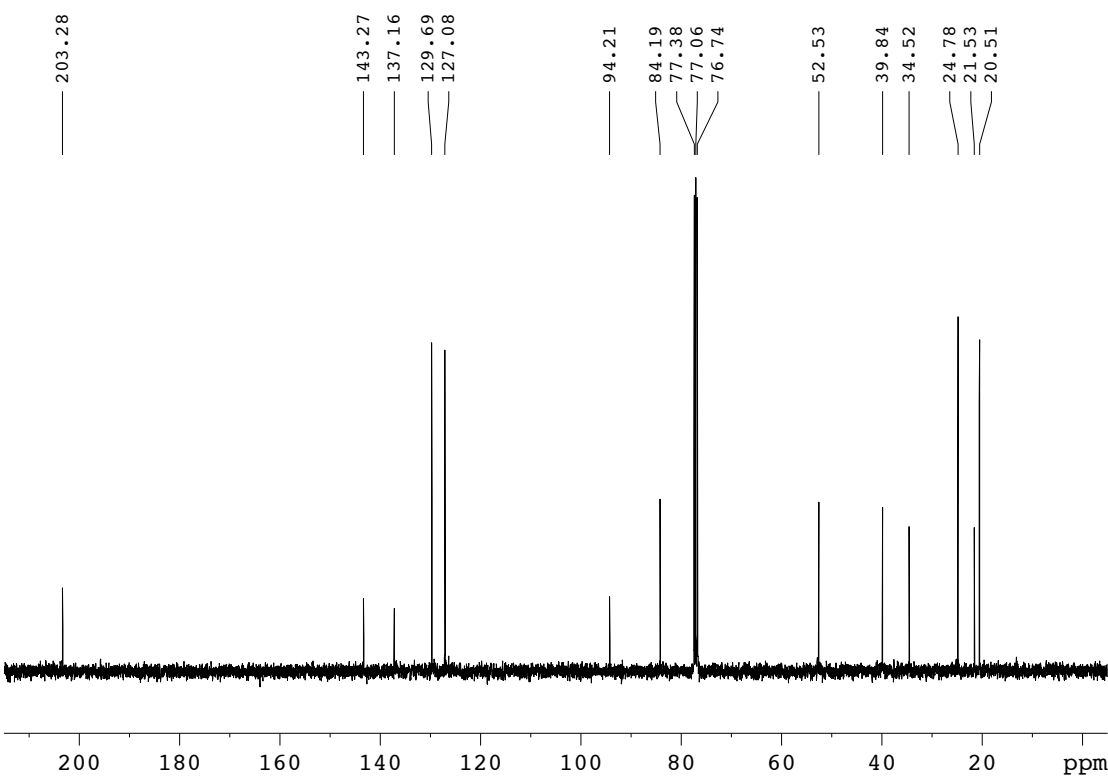
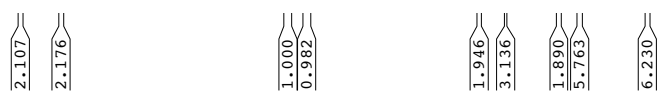
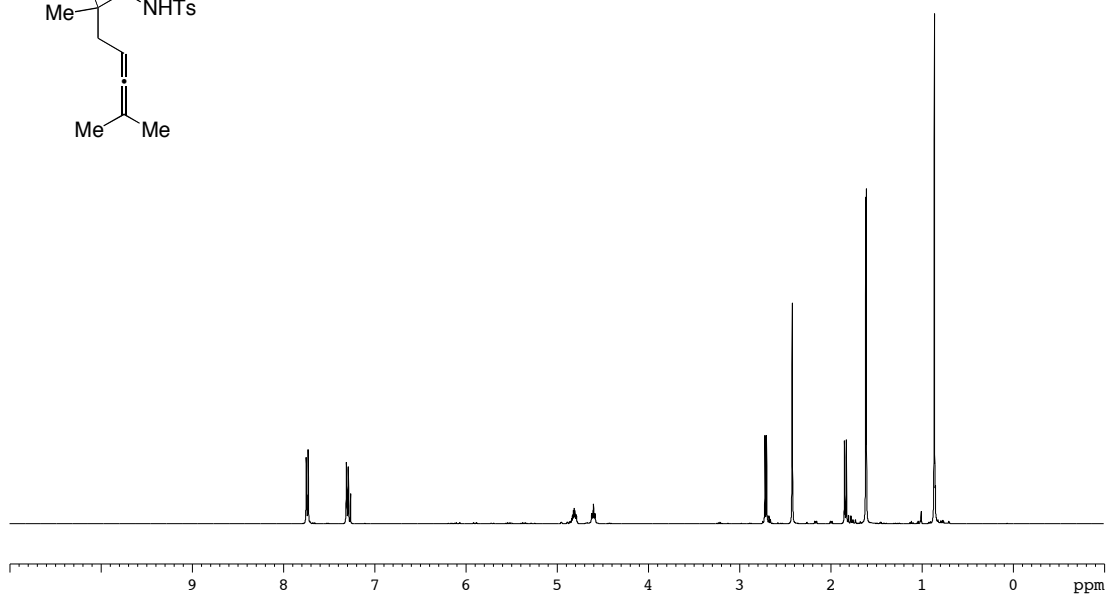
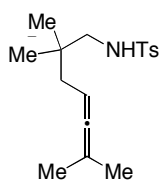
2.45 (*R*)-Segpos(AuOPNB)₂



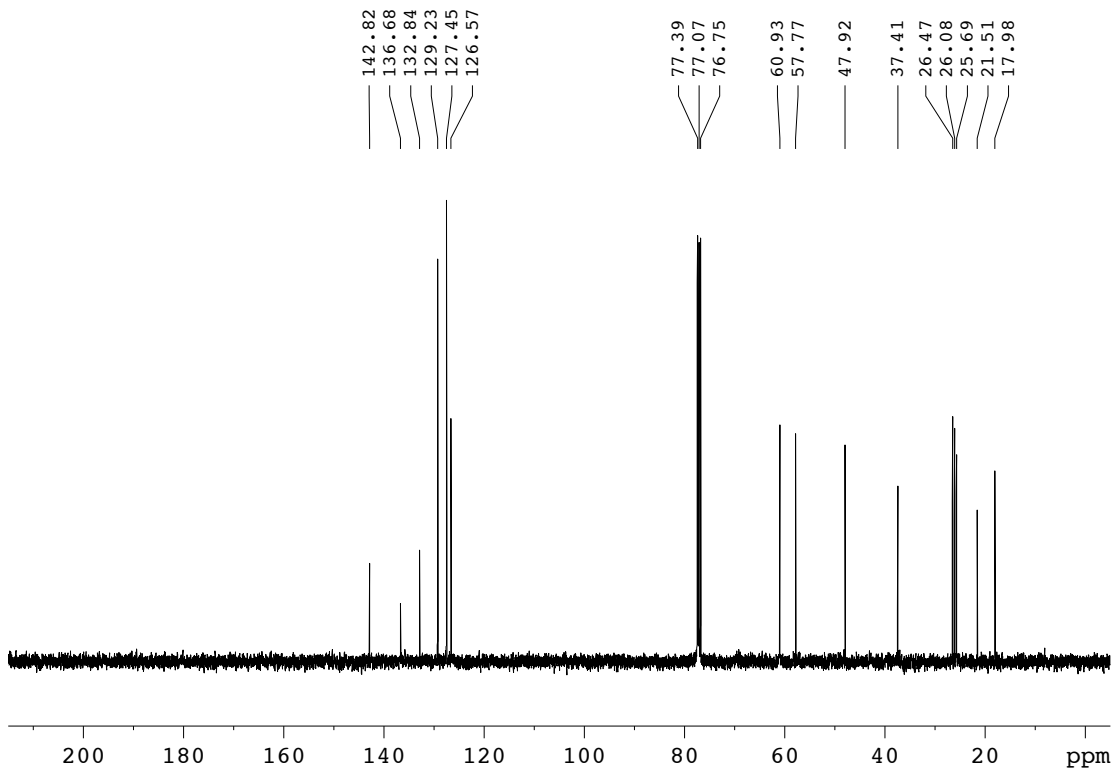
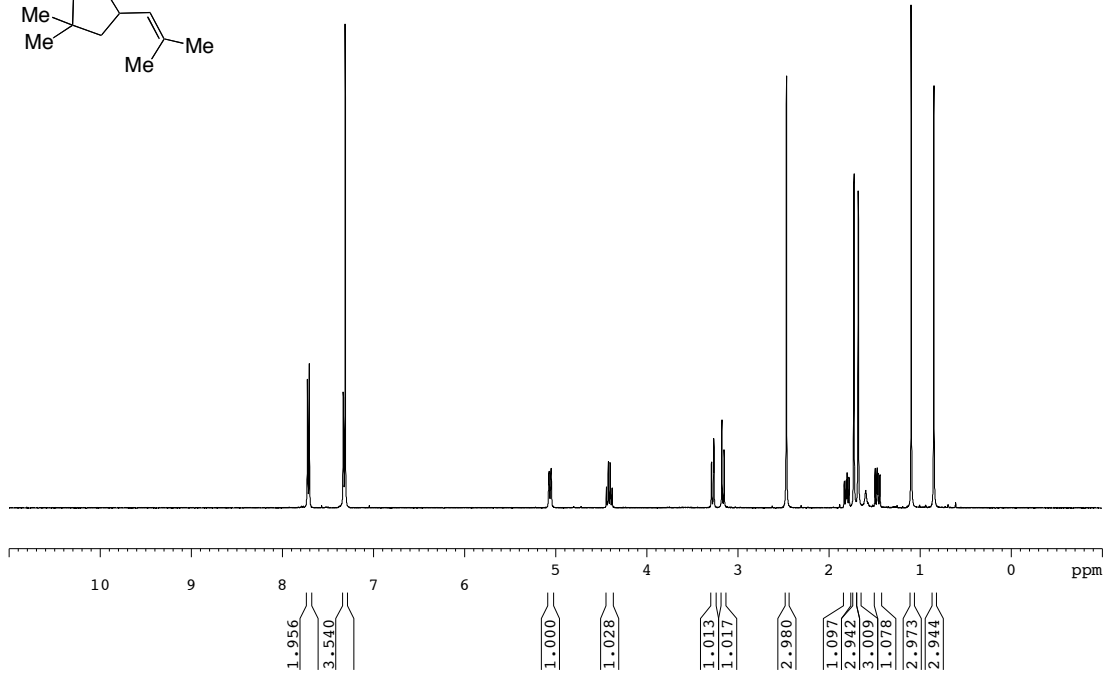
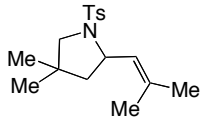
2.46 (*R*)-Synphos(AuOPNB)₂



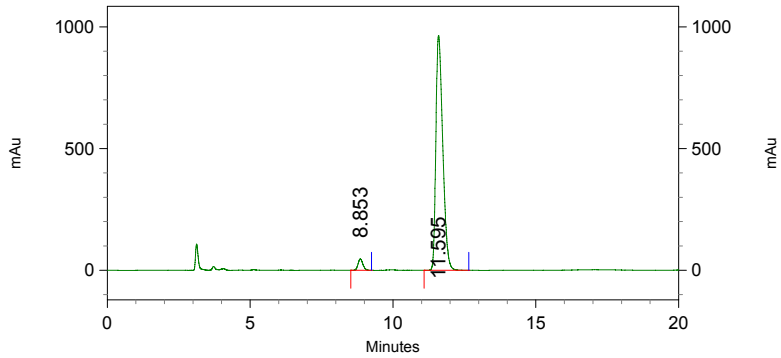
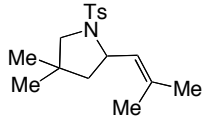
2.40



2.41

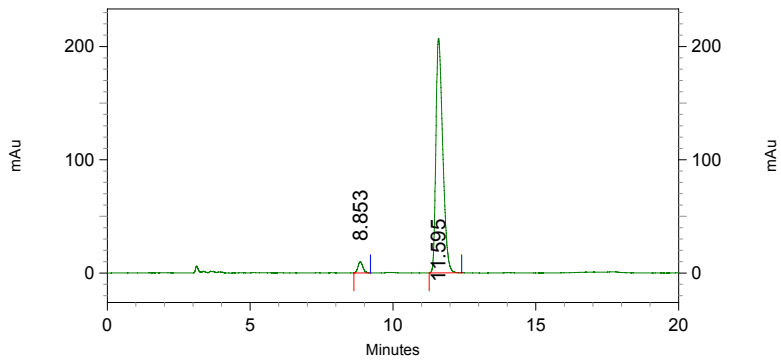


2.41



1: 230 nm, 4 nm Results

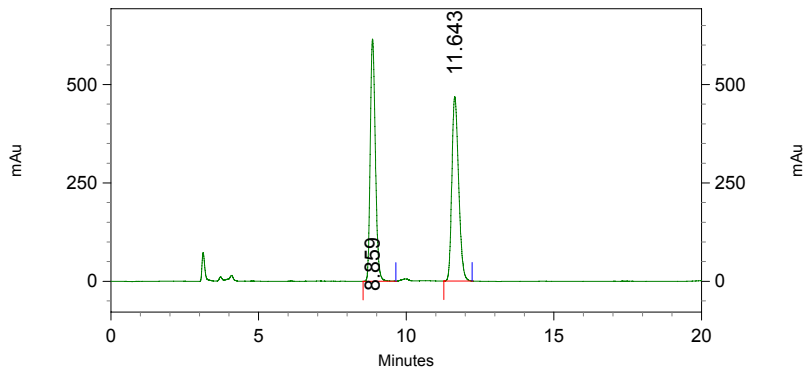
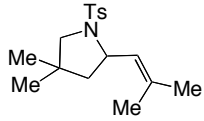
Retention Time	Area	Area Percent
8.853	546372	3.266
11.595	16183436	96.734



2: 254 nm, 4 nm Results

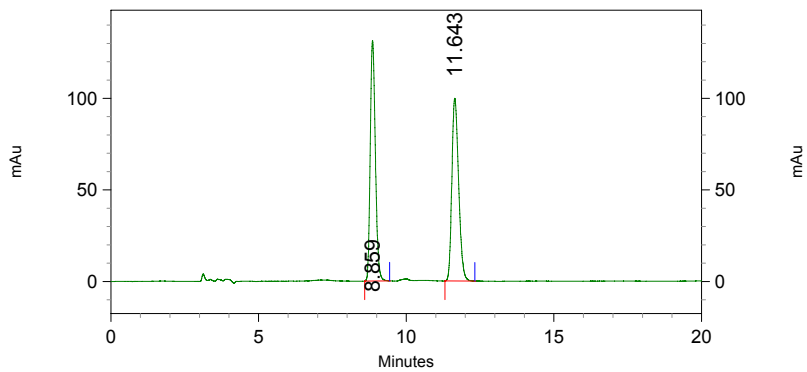
Retention Time	Area	Area Percent
8.853	114636	3.210
11.595	3456092	96.790

2.41



1: 230 nm, 4 nm Results

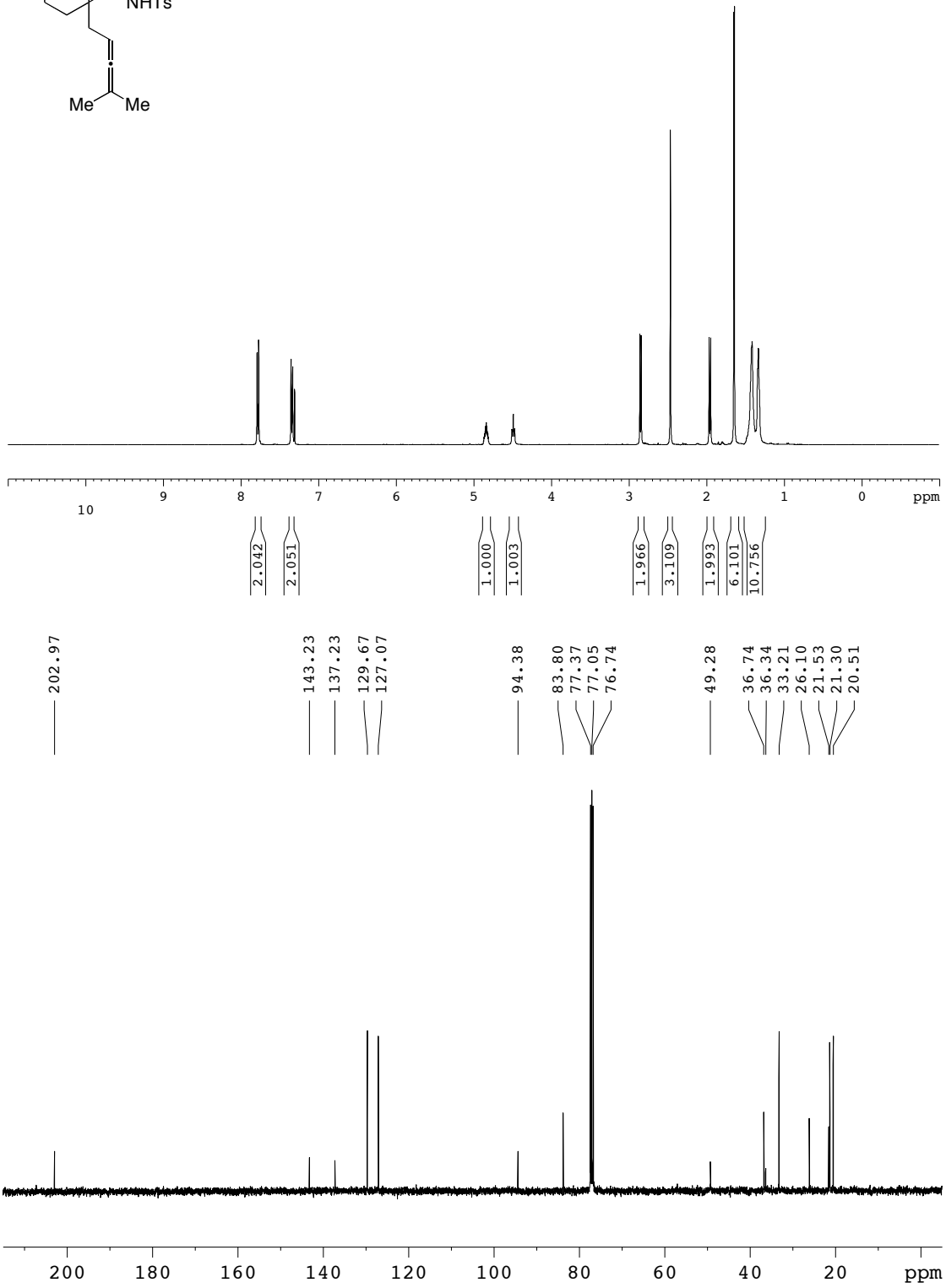
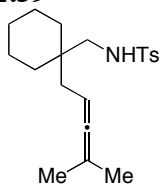
Retention Time	Area	Area Percent
8.859	7399804	49.816
11.643	7454412	50.184



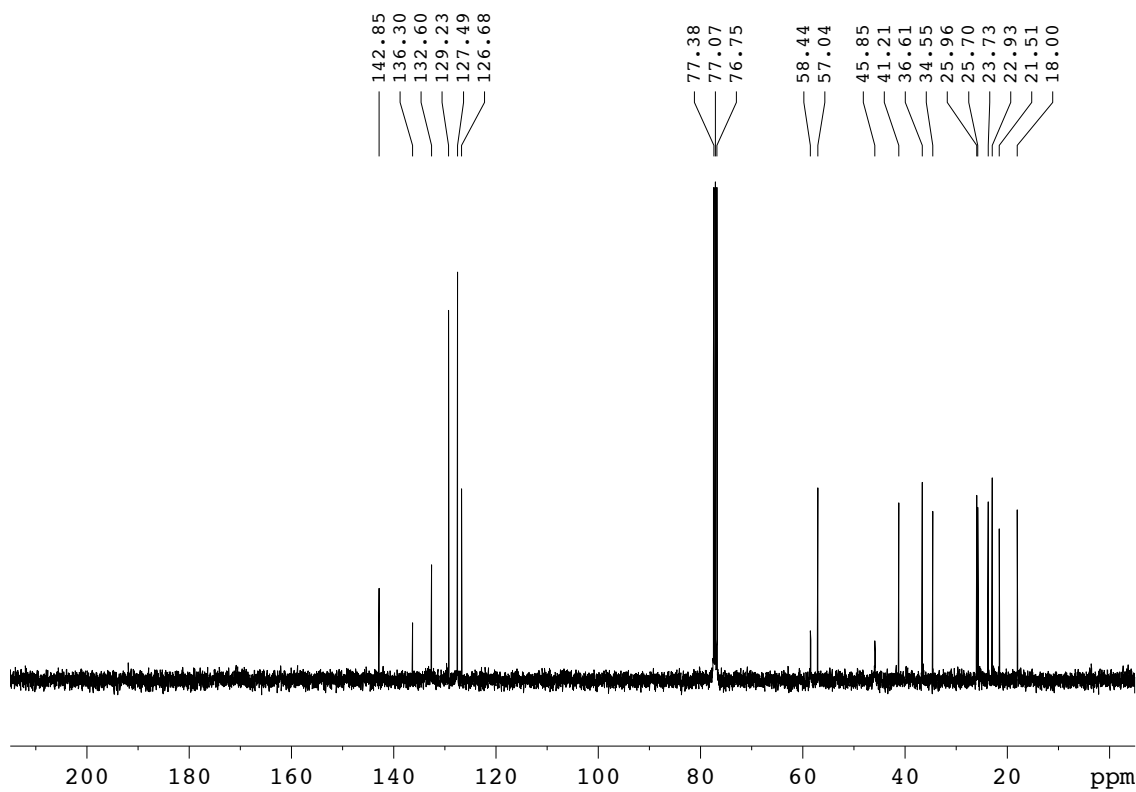
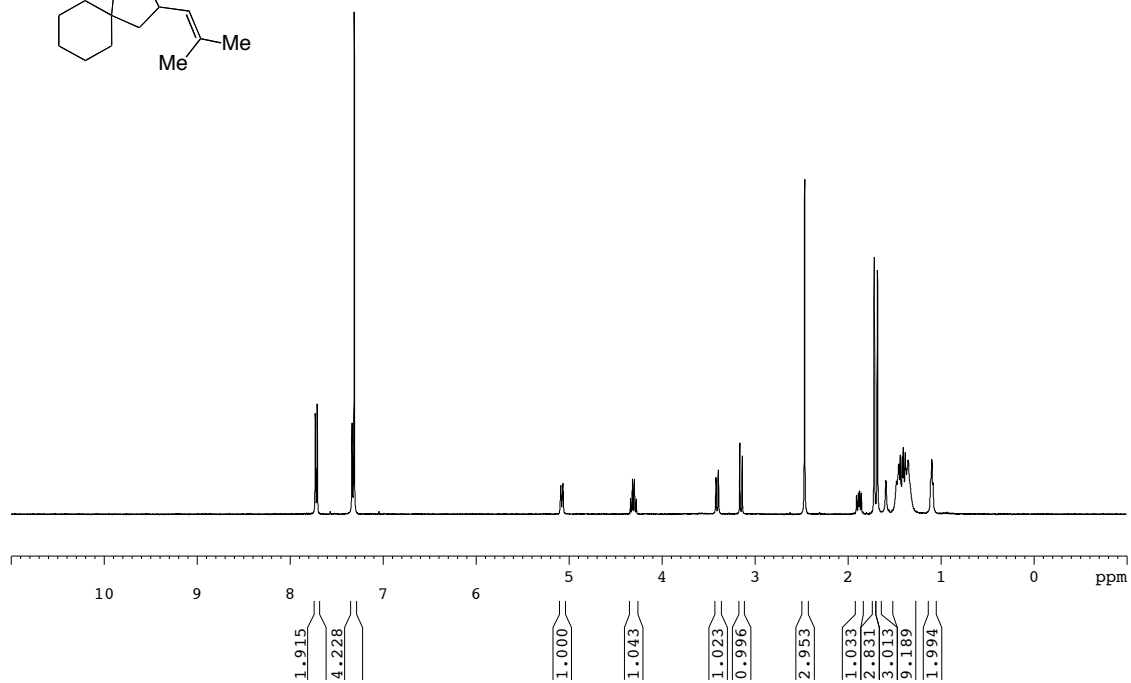
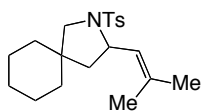
2: 254 nm, 4 nm Results

Retention Time	Area	Area Percent
8.859	1574011	49.766
11.643	1588801	50.234

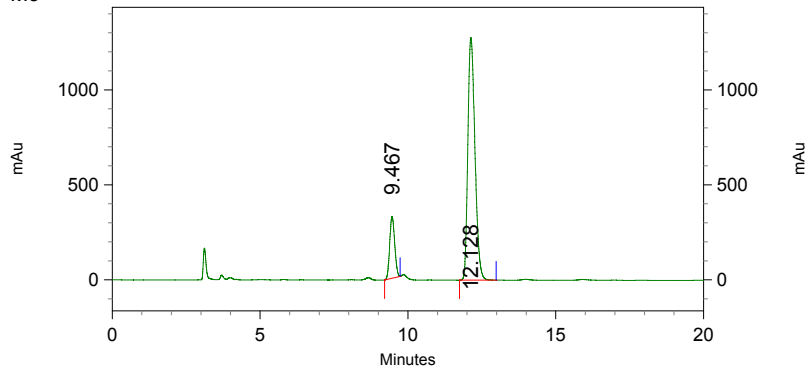
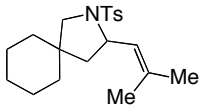
2.59



2.60

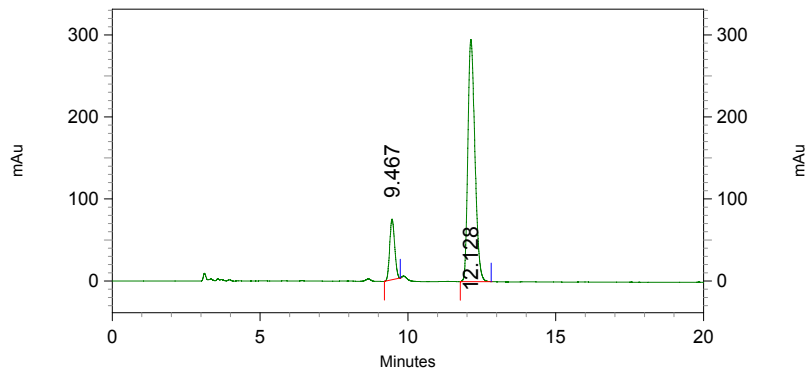


2.60



1: 230 nm, 4 nm Results

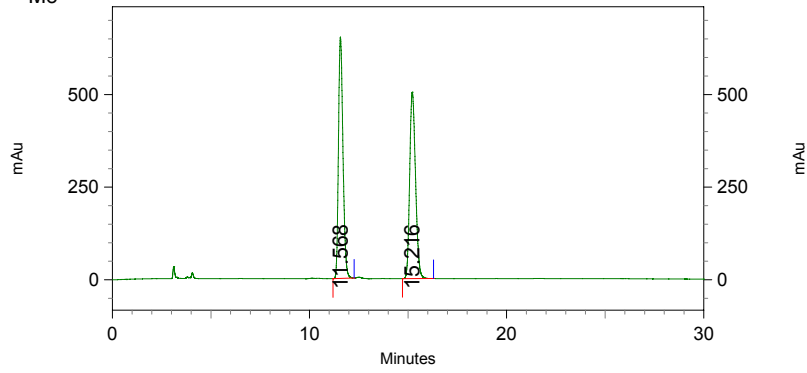
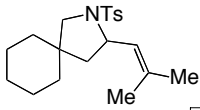
Retention Time	Area	Area Percent
9.467	3818564	15.198
12.128	21307085	84.802



2: 254 nm, 4 nm Results

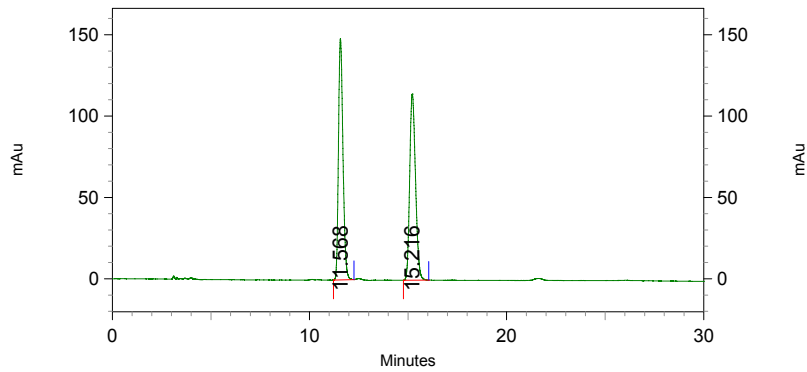
Retention Time	Area	Area Percent
9.467	864831	15.068
12.128	4874849	84.932

2.60



1: 230 nm, 4 nm Results

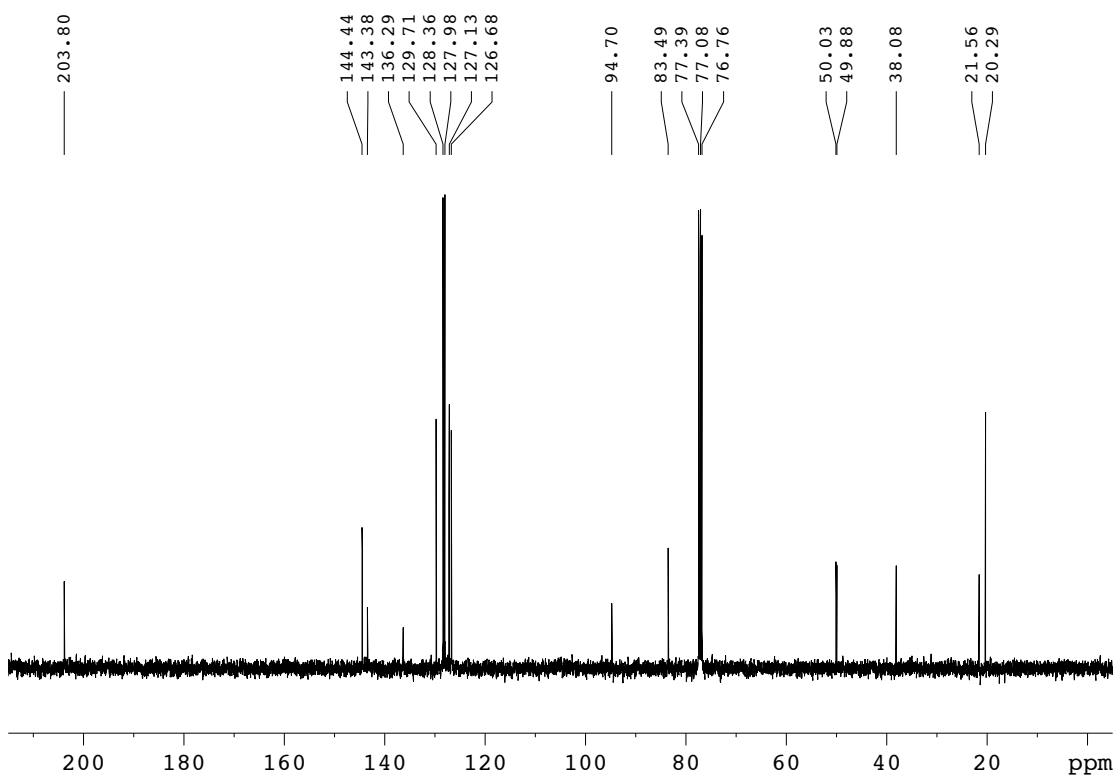
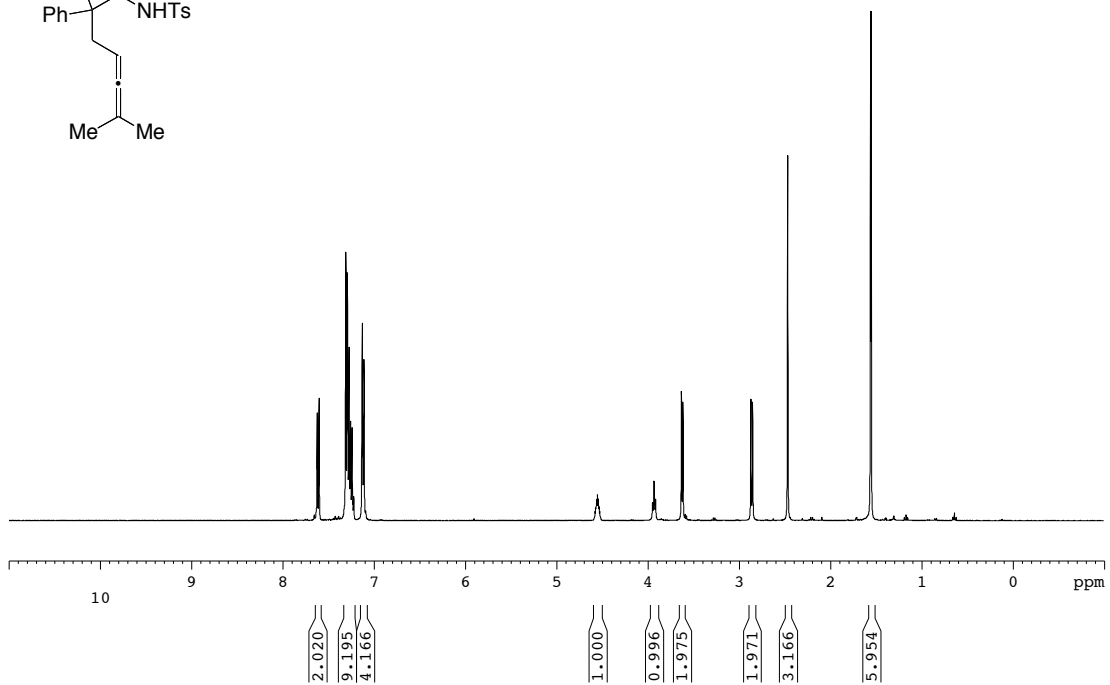
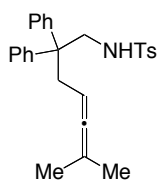
Retention Time	Area	Area Percent
11.568	10340132	49.954
15.216	10358970	50.046



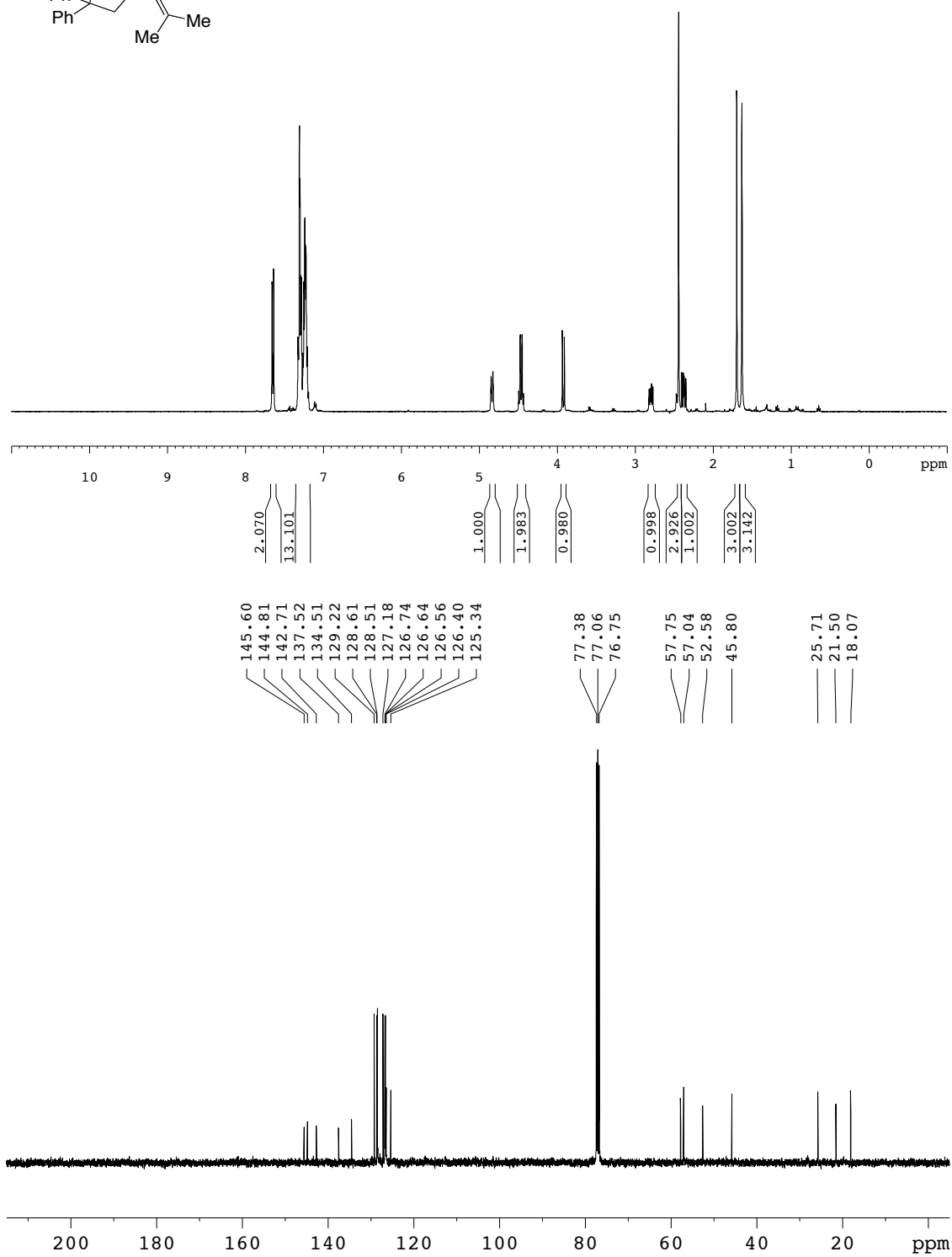
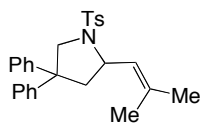
2: 254 nm, 4 nm Results

Retention Time	Area	Area Percent
11.568	2347967	49.989
15.216	2348959	50.011

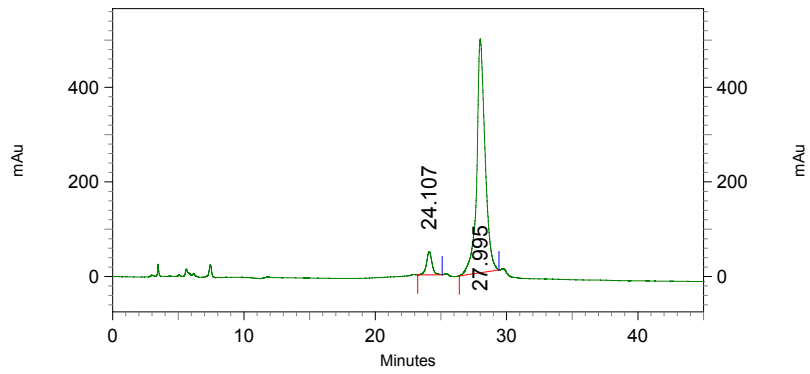
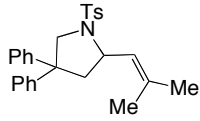
2.61



2.62

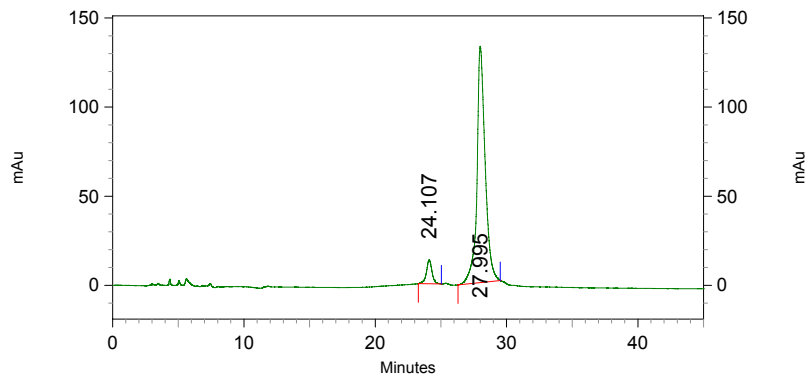


2.62



1: 230 nm, 4 nm Results

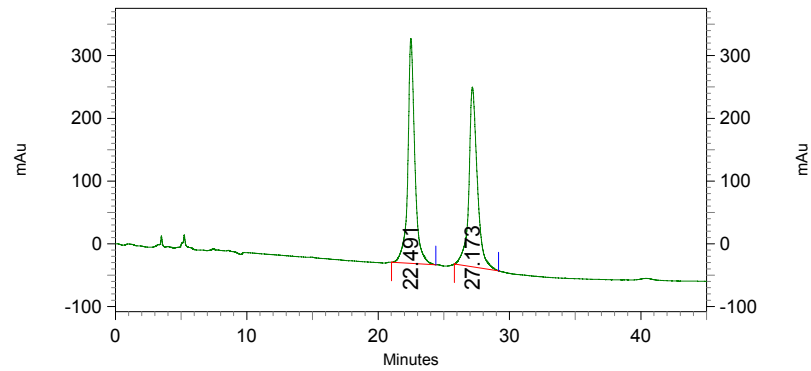
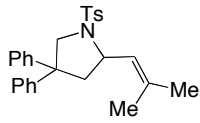
Retention Time	Area	Area Percent
24.107	1459521	6.278
27.995	21788825	93.722



2: 254 nm, 4 nm Results

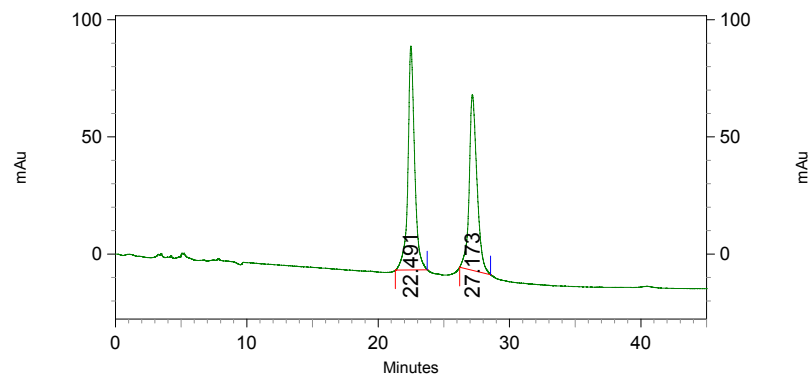
Retention Time	Area	Area Percent
24.107	398196	6.438
27.995	5786806	93.562

2.62



1: 230 nm, 4 nm Results

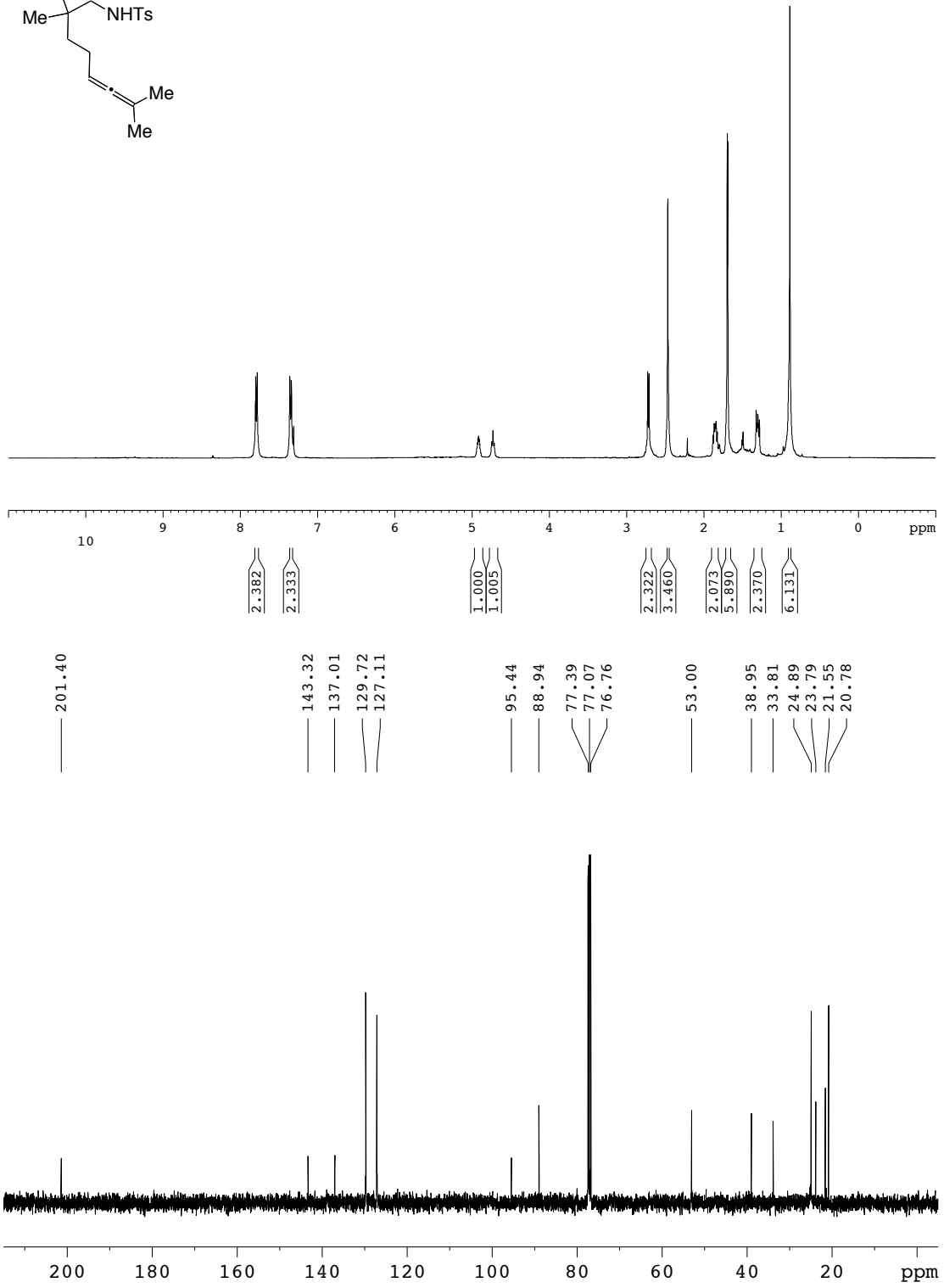
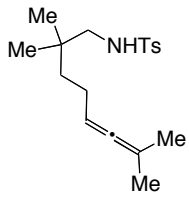
Retention Time	Area	Area Percent
22.491	13203817	50.705
27.173	12836463	49.295



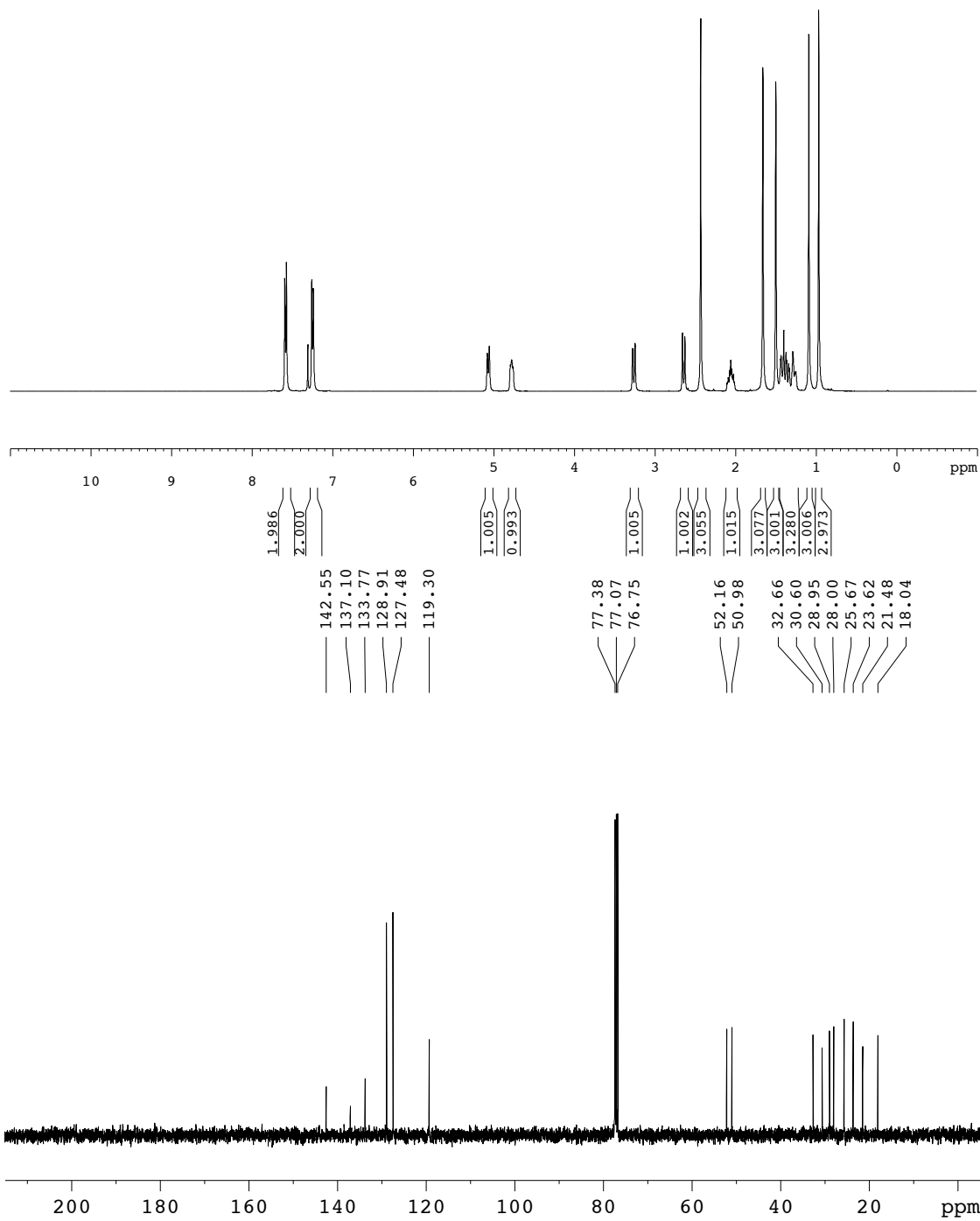
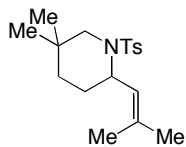
2: 254 nm, 4 nm Results

Retention Time	Area	Area Percent
22.491	3384669	52.172
27.173	3102908	47.828

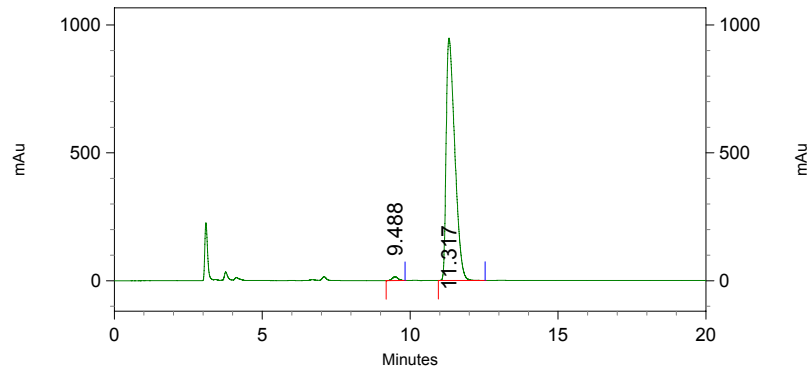
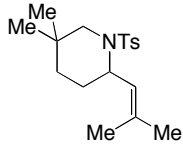
2.67



2.71

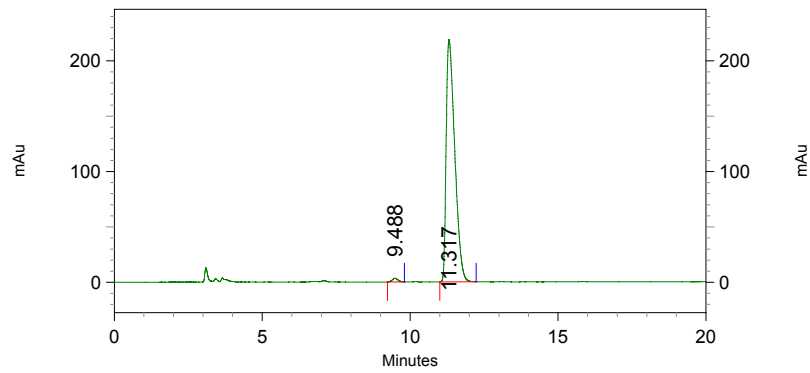


2.71



1: 230 nm, 4 nm Results

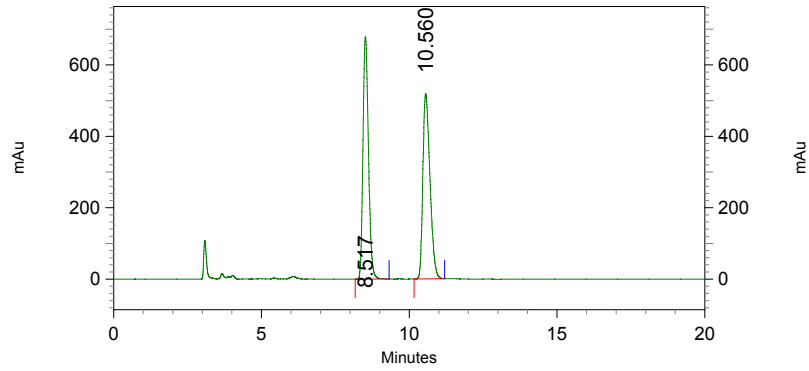
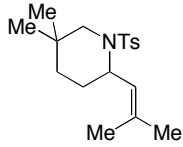
Retention Time	Area	Area Percent
9.488	194234	1.005
11.317	19126894	98.995



2: 254 nm, 4 nm Results

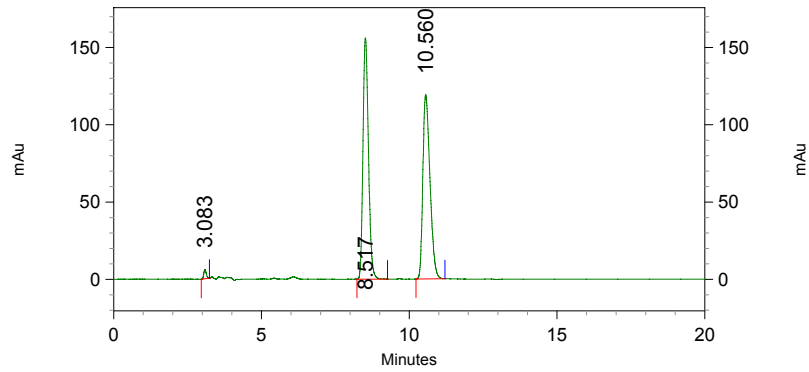
Retention Time	Area	Area Percent
9.488	44413	1.001
11.317	4394575	98.999

2.71



1: 230 nm, 4 nm Results

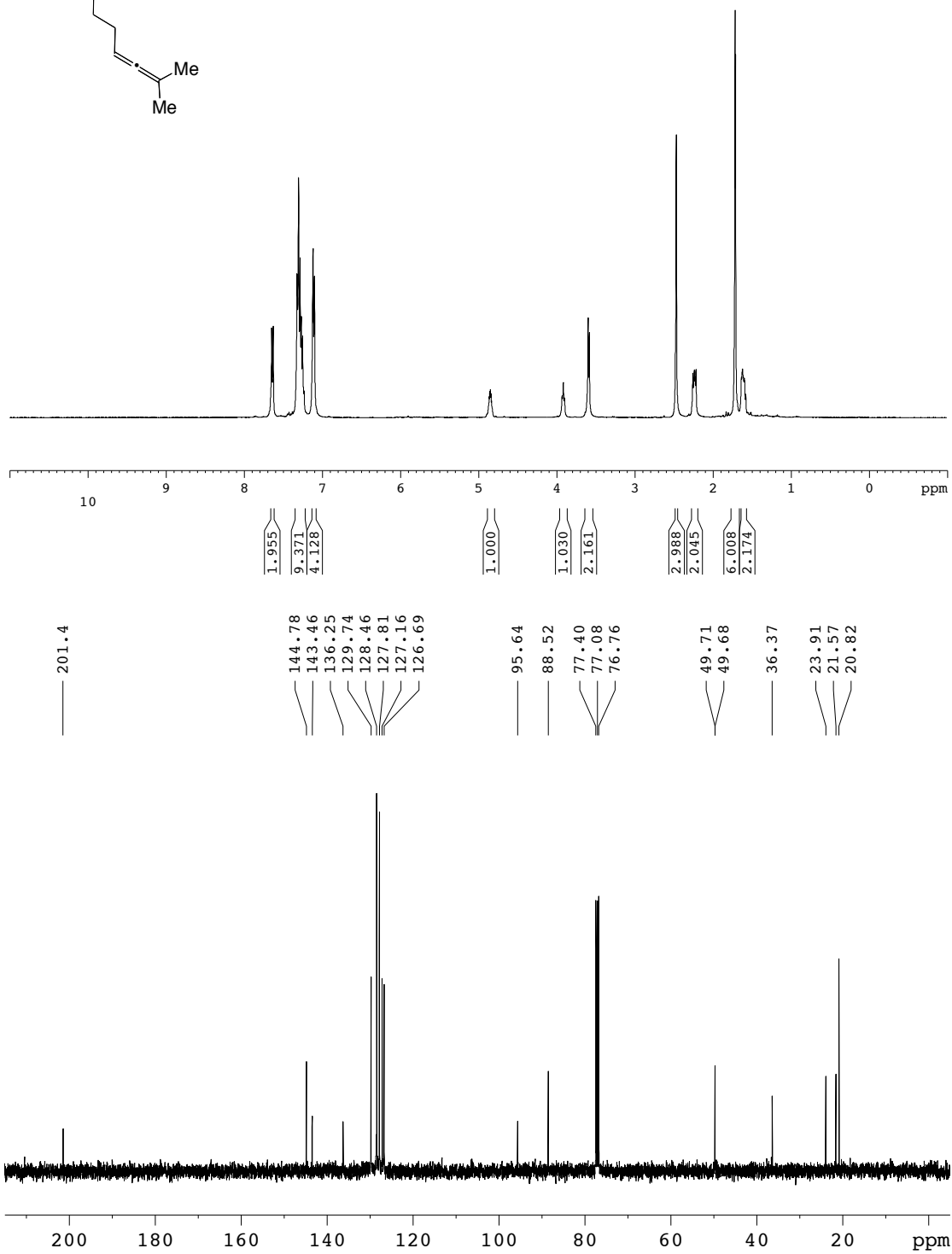
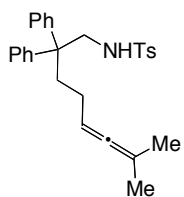
Retention Time	Area	Area Percent
8.517	8692423	50.011
10.560	8688658	49.989



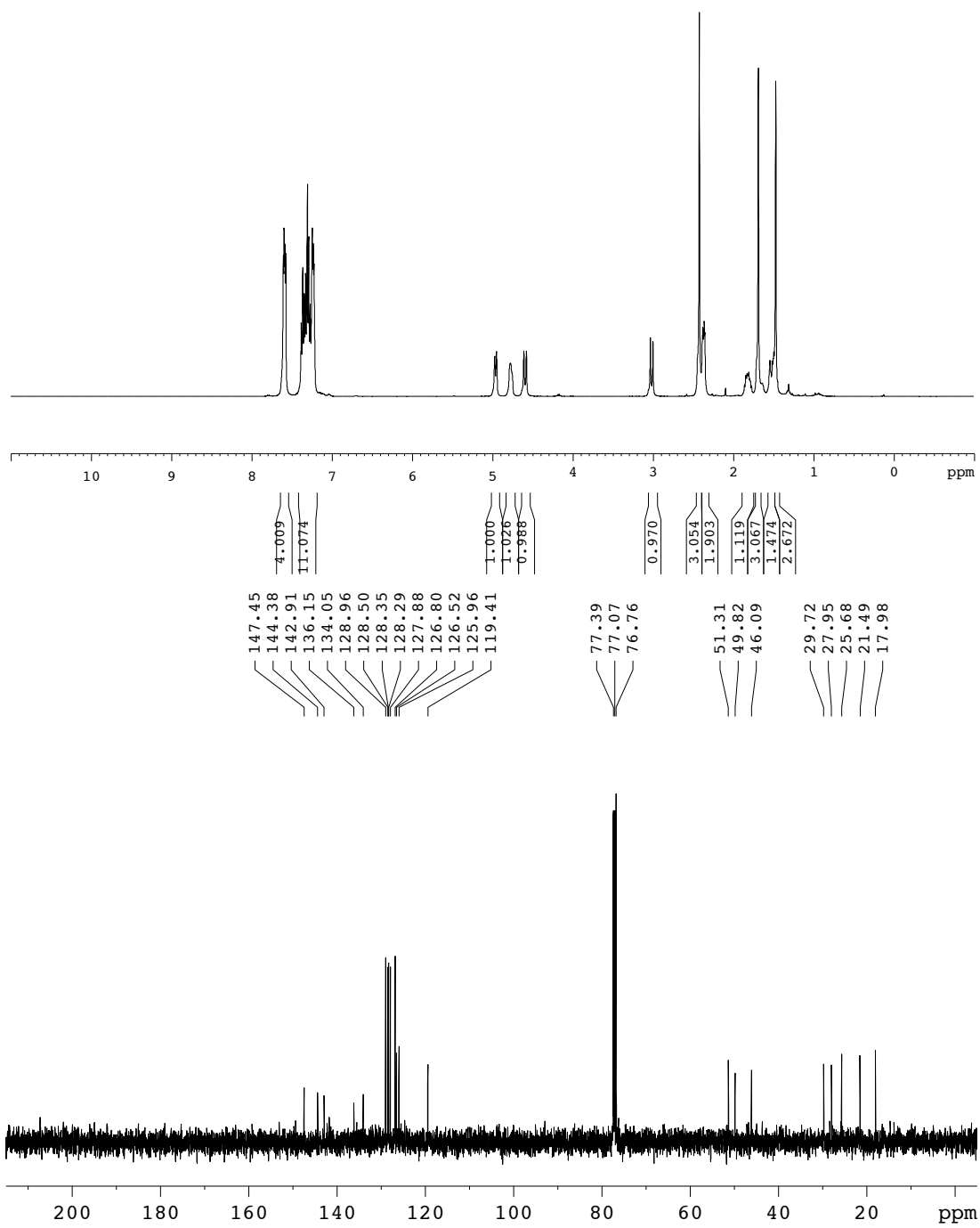
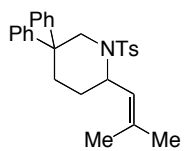
2: 254 nm, 4 nm Results

Retention Time	Area	Area Percent
3.083	34598	0.860
8.517	1995463	49.582
10.560	1994479	49.558

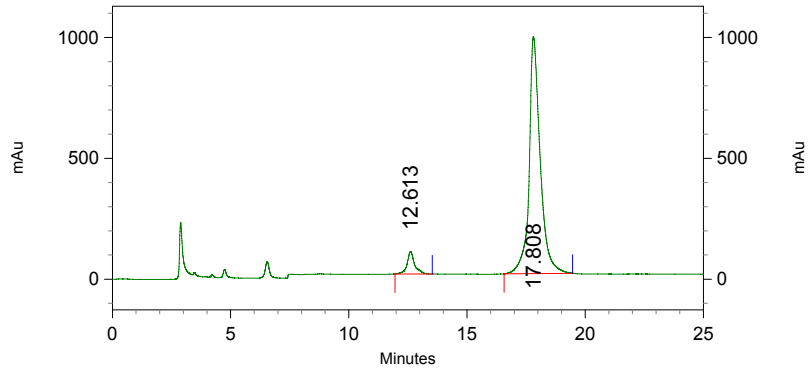
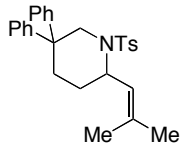
2.63



2.64

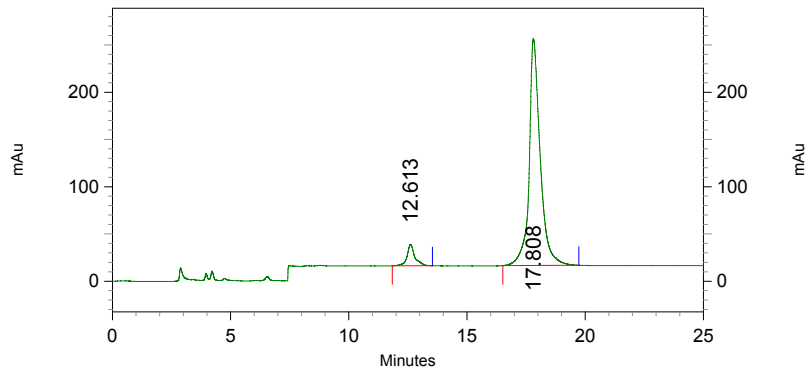


2.64



1: 230 nm, 4 nm Results

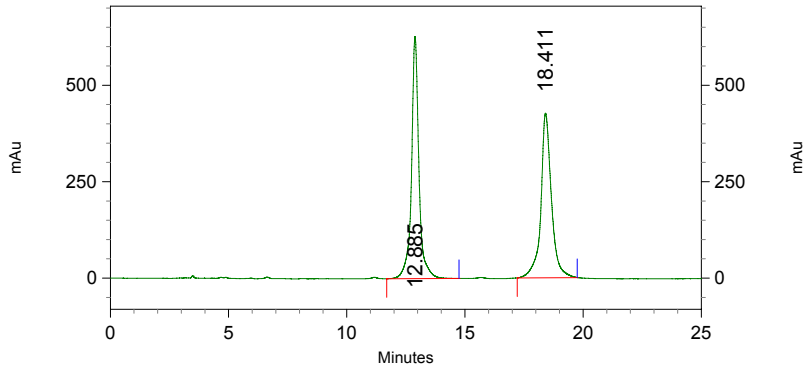
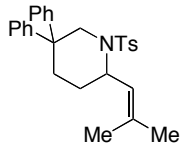
Retention Time	Area	Area Percent
12.613	2053488	6.057
17.808	31849716	93.943



2: 254 nm, 4 nm Results

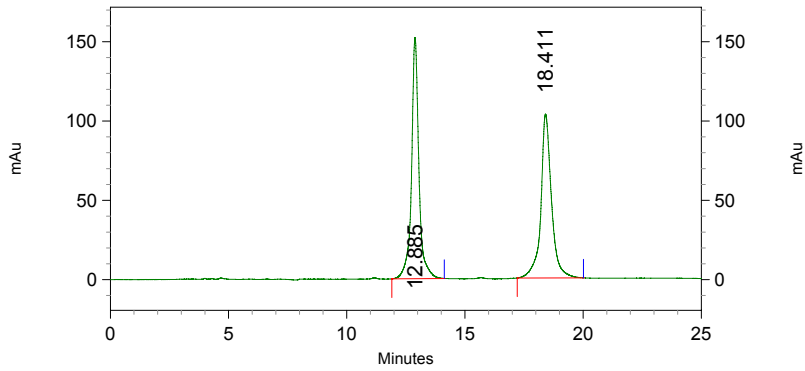
Retention Time	Area	Area Percent
12.613	515122	6.193
17.808	7803304	93.807

2.64



1: 230 nm, 4 nm Results

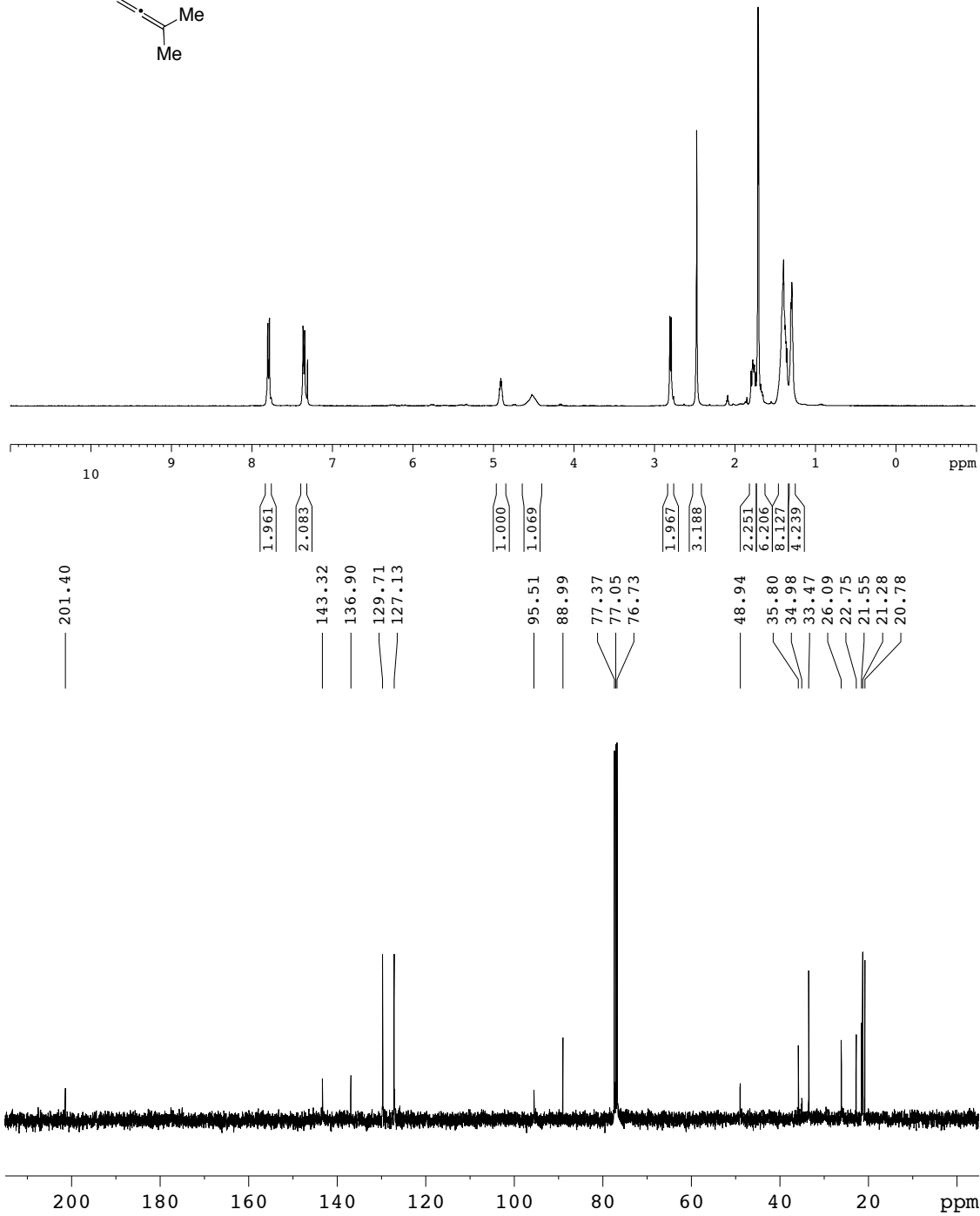
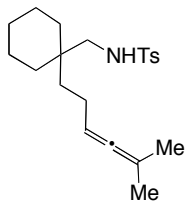
Retention Time	Area	Area Percent
12.885	13708930	50.893
18.411	13227691	49.107



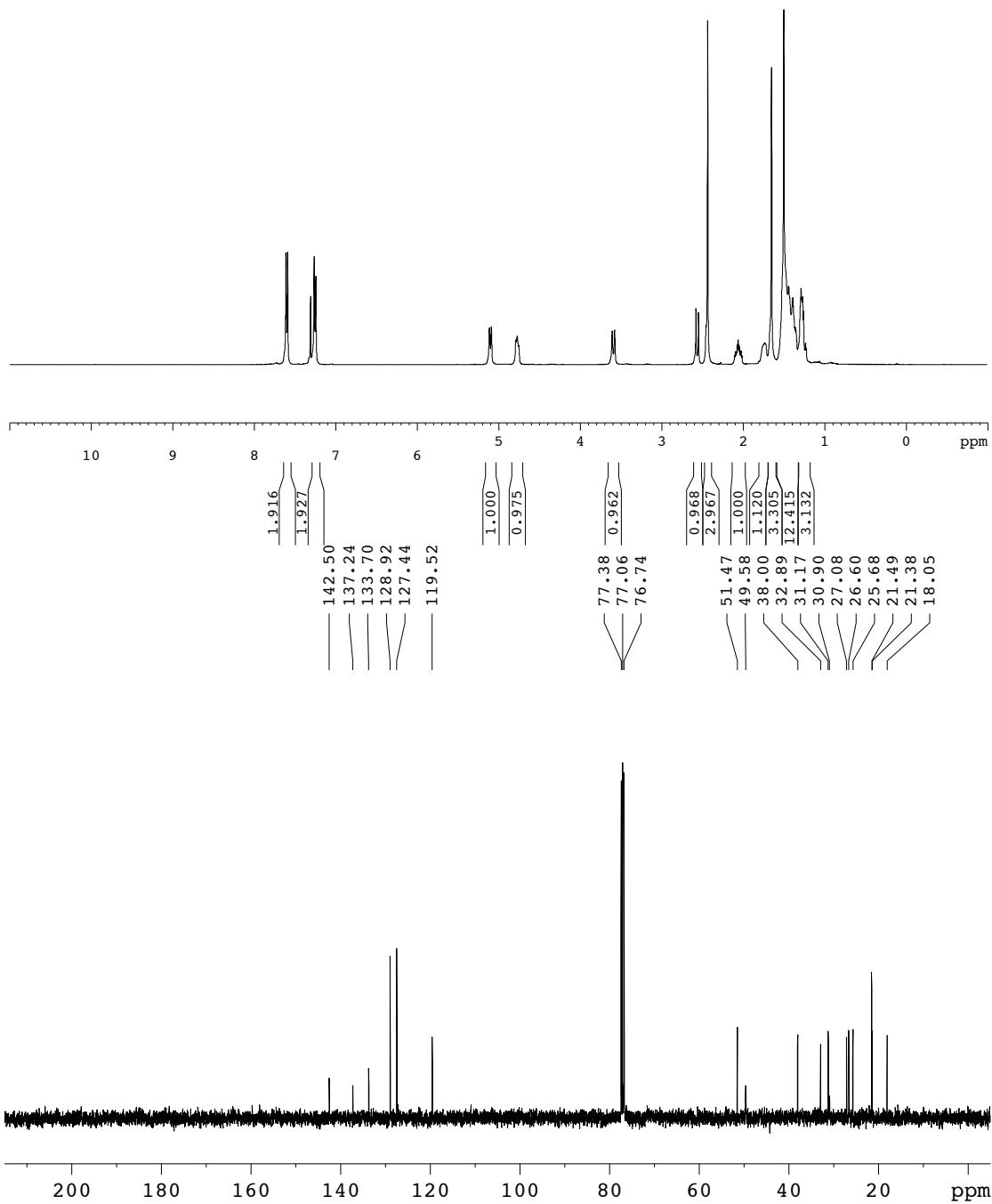
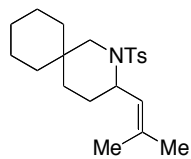
2: 254 nm, 4 nm Results

Retention Time	Area	Area Percent
12.885	3291382	50.517
18.411	3223987	49.483

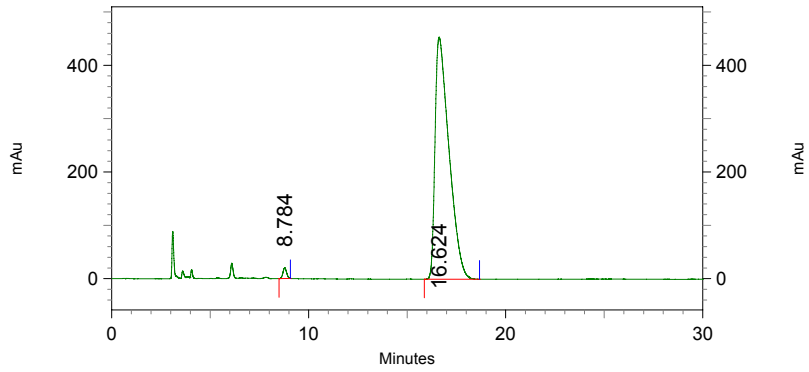
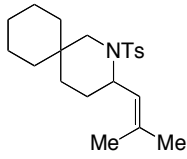
2.68



2.72

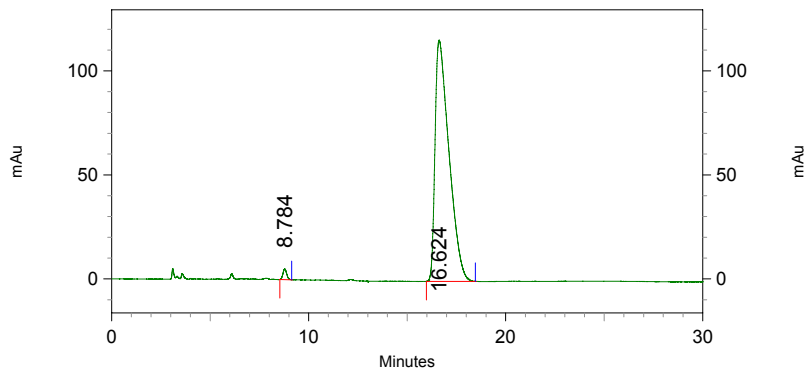


2.72



1: 230 nm, 4 nm Results

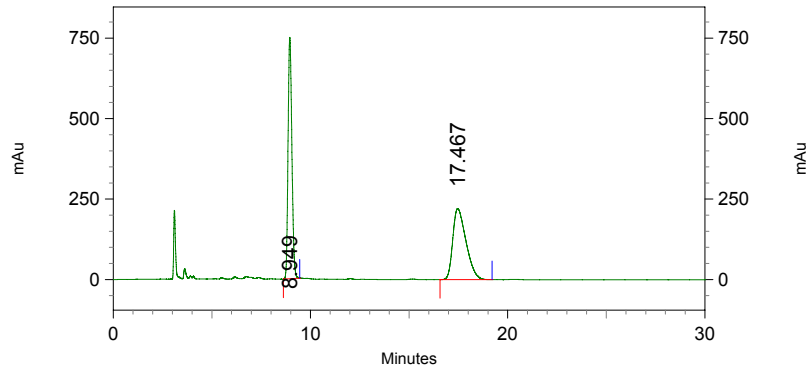
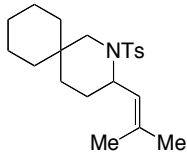
Retention Time	Area	Area Percent
8.784	262570	1.166
16.624	22248385	98.834



2: 254 nm, 4 nm Results

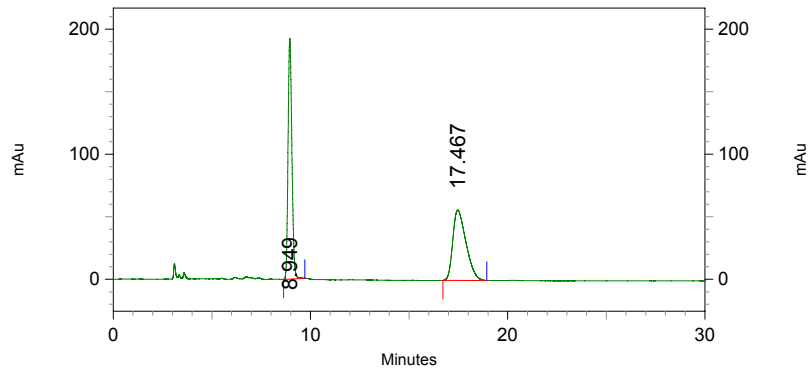
Retention Time	Area	Area Percent
8.784	66994	1.166
16.624	5678474	98.834

2.72



1: 230 nm, 4 nm Results

Retention Time	Area	Area Percent
8.949	10152251	49.733
17.467	10261438	50.267



2: 254 nm, 4 nm Results

Retention Time	Area	Area Percent
8.949	2623833	50.184
17.467	2604613	49.816

Chapter 3

Gold(I)-Catalyzed Enantioselective Synthesis of Pyrazolidines, Isoxazolidines, and Tetrahydrooxazines

A portion of this work has been published (LaLonde, R. L.; Wang, Z. J.; Mba, M.; Lackner, A. D.; Toste, F. D. “Gold(I)-Catalyzed Enantioselective Synthesis of Pyrazolidines, Isoxazolidines, and Tetrahydrooxazines” *Angew. Chem., Int. Ed. Engl.* **2010**, *49*, 598-601), but has been described here in greater detail.¹

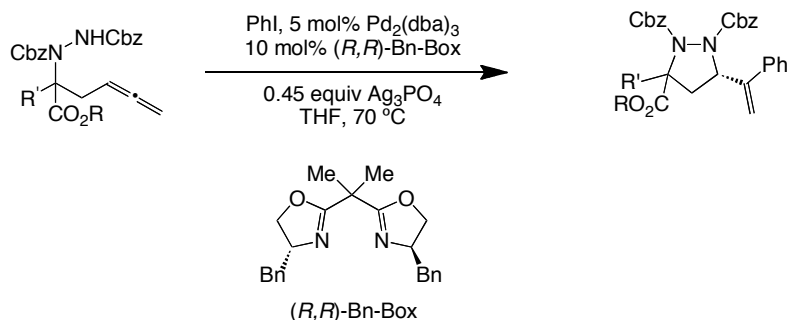
¹ Dr. Miriam Mba performed the initial reaction optimization. Z. Jane Wang was responsible for the hydroxylamine hydroamination. I carried out the hydrazine hydroamination, hydroxylamine hydroalkoxylation, and the functionalization studies. Aaron Lackner synthesized and tested (*S*)-Ag(**3.31**).

Introduction

As discussed in Chapter 2, the field of gold(I)-catalyzed addition of heteroatom nucleophiles to allenes¹ has recently been expanded to include enantioselective synthesis of heterocyclic products.^{2, 3} Despite the rapid growth in this area of research, as of 2009, the gold(I)-catalyzed enantioselective addition of hydroxylamines and hydrazines to allenes had not been reported. In addition to the area of gold-catalysis, this was also a deficiency found in general transition metal-catalysis. A literature search revealed a single enantioselective nucleophilic addition of hydrazines to allenes, but this transformation was an aminoarylation not a hydroamination. The enantioselective addition of hydroxylamine nucleophiles to allenes remained unknown.⁴ Other current methods for the synthesis of isoxazolidines⁵ and pyrazolidines,⁶ usually 1,3-dipolar cycloadditions, are limited by problems with regio- and diastereoselectivity. As these types of heterocycles appear frequently in biologically important molecules, it is imperative to have robust, flexible methods for their formation.⁷ In addition, these heterocycles serve as precursors to unnatural amino acid derivatives such as 5-oxaproline^{7, 8} as well as chiral allylic alcohols and 1,3-diamines, and thus are valuable for peptidomimetic studies.⁹

To the best of our knowledge, before 2009 there were no asymmetric transition metal-catalyzed allene hydroaminations with hydroxylamine and hydrazine nucleophiles. However, a related transformation, an enantioselective palladium-catalyzed aminoarylation of allenes was reported in 2007 (Table 3.1).¹⁰ While racemic keto-ester **3.1** was cyclized with poor diastereo- and enantioselectivity (entry 1), enantioenriched (*R*)-**3.1** reacted with much better results (entry 2). The desired pyrrolidine **3.2** was isolated with excellent enantioselectivity (99%) and good diastereoselectivity (94:6). In a subsequent report,¹¹ Ma tested this methodology on diester substrates. Unfortunately, the maximum ee obtained was much lower than with enantioenriched β -ketoesters. For example, upon treatment with palladium, diester **3.3** yielded **3.4** with 84% ee (entry 3). This method was also limited to hydrazines with matching protecting groups. This potentially presents a problem in differentiating the nitrogens for further functionalization.

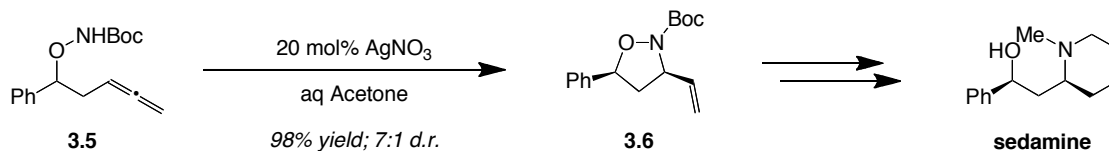
Table 3.1. Palladium-Catalyzed Asymmetric Aminoarylation with Hydrazine Nucleophiles.



entry	substrate	R =	R' =	product	% yield	cis:trans	cis % ee	trans % ee
1	3.1	Et	COMe	3.2	79	35:65	86	43
2	(<i>R</i>)- 3.1	Et	COMe	3.2	81	6:94	--	99
3	3.3	Me	CO ₂ Me	3.4	75	--	84	--

In addition to the lack of enantioselective allene hydroaminations with hydrazine and hydroxylamine nucleophiles, there were also very few analogous racemic transformations. One notable example is a silver-catalyzed intramolecular hydroamination of a mono-substituted allene reported by Bates in 2008 (Scheme 3.1). In addition to silver, the authors also tried using gold(III) chloride as a catalyst for this transformation. They found that the reaction was “less clean” than when catalyzed by silver, and proposed that this was “perhaps due to the stronger Lewis acidity” of gold(III) chloride. Silver nitrate-catalyzed the desired transformation in excellent yield (98%) and good diastereoselectivity (7:1). Isoxazolidine **3.6** was subsequently used in the total synthesis of the alkaloid sedamine.

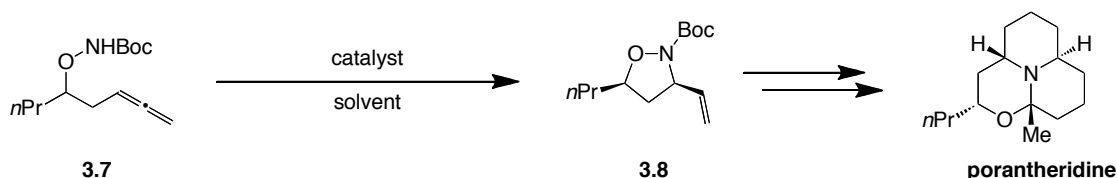
Scheme 3.1. Silver-Catalyzed Hydroxylamine Hydroamination.



This silver-catalyzed reaction was applied to another similar substrate in 2009.¹² In this report, a variety of gold(I), gold(III) and silver salts were screened for reactivity (Table 3.2). A combination of gold(III) chloride, calcium carbonate, and acetonitrile catalyzed the predicted cyclization, albeit with modest yield and diastereoselectivity (entry 1).¹³ The use of triphenylphosphinegold triflate did not improve the d.r. (entry 2). The authors posited that the decrease was due to “the lesser steric demand of linear gold(I).” This was an interesting

supposition due to the fact that simple silver salts, which are not particularly sterically demanding, catalyzed the reaction with greater diastereoselectivity (entries 3 and 4). Alternatively, the difference in selectivity could be explained by dissimilar reaction mechanisms. For example, phosphinegold(I) complexes generally activate C-C unsaturated bonds for *anti*-addition.¹⁴ In contrast, silver mediated hydroamination of allenes has been proposed to proceed by a *syn*-addition.¹⁵ Although the experimental evidence is circumstantial, it seems likely that a 6-membered ring cyclic transition state controlled by silver could be responsible for the observed high diastereoselectivity. Nonetheless, the synthetic utility of this transformation was demonstrated by using isoxazolidine **3.8** in the formal total synthesis of porantheridine and its epimer.

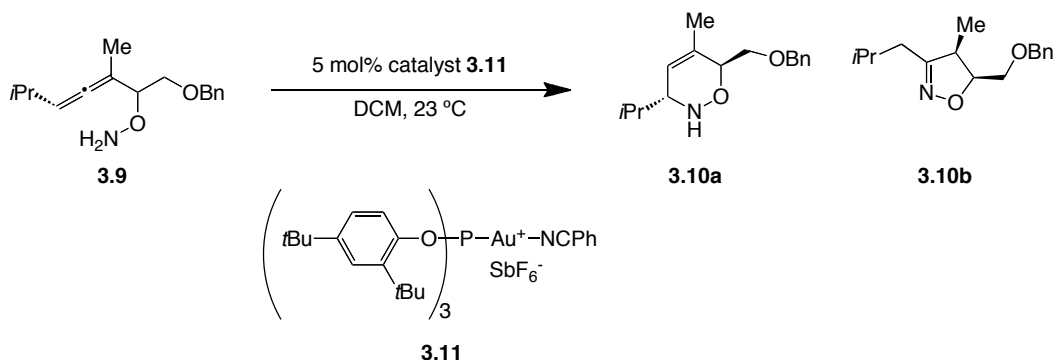
Table 3.2. Gold- and Silver-Catalyzed Hydroxylamine Hydroamination.



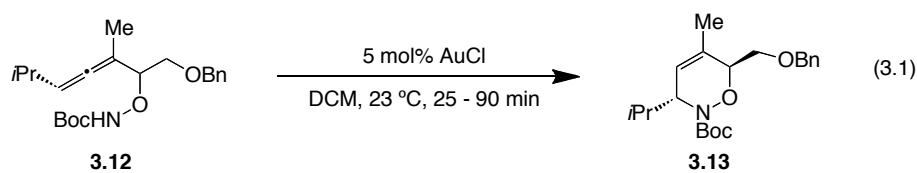
entry	catalyst	solvent	% yield	d.r.
1	5 mol% AuCl ₃ , CaCO ₃	DCM, CH ₃ CN	76	4:1
2	10 mol% Ph ₃ PAuCl 10 mol% AgOTf	DCM	86	2.6:1
3	10 mol% AgOTf	DCM	99	4.6:1
4	10 mol% AgBF ₄	DCM	94	11.5:1

Although Bates and coworkers had limited success with applying gold to their methodology, Krause recently reported the gold catalyzed synthesis of a diverse array of heterocycles via a similar method.^{3a} The use of either gold(III) or gold(I) chloride as catalysts favored the formation of dihydro-1,2-oxazole **3.10a** (Table 3.3, entries 1 and 2). Complete selectivity for **3.10a** could be obtained by simply protecting the hydroxylamine as a Boc carbamate (eq 3.1). Conversely, phosphinegold(I) catalysts were used to reverse the product distribution in preference of **3.10b**. For example, upon treatment with 5 mol% triphenylphosphinegold tetrafluoroborate, **3.9** was cyclized to form **3.10b** with 69% yield and 79:21 d.r. (entry 3). The yield was improved to 81% by employing a di-*tert*-butylphosphite ligand (entry 4). Increasing the steric bulk of the ligand also had a beneficial effect on the diastereoselectivity (11.5:1).

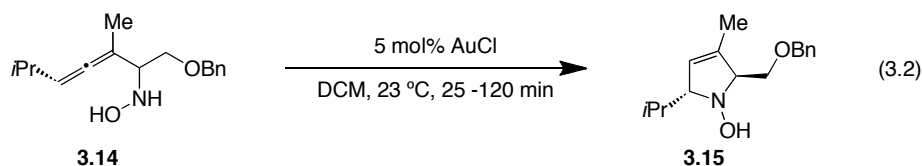
Table 3.3. Gold-Catalyzed Dihydrooxazole and Dihydroisoxazole Formation.



entry	catalyst	time (h)	3.10a % yield (d.r.)	3.10b % yield (d.r.)
1	AuCl ₃	2.5	49 (>99:1)	15 (89:11)
2	AuCl	2.5	47 (>99:1)	19 (87:13)
3	Ph ₃ PAuBF ₄	1.5	3	69 (79:21)
4	3.11	1.5	3	81 (94:6)



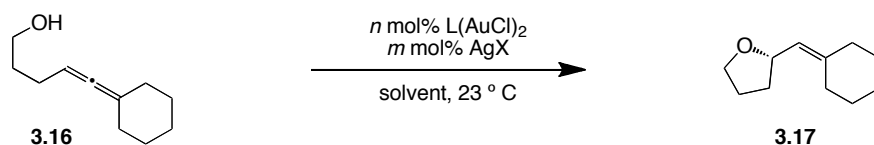
To complete the array of heterocycles, allene **3.14** was cyclized to exclusively form N-hydroxypyrroline **3.15** (eq 3.2). It is possible that blocking the amine with a protecting group would force 6-*endo* cyclization to take place. Unfortunately, the account was limited to hydroamination and did not record any attempts to execute the hydroalkoxylation of comparable substrates.



Even though Krause did not report the formation of the analogous hydroalkoxylation products, the enantioselective hydroalkoxylation of allenes is now well known.^{2e, f} While others have successfully utilized biarylphosphinegold(I) complexes,^{2e} in our hands gold(I) species such as (*R*)-3,5-xylyl-BINAP(AuCl)₂ did not produce favorable results with oxygen nucleophiles (Table 3.4, entry 1). As such, a team of researchers in our group approached this problem by means of an alternate strategy.^{2f} Our previous investigation showed that counterions played a crucial role in the transference of chiral information.^{2a} As such, a logical extension would be to

use the counterions as the source of chirality. The combination of an achiral bisphosphinegold(I) complex with a chiral counterion, (*R*)-TripAg, proved to be a remarkable catalyst for the enantioselective hydroalkoxylation of allenes.^{2f} For instance, in DCM, this combination catalyzed the formation of **3.17** with 65% ee (entry 2). The enantioselectivity was amplified to 97% by simply changing the solvent to benzene (entry 3).

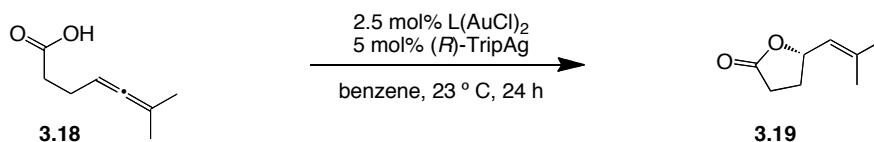
Table 3.4. Chiral Counterions Used For the Asymmetric Hydroalkoxylation of Allenes.



entry	<i>n</i> mol% L(AuCl) ₂	<i>m</i> mol% AgX	solvent	% yield	% ee
1	3 mol% (<i>R</i>)-3,5-xylyl-BINAP(AuCl) ₂	3 mol% AgBF ₄	DCM	68	0
2	2.5 mol% dppm(AuCl) ₂	5 mol% (<i>R</i>)-TriPAg	DCM	76	65
3	2.5 mol% dppm(AuCl) ₂	5 mol% (<i>R</i>)-TriPAg	benzene	90	97

The potential of this strategy was realized when chiral ligands and chiral counterions were used in conjunction. For substrates that were difficult to optimize, this option provided additional catalyst selection and often increased the observed enantioselectivity. As an example, carboxylic acids were challenging: when treated with a mixture of dppm(AuCl)₂ and (*R*)-TripAg, **3.18** cyclized to form **3.19** with only 12% ee (Table 3.5, entry 1). While a mis-matched ligand-counterion pair reduced the enantioselectivity even further (entry 2), the matched group produced the desired product with good enantioselectivity (82%, entry 3).

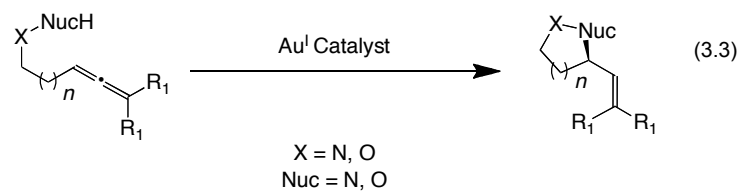
Table 3.5. Chiral Counterion Mediated Asymmetric Addition of Carboxylic Acids to Allenes.



entry	ligand	% yield	% ee
1	dppm	89	12
2	(<i>R</i>)-BINAP	91	3
3	(<i>S</i>)-BINAP	88	82

As detailed in Chapter 2, our group reported gold(I)-bis-*p*-nitrobenzoate complexes as excellent catalysts for the enantioselective hydroamination of allenes. We theorized that in

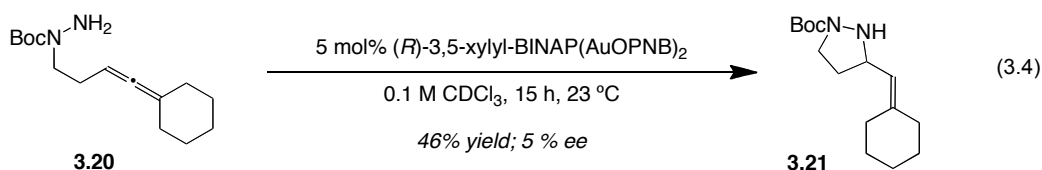
addition to tosyl amines, gold(I)-bis-*p*-nitrobenzoate complexes would perform as efficient catalysts for the enantioselective addition of hydroxylamines and hydrazines to allenes (eq 3.3). Moreover, we anticipated that the asymmetric hydroalkoxylation with hydroxylamines could be problematic, and would require the expanded flexibility of the chiral counterion strategy.



Results

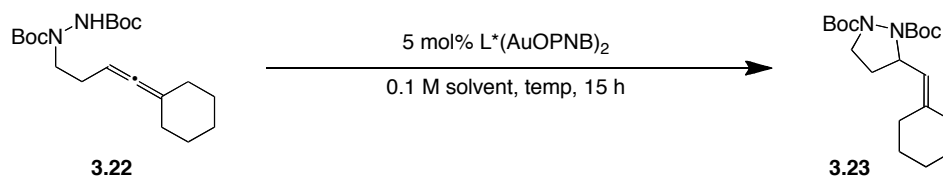
Initial Optimization

We began our studies with a mono-Boc protected homo-allenic hydrazine **3.20**, easily synthesized in four steps from the analogous homo-allenic alcohol. While unprotected amines are usually considered incompatible with cationic gold complexes, we hypothesized that the reduced Lewis basicity of the hydrazine would allow the use of an unprotected terminal amine. Upon treatment of **3.20** with 5 mol% (*R*)-3,5-xylyl-BINAP(AuOPNB)₂ in chloroform, the desired product (**3.21**) was formed, although in modest yield and low enantioselectivity (eq 3.4).



We theorized that adding a protecting group to the terminal nitrogen would constrain the transition state and thereby increase the observed enantioselectivity. Unfortunately, bis-Boc protected hydrazine **3.22** failed to cyclize at room temperature (Table 3.6, entry 1). Similar to our findings in the study of hydroamination with tosylamines, gentle heating in DCE or nitromethane restored quantitative conversion to **3.23** (entries 2 and 3). We were also pleased to find that **3.23** was obtained with good enantioselectivity in both solvents (70% and 73%, respectively). Nitromethane was selected as the optimal solvent due to a slight increase in ee. A brief ligand screen revealed that (*R*)-ClMeOBiPHEP(AuOPNB)₂ provided pyrazolidine **3.23** with the greatest enantioselectivity (78%, entry 4). Gold complexes with other ligands, such as (*R*)-Segphos and (*R*)-Synphos, catalyzed the reaction with similar conversion, but slightly lower enantioselectivities (70% and 60%, entries 5 and 6).

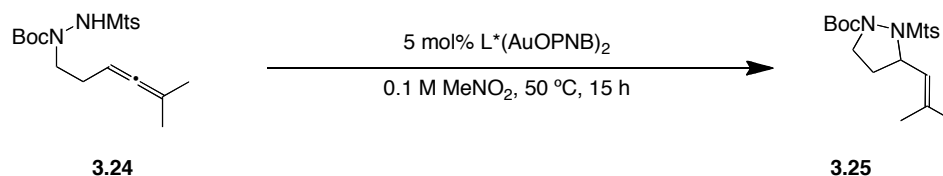
Table 3.6. Solvent and Ligand Optimization.



entry	ligand	solvent	temp (°C)	% conv	% ee
1	(<i>R</i>)-3,5-xylyl-BINAP	CHCl ₃	23	n.r.	--
2	(<i>R</i>)-3,5-xylyl-BINAP	DCE	50	>98	70
3	(<i>R</i>)-3,5-xylyl-BINAP	MeNO ₂	50	>98	73
4	(<i>R</i>)-ClMeOBiPHEP	MeNO ₂	50	>98	78
5	(<i>R</i>)-Segphos	MeNO ₂	50	>98	70
6	(<i>R</i>)-Synphos	MeNO ₂	50	>98	60

The dramatic increase in enantioselectivity when dual protecting groups were utilized led us to theorize that sterically differentiating the protecting groups would be necessary to further improve the enantioselectivity. Indeed, utilizing a mesitylenesulfonyl (Mts) protecting group on the terminal nitrogen raised the observed enantioselectivity to 80% ee (Table 3.7, entry 1). A detailed examination of chiral ligands revealed that a variety of biarylphosphine ligands catalyzed the desired hydroamination with adequate ee. For example, (*R*)-ClMeOBiPHEP(AuOPNB)₂, (*R*)-Synphos(AuOPNB)₂, and (*R*)-MeOBiPHEP(AuOPNB)₂ performed similarly, yielding **3.25** with approximately 85% ee (entries 2-4). Augmenting the steric size of the aryl groups on the phosphine ligands resulted in a large amplification of enantioselectivity. For instance, while using (*R*)-DM-MeOBiPHEP(AuOPNB)₂ provided a modest increase (87% ee, entry 5), an even bulkier ligand, (*R*)-DTBM-MeOBiPHEP(AuOPNB)₂ enhanced the enantioselectivity to 97% (entry 6). A similar trend was found in the Segphos family of ligands (entries 7 and 8). Ultimately, (*R*)-DTBM-Segphos was chosen as the optimal ligand, as its use yielded pyrazolidine **3.25** with 98% ee (entry 8).

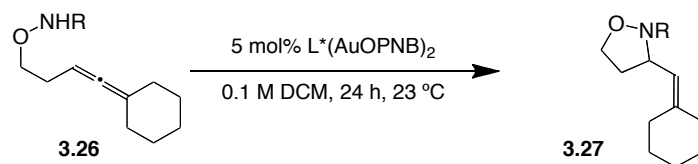
Table 3.7. Ligand Optimization for Hydrazine Hydroamination.



entry	ligand	% ee
1	(<i>R</i>)-3,5-xylyl-BINAP	80
2	(<i>R</i>)-ClMeOBiPHEP	85
3	(<i>R</i>)-Synphos	86
4	(<i>R</i>)-MeOBiPHEP	85
5	(<i>R</i>)-DM-MeOBiPHEP	87
6	(<i>R</i>)-DTBM-MeOBiPHEP	97
7	(<i>R</i>)-Segphos	90
8	(<i>R</i>)-DTBM-Segphos	98

Similar to hydroamination with hydrazines, we found that although unprotected hydroxylamine **3.26c** was transformed into isoxazolidine **3.27c** with excellent conversion (>98%), low enantioselectivity (10% ee) was observed (Table 3.8, entry 5).¹⁶ Fortunately, protection of the hydroxylamine resolved this issue. The cyclization of N-Boc-protected hydroxylamine **3.26a** was catalyzed by (*R*)-BINAP(AuOPNB)₂, yielding the desired product in 80% conversion and 89% ee (entry 1). Adding a methyl substituent to the ligand's aryl groups further increased the ee to 92% (entry 2). Upon treating hydroxylamine **3.26a** with 5 mol% (*R*)-3,5-xylyl-BINAP(AuOPNB)₂, isoxazolidine **3.27a** was formed with quantitative conversion and 93% ee (entry 3). Strangely, another carbamate protecting group, CBz, significantly reduced the conversion to 8% (entry 4). Additionally, a polar, non-coordinating solvent such as nitromethane was effective, producing **3.27a** in 98% conversion and 87% ee. However, a non-polar solvent (benzene) and a coordinating solvent (dioxane) completely eliminated catalyst activity.

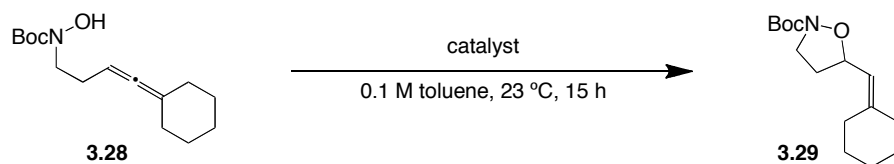
Table 3.8. Hydroxylamine Hydroamination Optimization.



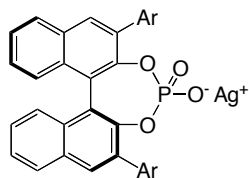
entry	3.26	R =	ligand	3.27	% conv	% ee
1	a	Boc	(<i>R</i>)-BINAP	a	80	89
2		Boc	(<i>R</i>)-tolyl-BINAP		>98	92
3		Boc	(<i>R</i>)-3,5-xylyl-BINAP		>98	93
4	b	Cbz	(<i>R</i>)-3,5-xylyl-BINAP	b	8	--
5	c	H	(<i>R</i>)-3,5-xylyl-BINAP	c	>98	0

While gold(I)-bis-*p*-nitrobenzoate complexes proved to be ineffective catalysts for the hydroalkoxylation of allenes (Table 3.9, entry 1), we hypothesized that employing a more non-coordinating counterion with a lower pKa would improve catalysis. A fellow graduate student, Aaron Lackner, synthesized chiral silver sulfonate (*S*)-Ag(**3.31**) in seven steps from (*S*)-BINOL.¹⁷ Gratifyingly, upon treatment with 3 mol% $dppm(AuCl)_2$ and 3 mol% (*S*)-Ag(**3.31**), isoxazolidine **3.29** was formed with quantitative conversion and 65% ee (entry 2). However, attempts to improve the enantioselectivity by matching the chiral counterion with chiral gold BINAP complexes were unsuccessful (entries 3 and 4). Both the matched and mismatched mixtures produced **3.29** with lower enantioselectivity (28% and 8% ee, respectively). Chiral silver phosphate (*S*)-AgTriP (**3.30**) proved to be the key to enhancing the enantioselectivity to 98% ee (entry 5).

Table 3.9. Hydroalkoxylation Optimization.^a

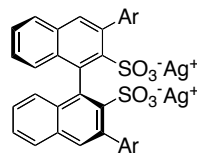


entry	catalyst	% yield	% ee
1	(<i>R</i>)-3,5-xylyl-BINAP(AuOPNB) ₂	0	--
2	3 mol% dppm(AuCl) ₂ 3 mol% (<i>S</i>)-Ag(3.31)	98 ^d	65
3	3 mol% (<i>R</i>)-BINAP(AuCl) ₂ 3 mol% (<i>S</i>)-Ag(3.31)	98 ^d	8
4	3 mol% (<i>S</i>)-BINAP(AuCl) ₂ 3 mol% (<i>S</i>)-Ag(3.31)	98	42
5	3 mol% dppm(AuCl) ₂ 6 mol% (<i>S</i>)-AgTriP (3.30)	98	98



(*S*)-AgTRIP (3.30)

Ar = 2,4,6-triisopropylphenyl



(*S*)-Ag(3.31)

Ar = 3,5-dinitrofluoromethylphenyl

^a Reaction conditions: 0.1 M in toluene, 23 °C, 15 h. ^b Isolated yield after column chromatography.

^c Determined by HPLC. ^d Conversion determined by ¹H NMR.

Reaction Scope: Hydroamination

We next sought to test the substrate scope of our optimized hydroamination conditions. Linear and cyclic alkyl substitutions were tolerated at the allene terminus in both the hydrazine and hydroxylamine hydroamination.¹⁶ For instance, methyl substituted substrates cyclized with excellent enantioselectivity (99% and 98%, entries 1 and 4, respectively). Cyclohexyl substituted allenes also reacted with high enantioselectivity (entries 3 and 6). Cyclopentyl substituted substrates **3.32** and **3.26** also provided pyrazolidine **3.42** and isoxazolidine **3.45** in good yield and slightly lower enantioselectivity (83% and 91%, entries 2 and 5). Furthermore,

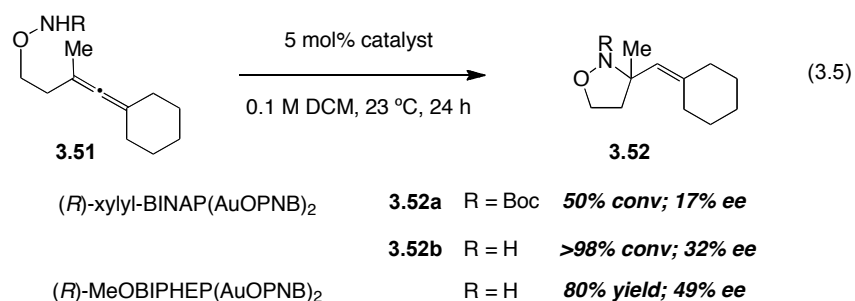
the formation of simple isoxazolidines was usually accomplished at room temperature, but allenes with sterically challenging backbone substitutions needed gentle heating (50 °C) in a polar, non-coordinating solvent (nitromethane). While substitution at the allenic position (entry 8) gave enhanced enantioselectivity (99%) with modest yield (73%), the homo-allenic position showed the reverse trend: modest enantioselectivity (63%) and excellent yield (94%).

Table 3.10. Hydrazine and Hydroxylamine Hydroamination Scope.

entry	substrate	conditions ^a	product	% yield ^b	% ee ^c	
1		3.24 R = Me	A		3.25 98	99
2		3.32 R = -CH ₂ (CH ₂) ₂ CH ₂ -	A		3.42 90	83
3		3.33 R = -CH ₂ (CH ₂) ₃ CH ₂ -	A		3.43 75	97
4		3.35 R = Me	B		3.44 91	98
5		3.36 R = -CH ₂ (CH ₂) ₂ CH ₂ -	B		3.45 98	91
6		3.26 R = -CH ₂ (CH ₂) ₃ CH ₂ -	B		3.27 93	93
7		3.37 R = Me; R' = H	C		3.46 94	63
8		3.38 R = H; R' = Me	C		3.47 73	99
9		3.39 R = -CH ₂ (CH ₂) ₃ CH ₂ -; R' = H	D ^d		3.48 63	89
10		3.40 R = -CH ₂ (CH ₂) ₃ CH ₂ -; R' = Me	D		3.49 85	89
11		3.41 R = Me; R' = Me	D		3.50 79	89

^a Reaction Conditions: A = 5 mol% (*R*)-DTBM-Segphos(AuOPNB)₂, 0.3 M in MeNO₂, 50 °C, 15 h; B = 3 mol% (*R*)-3,5-xylyl-BINAP(AuOPNB)₂, 0.1 M in DCM, 23 °C, 24 h; C = 5 mol% (*R*)-DM-MeOBiPHEP(AuOPNB)₂, 0.1 M in MeNO₂, 50 °C, 24 h; D = 5 mol% (*R*)-3,5-xylyl-BINAP(AuOPNB)₂, 0.3 M in MeNO₂, 50 °C, 24 h. ^b Isolated yield after column chromatography. ^c Determined by HPLC. ^d 36 h, 65 °C.

We also applied our hydroamination conditions to the formation of six-membered ring oxazine heterocycles (entries 9-11). Gentle heating in a polar non-coordinating solvent was required to produce oxazines in good yield (63-85%). Substrates with backbone substitutions (entries 10 and 11) were higher yielding than those without substitutions, presumably due to a Thorpe-Ingold effect. Also, both linear and cyclic alkyl substitutions were tolerated at the allene terminus providing the heterocycles with 89% ee in all cases.

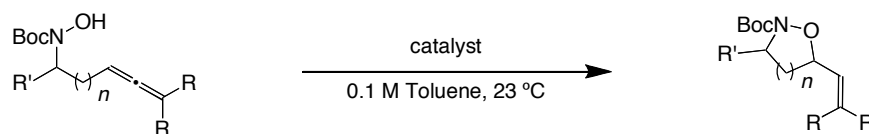


The advantage of the increased nucleophilicity of hydroxylamines was demonstrated in the cyclization onto tetrasubstituted allenes.¹⁶ Nucleophilic additions to tetrasubstituted allenes is challenging; only a handful of substrates have been reported.^{4a, 18} While the use of a protecting group was normally beneficial to enantioselectivity (*vide supra*), in the case of addition to sterically encumbered substrates such protecting groups were detrimental to both the observed enantioselectivity and conversion (eq 3.5). Unprotected hydroxylamines, however, when treated with the same catalyst produced the desired product in quantitative conversion and 32% ee. Modifying the catalyst ligand to (*R*)-MeOBiPHEP further improved the enantioselectivity to 49%.

Reaction Scope: Hydroalkoxylation

We were pleased to find that chiral silver salts used with gold(I) complexes catalyze the hydroalkoxylation of *N*-linked hydroxylamines with good to excellent enantioselectivity. Both cyclic and linear alkyl substitutions at the allene terminus were well tolerated, yielding the corresponding isomeric vinyl-isoxazolidines in good yield and high enantiomeric excess (Table 3.11, entries 1 and 2). Formation of oxazines proved to be more challenging, with the gold(I)-catalyzed reaction affording **3.58** in modest yield and 50% ee (entry 4).¹⁹ However, both the yield and enantioselectivity were greatly improved by combining a chiral ligand with the chiral silver salt (94% yield and 87% ee, entry 5). Additionally, while good diastereoselectivity was observed for substituted substrates (entry 3), the corresponding enantioselectivities favored the minor diastereomer.

Table 3.11. Hydroxylamine Hydroalkoxylation Reaction Scope.^a



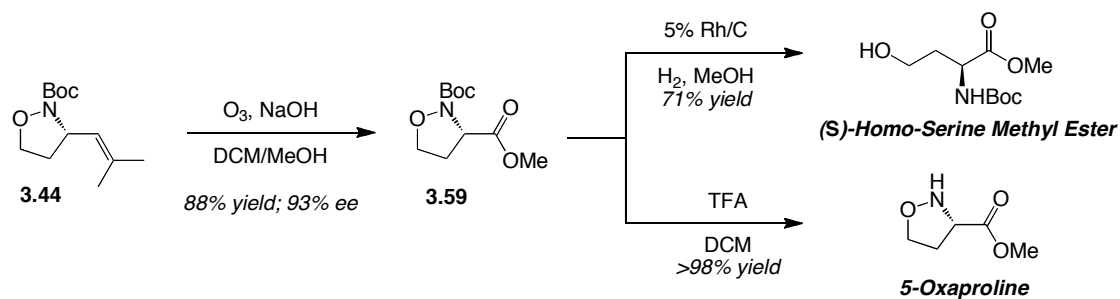
entry		R =	R' =	n =	catalyst	time (h)	product	% yield ^b	% ee ^c
1	3.53	Me	H	1	A	18	3.56	99	98
2	3.28	-CH ₂ (CH ₂) ₃ CH ₂ -	H	1	A	18	3.29	75	99
3	3.54	Me	Me	1	A	18	3.57	99 ^d	40/97
4	3.55	Me	H	2	A ^e	60	3.58	66	20
5		Me	H	2	B	60		94	87
6		Me	H	2	C	60		36	45

^a Reaction Conditions: A = 3 mol% dppm(AuCl)₂, 6 mol% (*S*)-AgTriP, 0.1 M in toluene, 23 °C, 18 h; B = 3 mol% (*S,S*)-DIPAMP(AuCl)₂, 6 mol% (*S*)-AgTriP, 0.1 M in toluene, 23 °C, 18 h; C = 3 mol% (*S,S*)-DIPAMP(AuCl)₂, 6 mol% (*R*)-AgTriP, 0.1 M in toluene, 23 °C, 18 h. ^b Isolated yield after column chromatography. ^c Determined by HPLC. ^d 5:1 dr. ^e 60 h.

Substrate Functionalization

Finally, we also showed that the products of our methodology could be easily modified for further use and transformed into unnatural amino acids. The Boc protecting group on these heterocycles can be easily deprotected using standard protocols allowing functionalization of the amine. Alternatively, the pendant alkene provided an additional handle for oxidative transformations. For instance, ozonolytic cleavage yielded **3.59** with 93% ee (Scheme 3.2). Furthermore, the N-O bond was reductively cleaved to yield the methyl ester of homo-serine.²⁰ The absolute configuration of **3.44** was assigned by Boc deprotection of **3.59** and Cbz protection to form (*S*)-methyl-2-benzyloxycarbonyl-3-isoxazolidinecarboxylate. The absolute configurations of the remaining hydroamination products were assigned by analogy to **3.44**.

Scheme 3.2. Synthesis of Unnatural Amino Acid Derivatives.



Conclusion

In summary, we have developed a series of enantioselective gold(I)-catalyzed hydroaminations and hydroalkoxylations of allenes with hydroxylamines and hydrazines. While chiral biarylphosphinegold(I) are suitable catalysts for the enantioselective addition of nitrogen nucleophiles to allenes, the addition of oxygen nucleophiles requires the use of chiral anions. These complementary methods allow rapid access to chiral vinyl isoxolidines, oxazines, and differentially protected pyrazolidines. Studies on the mechanism of enantioinduction in these transformations are ongoing in our laboratories.

Experimental

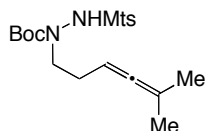
General Information

Unless otherwise noted commercial materials were used without further purification. Dichloromethane (DCM), toluene, and nitromethane (MeNO₂) utilized in gold(I)-catalyzed reactions was used as received from Aldrich Chemical Company. Gold(I)-catalyzed reactions were conducted in two dram vials equipped with a magnetic stir bar, fitted with a threaded cap, and protected from ambient light. All other reactions were conducted in flame-dried glassware under an inert (N₂) atmosphere with magnetic stirring and dried solvent. Solvents were dried by passage through an activated alumina column under nitrogen. Silver *p*-nitrobenzoate was prepared according to the method of Rubottom.²¹ Chiral gold(I) chloride complexes and phosphinegold(I)-bis-*p*-nitrobenzoate complexes were prepared according to procedures previously described by our group.^{22,2a} (*S*)-AgTriP was prepared according to procedures previously described by our group. Allenic alcohols were prepared by the method described by Widenhoefer,²³ and Landor.²⁴ *tert*-Butyltriisopropylsilyloxycarbamate was prepared according to the method of Mioskowski.²⁵ Thin-layer chromatography (TLC) analysis was performed using Merck silica gel 60 F254 TLC plates, and visualized by staining with I₂, UV, anisaldehyde, and/or permanganate. Flash column chromatography was carried out on Merck 60 silica gel (32-63 μm). ¹H and ¹³C NMR spectra were recorded with Bruker AVB-400, AVQ-400, DRX-500, and AV-600 spectrometers and chemical shifts are reported in ppm, relative to CHCl₃ (7.26 ppm for ¹H, and 77.23 ppm for ¹³C), unless otherwise noted. Enantiomeric excess was determined on a Shimadzu VP Series Chiral HPLC, using the Chiral PAK AD-H, Chiral PAK OD-H, or Regis Technologies WHELK-O 1 columns, eluting with a flow-rate of 1 mL/min. Mass spectral and analytical data were obtained via the Micro-Mass/Analytical Facility operated by the College of Chemistry, University of California, Berkeley.

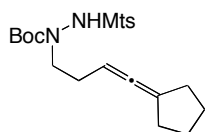
General Procedure for the Preparation of Hydrazine Substrates

To a solution of homo-allenic alcohol (1 equiv) and triethylamine (1.5 equiv) in DCM (1 M) at 0 °C was added methane sulfonyl chloride (1.2 equiv). The solution was stirred at 0 °C for 30 min or until TLC showed complete conversion. The solution was poured onto a 1:1 mixture of sat. aq. NaHCO₃ and brine, and extracted with DCM (3 x). The combined organics were washed with a 1:1 mixture of sat. aq. NaHCO₃ and brine, dried (MgSO₄) and concentrated. To a suspension of NaH (1.1 equiv) in dry DMF (1 M) was added a solution of N-(*tert*-butoxycarbonylamino)phthalimide (1.0 equiv) in dry DMF (1 M) at 0 °C. The mixture was stirred at 23 °C until gas evolution ceased. The solution was cooled to 0 °C before a solution of the crude mesylate in dry DMF (1 M) was transferred via cannula. The resulting solution was stirred at 80 °C overnight, before the mixture was quenched on sat. aq. NH₄Cl, and extracted with Et₂O (4 x). The combined organics were washed with water (4 x), dried (MgSO₄) and concentrated. The crude oil was purified by column chromatography (0-5% EtOAc/Hex). A

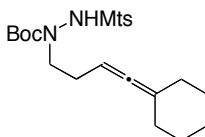
solution of the homo-allenic hydrazine in DCM (0.6 M) at 0 °C was treated with hydrazine (1 equiv, 60% in water). The solution was stirred at 23 °C for 4 h during which time a white precipitate formed. The mixture was filtered, washed with DCM (3 x), dried (Na₂SO₄) and concentrated. To solution of the crude hydrazine (1 equiv), and triethylamine (1.5 equiv) in DCM (0.5 M) was added metisylene chloride (1.2 equiv) and dimethylaminopyridine (DMAP) (0.1 equiv). The solution was diluted with sat. aq. NaHCO₃, extracted with DCM (3 x), dried (MgSO₄) and concentrated. Purification by column chromatography yielded the desired hydrazine substrates.



tert-Butyl 2-(mesitylsulfonyl)-1-(5-methylhexa-3,4-dienyl)hydrazinecarboxylate 3.24. The crude mixture was purified by flash column chromatography (0-10% EtOAc/Hexanes) to afford **3.24** as a clear oil. ¹H NMR shows a mixture of rotational isomers ¹H NMR (600 MHz): δ 6.93 (s, 2H), 5.04 (m, 0.3H), 4.80 (m, 0.7H), 3.64-3.49 (br s, 2H), 2.63 (s, 6H), 2.27 (s, 3H), 2.21 (q, *J* = 6.9 Hz, 1.5H), 1.89 (q, *J* = 7.2 Hz, 0.5H), 1.67 (s, 6H), 1.17 (s, 9H) ppm. ¹³C NMR (150 MHz): δ 202.6, 142.9, 140.9, 131.7, 123.4, 95.4, 85.1, 82.0, 27.67, 27.66, 25.6, 25.0, 23.4, 20.9, 20.5, 17.7 ppm. HRMS (ESI) calcd. for [C₂₁H₃₂O₄N₂NaS]⁺: *m/z* 431.1975, found 431.1976.



tert-Butyl 1-(4-cyclopentylidenebut-3-enyl)-2-(mesitylsulfonyl)hydrazine carboxylate 3.32. The crude mixture was purified by flash column chromatography (2-8% EtOAc/Hexanes) to afford **3.32** as a clear oil: ¹H NMR (600 MHz): δ 6.93 (s, 2H), 4.94-4.90 (m, 1H), 3.65-3.54 (br s, 2H), 2.63 (s, 3H), 2.35-2.19 (m, 10H), 1.68-1.57 (m, 5H), 1.19 (s, 9H) ppm. ¹³C NMR (150 MHz): δ 199.2, 142.9, 140.9, 131.7, 102.8, 85.0, 82.0, 31.4, 27.66, 27.61, 27.4, 26.1, 23.4, 20.9 ppm. HRMS (ESI) calcd. for [C₂₃H₃₄O₄N₂NaS]⁺: *m/z* 457.2131, found 457.2126.

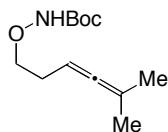


tert-Butyl 1-(4-cyclohexylidenebut-3-enyl)-2-(mesitylsulfonyl)hydrazine carboxylate 3.33. The crude mixture was purified by flash column chromatography (2-8% EtOAc/Hexanes) to afford **3.33** as a clear oil: ¹H NMR (600 MHz): δ 6.92 (s, 2H), 4.81 (t, *J* = 6.9 Hz, 1H), 3.61-3.57 (br s, 2H), 2.64 (s, 6H), 2.33-2.22 (m, 6H), 2.13-2.03 (m, 4H), 1.53-1.46 (m, 6H), 1.20 (s, 9H)

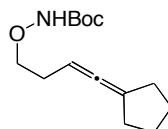
ppm. ppm. ^{13}C NMR (150 MHz): δ 198.1, 142.9, 140.9, 131.7, 104.0, 87.7, 81.9, 31.1, 27.7, 27.0, 23.4, 20.9 ppm. HRMS (ESI) calcd. for $[\text{C}_{24}\text{H}_{36}\text{O}_4\text{N}_2\text{NaS}]^+$: m/z 471.2288, found 471.2287.

General Procedure for the Preparation of *O*-Linked Hydroxylamine Substrates^{4a,26}

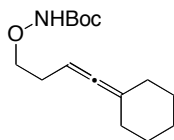
The corresponding alcohol was added to a stirring solution of PPh_3 and DEAD in THF (0.15 M in alcohol). The reaction mixture was stirred at 0 °C for 30 min before *N*-hydroxyphthalimide was added in one portion. The solution turned dark orange immediately upon addition. The reaction mixture was stirred at room temperature for 6 h, after which time, the reaction mixture was concentrated to afford a thick yellow oil. The crude oil was passed through a silica pad, eluting with 1:9 EtOAc:hexanes. The solution was concentrated and the crude product was redissolved in CH_2Cl_2 (15 mL) and $\text{NH}_2\text{NH}_2 \cdot \text{H}_2\text{O}$ (2.0 equiv) was added dropwise. The mixture was stirred overnight at room temperature and white precipitants were removed by filtration. Concentration of the organics afforded the deprotected hydroxylamine as a pale yellow oil. The oil was dissolved in 1:4 THF: H_2O (10 mL) and NaHCO_3 (1.5 equiv) and di-*tert*-butyl dicarbonate (1.2 equiv) was added. The biphasic solution was stirred vigorously at room temperature for 5 h, before it was diluted with Et_2O and extracted with brine (10 mL). The organic layer was dried with Na_2SO_4 , concentrated to provide the crude product.



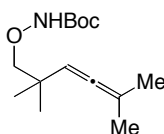
***tert*-Butyl 5-methylhexa-3,4-dienyloxycarbamate 3.35.** The crude mixture was purified by flash column chromatography (0-10% EtOAc/Hexanes) to afford **3.35** as a clear oil. ^1H NMR (400 MHz): δ 7.13 (s, 1H), 4.99 (m, 1H), 3.93 (t, $J = 7.0$ Hz, 2H), 2.33 (q, $J = 6.9$ Hz, 2H), 1.72 (s, 3H), 1.71 (s, 3H), 1.53 (s, 9H). ^{13}C NMR (150 MHz): δ 202.4, 156.9, 95.6, 84.5, 81.6, 76.0, 28.2, 27.9, 20.6 ppm. HRMS (FAB) calcd. for $[\text{C}_{12}\text{H}_{21}\text{O}_3\text{NNa}]^+$: m/z 250.1414, found 250.1409.



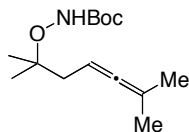
***tert*-Butyl 4-cyclopentylidenebut-3-enyloxycarbamate 3.36.** The crude oil was purified by column chromatography (1:24 EtOAc:hexanes) to yield **3.36** as a clear oil (0.40 g, 1.58 mmol, 42% yield overall). ^1H NMR (400 MHz): δ 7.12 (bs, 1 H), 5.08-5.03 (m, 1H), 3.89 (t, 2H, $J = 6.8$ Hz), 2.33-2.28 (m, 6H), 1.67-1.63 (m, 4H), 1.48 (s, 9H) ppm. ^{13}C NMR (100 MHz): δ 197.7, 156.9, 104.2, 87.0, 81.6, 76.0, 31.2, 28.2, 28.1, 27.0 ppm. HRMS (FAB) calcd. for $[\text{C}_{14}\text{H}_{23}\text{O}_3\text{N}]^+$: m/z 253.1678, found 253.1672.



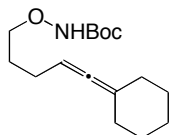
tert-Butyl 4-cyclohexylidenebut-3-enyloxycarbamate 3.26. The crude oil was purified by column chromatography (1:24 EtOAc:hexanes) to yield **3.26** as a clear oil (0.438 g, 1.63 mmol, 86% yield overall). ^1H NMR (400 MHz): δ 7.12 (br s, 1H), 4.97-4.93 (m, 1H), 3.89 (t, 2H, $J = 6.8$ Hz), 2.30 (q, 2H, $J = 6.8$ Hz), 2.09-2.07 (m, 4H), 1.60-1.55 (m, 6H), 1.48 (s, 9H) ppm. ^{13}C NMR (100 MHz): δ 199.0, 156.9, 103.0, 84.3, 81.6, 76.0, 31.6, 28.2, 28.1, 27.4, 26.1 ppm. HRMS (FAB) calcd. for $[\text{C}_{15}\text{H}_{25}\text{O}_3\text{N}]^+$: m/z 267.1834, found 267.1827.



tert-Butyl 2,2,5-trimethylhexa-3,4-dienyloxycarbamate 3.38. The crude oil was purified by flash chromatography, eluting with 1:24 EtOAc: hexanes to provide **3.38** as a clear oil (0.38 g, 1.48 mmol, 8% yield overall). ^1H NMR (500 MHz): δ 7.16 (br s, 1H), 4.95 (m, 1H), 3.63 (s, 2H), 1.68 (d, 6H, $J = 3.0$ Hz), 1.48 (s, 9H), 1.04 (s, 6H) ppm. ^{13}C NMR (500 MHz): δ 200.1, 156.7, 97.2, 96.7, 85.8, 81.5, 35.9, 28.2, 25.1, 20.7 ppm. HRMS (ESI) calcd. for $[\text{C}_{14}\text{H}_{23}\text{O}_3\text{N}+\text{Na}]^+$: m/z 278.1727, found 278.1726.

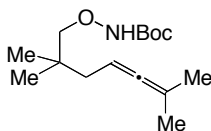


tert-Butyl 2,6-dimethylhepta-4,5-dien-2-yloxycarbamate 3.37. The crude oil was purified by column chromatography (3:97 EtOAc:hexanes) to yield **3.37** as a clear oil (0.45 g, 1.76 mmol, 10% yield overall). ^1H NMR (500 MHz): δ 6.70 (br s, 1H), 4.94 (m, 1H), 2.18 (d, 2H, $J = 7.5$ Hz), 1.67 (d, 6H, $J = 3.0$ Hz), 1.47 (s, 9H), 1.22 (s, 6H), ppm. ^{13}C NMR (125 MHz): δ 203.5, 157.5, 94.3, 84.2, 82.9, 81.3, 39.3, 28.2, 23.9, 20.5 ppm. HRMS (ESI) calcd. for $[\text{C}_{14}\text{H}_{25}\text{O}_3\text{N}+\text{Na}]^+$: m/z 278.1727, found 278.1727.

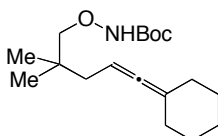


tert-Butyl 5-cyclohexylidenepent-4-enyloxycarbamate 3.39. The crude oil following protection with Boc_2O was purified by column chromatography (1:24 EtOAc:hexanes) to yield **3.39** as a

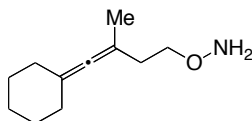
clear oil (0.57 g, 2.03 mmol, 34% yield overall). ^1H NMR (400 MHz): δ 7.10 (br s, 1H), 4.99-4.96 (m, 1H), 3.89-3.86 (t, 2H, $J = 6.8$ Hz), 2.09-2.01 (m, 6H), 1.76-1.69 (q, 2H, $J = 6.8$ Hz), 1.63-1.50 (m, 6H), 1.48 (s, 9H) ppm. ^{13}C NMR (100 MHz): δ 198.3, 176.0, 156.9, 103.1, 96.7, 87.9, 76.2, 31.7, 28.2, 27.4, 27.2, 26.1, 25.4 ppm. HRMS (EI) calcd. for $[\text{C}_{16}\text{H}_{27}\text{O}_3\text{N}+\text{Na}]^+$: m/z 304.1883, found 304.1890.



tert-Butyl 2,2,6-trimethylhepta-4,5-dienyloxycarbamate 3.41. The crude oil was purified by column chromatography (1:24 EtOAc:hexanes) to yield **3.41** as a clear oil (0.87 g, 3.2 mmol, 41% yield overall). ^1H NMR (500 MHz): δ 7.11 (br s, 1H), 0.93 (s, 6H), 4.90 (m, 1H), 3.16 (s, 2H), 1.93 (d, 2H, $J = 8.0$ Hz), 1.66 (d, 6H, $J = 2.5$ Hz), 1.48 (s, 9H) ppm. ^{13}C NMR (125 MHz): δ 203.4, 157.0, 93.5, 85.1, 84.4, 81.4, 39.4, 34.8, 28.2, 24.1, 20.1 ppm. HRMS (ESI) calcd. for $[\text{C}_{15}\text{H}_{27}\text{O}_3\text{N}+\text{Na}]^+$: m/z 292.1883 found 292.1884.



tert-Butyl 5-cyclohexylidene-2,2-dimethylpent-4-enyloxycarbamate 3.40. The crude oil was purified by column chromatography (1:49 EtOAc:hexanes) to yield **3.40** as a clear oil (0.866 g, 2.8 mmol, 33% yield overall). ^1H NMR (400 MHz): δ 7.10 (br s, 1H), 4.92 (m, 1H), 3.61 (s, 2H), 2.10-2.07 (m, 4H), 1.95 (d, 2H, $J = 7.6$ Hz), 1.62-1.56 (m, 2H), 1.55-1.48 (m, 4H), 1.48 (s, 9H), 0.94 (s, 6H) ppm. ^{13}C NMR (100 MHz): δ 200.2, 156.9, 101.0, 85.2, 84.4, 81.5, 39.8, 34.9, 31.7, 28.3, 27.4, 26.2, 24.1 ppm. HRMS (ESI) calcd. for $[\text{C}_{18}\text{H}_{31}\text{O}_3\text{N}+\text{Na}]^+$: m/z 332.2196 found 332.2197.

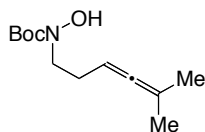


O-(4-Cyclohexylidene-3-methylbut-3-enyl)hydroxylamine 3.51b. 2-(4-Cyclohexylidene-3-methylbut-3-enyloxy)isoindoline-1,3-dione (0.64 g, 2.06 mmol) was dissolved in CH_2Cl_2 (10 mL) and $\text{NH}_2\text{NH}_2 \cdot \text{H}_2\text{O}$ (0.20 mL, 4.11 mmol) was added to the solution. The reaction mixture was stirred at room temperature for 16 h, and white precipitants appear. The reaction mixture was filtered and concentrated. The crude mixture was purified by column chromatography (1:9 EtOAc:hexanes) to yield a **3.51b** clear oil (0.24 g, 65% yield). ^1H NMR (400 MHz): δ 5.36 (br s, 2H), 3.75 (t, 2H, $J = 7.2$ Hz), 2.20 (t, 2H, $J = 7.2$ Hz), 2.08-2.05 (m, 4H), 1.68 (s, 3H), 1.59-

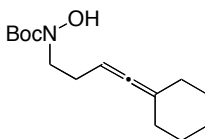
1.49 (m, 6H) ppm. ^{13}C NMR (100 MHz): δ 195.5, 102.1, 93.2, 74.4, 33.0, 32.0, 27.8, 26.3, 20.1 ppm. HRMS (EI) calcd. for $[\text{C}_{11}\text{H}_{19}\text{O}_1\text{N}+\text{H}]^+$: m/z 182.1539, found 182.1545.

General Procedure for the Preparation of *N*-Linked Hydroxylamine Substrates

To a solution of allenic or homo-allenic alcohol (1 equiv) and triethylamine (1.5 equiv) in DCM (1 M) at 0 °C was added methane sulfonyl chloride (1.2 equiv). The solution was stirred at 0 °C for 30 min or until TLC showed complete conversion. The solution was poured onto a 1:1 mixture of sat. aq. NaHCO_3 and brine, and extracted with DCM (3 x). The combined organics were washed with a 1:1 mixture of sat. aq. NaHCO_3 and brine, dried (MgSO_4) and concentrated. To a suspension of NaH (1.1 equiv) in dry DMF (1 M) was added a solution of *tert*-butyltriisopropylsilyloxycarbamate in dry DMF (1 M) at 0 °C. The mixture was stirred at 23 °C until gas evolution ceased. The solution was cooled to 0 °C before a solution of the crude mesylate in dry DMF (1 M) was transferred via cannula. The resulting solution was stirred at 23 °C overnight, before the mixture was quenched on sat. aq. NH_4Cl , and extracted with Et_2O (4 x). The combined organics were washed with water (4 x), dried (MgSO_4) and concentrated. The crude oil was purified by column chromatography (0-5% EtOAc/Hex). A solution of the TIPS protected hydroxyl amine in THF (0.6 M) at 0 °C was treated with TBAF (1 equiv, 1 M in THF). The solution was stirred at 23 °C for 4 h or until TLC showed complete conversion. The mixture was quenched on sat. aq. NH_4Cl , and extracted with EtOAc (3 x), dried (MgSO_4) and concentrated. Purification by column chromatography yielded the desired hydroxylamine substrates.

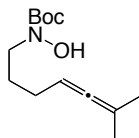


***tert*-Butyl hydroxy(5-methylhexa-3,4-dienyl)carbamate 3.53.** The crude mixture was purified by flash column chromatography (5-20% EtOAc/Hexanes) to afford **3.53** as a clear oil: ^1H NMR (400 MHz): δ 6.23 (br s, 1H), 4.97-4.94 (m, 1H), 3.58 (t, $J = 7.1$ Hz, 2H), 2.31 (q, $J = 7.1$ Hz, 2H), 1.72 (s, 3H), 1.71 (s, 3H), 1.53 (s, 9H). ^{13}C NMR (150 MHz): δ 202.4, 157.0, 95.5, 85.4, 81.6, 49.9, 28.3, 26.9, 20.5 ppm. HRMS (FAB) calcd. for $[\text{C}_{12}\text{H}_{21}\text{O}_3\text{NLi}_2]^+$: m/z 241.1841, found 2241.1808.

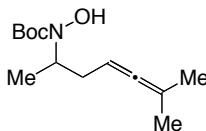


***tert*-Butyl 4-cyclohexylidenebut-3-enyl(hydroxy)carbamate 3.28.** The crude mixture was purified by flash column chromatography (10-20% EtOAc/Hexanes) to afford **3.28** as a clear oil: ^1H NMR (300 MHz): δ 6.13-6.07 (m, 1H), 4.93 (m, 1H), 3.53 (t, $J = 7.2$ Hz, 2H), 2.28-2.26 (q, J

= 9.2 Hz, 2H), 2.09-2.06 (m, 4H), 1.58-1.54 (m, 6H), 1.48 (s, 9H) ppm. ^{13}C NMR (150 MHz): δ 199.0, 156.9, 103.0, 85.2, 81.7, 49.8, 31.6, 28.3, 27.4, 27.1, 26.1 ppm. HRMS (FAB) calcd. for $[\text{C}_{15}\text{H}_{25}\text{O}_3\text{NLi}_2]^+$: m/z 281.2154, found 281.2109.



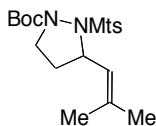
tert-Butyl hydroxy(6-methylhepta-4,5-dienyl)carbamate 3.55. The crude mixture was purified by flash column chromatography (5-20% EtOAc/Hexanes) to afford **3.55** as a clear oil: ^1H NMR (600 MHz): δ 7.50 (s, 1H), 4.95 (td, $J = 6.1, 3.0$ Hz, 1H), 3.49 (t, $J = 7.0$ Hz, 2H), 1.96 (q, $J = 6.9$ Hz, 2H), 1.71 (quintet, $J = 7.2$ Hz, 2H), 1.67 (s, 3H), 1.66 (s, 3H), 1.46 (s, 9H). ^{13}C NMR (150 MHz): δ 201.7, 157.1, 95.5, 88.0, 81.6, 49.7, 28.3, 26.4, 26.1, 20.7 ppm. HRMS (FAB) calcd. for $[\text{C}_{13}\text{H}_{23}\text{O}_3\text{NLi}_2]^+$: m/z 255.1998, found 255.1956.



tert-Butyl hydroxy(6-methylhepta-4,5-dien-2-yl)carbamate 3.54. The crude mixture was purified by flash column chromatography (10-15% EtOAc/Hexanes) to afford **3.54** as a clear oil: ^1H NMR (600 MHz): δ 6.11 (br s, 1H), 4.90-4.87 (m, 1H), 4.09-4.05 (m, 1H), 2.31 (dt, $J = 14.2, 7.9$ Hz, 1H), 2.08 (dt, $J = 13.9, 6.8$ Hz, 1H), 1.67 (dd, $J = 6.3, 2.8$ Hz, 6H), 1.48 (s, 9H), 1.20 (t, $J = 5.9$ Hz, 3H). ^{13}C NMR (150 MHz): δ 202.6, 156.9, 95.1, 85.6, 81.6, 54.8, 33.7, 28.3, 20.6, 20.3, 17.0 ppm. HRMS (FAB) calcd. for $[\text{C}_{13}\text{H}_{22}\text{O}_3\text{NLi}_2]^+$: m/z 254.1920, found 254.1919.

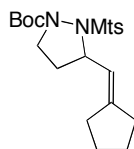
General Procedure A for Au(I)-Catalyzed Hydroamination

To a solution of allene (1 equiv) in the specified solvent was added the appropriate gold(I) complex (3-5 mol%). The resulting homogeneous mixture was protected from ambient light and left to stir at the indicated temperature (23° - 65° C). Upon completion, as judged by TLC analysis of the reaction mixture, the solution was loaded directly onto a silica gel column. Purification by column chromatography afforded the desired cyclized product.



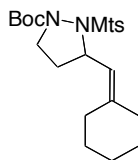
tert-Butyl 2-(mesitylsulfonyl)-3-(2-methylprop-1-enyl)pyrazolidine-1-carboxylate 3.25.

Following general procedure A, allene **3.24** (15 mg, 34 μmol), (*R*)-DTBM-Segphos(AuOPNB)₂ (3.2 mg, 1.7 μmol), and MeNO₂ (0.300 mL) was added and the mixture was stirred at 50 °C for 15 h. The crude mixture was purified by flash column chromatography (0-6% EtOAc/Hexanes) to afford **3.25** as a clear oil (10 mg, 66% yield, 98% ee): ¹H NMR (600 MHz): δ 6.92 (s, 2H), 5.13 (td, *J* = 8.2, 3.1 Hz, 1H), 4.91 (d, *J* = 8.6 Hz, 1H), 4.03 (ddd, *J* = 10.6, 8.9, 5.8 Hz, 1H), 3.59 (ddd, *J* = 10.6, 9.6, 5.8 Hz, 1H), 2.62 (s, 6H), 2.55-2.49 (m, 1H), 2.29 (s, 3H), 1.83 (td, *J* = 6.0, 3.0 Hz, 1H), 1.78 (s, 3H), 1.70 (s, 3H), 1.09 (s, 9H) ppm. ¹³C NMR (100 MHz): δ 156.8, 142.9, 142.1, 135.9, 131.4, 130.9, 123.5, 81.0, 56.8, 47.6, 33.5, 27.5, 25.6, 22.9, 20.9, 18.3 ppm. HRMS (ESI) calcd. for [C₂₁H₃₂O₄N₂NaS]⁺: *m/z* 431.1975, found 431.1978. HPLC Regis Technologies Whelk-O 1 column (99:1 Hex:isopropanol; 1 mL/min) *t_R* 20.2min (major), 26.8 min (minor): 98% ee.



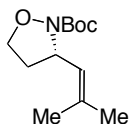
tert-Butyl 3-(cyclopentylidenemethyl)-2-(mesitylsulfonyl)pyrazolidine-1-carboxylate 3.42.

Following general procedure A, allene **3.32** (50 mg, 115 μmol), (*R*)-DTBM-Segphos(AuOPNB)₂ (10.6 mg, 5.6 μmol), and MeNO₂ (0.380 mL) was added and the mixture was stirred at 50 °C for 15 h. The crude mixture was purified by flash column chromatography (0-7% EtOAc/Hexanes) to afford **3.42** as a clear oil (30 mg, 60% yeild, 90% ee). ¹H NMR (400 MHz) δ 6.96 (s, 2H), 5.10-5.05 (m, 2H), 4.11-4.05 (m, 1H), 3.62 (ddd, *J* = 10.8, 9.2, 6.3 Hz, 1H), 2.66 (s, 6H), 2.58-2.51 (m, 2H), 2.33 (s, 3H), 2.28-2.24 (t, 2H, *J* = 7.6 Hz), 1.91-1.85 (m, 1H), 1.78-1.71 (m, 2H), 1.66 (quintet, *J* = 6.7 Hz, 3H), 1.13 (s, 9H) ppm. ¹³C NMR (101 MHz): δ 156.8, 147.6, 142.9, 142.1, 131.4, 131.0, 119.0, 81.1, 76.7, 58.3, 47.7, 33.8, 33.3, 29.0, 27.6, 26.38, 26.19, 23.0, 21.0 ppm. HRMS (ESI) calcd. for [C₂₃H₃₄O₄N₂NaS]⁺: *m/z* 457.2131, found 457.2132. HPLC Regis Technologies Whelk-O 1 column (98:2 hexanes:isopropanol; 1 mL/min) *t_R* 18.8 min (major), 24.9 min (minor): 90% ee.



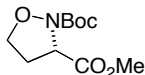
tert-Butyl 3-(cyclohexylidenemethyl)-2-(mesitylsulfonyl)pyrazolidine-1-carboxylate 3.43.

Following general procedure A, allene **3.33** (50 mg, 111 μmol), (*R*)-DTBM-Segphos(AuOPNB)₂ (10.6 mg, 5.6 μmol), and MeNO₂ (0.375 mL) was added and the mixture was stirred at 50 °C for 15 h. The crude mixture was purified by flash column chromatography (0-9% EtOAc/Hexanes) to afford **3.43** as a clear oil (38 mg, 76% yield, 97% ee). ¹H NMR (400 MHz): δ 6.96 (s, 2H), 5.23 (td, *J* = 8.2, 3.0 Hz, 1H), 4.87 (d, *J* = 8.7 Hz, 1H), 4.12-4.06 (m, 1H), 3.64 (ddd, *J* = 10.8, 9.5, 5.7 Hz, 1H), 2.67 (s, 6H), 2.61-2.52 (m, 1H), 2.46-2.41 (m, 1H), 2.33 (s, 3H), 2.27-2.21 (m, 1H), 2.08 (d, *J* = 2.0 Hz, 2H), 1.88 (dddd, *J* = 12.0, 8.9, 5.8, 3.0 Hz, 1H), 1.62-1.52 (m, 6H), 1.13 (s, 9H); ¹³C NMR (101 MHz): δ 156.9, 144.0, 142.1, 131.4, 131.0, 120.1, 81.09, 81.09, 77.27, 55.93, 47.62, 37.0, 33.7, 29.3, 28.5, 27.6, 26.6, 23.1, 21.0. HRMS (ESI) calcd. for [C₂₄H₃₆O₄N₂NaS]⁺: *m/z* 471.2288, found 471.2282. HPLC Regis Technologies Whelk-O 1 column (98:2 hexanes:Ethanol; 1 mL/min) *t_R* 19.8 min (major), 25.8 min (minor): 97% ee.

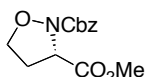


tert-Butyl 3-(2-methylprop-1-enyl)isoxazolidine-2-carboxylate 3.44. Following general procedure A, allene **3.35** (159 mg, 700 μmol), (*R*)-xylyl-BINAP(AuOPNB)₂ (30 mg, 21 μmol), and CH₂Cl₂ (1.4 mL) was added and the mixture was stirred at room temperature for 24 h. The crude mixture was purified by column chromatography (5-12.5% EtOAc/hexanes) to afford **3.44** as a clear oil (145 mg, 91% yield, 93% ee): ¹H NMR (600 MHz): δ 5.18 (dd, *J* = 9.1, 0.9 Hz, 1H), 4.83 (td, *J* = 8.7, 5.1 Hz, 1H), 4.09-4.05 (m, 1H), 3.74 (q, *J* = 8.0 Hz, 1H), 2.45 (dtd, *J* = 11.8, 7.9, 4.0 Hz, 1H), 1.95 (dtd, *J* = 12.4, 8.1, 4.6 Hz, 1H), 1.72 (s, 3H), 1.70 (s, 3H), 1.46 (s, 9H) ppm. ¹³C NMR (150 MHz): δ 157.3, 134.0, 125.2, 81.6, 68.7, 57.1, 36.1, 28.2, 25.6, 17.9 ppm. HRMS (FAB) calcd. for [C₁₂H₂₁O₃NNa]⁺: *m/z* 250.1414, found 250.1409. HPLC Regis Technologies Whelk-O 1 column (98:2 Hexanes:Ethanol; 1 mL/min) *t_R* 11.9 min (minor), 12.6 min (major): 93% ee.

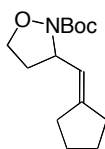
Determination of Absolute Stereochemistry



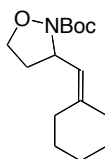
2-tert-Butyl 3-methyl isoxazolidine-2,3-dicarboxylate 3.59. To a solution of isoxazolidine **3.44** (100 mg, 0.238 mmol) in CH₂Cl₂ (2.4 mL) was added a solution of NaOH in MeOH (1.2 mL, 3.06 mmol, 2.5 M). The resulting mixture was cooled to -78 °C and O₃ was bubbled through continuously. After approximately 10 min the initially pale yellow solution took on the characteristic blue color of ozone and a yellow precipitate was observed. The reaction mixture was diluted with H₂O (4 mL) and Et₂O (4 mL) and warmed to rt. The aqueous layer was extracted with Et₂O (4 x 20 mL), the combined organic extracts were washed with brine (10 mL), dried over MgSO₄, filtered, and concentrated. The crude mixture was purified by flash column chromatography (20-30% EtOAc/hexanes) to afford **3.59** as a clear oil (70 mg, 0.3 mmol, 68% yield, 93% ee). ¹H NMR (600 MHz): δ 4.71 (dd, *J* = 9.4, 4.8 Hz, 1H), 4.13 (td, *J* = 7.9, 4.4 Hz, 1H), 3.80 (q, *J* = 7.9 Hz, 1H), 3.77 (s, 3H), 2.60 (dddd, *J* = 12.3, 9.3, 7.6, 4.5 Hz, 1H), 2.47 (dtd, *J* = 12.5, 7.9, 4.7 Hz, 1H), 1.47 (s, 9H) ppm. ¹³C NMR (150 MHz): δ 171.2, 156.0, 82.7, 68.4, 59.5, 52.6, 32.8, 28.1 ppm. HRMS (FAB) calcd. for [C₁₀H₁₇O₅N]⁺: *m/z* 231.1107, found 231.1109. HPLC Chiralpak AS column (90:10 hexanes:isopropanol, 1 mL/min) *t_R* 8.1 min (minor), 9.4 min (major): 93% ee.



(S)-Methyl-2-benzyloxycarbonyl-3-isoxazolidinecarboxylate. Trifluoroacetic acid (0.25 mL) was added to a solution of methyl ester **3.59** (25 mg, 0.11 mmol) in DCM cooled to 0 °C. The resulting mixture was stirred at 0 °C for 40 min before concentrating to a yellow oil. The oily residue was dissolved in THF (0.2 mL), then, water (0.2 mL), and sodium carbonate (30 mg, 0.275 mmol 2.5 equiv) were added. The solution was cooled to 0 °C and benzyl chloroformate (20 uL, 0.13 mmol, 1.2 equiv) was added. The solution was stirred at 0 °C for 30 min, poured onto sat. aq. NaHCO₃ (10 mL), extracted with EtOAc (3 x 10 mL), dried (MgSO₄) and concentrated to yield an oily residue. The crude mixture was purified by flash column chromatography (25-40% EtOAc/hexanes) to afford the title compound as a clear oil (24 mg, 0.09 mmol, 82% yield): ¹H NMR (600 MHz): δ 7.38-7.30 (m, 5H), 5.21 (m, 2H), 4.78 (dd, *J* = 9.4, 4.9 Hz, 1H), 4.16 (td, *J* = 7.9, 4.3 Hz, 1H), 3.82 (q, *J* = 7.8 Hz, 1H), 3.75 (s, 3H), 2.65-2.60 (m, 1H), 2.50 (dtd, *J* = 12.4, 8.1, 4.6 Hz, 1H) ppm. ¹³C NMR (150 MHz): δ 170.8, 156.8, 135.5, 128.54, 128.39, 128.26, 68.9, 68.4, 59.5, 52.7, 32.9 ppm. [α]_D = -91.1 (c = 1.0, CHCl₃) (lit. -97.8 (c = 1.5, CHCl₃)). Spectral data are consistent with previously published literature values.²⁷

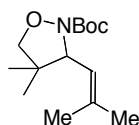


tert-Butyl 3-(cyclopentylidenemethyl)isoxazolidine-2-carboxylate 3.45. Following general procedure A, allene **3.36** (62.5 mg, 247 μmol), (*R*)-xylyl-BINAP(AuOPNB)₂ (10.8 mg, 5.9 μmol), and CH₂Cl₂ (0.6 mL) was added and the mixture was stirred at room temperature for 24 h. The crude mixture was purified by column chromatography (3:97 EtOAc:hexanes) to yield **3.45** as a clear oil (61.0 mg, 241 μmol , 98% yield, 91% ee). ¹H NMR (500 MHz): δ 5.31 (dt, 1H, *J* = 9, 2.5 Hz), 4.73 (dt, 1H, *J* = 5.0, 8.5 Hz), 4.07 (dt, 1H, *J* = 4.0, 8.0 Hz), 3.75 (q, 1H, *J* = 8.0 Hz), 2.49-2.43 (m, 2H), 2.33-2.17 (m, 3H), 2.01-1.95 (m, 1H), 1.71-1.67 (m, 2H), 1.66-1.62 (m, 2H), 1.48 (s, 9H) ppm. ¹³C NMR (125 MHz): δ 157.4, 145.9, 120.4, 81.6, 68.7, 58.5, 35.8, 33.6, 28.6, 28.2, 26.3, 26.1 ppm. HPLC Regis Technologies WHELK-O1 (98:2 hexanes:isopropanol; 1 mL/min): *t*_R 24.4 min (major), 25.8 min (minor). HRMS (FAB) calcd. for [C₁₄H₂₃O₃N]⁺: *m/z* 253.1678, found 253.1672.

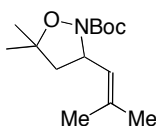


tert-Butyl 3-(cyclohexylidenemethyl)isoxazolidine-2-carboxylate 3.27. Following general procedure A, **3.26** (53.4 mg, 0.20 mmol), (*S*)-xylyl-BINAP(AuOPNB)₂ (8.8 mg, 0.006 mmol) and CH₂Cl₂ (0.60 mL) were combined and stirred for 24 h at room temperature. The crude oil was purified by column chromatography (1:24 EtOAc:hexanes) to yield a white solid (49.7 mg, 0.183 mmol, 93% yield, 99% ee): ¹H NMR (400 MHz): δ 5.14 (d, 1H, *J* = 8.8 Hz), 4.93-4.87 (m, 1H), 4.08 (sextet, 1H, *J* = 4.0 Hz), 4.74 (q, 1H, *J* = 8.0 Hz), 2.49-2.41 (m, 1H), 2.23 (t, 2H, *J* = 2.8 Hz), 2.07 (t, 2H, *J* = 2.8 Hz), 2.01-1.91 (m, 1H), 1.67-1.53 (m, 6H), 1.48 (s, 9H) ppm. ¹³C NMR (100 MHz): δ 157.4, 141.8, 122.2, 81.7, 68.7, 56.3, 36.8, 36.6, 29.0, 28.3, 28.3, 27.7, 26.7 ppm; HRMS (FAB) calcd. for [C₁₅H₂₅O₃N]⁺: *m/z* 267.1834, found 267.1827; HPLC Regis Technologies Whelk-O 1 column (99:1 hexanes:isopropanol; 1 mL/min) *t*_R 36.4 min (minor), 42.8 min (major): 99% ee. Results for other solvents are reported below:

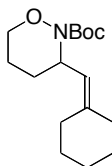
Solvent	Conversion	%ee
MeNO ₂	>98%	87%
Benzene	0%	--
Dioxane	0%	--



tert-Butyl 4,4-dimethyl-3-(2-methylprop-1-enyl)isoxazolidine-2-carboxylate 3.47. Following general procedure A, **3.38** (30.4 mg, 127 μmol), (*R*)-DM-MeOBIPHEP (AuOPNB)₂ (9.0 mg, 6.3 μmol), and MeNO₂ (1.2 mL) were combined and stirred at 50 °C for 24 h. The crude mixture was purified by column chromatography (1:99 EtOAc:DCM) to yield white crystals (22.2 mg, 73 % yield, 99% ee). ¹H NMR (500 MHz): δ 5.09 (d, 1H, *J* = 8.0 Hz), 4.31 (d, 1H, *J* = 8.0 Hz), 3.71 (d, 1H, *J* = 7.5 Hz), 3.65 (d, 1H, *J* = 7.5 Hz), 1.77 (s, 3H), 1.71 (s, 3H), 1.47 (s, 9H), 1.02 (s, 3H), 0.89 (s, 3H) ppm. ¹³C NMR (125 MHz): δ 156.8, 135.2, 121.4, 81.2, 79.9, 66.6, 46.3, 28.2, 25.9, 24.6, 21.1, 18.0 ppm. HPLC Chiralpak OD-H (99:1 hexanes:isopropanol; 1 mL/min) *t*_R 10.7 min (major), 13.2 min (minor). HRMS (ESI) calcd. for [C₁₄H₂₅O₃N+Na]⁺: *m/z* 278.1727, found 278.1726.

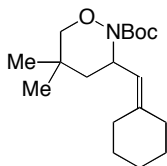


tert-Butyl 5,5-dimethyl-3-(2-methylprop-1-enyl)isoxazolidine-2-carboxylate 3.46. Following general procedure A, **3.37** (50.0 mg, 196 μmol), (*R*)-DM-MeOBIPHEP (AuOPNB)₂ (13.9 mg, 9.8 μmol), and MeNO₂ (0.65 mL) were combined and stirred at 50 °C for 24 h. The crude mixture was purified by column chromatography (1:99 EtOAc:DCM) to yield a clear oil (46.7 mg, 94% yield, 63% ee). ¹H NMR (400 MHz): δ 5.21 (d, 1H, *J* = 7.6 Hz), 4.89 (dd, 1H, *J* = 7.6, 8.4 Hz), 2.28 (dd, 1H, *J* = 8.4, 12.4 Hz), 1.77-1.74 (m, 1H), 1.74-1.70, (m, 6H), 1.48 (s, 9H), 1.39 (s, 3H), 1.19 (s, 3H) ppm. ¹³C NMR (125MHz): δ 157.5, 133.3, 125.6, 83.2, 81.0, 57.7, 48.0, 28.3, 25.6, 25.4, 24.8, 17.9 ppm. HPLC Regis Technologies WHELK-O1 column (99:1 hexanes:isopropanol; 1 mL/min): *t*_R 20.4 min (major), 27.8 min (minor). HRMS (ESI) calcd. for [C₁₄H₂₅O₃N+Na]⁺: *m/z* 278.1727, found 278.1727.



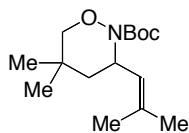
tert-Butyl 3-(cyclohexylidenemethyl)morpholine-2-carboxylate 3.48. Following general procedure A, **3.39** (50.0 mg, 178 μmol), (*R*)-xylyl-BINAP(AuOPNB)₂ (13.0 mg, 8.9 μmol), and MeNO₂ (0.60 mL) were combined and stirred at 65 °C for 24 h. The crude mixture was purified by column chromatography (1:99 EtOAc:CH₂Cl₂) to yield white solids (31.3 mg, 111 μmol , 63% yield, 89% ee). ¹H NMR (500 MHz): δ 5.69 (d, 1H, *J* = 8.8 Hz), 4.87 (t, 1H, *J* = 6.4 Hz), 4.07 (dd, 1H, *J* = 10.8, 4.0 Hz), 3.88 (dt, 1H, *J* = 2, 12.5 Hz), 2.21-2.02 (m, 5H), 1.92 (m, 1H), 1.66-1.47 (m, 8H), 1.47 (s, 9H) ppm. ¹³C NMR (125 MHz): δ 154.9, 142.1, 117.8, 81.0, 71.6, 36.9,

29.2, 28.5, 28.3, 27.8, 26.7, 20.4 ppm. HPLC Chiralpak AD-H column (99:1 hexanes:isopropanol, 1 mL/min) t_R 11.6 min (minor), 12.9 min (major): 89% ee. HRMS (FAB) calcd. for $[C_{16}H_{27}O_3N]^+$: m/z 281.1991, found 281.1983.

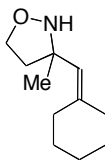


tert-Butyl 3-(cyclohexylidene)methyl-4,4-dimethylisoxazolidine-2-carboxylate 3.49.

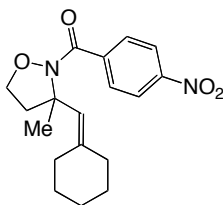
Following general procedure A, **3.40** (35.4 mg, 127 μ mol), (*R*)-DM-MeOBIPHEP (AuOPNB)₂ (9.0 mg, 6.3 μ mol), and MeNO₂ (1.2 mL) were combined and stirred at 50 °C for 24 h. The crude mixture was purified by column chromatography (1:99 EtOAc:DCM) to yield clear crystals (30.0 mg, 85 % yield, 89% ee). ¹H NMR (400 MHz): δ 5.04 (d, 1H, J = 9.6 Hz), 4.37 (d, 1H, J = 9.6 Hz), 3.72 (d, 1H, J = 7.6 Hz), 3.65 (d, 1H, J = 7.6 Hz), 2.29-2.19 (m, 1H), 2.16-2.08 (m, 3H), 1.75 (m, 1 H), 1.71-1.59 (m, 2H), 1.47 (s, 9H), 1.56-1.46 (m, 5H), 1.12 (s, 3H), 1.03 (s, 3H) ppm. ¹³C NMR (125 MHz): δ 156.8, 143.0, 118.4, 81.3, 79.9, 65.9, 46.3, 37.3, 29.1, 28.6, 28.3, 28.1, 26.7, 24.7, 21.3 ppm. HPLC Chiralpak OD-H column (99:1 Hex:isopropanol; 1 mL/min) t_R 18.1 min (minor), 20.2 min (major): 89% ee. HRMS (ESI) calcd. for $[C_{17}H_{29}O_3N+Na]^+$: m/z 318.2040 found 318.2040.



tert-Butyl 5,5-dimethyl-3-(2-methylprop-1-enyl)morpholine-2-carboxylate 3.50. Following general procedure A, **3.41** (50.0 mg, 162 μ mol), (*R*)-xylyl-BINAP(AuOPNB)₂ (11.8 mg, 8.9 μ mol), and MeNO₂ (0.53 mL) were combined and stirred at 50 °C for 24 h. The crude mixture was purified by column chromatography (1:99 EtOAc:CH₂Cl₂) to yield white solids (39.5 mg, 128 μ mol, 79% yield, 89% ee). ¹H NMR (500 MHz): δ 5.60 (d, 1H, J = 8.4 Hz), 4.78 (m, 1H), 3.63 (d, 1H, J = 11.2 Hz), 3.58 (d, 1H, J = 11.2 Hz), 1.75 (m, 1H), 1.71 (s, 3H), 1.50 (m, 1H), 1.64 (s, 3H), 1.47 (s, 9H), 1.10 (s, 3H), 0.86 (s, 3H) ppm. ¹³C NMR (125 MHz): δ 155.0, 132.3, 124.1, 81.1, 81.0, 52.7, 40.9, 29.6, 28.3, 27.5, 26.5, 25.5, 17.8 ppm. HPLC Regis Technologies Whelk-O 1 column (98:2 hexanes:ethanol; 1 mL/min) t_R 14.7 min (minor), 20.3 min (major): 89% ee; HRMS (ESI) calcd. for $[C_{15}H_{27}O_3N+Na]^+$: m/z 292.1883 found 292.1884.



3-(Cyclohexylidenemethyl)-3-methylisoxazolidine 3.52b. Following general procedure A, **3.51b** (40.0 mg, 221 μmol), (*R*)-MeO-BIPHEP(AuOPNB)₂ (14.4 mg, 11.0 μmol) and CH₂Cl₂ (0.74 mL) were combined and stirred for 24 h at room temperature. The reaction mixture was purified by column chromatography (1:24 EtOAc:hexanes) to afford a clear oil (31.9 mg, 176 μmol , 80% yield). ¹H NMR (400 MHz): δ 5.35 (s, 1H), 4.02 (dd, 1H, *J* = 6.4, 11.6 Hz), 3.83 (dd, 1H, *J* = 6.4, 12.6 Hz), 2.35-2.23 (m, 2H), 2.23-2.11 (m, 2H), 2.11-1.99 (m, 2H), 1.54-1.45 (m, 6H), 1.32 (s, 3H) ppm. ¹³C NMR (100 MHz): 143.8, 124.8, 70.4, 64.1, 44.3, 37.5, 30.6, 28.7, 27.8, 26.4, 26.1 ppm. HRMS (EI) calcd. for [C₁₁H₁₉O₁N+H]⁺: *m/z* 182.1539, found 182.1545.

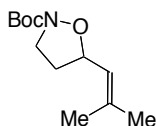


(3-(Cyclohexylidenemethyl)-3-methylisoxazolidin-2-yl) (4-nitrophenyl) methanone 3.60. 3-(Cyclohexylidenemethyl)-3-methylisoxazolidine (**3.52b**) (8.0 mg, 44.1 μmol) was dissolved in CH₂Cl₂ (0.5 mL) and pyridine (5.6 μL , 69.0 μmol) and 4-nitrobenzoyl chloride (10.6 mg, 57.4 μmol) were added. The reaction mixture was stirred for 16 h at room temperature and the crude reaction mixture was purified by column chromatography (1:19 THF:hexanes) to afford a pale yellow solid (9.0 mg, 27.3 μmol , 62% yield). ¹H NMR (400 MHz) δ 8.24 (d, 2H, *J* = 9.2 Hz), 7.88 (d, 2H, *J* = 9.2 Hz), 5.62 (s, 1H), 4.20-4.15 (m, 1H), 4.10-4.04 (m, 1H), 2.68-2.61 (m, 1H), 2.49-2.43 (m, 1H), 2.32-2.16 (m, 2H), 2.19-2.05 (m, 2H), 2.12 (s, 3H), 1.64-1.44 (m, 6H) ppm. ¹³C NMR (100 MHz) δ 160.4, 148.7, 142.2, 141.1, 129.6, 124.6, 123.0, 68.4, 64.3, 45.2, 37.5, 30.3, 29.6, 28.6, 27.5, 26.4 ppm. HPLC Chiralpak AD-H column (95:5 hexanes:isopropanol, 1 mL/min) *t*_R 21.6 min (minor), 29.4 min (major): 49% ee. HRMS (EI) calcd. for [C₁₈H₂₂O₄N₄+H]⁺: *m/z* 331.1652, found 331.1658 ppm.

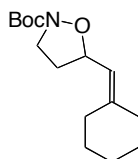
General Procedure B for Au(I)-Catalyzed Hydroalkoxylation

A solution of silver salt (3 mol %) and the appropriate dinuclear gold catalyst (3-6 mol %) in toluene. The reaction mixture was protected from ambient light and allowed to stir in the dark for 30 min. A solution of allene (1 equiv) in toluene (0.1 M) was added to the catalyst mixture. The

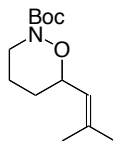
reaction mixture was stirred at rt for 15 h. Purification by column chromatography afforded the desired cyclized product.



tert-Butyl 5-(2-methylprop-1-enyl)isoxazolidine-2-carboxylate 3.56. Following general procedure B, **3.53** (50 mg, 100 μmol), $\text{dppm}(\text{AuCl})_2$ (2.6 mg, 3 μmol), and (*S*)-AgTriP (5.2 mg, 6 μmol) were combined and stirred at 23 $^\circ\text{C}$ for 15 h. The crude mixture was purified by flash column chromatography (5-15% EtOAc/hexanes) to afford **3.56** as a clear oil: ^1H NMR (600 MHz): δ 5.17-5.15 (m, 1H), 4.60 (q, $J = 7.8$ Hz, 1H), 3.83-3.78 (m, 1H), 3.56-3.52 (m, 1H), 2.35-2.29 (m, 1H), 1.92-1.87 (m, 1H), 1.73 (s, 6H), 1.47 (s, 9H) ppm. ^{13}C NMR (150 MHz): δ 158.0, 140.3, 121.5, 81.5, 77.1, 47.8, 34.3, 28.2, 25.8, 18.4 ppm. HPLC Regis Technologies Whelk-O 1 column (98:2 hexanes:Ethanol; 1 mL/min) t_{R} 14.7 min (minor), 20.3 min (major): 98% ee; HRMS (FAB) calcd. for $[\text{C}_{12}\text{H}_{21}\text{O}_3\text{NNa}]^+$: m/z 250.1414, found 250.1409.

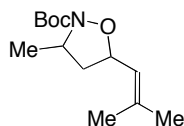


tert-Butyl 5-(cyclohexylidenemethyl)isoxazolidine-2-carboxylate 3.29. Following general procedure B, **3.28** (27 mg, 100 μmol), $\text{dppm}(\text{AuCl})_2$ (2.6 mg, 3 μmol), and (*S*)-AgTriP (5.2 mg, 6 μmol) were combined and stirred at 23 $^\circ\text{C}$ for 15 h. The crude mixture was purified by flash column chromatography (5-8% EtOAc/hexanes) to afford **3.29** as a clear oil: ^1H NMR (600 MHz): δ 5.12 (d, $J = 8.3$ Hz, 1H), 4.66 (q, $J = 7.6$ Hz, 1H), 3.82 (ddd, $J = 10.6, 8.8, 6.5$ Hz, 1H), 3.56 (td, $J = 10.1, 4.9$ Hz, 1H), 2.35-2.26 (m, 2H), 2.21-2.09 (m, 3H), 1.91 (dtd, $J = 11.9, 9.0, 6.4$ Hz, 1H), 1.62-1.52 (m, 6H), 1.51-1.48 (s, 9H) ppm. ^{13}C NMR (150 MHz): δ 158.0, 148.0, 118.1, 81.5, 76.3, 47.8, 37.0, 34.7, 29.5, 28.2 (2), 27.7, 26.5 ppm. HPLC Regis Technologies Whelk-O 1 column (96:4 Hexanes:isopropanol; 1 mL/min) t_{R} 10.5 min (major), 13.6 min (minor): 99% ee. HRMS (FAB) calcd. for $[\text{C}_{15}\text{H}_{25}\text{O}_3\text{NNa}]^+$: m/z 290.1724, found 290.1727.

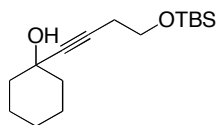


tert-Butyl 6-(2-methylprop-1-enyl)morpholine-2-carboxylate 3.58. Following general procedure B, **3.55** (30 mg, 238 μmol), (*S,S*)-DiPAMP(AuCl) $_2$ (6.6mg, 7.4 μmol), and (*S*)-AgTriP (12.3 mg, 14.3 μmol) were combined and stirred at 23 $^\circ\text{C}$ for 15 h. The crude mixture was purified by flash column chromatography (0-15% EtOAc/hexanes) to afford **3.58** as a clear oil

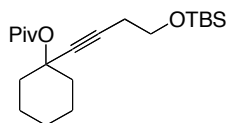
(28 mg, 93% yield): ^1H NMR (600 MHz): δ 5.09 (dt, $J = 7.9, 1.3$ Hz, 1H), 4.40 (td, $J = 9.1, 2.3$ Hz, 1H), 4.04-4.02 (m, 1H), 3.18-3.13 (m, 1H), 1.82 (s, 3H), 1.74 (s, 3H), 1.71-1.62 (m, 4H), 1.48 (s, $J = 9.9$ Hz, 9H) ppm. ^{13}C NMR (150 MHz): δ 155.0, 140.8, 122.9, 81.0, 77.4, 45.4, 30.4, 28.4, 25.7, 22.6, 18.8 ppm. HPLC Regis Technologies Whelk-O 1 column (97:3 Hexanes:isopropanol; 1 mL/min) t_{R} 9.2 min (major), 12.2 min (minor): 87% ee. HRMS (FAB) calcd. for $[\text{C}_{15}\text{H}_{23}\text{O}_3\text{NNa}]^+$: m/z 264.1565, found 264.1570.



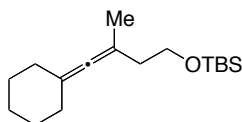
***tert*-Butyl 3-methyl-5-(2-methylprop-1-enyl)isoxazolidine-2-carboxylate 3.57.** Following general procedure B, **3.54** (25 mg, 100 μmol), $\text{dppm}(\text{AuCl})_2$ (2.5 mg, 3 μmol), and (*S*)-AgTriP (5.2 mg, 6 μmol) were combined and stirred at 23 $^\circ\text{C}$ for 15 h. The crude mixture was purified by flash column chromatography (0-4% EtOAc/hexanes) to afford **3.57** as a clear oil (24 mg, 99% yield, 40% ee). ^1H NMR (500 MHz): δ 5.21 (d, $J = 8.1$ Hz, 1H), 4.55-4.50 (m, 1H), 4.34-4.27 (m, 1H), 2.54 (ddd, $J = 12.1, 8.0, 6.3$ Hz, 1H), 1.77 (s, 3H), 1.76 (s, 3H), 1.59 (m, 1H), 1.51 (s, 9H), 1.33 (d, $J = 6.5$ Hz, 3H) ppm. ^{13}C NMR (160 MHz): δ 156.6, 138.6, 122.4, 81.1, 76.2, 55.0, 42.0, 28.3, 25.8, 21.1, 18.4 ppm. HPLC Regis Technologies Whelk-O 1 column (98:2 hexanes:isopropanol; 1 mL/min) t_{R} 16.9 min (minor), 21.8 min (major): 40% ee. HRMS (FAB) calcd. for $[\text{C}_{13}\text{H}_{23}\text{O}_3\text{NNa}]^+$: m/z 264.1564, found 264.1570.



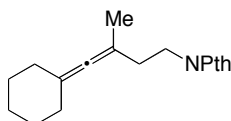
1-(4-(*tert*-Butyldimethylsilyloxy)but-1-ynyl)cyclohexanol 3.61. To a solution of (but-3-ynyl)oxy(*tert*-butyl)dimethylsilane (4.00 g, 21.7 mmol) in anhydrous THF (42 mL) was added 11.9 mL (23.9 mmol) of *n*-BuLi at -78 $^\circ\text{C}$ under N_2 . The solution was stirred for 60 min at -78 $^\circ\text{C}$. Next, a solution of cyclohexanone (2.47 mL, 23.9 mmol) in THF (3 mL) was added and the mixture was allowed to warm to 23 $^\circ\text{C}$ over 2 h. The reaction mixture was quenched by dropwise addition of saturated NH_4Cl (20 mL). The mixture was transferred to a separatory funnel and Et_2O (40 mL) was added. The layers were separated and the aqueous layer was washed with two portions of Et_2O (40 mL each). The organic layer was combined, dried with Na_2SO_4 , and concentrated. The oil was purified by column chromatography (1:15 EtOAc:hexanes) to afford **3.61** (5.08 g, 18.0 mmol, 83% yield) as a clear oil. ^1H NMR (400 MHz): δ 3.72-3.68 (t, 2H, $J = 9.6$), 2.45-2.40 (t, 2H, $J = 9.6$ Hz), 1.69-1.42 (m, 8H), 1.33-1.27 (m, 2H), 0.90 (s, 9H), 0.08 (s, 6H) ppm. The ^1H NMR data matched the spectroscopic data reported in literature.²⁸



1-(4-(Isopropylidimethylsilyloxy)but-1-ynyl)cyclohexyl pivalate 3.62. To a solution of **3.61** (3.00 g, 10.6 mmol) in anhydrous THF (25 mL) at 0 °C under N₂ was added LiHMDS (1.78 g, 10.6 mmol) in one portion. The solution was stirred at 0 °C for 15 min and pivaloyl chloride (1.31 mL, 10.6 mmol) was added. The mixture was allowed to warm to room temperature over 1 h and quenched with saturated aq. NH₄Cl (20 mL). The mixture was transferred to a separatory funnel and extracted with Et₂O (100 mL). The organic layer was dried with MgSO₄ and concentrated. The oil was purified by chromatography (1:24 EtOAc:hexanes) to afford **3.62** (3.40 g, 9.33 mmol, 88% yield) as a clear oil. ¹H NMR (400 MHz): δ 3.72-3.67 (t, 2H, *J* = 9.6 Hz), 2.46-2.41 (t, 2H, *J* = 9.6 Hz), 1.95-1.91 (m, 4H), 1.69-1.53 (m, 4H), 1.43-1.40 (m, 2H), 1.19 (s, 9H), 0.89 (s, 9H), 0.06 (s, 6H) ppm. The ¹H NMR data are consistent with literature data.²⁸



tert-Butyl(4-cyclohexylidene-3-methylbut-3-enyloxy)dimethylsilane 3.63. A flame dried flask was charged with anhydrous CuI (3.43 g, 18.0 mmol), LiBr (1.57 g, 18.0 mmol), and THF (40 mL). The solution was cooled to 0 °C and MeMgBr (6.75 mL, 18.0 mmol) was added. The mixture was stirred for 25 min and a solution of **3.62** (1.1 g, 3.0 mmol) in THF (5 mL) was added dropwise over 5 min. The solution was warmed to room temperature over 4 h and quenched by the addition of 40 mL of 1:4 NH₄OH and NH₄Cl solution. The mixture was extracted twice with Et₂O (50 mL each) and the organic layer was dried with Na₂SO₄ and concentrated. The crude oil was purified by column chromatography, eluting with hexanes to give **3.63** as a pale yellow oil (0.62 g, 2.33 mmol, 78% yield). ¹H NMR (400 MHz): δ 3.69-3.65 (t, 2H, *J* = 9.6 Hz), 2.16-2.12 (t, 2H, *J* = 9.6 Hz), 2.05-2.02 (m, 4H), 1.65-1.57 (m, 2H), 1.55-1.43 (m, 4H), 0.90 (s, 9H), 0.06 (s, 6H) ppm. ¹³C NMR (100 MHz) δ 195.6, 101.7, 93.4, 62.4, 37.7, 32.1, 27.8, 26.3, 26.0, 20.1, 18.4, -5.3 ppm. HRMS (EI) calcd. for [C₁₇H₃₂O₁Si₁-C₄H₉]⁺: *m/z* 223.1518, found 223.1519.



2-(4-Cyclohexylidene-3-methylbut-3-enyloxy)isoindoline-1,3-dione 3.65. A solution of **3.64** (0.62 g, 2.33 mmol) in THF (15 mL) was cooled to 0 °C and TBAF (2.56 mL, 2.56 mmol) was added. The reaction mixture was warmed to room temperature and stirred for 2 hr. Saturated NH₄Cl (40 mL) was added and mixture was extracted with Et₂O (50 mL). The organic layer was

dried with Na₂SO₄ and concentrated to yield 4-cyclohexylidene-3-methylbut-3-en-1-ol as a pale yellow oil (0.43 g). The crude oil was redissolved in dry THF (5 mL) and the solution was added to a prestirred mixture of PPh₃ (0.766 g, 2.84 mmol) and DEAD (1.3 mL, 2.84 mmol) in dry THF (20 mL) at 0 °C. The reaction mixture was stirred at 0 °C for 30 min before *N*-hydroxyphthalimide (0.464 g, 2.84 mmol) was added in one portion. The solution became deep red immediately upon addition of hydroxyphthalimide but turned clear as it is stirred at room temperature for 2 h. The reaction mixture was concentrated slowly under reduced pressure and the crude mixture was purified via flash chromatography (3:47 EtOAc:hexanes) afford (**3.65**) as a white solid (0.64 g, 2.06 mmol, 82% yield over 2 steps). ¹H NMR (400 MHz): δ 4.27 (t, 2H, *J* = 7.6 Hz), 2.44 (t, 2H, *J* = 7.6 Hz), 2.03-2.06 (m, 4H), 1.46-1.56 (m, 6H), 1.72 (s, 3H) ppm. ¹³C NMR (100 MHz) δ 195.2, 163.7, 134.4, 129.0, 123.5, 103.1, 92.1, 77.1, 32.5, 31.9, 27.7, 26.2, 20.3 ppm. HRMS (FAB) calcd. for [C₁₆H₂₆O₃N+H]⁺: *m/z* 312.1600, found 312.1604.

References

- ¹ For examples of gold-catalyzed hydroamination of allenes, see: (a) Krause, N.; Morita, N. *Org. Lett.* **2004**, *6*, 4121. (b) Nishina, N.; Yamamoto, Y. *Angew. Chem., Int. Ed. Engl.* **2006**, *45*, 3314. (c) Patil, N. T.; Lutet, L. M.; Nishina, N.; Yamamoto, Y. *Tetrahedron Lett.* **2006**, *47*, 4749. (d) Zhang, Z.; Liu, C.; Kinder, R. E.; Han, X.; Qian, H.; Widenhoefer, R. A. *J. Am. Chem. Soc.* **2006**, *128*, 9066. (e) Morita, N.; Krause, N. *Eur. J. Org. Chem.* **2006**, 4634. For a recent review of gold(I)-catalyzed heterocyclic synthesis, see: (f) Shen, H. C. *Tetrahedron* **2008**, *64*, 3885.
- ² (a) LaLonde, R. L.; Sherry, B. D.; Kang, E. J.; Toste, F. D. *J. Am. Chem. Soc.* **2007**, *129*, 2452. (b) Zhang, Z.; Bender, C. F.; Widenhoefer, R. A. *Org. Lett.* **2007**, *9*, 2887. For a dynamic kinetic resolution, see: (c) Zhang, Z.; Bender, C. F.; Widenhoefer, R. A. *J. Am. Chem. Soc.* **2007**, *129*, 14148. For a previous report of asymmetric hydroamination of allenes (maximum ee was 16%), see: (d) Hoover, J. M.; Peterson, J. R.; Pikul, J. H.; Johnson, A. R. *Organometallics* **2004**, *23*, 4614. For an Au(I)-catalyzed asymmetric hydroalkoxylation of allenes, see: (e) Zhang, Z.; Widenhoefer, R. A. *Angew. Chem., Int. Ed. Engl.* **2007**, *46*, 283. (f) Hamilton, G. L.; Kang, E. J.; Mba, M.; Toste, F. D. *Science* **2007**, *317*, 496.
- ³ For a review of recent developments in enantioselective gold-catalysis, see: (a) Widenhoefer, R. A. *Chem. Eur. J.* **2008**, *14*, 5382. For reviews of enantioselective alkene hydroamination, see: (b) Hultsch, K. C. *Org. Biomol. Chem.* **2005**, *3*, 1819. (c) Hultsch, K. C. *Adv. Synth. Catal.* **2005**, *347*, 367.
- ⁴ For a racemic gold catalyzed synthesis of *N*-hydroxypyrrolines, dihydroisoxazoles and dihydro-1,2-oxazines, see: (a) Winter, C.; Krause, N. *Angew. Chem., Int. Ed. Engl.* **2009**, *48*, 6339. For a gold(I)-catalyzed addition of hydroxylamines to alkynes, see: (b) Yeom, H.-S.; Lee, E.-S.; Shin, S. *Synlett* **2007**, 2292. For a silver catalyzed addition of hydroxylamines to allenes, see: (c) Bates, R.; Nemeth, J.; Snell, R. *Synthesis* **2008**, *7*, 1033.
- ⁵ For selected enantioselective syntheses of isoxazolidines, see: (a) Rios, R.; Ibrahim, I.; Wesely, J.; Zhao, G.-L.; Cordova, A. *Tetrahedron Lett.* **2007**, *48*(32), 5701. (b) Troisi, L.; De Lorenzis, S.; Fabio, M.; Rosato, F.; Granito, C. *Tetrahedron Asymm.* **2008**, *19*, 2246. (c) Tokizana, M.; Sato, K.; Ohta, T.; Ito, Y. *Tetrahedron Asymm.* **2008**, *19*, 2519.
- ⁶ For selected methods to synthesize pyrazolines and pyrazolidines, see: (a) Whitlock, G. A.; Carreira, E. M. *J. Org. Chem.* **1997**, *62*, 7916. (b) Yamashita, Y.; Kobayashi, S. *J. Am. Chem. Soc.* **2004**, *126*, 11279. (c) Shintani, R.; Fu, G. C. *J. Am. Chem. Soc.* **2003**, *125*, 10778. (d) Giampietro, N. C.; Wolfe, J. P. *J. Am. Chem. Soc.* **2008**, *130*, 12907.
- ⁷ For an isoxazoline artificial transcription activator, see: (a) Buhrlage, S. J.; Brennan, B. B.; Minter, A. R.; Mapp, A. K. *J. Am. Chem. Soc.* **2005**, *127*, 12456. For a recent study of isoxazolidine HIV-1 replication inhibitors, see: (b) Loh, B.; Vozzollo, L.; Mok, B. J.;

-
- Lee, C. C.; Fitzmaurice, R. J.; Caddick, S.; Fassati, A. *Chem. Bio. Drug Des.* **2010**, *75*, 461.
- ⁸ Vasella, A.; Voefray, R. *J. Chem. Soc., Chem. Commun.* **1981**, 97.
- ⁹ (a) Hill, D. J.; Mio, M. J.; Prince, R. B.; Hughes, T. S.; Moore, J. S. *Chem. Rev.* **2001**, *101*, 3893. (b) Cheng, R. P.; Gellman, S. H.; DeGrado, W. F. *Chem. Rev.* **2001**, *101*, 3219.
- ¹⁰ (a) Yang, Q.; Jiang, X.; Ma, S. *Chem. Eur. J.* **2007**, *13*, 9310.
- ¹¹ Shu, W.; Yang, Q.; Jia, G.; Ma, S. *Tetrahedron* **2008**, *64*, 11159.
- ¹² Bates, R. W.; Lu, Y. *J. Org. Chem.* **2009**, *74*, 9460.
- ¹³ Bates, R. W.; Dewey, M. R. *Org. Lett.* **2009**, *11*, 3706.
- ¹⁴ (a) Kennedy-Smith, J. J.; Staben, S. T.; Toste, F. D. *J. Am. Chem. Soc.* **2004**, *126*, 4526. (b) Staben, S. T.; Kennedy-Smith, J. J.; Toste, F. D. *Angew. Chem., Int. Ed. Engl.* **2004**, *43*, 5350.
- ¹⁵ (a) Kinsman, R.; Lathbury, D.; Vernon, P.; Gallagher, T. *J. Chem. Soc., Chem. Commun.* **1987**, 243. (b) Fox, D. N. A.; Gallagher, T. *Tetrahedron* **1990**, *46*, 4697. (c) Davies, I. W.; Gallagher, T.; Lamont, R. B.; Scopes, D. I. C. *J. Chem. Soc., Chem. Commun.* **1992**, 335.
- ¹⁶ Z. Jane Wang performed the optimization of hydroxylamine hydroamination and explored the substrate scope (except **3.35**).
- ¹⁷ (a) Hatano, M.; Maki, T.; Moriyama, K.; Arinobe, M.; Ishihara, K. *J. Am. Chem. Soc.* **2008**, *130*, 16858. (b) Garcia-Garcia, P.; Lay, F.; Garcia-Garcia, P.; Rabalakos, C.; List, B. *Angew. Chem., Int. Ed. Engl.* **2009**, *48*, 4363.
- ¹⁸ (a) For a single example of an intermolecular gold(I)-catalyzed addition of methyl carbamate to tetramethyl allene (61% yield), see: Kinder, R. E.; Zhang, Z.; Widenhoefer, R. A. *Org. Lett.* **2008**, *10*, 3157. (b) For a single example of an intermolecular gold(I)-catalyzed addition of indole to tetramethyl allene (56% yield), see: Toups, K.; Liu, G.; Widenhoefer, R. A. *J. Organomet. Chem.* **2009**, *694*, 571.
- ¹⁹ Use of 3 mol% dppm(AuCl)₂, 6 mol% (S)-Ag(**3.31**), 0.1 M in toluene, 23 °C, 18 h gave oxazine **3.58** in 60% yield and 34% ee.
- ²⁰ For a representative procedure to cleave the N-O bond, see: Vasella, A.; Voefray, R.; Pless, J.; Hugenin, R. *Helv. Chim. Acta* **1983**, *66*, 1241.
- ²¹ Rubottom, G. M.; Mott, R. C.; Henrik D. Juve, J. *J. Org. Chem.* **1981**, *46*, 2717.
- ²² Johansson, M. J.; Gorin, D. J.; Staben, S. T.; Toste, F. D. *J. Am. Chem. Soc.* **2005**, *127*, 18002.
- ²³ Zhang, Z.; Liu, C.; Kinder, R. E.; Han, X.; Qian, H.; Widenhoefer, R. A. *J. Am. Chem. Soc.* **2006**, *128*, 9066.
- ²⁴ Black, D. K.; Landor, S. R. *J. Chem. Soc.* **1965**, 6784.

²⁵ Altenurger, J. M.; Mioskowski, C.; d'Orchymont, H.; Schirlin, D.; Schalk, C.; Tarnus, C., *Tetrahedron Lett.* **1992**, 33(35), 5055.

²⁶ Bates, R. W.; Kanicha, S.-E. *Org. Lett.* **2002**, 4, 4225.

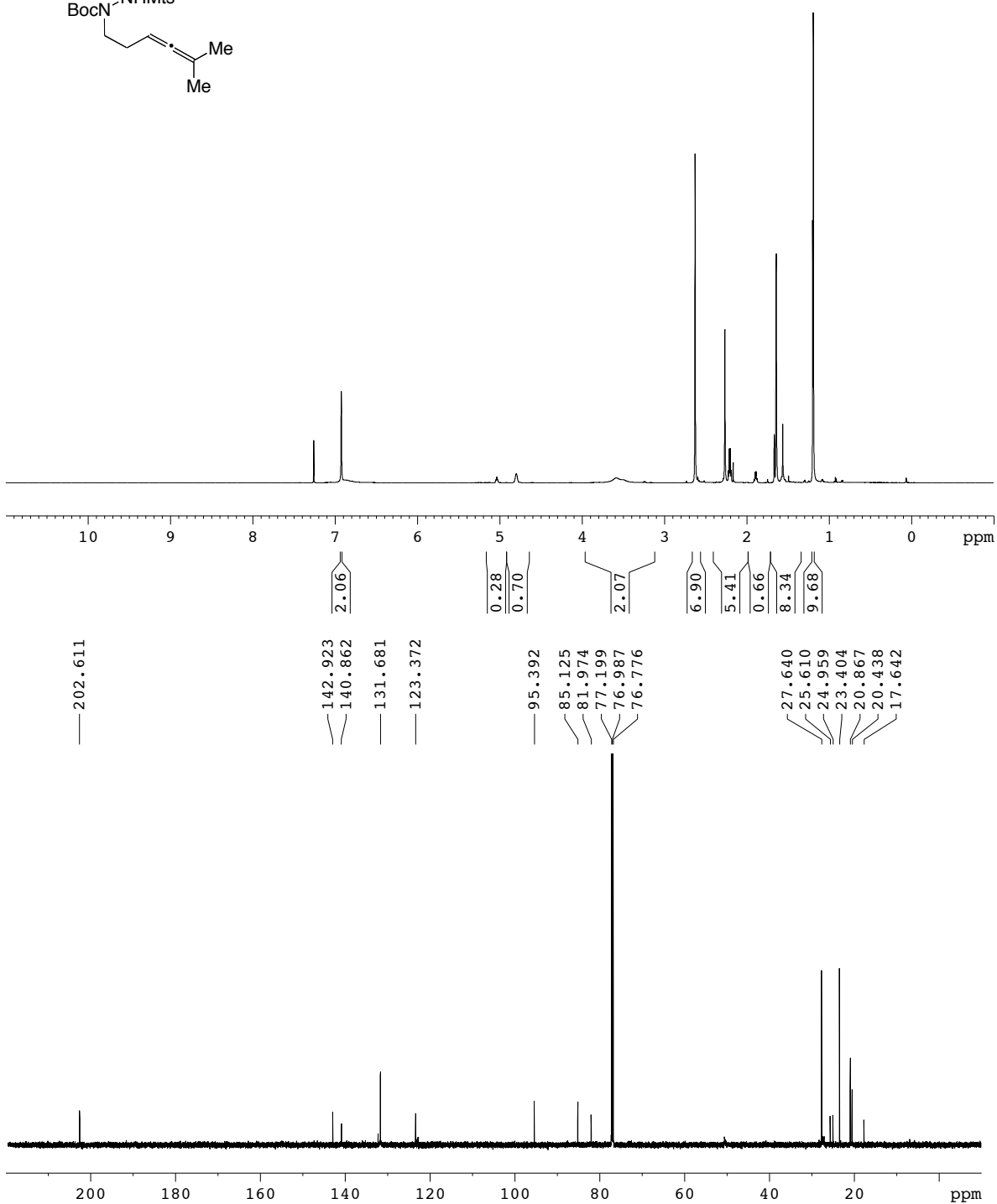
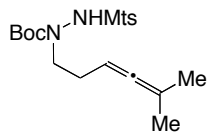
²⁷ Cossu, S.; De Lucchi, O.; Fabbri, D.; Valle, G.; Painter, G. F.; Smith, R. A. J. *Tetrahedron* **1997**, 53, 6073.

²⁸ Zhurnal, O. K. U.S. Patent 75722, **1967**.

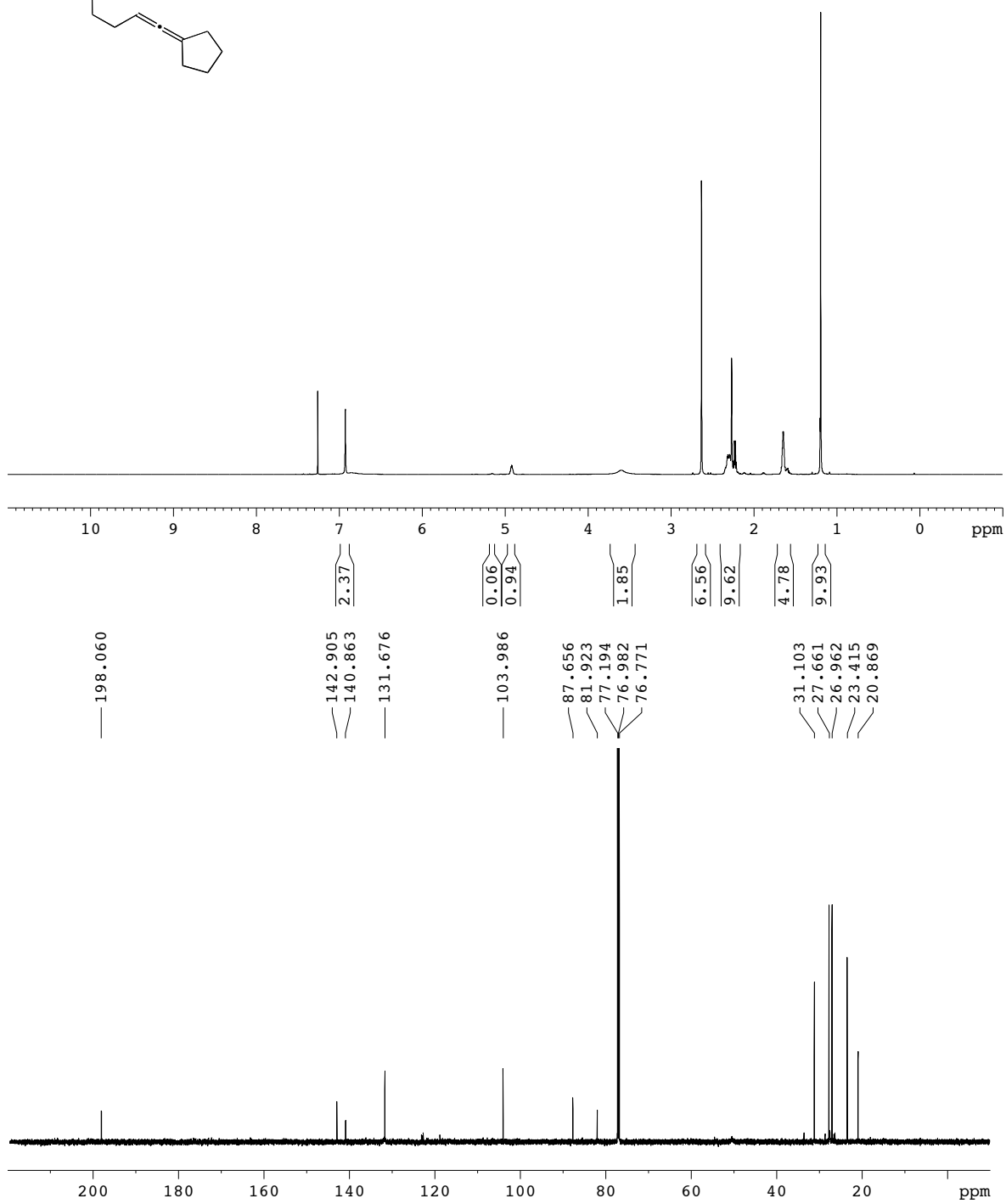
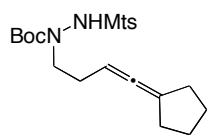
Appendix 3A

Copies of ^1H and ^{13}C NMR characterization data are included for compounds **3.24, 3.25, 3.28, 3.29, 3.32, 3.33, 3.35, 3.42-3.44, 3.53-3.59**.
Copies of HPLC chromatographs are included for compounds **3.25, 3.29, 3.42-3.44, 3.57-3.59**.

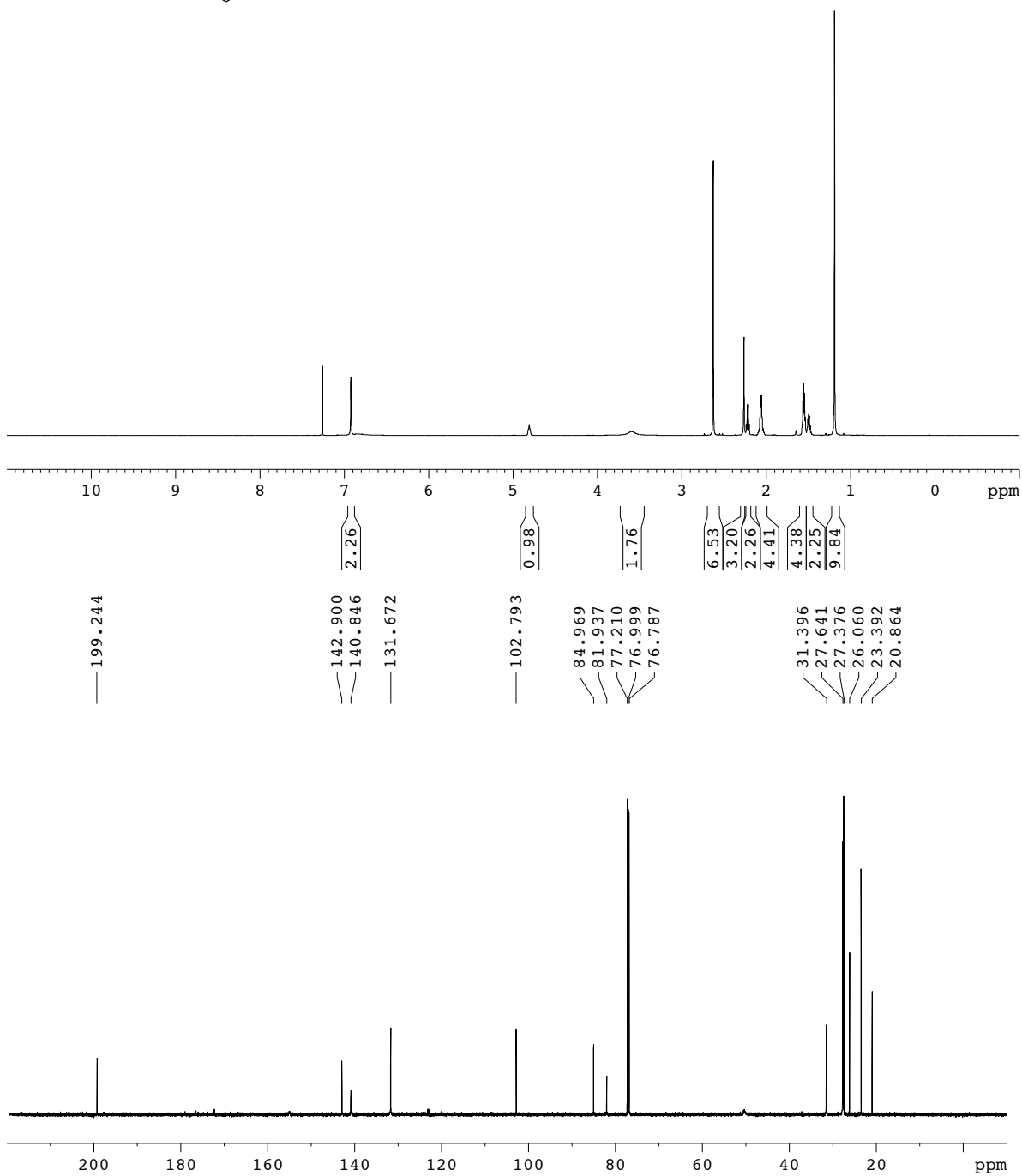
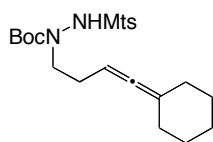
3.24



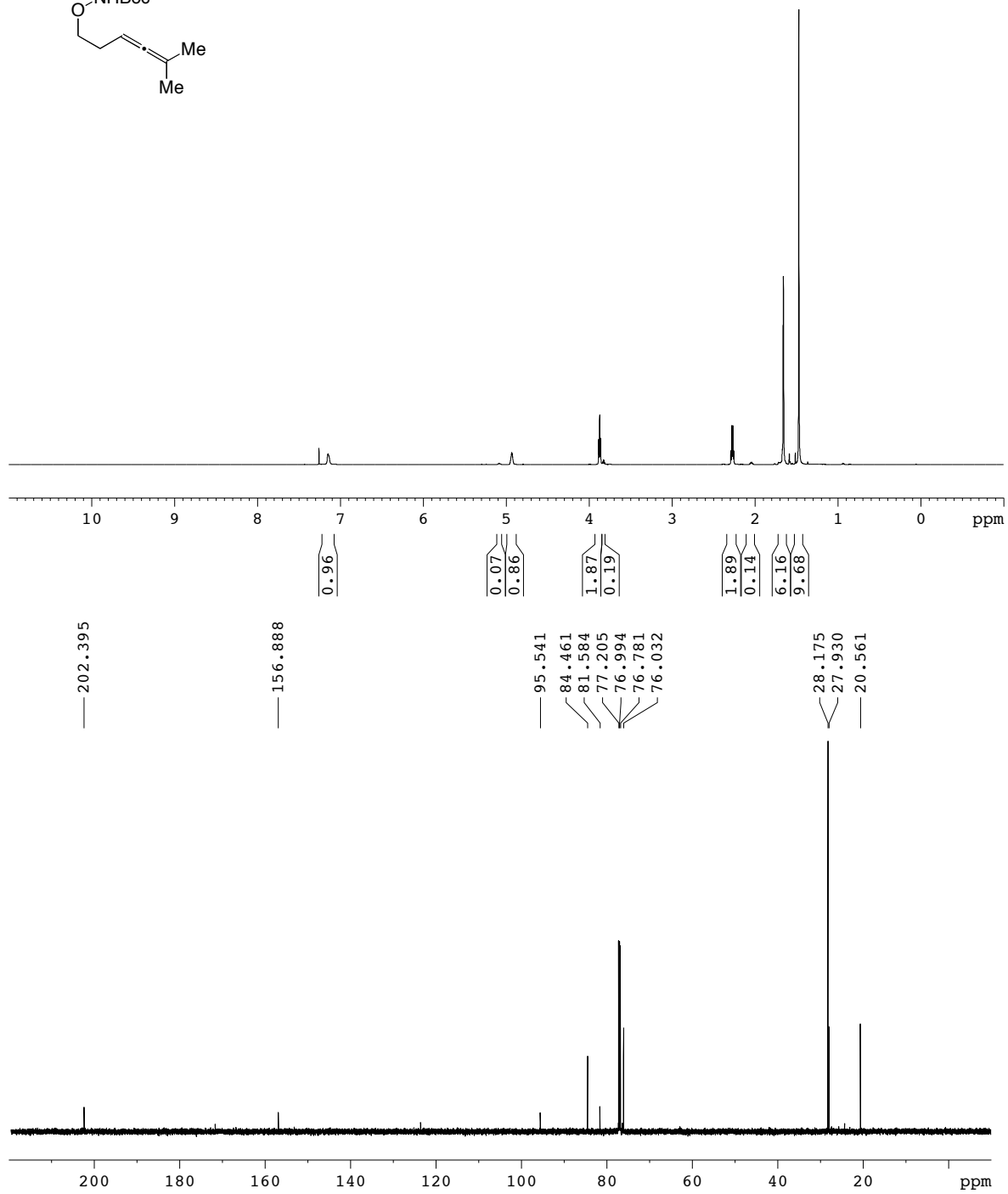
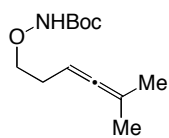
3.32



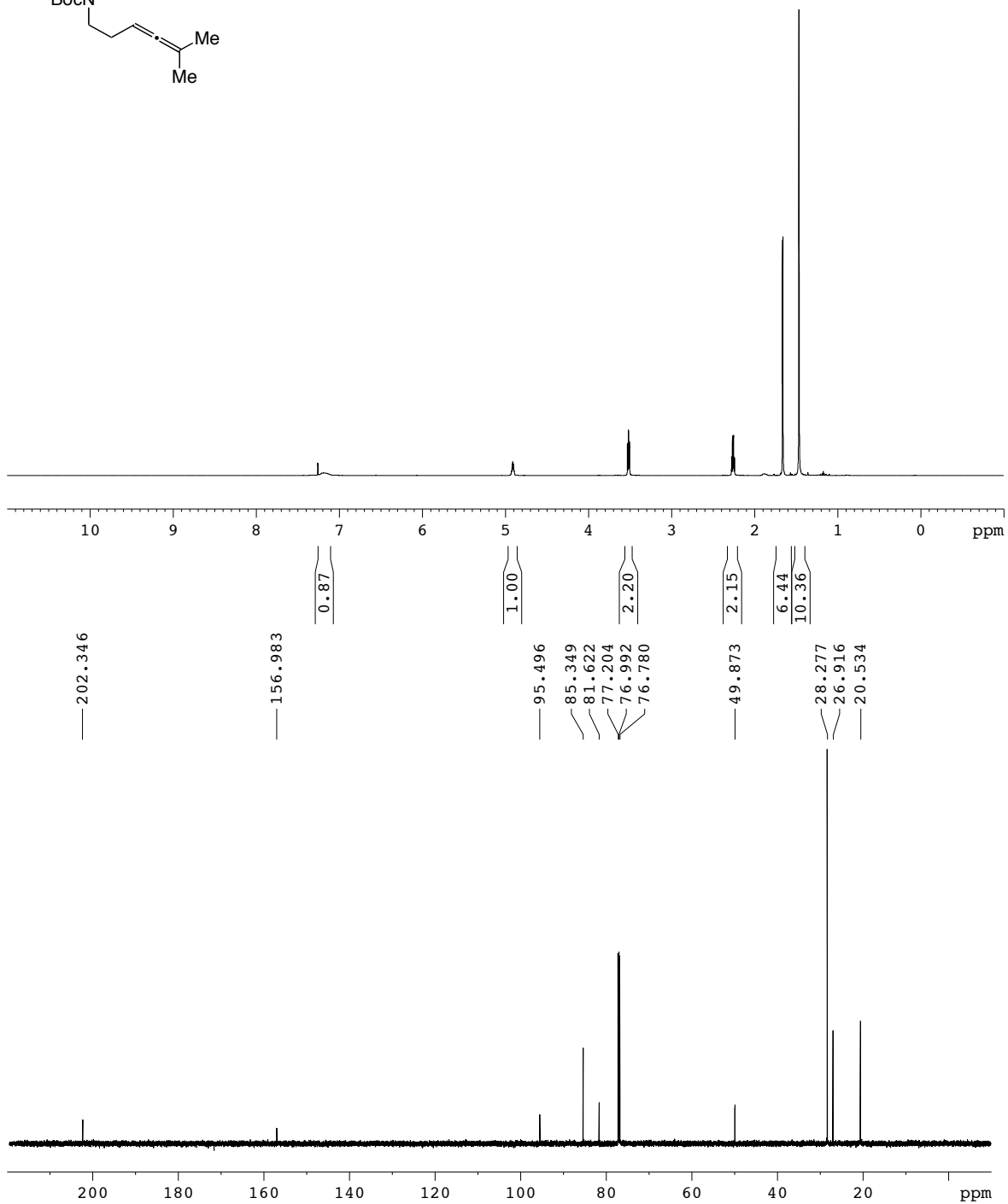
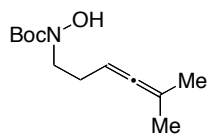
3.33



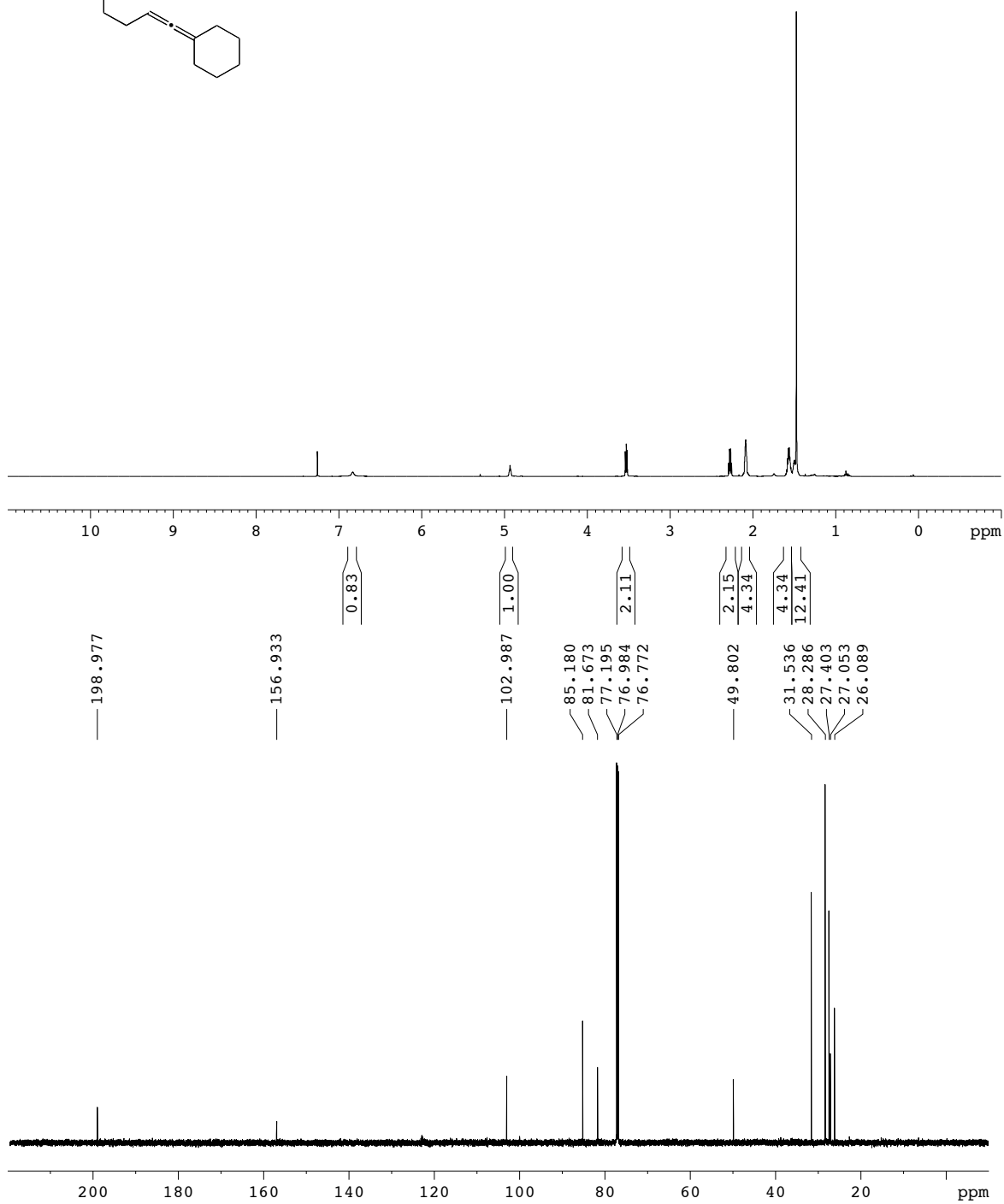
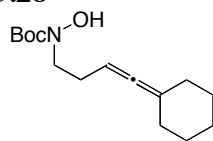
3.35



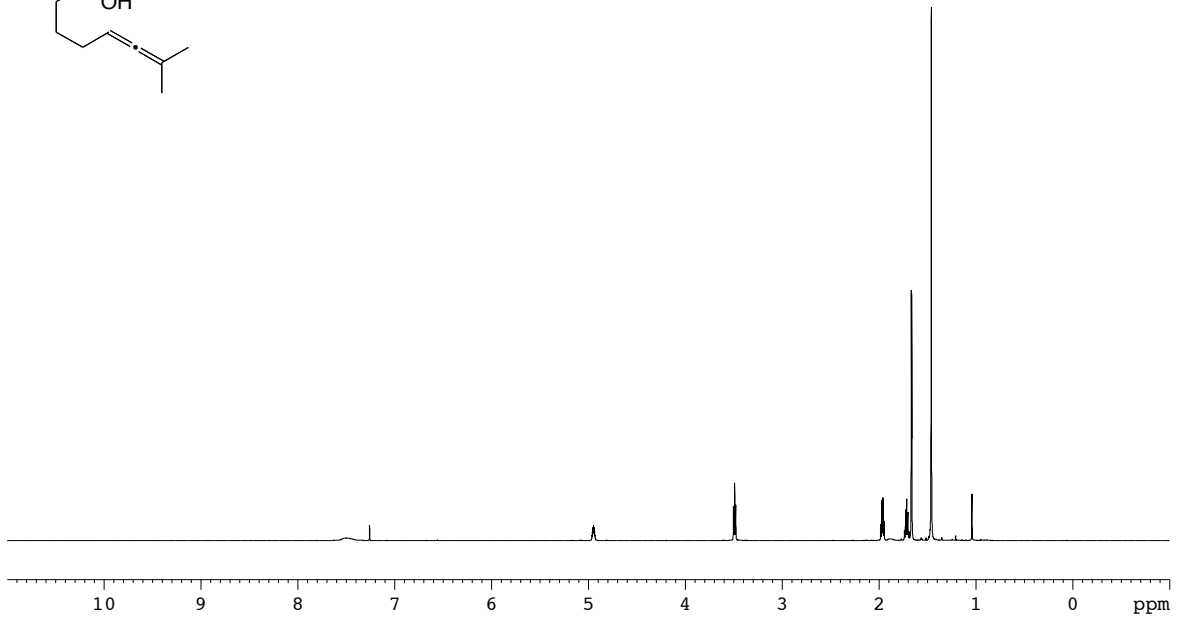
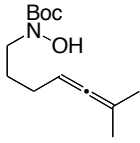
3.53



3.28



3.55



201.682

157.051

95.444

87.960

81.543

77.203

76.992

76.780

49.657

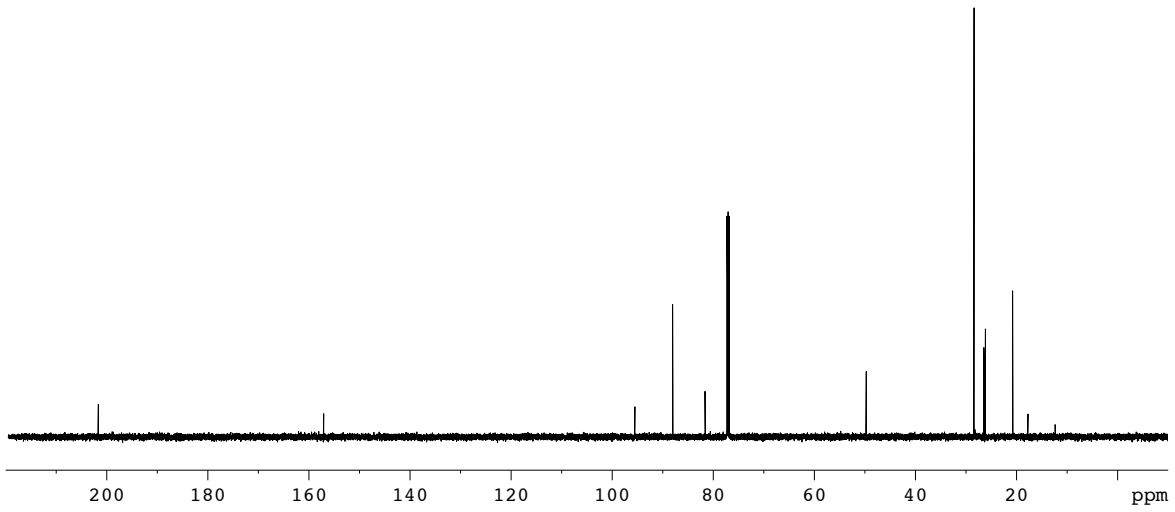
28.303

26.344

26.085

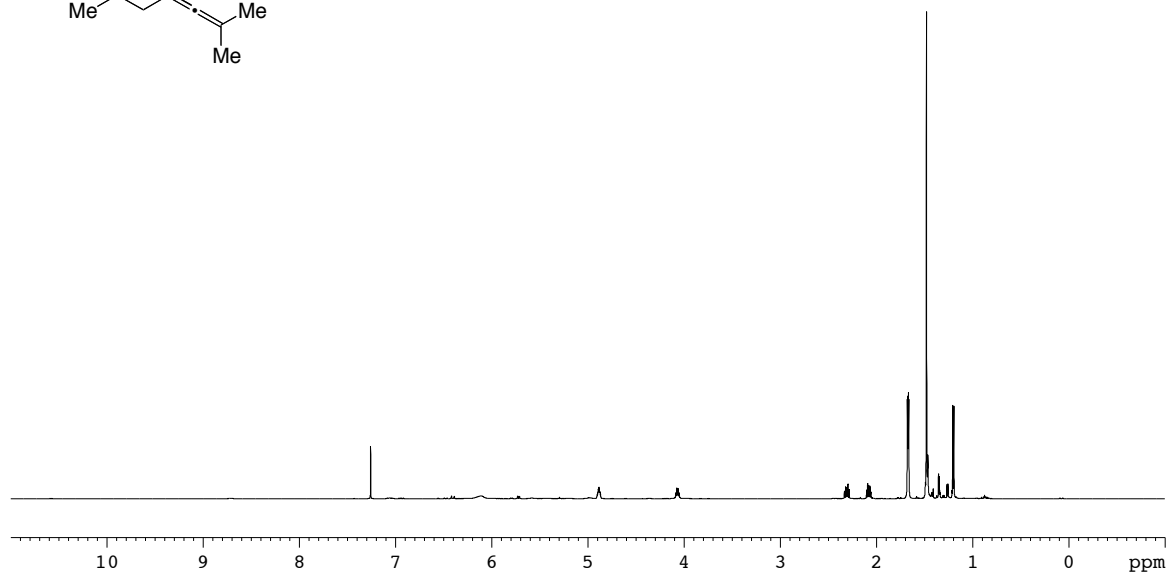
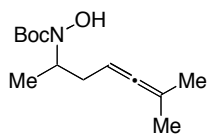
20.663

17.649



54

3.54



— 202.572

— 156.880

— 95.120

— 85.546

— 81.546

— 77.184

— 76.972

— 76.760

— 54.775

— 33.647

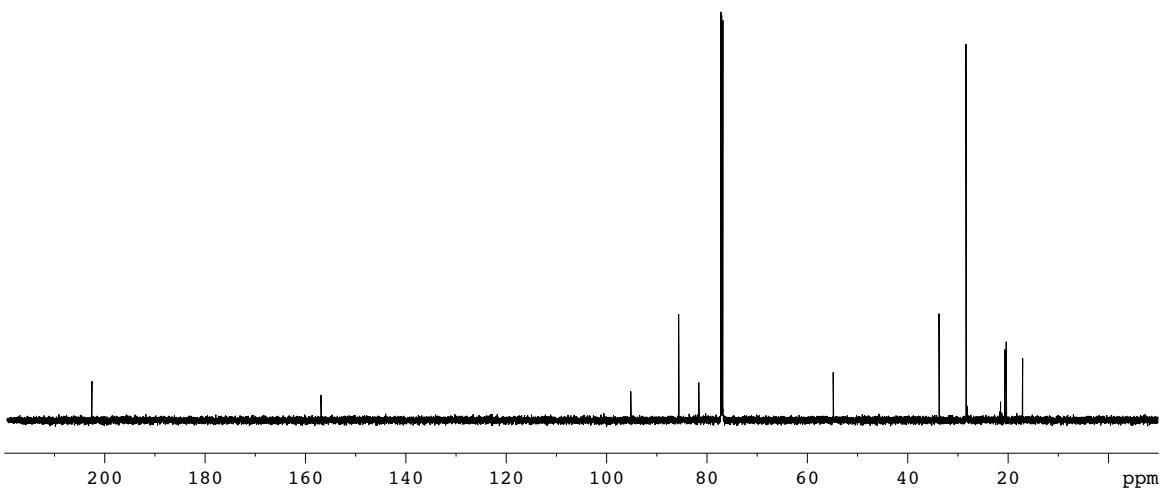
— 28.313

— 28.242

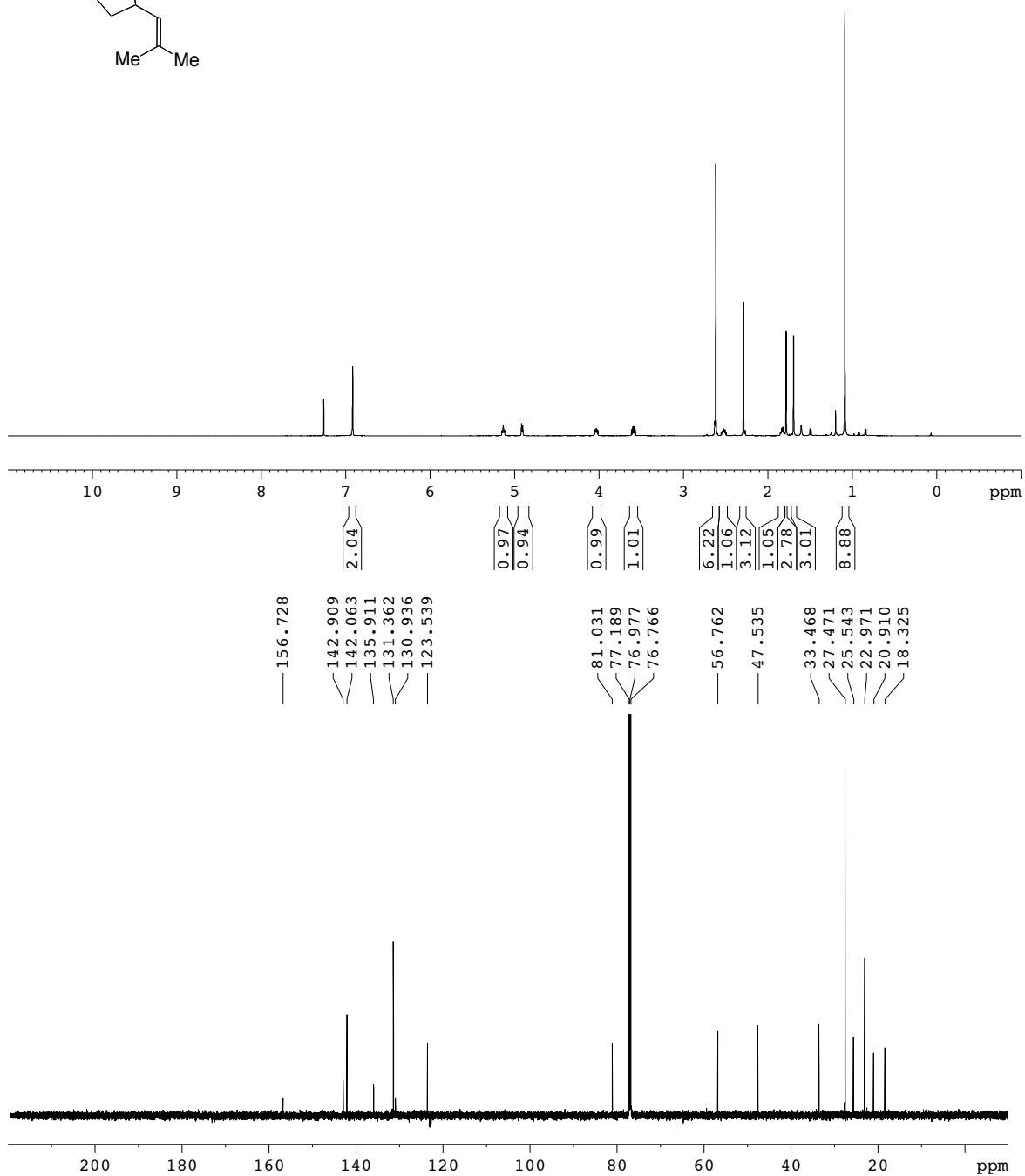
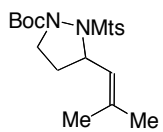
— 20.556

— 20.290

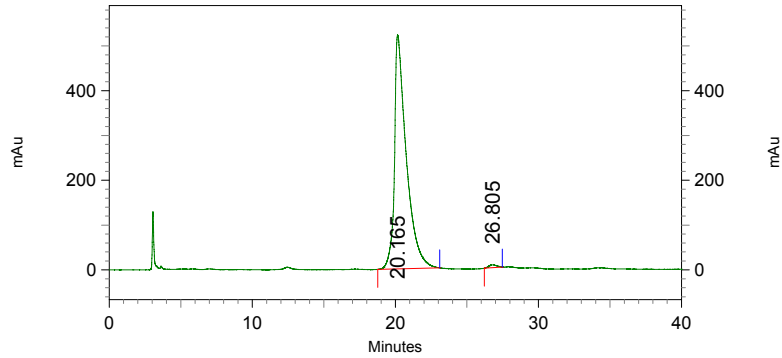
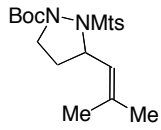
— 17.015



3.25

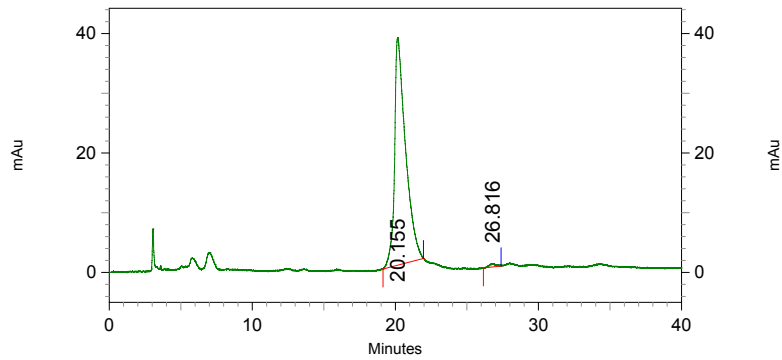


3.25



1: 230 nm, 4 nm Results

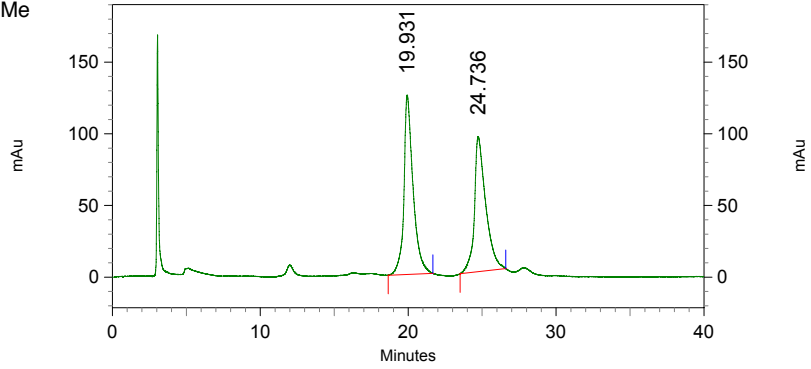
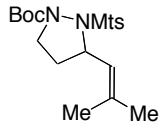
Retention Time	Area	Area Percent
20.165	30024208	99.179
26.805	248513	0.821



2: 254 nm, 4 nm Results

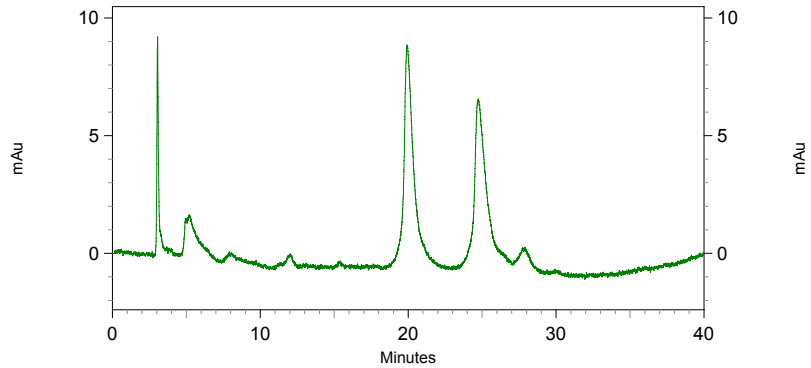
Retention Time	Area	Area Percent
20.155	2040144	99.120
26.816	18122	0.880

3.25



1: 230 nm, 4 nm Results

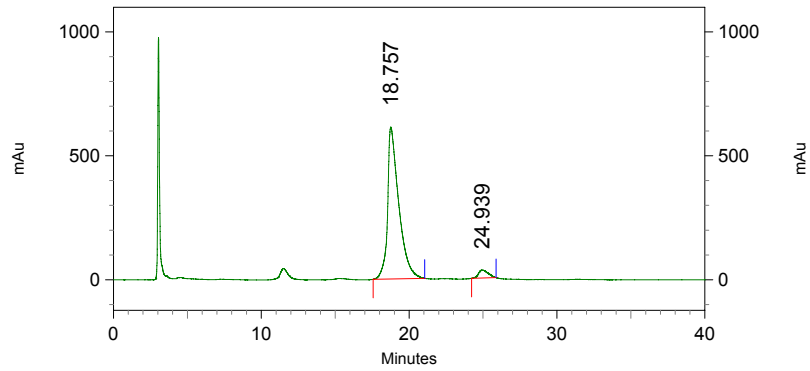
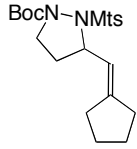
Retention Time	Area	Area Percent
19.931	5398688	51.840
24.736	5015495	48.160



2: 254 nm, 4 nm Results

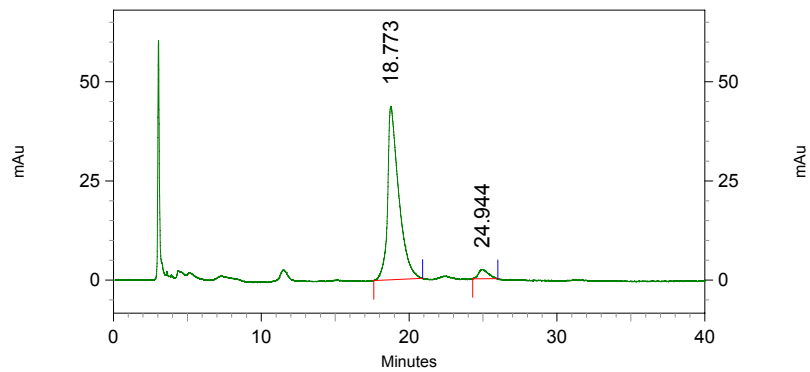
Retention Time	Area	Area Percent
----------------	------	--------------

3.42



1: 230 nm, 4 nm Results

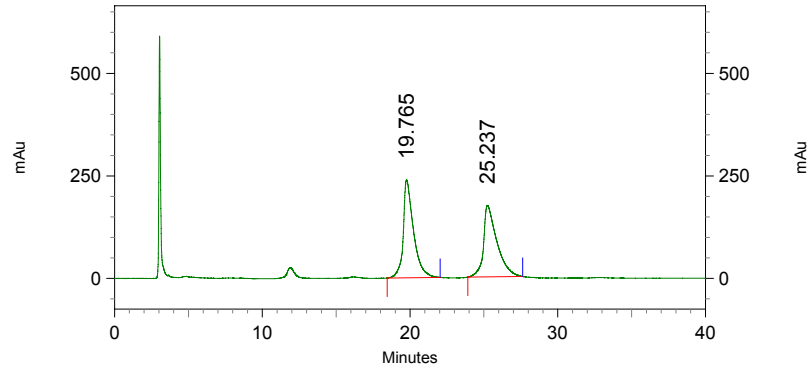
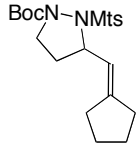
Retention Time	Area	Area Percent
18.757	32207050	95.715
24.939	1441955	4.285



2: 254 nm, 4 nm Results

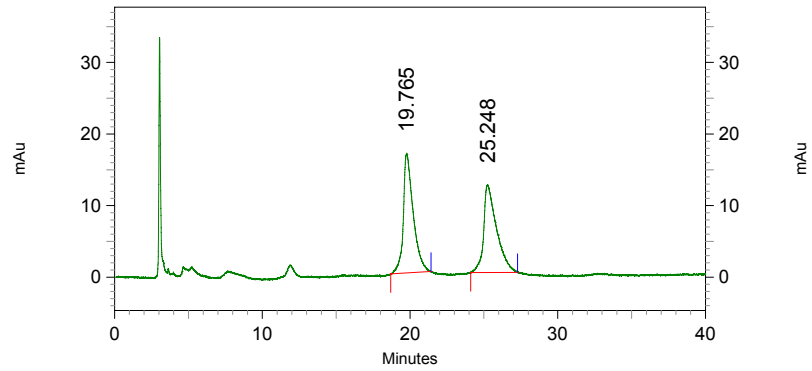
Retention Time	Area	Area Percent
18.773	2290612	95.559
24.944	106465	4.441

3.42



1: 230 nm, 4 nm Results

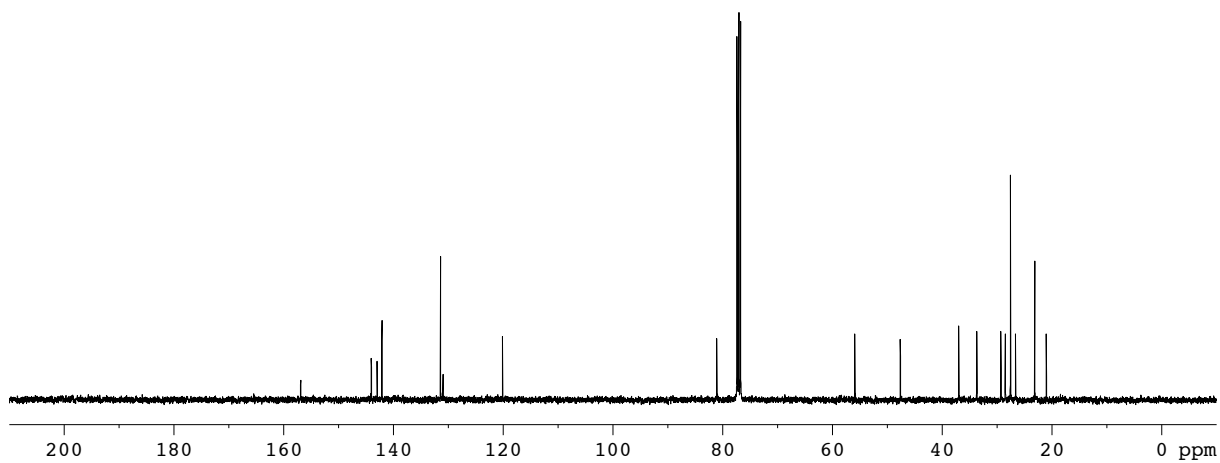
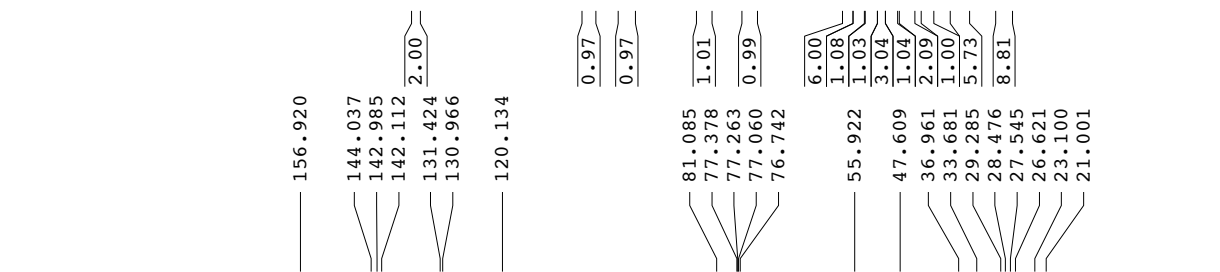
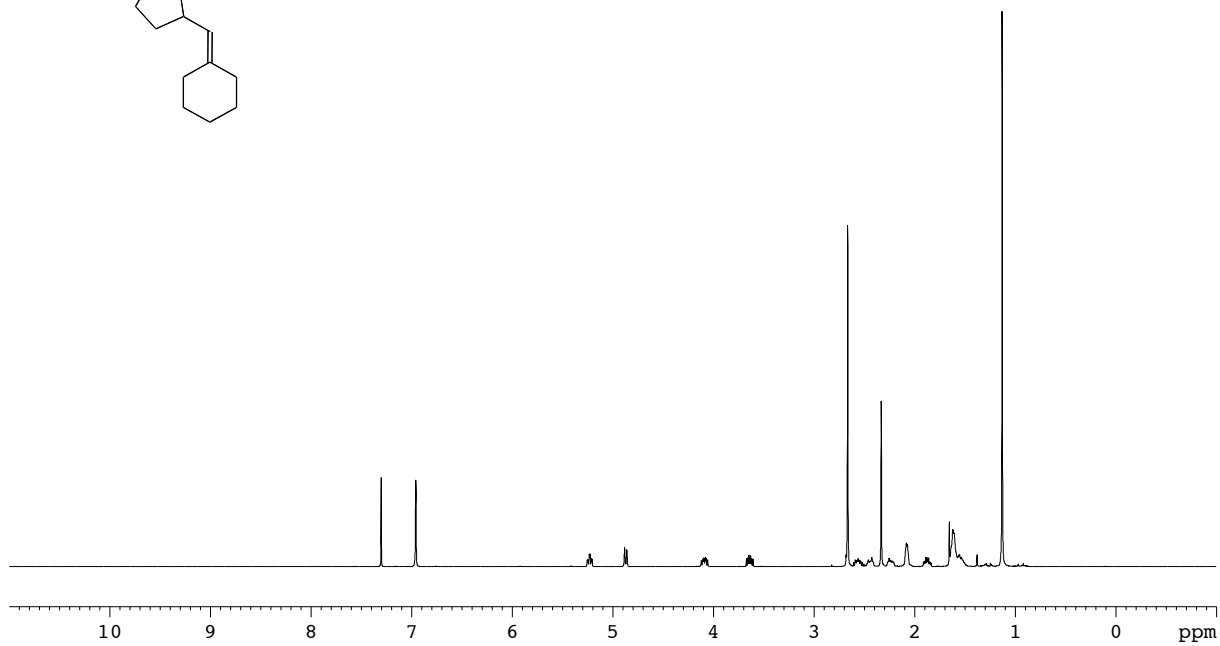
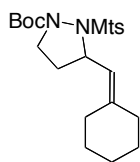
Retention Time	Area	Area Percent
19.765	11568041	51.228
25.237	11013561	48.772



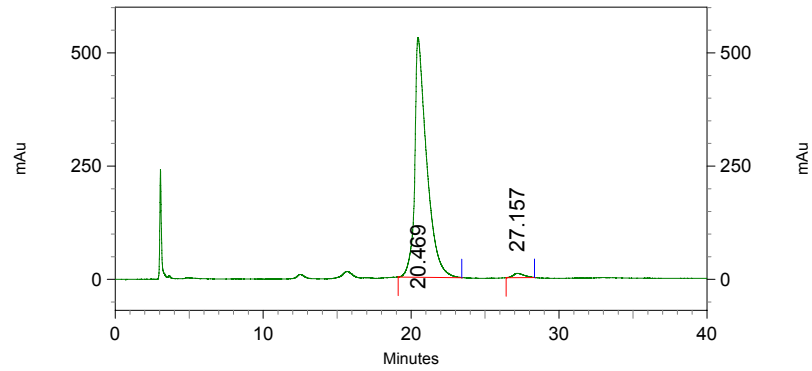
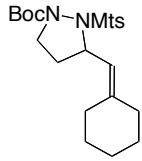
2: 254 nm, 4 nm Results

Retention Time	Area	Area Percent
19.765	777269	50.988
25.248	747159	49.012

3.43

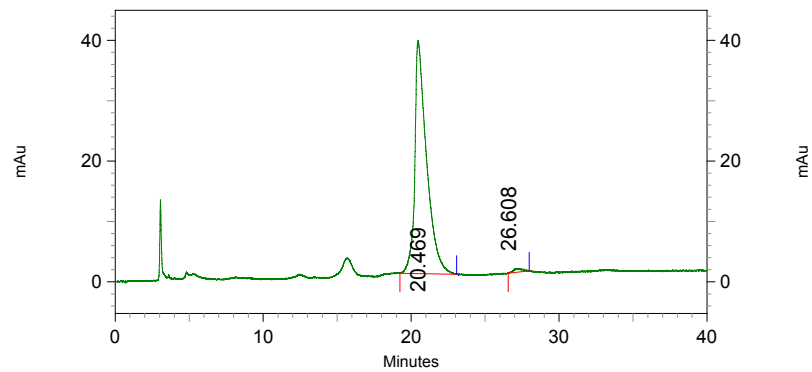


3.43



1: 230 nm, 4 nm Results

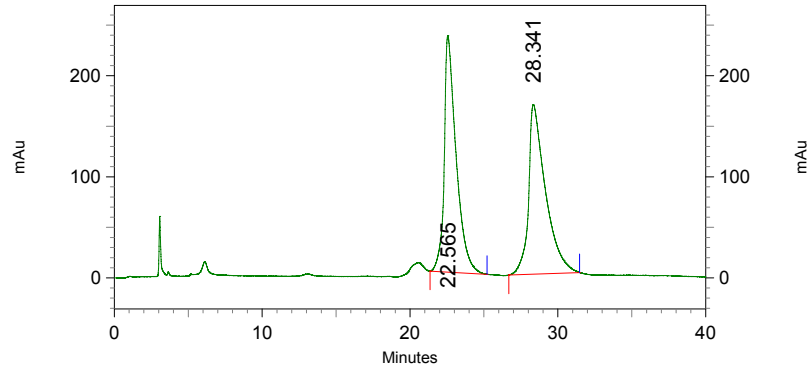
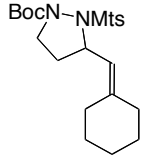
Retention Time	Area	Area Percent
20.469	29776859	98.393
27.157	486388	1.607



2: 254 nm, 4 nm Results

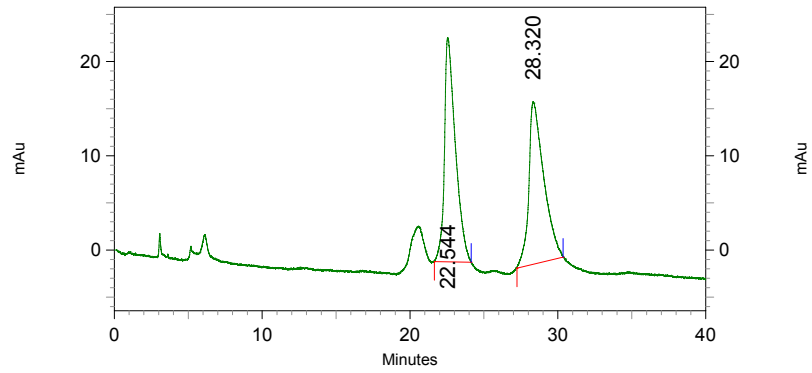
Retention Time	Area	Area Percent
20.469	2142599	98.941
26.608	22930	1.059

3.43



1: 230 nm, 4 nm Results

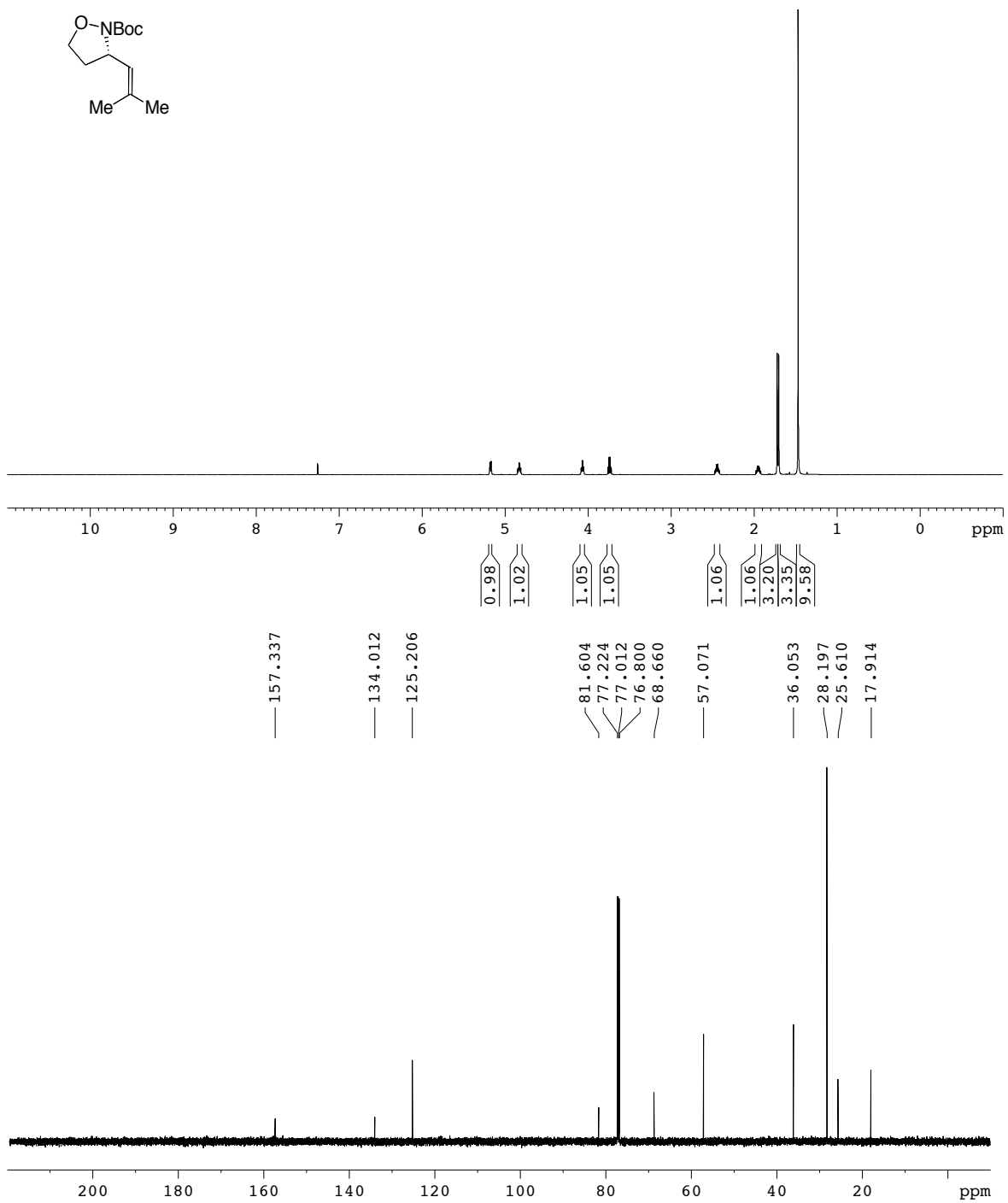
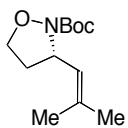
Retention Time	Area	Area Percent
22.565	13150309	49.588
28.341	13368955	50.412



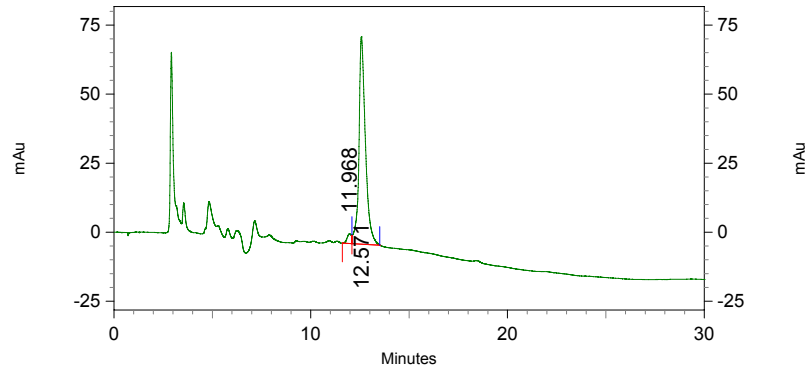
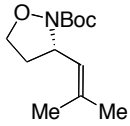
2: 250 nm, 4 nm Results

Retention Time	Area	Area Percent
22.544	1229759	50.287
28.320	1215742	49.713

3.44

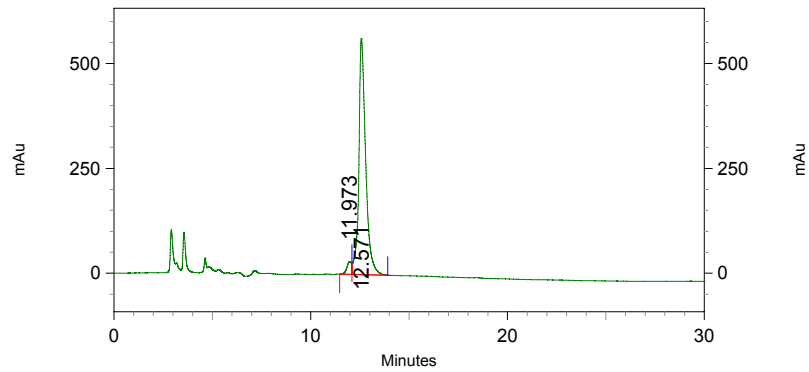


3.44



1: 230 nm, 4 nm Results

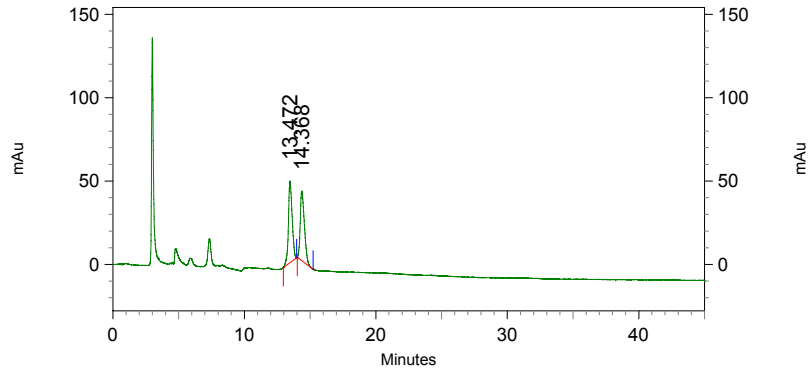
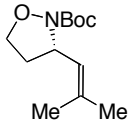
Retention Time	Area	Area Percent
11.968	54402	3.058
12.571	1724371	96.942



2: 214 nm, 4 nm Results

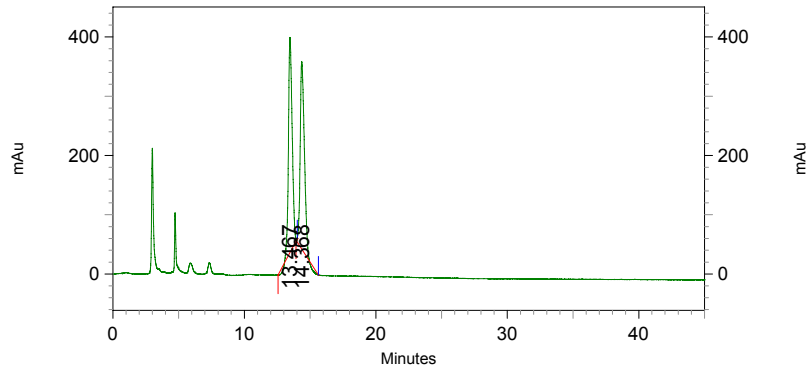
Retention Time	Area	Area Percent
11.973	487661	3.452
12.571	13639486	96.548

3.44



1: 230 nm, 4 nm Results

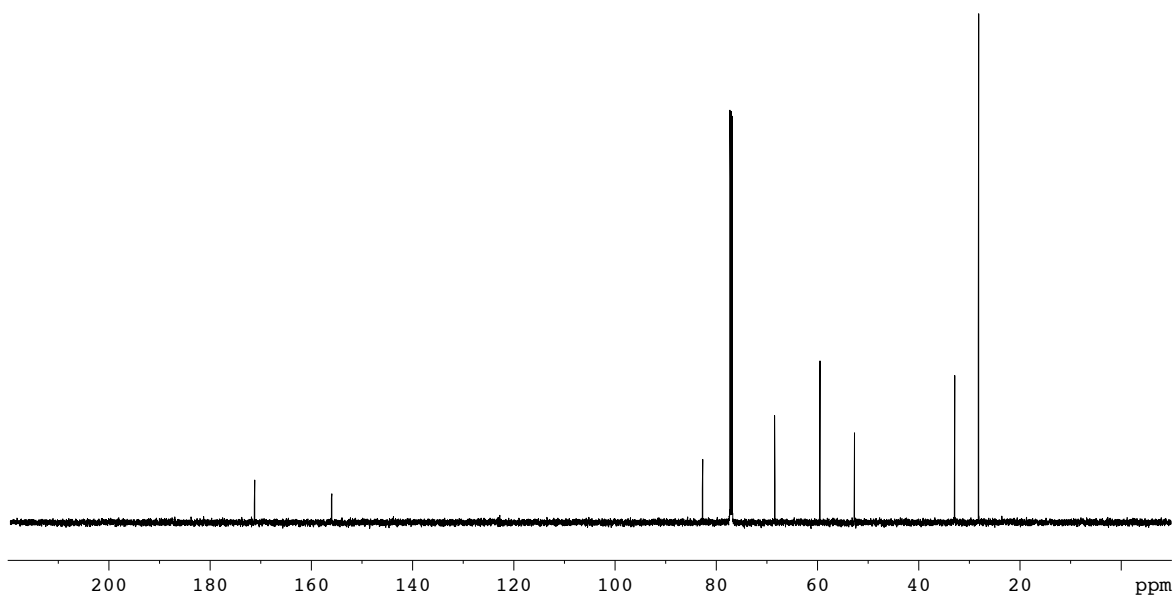
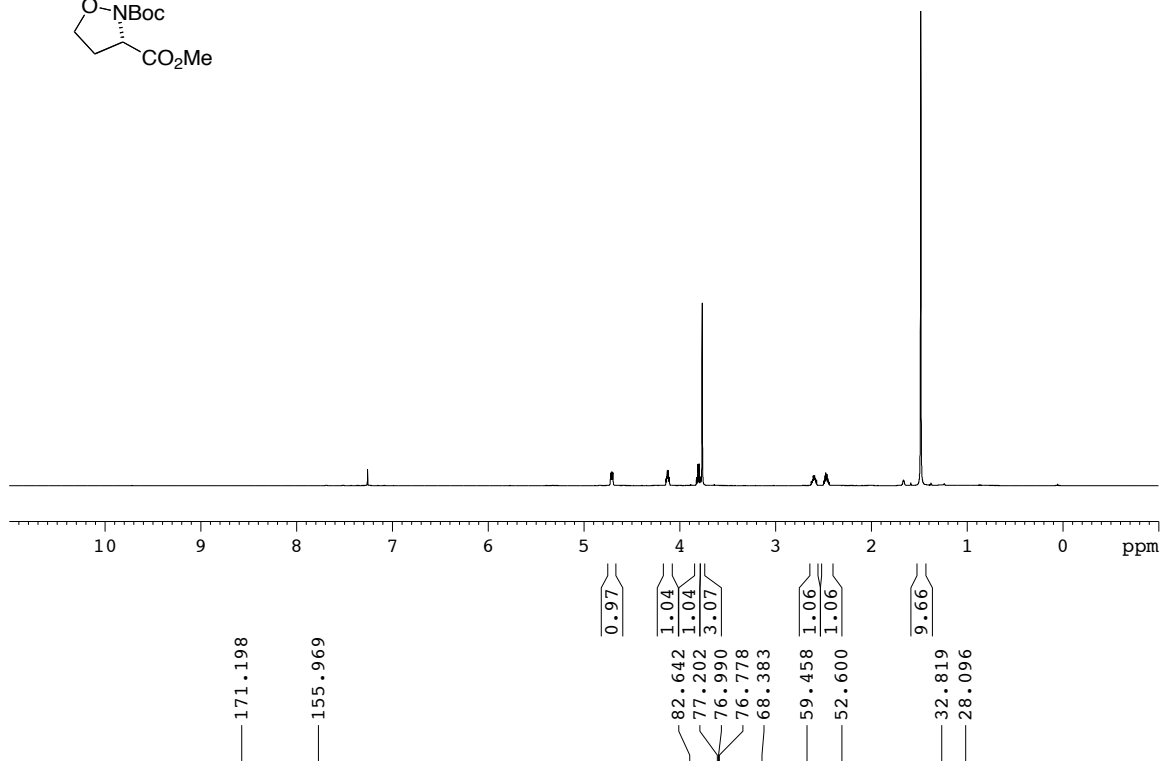
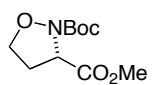
Retention Time	Area	Area Percent
13.472	967163	51.293
14.368	918412	48.707



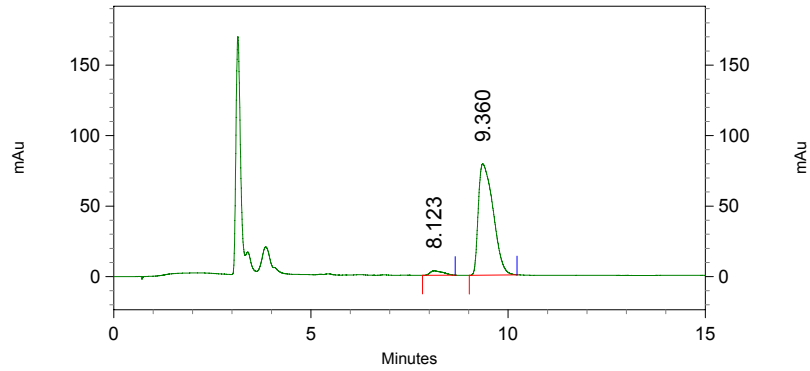
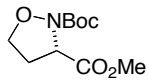
2: 214 nm, 4 nm Results

Retention Time	Area	Area Percent
13.467	7007712	50.479
14.368	6874689	49.521

3.59

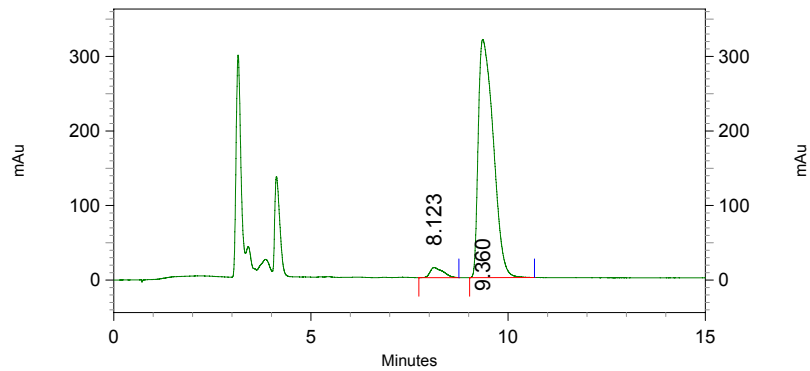


3.59



1: 230 nm, 4 nm Results

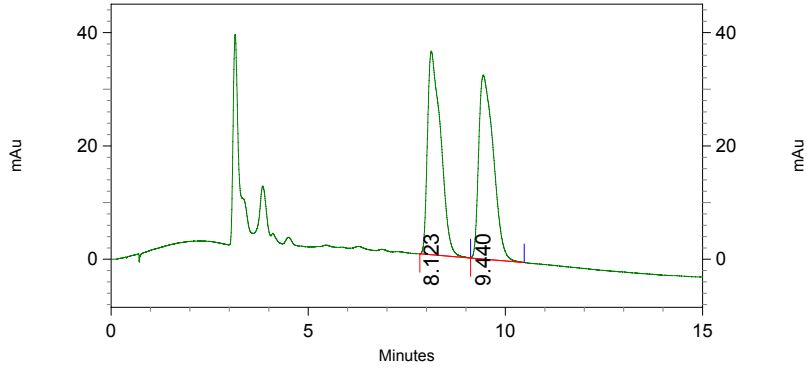
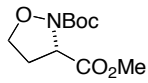
Retention Time	Area	Area Percent
8.123	71359	3.355
9.360	2055661	96.645



2: 214 nm, 4 nm Results

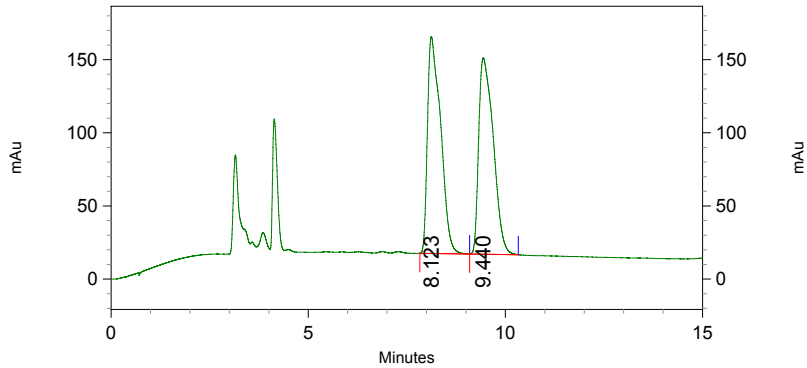
Retention Time	Area	Area Percent
8.123	304957	3.495
9.360	8421287	96.505

3.59



1: 230 nm, 4 nm Results

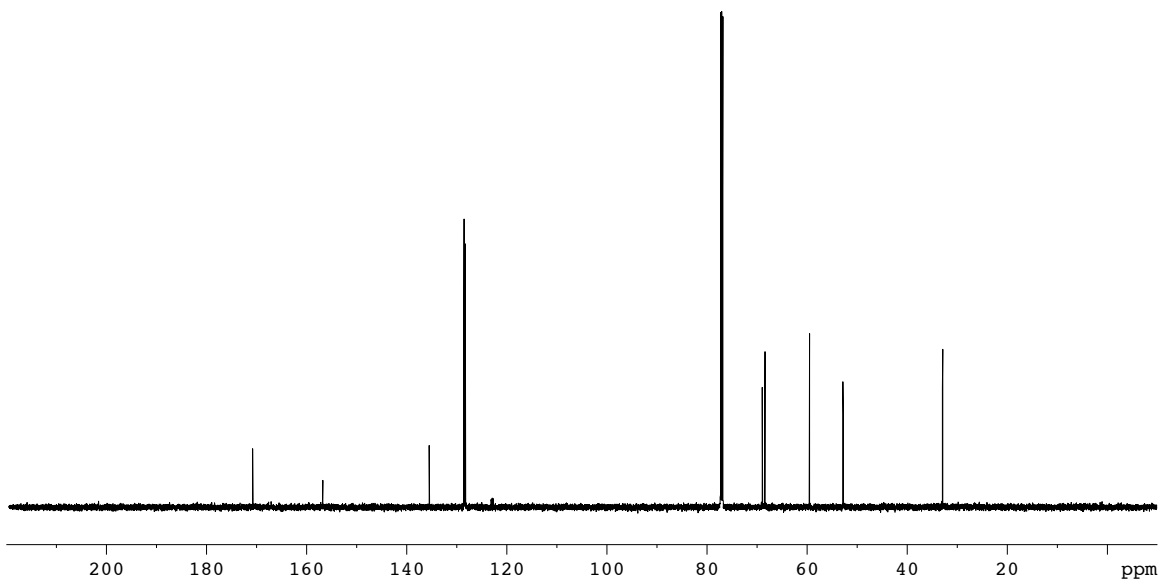
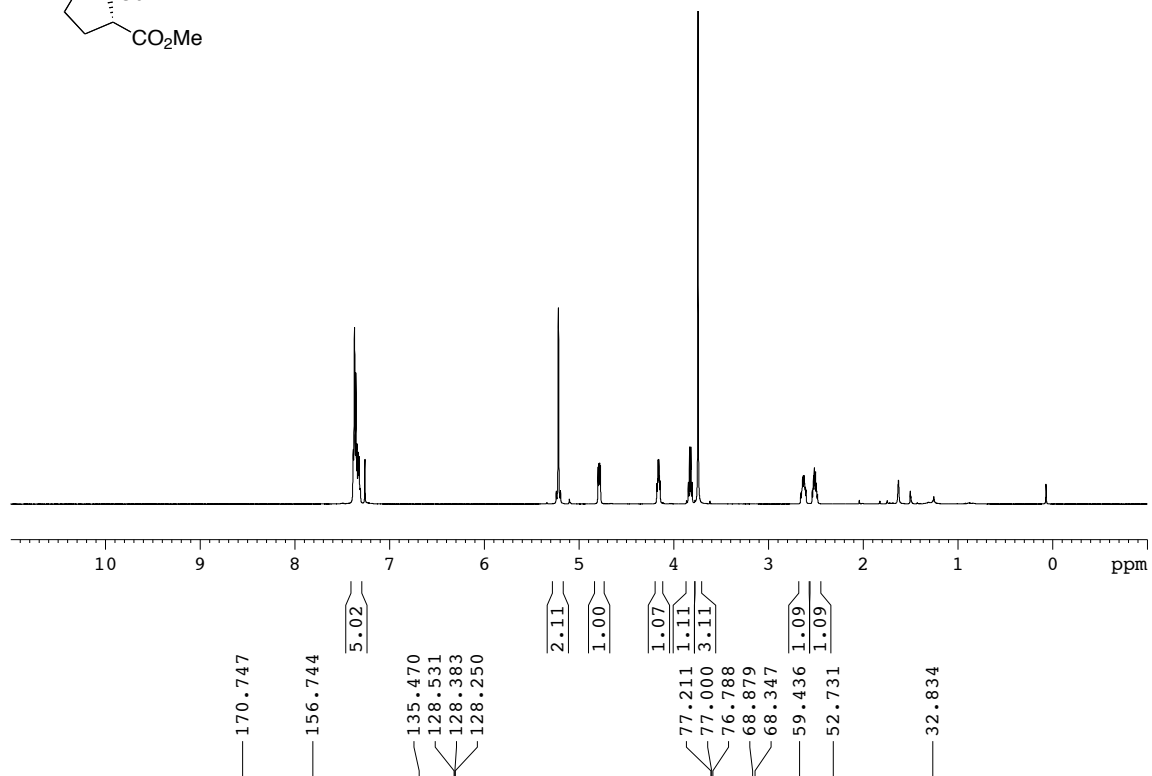
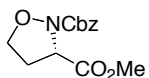
Retention Time	Area	Area Percent
8.123	829975	49.885
9.440	833806	50.115

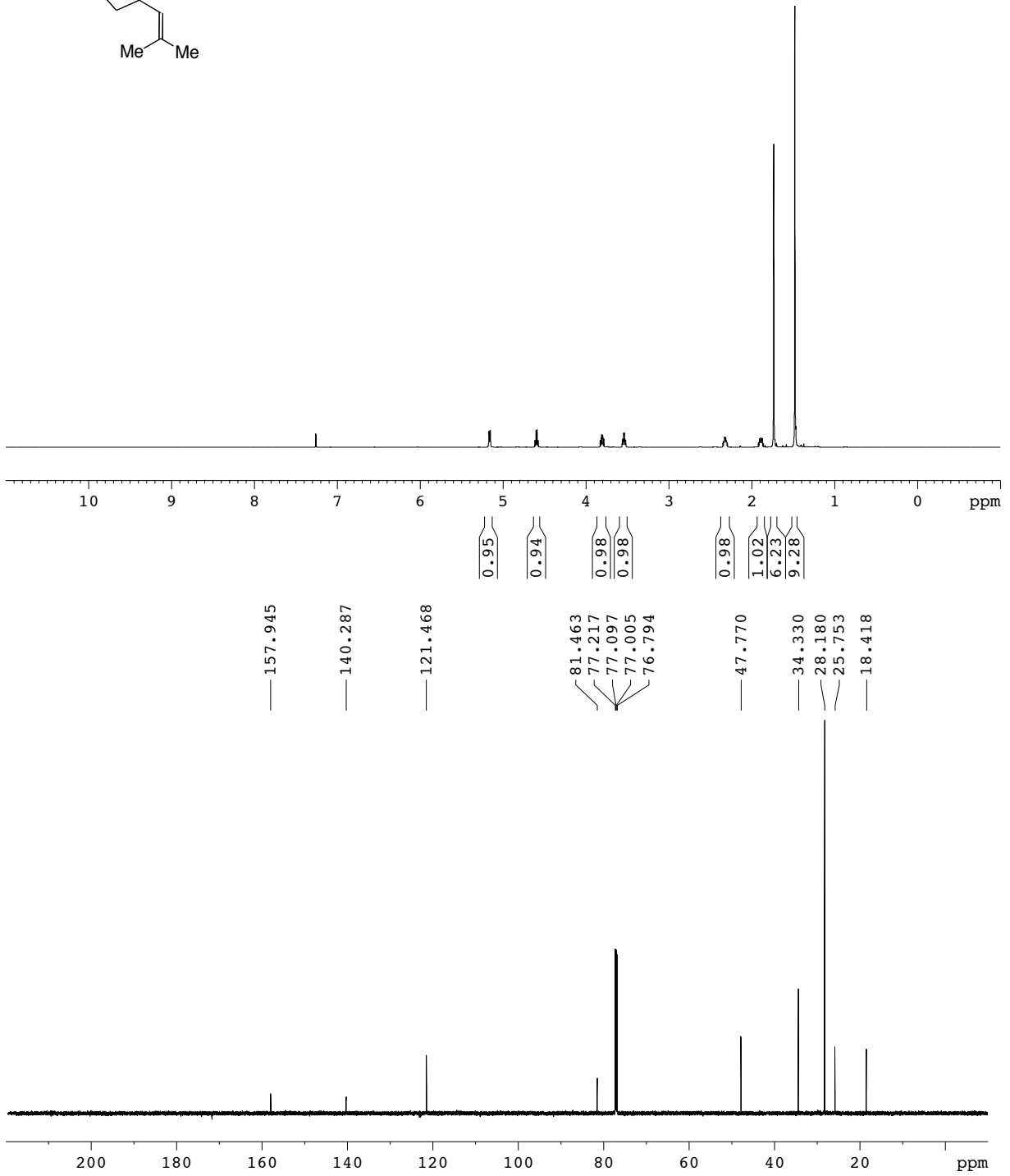
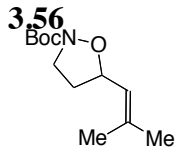


2: 214 nm, 4 nm Results

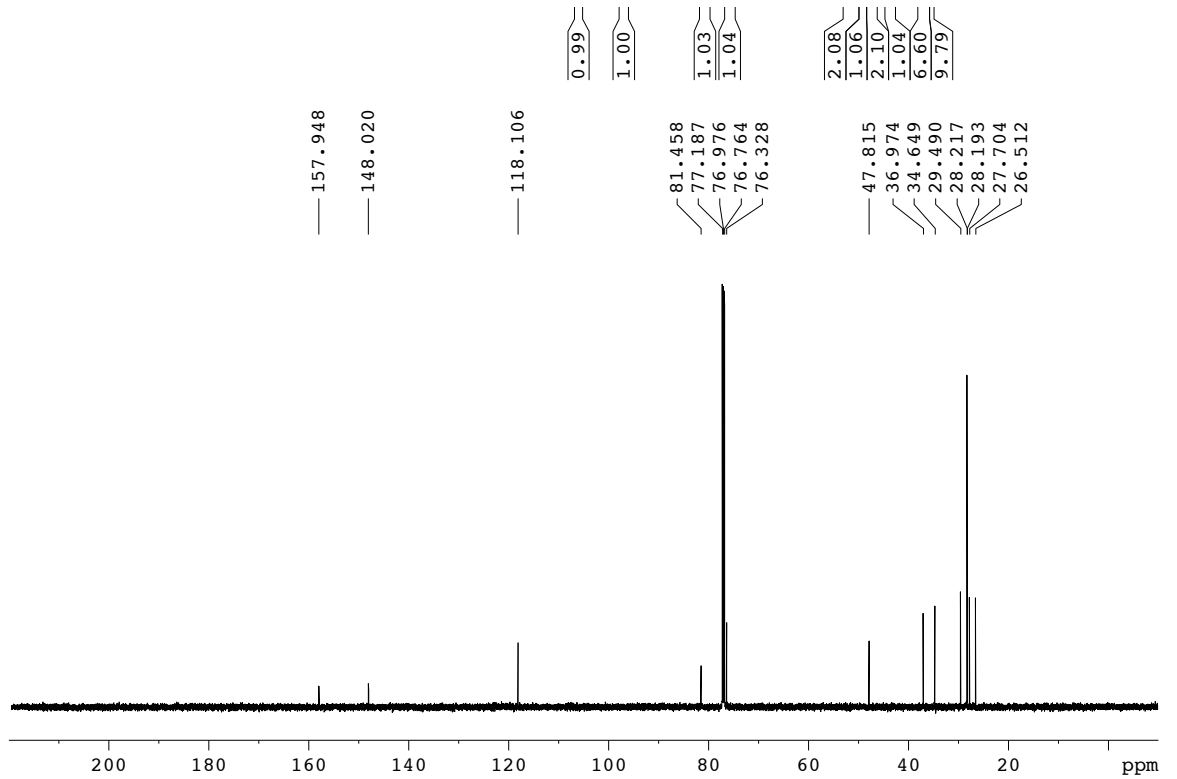
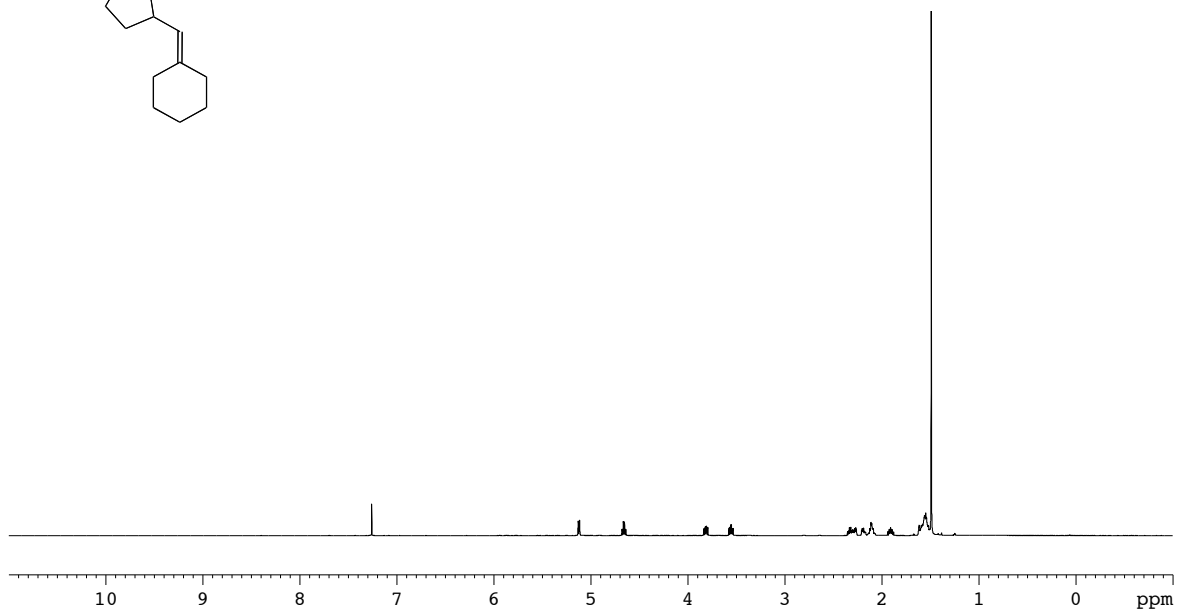
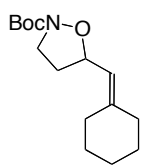
Retention Time	Area	Area Percent
8.123	3430726	49.931
9.440	3440247	50.069

(S)-methyl-2-benzyloxycarbonyl-3-isoxazolidinecarboxylate

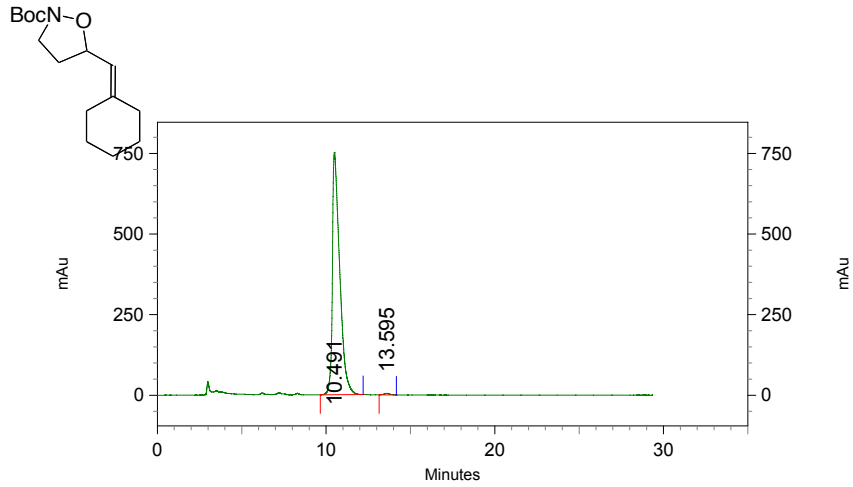




3.29

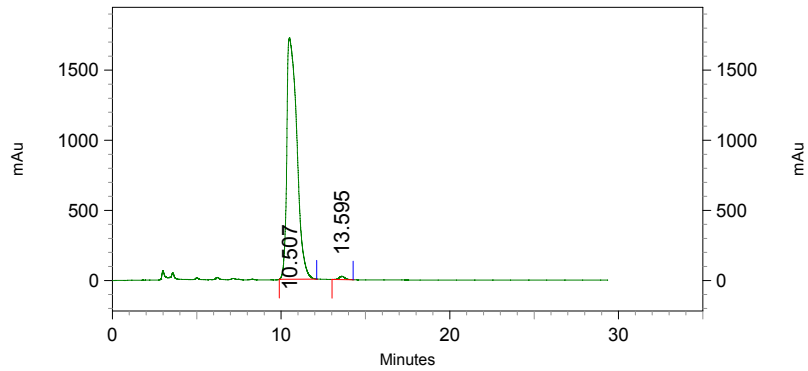


3.29



1: 230 nm, 4 nm Results

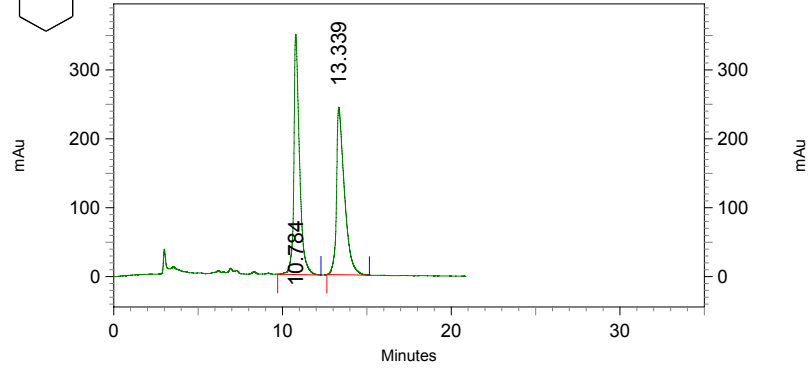
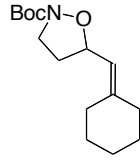
Retention Time	Area	Area Percent
10.491	22652804	99.549
13.595	102568	0.451



2: 214 nm, 4 nm Results

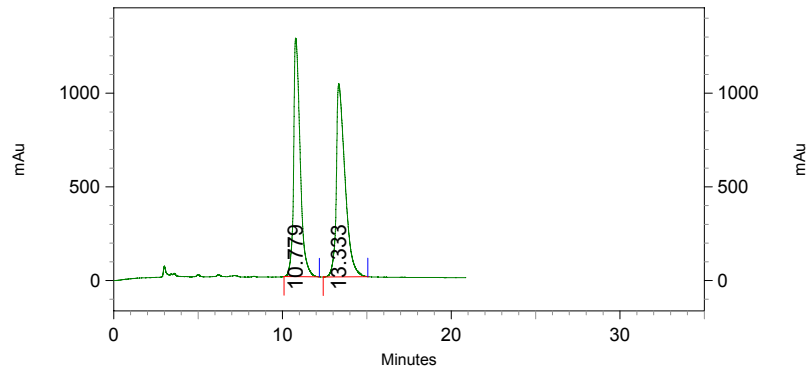
Retention Time	Area	Area Percent
10.507	71417480	99.222
13.595	560099	0.778

3.29



1: 230 nm, 4 nm Results

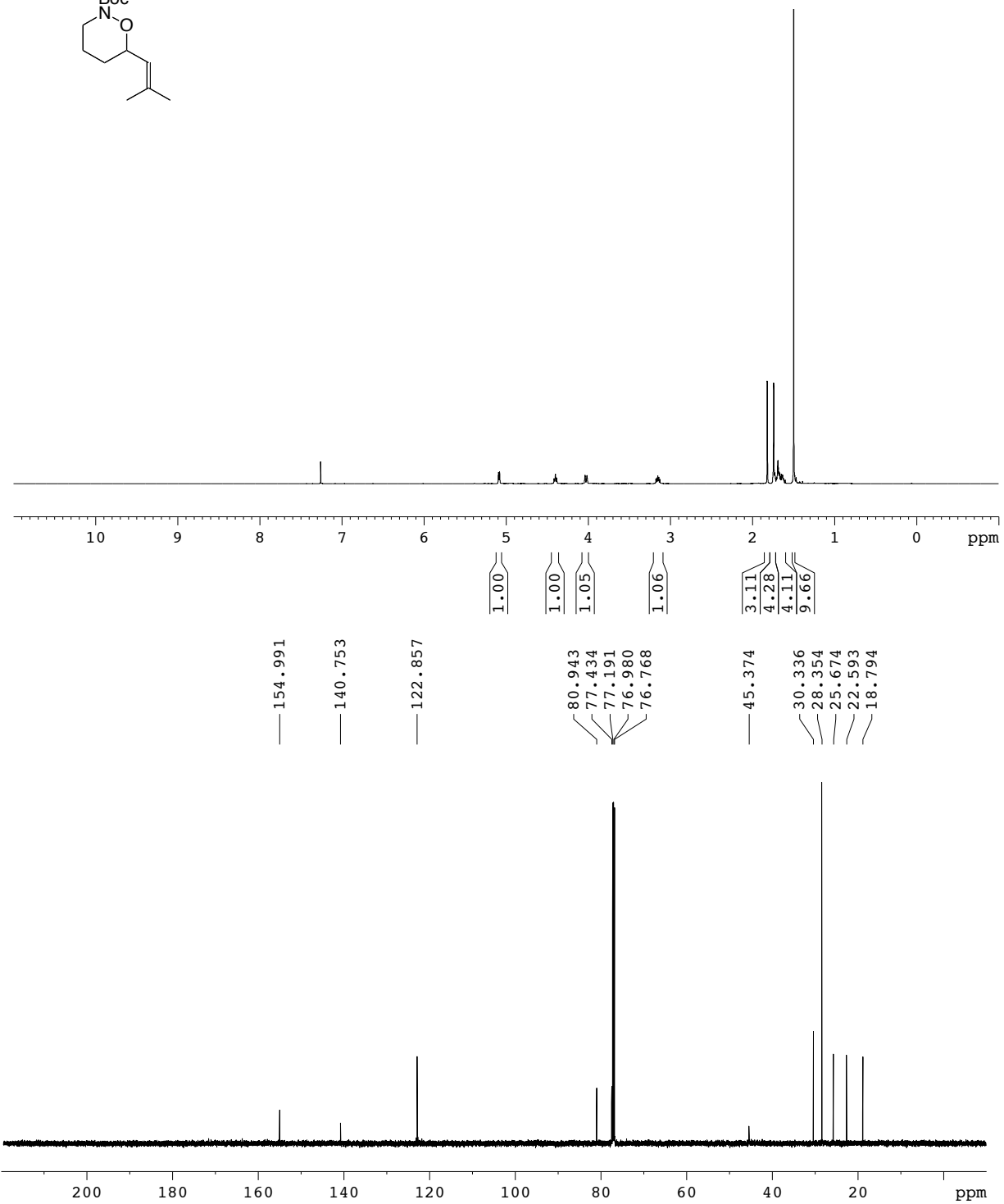
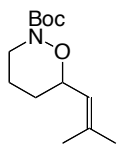
Retention Time	Area	Area Percent
10.784	8096816	50.387
13.339	7972500	49.613



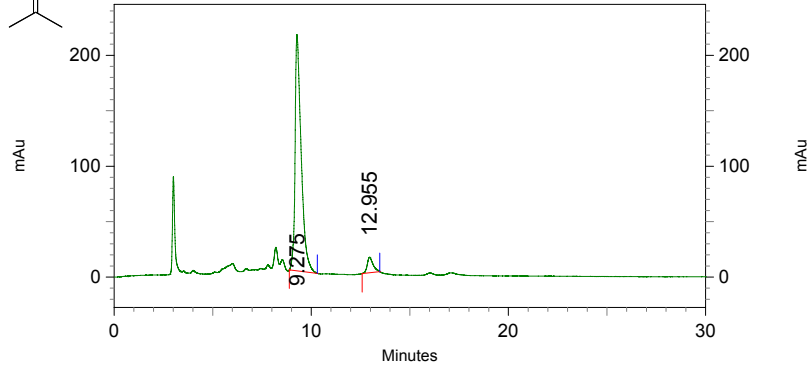
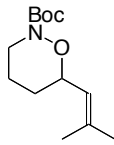
2: 214 nm, 4 nm Results

Retention Time	Area	Area Percent
10.779	34355496	48.052
13.333	37140850	51.948

3.58

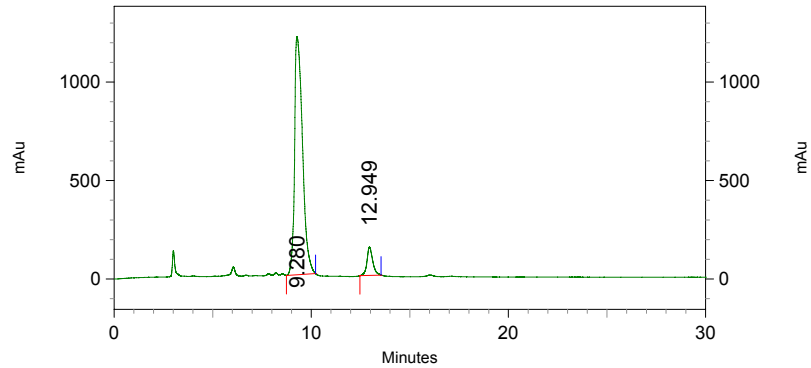


3.58



1: 230 nm, 4 nm Results

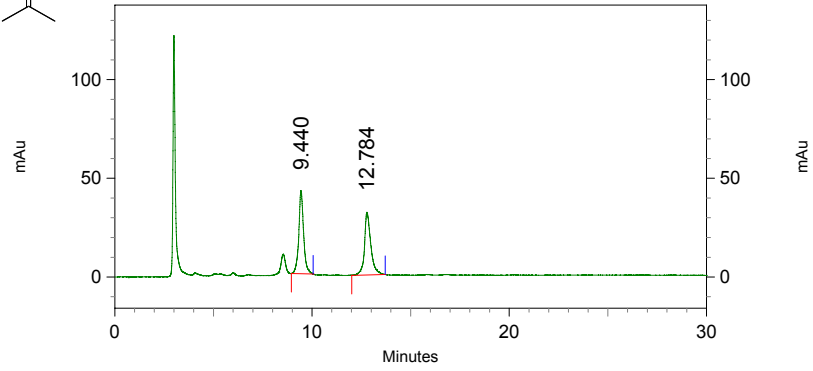
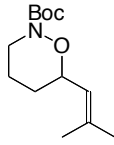
Retention Time	Area	Area Percent
9.275	4581615	94.081
12.955	288255	5.919



2: 215 nm, 4 nm Results

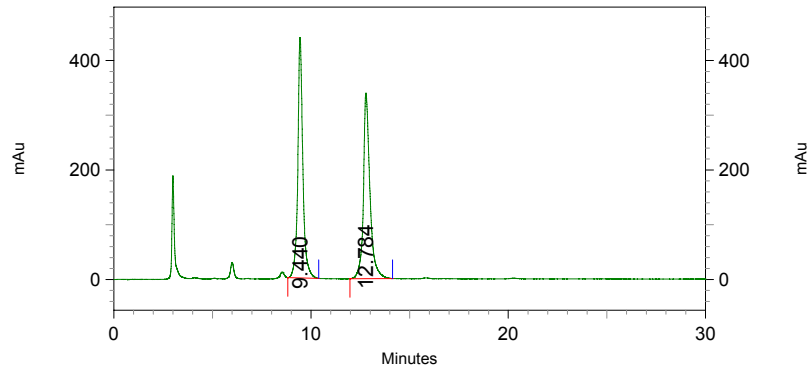
Retention Time	Area	Area Percent
9.280	33884258	92.031
12.949	2934039	7.969

3.58



1: 230 nm, 4 nm Results

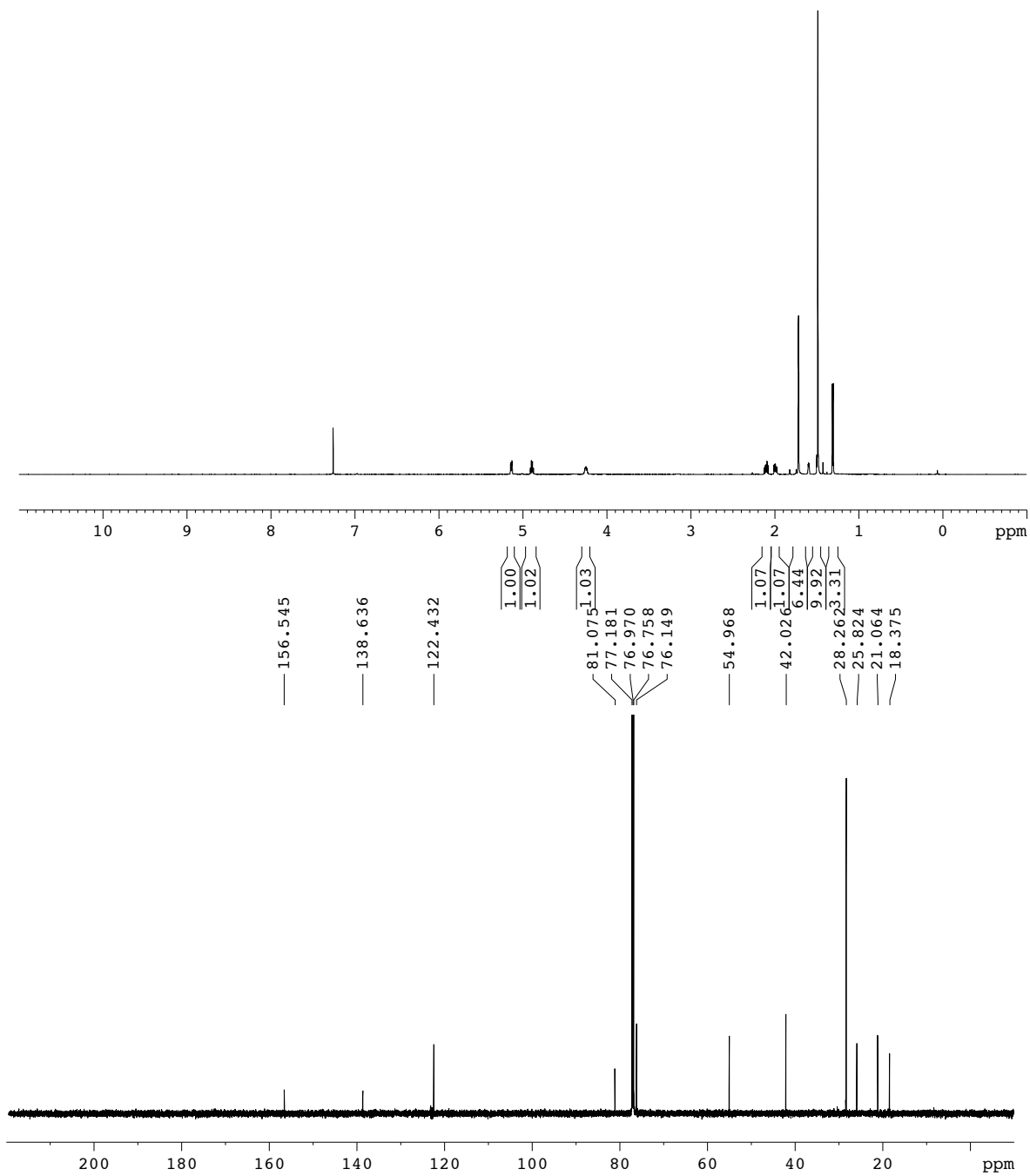
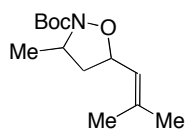
Retention Time	Area	Area Percent
9.440	718020	50.163
12.784	713359	49.837



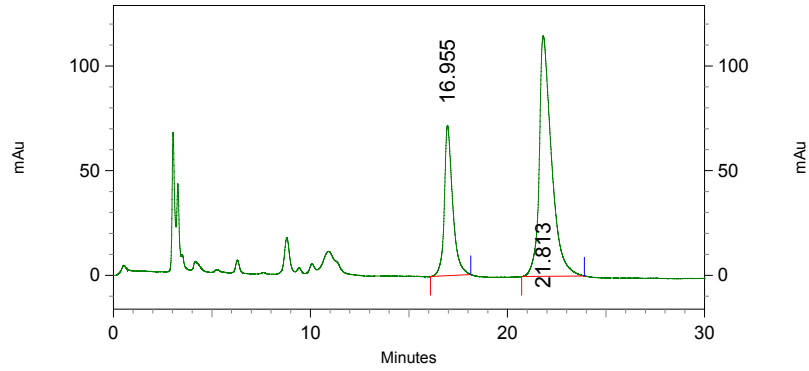
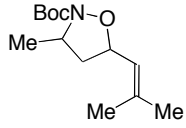
2: 214 nm, 4 nm Results

Retention Time	Area	Area Percent
9.440	7817904	50.008
12.784	7815389	49.992

3.57

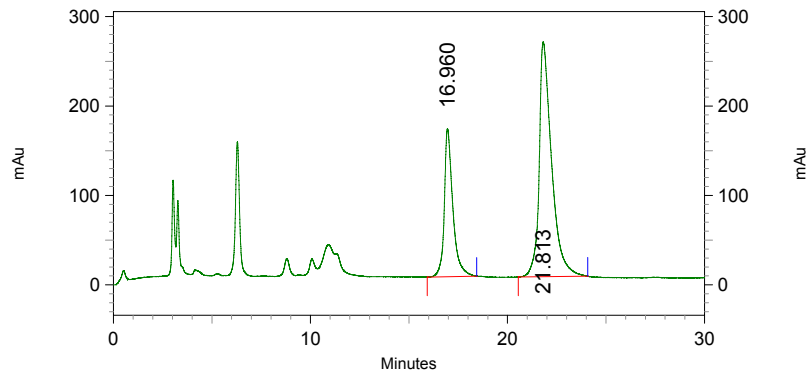


3.57



1: 230 nm, 4 nm Results

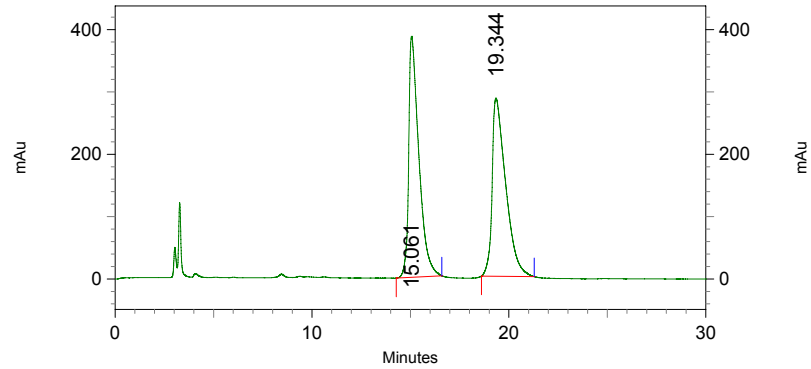
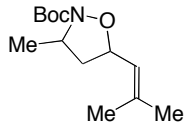
Retention Time	Area	Area Percent
16.955	2104327	29.651
21.813	4992741	70.349



2: 214 nm, 4 nm Results

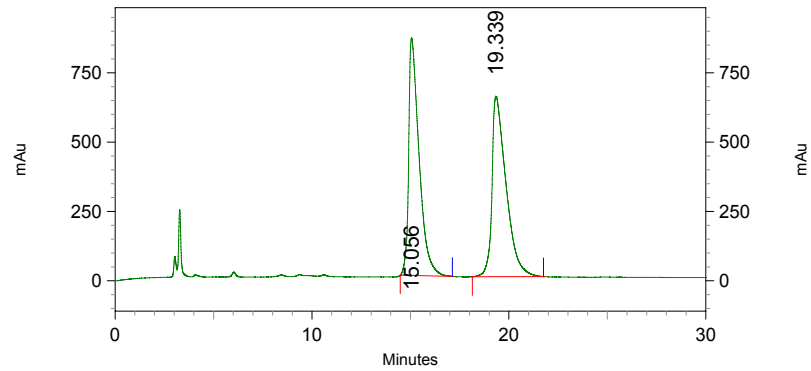
Retention Time	Area	Area Percent
16.960	4974519	30.139
21.813	11530464	69.861

3.57



1: 230 nm, 4 nm Results

Retention Time	Area	Area Percent
15.061	13875845	50.308
19.344	13705702	49.692



2: 214 nm, 4 nm Results

Retention Time	Area	Area Percent
15.056	31490794	49.278
19.339	32413056	50.722

Chapter 4

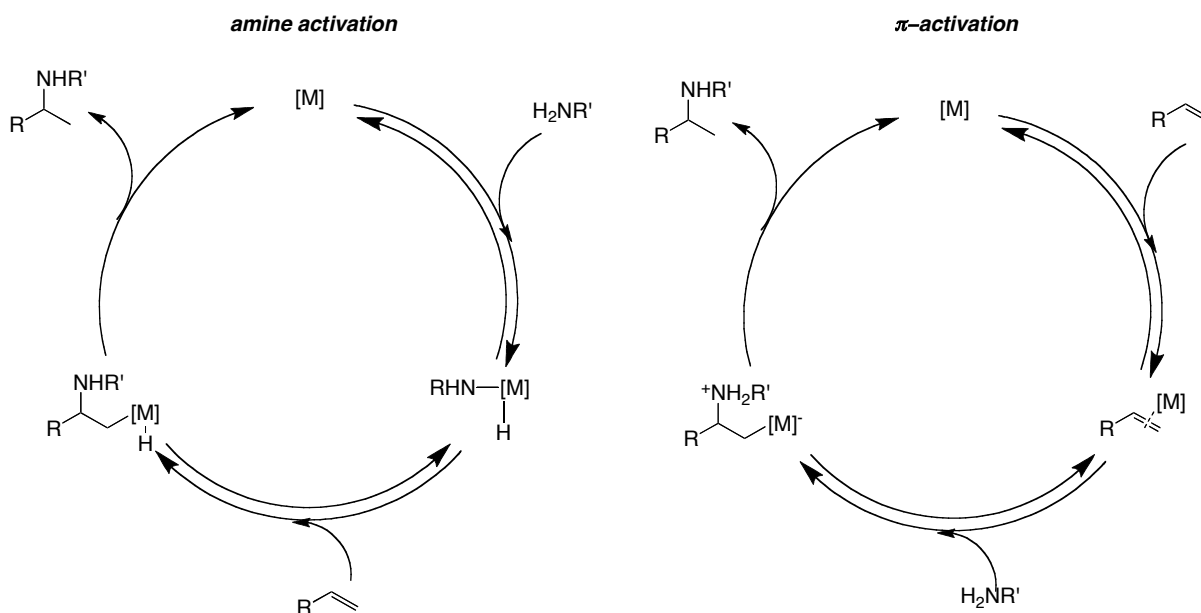
Intramolecular Aminoauration of Unactivated Alkenes

A portion of this work has been accepted for publication (LaLonde, R. L.; Brenzovich, W. E.; Benitez, D.; Tkatchouk, K.; Kelley, K.; Goddard, W. A.; Toste, F. D. “Alkylgold Complexes by the Intramolecular Aminoauration of Unactivated Alkenes” *Chem. Science* **2010**, DOI: 10.1039/c0sc00255k), but has been described here in greater detail.¹

¹I initially discovered the aminoauration reaction and carried out the deuteration, kinetic studies, investigations of gold-amide reactivity, and zinc transmetallation. Dr. William ‘Skip’ Brenzovich was responsible for testing the substrate scope, performing the ligand exchange reaction, and transmetallation studies with palladium. Kotaro Kelley, an undergrad under my supervision performed the studies on piperidine formation. Dr. Diego Benitez was responsible for the computational studies.

Introduction

Metal-catalyzed alkene hydroamination constitutes a vast area of research, which spans the periodic table, from lanthanides to early and late transition metals.¹ The primary goal in this field is clear: a general, practical method to install nitrogen on simple alkenes. The generation of an enantioselective process is an ancillary objective. The breadth of this field is a testament to the difficulty in achieving these goals. In general, there are two mechanistic paradigms (Scheme 4.1). The first, which is usually favored by lanthanide² and group IV early metals,³ involves the formation of amido- or imidometal complexes, respectively. After migratory insertion, an alkylmetal intermediate is generated. Although these reaction systems have been developed into enantioselective methods,⁴ the utility of these processes is greatly hindered by the extreme air and moisture sensitivity of the metals involved.



Scheme 4.1. Two Mechanistic Paradigms for Alkene Hydroamination.

Late metals commonly proceed via an alternative mechanism, π -activation. The foundations to this area of research were laid over a century ago, with the formation of organomercurials using mercuric salts.⁵ It was subsequently discovered that platinum⁶ and palladium⁷ were capable of effecting related alkene addition reactions as well. Moreover, the reaction of alkene complexes with amine nucleophiles was shown to give rise to β -aminoalkyl-mercury,⁸ -platinum⁹ and -palladium¹⁰ complexes. These discoveries formed the basis for the development of late transition metal-catalyzed hydroamination reactions¹ in which the catalyst may be regenerated from the alkylmetal intermediate by protonolysis of the alkylmetal bond.

While the π -activation paradigm has been proposed and studied in platinum-¹¹ and palladium¹²-catalyzed hydroamination reactions of alkenes, the mechanism appears to vary in

different systems. For example, a recent report by Wolfe and co-workers provided evidence for initial formation of a palladium-amine complex followed by *syn* migratory insertion into the alkene.¹³ Although the authors spectroscopically observed an alkylpalladium intermediate, they did not report crystallographic evidence. In contrast, Michael and co-workers found that with less basic amines, carbamates and acetamides, fast and reversible π -complexation was followed by nucleophilic attack.¹⁴ In this case, protodemetalation was found to be rate limiting, and the crystal structure of an alkylpalladium intermediate was described.

Another common theme in metal catalyzed hydroamination is the mechanistic debate about the role of acid in these reactions. In particular, metal triflate catalysts, which could potentially generate triflic acid, have subjected to intense scrutiny. One of the best understood systems, a platinum-mediated hydroamination, was subjected to a thorough analysis.¹⁵ After this investigation, the mechanism of this transformation was accepted not as acid or metal catalyzed, but instead as a “metal-mediated proton transfer”. This serves as a prime example of the complexity of differentiating between acid and metal catalyzed processes, since the true mechanism may lie somewhere in between.

Gold Alkene Activation

Gold-catalyzed reactions that proceed through the activation of alkynes and allenes are now well-established,¹⁶ though there have been significantly fewer reports of related additions to alkenes.¹⁷ In addition, gold(I) has in the past been referred to as an ‘alkynophilic’ Lewis acid, which has added to the confusion about gold(I)-alkene activation. Although this term could be used to suggest that gold could not activate alkenes for nucleophilic attack, it has been made clear, in computational and crystallographic studies, that gold(I) complexes both alkynes and alkenes. In fact, computational studies demonstrated that a gold(I)-ethylene complex was stabilized ~10 kcal/mol more relative to the corresponding gold(I)-ethyne species.¹⁸ In addition, a variety of gold(I)-alkene complexes have recently been isolated and analyzed by X-ray crystallography (Figure 4.1).¹⁹

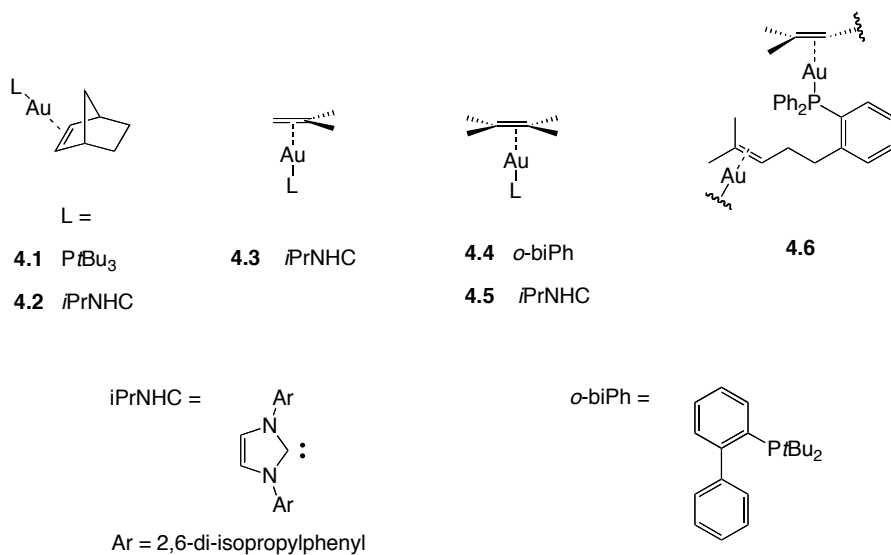
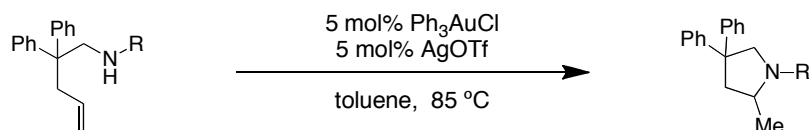


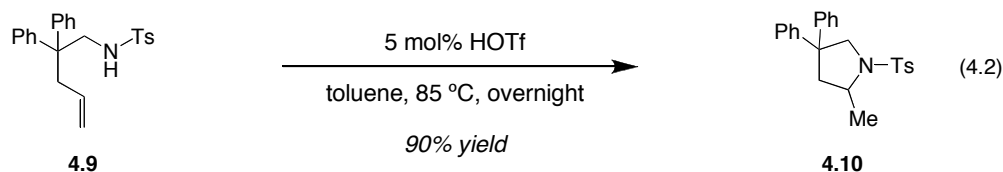
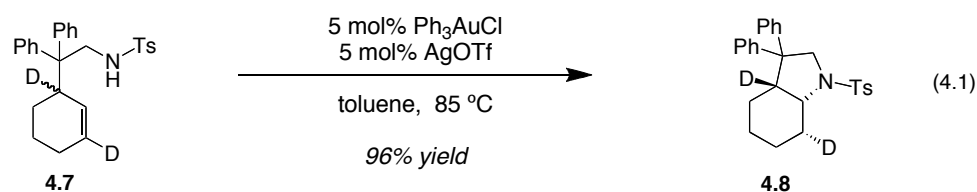
Figure 4.1. Gold(I)-Alkene Complexes.

Despite the experimental evidence for gold(I)-alkene complexes, the role of gold in alkene hydroamination remains unclear. The majority of the reported gold-catalyzed additions require elevated temperatures and extended reaction times; conditions under which the analogous Brønsted acid-catalyzed reactions also occur.^{15, 20} Therefore, one may deduce that gold may not be involved in the catalytic cycle at all by comparing the accounts of gold(I) to the equivalent acid reactivity. For example, He reported an inter- and intramolecular alkene hydroamination which was initially believed to be gold(I)-catalyzed (Table 4.1).^{17a} The reaction was found to be limited to sulfonamide nucleophiles (entries 1 and 2), such as *o*-nitrosulfonyl (Ns) and *p*-toluenesulfonyl (Ts). In addition, deuterated cyclohexene **4.7** cyclized to form a single diastereomer (eq 4.1). The authors interpreted this result as support for *anti*-nucleophilic addition to the alkene. However, it must be emphasized that the stereochemical consequences of protodeauration are unknown. Although these results seemed promising, Hartwig showed that the exact same transformation could be catalyzed by triflic acid under practically identical conditions (eq 4.2).^{20a} This information, coupled with the fact that acetamides exhibited no reactivity (entry 3), leads to the conclusion that the reactivity described by He was not gold(I)-catalyzed.

Table 4.1. Intramolecular Hydroamination with Tosylamines.

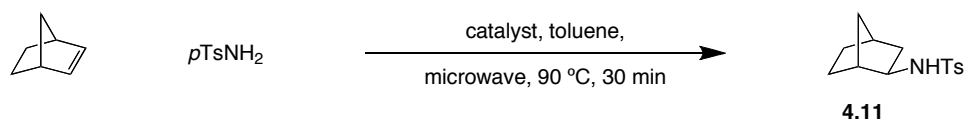


entry	R =	time (h)	% yield
1	Ts	17	96
2	Ns	48	99
3	Ac	48	0



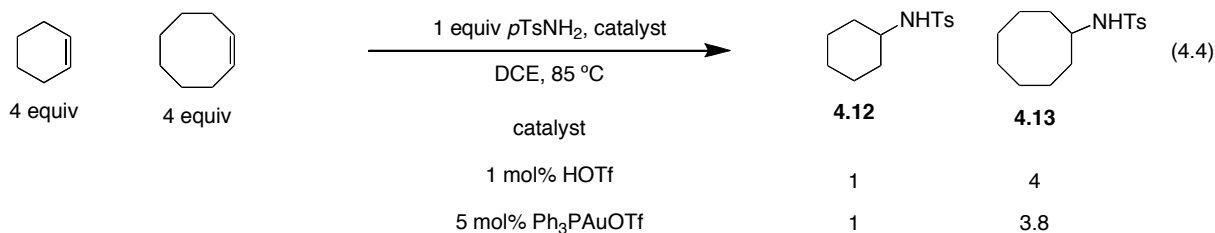
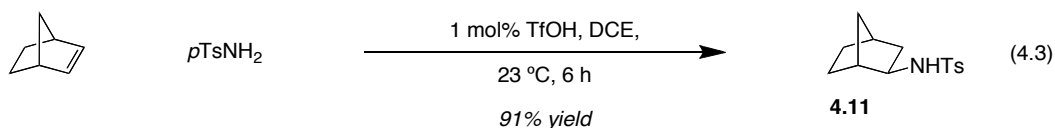
More examples of the parallel reactivity between gold and Brønsted acid were found in intermolecular hydroamination. The analogous intermolecular hydroamination was achieved with 85% yield (Table 4.2, entry 1).^{17a} In this case, the corresponding acid catalyzed reaction (eq 4.3) was reported to have an even higher yield (91%) and lower catalyst loading (1 mol%).^{20a} Furthermore, Hartwig performed a competition experiment between cyclohexene and cyclooctene. A comparison of the resulting product distribution for acid catalysis and gold catalysis revealed minimal differences (eq 4.4).

Table 4.2. Ligand Effects on Microwave Assisted Intermolecular Hydroamination of Alkenes.



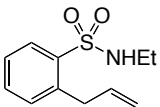
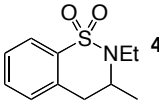
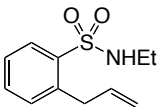
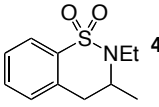
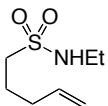
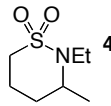
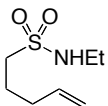
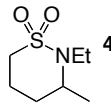
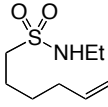
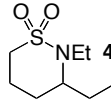
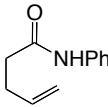
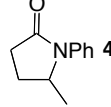
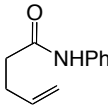
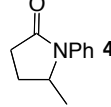
entry	catalyst	% conv
1	5 mol% Ph ₃ PAuCl/AgOTf ^a	85 ^b
2	0.1 mol% Ph ₃ PAuCl/AgOTf	58
3	0.1 mol% (PhO) ₃ PAuCl/AgOTf	99
4	0.05 mol% (PhO) ₃ PAuCl/AgOTf	94
5	0.01 mol% (PhO) ₃ PAuCl/AgOTf	60
6	0.01 mol% HOTf	8

^a Thermal heating to 85 °C. ^b Isolated yield.

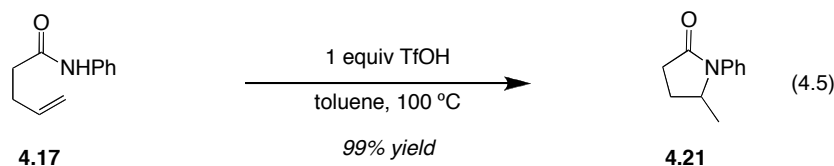


Nájera later combined microwave heating with ligand effects to affect the same transformation with reduced catalyst loading (Table 4.2).²¹ Lowering the amount of triphenylphosphinegold triflate also diminished the observed conversion to 58% (entry 2). Employing triphenylphosphite as a ligand generated the product with near perfect conversion (entry 3). The catalyst loading could be minimized (0.05 mol%) even further without significantly decreasing the conversion (94%). Under comparable conditions, 0.01 mol% triflic acid did not perform as an efficient catalyst. As such, when methods use extremely low catalyst loadings the role of acid in the reaction appears to be small, but measurable. However, the amount of gold is usually much larger, typically in the range of 5 mol%.

Table 4.3. Thermal and Microwave-Assisted Gold(I)-Catalyzed Hydroamination.^a

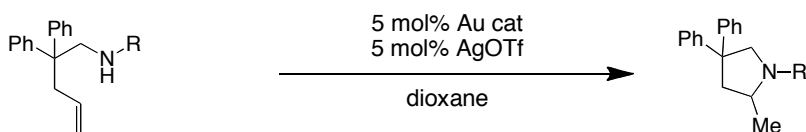
entry	substrate	temp (°C)	time	product	% yield
1		100	24 h		95
2		140	40 min		90
3		100	72 h		95
4		140	40 min		95
5		100	48 h		88
6		100	30 h		50
7		140	30 min		57

^a Thermal reaction conditions: 5 mol% Ph₃PAuOTf, toluene, 100 °C; Microwave reaction conditions: 5 mol% Ph₃PAuOTf, DCE, 140 °C.



Microwave irradiation was also found to be useful for reducing the extended reaction times required to cyclize sulfonamides (Table 4.3).^{17b} For example, cyclization of **4.14** with thermal heating took 24 h, whereas with microwave heating to 140 °C the reaction time was only 40 min (entry 2). The time needed to catalyze the formation of **4.15** was even more dramatically decreased from 72 h to 40 min. Although this report seemed to describe progress towards creating a more practical gold(I)-catalyzed hydroamination, some evidence suggests that this transformation was actually acid mediated. Under both thermal and microwave conditions, benzamide **4.17** reacted with poor yield (50% and 57% yield, respectively). In this case, a triflic acid mediated cyclization produced the desired product with near quantitative yield (eq 4.5).^{20b}

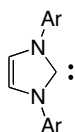
Table 4.4. Gold(I)-Catalyzed Hydroamination of Alkenes.



entry	substrate	R =	ligand	temp (° C)	time (h)	product	% yield
1	4.22	Cbz	Ph ₃ P	100	24	4.25	70
2			Me ₂ PhP	100	24		7
3			<i>o</i> -BiPh	100	24		98
4			<i>o</i> -BiPh	60	18		97
5			iPrNHC	23	18		20 ^a
6			iPrNHC	45	15		96
7	4.23	Ac	<i>o</i> -BiPh	80	21	4.26	99
8			iPrNHC	23	18		83
9	4.24	NHCONHPh	<i>o</i> -BiPh	80	15	4.27	92
10			iPrNHC	23	18		96

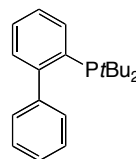
^a % conversion.

iPrNHC =



Ar = 2,6-di-*iso*-propylphenyl

o-biPh =



A clear trend can be extracted from the previous examples: the addition of sulfonamides, often appear to be acid-catalyzed. On the other hand, the parallel acid-catalyzed transformations have not yet been illustrated for acetamides and carbamates. In a series of reports, Widenhoefer described the addition of carbamates, acetates and ureas to unactivated alkenes.²² Interestingly, the authors found that adding steric bulk to the catalyst significantly improved the observed yield. For example, triphenylphosphinegold triflate catalyzed the desired cyclization in 70% yield (Table 4.4, entry 1). The yield was increased to 98% by employing *o*-BiPhAuOTf (**4.28**) as the catalyst (entry 3 and 4). By comparing this result to the use Me₂PhPAuOTf (entry 2), the authors deduced that sterics, rather than electronics were responsible for the enhanced reactivity. The sterically hindered complex **4.28** catalyzed the hydroamination of a variety of alkenyl carbamates, although high temperatures (60-100 °C) and extended reaction times (18-68 h) were required. In a subsequent paper, Widenhoefer extended the use of sterically encumbered ligands by employing an N-heterocyclic carbenegold(I) complex **4.29**. To illustrate the enhanced

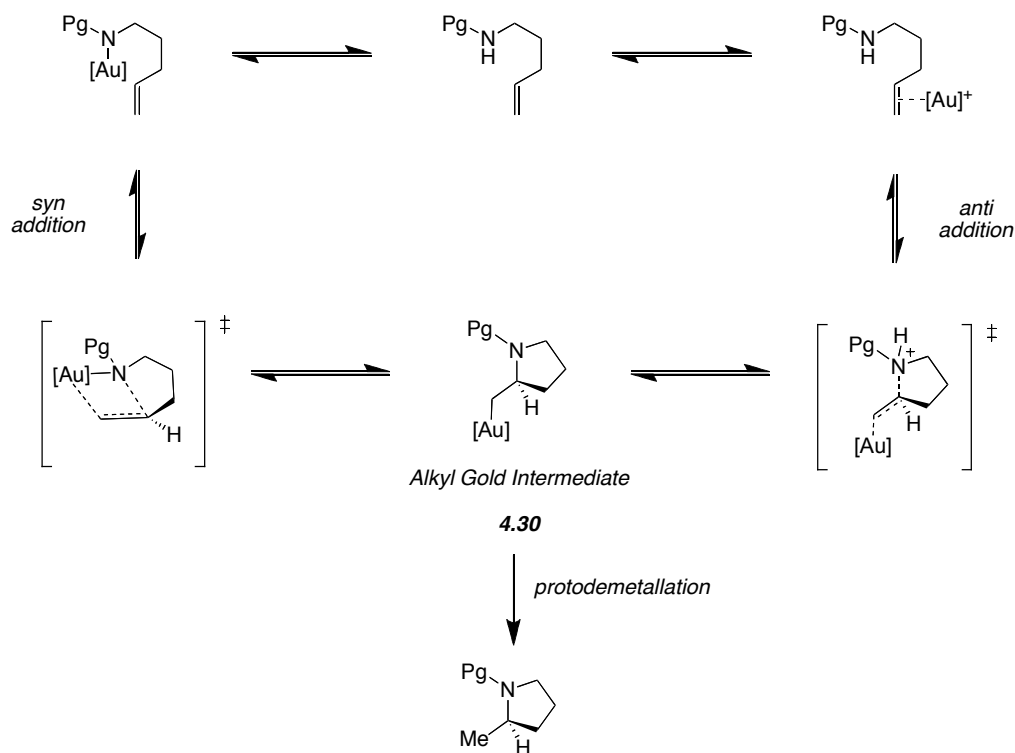
reactivity of complex **4.29**, the reaction temperature could be lowered to 23-45 °C while maintaining reactivity. For example, both acetamide **4.23** and urea **4.24** cyclized in good yield (83% and 96%, respectively) at room temperature.

To our knowledge, the gold(I)-catalyzed hydroamination systems described above have not been subjected to mechanistic analysis. We identified distinguishing between acid and metal catalyzed processes as a critical step in advancing gold(I)-catalyzed alkene hydroamination. Finding direct experimental evidence for the elementary step of gold-promoted nucleophilic addition to an alkene is necessary before the two processes can be distinguished. Although several vinylgold intermediates derived from the gold-promoted addition of nucleophiles to alkynes and allenes have been isolated and characterized, the analogous alkylgold complexes were unknown at the time of this work.²³ In fact, relatively few of the analogous mercury, palladium and platinum complexes have been characterized by X-ray crystallography.^{14, 24, 25} Furthermore, the isolation of such intermediates could enable the discovery of new reactivity. Finally, until the mechanism of this transformation is clear, efforts at creating enantioselective versions will be complicated. Herein we report the isolation and characterization of the first compounds derived from the gold-activated nucleophilic addition to an olefin.

Results

Synthesis and Isolation of Alkylgold Complexes

Mechanisms involving either the gold-promoted *anti*- or *syn*-addition of nucleophiles to π -bonds have been previously proposed (Scheme 4.2). Both of these pathways necessitate the intermediacy of an alkylgold species (**4.30**) that subsequently undergoes protodemetalation to provide product and regenerate the gold catalyst. We reasoned that the addition of an exogenous base might prevent protodemetalation, allowing for the observation and isolation of intermediates like **4.30**. However, previous reports have suggested that basic amines might “bind gold(I) and thus inhibit the addition step”.^{17a}

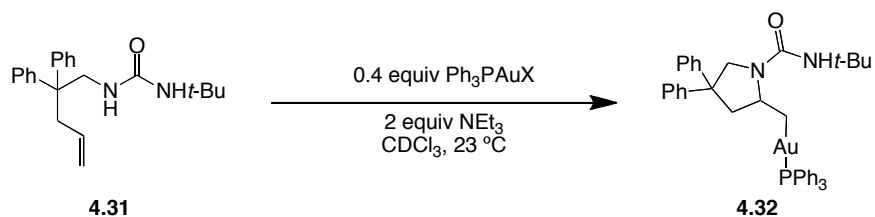


Scheme 4.2. Proposed *Syn*- and *Anti*- Addition Mechanisms for Gold(I)-Catalyzed Hydroamination of Alkenes.

Thus, we initially chose proton sponge, a hindered, non-nucleophilic base, and a gold(I) complex stabilized by a strongly coordinating *p*-nitrobenzoate counterion. We were pleased to find that under these conditions alkene **4.31** was converted to the desired alkylgold complex **4.32**, as indicated by ³¹P and ¹H NMR, in modest yields (Table 4.5, entry 1). Replacing the starting gold complex with a gold-oxo trimer, [(Ph₃PAu)₃O]BF₄, resulted in near quantitative conversion of **4.31** to alkylgold **4.32** (entry 2). Surprisingly, even excess amounts of other less-

hindered amine bases (entries 3, 4) were competent at sequestering protons without hindering the activity of the cationic gold complex. 2,6-Di-*tert*-butylpyridine, however, was not sufficiently basic, yielding only 33% of the desired alkylgold complex and 59% of the pyrrolidine resulting from hydroamination (entry 5). Ultimately, we identified triethylamine as the optimal base, as isolation of alkylgold complex **4.32** was simplified by performing an aqueous work up.

Table 4.5. Optimization of Alkylgold Formation.^a

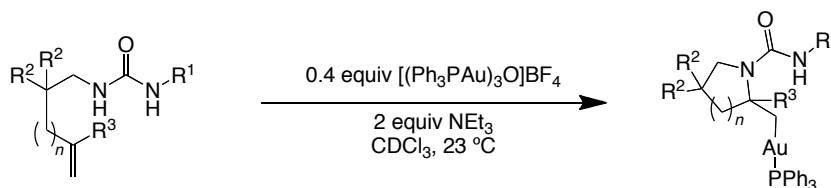


entry	Ph ₃ AuX	base	% conv ^b
1	Ph ₃ PAuOPNB	proton sponge	~10
2	[(Ph ₃ PAu) ₃ O]BF ₄	proton sponge	100
3	[(Ph ₃ PAu) ₃ O]BF ₄	DABCO	92
4	[(Ph ₃ PAu) ₃ O]BF ₄	NEt ₃	98
5	[(Ph ₃ PAu) ₃ O]BF ₄	2,6-di- <i>t</i> -butylpyridine	33(59) ^c

^a Reaction Conditions: To a solution of alkene (1 equiv) and base (2 equiv) in CDCl₃ was added a molar equivalent of gold. ^b Determined by ¹H and ³¹P NMR. ^c Yield in parentheses is protodemetalated product.

Under these optimized reaction conditions, a variety of urea substrates underwent the intramolecular aminoauration reaction (Table 4.6).²⁶ The conversions, as judged by ¹H and ³¹P NMR, are generally high and the reported yields are reflective of difficulties in the purification step. 1,1-Disubstituted alkenes also proved to be competent substrates, forming tertiary amine products (entries 6, 7); however, 1,2-disubstituted olefins (eq 4.6) did not form the desired alkylgold complex in any appreciable amount, even at elevated temperatures. The aminoauration to produce piperidine **4.46** in 30% yield required an excess of gold and extended reaction time (entry 8). The conversion could be improved by increasing the reaction temperature, although purification was then complicated by the formation of intractable byproducts.

Table 4.6. Scope of Aminoauration with Urea Substrates.^a



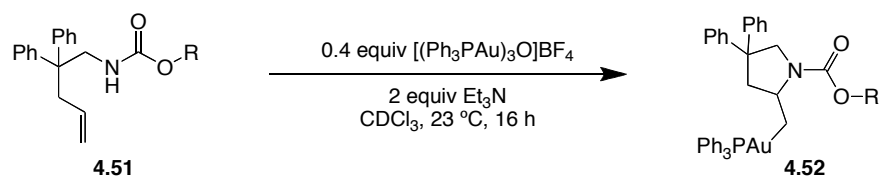
entry	substrate	<i>n</i> =	R ¹	R ²	R ³	time (h)	product	% yield ^b
1	4.31	1	<i>t</i> -Bu	Ph	H	2	4.32	80
2	4.33	1	Me	Ph	H	2	4.40	59
3	4.34	1	Et	Ph	H	2	4.41	63
4	4.35	1	Ph	Ph	H	2	4.42	66
5	4.36	1	Et	-C ₅ H ₁₀ -	H	2	4.43	49
6	4.37	1	Me	Ph	Me	14	4.44	60
7	4.38	1	Et	Ph	Me	14	4.45	40
8	4.39	2	Me	Ph	H	48	4.46	30 ^c

^a Reaction Conditions: To a solution of alkene (1 equiv) and base (2 equiv) in CDCl₃ was added 0.4 equiv of [(Ph₃PAu)₃O]BF₄. ^b Isolated yield after column chromatography on Al₂O₃ buffered with 1% Et₃N. ^c 1.0 equiv of [(Ph₃PAu)₃O]BF₄ used.



Previous reports of gold-catalyzed hydroamination reactions using carbamate nucleophiles generally required elevated temperatures (60–100 °C).^{17b} Therefore, we were surprised to find that, even at room temperature, substrates protected as carbamates underwent significant conversion to the corresponding alkylgold complexes (Table 4.7).²⁶ For example, Boc protected amine **4.51a** cyclized equally as well as less sterically encumbered allyl carbamate **4.51c**. Again, conversions were generally high, and the decrease in isolated yield was due to decomposition during purification. In addition to sterics, electronic did not affect the formation of the alkyl gold complexes. Trichloroethylcarbamate **4.52d** was formed in similar conversion and yield.

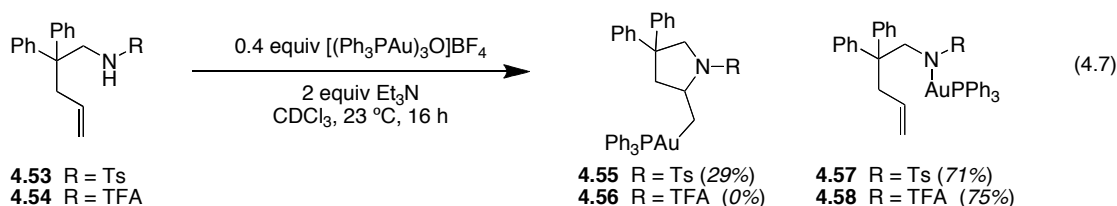
Table 4.7. Scope of Aminoauration with Carbamates. ^a



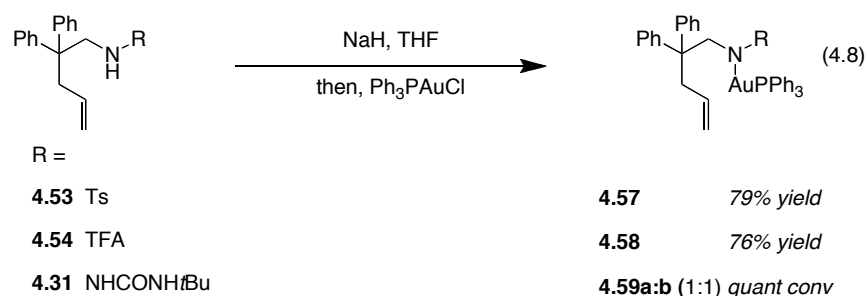
entry	4.51	R	4.52	% yield ^b
1	4.51a	<i>t</i> -Bu	4.52a	53%
2	4.51b	Bn	4.52b	49%
3	4.51c	Allyl	4.52c	37%
4	4.51d	CH ₂ CCl ₃	4.52d	43%
5	4.51e	Ph	4.52e	69%

^a Reaction Conditions: To a solution of alkene (1 equiv) and triethylamine (2 equiv) in CDCl₃ was added 0.4 equiv of [(Ph₃PAu)₃O]BF₄. ^b Isolated yield.

More electron-withdrawing protecting groups, such as tosylamide **4.53** and trifluoroacetamide **4.54**, primarily lead to the formation of gold(I)amide complexes instead of cyclizing to form the alkylgold (eq 4.7). The synthesis of gold amides under similar conditions has been previously reported.²⁷ This result indicated that for these protecting groups *syn*-addition intermediates were accessible under the reaction conditions.

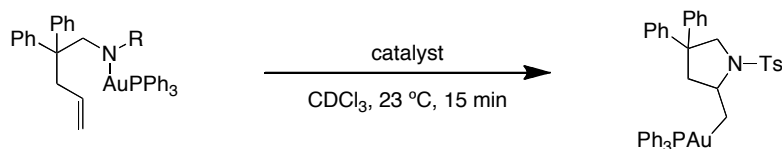


We were curious to explore the reactivity of the gold(I)amide complexes, and thus devised an independent synthesis and isolation method (eq 4.8). Stoichiometric deprotonation with sodium hydride followed by treatment with triphenylphosphinegold chloride quantitatively formed the desired complexes. Purification was straightforward; sodium chloride was removed by filtration through celite, and after trituration, analytically pure samples were isolated. Once in solid form these complexes were bench stable. However, when in solution they are prone to decomposition in the presence of adventitious moisture. Therefore, we found preparation was easiest in the controlled environment of a glove box. In addition to gold(I)amides, we also applied this procedure to *N-t*BuUrea **4.31**. Although we were able to generate a 1:1 mixture of gold(I)ureas **4.59a** and **4.59b** as indicated by ¹H and ³¹P NMR, the complexes were unstable and we were not able to isolate an analytically pure sample.



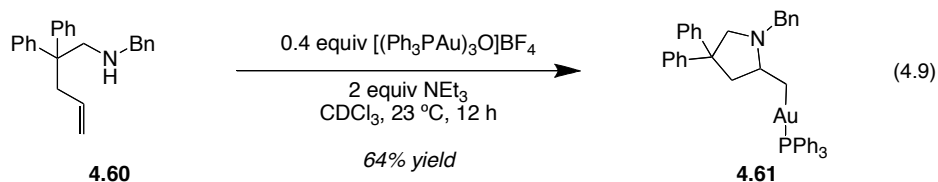
We then treated the gold(I)amide complexes with cationic gold catalysts (Table 4.8). Interestingly, while 10 mol% Ph₃PAuOTf catalyzed the formation of **4.55** (40%, entry 1), the use of a gold trimer complex resulted in no reaction (entry 2). A mixture of gold(I)ureas **4.59a** and **4.59b** also did not cyclize upon treatment with trimer (entry 4). We interpreted this result as evidence against the *syn*-addition pathway for urea protected substrates. We were surprised to find that when **4.58** was treated with 10 mol% zinc triflate, **4.56** was formed with nearly quantitative conversion (entry 3). We propose that this transformation could proceed via a transmetalation between zinc and gold, which would produce free cationic gold and a zinc amide. Subsequent gold alkene activation and addition of the zinc amide could produce the observed product. While detailed experimental evidence for the mechanism of this transformation is lacking, we have established that neither zinc triflate alone nor a 1:1 mixture of zinc triflate and Ph₃PAuOTf catalyze the hydroamination of triflamide **4.56**. In addition these results provided an interesting precedent for bimetallic hydroamination systems.

Table 4.8. Cyclization of Gold(I)-Amide and Gold(I)-Urea Complexes.



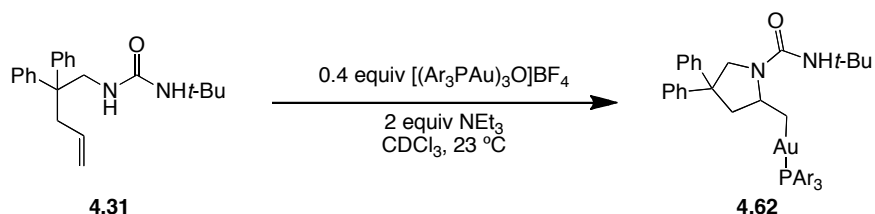
entry		R =	catalyst	product	% conv
1	4.57	Ts	10 mol% Ph ₃ PAuOTf	4.55	40
2			3 mol% [(Ph ₃ PAu) ₃ O]BF ₄		0
3	4.58	TFA	10 mol% Zn(OTf) ₂	4.56	90
4	1:1 4.59a:4.59b	NHCONH <i>t</i> Bu	2 mol% [(Ph ₃ PAu) ₃ O]BF ₄	4.32	0

With the recent reports of hydroaminations with secondary ammonium salts, we were interested in attempting the reaction with amines. We were intrigued to find that benzyl amine **4.60** reacted readily with the trinuclear gold-oxo complex to provide **4.61** (eq 4.9).²⁸ Pyrrolidine



4.61 proved to be highly unstable, and we were therefore unable to successfully isolate and purify this alkylgold complex, though the diagnostic peaks were identified in both the crude ^1H and ^{31}P NMR spectra. Interestingly, the alkylgold complex was formed even in the absence of an added base, as the amine is capable of sequestering the proton to prevent protodeauration. This suggests that catalytic hydroamination with amines was not necessarily precluded due to coordination of the gold to the amine as previously predicted,^{17a} but rather by the prevention of efficient protodeauration of the β -aminoalkylgold complex by means of an internal base.

Table 4.9. Scope of Aminoauration with Arylphosphine Ligands.^a



entry	Ar =	4.62	% yield ^b
1	<i>p</i> -F ₃ CC ₆ H ₄	4.62a	79%
2	<i>p</i> -ClC ₆ H ₄	4.62b	67%
3	<i>p</i> -FC ₆ H ₄	4.62c	75%
4	<i>p</i> -MeC ₆ H ₄	4.62d	72%
5	<i>o</i> -MeC ₆ H ₄	4.62e	73%
6	<i>p</i> -MeOC ₆ H ₄	4.62f	56%

^a Reaction Conditions: To a solution of alkene (1 equiv) and base (2 equiv) in CDCl₃ was added 0.4 equiv of [(Ar₃PAu)₃O]BF₄. ^b Isolated yield.

In order to determine the effect of the ligand on the formation of the alkylgold complex, we utilized several trinuclear gold-oxo complexes with various monophosphine ligands (Table 4.9).²⁸ We were gratified to find that the reaction proceeded smoothly for a variety of electron-rich and electron-poor phosphine ligands. Electron poor phosphines, such as the (*p*-F₃CC₆H₄)₃P (entry 1) appear to enhance the formation of the gold complex, while the analogous reaction with the electron-rich (*p*-MeOC₆H₄)₃P (entry 5) failed to go to completion, providing only about 80% conversion by ^1H NMR.

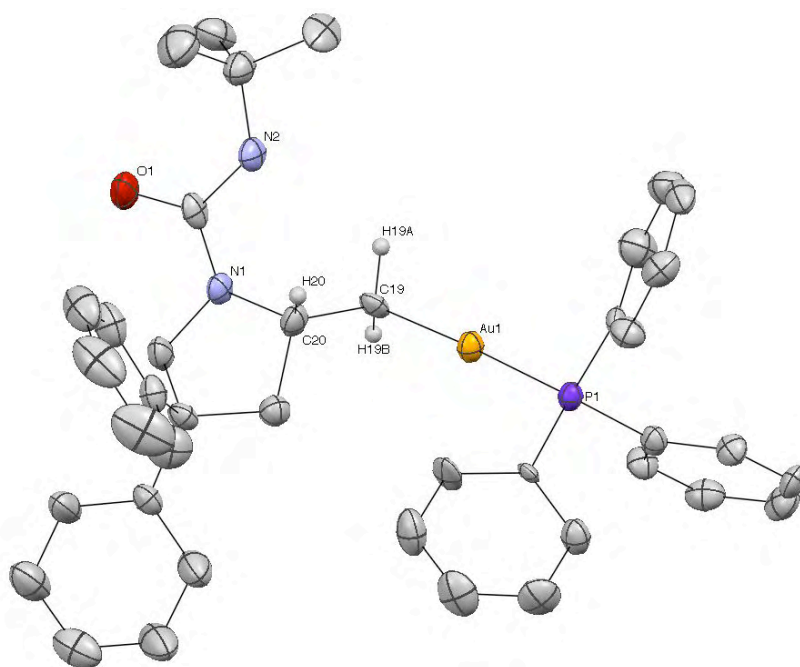


Figure 4.2. ORTEP of alkylgold **4.32**. Thermal ellipsoids shown at 50% probability. Hydrogens (except H19A, H19B, and H20) and DME solvent molecule omitted for clarity.

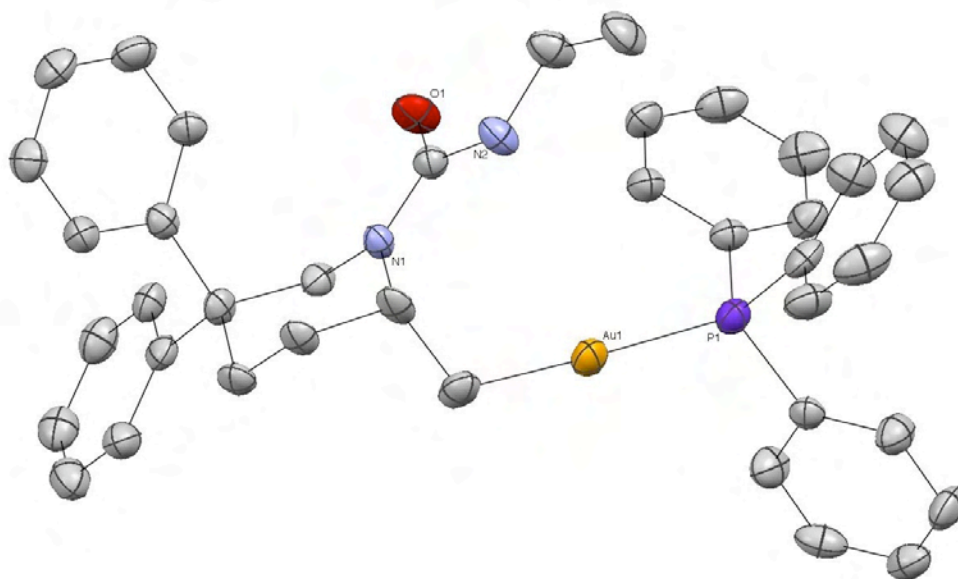


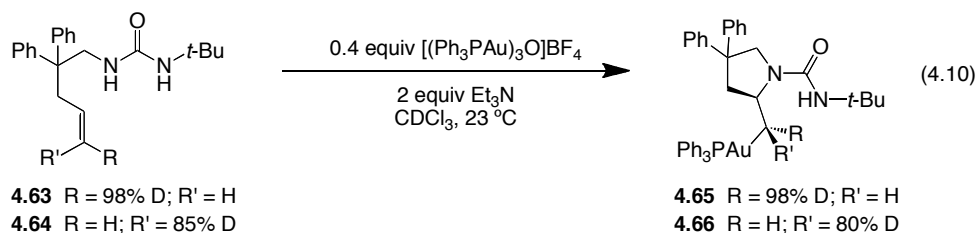
Figure 4.3. ORTEP of alkylgold **4.46**. Thermal ellipsoids shown at 50% probability. Hydrogens (except H19A, H19B, and H20) and DME solvent molecule omitted for clarity.

Recrystallization of **4.32** from DME and diethyl ether provided crystals suitable for X-ray analysis (Figure 4.2). The structure displays the characteristic linear, two-coordinate, geometry

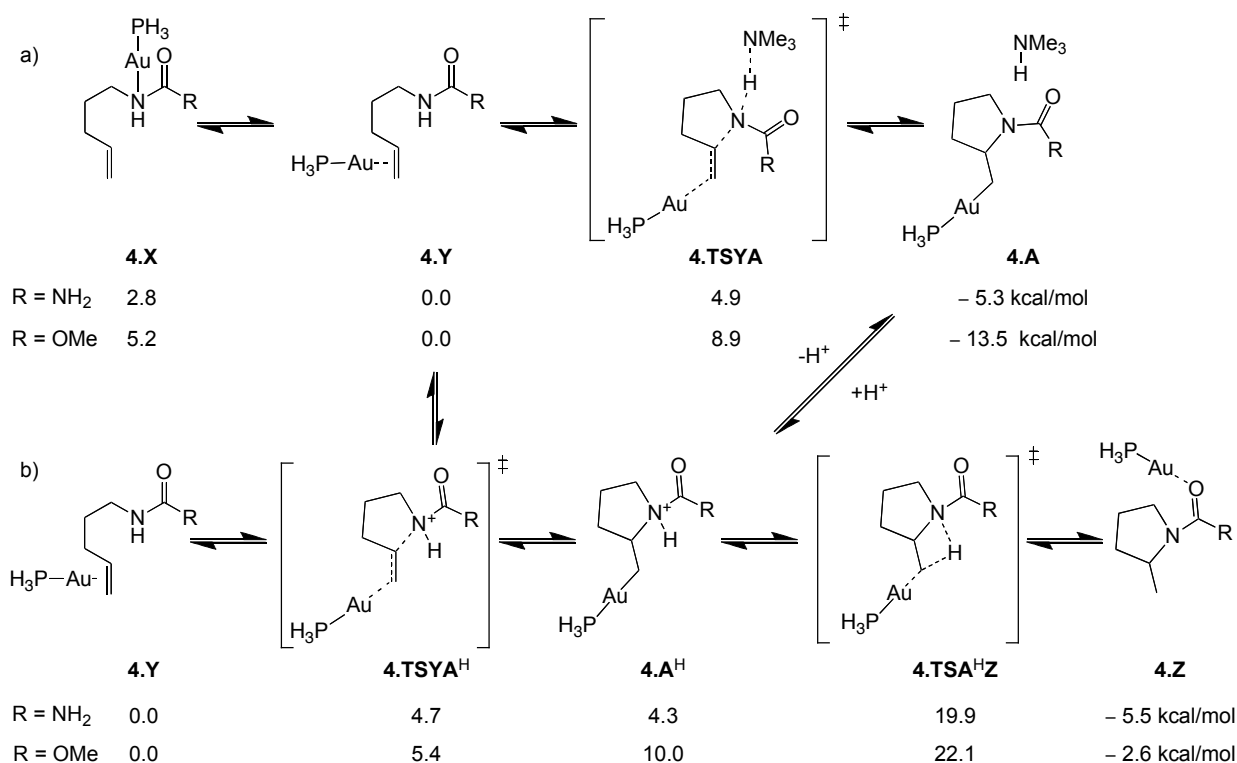
around gold (P-Au-C19 176°). The phosphine-gold bond length of 2.29 Å is typical for a phosphine gold(I) complex.²⁹ The C19-Au bond length (2.07 Å) is comparable to that of MeAuPPh₃ (2.12 Å).³⁰ The N-C-C-Au dihedral angle is an almost perfect antiperiplanar arrangement. The crystal structure of piperidine alkylgold complex, **4.46**, displayed similar characteristics with a C-Au-P angle of 177° and bond lengths of 2.08, and 2.28 Å for the C-Au and Au-P bonds, respectively (Figure 4.3).

Mechanism of Aminoauration

As mentioned previously, activation of the alkene could lead to addition of a nucleophile either *syn*- or *anti*- to the forming gold-carbon bond. The stereochemical course of the aminoauration was examined experimentally through the use of deuterated olefins **4.63** and **4.64** (eq 4.10).³¹ On the basis of the dihedral angles in the X-ray crystal structure of alkyl gold **4.32**, we predicted J^3 values of 1.2, and 9.1 Hz, for H19A and H19B protons, respectively. Upon treatment with [(Ph₃PAu)₃O]BF₄ under standard conditions, *trans*-deuterated alkene **4.63** cyclized to form exclusively the *anti*-addition product **4.65** (methylene proton, $J^3 = 8.4$ Hz). As expected, the *cis*-deuterated alkene **4.64** underwent aminoauration reaction to furnish **4.66** (methylene proton, $J^3 = 2.0$ Hz), confirming the *anti*-addition of the nucleophile relative to the activating gold.



Further mechanistic insight into the aminoauration reaction was gained through the use of a density functional theory (DFT) computational study³² employing the M06 functional.³³ As shown in Scheme 4.3, we hypothesized that during the course of the reaction, the active gold species could bind to, and therefore activate, either the alkene (**4.Y**) or nitrogen nucleophile (**4.X**). We found that the gold preferentially coordinated to the olefin by $\Delta H = 2.8$ kcal/mol relative to N for the urea (R = NH₂), and $\Delta H = 5.2$ kcal/mol relative the N for the carbamate (R = OMe). A series of relaxed coordinate scans found a single pathway for hydroamination: one which involves *anti*-addition of the nucleophile following activation of the alkene. For the case where the gold is bound to the nitrogen (**4.X**), calculations indicate that the metal shifts to bind the alkene, due to proximity. This leads to the same pathway on the potential energy surface as the Au-alkene complex (**4.Y**), indicating that a *syn*-addition pathway is not available for aminoauration.



Scheme 4.3. DFT computed potential enthalpies (ΔH) at 298 K for key hydroamination intermediates and transition structures: a) in basic media, and b) in acidic media.

Having established the stereochemical course of the aminoauration reaction, we next investigated the role of the base. We found a concerted transition state for the simultaneous nucleophilic addition and deprotonation by an exogenous base (**4.TSYA**) with an activation enthalpy of 4.9 kcal/mol for the model urea and 8.9 kcal/mol for the model carbamate. Another step-wise process where aminoauration precedes proton abstraction (**4.TSYA^H**) was also discovered, having similar energies to the concerted process. We established that the cationic (non-deprotonated) product of aminoauration (**4.A^H**) was a moderately unstable intermediate, where its stability may be determined by the electronic nature of L and R.

Electron-withdrawing phosphine ligands and protecting groups (urea vs. carbamate) may lower the barrier for hydroamination and stabilize the intermediate. These two related mechanisms could be in competition depending on the electronic nature of L and R, the concentration, and the relative strength of the base. Our results predicted that for the carbamate (R = OMe), the concerted pathway might be lower in energy, while for the urea (R = NH₂) the step-wise pathway might be lower in energy. We believe that a key characteristic of this transformation is the difference in acidity of **4.A^H** before and after (or during) hydroamination.

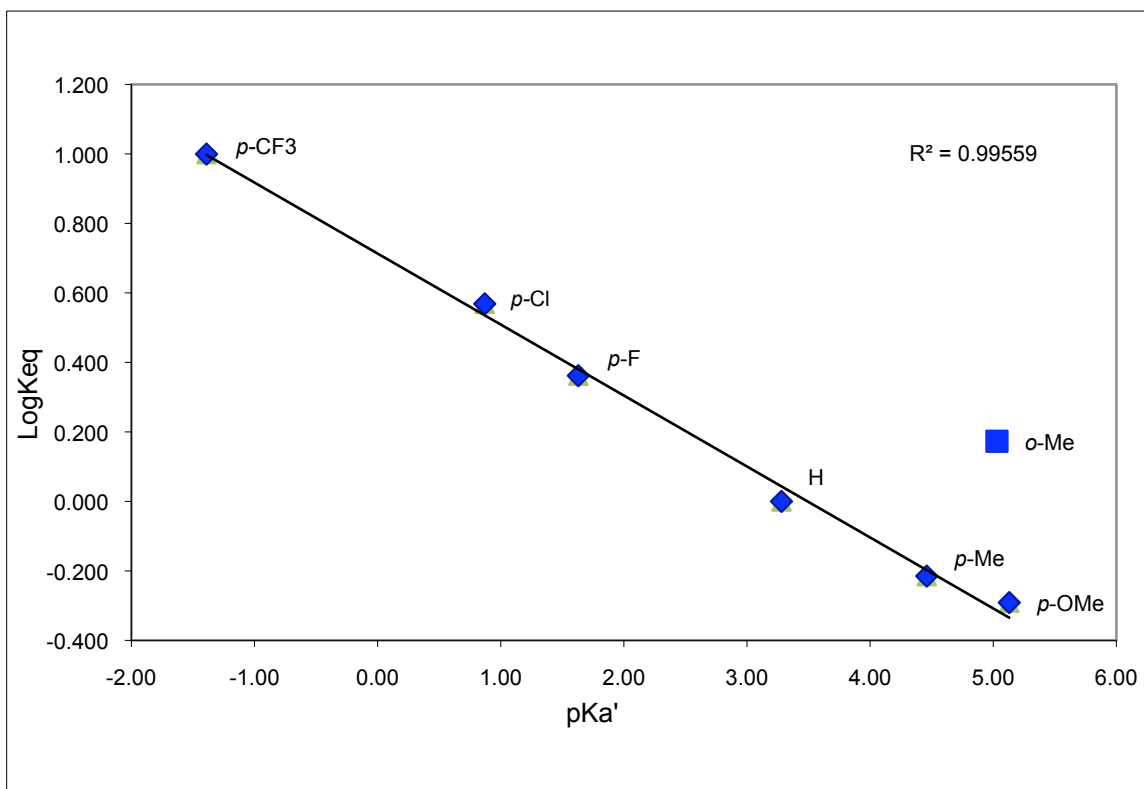
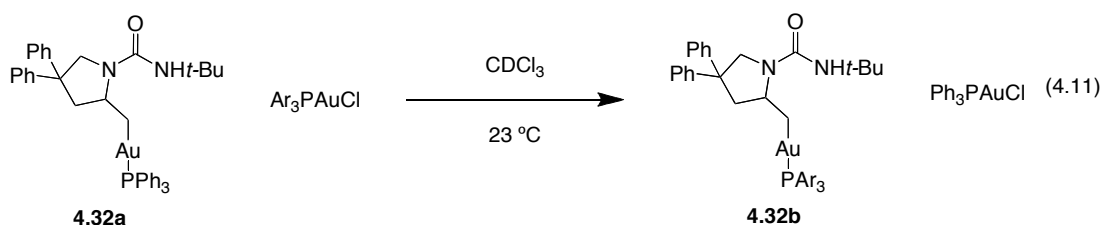


Figure 4.4. Hammett plot for the ligand exchange reaction of Ar_3PAuCl with **4.32** for the isosteric ligand set ($p\text{-XC}_6\text{H}_4$)₃P. Reactions were run at 0.1 M in CDCl_3 at room temperature for 12 hours.

During the course of our initial investigations, we discovered that the addition of a cationic gold species to the isolated alkylgold complex **4.32** leads to a rapid equilibrium of the gold species.²⁸ Surprisingly, gold(I) chloride complexes were shown to participate in this exchange reaction as well (eq 4.11). When **4.32** was treated with a stoichiometric amount of ($p\text{-F}_3\text{CC}_6\text{H}_4$)₃PAuCl, the mixture rapidly equilibrated to a 1:3.5 mixture of **4.32**:**4.62a**. The equilibrium with an electron-donating ligand (such as MeO) favored the starting material. We found a linear relationship between the pK_a' of the arylphosphine and the $\log(K_{\text{eq}})$ of the exchange reaction with the isosteric ligand set Ar_3PAuCl (Figure 4.4), with the alkylgold complex favoring the more electron-poor ligand. Interestingly, the more sterically encumbered (*o*-tolyl)₃P ligand favored the formation of the alkylgold complex, indicating a large steric component to the reaction as well. Attempts to utilize more electron rich ligands, such as NHCs and alkylphosphines, led to no significant exchange from **4.32**.

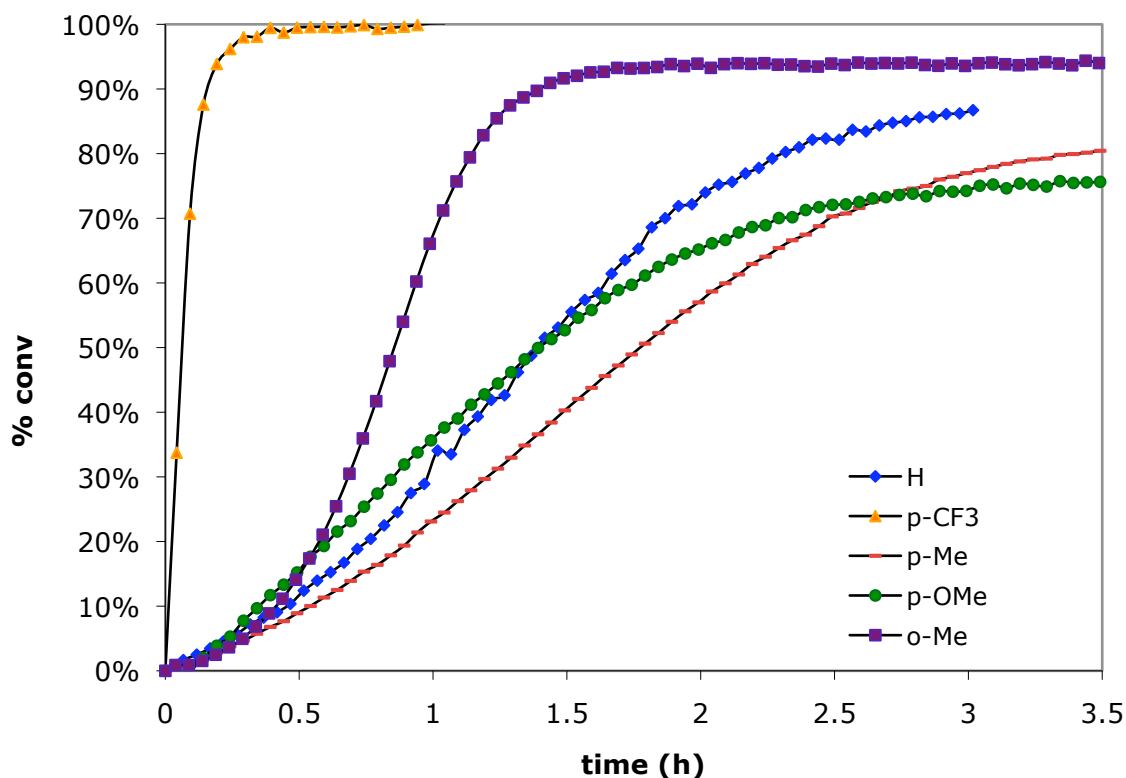


Figure 4.5. Time Course of the Aminoauration Reaction with Various Arylphosphine Ligands.

We surmised that the more electrophilic gold(I)-complexes should also enhance the rate of cyclization. To explore this effect, we observed the course of the reaction for five electronically differentiated arylphosphine ligands (Figure 4.5). We noted a clear induction period in which the gold-oxo complex is presumably transformed into the active cationic species. This induction period was absent when an electron-withdrawn ligand was employed. For example, *p*-CF₃ substituted phosphine, showed little to no induction period and an enhanced rate, reaching completion in under 30 minutes. After the induction period, the rate of alkylgold formation for PPh₃, -OMe, and *p*-tolyl substituted phosphines was similar, reaching equilibrium in 3–5 hours. In accord with our exchange experiments, the equilibrium concentrations of alkylgold complexes are greatest for electron withdrawn ligands (*p*-CF₃), although the sterically bulky *o*-Me also exhibits enhanced stability.

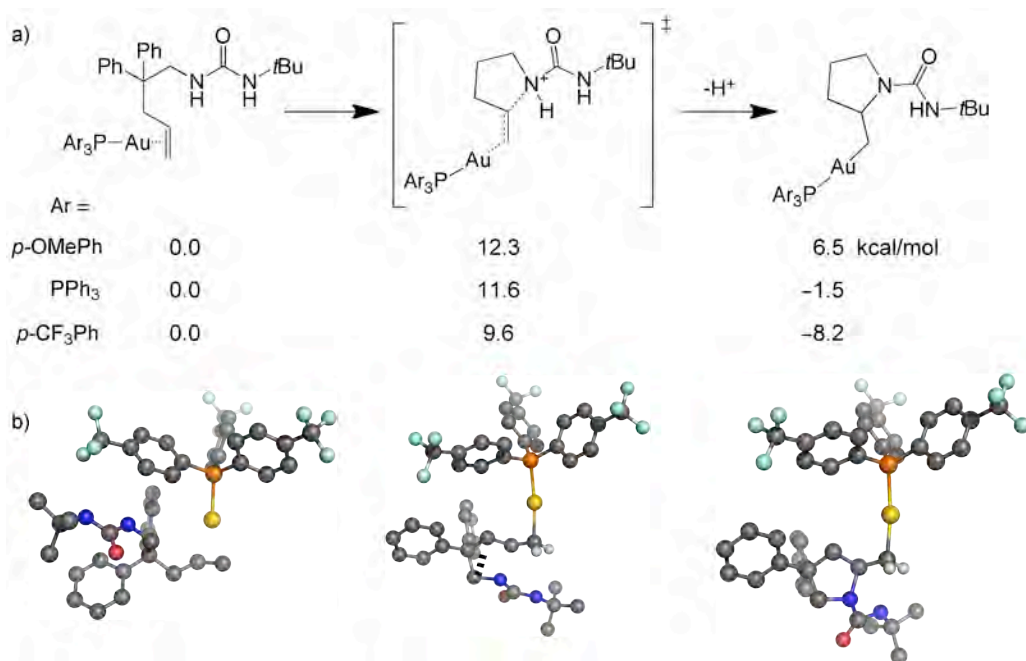


Figure 4.6. Comparison of aminoauration between *p*-substituted triphenylphosphine Au(I) species. a) enthalpic comparison and b) representative structures for (*p*-CF₃Ph)₃PAu(I) aminoauration reaction.

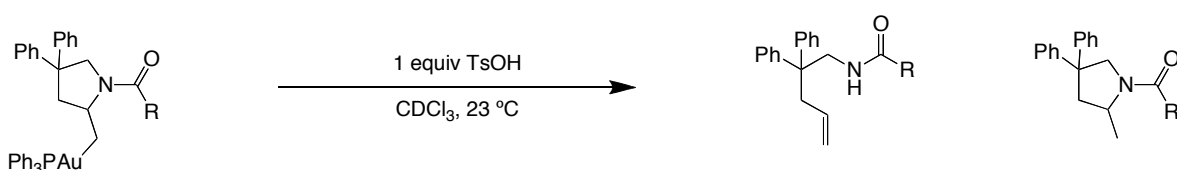
Our calculations³² support the experimentally observed stabilization of the alkylgold complexes by electron poor ligands (Figure 4.6). More electron-donating phosphines will populate the 6s orbital of the gold to a higher degree, thereby reducing the interaction with the substrate.³⁴ This results in a less activated alkene and a higher barrier to the generation of sp³ C-bound alkylgold(I) complex. In our calculations we found that the activation barrier for the cyclization with the electron-withdrawing phosphine (*p*-F₃CC₆H₄)₃P is 1.9 kcal/mol lower than with PPh₃. On the other hand, the barrier with the electron-donating (*p*-MeOC₆H₄)₃P is predicted to be 0.3 kcal/mol higher than for PPh₃. Even though the differences in the barriers are close to the limit of the accuracy of the method, the trend is consistent with our experiments. Minor structural differences, especially in the Au–C and N–C bond distances, suggest a later transition state for the more electron-donating phosphine. This is a consequence of the 5d¹⁰ configuration of Au(I) and the relative population of the 6s orbital in each of the complexes.

To help determine the origin of the increased rate with the more electron withdrawing phosphine, we performed a natural bond orbital (NBO) study on the charge distribution of the transition state **4.TSYA**^H.³⁵ We found that the charge on L for Ph₃P is +0.35, while it was only +0.31 for (*p*-F₃CC₆H₄)₃P, consistent with the higher electronegativity of the CF₃ substituted ligand. Analogously, the charge on the substrate shows +0.40 for Ph₃P and +0.38 for (*p*-F₃CC₆H₄)₃P. The higher charge on the substrate for the electron withdrawing phosphine was consistent with the destabilization of the cyclized intermediate and its increased acidity.

Protonation of Alkylgold Complexes

Protonation of an alkylgold(I) intermediate has been proposed in the mechanism of gold-catalyzed alkene hydroamination reactions. We were therefore surprised to find that upon treatment with *p*-toluenesulfonic acid, **4.32** and **4.52e** initially reverted to the starting alkenes **4.31** and **4.51e**, respectively (Table 4.10).³⁶ Moreover, while the hydroamination product from **4.52e** was formed on prolonged exposure to acid, the product from carbamate cyclization was not observed even after 18 h. A screen of various Brønsted and Lewis acids led almost exclusively to reversion of the alkylgold complex to the alkene precursor. As the crystal structures of the aminoauration products confirm a perfect anti-periplanar arrangement of the amine nucleophile to the gold, activation of the nitrogen by protonation would therefore allow for a facile E2 reaction to provide the starting olefin. Recent reports on the kinetics of protodeauration have indicated that the reaction can be surprisingly slow,³⁷ allowing the elimination ample time to occur. For instance, reaction of a 1:1 mixture of alkylgold complex **4.32** and PhAuPPh₃ with HCl, TsOH, or BzOH showed that the rate of reversion of **4.32** to olefin **4.31** far exceeds protodeauration of PhAuPPh₃ to form benzene.

Table 4.10. Treatment of Alkylgold Complexes with Acid.^a

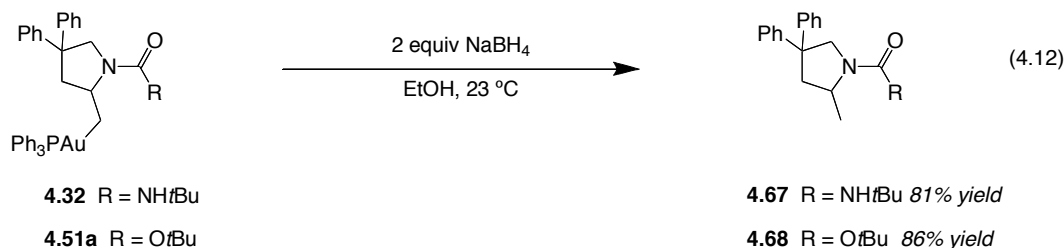


entry	R	time (h)	% alkylgold	% alkene	% pyrrolidine
1	NH <i>t</i> -Bu (4.32)	1	40	0	60
2		15	0	100	0
3	OPh (4.52e)	1	79	0	19
4		15	64	0	33

^a Yields determined by ¹H NMR.

Our calculations³² showed that upon protonation of alkylgold(I) complex **4.A**, complex **4.A^H** is formed, which is 4.3 kcal/mol higher in energy than the gold-substrate complex **4.Y**, with virtually no barrier (~0.3 kcal/mol **4.A^H** to **4.TSYA^H**) for R = NH₂ and 10.0 kcal/mol with no barrier for R = OMe (Scheme 4.3). This is consistent with the apparent reversibility of the aminoauration reaction in which upon protonation of **4.A**, starting material is observed initially. We then examined the protodeauration step; we find an internal barrier to protodeauration of 19.9 kcal/mol for R = NH₂ and 22.1 kcal/mol for R = OMe. We envision that the internal proton transfer could be operative, although external protodeauration may be possible from a weak acid that does not readily protonate **4.A**. While it is difficult to draw conclusions on the validity of these alkylgold(I) complexes as intermediates in the reported alkene hydroamination reactions, these results are in accord with the hypothesis that the gold(I)-promoted addition of amines to

alkenes is reversible. Under catalytic conditions it is possible that the formation of an alkylgold complex merely serves to liberate an equivalent of Brønsted acid, which catalyzes the observed hydroamination reactions.³⁸

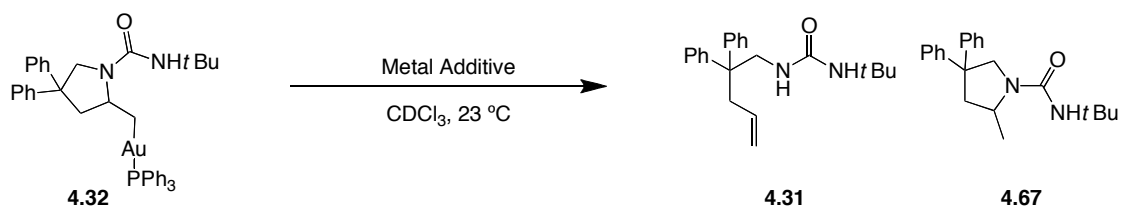


Given our inability to deaurate the alkylgold complexes by protonation, we examined other means to functionalize the carbon-gold bond.³⁹ In early studies with related metals, such as platinum, palladium, and mercury, it was demonstrated that the metal could be removed under reductive or hydrogenation conditions.¹⁰ No reaction was observed when alkylgold **4.32** was treated to hydrogenation conditions (H₂, 1 atm); however, treatment with NaBH₄ in THF led to 27% of the protodeauration product after 12 hours with no indication of reversion to starting olefin.²⁸ The conversions were improved through the use of a protic solvent, such as EtOH, which provided 81% yield of the purported hydroamination product (eq 4.12). Similar yields were observed for the formation of **4.68** from alkylgold **4.51a**. While reductive removal of the metal could be useful for stoichiometric reactions, it would be difficult to use in a catalytic sense, due to the formation of Au(0) clusters from the reduction of the gold, which prevents catalyst turnover.

Transmetalation of Alkylgold Complexes

The work described above solved one mystery: alkene activation by gold(I) is not only possible, but facile. But importantly, due to the reversibility of aminoauration, the role of gold(I) in catalytic hydroamination remains ambiguous. It follows that the barrier to such a process is solely due to protodeauration. As such, we conceived of three possible ways to enhance the rate of protodemetalation. First, an electron donating ligand, such as an N-heterocyclic carbene, could be employed to increase the electron density on the alkylgold methylene carbon. Second, a modified protecting group could be designed to facilitate intramolecular proton transfer. And third, transmetalation could create a more electrophilic metal species. While the first two tactics were not particularly successful, the transmetalation strategy yielded some interesting results.

Table 4.11. Enhancing Protodemetalation with Metal Additives.



entry	metal	time	% 4.32	% 4.31	% 4.67
1	TIPSCl	45 min	66	33	0
2		15 h	0	0	100
3	MgO	4 d	100	0	0
4	Mg(OTf) ₂	45 min	75	25	0
5		4 d	0	0	100
6	CuSO ₄	30 min	100	0	0
7	Cu(OTf) ₂	30 min	decomp	--	--
8	PtCl ₂	4 d	100	0	0
9	ZnCl ₂	30 min	0	100	0
10	ZnCO ₃	30 min	100	0	0
11	ZnO	30 min	100	0	0
12	Zn(OTf) ₂	30 min	0	0	100

We began by treating alkylgold **4.32** with a variety of metal species (Table 4.11). While most salts produced no reaction, we noticed that some metal species first yielded the alkene, which was then slowly converted to pyrrolidine **4.67** (entries 1 and 4). We theorized that this reactivity was due to the proclivity of these compounds to generate acidic residue in the presence of atmospheric moisture. Zinc triflate (entry 12) immediately produced the desired protodemetalated product. The rapidity with which this process occurred supported our hypothesis of transmetalation followed by fast protodemetalation by adventitious water. We next attempted to observe the alkylzinc species by repeating the experiment under rigorously dry conditions. The reaction mixture, however, rapidly equilibrated to a mixture compounds. Upon quenching with methanol alkene **4.31** was re-isolated. We hypothesized that in the absence of an external proton source, the alkylzinc species eliminates to form an aminozinc complex. Although the initial attempts at creating a gold-zinc catalytic system were not successful, further work is clearly needed.

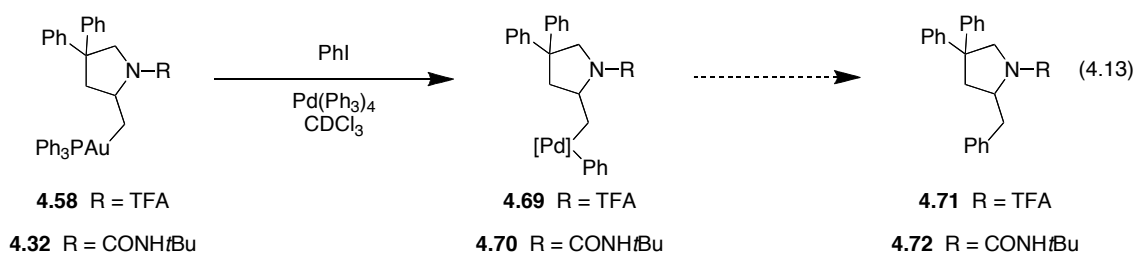
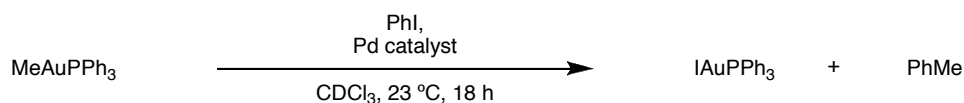


Table 4.12. Palladium Catalyzed Cross-Coupling with MeAuPh₃.



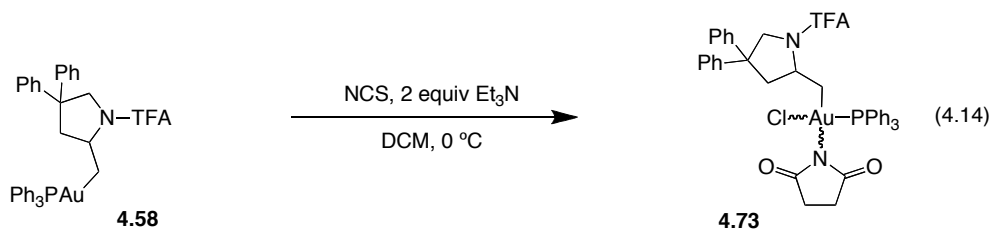
entry	Pd catalyst	% conv ^a
1	Pd(PPh ₃) ₄	decomp
2	Pd ₂ (dba) ₃	decomp
3	Pd ₂ (dba) ₃ , PPh ₃	n.r.
4	Pd ₂ (dba) ₃ , PCy ₃	n.r.
5	Pd ₂ (dba) ₃ , dppb ₃	trace
6	Pd ₂ (dba) ₃ , DPEPHOS	47
7	PdCl ₂ (MeCN) ₂ , DPEPHOS	trace
8	PdCl ₂ (MeCN) ₂ , XANTPHOS	9
9	Pd ₂ (dba) ₃ , XANTPHOS	84

^a Conversion was determined by ¹H NMR vs. an internal standard.

In addition to simple protodemetalation, we were also interested in establishing a cross-coupling protocol. A similar method for the coupling of vinylgold(I) species was reported by Blum in 2009.⁴⁰ However, the transition metal catalyzed cross-coupling of sp³ hybridized components remains challenging.⁴¹ Therefore, we embarked on our studies with the treatment of alkylgold **4.32** and **4.58** with various palladium species. Although transmetalation was verified by ¹H and ³¹P NMR studies, we were unable to isolate the palladium intermediate (eq 4.13). Efforts to force the palladium complex to reductively eliminate were also unsuccessful. Dr. William Brenzovich performed a detailed study of conditions for the palladium-catalyzed coupling of MeAuPPh₃ with Ph-I (Table 4.12). However, application of these conditions to various alkylgold(I) complexes merely returned the starting alkene.

Oxidation of Alkylgold Complexes

We also attempted to react alkylgold(I) complexes with various electrophiles. Treatment with aldehyde and anhydride reagents all produced no observable reaction. Because organogold(I) complexes have been reported to react with electrophilic halogen sources,⁴² we selected N-chlorosuccinimide as a potential electrophile. At first, a complex assortment of alkene and other compounds was observed due to acidic impurities. Buffering the reaction mixture with base and cooling to 0 °C simplified the mixture to a single component, which was distinctly not the expected alkylchloride. The product of the reaction was surprisingly stable to purification by silica gel chromatography. On the basis of NMR studies (¹H, {³¹P}¹H, ¹³C, ³¹P, gCOSY) we tentatively identified the complex as **4.73**. In addition to the expected ¹H-¹H coupling, ³¹P coupling was clearly evident to both the succinimide and pyrrolidine moieties. As anticipated, broadband ³¹P decoupling simplified the coupled proton signals. Unfortunately structural confirmation by X-ray analysis was not possible due to our inability to crystallize this material.



Conclusion and Future Directions

We have provided the first direct crystallographic evidence for electrophilic activation of alkenes for nucleophilic addition by isolation of the products of olefin aminoauration. A variety of protected amine nucleophiles proved competent, and the use of electron deficient ligands on the gold center accelerated the formation of the aminoauration product. In addition, we have provided the first experimental verification of an *anti*-addition mechanism for alkene aminoauration, which is supported by DFT calculations.

While these complexes potentially provide support for gold(I)-catalyzed hydroamination reactions, all attempts to complete the catalytic cycle by means of protodeauration of the purported hydroamination intermediates lead only to reversion to the starting alkenes. Furthermore, taking into account the high energy barrier calculated for protodeauration, the precise involvement of gold complexes in catalytic hydroamination reactions remains unclear.

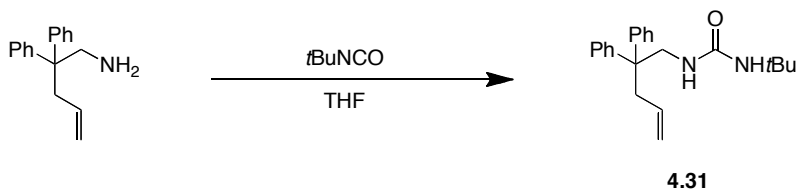
As we have shown, the isolation of alkylgold(I) complexes provided a helpful tool for probing the fundamental chemistry of gold, the limits of which we are still exploring. For example, the oxidation potential for gold(I) species bearing intricate ligands is as of yet unexplored. The converse, reductive elimination, from gold(III) has been the subject of only cursory study.⁴³ Finally, we hope that these complexes will enable the discovery of new dual metal catalytic activity.

Experimental

General Information

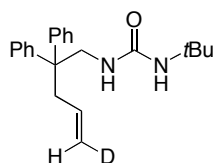
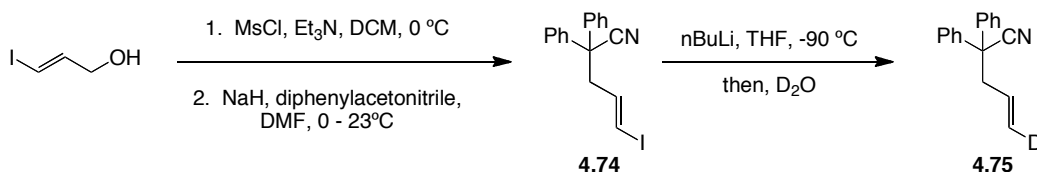
Unless otherwise noted commercial materials were used without further purification. Dichloromethane (DCM) and chloroform utilized in gold(I)-catalyzed reactions was used as received from Aldrich Chemical Company. Gold(I)-catalyzed reactions were conducted in two dram vials equipped with a magnetic stir bar, fitted with a threaded cap, and protected from ambient light. All other reactions were conducted in flame-dried glassware under an inert (N_2) atmosphere with magnetic stirring and dried solvent. Solvents were dried by passage through an activated alumina column under nitrogen. Phosphine gold(I) chloride complexes and $[(Ph_3PAu)_3O]BF_4$ complexes were prepared according to procedures previously described.^{44, 45} Alkene substrates were prepared according to the methods of Widenhoefer.^{11b, 22c} Thin-layer chromatography (TLC) analysis was performed using Merck silica gel 60 F254 TLC plates, and visualized by staining with I_2 , and UV. Flash column chromatography was carried out on Merck 60 silica gel (32 – 63 μm) or MicroSolv Basic Alumina (50 – 200 μm). 1H and ^{13}C NMR spectra were recorded with Bruker AVB-400, AVQ-400, DRX-500, and AV-600 spectrometers and chemical shifts are reported in ppm, relative to $CHCl_3$ (7.26 ppm for 1H , and 77.23 ppm for ^{13}C), unless otherwise noted. Mass spectral and analytical data were obtained via the QB3/College of Chemistry Mass Spectrometry Facility operated by the College of Chemistry, University of California, Berkeley.

Synthesis of Urea and Carbamate Substrates



Urea 4.31. Amine (0.237 g, 1.0 mmol) was dissolved in THF (2 mL) at room temperature, then *tert*-butyl isocyanate (0.08 mL, 1.0 mmol) was added slowly and the solution was allowed to stir overnight. The reaction was concentrated *in vacuo*. The residue was purified by column chromatography on silica gel (0 – 10% EtOAc in hexanes with 2% MeOH) to provide **4.31** (0.300 g, 90%) as a fluffy white solid: 1H NMR (600 MHz, $CDCl_3$) δ 7.29 (s, 4H), 7.22 – 7.17 (m, 6H), 5.43 (ddt, 1H, $J = 17.1, 10.1, 7.1$ Hz), 5.01 – 4.95 (m, 2H), 4.03 (dt, 1H, $J = 1.2, 0.6$ Hz), 3.85 (d, 2H, $J = 5.9$ Hz), 3.78 (s, 1H), 2.87 (d, 2H, $J = 7.1$ Hz), 1.19 (s, 9H) ppm; ^{13}C NMR (150 MHz, $CDCl_3$) δ 157.2, 145.7, 134.0, 128.2, 128.1, 126.3, 118.4, 50.3, 50.2, 47.0, 41.9, 29.4 ppm. HRMS (ESI) calcd. for $[C_{22}H_{29}ON_2]^+$: m/z 337.2274, found 337.2283.

Synthesis of *trans*-Deuterated Alkene **4.63**

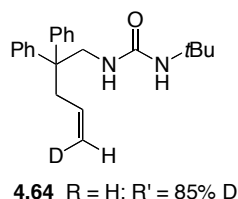
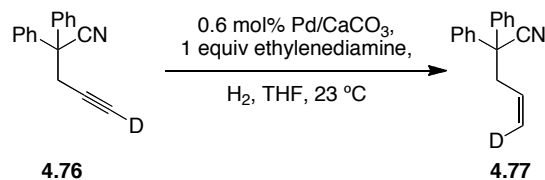


4.63 R = 98% D; R' = H

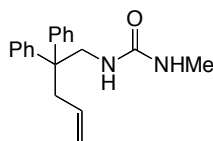
4.63: Mesyl chloride (1.8 mL, 22.8 mmol, 1.2 equiv) was added dropwise to a solution of (E)-prop-2-ene-1-ol⁴⁶ (3.5 g, 19 mmol) and triethylamine (3.96 mL, 28.5 mmol, 1.5 equiv) in DCM (30 mL) at 0 °C. The solution was stirred at 0 °C for 30 min at which point TLC indicated complete reaction. The reaction mixture was poured onto sat. aq. NaHCO₃/Brine (50 mL, 1:3), extracted with DCM (3 x 50 mL), washed with sat. aq. NaHCO₃/Brine (50 mL, 1:3), dried (MgSO₄) and concentrated to yield 4.24 g (E)-prop-2-ene-1-methanesulfonate as a clear yellow oil. The crude oil was used without further purification. Diphenylacetonitrile (2.85 g, 14.7 mmol) in DMF (10 mL) was via cannula to a suspension of NaH (600 mg, 15 mmol) in DMF (2 mL) at 0 °C. The solution was warmed to 23 °C and stirred until gas evolution ceased (~30 min). The solution was re-cooled to 0 °C and (E)-prop-2-ene-1-methanesulfonate (4.2 g, 16 mmol) was added. The solution was warmed to 23 °C and stirred overnight. The reaction was quenched on sat. aq. NH₄Cl (50 mL), extracted with Et₂O (4 x 50 mL), washed with water (4 x 50 mL), dried (MgSO₄) and concentrated to yield a crude yellow oil (2.8 g). The crude oil was purified by column chromatography (SiO₂; 0-4% EtOAc/Hex; 1% inc; collect at 2%) to yield 2.1 g clear oil contaminated with ~5% diphenylacetonitrile. The clear oil was dissolved in EtOAc (4 mL) and diluted with hexanes (50 mL) and allowed to recrystallize by slow evaporation. The crystals were collected by filtration and washed with cold hexanes to yield **4.74** as clear colorless crystals (1.5 g, 4.2 mmol, 28%): ¹H NMR (600 MHz, CDCl₃) δ 7.41-7.37 (m, 8H), 7.34-7.31 (m, 2H), 6.46 (dt, 1H, *J* = 7.7, 1.6 Hz), 6.28 (dt, 1H, *J* = 7.6, 6.4 Hz), 3.24 (dd, 2H, *J* = 6.3, 1.7 Hz). Deuterium was incorporated by the method of Seebach.⁴⁷ To a solution of **4.74** (294 mg, 0.82 mmol) in dry THF at -90 °C was added nBuLi (315 μL, 0.82 mmol, 1 equiv). The solution was quenched with MeOD (0.2 mL, from an ampule). The solution was diluted with ethyl acetate (50 mL), washed with water (15 mL), dried with MgSO₄ and concentrated to yield **4.75** as a clear oil (185 mg, 0.79 mmol, 96%, 98% D): ¹H NMR (600 MHz, CDCl₃) δ 7.42-7.36 (m, 8H), 7.32-7.30 (m, 2H), 5.73 (dt, 1H, *J* = 16.9, 7.1 Hz), 5.23-5.20 (m, 1H), 3.16 (dd, 2H, *J* = 7.0, 1.2 Hz); ¹³C NMR (150 MHz, CDCl₃) δ 139.74, 131.67, 128.85, 127.94, 121.96, 120.14 (t, *J* = 22 Hz), 51.73, 43.90. Compound **4.75** was reduced with LAH and treated with *tert*-butylisocyanate according to the methods of Widenhoefer^{11b,22c} to yield **4.63**: ¹H NMR (600 MHz, CDCl₃) δ 7.30 – 7.18 (m, 10H), 5.43 (dt, 1H, *J* = 16.8, 7.2 Hz), 4.98 (d, 1H, *J* = 17.1 Hz), 4.05 (s, 1H), 3.85 (d, 3H, *J* = 5.8 Hz), 2.87 (d, 2H, *J* = 7.0 Hz), 1.26 (s, 9H) ppm; ²H NMR (92 MHz, CDCl₃) δ 4.97 (s, 1H); ¹³C NMR

(150 MHz, CDCl₃) δ 157.2, 145.7, 133.9, 128.2, 128.1, 126.3, 118.1 (t, *J* = 22 Hz), 50.3, 50.2, 47.1, 41.8, 29.4 ppm; HRMS (ESI) calcd. for [C₂₂H₂₈DON₂]⁺: *m/z* 338.2337, found 338.2343.

Synthesis of *cis*-Deuterated Alkene **4.64**

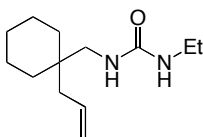


4.64. Alkyne **4.76** (98% D) was prepared according to the methods of Chang.⁴⁸ A solution of alkyne **4.76** (100 mg, 0.43 mmol), ethylene diamine (30 μ L, 0.43 mmol) and Pd/CaCO₃ (5 mg, 0.0025 mmol, 0.6 mol%) in THF (5 mL) was stirred rapidly under H₂ (1 atm) for 50 min. TLC showed complete conversion to a higher R_f spot. The reaction mixture was filtered thru celite, washed with EtOAc (3 x 10 mL), concentrated in vacuo to yield 110 mg crude clear yellow oil. ¹H NMR showed alkene **4.77** with approximately ~15% E/Z isomerization: ¹H NMR (600 MHz, CDCl₃) δ 7.42-7.34 (m, 8H), 7.32-7.28 (m, 2H), 5.72-5.69 (m, 1H), 5.16 (d, 1H, *J* = 10.2 Hz), 3.14 (d, 2H, *J* = 7.0 Hz). The crude material was used without further purification to prepare **4.64** according to the methods of Widenhoefer:^{11b, 22c} ¹H NMR (600 MHz, CDCl₃) δ 7.30 (t, 4H, *J* = 7.6 Hz), 7.20 (m, 6H), 5.42 (m, 1H), 4.95 (d, 1H, *J* = 10.2 Hz), 3.97 (s, 1H), 3.85 (d, 2H, *J* = 5.9 Hz), 3.73 (s, 1H), 2.87 (d, 2H, *J* = 7.1 Hz), 1.26 (s, 9H) ppm; ²H NMR (92 MHz, CDCl₃) δ 4.93 (s, 1H); ¹³C NMR (150 MHz, CDCl₃): δ 157.2, 145.7, 133.9, 128.2, 128.1, 126.3, 118.1 (t, *J* = 22 Hz), 50.3, 50.2, 47.1, 41.8, 29.4 ppm; HRMS (ESI) calcd. for [C₂₂H₂₈DON₂]⁺: *m/z* 338.2337, found 338.2349.

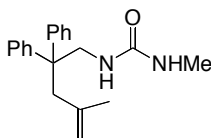


Methyl Urea 4.33. Amine (0.237 g, 1.0 mmol) and 4-methylmorpholine (0.22 mL, 2.0 mmol) were dissolved in CH₂Cl₂ (3.0 mL) was added dropwise over 10 minutes to a solution of carbonyl diimidazole (0.243 g, 1.5 mmol) in CH₂Cl₂ (10.0 mL) at -10 °C. After slowly warming to room temperature over 1 hour, the solution was recooled to -10 °C, and methylamine (0.50 mL, 33% in EtOH, 4.0 mmol) was added and the solution warmed to room temperature

overnight. The reaction mixture was diluted with CH₂Cl₂ (30 mL), and washed with 1 N HCl (15 mL), water (15 mL), and brine (15 mL). The organic layer was then dried over MgSO₄, filtered, and concentrated *in vacuo*. The residue was suspended in CH₂Cl₂ (2.0 mL) and then pentanes was added (30 mL), giving a voluminous white precipitate, which was collected by suction filtration, washing with pentanes, then collected and dried under vacuum, providing **4.33** (0.2587 g, 88% yield) as a fluffy white solid: ¹H NMR (500 MHz, CDCl₃) δ 7.31 – 7.28 (m, 4H), 7.23 – 7.15 (m, 6H), 5.44 (ddt, 1H, *J* = 17.2, 10.1, 7.1 Hz), 5.01 – 4.97 (m, 2H), 4.18 (brs, 1H), 3.91 (brs, 1H), 3.87 (d, 2H, *J* = 5.2 Hz), 2.87 (d, 2H, *J* = 7.1 Hz), 2.61 (d, 3H, *J* = 4.9 Hz) ppm; ¹³C NMR (125 MHz, CDCl₃) δ 158.7, 145.6, 134.0, 128.3, 128.1, 126.5, 118.5, 50.4, 47.2, 41.8, 27.2 ppm; HRMS (ESI) calcd. for [C₁₉H₂₃N₂O]⁺: *m/z* 295.1810, found 295.1812.

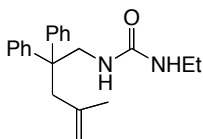


Ethyl Urea 4.36. Amine (0.153 g, 1.0 mmol) was dissolved in THF (2 mL) at room temperature, then ethyl isocyanate (0.08 mL, 1.0 mmol) was added slowly and the solution was allowed to stir overnight. The reaction was concentrated *in vacuo*. The residue was purified by column chromatography on silica gel (10 – 14% EtOAc in hexanes with 2% MeOH) to provide **4.36** (0.200 g, 89%) as a fluffy white solid: ¹H NMR (600 MHz, CDCl₃) δ 5.80 (m, 1H), 5.08 (m, 2H), 3.16 (m, 2H), 3.05 (d, 2H, *J* = 6.1 Hz), 2.03 (d, 2H, *J* = 7.4 Hz), 1.48 – 1.33 (m, 6H), 1.33 – 1.22 (m, 4H), 1.09 (td, 3H, *J* = 7.2, 1.8 Hz) ppm; ¹³C NMR (150 MHz, CDCl₃) δ 159.0, 134.9, 117.1, 46.7, 40.3, 36.9, 35.1, 33.3, 26.2, 21.4, 15.5 ppm; HRMS (ESI) calcd. for [C₁₃H₂₄ON₂]⁺: *m/z* 224.1889, found 224.1888.

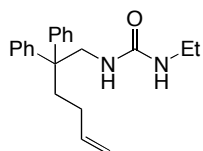


Methyl Urea 4.37. Amine (0.251 g, 1.0 mmol) and 4-methylmorpholine (0.22 mL, 2.0 mmol) were dissolved in CH₂Cl₂ (3.0 mL) was added dropwise over 10 minutes to a solution of carbonyl diimidazole (0.243 g, 1.5 mmol) in CH₂Cl₂ (10.0 mL) at –10 °C. After slowly warming to room temperature over 1 hour, the solution was recooled to –10 °C, and methylamine (0.50 mL, 33% in EtOH, 4.0 mmol) was added and the solution was warmed to room temperature overnight. The reaction mixture was diluted with CH₂Cl₂ (30 mL), and washed with 1 N HCl (15 mL), water (15 mL), and brine (15 mL). The organic layer was then dried over MgSO₄, filtered, and concentrated *in vacuo*. The residue was suspended in CH₂Cl₂ (2.0 mL) and then pentanes was added (30 mL), giving a voluminous white precipitate, which was collected by suction filtration, washing with pentanes, then collected and dried under vacuum, providing **4.37** (0.2633 g, 85% yield) as a fluffy white solid: ¹H NMR (500 MHz, CDCl₃) δ 7.31 – 7.23 (m, 4H), 7.23 – 7.19 (m, 6H), 4.84 (s, 1H), 4.66 (s, 1H), 4.28 (brs, 1H), 3.93 (d, 2H, *J* = 5.0 Hz), 3.90 (brs, 1H), 2.86 (s, 2H), 2.59 (d, 3H, *J* = 4.8 Hz), 1.04 (s, 3H) ppm; ¹³C NMR (125 MHz, CDCl₃) δ 158.7,

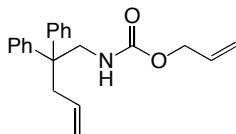
146.1, 141.9, 128.2, 126.5, 116.3, 49.9, 46.7, 44.7, 27.1, 24.3 ppm; HRMS (ESI) calcd. for $[C_{20}H_{25}N_2O]^+$: m/z 309.1967, found 309.1966.



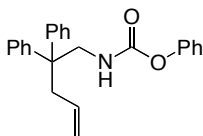
Ethyl Urea 4.34. Amine (0.241 g, 1.0 mmol) was dissolved in CH_2Cl_2 (10 mL) at room temperature, then ethyl isocyanate (0.08 mL, 1.0 mmol) was added slowly and the solution was allowed to stir overnight. The reaction was quenched by the addition of 1 N HCl (20 mL) and extracted with CH_2Cl_2 (3×10 mL). The combined organic layers were washed with H_2O (10 mL) and brine (10 mL), dried over $MgSO_4$, filtered and concentrated *in vacuo*. The residue was purified by crystallization from CH_2Cl_2 /hexanes to provide **4.34** (0.2658g, 86%) as a fluffy white solid: 1H NMR (500 MHz, $CDCl_3$) δ 7.31 – 7.23 (m, 4H), 7.23 – 7.19 (m, 6H), 4.87 (s, 1H), 4.69 (s, 1H), 4.11 (brs, 1H), 3.97 (d, 2H, $J = 5.6$ Hz), 3.10 – 3.02 (m, 2H), 2.90 (s, 2H), 1.07 (s, 3H), 1.05 (t, 3H, $J = 7.2$ Hz) ppm; ^{13}C NMR (150 MHz, $CDCl_3$) δ 157.9, 146.1, 141.8, 128.2, 128.1, 126.5, 116.2, 49.9, 46.7, 44.8, 35.3, 24.3, 15.3 ppm; HRMS (ESI) calcd. for $[C_{21}H_{27}ON_2]^+$: m/z 323.2118, found 323.2130.



Ethyl Urea 4.39. To amine (0.616 g, 2.45 mmol) in THF (6.0 mL) was added dropwise ethyl isocyanate (0.193 mL, 2.45 mmol) and stirred overnight. The reaction mixture was concentrated *in vacuo* to giving an off-white solid. The residue was recrystallized in toluene yielding a voluminous white precipitate, which was collected under suction filtration and dried under vacuum, providing **4.39** (0.2993 g, 38% yield) as a fluffy white solid: 1H NMR (400 MHz, $CDCl_3$) δ 7.36 – 7.30 (m, 4H), 7.27 – 7.22 (m, 6H), 5.78 (ddt, 1H, $J = 17.1, 10.2, 6.8$ Hz), 4.98 (dd, 1H, $J = 17.1, 1.8$ Hz), 4.93 (d, 1H, $J = 10.2$ Hz), 4.15 (t, 1H, $J = 5.3$ Hz), 3.96 (d, 2H, $J = 5.5$ Hz), 3.86 (t, 1H, $J = 5.7$ Hz), 3.15 (dq, 2H, $J = 7.2, 5.6$ Hz), 2.21 – 2.17 (m, 2H), 1.87 – 1.81 (m, 2H), 1.07 (t, 3H, $J = 7.2$ Hz) ppm; ^{13}C NMR (100 MHz, $CDCl_3$) δ 158.0, 146.0, 138.8, 128.3, 128.1, 126.4, 114.4, 50.6, 47.1, 36.5, 35.4, 28.7, 15.4 ppm; IR (neat): 3329, 1624, 1495, 1282, 1141, 703 cm^{-1} ; HRMS (ESI) calcd. for $[C_{21}H_{27}ON_2]^+$: m/z 323.2118, found 323.2124.

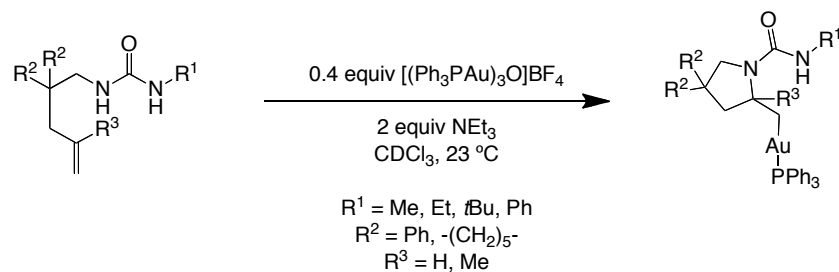


Allyl Carbamate 4.51c. Amine (0.593 g, 2.5 mmol) and triethylamine (0.52 mL, 3.75 mmol) were combined in CH_2Cl_2 (10 mL) and cooled to 0 °C. Then allyl chloroformate (0.29 mL, 2.75 mmol) was added dropwise and the solution was allowed to slowly warm to room temperature overnight. The reaction was quenched by the addition of 0.5 N HCl (20 mL) and extracted with Et_2O (3×10 mL). The combined organic layers were washed with sat. aq. NaHCO_3 (10 mL) and brine (10 mL), dried over MgSO_4 , filtered and concentrated *in vacuo*. The residue was purified by flash chromatography on silica gel (10% EtOAc in hexanes) to give **4.51c** (0.4223, 52%) as a colorless viscous oil that solidified upon standing: ^1H NMR (500 MHz, CDCl_3) δ 7.32 – 7.28 (m, 4H), 7.24 – 7.20 (m, 2H), 7.17 (d, 4H, $J = 7.6$ Hz), 5.87 (m, 1H), 5.43 (m, 1H), 5.24 (d, 1H, $J = 17.3$ Hz), 5.18 (d, 1H, $J = 10.4$ Hz), 5.05 (m, 2H), 4.51 (d, 2H, $J = 5.5$ Hz), 4.30 (s, 1H), 3.92 (d, 2H, $J = 5.9$ Hz), 2.87 (d, 2H, $J = 6.9$ Hz) ppm; ^{13}C NMR (125 MHz, CDCl_3) δ 156.1, 145.2, 133.7, 132.9, 128.3, 128.0, 126.5, 118.7, 117.8, 65.6, 50.1, 47.6, 41.7 ppm; HRMS (ESI) calcd. for $[\text{C}_{21}\text{H}_{24}\text{O}_2\text{N}]^+$: m/z 322.1808, found 322.1802.

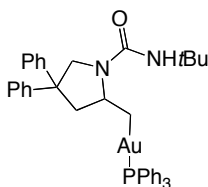


Phenyl Carbamate 4.51e. Amine (0.593 g, 2.5 mmol) and triethylamine (0.52 mL, 3.75 mmol) were combined in CH_2Cl_2 (10 mL) and cooled to 0 °C. Then phenyl chloroformate (0.38 mL, 3.0 mmol) was added dropwise and the solution was allowed to slowly warm to room temperature overnight. The reaction was quenched by the addition of 0.5 N HCl (20 mL) and extracted with Et_2O (3×10 mL). The combined organic layers were washed with sat. aq. NaHCO_3 (10 mL) and brine (10 mL), dried over MgSO_4 , filtered and concentrated *in vacuo*. The residue was purified by flash chromatography on silica gel (8% EtOAc in hexanes) to give **4.51e** (0.5262, 59%) as an amorphous solid. At room temperature in CDCl_3 , **4.51e** exists as a 6:1 mixture of rotamers. Spectroscopic data is reported only for the major rotamer: ^1H NMR (500 MHz, CDCl_3) δ 7.40 – 7.35 (m, 6H), 7.32 – 7.25 (m, 6H), 7.22 (t, 1H, $J = 7.3$ Hz), 7.09 (d, 2H, $J = 8.1$ Hz), 5.55 – 5.46 (m, 1H), 5.09 (d, 1H, $J = 17.3$ Hz), 5.05 (d, 1H, $J = 10.5$ Hz), 4.68 (brs, 1H), 4.05 (d, 2H, $J = 6.0$ Hz), 2.98 (d, 2H, $J = 7.0$ Hz) ppm; ^{13}C NMR (125 MHz, CDCl_3) δ 154.5, 151.0, 145.1, 133.6, 129.3, 128.4, 128.0, 126.7, 125.3, 121.5, 118.9, 50.3, 47.8, 41.9 ppm; HRMS (ESI) calcd. for $[\text{C}_{24}\text{H}_{24}\text{O}_2\text{N}]^+$: m/z 358.1808, found 358.1802.

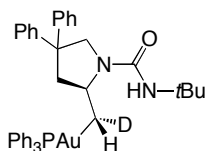
General Procedure for Cyclization of Urea Substrates to Pyrrolidines



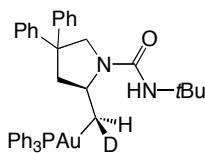
Urea (100 μmol) and triethylamine (200 μmol) were combined in CDCl_3 (1.0 mL) and let stir for five minutes before the addition of the gold trimer (40 μmol) in one portion. After 12 hours, the reaction mixture was concentrated to dryness. The residue was then suspended in EtOAc and filtered through a pad of basic alumina, then concentrated *in vacuo*. Alternatively, the crude reaction mixture was diluted with chloroform (20 mL), washed with sat. aq. NaHCO_3 (10 mL), dried (MgSO_4) and concentrated to yield a crude foam.



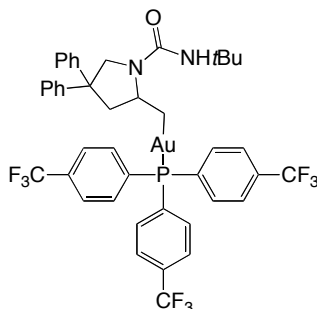
Alkylgold 4.32. Purified by flash column chromatography on basic alumina (5% EtOAc in toluene with 1% NEt_3) to afford **2** (80%) as a white foam: ^1H NMR (600 MHz, CDCl_3) δ 7.48 (m, 9H), 7.39 (m, 6H), 7.21 (m, 10H), 4.94 (dd, 1H, $J = 11.5, 2.0$ Hz), 4.48 (s, 1H), 4.02 (m, 1H), 3.52 (d, 1H, $J = 11.6$ Hz), 2.95 (m, 1H), 2.74 (dd, 1H, $J = 12.1, 9.7$ Hz), 1.76 (m, 1H), 1.66 (m, 1H), 1.37 (s, 9H); ^{13}C NMR (150 MHz, CDCl_3) δ 156.8, 146.8, 146.4, 134.2 (d, $J_{31\text{P}-13\text{C}} = 13.7$ Hz), 131.2 (d, $J_{31\text{P}-13\text{C}} = 47.7$ Hz), 130.99 (d, $J_{31\text{P}-13\text{C}} = 4.4$ Hz), 128.9 (d, $J_{31\text{P}-13\text{C}} = 10.6$ Hz), 128.3, 128.2, 127.1, 127.0, 126.0, 125.7, 58.5 (d, $J_{31\text{P}-13\text{C}} = 3$ Hz), 54.8, 52.2, 52.1, 50.4, 37.1 (d, $J_{31\text{P}-13\text{C}} = 92$ Hz), 36.8, 29.8 ppm; ^{31}P NMR (240 MHz, CDCl_3) δ 45.4 ppm; HRMS (ESI) calcd. for $[\text{C}_{40}\text{H}_{43}\text{AuN}_2\text{OP}]^+$: m/z 795.2773, found 795.2791.



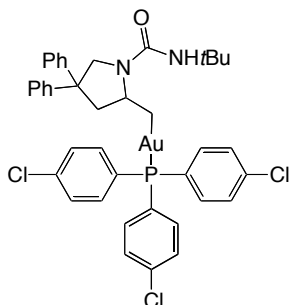
4.65. ^1H NMR (600 MHz, CDCl_3) δ 7.49 – 7.44 (m, 9H), 7.40– 7.37 (m, 6H), 7.27–7.11 (m, 10H), 4.92 (dd, 1H, $J = 11.5, 2.2$ Hz), 4.45 (s, 1H), 3.99 (m, 1H), 3.50 (d, 1H, $J = 11.6$ Hz), 2.72 (dd, 1H, $J = 12.1, 9.7$ Hz), 1.61 (t, 1H, $J = 8.4$ Hz), 1.36 (s, 9H); ^2H NMR (92 MHz, CDCl_3) δ 1.64 (br s, 1H); HRMS (ESI) calcd. for $[\text{C}_{40}\text{H}_{42}\text{DAuN}_2\text{OP}]^+$: m/z 796.2836, found 796.2856.



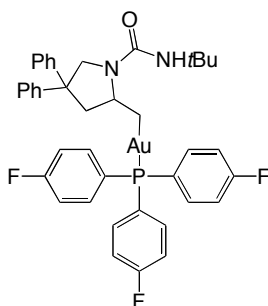
4.66. ^1H NMR (500 MHz, CDCl_3) δ 7.52 – 7.46 (m, 9 H), 7.42 – 7.38 (m, 6H), 7.30 – 7.13 (m, 10H), 4.95 (dd, 1H, $J = 11.5, 2.2$ Hz), 4.48 (s, 1H), 4.03 (m, 1H), 3.53 (d, 1H, $J = 11.5$ Hz), 2.95 (m, 1 H), 2.75 (dd, 1H, $J = 12.1, 9.7$ Hz), 1.75 (dd, 1H, $J = 9.0, 2.2$ Hz), 1.38 (s, 9H); ^2H NMR (92 MHz, CDCl_3) δ 1.54 (br s, 1H); HRMS (ESI) calcd. for $[\text{C}_{40}\text{H}_{42}\text{DAuN}_2\text{OP}]^+$: m/z 796.2836, found 796.2853.



***para*-Trifluoromethyl Phosphine 4.62a:** Purified by flash column chromatography on basic alumina (99:1 toluene/EtOAc with 1% NEt_3) to afford **4.62a** (68%) as a white foam: ^1H NMR (600 MHz, CDCl_3) δ 7.66 (d, 6H, $J = 6.9$ Hz), 7.64 – 7.58 (m, 6H), 7.35 – 7.21 (m, 9H), 7.18 – 7.13 (m, 1H), 4.94 (d, 1H, $J = 11.4$ Hz), 4.41 (brs, 1H), 4.28 – 4.16 (m, 1H), 3.51 (d, 1H, $J = 11.4$ Hz), 2.95 (ddd, 1H, $J = 12.1, 6.0, 2.2$ Hz), 2.77 (dd, 1H, $J = 12.1, 9.5$ Hz), 1.90 – 1.73 (m, 2H), 1.38 (s, 9H) ppm; ^{13}C NMR (150 MHz, CDCl_3) δ 156.6, 146.9, 146.3, 134.6 (d, $J_{31\text{P}-13\text{C}} = 15.0$ Hz), 134.2 (d, $J_{31\text{P}-13\text{C}} = 44.2$ Hz), 133.7 (qd, $J_{19\text{F}-13\text{C}} = 33.6$ Hz, $J_{31\text{P}-13\text{C}} = 1.8$ Hz), 128.4, 128.3, 127.0, 126.8, 126.2 (dq, $J_{31\text{P}-13\text{C}} = 11.2$ Hz, $J_{19\text{F}-13\text{C}} = 3.9$ Hz), 125.8, 123.3 (q, $J_{19\text{F}-13\text{C}} = 273.5$ Hz), 57.8 (d, $J_{31\text{P}-13\text{C}} = 4.0$ Hz), 54.9, 52.1, 52.0, 50.5, 33.0 (d, $J_{31\text{P}-13\text{C}} = 93.4$ Hz), 29.8 ppm; ^{31}P NMR (160 MHz, CDCl_3) δ 45.3 ppm; HRMS (ESI) calcd. for $[\text{C}_{43}\text{H}_{40}\text{AuF}_9\text{N}_2\text{OP}]^+$: m/z 999.2400, found 999.2406.

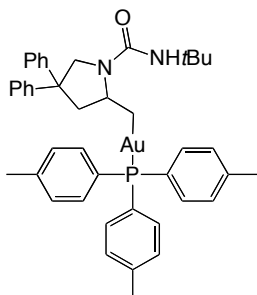


***para*-Chlorophosphine 4.62b:** Purified by flash column chromatography on basic alumina (99:1 toluene/EtOAc with 1% NEt₃) to afford **4.62b** (67%) as a red foam: ¹H NMR (600 MHz, CDCl₃) δ 7.39 – 7.31 (m, 11H), 7.30 – 7.20 (m, 10H), 7.15 – 7.10 (m, 1H), 4.92 (dd, 1H, *J* = 11.5, 2.2 Hz), 4.40 (s, 1H), 4.17 – 4.05 (m, 1H), 3.47 (d, 1H, *J* = 11.5 Hz), 2.91 (ddd, 1H, *J* = 12.0, 6.0, 2.2 Hz), 2.71 (dd, 1H, *J* = 12.0, 9.6 Hz), 1.75 – 1.70 (m, 1H), 1.36 (s, 1H) ppm; ¹³C NMR (150 MHz, CDCl₃) δ 156.6, 146.8, 146.3, 138.1 (d, *J*_{31P-13C} = 2.2 Hz), 135.3, (d, *J*_{31P-13C} = 15.2 Hz), 129.5, (d, *J*_{31P-13C} = 11.2 Hz), 128.9 (d, *J*_{31P-13C} = 47.8 Hz), 128.4, 128.2, 127.0, 126.8, 126.2, 125.8, 58.0 (d, *J*_{31P-13C} = 3.6 Hz), 54.8, 52.1, 52.0, 50.4, 37.5 (d, *J*_{31P-13C} = 92.9 Hz), 29.8 ppm; ³¹P NMR (160 MHz, CDCl₃) δ 44.1 ppm; HRMS (ESI) calcd. for [C₄₀H₄₀AuN₂OPCl₃]⁺: *m/z* 891.1604, found 891.1614.

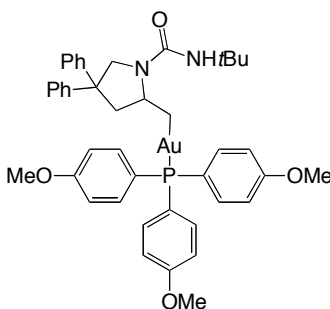


***para*-Fluorophosphine 4.62c.** Purified by flash column chromatography on basic alumina (99:1 toluene/EtOAc with 1% NEt₃) to afford **4.62c** (75%) as a faint pink foam: ¹H NMR (500 MHz, CDCl₃) δ 7.49 – 7.44 (m, 6H), 7.36 – 7.22 (m, 9H), 7.17 – 7.08 (m, 7H), 4.95 (dd, 1H, *J* = 11.5, 1.3 Hz), 4.45 (brs, 1H), 4.19 – 4.11 (m, 1H), 3.51 (d, *J* = 11.5 Hz, 1H), 2.94 (ddd, 1H, *J* = 12.1, 6.0, 2.0 Hz), 2.75 (dd, *J* = 12.1, 9.7 Hz, 1H), 1.74 – 1.71 (m, 2H), 1.39 (s, 9H) ppm; ¹³C NMR (125 MHz, CDCl₃) δ 164.6 (d, *J*_{19F-13C} = 253.7 Hz), 156.7, 146.9, 146.4, 136.3 (dd, *J*_{31P-13C} = 15.7, *J*_{19F-13C} = 8.6 Hz), 128.4, 128.3, 127.1, 127.0, 126.6 (d, *J*_{31P-13C} = 51.8 Hz), 126.2, 125.8, 116.6 (dd, *J*_{19F-13C} = 21.5, *J*_{31P-13C} = 11.8 Hz), 58.1 (d, *J*_{31P-13C} = 1.9 Hz), 54.8, 52.1, 52.1, 50.4, 37.4 (d,

$J_{31\text{P}-13\text{C}} = 93.0$ Hz), 29.8 ppm; ^{31}P NMR (160 MHz, CDCl_3) δ 43.6 ppm; HRMS (ESI) calcd. for $[\text{C}_{40}\text{H}_{40}\text{AuN}_2\text{OPF}_3]^+$: m/z 849.2490, found 849.2496.

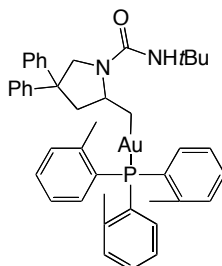


***para*-Methylphosphine 4.62d.** Purified by flash column chromatography on basic alumina (99:1 toluene/EtOAc with 1% NEt_3) to afford **4.62d** (72%) as an off-white foam: ^1H NMR (600 MHz, CDCl_3) δ 7.42 – 7.38 (m, 6H), 7.34 – 7.24 (m, 8H), 7.24 – 7.16 (m, 7H), 7.16 – 7.13 (m, 1H), 4.96 (dd, 1H, $J = 11.6, 1.5$ Hz), 4.50 (s, 1H), 4.08 – 3.96 (m, 1H), 3.53 (d, 1H, $J = 11.6$ Hz), 3.00 – 2.92 (m, 1H), 2.75 (dd, 1H, $J = 12.0, 9.8$ Hz), 2.40 (s, 9H), 1.76 (ddd, 1H, $J = 12.4, 8.4, 3.8$ Hz), 1.64 (ddd, 1H, $J = 12.9, 8.4, 8.3$ Hz), 1.39 (s, 9H) ppm; ^{13}C NMR (150 MHz, CDCl_3) δ 156.9, 146.9, 146.5, 141.2, (d, $J_{31\text{P}-13\text{C}} = 2.2$ Hz), 134.1 (d, $J_{31\text{P}-13\text{C}} = 14.0$ Hz), 129.7 (d, $J_{31\text{P}-13\text{C}} = 10.9$ Hz), 128.3 (d, $J_{31\text{P}-13\text{C}} = 49.6$ Hz), 128.2, 128.2, 127.2, 127.1, 126.0, 125.7, 58.6 (d, $J_{31\text{P}-13\text{C}} = 2.9$ Hz), 54.76, 52.24, 52.11, 50.37, 36.9 (d, $J_{31\text{P}-13\text{C}} = 92.1$ Hz), 29.8, 21.4 ppm; ^{31}P NMR (160 MHz, CDCl_3) δ 43.7 ppm; HRMS (ESI) calcd. for $[\text{C}_{43}\text{H}_{49}\text{AuN}_2\text{OP}]^+$: m/z 837.3243, found 837.3258.

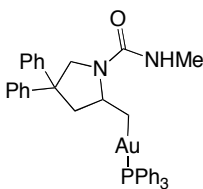


***para*-Methoxyphosphine 4.62f.** Purified by flash column chromatography on basic alumina (9:1 pentanes/EtOAc with 1% NEt_3) to afford **4.62f** (56%) as a white foam: ^1H NMR (600 MHz, CDCl_3) δ 7.41 – 7.36 (m, 6H), 7.31 – 7.20 (m, 8H), 7.20 – 7.16 (m, 1H), 7.12 (t, 1H, $J = 7.0$ Hz), 6.87 (d, $J = 7.5$ Hz, 6H), 4.94 (d, 1H, $J = 11.7$ Hz), 4.48 (s, 1H), 4.02 (d, 1H, $J = 8.1$ Hz), 3.81 (s, 9H), 3.52 (d, 1H, $J = 11.6$ Hz), 2.95 – 2.89 (m, 1H), 2.76 (dd, 1H, $J = 11.9, 9.9$ Hz), 1.69 (ddd, 1H, $J = 12.8, 9.1, 2.7$ Hz), 1.61 (ddd, 1H, $J = 13.1, 9.1, 8.2$ Hz), 1.36 (s, 9H) ppm; ^{13}C NMR (150 MHz, CDCl_3) δ 161.6 (d, $J_{31\text{P}-13\text{C}} = 2.0$ Hz), 156.9, 147.0, 146.5, 135.6 (d, $J_{31\text{P}-13\text{C}} = 15.2$ Hz), 128.3, 128.2, 127.2, 127.1, 126.0, 125.7, 123.0 (d, $J_{31\text{P}-13\text{C}} = 52.8$ Hz), 114.6 (d, $J_{31\text{P}-13\text{C}} = 11.7$ Hz), 58.5 (d, $J_{31\text{P}-13\text{C}} = 3.3$ Hz), 55.4, 54.8, 52.2, 52.1, 50.4, 37.1 (d, $J_{31\text{P}-13\text{C}} = 92.4$ Hz), 29.8 ppm;

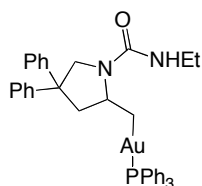
^{31}P NMR (160 MHz, CDCl_3) δ 42.2 ppm; HRMS (ESI) calcd. for $[\text{C}_{43}\text{H}_{49}\text{AuN}_2\text{O}_4\text{P}]^+$: m/z 885.3090, found 885.3097.



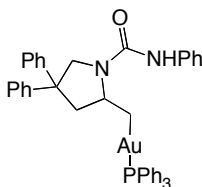
ortho-Methylphosphine 4.62e. Purified by flash column chromatography on basic alumina (49:1 toluene/EtOAc with 1% NEt_3) to afford **4.62e** (73%) as a white foam: ^1H NMR (500 MHz, CDCl_3) δ 7.40 (t, 3H, $J = 7.5$ Hz), 7.29 (m, 3H), 7.27 – 7.19 (m, 6H), 7.19 – 7.07 (m, 7H), 6.87 (dd, 3H, $J = 10.7, 8.0$ Hz), 4.89 (dd, 1H, $J = 11.5, 1.7$ Hz), 4.38 (s, 1H), 3.87 – 3.79 (m, 1H), 3.36 (d, 1H, $J = 11.5$ Hz), 2.85 (ddd, 1H, $J = 12.0, 5.9, 2.0$ Hz), 2.67 (s, 9H), 2.56 (dd, 1H, $J = 12.0, 9.7$ Hz), 1.70 (ddd, 1H, $J = 12.8, 8.8, 2.5$ Hz), 1.53 (dt, $J = 12.8, 8.8$ Hz, 1H), 1.32 (s, 9H) ppm; ^{13}C NMR (125 MHz, CDCl_3) δ 156.8, 146.8, 146.4, 143.0 (d, $J_{31\text{P}-13\text{C}} = 14.1$ Hz), 133.6 (d, $J_{31\text{P}-13\text{C}} = 7.2$ Hz), 131.9 (d, $J_{31\text{P}-13\text{C}} = 8.2$ Hz), 131.0 (d, $J_{31\text{P}-13\text{C}} = 1.9$ Hz), 128.2, 128.2, 127.9 (d, $J_{31\text{P}-13\text{C}} = 45.4$ Hz), 127.1, 127.0, 126.5 (d, $J_{31\text{P}-13\text{C}} = 8.2$ Hz), 126.0, 125.7, 58.7 (d, $J_{31\text{P}-13\text{C}} = 2.6$ Hz), 54.5, 52.1, 51.9, 50.3, 33.8 (d, $J_{31\text{P}-13\text{C}} = 91.3$ Hz), 29.7, 23.5 (d, $J_{31\text{P}-13\text{C}} = 9.9$ Hz) ppm; ^{31}P NMR (160 MHz, CDCl_3) δ 34.7 ppm; HRMS (ESI) calcd. for $[\text{C}_{43}\text{H}_{49}\text{AuN}_2\text{OP}]^+$: m/z 837.3243, found 837.3255.



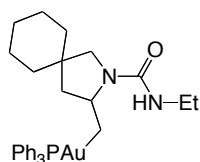
Alkylgold 4.40. Purified by flash column chromatography on basic alumina (10% EtOAc in toluene with 1% NEt_3) to afford **4.40** (59%) as a white foam: ^1H NMR (600 MHz, CDCl_3) δ 7.47 (m, 8H), 7.43 – 7.36 (m, 6H), 7.31 – 7.21 (m, 9H), 7.21 – 7.15 (m, 1H), 7.12 (m, 1H), 4.94 (d, 1H, $J = 11.4$ Hz), 4.51 (q, 1H, $J = 4.6$ Hz), 4.13 – 3.99 (m, 1H), 3.60 (d, 1H, $J = 11.4$ Hz), 3.00 (ddd, 1H, $J = 12.1, 6.3, 1.5$ Hz), 2.81 (d, 3H, $J = 4.6$ Hz), 2.70 (dd, 1H, $J = 12.1, 9.6$ Hz), 1.76 (ddd, 1H, $J = 12.3, 8.7, 3.1$ Hz), 1.61 (ddd, 1H, $J = 13.0, 8.7, 8.4$ Hz) ppm; ^{13}C NMR (150 MHz, CDCl_3) δ 157.9, 146.8, 146.3, 134.2 (d, $J_{31\text{P}-13\text{C}} = 13.7$ Hz), 131.2 (d, $J_{31\text{P}-13\text{C}} = 50.0$ Hz), 131.0, 129.0 (d, $J_{31\text{P}-13\text{C}} = 10.6$ Hz), 128.3, 128.2, 127.1, 126.9, 126.0, 125.7, 58.5 (d, $J_{31\text{P}-13\text{C}} = 2.5$ Hz), 55.2, 52.2, 52.0, 37.10 (d, $J_{31\text{P}-13\text{C}} = 92.0$ Hz), 27.3 ppm; ^{31}P NMR (160 MHz, CDCl_3) δ 45.6 ppm; HRMS (ESI) calcd. for $[\text{C}_{37}\text{H}_{37}\text{AuN}_2\text{OP}]^+$: m/z 753.2309, found 753.2319.



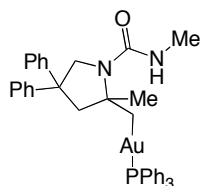
Alkylgold 4.41. Purified by flash column chromatography on basic alumina (5% EtOAc in toluene with 1% NEt₃) to afford **4.41** (63%) as a white foam: ¹H NMR (600 MHz, CDCl₃) δ 7.53 – 7.46 (m, 8H), 7.45 – 7.39 (m, 6H), 7.30 – 7.25 (m, 9H), 7.20 – 7.17 (m, 1H), 7.15 – 7.13 (m, 1H), 4.96 (d, 1H, *J* = 10.4 Hz), 4.53 (t, 1H, *J* = 5.4 Hz), 4.13 – 4.02 (m, 1H), 3.60 (d, 1H, *J* = 11.5 Hz), 3.38 – 3.25 (m, 1H), 3.00 (ddd, 1H, *J* = 12.1, 6.0, 2.1 Hz), 2.73 (dd, 1H, *J* = 12.2, 9.6 Hz), 1.79 (ddd, 1H, *J* = 12.4, 9.0, 3.1 Hz), 1.65 (dt, 1H, *J* = 13.0, 8.5 Hz), 1.13 (t, *J* = 7.2 Hz, 3H) ppm; ¹³C NMR (150 MHz, CDCl₃) δ 157.3, 146.9, 146.4, 134.2 (d, *J*_{31P-13C} = 13.7 Hz), 131.2 (d, *J*_{31P-13C} = 47.7 Hz), 131.0 (d, *J*_{31P-13C} = 2.2 Hz), 129.0 (d, *J*_{31P-13C} = 10.6 Hz), 128.3, 127.1, 126.9, 126.0, 125.8, 58.5 (d, *J*_{31P-13C} = 3.0 Hz), 55.2, 52.2, 52.1, 37.1 (d, *J*_{31P-13C} = 92.0 Hz), 35.4, 16.0 ppm; ³¹P NMR (160 MHz, CDCl₃) δ 45.6 ppm; HRMS (ESI) calcd. for [C₃₈H₃₉AuN₂OP]⁺: *m/z* 767.2466, found 767.2474.



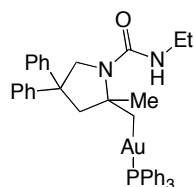
Alkylgold 4.42. Purified by flash column chromatography on basic alumina (1% EtOAc in toluene with 1% NEt₃) to afford **4.42** (66%) as a white foam: ¹H NMR (600 MHz, CDCl₃) δ 7.55 – 7.45 (m, 10H), 7.45 – 7.37 (m, 6H), 7.35 (d, 2H, *J* = 7.8 Hz), 7.33 – 7.20 (m, 10H), 7.16 (t, 1H, *J* = 7.3 Hz), 6.99 (t, 1H, *J* = 7.4 Hz), 6.71 (brs, 1H), 5.01 (d, 1H, *J* = 11.4 Hz), 4.35 – 4.31 (m, 1H), 3.70 (d, 1H, *J* = 11.4 Hz), 3.09 (ddd, 1H, *J* = 12.2, 5.9, 2.0 Hz), 2.81 (dd, 1H, *J* = 12.2, 9.6 Hz), 1.88 (ddd, 1H, *J* = 12.9, 9.1, 3.1 Hz), 1.81 (ddd, 1H, *J* = 12.9, 8.2, 8.1 Hz) ppm; ¹³C NMR (150 MHz, CDCl₃) δ 154.2, 146.6, 146.0, 139.9, 134.2 (d, *J*_{31P-13C} = 13.8 Hz), 131.1 (d, *J*_{31P-13C} = 48.6 Hz), 131.0 (d, *J*_{31P-13C} = 2.0 Hz), 129.0 (d, *J*_{31P-13C} = 10.9 Hz), 128.7, 128.4, 128.4, 127.1, 126.8, 126.2, 126.0, 122.0, 119.1, 58.9 (d, *J*_{31P-13C} = 2.8 Hz), 55.1, 52.1, 51.9, 37.4 (*J*_{31P-13C} = 92.2 Hz) ppm; ³¹P NMR (160 MHz, CDCl₃) δ 45.5 ppm; HRMS (ESI) calcd. for [C₄₂H₃₉AuN₂OP]⁺: *m/z* 815.2466, found 815.2471.



Alkylgold 4.43. Purified by flash column chromatography on basic alumina (5% EtOAc in toluene with 1% NEt₃) to afford **4.43** (49%) as white foam: ¹H NMR (600 MHz, CDCl₃) δ 7.54 – 7.43 (m, 15H), 4.45 (m, 1H), 4.21 (m, 1H), 3.77 (d, *J* = 10.6 Hz, 1H), 3.32 – 3.18 (m, 2H), 2.98 (d, *J* = 10.7 Hz, 1H), 2.23 (dd, *J* = 12.3, 7.1 Hz, 1H), 1.74 (ddd, *J* = 12.6, 9.0, 3.5 Hz, 1H), 1.56 (dt, *J* = 12.6, 8.8 Hz, 2H), 1.48 – 1.21 (m, 10H), 1.10 (t, *J* = 7.2 Hz, 3H) ppm; ¹³C NMR (150 MHz, CDCl₃): δ 157.6, 134.2 (d, *J*_{31P-13C} = 13.7 Hz), 131.3 (d, *J*_{31P-13C} = 47.3 Hz), 130.96 (d, *J*_{31P-13C} = 2.0 Hz), 128.95 (d, *J*_{31P-13C} = 10.6 Hz), 58.5 (d, *J*_{31P-13C} = 2.6 Hz), 40.4, 37.9 (d, *J*_{31P-13C} = 91.9 Hz), 37.0, 35.3, 34.7, 26.4, 24.0, 22.9, 15.9 ppm; ³¹P NMR (240 MHz, CDCl₃) δ 45.8 ppm; HRMS (ESI) calcd. for [C₃₁H₃₉AuNO₂P]⁺: *m/z* 683.2460, found 683.2483.

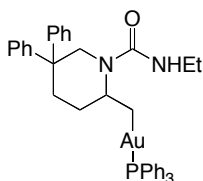


Alkylgold 4.44. Purified by flash column chromatography on basic alumina (5% EtOAc in toluene! with 1% NEt₃) to afford **4.44** (60%) as white foam: ¹H NMR (600 MHz, CDCl₃) δ 7.53 – 7.42 (m, 9H), 7.42 – 7.33 (m, 8H), 7.31 – 7.24 (m, 6H), 7.22 – 7.16 (m, 1H), 7.12 (dd, 1H, *J* = 18.3, 11.0 Hz), 4.84 (d, 1H, *J* = 11.4 Hz), 4.65 (brs, 1H), 3.84 (d, 1H, *J* = 11.4 Hz), 3.28 (d, 1H, *J* = 12.3 Hz), 2.86 (d, 1H, *J* = 4.7 Hz), 2.81 (d, 1H, *J* = 12.3 Hz), 1.91 (dd, 1H, *J* = 13.0, 9.1 Hz), 1.75 (dd, 1H, *J* = 12.4, 9.1 Hz), 1.15 (s, 1H) ppm; ¹³C NMR (151 MHz, CDCl₃) δ 157.6, 147.8, 146.8, 134.2 (d, *J*_{31P-13C} = 13.8 Hz), 131.2 (d, *J*_{31P-13C} = 47.6 Hz), 131.0 (d, *J*_{31P-13C} = 2.2 Hz), 129.0 (d, *J*_{31P-13C} = 10.6 Hz), 128.3, 128.2, 127.2, 127.0, 125.8, 125.7, 66.5, 58.6, 56.1, 50.1, 47.8 (d, *J*_{31P-13C} = 92.6 Hz), 31.6 (d, *J*_{31P-13C} = 5.2 Hz), 27.31 ppm; ³¹P NMR (160 MHz, CDCl₃) δ 45.4 ppm; HRMS (ESI) calcd. for [C₃₈H₃₉AuN₂OP]⁺: *m/z* 767.2466, found 767.2443.



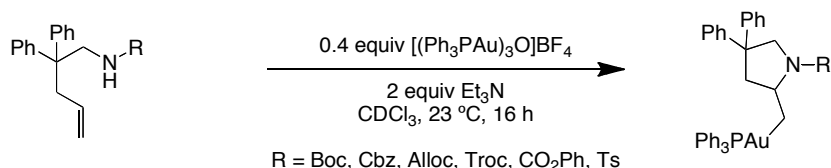
Alkylgold 4.45. Purified by flash column chromatography on basic alumina (5% EtOAc in toluene with 1% NEt₃) to afford **4.45** (40%) as white foam: ¹H NMR (500 MHz, CDCl₃) δ 7.54

– 7.42 (m, 9H), 7.42 – 7.34 (m, 8H), 7.31 – 7.24 (m, 6H), 7.18 (dd, 1H, $J = 13.4, 6.3$ Hz), 7.13 (dd, 1H, $J = 16.4, 9.1$ Hz), 4.86 (d, 1H, $J = 11.4$ Hz), 4.67 (brs, 1H), 3.85 (d, 1H, $J = 11.4$ Hz), 3.44 – 3.28 (m, 3H), 2.82 (dd, $J = 12.2, 1.6$ Hz, 1H), 1.93 (dd, $J = 13.0, 9.1$ Hz, 1H), 1.74 (dd, $J = 12.8, 7.9$ Hz, 1H), 1.16 (s, 3H), 1.15 (t, 3H, $J = 7.3$ Hz) ppm; ^{13}C NMR (125 MHz, CDCl_3) δ 156.9, 147.9, 146.8, 134.3 (d, $J_{31\text{P}-13\text{C}} = 13.8$ Hz), 131.2 (d, $J_{31\text{P}-13\text{C}} = 47.6$ Hz), 131.0 (d, $J_{31\text{P}-13\text{C}} = 2.2$ Hz), 129.0 (d, $J_{31\text{P}-13\text{C}} = 10.6$ Hz), 128.3, 128.2, 127.2, 127.0, 125.8, 125.7, 66.4 (d, $J_{31\text{P}-13\text{C}} = 4.5$ Hz), 58.7, 56.0, 47.9 (d, $J_{31\text{P}-13\text{C}} = 92.6$ Hz), 47.5, 35.3, 31.6 (d, $J_{31\text{P}-13\text{C}} = 5.2$ Hz), 15.9 ppm; ^{31}P NMR (160 MHz, CDCl_3) δ 45.3 ppm; HRMS (ESI) calcd. for $[\text{C}_{39}\text{H}_{41}\text{AuN}_2\text{OP}]^+$: m/z 781.2617, found 781.2620.



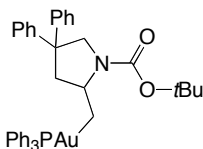
Alkylgold 4.46. To a solution of ethyl urea **4.39** (0.027 g, 0.084 mmol) and triethylamine (24 μL , 0.17 mmol) in DCM (0.5 mL) was added $[(\text{Ph}_3\text{P}_3\text{Au})_3\text{O}]\text{BF}_4$ and stirred overnight. The reaction was diluted with DCM (3 mL) and washed with saturated NaHCO_3 (2×3 mL), dried over MgSO_4 , filtered, and concentrated *in vacuo*, to yield a yellow foam. The crude material was purified by flash column chromatography on basic alumina (40:20:1 toluene/DCM/EtOAc with 1% NEt_3) to afford **4.46** (20 mg, 30% yield) as a white foam: ^1H NMR (600 MHz, CD_2Cl_2) δ 7.52 – 7.44 (m, 17H), 7.28 – 7.24 (m, 4H), 7.17 – 7.08 (m, 4H), 5.07 (dd, 1H, $J = 13.9, 2.3$ Hz), 4.67 (t, 1H, $J = 5.2$ Hz), 4.23 (br s, 1H), 3.30 (d, 1H, $J = 13.9$ Hz), 3.25 – 3.19 (m, 1H), 3.15 – 3.08 (m, 1H), 2.91 (dt, 1H, $J = 13.3, 3.42$ Hz), 2.43 – 2.40 (m, 1H), 1.74 – 1.60 (m, 4H), 1.03 (t, 3H, $J = 7.2$ Hz) ppm; ^{13}C NMR (150 MHz, CD_2Cl_2) δ 157.4, 148.6, 145.9, 134.2 (d, $J_{31\text{P}-13\text{C}} = 13.7$ Hz), 131.3 (d, $J_{31\text{P}-13\text{C}} = 47.5$ Hz), 131.0, 128.9 (d, $J_{31\text{P}-13\text{C}} = 10.5$ Hz), 128.0, 128.0, 128.0, 126.7, 125.75, 125.4, 46.6, 45.4, 35.6, 30.8 (d, $J_{31\text{P}-13\text{C}} = 93.4$ Hz), 30.4, 30.4, 29.5, 15.4 ppm; ^{31}P NMR (160 MHz, CD_2Cl_2) δ 45.4 ppm; IR (neat): 3449, 2092, 1624.3, 1496, 1435, 1272, 1124, 1027, 1011 cm^{-1} ; HRMS (ESI) calcd. for $[\text{C}_{39}\text{H}_{41}\text{AuN}_2\text{OP}]^+$: m/z 781.2617, found 781.2625.

General Procedure for Cyclization of Carbamate and Sulfonyl Substrates

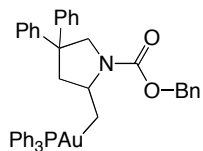


Protected amine (100 μmol) and triethylamine (200 μmol) were combined in CDCl_3 (1.0 mL) and let stir for five minutes before the addition of the gold trimer (40 μmol) in one portion. After 12 hours, the reaction mixture was diluted with CHCl_3 (10 mL) and washed with H_2O (2×5 mL). The organic layer was then dried over Na_2SO_4 , filtered and concentrated *in vacuo*. The

residue was then suspended in EtOAc and filtered through a pad of basic alumina, the concentrated *in vacuo*.

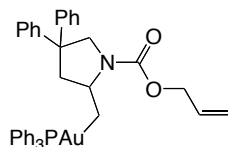


Alkylgold 4.52a. Purified by flash chromatography on silica gel (gradient: 5% – 10% EtOAc in pentanes with 0.5% NEt₃) to afford **4.52a** (53%) as a white foam. ¹H NMR shows a 3:1 mixture of rotamers in C₆D₆, confirmed by heating to 60 °C, where peaks coalesced to broad singlets. Major rotamer: ¹H NMR (600 MHz, CDCl₃, 298 K) δ 7.45 – 7.35 (m, 8H), 7.13 – 7.07 (m, 4H), 7.01 – 6.91 (m, 13H), 5.14 (d, 1H, *J* = 11.5, 1.4 Hz), 4.89 – 4.83 (m, 1H), 3.90 (d, 1H, *J* = 11.5 Hz), 3.07 (ddd, 1H, *J* = 12.1, 6.3, 1.8 Hz), 2.91 (dd, 1H, *J* = 12.1, 9.9 Hz), 2.62 (ddd, 1H, *J* = 12.5, 8.4, 8.0 Hz), 2.44 (ddd, 1H, *J* = 11.3, 8.4, 1.7 Hz), 1.60 (s, 9H) ppm; ¹³C NMR (150 MHz, C₆D₆, 298 K) δ 155.1, 147.3, 146.7, 134.2 (d, *J*_{31P-13C} = 13.8 Hz), 131.7 (d, *J*_{31P-13C} = 46.2 Hz), 130.5, 128.8 (d, *J*_{31P-13C} = 10.5 Hz), 128.2, 128.2, 127.2, 127.1, 125.7, 125.6, 77.4, 59.7 (d, *J*_{31P-13C} = 3.5 Hz), 55.8, 52.9, 51.4, 39.1 (d, *J*_{31P-13C} = 91.7 Hz), 28.6 ppm; ³¹P NMR (240 MHz, C₆D₆, 298 K) δ 45.7 ppm; Minor rotamer: ¹H NMR (600 MHz, CDCl₃, 298 K) δ 7.45 – 7.35 (m, 8H), 7.13 – 7.07 (m, 4H), 7.01 – 6.91 (m, 13H), 5.09 – 5.02 (m, 1H), 4.80 (d, 1H, *J* = 11.0 Hz), 3.98 (d, 1H, *J* = 11.0 Hz), 3.13 (dd, 1H, *J* = 11.5, 6.7 Hz), 2.80 (app t, 1H, *J* = 9.1 Hz), 2.74 (dd, 1H, *J* = 11.5, 10.6 Hz), 2.53 – 2.58 (m, 1H), 1.53 (s, 9H) ppm; ³¹P NMR (240 MHz, C₆D₆, 298 K) δ 45.6 ppm; HRMS (ESI) calcd. for [C₄₀H₄₂AuNO₂P]⁺: *m/z* 796.2626, found 796.2613.

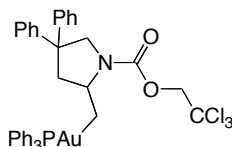


Alkylgold 4.52b. Purified by flash chromatography on silica gel (gradient: 10% – 20% EtOAc in pentanes with 0.5% NEt₃) to afford **4.52b** (49%) as an off-white foam. ¹H NMR shows a 1.5:1 mixture of rotamers in CDCl₃, confirmed by heating to 60 °C in C₆D₆ where peaks coalesced to broad singlets. Major rotamer: ¹H NMR (600 MHz, CDCl₃, 298 K) δ 7.53 – 7.46 (m, 10H), 7.43 – 7.32 (m, 9H), 7.31 – 7.13 (m, 11H), 5.24 (d, 1H, *J* = 13.0 Hz), 5.22 (d, 1H, *J* = 13.0 Hz), 4.77 (dd, 1H, *J* = 11.5, 1.7 Hz), 4.52 – 4.43 (m, 1H), 3.75 (d, 1H, *J* = 11.5 Hz), 3.02 – 3.07 (m, 1H), 2.67 (dd, 1H, *J* = 12.3, 9.8 Hz), 1.95 (ddd, 1H, *J* = 11.9, 9.1, 2.7 Hz), 1.87 – 1.82 (m, 1H) ppm; ¹³C NMR (150 MHz, CDCl₃, 298 K) δ 155.5, 146.8, 146.1, 137.8, 134.3 (d, *J*_{31P-13C} = 13.4 Hz), 131.4 (d, *J*_{31P-13C} = 46.9 Hz), 130.9 (d, *J*_{31P-13C} = 2.1 Hz), 128.9 (d, *J*_{31P-13C} = 10.3 Hz), 128.9, 128.4, 128.3, 128.3, 127.9, 127.3, 127.1, 126.8, 126.1, 125.9, 66.2, 60.0 (d, *J*_{31P-13C} = 2.4 Hz), 55.8, 52.7, 51.0, 37.8 (d, *J*_{31P-13C} = 92.1 Hz) ppm; ³¹P NMR (240 MHz, CDCl₃, 298 K) δ 45.8 ppm; Minor rotamer: ¹H NMR (600 MHz, CDCl₃, 298 K) δ 7.53 – 7.46 (m, 10H), 7.43 – 7.32 (m, 9H), 7.31 – 7.13 (m, 11H), 5.35 (d, 1H, *J* = 12.5 Hz), 5.07 (d, 1H, *J* = 12.5 Hz), 4.63 (dd, 1H, *J* = 11.45, 1.2 Hz), 4.52 – 4.43 (m, 1H), 3.79 (d, 1H, *J* = 11.4 Hz), 3.02 – 3.07 (m, 1H), 2.57

(dd, 1H, $J = 12.4, 9.8$ Hz), 2.08 (ddd, 1H, $J = 11.8, 9.2, 2.6$ Hz), 1.85 – 1.79 (m, 1H) ppm; ^{13}C NMR (150 MHz, CDCl_3 , 298 K) δ 154.3, 146.8, 146.2, 137.8, 134.2 (d, $J_{31\text{P}-13\text{C}} = 13.6$ Hz), 131.6 (d, $J_{31\text{P}-13\text{C}} = 46.5$ Hz), 130.9 (d, $J_{31\text{P}-13\text{C}} = 1.8$ Hz), 129.2 (d, $J_{31\text{P}-13\text{C}} = 11.8$ Hz), 128.5, 128.3, 128.3, 127.7, 127.3, 127.1, 126.8, 126.1, 125.9, 66.2, 60.6 (d, $J_{31\text{P}-13\text{C}} = 2.7$ Hz), 55.8, 52.8, 50.1, 36.7 (d, $J_{31\text{P}-13\text{C}} = 91.8$ Hz) ppm; ^{31}P NMR (240 MHz, CDCl_3 , 298 K) δ 45.7 ppm; HRMS (ESI) calcd. for $[\text{C}_{43}\text{H}_{40}\text{AuNO}_2\text{P}]^+$: m/z 830.2476, found 830.2457.

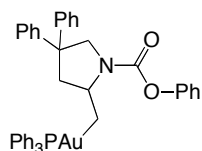


Alkylgold 4.52c. Purified by flash chromatography on silica gel (gradient: 10% – 20% EtOAc in pentanes with 0.5% NEt_3) to afford **4.52c** (37%) as a white foam. ^1H NMR shows a 1.5:1 mixture of rotamers in CDCl_3 , confirmed by heating to 60 °C in C_6D_6 where peaks coalesced to broad singlets. Major rotamer: ^1H NMR (600 MHz, CDCl_3 , 298 K) δ 7.53 – 7.46 (m, 10H), 7.43 – 7.39 (m, 6H), 7.32 – 7.19 (m, 8H), 7.17 – 7.13 (m, 1H), 6.01 – 5.93 (m, 1H), 5.31 (dd, 1H, $J = 17.1, 1.4$ Hz), 5.14 (dd, 1H, $J = 10.6, 1.4$ Hz), 4.76 – 4.58 (m, 3H), 4.43 – 4.37 (m, 1H), 3.73 (d, 1H, $J = 11.4$ Hz), 3.08 – 3.03 (m, 1H), 2.66 (dd, 1H, $J = 12.5, 9.9$ Hz), 1.96 (ddd, 1H, $J = 12.0, 9.1, 2.8$ Hz), 1.84 – 1.75 (m, 1H) ppm; ^{13}C NMR (150 MHz, CDCl_3 , 298 K) δ 155.4, 146.9, 146.1, 134.3 (d, $J_{31\text{P}-13\text{C}} = 14.0$ Hz), 133.8, 132.0, 131.4 (d, $J_{31\text{P}-13\text{C}} = 46.7$ Hz), 130.9 (d, $J_{31\text{P}-13\text{C}} = 1.7$ Hz), 129.0 (d, $J_{31\text{P}-13\text{C}} = 10.4$ Hz), 128.9, 128.3, 127.0, 126.8, 126.1, 125.9, 116.2, 65.2, 60.0 (d, $J_{31\text{P}-13\text{C}} = 2.7$ Hz), 55.7, 52.7, 51.0, 37.6 (d, $J_{31\text{P}-13\text{C}} = 91.6$ Hz) ppm; ^{31}P NMR (240 MHz, CDCl_3 , 298 K) δ 45.8 ppm; Minor rotamer: ^1H NMR (600 MHz, CDCl_3 , 298 K) δ 7.53 – 7.46 (m, 10H), 7.43 – 7.39 (m, 6H), 7.32 – 7.19 (m, 8H), 7.17 – 7.13 (m, 1H), 6.01 – 5.93 (m, 1H), 5.29 (dd, 1H, $J = 17.1, 1.3$ Hz), 5.14 (dd, 1H, $J = 10.4, 1.3$ Hz), 4.76 – 4.58 (m, 3H), 4.53 – 4.46 (m, 1H), 3.80 (d, 1H, $J = 11.3$ Hz), 3.08 – 3.03 (m, 1H), 2.56 (dd, 1H, $J = 12.3, 9.6$ Hz), 2.05 (ddd, 1H, $J = 12.0, 9.2, 2.6$ Hz), 1.84 – 1.73 (m, 1H) ppm; ^{13}C NMR (150 MHz, CDCl_3 , 298 K) δ 154.1, 146.9, 146.3, 143.1 (d, $J_{31\text{P}-13\text{C}} = 13.4$ Hz), 133.9, 132.0, 131.6 (d, $J_{31\text{P}-13\text{C}} = 47.0$ Hz), 130.9 (d, $J_{31\text{P}-13\text{C}} = 1.5$ Hz), 129.3 (d, $J_{31\text{P}-13\text{C}} = 11.8$ Hz), 128.9, 128.3, 127.0, 126.8, 126.1, 125.9, 116.7, 65.1, 60.5 (d, $J_{31\text{P}-13\text{C}} = 1.9$ Hz), 55.8, 52.9, 50.1, 37.8 (d, $J_{31\text{P}-13\text{C}} = 91.6$ Hz) ppm; ^{31}P NMR (240 MHz, CDCl_3 , 298 K) δ 45.7 ppm; HRMS (ESI) calcd. for $[\text{C}_{39}\text{H}_{38}\text{AuNO}_2\text{P}]^+$: m/z 780.2313, found 780.2300.

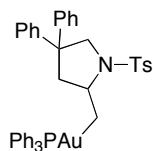


Alkylgold 4.52d. Purified by flash chromatography on silica gel (gradient: 5% – 10% EtOAc in pentanes with 0.5% NEt_3) to afford **4.52d** (43%) as a white foam. ^1H NMR shows a 1.3:1 mixture of rotamers in CDCl_3 , confirmed by heating to 60 °C in C_6D_6 where peaks coalesced to broad singlets. Major rotamer: ^1H NMR (600 MHz, CDCl_3 , 298 K) δ 7.54 – 7.47 (m, 9H), 7.45 –

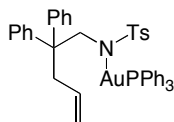
7.39 (m, 6H), 7.33 – 7.20 (m, 9H), 7.17 – 7.14 (m, 1H), 4.85 (d, 1H, $J = 12.1$ Hz), 4.83 (d, 1H, $J = 12.1$ Hz), 4.77 (dd, 1H, $J = 11.5, 2.3$ Hz), 4.60 – 4.54 (m, 1H), 3.79 (d, 1H, $J = 11.5$ Hz), 3.10 – 3.06 (m, 1H), 2.69 (dd, 1H, $J = 12.5, 9.8$ Hz), 1.98 – 1.94 (m, 2H) ppm; ^{13}C NMR (150 MHz, CDCl_3 , 298 K) δ 153.7, 146.6, 145.7, 134.2 (d, $J_{31\text{P}-13\text{C}} = 13.8$ Hz), 131.4 (d, $J_{31\text{P}-13\text{C}} = 47.1$ Hz), 130.9, 129.0 (d, $J_{31\text{P}-13\text{C}} = 10.5$ Hz), 128.4, 128.4, 127.0, 126.8, 126.2, 126.0, 96.2, 74.6, 60.5 (d, $J_{31\text{P}-13\text{C}} = 3.2$ Hz), 55.9, 52.8, 50.7, 37.6 (d, $J_{31\text{P}-13\text{C}} = 91.6$ Hz) ppm; ^{31}P NMR (240 MHz, CDCl_3 , 298 K) δ 45.8 ppm. Minor rotamer: ^1H NMR (600 MHz, CDCl_3 , 298 K) δ 7.54 – 7.47 (m, 9H), 7.45 – 7.39 (m, 6H), 7.33 – 7.20 (m, 9H), 7.17 – 7.14 (m, 1H), 5.03 (d, 1H, $J = 12.0$ Hz), 4.75 (dd, 1H, $J = 11.4, 2.3$ Hz), 4.58 (d, 1H, $J = 12.0$ Hz), 4.53 – 4.48 (m, 1H), 3.86 (d, 1H, $J = 11.4$ Hz), 3.12 – 3.08 (m, 1H), 2.59 (dd, 1H, $J = 12.6, 9.8$ Hz), 2.06 (ddd, 1H, $J = 12.2, 9.1, 3.0$ Hz), 1.81 (dt, 1H, $J = 12.2, 8.5$ Hz) ppm; ^{13}C NMR (150 MHz, CDCl_3 , 298 K) δ 152.1, 146.5, 145.7, 134.2 (d, $J_{31\text{P}-13\text{C}} = 13.8$ Hz), 134.4 (d, $J_{31\text{P}-13\text{C}} = 47.1$ Hz), 130.9, 129.0 (d, $J_{31\text{P}-13\text{C}} = 10.5$ Hz), 128.4, 128.4, 127.0, 126.8, 126.2, 126.1, 96.4, 74.4, 61.0 (d, $J_{31\text{P}-13\text{C}} = 2.6$ Hz), 55.8, 52.9, 50.0, 36.3 (d, $J_{31\text{P}-13\text{C}} = 91.9$ Hz) ppm; ^{31}P NMR (240 MHz, CDCl_3 , 298 K) δ 45.8 ppm; HRMS (ESI) calcd. for $[\text{C}_{38}\text{H}_{35}\text{AuNO}_2\text{PCl}_3]^+$: m/z 870.1151, found 870.1131.



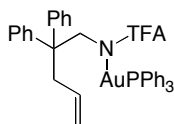
Alkylgold 4.52e. Purified by flash chromatography on silica gel (gradient: 10% – 20% EtOAc in pentanes with 0.5% NEt_3) to afford **4.52e** (69%) as a white foam. ^1H NMR shows a 2:1 mixture of rotamers in CDCl_3 , confirmed by heating to 60 °C in C_6D_6 where peaks coalesced to broad singlets. Major rotamer: ^1H NMR (600 MHz, CDCl_3 , 298 K) δ 7.56 – 7.47 (m, 9H), 7.44 – 7.27 (m, 16H), 7.23 – 7.16 (m, 5H), 4.78 (dd, 1H, $J = 11.4, 2.1$ Hz), 4.64 – 4.58 (m, 1H), 3.82 (d, 1H, $J = 11.4$ Hz), 3.12 (ddd, 1H, $J = 12.2, 6.3, 2.2$ Hz), 2.72 (dd, 1H, $J = 12.5, 9.8$ Hz), 2.06 – 2.02 (m, 1H), 1.95 (dt, 1H, $J = 12.3, 8.5$ Hz) ppm; ^{13}C NMR (150 MHz, CDCl_3 , 298 K) δ 153.9, 152.1, 146.7, 145.9, 134.3 (d, $J_{31\text{P}-13\text{C}} = 13.7$ Hz), 131.3 (d, $J_{31\text{P}-13\text{C}} = 47.2$ Hz), 137.0 (d, $J_{31\text{P}-13\text{C}} = 2.1$ Hz), 129.0, 129.0 (d, $J_{31\text{P}-13\text{C}} = 10.8$ Hz), 128.4, 128.4, 127.1, 126.8, 126.2, 126.0, 124.6, 121.9, 60.6 (d, $J_{31\text{P}-13\text{C}} = 2.7$ Hz), 55.8, 52.7, 50.8, 37.7 (d, $J_{31\text{P}-13\text{C}} = 91.3$ Hz) ppm; ^{31}P NMR (240 MHz, CDCl_3 , 298 K) δ 45.9 ppm; Minor rotamer: ^1H NMR (600 MHz, CDCl_3 , 298 K) δ 7.56 – 7.47 (m, 9H), 7.44 – 7.27 (m, 16H), 7.23 – 7.16 (m, 4H), 7.12 (d, 2H, $J = 7.1$ Hz), 4.83 (dd, 1H, $J = 11.4, 1.8$ Hz), 4.64 – 4.58 (m, 1H), 3.96 (d, 1H, $J = 11.4$ Hz), 3.17 – 3.12 (m, 1H), 2.63 (dd, 1H, $J = 12.6, 9.8$ Hz), 2.08 – 2.05 (m, 1H), 1.91 (dt, 1H, $J = 12.2, 8.4$ Hz) ppm; ^{13}C NMR (150 MHz, CDCl_3 , 298 K) δ 152.5, 151.8, 146.7, 146.0, 134.3 (d, $J_{31\text{P}-13\text{C}} = 13.6$ Hz), 130.9 (d, $J_{31\text{P}-13\text{C}} = 2.0$ Hz), 129.0 (d, $J_{31\text{P}-13\text{C}} = 10.6$ Hz), 128.4, 128.4, 127.1, 126.8, 126.2, 126.1, 124.6, 121.9, 60.9 (d, $J_{31\text{P}-13\text{C}} = 3.0$ Hz), 56.3, 53.1, 50.8, 36.6 (d, $J_{31\text{P}-13\text{C}} = 91.5$ Hz) ppm; ^{31}P NMR (240 MHz, CDCl_3 , 298 K) δ 45.8 ppm; HRMS (ESI) calcd. for $[\text{C}_{42}\text{H}_{38}\text{AuNO}_2\text{P}]^+$: m/z 816.2325, found 816.2300.



Alkylgold 4.55. Purified by flash chromatography on silica gel (10% EtOAc in pentanes with 0.5% NEt₃) to afford **4.55** (29%) as a white foam: ¹H NMR (600 MHz, CDCl₃) δ 7.69 (d, 2H, *J* = 8.2 Hz), 7.54 – 7.41 (m, 8H), 7.31 – 7.29 (m, 3H), 7.26 – 7.11 (m, 8H), 7.09 (d, 2H, *J* = 8.2 Hz), 4.53 (dd, 1H, *J* = 10.3, 1.1 Hz), 4.52 – 4.46 (m, 1H), 3.93 (d, 1H, *J* = 10.3 Hz), 3.08 (ddd, 1H, *J* = 12.5, 6.0, 1.1 Hz), 2.58 (dd, 1H, *J* = 12.5, 9.5 Hz), 2.33 (s, 3H), 2.05 (ddd, 1H, *J* = 12.3, 8.9, 3.4 Hz), 1.52 (ddd, 1H, *J* = 11.8, 10.1, 8.9 Hz) ppm; ¹³C NMR (150 MHz, CDCl₃) δ 146.8, 145.6, 141.7, 139.1, 134.3 (d, *J*_{31P-13C} = 13.7 Hz), 131.4 (d, *J*_{31P-13C} = 47.2 Hz), 131.0 (d, *J*_{31P-13C} = 2.2 Hz), 129.1, 129.0 (d, *J*_{31P-13C} = 10.5 Hz), 128.3, 127.0, 127.0, 126.9, 126.1, 125.9, 64.6 (d, *J*_{31P-13C} = 1.5 Hz), 58.3, 52.5, 51.2, 37.4 (d, *J*_{31P-13C} = 90.5 Hz), 21.4 ppm; ³¹P NMR (240 MHz, CDCl₃) δ 45.34 ppm; HRMS (ESI) calcd. for [C₄₂H₄₀AuNO₂PS]⁺: *m/z* 850.2203, found 850.2177.



4.57. Gold Tosylamide **4.57** was independently synthesized by the following method: In the glove box, sodium hydride (1.9 mg, 0.075 mmol, 1 equiv) was added to a solution of tosylamide (30 mg, 0.075 mmol, 1 equiv) in THF (1 mL). The solution was stirred until gas evolution ceased (30 min). Triphenylphosphine gold chloride (37 mg, 0.075 mmol, 1 equiv) was added and the reaction mixture was stirred for 30 min. The resulting white suspension was filtered through a glass microfilter fiber plug and concentrated in vacuo to yield **4.57** as an off-white solid (50 mg, 79%): H NMR (600 MHz, d₈-THF) δ 7.81 (d, 2H, *J* = 8.1 Hz), 7.55 (ddt, 3H, *J* = 9.4, 5.3, 1.8 Hz), 7.49 (m, 6H), 7.42 (m, 6H), 7.13 (m, 6H), 6.93 (dd, 4H, *J* = 8.2, 7.5 Hz), 6.77 (t, 2H, *J* = 7.3 Hz), 5.70 (m, 1H), 4.74 (m, 2H), 4.11 (s, 2H), 3.10 (d, 2H, *J* = 7.1 Hz), 2.35 (s, 3H) ppm; ¹³C NMR (150 MHz, d₈-THF): δ 147.0, 143.0, 139.5, 135.2, 134.35 (d, *J*_{31P-13C} = 13.9 Hz), 131.30 (d, *J*_{31P-13C} = 2.7 Hz), 129.8 (d, *J*_{31P-13C} = 60.5 Hz), 128.7 (d, *J*_{31P-13C} = 11.5 Hz), 128.38, 128.35, 127.5, 126.9, 125.3, 116.3, 55.6, 50.5, 41.6, 20.3 ppm; ³¹P NMR (240 MHz, d₈-THF) δ 31.7 ppm; HRMS (ESI) calcd. for M+(Ph₃P)₂Au⁺ [C₆₀H₅₄AuNO₂PS]⁺: *m/z* 1308.2676, found 1308.2713.



4.58. Gold Amide **4.58** was independently synthesized by the following method: In the glove box, sodium hydride (1.9 mg, 0.075 mmol, 1 equiv) was added to a solution of amide (25 mg, 0.075 mmol, 1 equiv) in THF (1 mL). The solution was stirred until gas evolution ceased (30

min). Triphenylphosphine gold chloride (37 mg, 0.075 mmol, 1 equiv) was added and the reaction mixture was stirred for 30 min. The resulting white suspension was filtered through a glass microfilter fiber plug and concentrated in vacuo to yield **4.58** as an off-white solid (45 mg, 76%): ^1H NMR (600 MHz, d_8 -THF) δ 7.56 (t, 3H, $J = 7.1$ Hz), 7.50 (t, 6H, $J = 6.7$ Hz), 7.35 (m, 6H), 7.19 (d, 4H, $J = 7.7$ Hz), 6.97 (t, 4H, $J = 7.5$ Hz), 6.77 (t, 2H, $J = 7.1$ Hz), 4.70 (m, 2H), 4.57 (s, 2H), 2.89 (d, 2H, $J = 6.7$ Hz) ppm; ^{13}C NMR (150 MHz, d_8 -THF) δ 163.6 (m) 147.5, 135.7, 134.2 (d, $J_{31\text{P}-13\text{C}} = 13.7$ Hz), 131.6, 128.90, 128.85 (d, $J_{31\text{P}-13\text{C}} = 11.6$ Hz), 128.6 (d, $J_{31\text{P}-13\text{C}} = 46.2$ Hz), 127.5, 125.4, 116.1, 54.5, 51.5, 41.4 ppm; ^{31}P NMR (240 MHz, d_8 -THF) δ 31.2 ppm; HRMS (ESI) calcd. for $\text{M}+(\text{Ph}_3\text{P})_2\text{Au}^+ [\text{C}_{55}\text{H}_{47}\text{AuNO}_2\text{PCl}_3]^+$: m/z 1250.2411, found 1250.2434.

References

- ¹ For general reviews of transition metal catalyzed hydroamination, see: (a) Müller, T. E.; Hultsch, K. C.; Yus, M.; Foubelo, F.; Tada, M. *Chem. Rev.* **2008**, *108*, 3795. For a review of Pt-Catalyzed hydroamination see: (b) Brunet, J.-J.; Chu, N.-C.; Rodriguez-Zubiri, M. *Eur. J. Inorg. Chem.* **2007**, 4711.
- ² For examples of lanthanide catalysis, see: (a) Thomson, R. K.; Bexrud, J. A.; Schafer, L. L. *Organometallics* **2006**, *25*, 4069. (b) Douglass, M. R.; Ogasawara, M.; Hong, S.; Metz, M. V.; Marks, T. J. *Organometallics* **2002**, *21*, 283.
- ³ For examples of zirconium and titanium catalysis, see: (a) Watson, D. A.; Chiu, M.; Bergman, R. G. *Organometallics* **2006**, *25*, 4731. (b) Wood, M. C.; Leitch, D. C.; Yeung, C. S.; Kozak, J. A.; Schafer, L. L. *Angew. Chem., Int. Ed. Engl.* **2007**, *46*, 354.
- ⁴ For recent reviews of enantioselective hydroamination, see: (a) Hultsch, K. C. *Org. Biomol. Chem.* **2005**, *3*, 1819. (b) Aillaud, I.; Collin, J.; Hannedouche, J.; Schulz, E. *Dalton Trans.* **2007**, 5105. (c) Roesky, P. W.; Muller, T. E. *Angew. Chem., Int. Ed. Engl.* **2003**, *42*, 2708. (d) Hultsch, K. C. *Adv. Synth. Catal.* **2005**, 347, 367.
- ⁵ (a) Hofmann, K. A.; Sand, J. *Ber.* **1900**, 1340. (b) Hofmann, K. A.; Sand, J. *Ber.* **1900**, 1353. (c) For an early review see: Chatt, J. *Chem. Rev.* **1950**, *48*, 7.
- ⁶ Chatt, J.; Venanzi, L. M. *J. Chem. Soc.* **1957**, 2445.
- ⁷ Chatt, J.; Vallarino, L. M.; Vananzi, L. M. *J. Chem. Soc.* **1957**, 3413.
- ⁸ For selected examples from Hg-promoted intramolecular hydroamination see: (a) Perie, J. J.; Laval, J. P.; Roussel, J.; Lattes, A. *Tetrahedron* **1972**, *28*, 675. (b) Danishefsky, S.; Taniyama, E.; Webb II, R. R. *Tetrahedron Lett.* **1983**, *24*, 11.
- ⁹ (a) Panunzi, A.; De Renzi, A.; Palumbo, R.; Paiaro, G. *J. Am. Chem. Soc.* **1969**, *91*, 3879. (b) Hollings, D.; Green, M.; Claridge, D. V. *J. Organomet. Chem.* **1973**, *54*, 399. (c) Sarhan, J. K. K.; Green, M.; Al-Najjar, I. M. *J. Chem. Soc. Dalton Trans.* **1984**, 771. (d) For an example of Pt-promoted intermolecular hydroamination see: Ambühl, J.; Pregosin, P. S.; Venanzi, L. M.; Ughetto, G.; Zambonelli, L. *Angew. Chem., Int. Ed. Engl.* **1975**, *14*, 369.
- ¹⁰ (a) Åkermark, B.; Bäckvall, J.; Hegedus, L. S.; Zetterberg, K.; Siirala-Hansén, K.; Sjöberg, K. *J. Organomet. Chem.* **1974**, *72*, 127. (b) Hegedus, L. S.; McKearin, J. M. *J. Am. Chem. Soc.* **1982**, *104*, 2444. (c) For a recent review of aminopalladation reactions, see: A. Minatti, K. Muñoz, K., *Chem. Soc. Rev.* **2007**, *36*, 1142.
- ¹¹ (a) Wang, X.; Widenhofer, R. A. *Organometallics* **2004**, *23*, 1649. (b) Bender, C. F.; Widenhofer, R. A. *J. Am. Chem. Soc.* **2005**, *127*, 1070. (c) Liu, C.; Bender, C. F.; Han, X.; Widenhofer, R. A. *Chem. Comm.* **2007**, 3607.
- ¹² Cochran, B. M.; Michael, F. E. *J. Am. Chem. Soc.* **2006**, *128*, 4246.

-
- ¹³ Neukom, J. D.; Perch, N. S.; Wolfe, J. P. *J. Am. Chem. Soc.* **2010**, *132*, 6276.
- ¹⁴ Cochran, B. M.; Michael, F. E. *J. Am. Chem. Soc.* **2008**, *130*, 2786.
- ¹⁵ McBee, J. L.; Bell, A. T.; Tilley, T. D. *J. Am. Chem. Soc.* **2008**, *130*, 16562.
- ¹⁶ For recent reviews on gold-catalyzed reactions see: (a) Fürstner, A. *Chem. Soc. Rev.*, **2009**, *38*, 3208. (b) Li, Z.; Brouwer, C.; He, C. *Chem. Rev.* **2008**, *108*, 3239. (c) Gorin, D. J.; Sherry, B. D.; Toste, F. D. *Chem. Rev.* **2008**, *108*, 3351. (d) Shen, H. C. *Tetrahedron* **2008**, *64*, 3885.
- ¹⁷ For examples of gold-catalyzed hydroamination of alkenes, see: (a) Zhang, J.; Yang, C.-G.; He, C. *J. Am. Chem. Soc.* **2006**, *128*, 1798. (b) Liu, X.-Y.; Li, C.-H.; Che, C.-M. *Org. Lett.* **2006**, *8*, 2707. For examples of gold(I)-catalyzed additions of other nucleophiles to alkenes, see: (c) Yang, C.-G.; He, C. *J. Am. Chem. Soc.* **2005**, *127*, 6966. (d) Zhou, C.-Y.; Ming, C.-M. *J. Am. Chem. Soc.* **2007**, *129*, 5828. (e) Wang, M.-Z.; Wong, M.-K.; Che, C.-M. *Chem – Eur. J.* **2009**, *14*, 8353. (f) Iglesias, A.; Muñoz, K. *Chem. Eur. J.* **2009**, *15*, 10563. (g) Zhang, G.; Cui, L.; Wang, Y.; Zhang, L. *J. Am. Chem. Soc.* **2010**, *132*, 1474. For a review, see: (h) Widenhoefer, R. A.; Han, X. *Eur. J. Org. Chem.* **2006**, 4555.
- ¹⁸ (a) Hertwig, R. H.; Koch, W.; Schröder, D.; Schwarz, H. *J. Phys. Chem.* **1996**, *100*, 12253. (b) Nechaev, M. S.; Rayón, V. M.; Frenking, G. *J. Phys. Chem. A* **2004**, *108*, 3134.
- ¹⁹ For X-ray structure of L-gold(I)-alkene complexes see: (a) Shapiro, N. D.; Toste, F. D. *Proc. Natl. Acad. Sci. USA*, **2008**, *105*, 2779. (b) Brown, T. J.; Dickens, M. G.; Widenhoefer, R. A. *J. Am. Chem. Soc.* **2009**, *131*, 6350. (c) Hooper, T. N.; Green, M.; McGrady, J. E.; Patel, J. R.; Russell, C. A. *Chem. Commun.* **2009**, 3877. (d) Brown, T. J.; Dickens, M. G.; Widenhoefer, R. A. *Chem. Commun.* **2009**, 6451. (e) Hooper, T. N.; Butts, C. P.; Green, M.; Haddow, M. F.; McGrady, J. E.; Russell, C. A. *Chem. Eur. J.* **2009**, *15*, 12196.
- ²⁰ (a) Rosenfeld, D. C.; Shekhar, S.; Takemiya, A.; Utsunomiya, M.; Hartwig, J. F. *Org. Lett.* **2006**, *8*, 4179. (b) Schlummer, B.; Hartwig, J. F. *Org. Lett.* **2002**, *4*, 1471. (d) Zigang, L.; Zhang, J.; Brouwer, C.; Yang, C. G.; Reich, N. W.; He, C. *Org. Lett.* **2006**, *8*, 4175. For a review, see (c) Taylor, J. G.; Adrio, L. A.; Hii, K. K. *Dalton Trans.* **2010**, *39*, 1171.
- ²¹ Giner, X.; Nájera, C. *Org. Lett.* **2008**, *10*, 2919.
- ²² (a) Han, X.; Widenhoefer, R. A. *Angew. Chem., Int. Ed. Engl.* **2006**, *45*, 1747. (b) Bender, C. F.; Widenhoefer, R. A. *Chem. Commun.* **2006**, 4143. (c) Bender, C. F.; Widenhoefer, R. A. *Org. Lett.* **2006**, *8*, 5303.
- ²³ For isolation of vinylgold(I) intermediates from additions to alkynes and allenes see: (a) Akana, J. A.; Bhattacharyya, K. X.; Muller, P.; Sadighi, J. P. *J. Am. Chem. Soc.* **2007**, *129*, 7736. (b) Liu, L.-P.; Hammond, G. B. *Chem. – Asian J.* **2009**, *4*, 1230. (c) Liu, L.-P.; Xu, B.; Mashita, M. A.; Hammond, G. B. *J. Am. Chem. Soc.* **2008**, *130*, 17642. (d) Shi,

Y.; Ramgren, S. D.; Blum, S. A. *Organometallics* **2009**, *28*, 1275. (e) Hashmi, A. S. K.; Schuster, A. M.; Rominger, F. *Angew. Chem., Int. Ed. Engl.* **2009**, *48*, 8247. (f) Zeng, X.; Kinjo, R.; Donnadiou, B.; Bertrand, G. *Angew. Chem., Int. Ed. Engl.* **2010**, *49*, 942.

²⁴ For an example of a mercury complex, see: (a) Pathak, R.; Naicker, P.; Thompson, W. A.; Fernandes, A.; de Konig, C. B.; van Otterol, W. A. L. *Eur. J. Org. Chem.* **2007**, 5337. For an example of a platinum complex, see: (b) Hoover, J. M.; Freudenthal, J.; Michael, F. E.; Mayer, J. M. *Organometallics* **2008**, *27*, 2238.

²⁵ Late transition metal alkyl complexes readily undergo β -hydride elimination: Hegedus, L. *Angew. Chem., Int. Ed. Engl.* **1988**, *27*, 1113.

²⁶ The scope of aminoauration was explored in collaboration with Dr. William Brenzovich and Kotaro Kelley.

²⁷ (a) Perevalova, E. G.; Bolesov, I. G.; Grandberg, K.I.; Kalyuzhnaya, E. S.; Voyevodskaya, T. I.; Kuzmina, L. G. *Metalloorg. Khim.* **1988**, 183. (b) Perevalova, E. G.; Bolesov, I. G.; Kalyuzhnaya, E. S.; Voyevodskaya, T. I.; Kuzmina, L. G.; Korsunsky, V. I.; Grandberg, K.I. *J. Organomet. Chem.* **1989**, *369*, 267. (c) Perevalova, E. G.; Struchkov, Y. T.; Kravtsov, D. N.; Kuzmina, L. G.; Smyslova, E. I.; Grandberg, K. I.; Kalinina, O. N.; Dyadchenko, V. P. *Zh. Obshch. Khim.* **1988**, *58*, 62. (d) Perevalova, E. G.; Grandberg, K. I.; Smyslova, E. I.; Kuzmina, L. G.; Korsunsky, V. I.; Kravtsov, D. N. *Metalloorg. Khim.* **1989**, 100.

²⁸ These experiments were performed by Dr. William Brenzovich.

²⁹ Baenziger, N. C.; Bennett, W. E.; Soborofe, D. M. *Acta. Cryst. B.* **1976**, *32*, 962.

³⁰ Gavens, P. D.; Guy, J. J.; Mays, M.; Sheldrick, G. M. *Acta. Cryst. B.* **1977**, *33*, 139.

³¹ For D-labelling studies probing the stereochemistry of alkyne addition, see: (a) Kennedy-Smith, J. J.; Staben, S. T.; Toste, F. D. *J. Am. Chem. Soc.* **2004**, *126*, 4526. (b) Hashmi, A. S. K.; Weyrauch, J. P.; Frey, W.; Bats, J. W. *Org. Lett.* **2004**, *6*, 4391.

³² The computational studies were carried out by Dr. Diego Benitez.

³³ Zhao, Y.; Truhlar, D. G. *Acc. Chem. Res.* **2008**, *41*, 157.

³⁴ Benitez, D.; Shapiro, N. D.; Tkatchouk, E.; Wang, Y.; Goddard III., W. A.; Toste, F. D. *Nature Chem.* **2009**, *1*, 482.

³⁵ NBO 5.0: E. D. Glendening, J. K. Badenhoop, A. E. Reed, J. B. Carpenter, J. A. Bohmann, C. M. Morales, F. Weinhold, Theoretical Chemistry Institute, University of Wisconsin, Madison (2001).

³⁶ The protonation of carbamate **4.52e** was performed by Dr. William Brenzovich.

³⁷ Roth, K. E.; Blum, S. A. *Organometallics* **2010**, *29*, 1712-1716.

³⁸ Szuromi, E.; Sharp, P. R. *Organometallics* **2006**, *25*, 558.

³⁹ Murakami, M.; Inouye, M.; Suginome, M.; Ito, Y. *Bull. Chem. Soc. Jpn.* **1988**, *61*, 3649.

-
- ⁴⁰ For Pd-catalyzed coupling of vinylgold(I) complexes, see: Shi, Y.; Ramgren, D.; Blum, S. A. *Organometallics* **2009**, 28, 1275.
- ⁴¹ For selected reviews, see: (a) Frisch, A. C.; Beller, M. *Angew. Chem., Int. Ed. Engl.* **2005**, 44, 674. (b) Netherton, M. R.; Fu, G. C. *Adv. Synth. Catal.* **2004**, 346, 1525.
- ⁴² Tamaki, A.; Kochi, J. K. *J. Chem. Soc.* **1973**, 2620.
- ⁴³ (a) Komiya, S.; Albright, T. A.; Hoffmann, R.; Kochi, J. K. *J. Am. Chem. Soc.* **1976**, 98, 7255. (b) Zhu, D.; Lindeman, S. V.; Kochi, J. K. *Organometallics* **1999**, 18, 2241. (c) Komiya, S.; Kochi, J. K. *J. Am. Chem. Soc.* **1976**, 98, 7599.
- ⁴⁴ Bruce, M.I.; Nicholson, B.K.; Bin Shawkataly, O. *Inorg. Syn.* **1989**, 26, 324.
- ⁴⁵ (a) Yang, Y.; Ramamoorthy, V.; Sharp, P.R. *Inorg. Chem.* **1993**, 32, 1946. (b) Nesmeyanov, A.N.; Perevalova, E.G.; Struchkov, Yu. T.; Antipin, M. Yu.; Grandberg, K.I.; Dyadchenko, V.P. *J. Organomet. Chem.* **1980**, 201, 343.
- ⁴⁶ Cox, L. R.; DeBoos, G. A.; Fullbrook, J. J.; Percy, J. M.; Spencer, N. S.; Tolley, M. *Org. Lett.* **2003**, 5, 337.
- ⁴⁷ Neuman, H.; Seebach, D. *Tetrahedron Lett.* **1976**, 17(52), 4839.
- ⁴⁸ Chang, S.; Lee, M.; Jung, D. Y.; Yoo, E. J.; Cho, S. H.; Han, S. K. *J. Am. Chem. Soc.* **2006**, 128, 12366.

Appendix 4A

Data acquisition details for X-ray crystal structure of alkylgold complex **4.32**

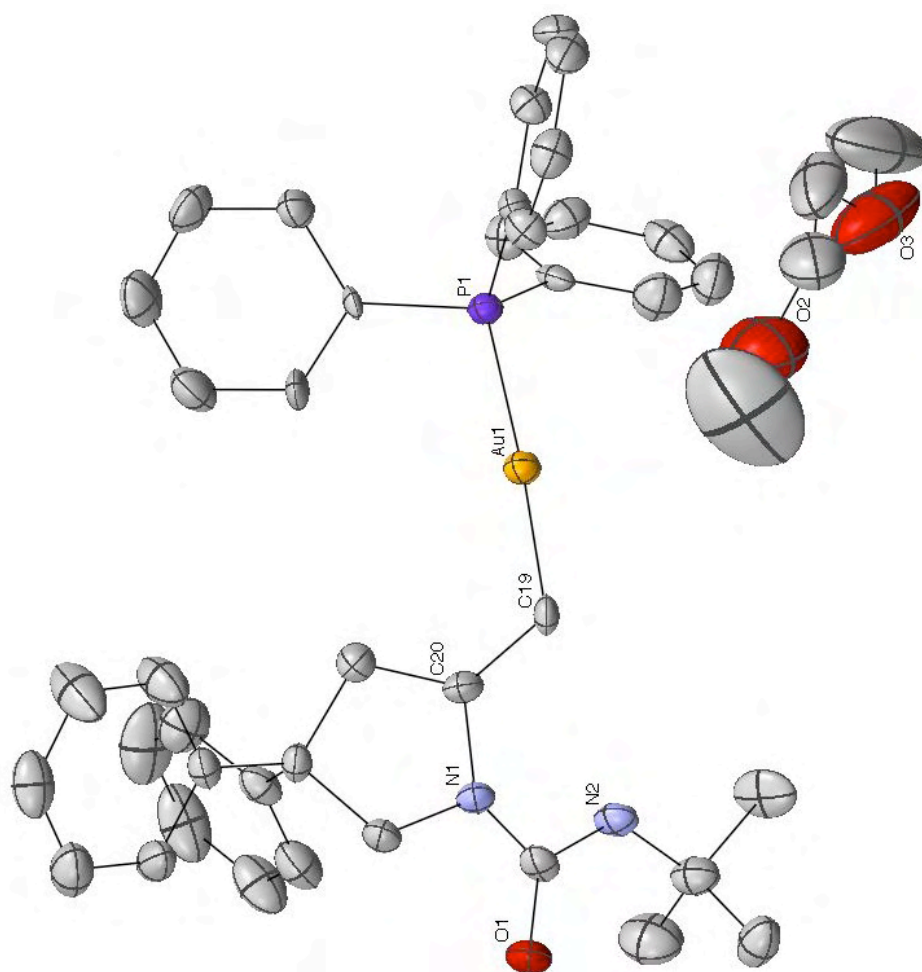


Figure 4A.1. ORTEP of Alkyl gold complex **4.32**. Thermal ellipsoids shown at 50% probability. Hydrogens and solvent molecules omitted for clarity.

Experimental

Data Collection

A yellow plate 0.10 x 0.10 x 0.02 mm in size was mounted on a Cryoloop with Paratone oil. Data were collected in a nitrogen gas stream at 123(2) K using phi and omega scans. Crystal-to-detector distance was 60 mm and exposure time was 10 seconds per frame using a scan width of 0.3°. Data collection was 99.9% complete to 25.00° in θ . A total of 49189 reflections were collected covering the indices, $-10 \leq h \leq 10$, $-32 \leq k \leq 31$, $-20 \leq l \leq 20$. 7475 reflections were found to be symmetry independent, with an R_{int} of 0.0785. Indexing and unit cell refinement indicated a primitive, monoclinic lattice. The space group was found to be P2(1)/n (No. 14). The data were integrated using the Bruker SAINT software program and scaled using the SADABS software program. Solution by direct methods (SIR-2004) produced a complete heavy-atom phasing model consistent with the proposed structure. All non-hydrogen atoms were refined anisotropically by full-matrix least-squares (SHELXL-97). All hydrogen atoms were placed using a riding model. Their positions were constrained relative to their parent atom using the appropriate HFIX command in SHELXL-97.

Crystal Data

Empirical formula	C ₄₄ H ₅₂ Au N ₂ O ₃ P	
Formula weight	884.81	
Temperature	123(2) K	
Wavelength	0.71073 Å	
Crystal system	Monoclinic	
Space group	P2(1)/n	
Unit cell dimensions	a = 8.8343(11) Å	$\alpha = 90^\circ$.
	b = 27.110(4) Å	$\beta = 92.118(2)^\circ$.
	c = 17.039(2) Å	$\gamma = 90^\circ$.
Volume	4078.1(9) Å ³	
Z	4	
Density (calculated)	1.441 Mg/m ³	
Absorption coefficient	3.687 mm ⁻¹	
F(000)	1792	

Crystal size	0.10 x 0.10 x 0.02 mm ³
Crystal color/habit	yellow plate
Theta range for data collection	1.41 to 25.37°.
Index ranges	-10<=h<=10, -32<=k<=31, -20<=l<=20
Reflections collected	49189
Independent reflections	7475 [R(int) = 0.0785]
Completeness to theta = 25.00°	99.9 %
Absorption correction	Semi-empirical from equivalents
Max. and min. transmission	0.9299 and 0.7094
Refinement method	Full-matrix least-squares on F ²
Data / restraints / parameters	7475 / 0 / 465
Goodness-of-fit on F ²	1.251
Final R indices [I>2sigma(I)]	R1 = 0.0656, wR2 = 0.1566
R indices (all data)	R1 = 0.0844, wR2 = 0.1636
Largest diff. peak and hole	3.177 and -1.607 e.Å ⁻³

Table 4A.I. Atomic coordinates ($\times 10^4$) and equivalent isotropic displacement parameters ($\text{\AA}^2 \times 10^3$)

atom	x	y	z	U_{eq}^a
C(1)	4631(10)	2404(4)	5088(5)	16(2)
C(2)	4098(15)	2880(5)	5109(7)	35(3)
C(3)	3507(16)	3094(5)	5772(8)	44(3)
C(4)	3414(17)	2820(6)	6445(8)	46(4)
C(5)	3915(16)	2343(5)	6468(7)	42(3)
C(6)	4552(14)	2133(4)	5809(6)	30(3)
C(7)	4956(13)	1500(4)	4203(6)	24(2)
C(8)	3750(13)	1328(4)	3728(7)	28(3)
C(9)	3417(15)	829(5)	3676(7)	35(3)
C(10)	4347(16)	494(5)	4112(7)	37(3)
C(11)	5517(14)	661(4)	4580(7)	31(3)
C(12)	5846(13)	1152(4)	4626(7)	28(3)
C(13)	7414(12)	2193(4)	4299(7)	23(2)
C(14)	8230(16)	2118(5)	3655(8)	43(3)
C(15)	9751(16)	2164(5)	3674(8)	45(4)
C(16)	10549(14)	2285(4)	4343(8)	37(3)
C(17)	9797(15)	2360(5)	5026(7)	38(3)
C(18)	8211(13)	2319(5)	5023(7)	33(3)
C(19)	3344(13)	2978(4)	2246(6)	23(2)
C(20)	2910(14)	3494(4)	2560(6)	28(3)
C(21)	1638(14)	3469(4)	3147(7)	29(3)
C(22)	814(12)	3961(4)	3080(6)	23(2)
C(23)	791(13)	4023(5)	2176(7)	29(3)
C(24)	-818(13)	3955(4)	3364(6)	26(3)
C(25)	-1384(16)	3574(5)	3811(9)	50(4)
C(26)	-2866(18)	3598(6)	4054(11)	65(5)
C(27)	-3770(16)	3992(6)	3886(8)	48(4)
C(28)	-3231(17)	4372(6)	3453(8)	50(4)
C(29)	-1745(15)	4358(5)	3209(8)	43(3)

C(30)	1707(14)	4363(4)	3529(7)	30(3)
C(31)	1772(17)	4341(6)	4336(8)	49(4)
C(32)	2555(19)	4702(8)	4774(10)	72(6)
C(33)	3232(18)	5087(7)	4410(11)	63(5)
C(34)	3172(16)	5116(5)	3608(10)	52(4)
C(35)	2410(15)	4750(5)	3166(8)	42(3)
C(36)	3103(13)	4109(4)	1457(6)	26(3)
C(37)	5656(14)	4177(5)	862(8)	35(3)
C(38)	5047(15)	4157(6)	-2(8)	44(4)
C(39)	6070(19)	4696(6)	1120(10)	59(4)
C(40)	7071(13)	3853(6)	943(9)	48(4)
C(41)	3850(40)	1471(14)	1470(20)	210(20)
C(42)	5650(30)	936(7)	1868(14)	85(6)
C(43)	6940(30)	824(8)	2398(14)	103(9)
C(44)	9420(40)	945(9)	2718(16)	155(14)
N(1)	2263(10)	3840(3)	1945(5)	24(2)
N(2)	4593(11)	3957(4)	1382(5)	28(2)
P(1)	5367(3)	2153(1)	4217(2)	21(1)
Au(1)	4325(1)	2566(1)	3155(1)	24(1)
O(1)	2607(10)	4480(3)	1117(5)	38(2)
O(2)	5260(20)	1427(6)	1870(11)	125(6)
O(3)	8160(30)	1035(6)	2170(9)	126(7)

^a. U(eq) is defined as one third of the trace of the orthogonalized Uij tensor.

Table 4A.2. Anisotropic displacement parameters ($\text{\AA}^2 \times 10^3$).

atom	U¹¹	U²²	U³³	U²³	U¹³	U¹²
C(1)	13(5)	15(5)	20(5)	-4(4)	8(4)	3(4)
C(2)	47(8)	39(8)	20(6)	-2(5)	14(5)	22(6)
C(3)	54(9)	36(8)	42(8)	-8(6)	-5(7)	18(7)
C(4)	54(9)	53(9)	31(7)	-18(6)	-4(6)	10(7)
C(5)	52(8)	55(9)	18(6)	1(6)	1(6)	2(7)
C(6)	37(7)	29(7)	25(6)	-3(5)	0(5)	8(5)
C(7)	30(6)	22(6)	21(6)	-1(4)	3(5)	5(5)
C(8)	21(6)	30(7)	32(6)	-2(5)	-4(5)	-1(5)
C(9)	34(7)	39(8)	31(7)	-5(5)	3(6)	-9(6)
C(10)	54(9)	22(7)	36(7)	-3(5)	9(6)	-6(6)
C(11)	39(7)	25(7)	31(6)	11(5)	1(6)	4(5)
C(12)	28(6)	23(6)	32(6)	-3(5)	0(5)	-4(5)
C(13)	18(6)	16(6)	34(6)	8(5)	2(5)	4(4)
C(14)	38(8)	55(9)	37(7)	4(6)	-3(6)	5(7)
C(15)	49(9)	48(9)	40(8)	-2(6)	14(7)	-1(7)
C(16)	27(7)	24(7)	62(9)	0(6)	4(6)	-3(5)
C(17)	45(8)	34(7)	34(7)	4(6)	-1(6)	-7(6)
C(18)	25(6)	37(8)	36(7)	-1(5)	1(5)	-2(5)
C(19)	23(6)	29(6)	19(5)	-5(4)	8(5)	4(5)
C(20)	35(7)	25(6)	24(6)	7(5)	0(5)	5(5)
C(21)	32(7)	28(7)	27(6)	1(5)	3(5)	1(5)
C(22)	22(6)	30(6)	18(5)	-3(4)	3(4)	3(5)
C(23)	30(7)	31(7)	27(6)	5(5)	1(5)	12(5)
C(24)	25(6)	29(7)	25(6)	-6(5)	3(5)	4(5)
C(25)	36(8)	36(8)	79(11)	3(7)	15(8)	4(6)
C(26)	46(10)	34(9)	118(16)	1(9)	35(10)	-4(7)
C(27)	37(8)	61(10)	48(9)	-25(7)	5(7)	-9(7)
C(28)	43(9)	69(11)	38(8)	0(7)	6(7)	16(8)
C(29)	39(8)	54(9)	37(7)	15(6)	13(6)	19(7)

C(30)	28(6)	28(7)	33(7)	-3(5)	-7(5)	7(5)
C(31)	52(9)	60(10)	35(8)	-4(7)	-7(7)	-3(8)
C(32)	54(11)	120(17)	43(9)	-31(10)	-13(8)	-7(11)
C(33)	38(9)	70(12)	80(13)	-45(10)	-4(8)	-9(8)
C(34)	41(9)	34(8)	79(12)	-18(7)	3(8)	-5(7)
C(35)	41(8)	39(8)	46(8)	-11(6)	-5(6)	10(6)
C(36)	23(6)	33(7)	22(6)	-2(5)	-9(5)	10(5)
C(37)	30(7)	35(7)	40(7)	10(6)	-2(6)	1(6)
C(38)	31(7)	68(10)	33(7)	7(7)	4(6)	7(7)
C(39)	56(10)	45(9)	77(12)	10(8)	2(9)	-8(8)
C(40)	14(6)	58(10)	71(10)	18(8)	-10(6)	-2(6)
C(41)	140(30)	270(50)	210(40)	-80(30)	-130(30)	60(30)
C(42)	106(17)	55(12)	96(16)	17(12)	30(13)	1(13)
C(43)	160(30)	57(13)	98(17)	9(12)	73(19)	-8(15)
C(44)	280(40)	74(17)	110(20)	0(15)	-50(20)	60(20)
N(1)	25(5)	27(5)	20(5)	4(4)	-4(4)	5(4)
N(2)	24(5)	31(6)	29(5)	8(4)	-6(4)	5(4)
P(1)	24(2)	21(2)	19(1)	2(1)	-2(1)	2(1)
Au(1)	27(1)	24(1)	22(1)	2(1)	-2(1)	4(1)
O(1)	43(5)	37(5)	35(5)	11(4)	1(4)	15(4)
O(2)	137(16)	91(12)	147(16)	35(11)	19(13)	-5(11)
O(3)	210(20)	94(12)	77(11)	23(9)	12(12)	-48(13)

The anisotropic displacement factor exponent takes the form: $-2\pi^2 [h^2 a^{*2} U^{11} + \dots + 2 h k a^* b^* U^{12}]$

Table 4A.3. Bond lengths (Å) and angles (°).

C(1)-C(2)	1.375(15)	C(15)-C(14)-H(14)	119
C(1)-C(6)	1.435(15)	C(13)-C(14)-H(14)	119
C(1)-P(1)	1.778(9)	C(14)-C(15)-C(16)	121.9(13)
C(2)-C(3)	1.389(17)	C(14)-C(15)-H(15)	119.1
C(2)-H(2)	0.95	C(16)-C(15)-H(15)	119.1
C(3)-C(4)	1.371(19)	C(15)-C(16)-C(17)	119.6(12)
C(3)-H(3)	0.95	C(15)-C(16)-H(16)	120.2
C(4)-C(5)	1.368(19)	C(17)-C(16)-H(16)	120.2
C(4)-H(4)	0.95	C(16)-C(17)-C(18)	119.8(12)
C(5)-C(6)	1.395(16)	C(16)-C(17)-H(17)	120.1
C(5)-H(5)	0.95	C(18)-C(17)-H(17)	120.1
C(6)-H(6)	0.95	C(17)-C(18)-C(13)	118.7(11)
C(7)-C(8)	1.395(15)	C(17)-C(18)-H(18)	120.7
C(7)-C(12)	1.408(16)	C(13)-C(18)-H(18)	120.7
C(7)-P(1)	1.807(11)	C(20)-C(19)-Au(1)	109.3(7)
C(8)-C(9)	1.385(17)	C(20)-C(19)-H(19A)	109.8
C(8)-H(8)	0.95	Au(1)-C(19)-H(19A)	109.8
C(9)-C(10)	1.417(18)	C(20)-C(19)-H(19B)	109.8
C(9)-H(9)	0.95	Au(1)-C(19)-H(19B)	109.8
C(10)-C(11)	1.359(18)	H(19A)-C(19)-H(19B)	108.3
C(10)-H(10)	0.95	N(1)-C(20)-C(21)	102.4(9)
C(11)-C(12)	1.363(16)	N(1)-C(20)-C(19)	114.4(9)
C(11)-H(11)	0.95	C(21)-C(20)-C(19)	112.4(9)
C(12)-H(12)	0.95	N(1)-C(20)-H(20)	109.1
C(13)-C(14)	1.351(17)	C(21)-C(20)-H(20)	109.1
C(13)-C(18)	1.438(16)	C(19)-C(20)-H(20)	109.1
C(13)-P(1)	1.812(11)	C(22)-C(21)-C(20)	105.7(9)
C(14)-C(15)	1.348(19)	C(22)-C(21)-H(21A)	110.6
C(14)-H(14)	0.95	C(20)-C(21)-H(21A)	110.6
C(15)-C(16)	1.359(19)	C(22)-C(21)-H(21B)	110.6

C(15)-H(15)	0.95	C(20)-C(21)-H(21B)	110.6
C(16)-C(17)	1.377(18)	H(21A)-C(21)-H(21B)	108.7
C(16)-H(16)	0.95	C(21)-C(22)-C(30)	110.4(9)
C(17)-C(18)	1.405(17)	C(21)-C(22)-C(24)	114.8(10)
C(17)-H(17)	0.95	C(30)-C(22)-C(24)	108.7(9)
C(18)-H(18)	0.95	C(21)-C(22)-C(23)	99.2(9)
C(19)-C(20)	1.551(15)	C(30)-C(22)-C(23)	114.0(10)
C(19)-Au(1)	2.073(11)	C(24)-C(22)-C(23)	109.6(9)
C(19)-H(19A)	0.99	N(1)-C(23)-C(22)	104.6(9)
C(19)-H(19B)	0.99	N(1)-C(23)-H(23A)	110.8
C(20)-N(1)	1.503(13)	C(22)-C(23)-H(23A)	110.8
C(20)-C(21)	1.533(16)	N(1)-C(23)-H(23B)	110.8
C(20)-H(20)	1	C(22)-C(23)-H(23B)	110.8
C(21)-C(22)	1.521(16)	H(23A)-C(23)-H(23B)	108.9
C(21)-H(21A)	0.99	C(29)-C(24)-C(25)	118.0(12)
C(21)-H(21B)	0.99	C(29)-C(24)-C(22)	119.1(11)
C(22)-C(30)	1.533(16)	C(25)-C(24)-C(22)	122.7(11)
C(22)-C(24)	1.538(15)	C(24)-C(25)-C(26)	119.4(14)
C(22)-C(23)	1.549(15)	C(24)-C(25)-H(25)	120.3
C(23)-N(1)	1.459(14)	C(26)-C(25)-H(25)	120.3
C(23)-H(23A)	0.99	C(27)-C(26)-C(25)	121.8(15)
C(23)-H(23B)	0.99	C(27)-C(26)-H(26)	119.1
C(24)-C(29)	1.385(17)	C(25)-C(26)-H(26)	119.1
C(24)-C(25)	1.388(18)	C(26)-C(27)-C(28)	119.6(14)
C(25)-C(26)	1.389(19)	C(26)-C(27)-H(27)	120.2
C(25)-H(25)	0.95	C(28)-C(27)-H(27)	120.2
C(26)-C(27)	1.36(2)	C(27)-C(28)-C(29)	119.6(14)
C(26)-H(26)	0.95	C(27)-C(28)-H(28)	120.2
C(27)-C(28)	1.36(2)	C(29)-C(28)-H(28)	120.2
C(27)-H(27)	0.95	C(24)-C(29)-C(28)	121.4(13)
C(28)-C(29)	1.392(19)	C(24)-C(29)-H(29)	119.3
C(28)-H(28)	0.95	C(28)-C(29)-H(29)	119.3

C(29)-H(29)	0.95	C(31)-C(30)-C(35)	118.6(12)
C(30)-C(31)	1.375(18)	C(31)-C(30)-C(22)	118.1(12)
C(30)-C(35)	1.378(19)	C(35)-C(30)-C(22)	123.3(11)
C(31)-C(32)	1.40(2)	C(30)-C(31)-C(32)	120.3(15)
C(31)-H(31)	0.95	C(30)-C(31)-H(31)	119.8
C(32)-C(33)	1.37(3)	C(32)-C(31)-H(31)	119.8
C(32)-H(32)	0.95	C(33)-C(32)-C(31)	120.7(16)
C(33)-C(34)	1.37(2)	C(33)-C(32)-H(32)	119.7
C(33)-H(33)	0.95	C(31)-C(32)-H(32)	119.7
C(34)-C(35)	1.403(18)	C(32)-C(33)-C(34)	119.7(14)
C(34)-H(34)	0.95	C(32)-C(33)-H(33)	120.1
C(35)-H(35)	0.95	C(34)-C(33)-H(33)	120.1
C(36)-O(1)	1.234(13)	C(33)-C(34)-C(35)	119.6(15)
C(36)-N(1)	1.349(15)	C(33)-C(34)-H(34)	120.2
C(36)-N(2)	1.389(14)	C(35)-C(34)-H(34)	120.2
C(37)-N(2)	1.443(15)	C(30)-C(35)-C(34)	120.9(14)
C(37)-C(39)	1.514(19)	C(30)-C(35)-H(35)	119.5
C(37)-C(40)	1.530(17)	C(34)-C(35)-H(35)	119.5
C(37)-C(38)	1.550(18)	O(1)-C(36)-N(1)	122.4(11)
C(38)-H(38A)	0.98	O(1)-C(36)-N(2)	121.3(11)
C(38)-H(38B)	0.98	N(1)-C(36)-N(2)	116.2(10)
C(38)-H(38C)	0.98	N(2)-C(37)-C(39)	111.1(12)
C(39)-H(39A)	0.98	N(2)-C(37)-C(40)	104.8(10)
C(39)-H(39B)	0.98	C(39)-C(37)-C(40)	108.7(12)
C(39)-H(39C)	0.98	N(2)-C(37)-C(38)	111.0(10)
C(40)-H(40A)	0.98	C(39)-C(37)-C(38)	112.3(12)
C(40)-H(40B)	0.98	C(40)-C(37)-C(38)	108.6(11)
C(40)-H(40C)	0.98	C(37)-C(38)-H(38A)	109.5
C(41)-O(2)	1.40(3)	C(37)-C(38)-H(38B)	109.5
C(41)-H(41A)	0.9809	H(38A)-C(38)-H(38B)	109.5
C(41)-H(41B)	0.9809	C(37)-C(38)-H(38C)	109.5
C(41)-H(41C)	0.9809	H(38A)-C(38)-H(38C)	109.5

C(42)-O(2)	1.38(2)	H(38B)-C(38)-H(38C)	109.5
C(42)-C(43)	1.46(3)	C(37)-C(39)-H(39A)	109.5
C(42)-H(42A)	0.99	C(37)-C(39)-H(39B)	109.5
C(42)-H(42B)	0.99	H(39A)-C(39)-H(39B)	109.5
C(43)-O(3)	1.30(3)	C(37)-C(39)-H(39C)	109.5
C(43)-H(43A)	0.99	H(39A)-C(39)-H(39C)	109.5
C(43)-H(43B)	0.99	H(39B)-C(39)-H(39C)	109.5
C(44)-O(3)	1.44(3)	C(37)-C(40)-H(40A)	109.5
C(44)-H(44A)	0.98	C(37)-C(40)-H(40B)	109.5
C(44)-H(44B)	0.98	H(40A)-C(40)-H(40B)	109.5
C(44)-H(44C)	0.98	C(37)-C(40)-H(40C)	109.5
N(2)-H(2A)	0.88	H(40A)-C(40)-H(40C)	109.5
P(1)-Au(1)	2.293(3)	H(40B)-C(40)-H(40C)	109.5
C(2)-C(1)-C(6)	115.5(9)	O(2)-C(41)-H(41A)	109.7
C(2)-C(1)-P(1)	121.1(8)	O(2)-C(41)-H(41B)	109.5
C(6)-C(1)-P(1)	123.3(8)	H(41A)-C(41)-H(41B)	109.4
C(1)-C(2)-C(3)	123.5(12)	O(2)-C(41)-H(41C)	109.5
C(1)-C(2)-H(2)	118.3	H(41A)-C(41)-H(41C)	109.4
C(3)-C(2)-H(2)	118.3	H(41B)-C(41)-H(41C)	109.4
C(4)-C(3)-C(2)	119.4(13)	O(2)-C(42)-C(43)	113(2)
C(4)-C(3)-H(3)	120.3	O(2)-C(42)-H(42A)	109
C(2)-C(3)-H(3)	120.3	C(43)-C(42)-H(42A)	109
C(5)-C(4)-C(3)	120.4(13)	O(2)-C(42)-H(42B)	109
C(5)-C(4)-H(4)	119.8	C(43)-C(42)-H(42B)	109
C(3)-C(4)-H(4)	119.8	H(42A)-C(42)-H(42B)	107.8
C(4)-C(5)-C(6)	120.1(12)	O(3)-C(43)-C(42)	111(2)
C(4)-C(5)-H(5)	119.9	O(3)-C(43)-H(43A)	109.4
C(6)-C(5)-H(5)	119.9	C(42)-C(43)-H(43A)	109.4
C(5)-C(6)-C(1)	121.0(11)	O(3)-C(43)-H(43B)	109.4
C(5)-C(6)-H(6)	119.5	C(42)-C(43)-H(43B)	109.4
C(1)-C(6)-H(6)	119.5	H(43A)-C(43)-H(43B)	108
C(8)-C(7)-C(12)	118.3(10)	O(3)-C(44)-H(44A)	109.5

C(8)-C(7)-P(1)	118.9(9)	O(3)-C(44)-H(44B)	109.5
C(12)-C(7)-P(1)	122.8(9)	H(44A)-C(44)-H(44B)	109.5
C(9)-C(8)-C(7)	121.2(11)	O(3)-C(44)-H(44C)	109.5
C(9)-C(8)-H(8)	119.4	H(44A)-C(44)-H(44C)	109.5
C(7)-C(8)-H(8)	119.4	H(44B)-C(44)-H(44C)	109.5
C(8)-C(9)-C(10)	118.4(12)	C(36)-N(1)-C(23)	119.9(9)
C(8)-C(9)-H(9)	120.8	C(36)-N(1)-C(20)	124.3(9)
C(10)-C(9)-H(9)	120.8	C(23)-N(1)-C(20)	110.1(9)
C(11)-C(10)-C(9)	120.4(12)	C(36)-N(2)-C(37)	125.1(10)
C(11)-C(10)-H(10)	119.8	C(36)-N(2)-H(2A)	117.4
C(9)-C(10)-H(10)	119.8	C(37)-N(2)-H(2A)	117.4
C(10)-C(11)-C(12)	121.1(11)	C(1)-P(1)-C(7)	107.9(5)
C(10)-C(11)-H(11)	119.5	C(1)-P(1)-C(13)	107.9(5)
C(12)-C(11)-H(11)	119.5	C(7)-P(1)-C(13)	105.0(5)
C(11)-C(12)-C(7)	120.6(11)	C(1)-P(1)-Au(1)	108.9(3)
C(11)-C(12)-H(12)	119.7	C(7)-P(1)-Au(1)	113.2(4)
C(7)-C(12)-H(12)	119.7	C(13)-P(1)-Au(1)	113.7(4)
C(14)-C(13)-C(18)	118.2(11)	C(19)-Au(1)-P(1)	176.1(3)
C(14)-C(13)-P(1)	119.3(10)	C(42)-O(2)-C(41)	107(2)
C(18)-C(13)-P(1)	122.5(9)	C(43)-O(3)-C(44)	111(2)
C(15)-C(14)-C(13)	121.9(13)		

Table 4A.4. Hydrogen coordinates (x 104) and isotropic displacement parameters ($\text{\AA}^2 \times 10^3$).

atom	x	y	z	U(eq)
H(2)	4137	3073	4644	42
H(3)	3170	3427	5759	53
H(4)	2999	2963	6898	56
H(5)	3829	2154	6933	50
H(6)	4938	1807	5838	36
H(8)	3145	1557	3434	34
H(9)	2586	715	3356	42
H(10)	4151	150	4078	45
H(11)	6115	433	4878	38
H(12)	6683	1260	4947	33
H(14)	7718	2030	3175	52
H(15)	10279	2109	3206	54
H(16)	11619	2319	4339	45
H(17)	10348	2439	5499	45
H(18)	7677	2373	5489	39
H(19A)	4065	3014	1819	28
H(19B)	2428	2808	2031	28
H(20)	3823	3650	2822	34
H(21A)	939	3193	3015	34
H(21B)	2061	3420	3688	34
H(23A)	-40	3829	1924	35
H(23B)	660	4374	2028	35
H(25)	-763	3299	3949	60
H(26)	-3257	3331	4346	78
H(27)	-4772	4003	4068	58
H(28)	-3864	4645	3320	60
H(29)	-1359	4631	2929	52
H(31)	1282	4079	4597	59
H(32)	2616	4678	5330	87

H(33)	3743	5335	4713	76
H(34)	3643	5383	3351	62
H(35)	2380	4768	2609	51
H(38A)	4932	3813	-167	66
H(38B)	5763	4324	-340	66
H(38C)	4063	4324	-46	66
H(39A)	5161	4903	1099	89
H(39B)	6820	4831	770	89
H(39C)	6497	4688	1659	89
H(40A)	7386	3824	1499	72
H(40B)	7890	4002	652	72
H(40C)	6844	3524	730	72
H(41A)	3519	1816	1482	313
H(41B)	3108	1263	1725	313
H(41C)	3945	1366	924	313
H(42A)	5900	839	1328	102
H(42B)	4770	738	2022	102
H(43A)	6720	938	2934	124
H(43B)	7092	462	2418	124
H(44A)	9269	1131	3203	232
H(44B)	10364	1053	2486	232
H(44C)	9482	592	2838	232
H(2A)	4914	3708	1675	34

Appendix 4B

Data acquisition details for X-ray crystal structure of piperidine alkylgold complex **4.46**

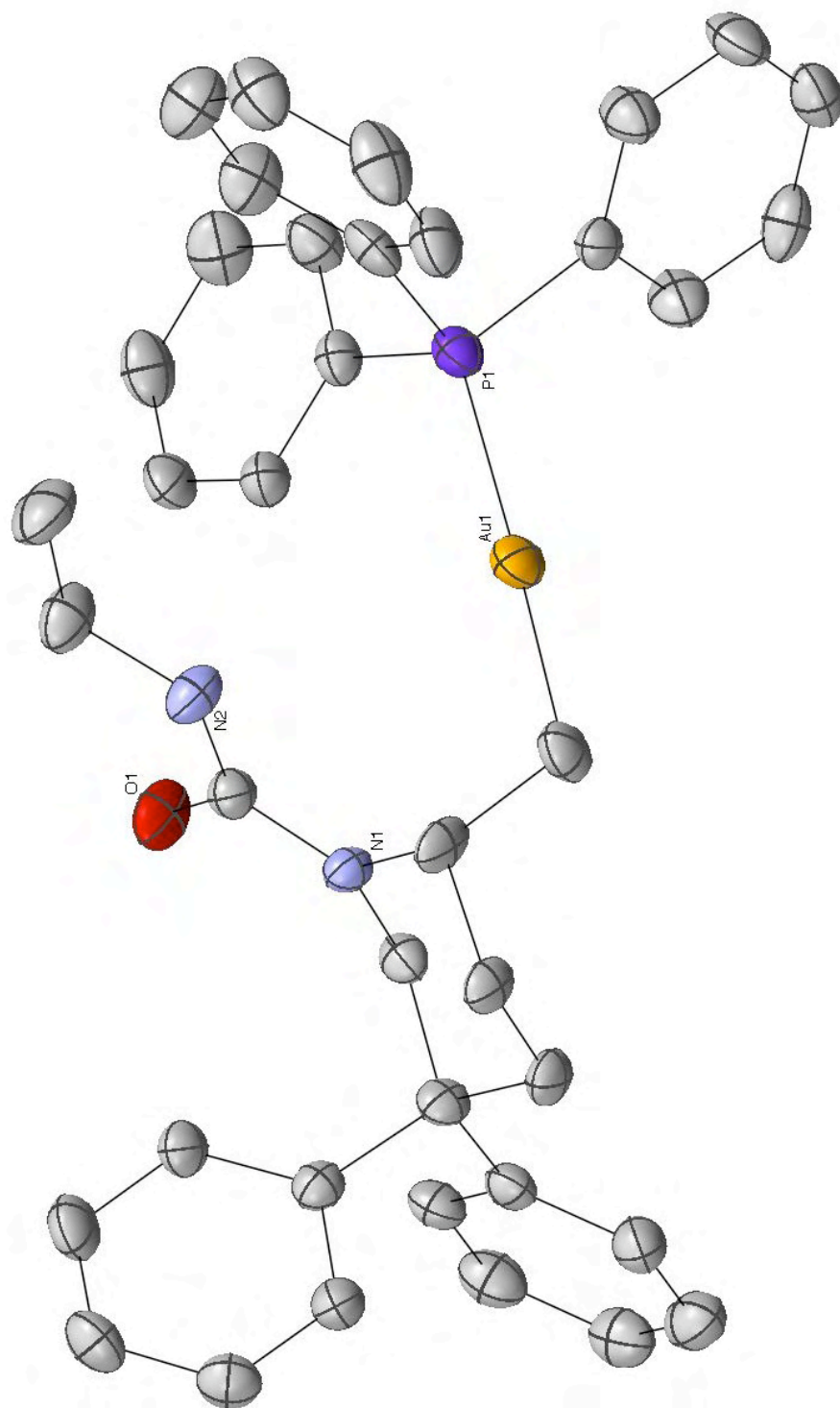


Figure 4B.1. ORTEP of Alkyl gold complex **4.46**. Thermal ellipsoids shown at 50% probability. Hydrogens omitted for clarity.

Experimental

Data Collection

A colorless plate 0.12 x 0.10 x 0.02 mm in size was mounted on a Cryoloop with Paratone oil. Data were collected in a nitrogen gas stream at 139(2) K using phi and omega scans. Crystal-to-detector distance was 60 mm and exposure time was 20 seconds per frame using a scan width of 1.0°. Data collection was 99.4% complete to 25.00° in θ . A total of 15093 reflections were collected covering the indices, $-11 \leq h \leq 11$, $-14 \leq k \leq 15$, $-18 \leq l \leq 17$. 6009 reflections were found to be symmetry independent, with an R_{int} of 0.0569. Indexing and unit cell refinement indicated a primitive, triclinic lattice. The space group was found to be P-1 (No. 2). The data were integrated using the Bruker SAINT software program and scaled using the SADABS software program. Solution by direct methods (SIR-97) produced a complete heavy-atom phasing model consistent with the proposed structure. All non-hydrogen atoms were refined anisotropically by full-matrix least-squares (SHELXL-97). All hydrogen atoms were placed using a riding model. Their positions were constrained relative to their parent atom using the appropriate HFIX command in SHELXL-97.

Crystal Data

Empirical formula	C ₃₉ H ₃₉ Au N ₂ O P	
Formula weight	779.66	
Temperature	139(2) K	
Wavelength	0.71073 Å	
Crystal system	Triclinic	
Space group	P-1	
Unit cell dimensions	a = 9.2568(19) Å	$\alpha = 95.195(3)^\circ$.
	b = 12.331(3) Å	$\beta = 105.262(3)^\circ$.
	c = 15.174(3) Å	$\gamma = 101.577(3)^\circ$.
Volume	1618.1(6) Å ³	
Z	2	
Density (calculated)	1.600 Mg/m ³	
Absorption coefficient	4.630 mm ⁻¹	

F(000)	778
Crystal size	0.12 x 0.10 x 0.02 mm ³
Crystal color/habit	colorless plate
Theta range for data collection	1.71 to 26.15°.
Index ranges	-11<=h<=11, -14<=k<=15, -18<=l<=17
Reflections collected	15093
Independent reflections	6009 [R(int) = 0.0569]
Completeness to theta = 25.00°	99.4 %
Absorption correction	Semi-empirical from equivalents
Max. and min. transmission	0.9131 and 0.6065
Refinement method	Full-matrix least-squares on F ²
Data / restraints / parameters	6009 / 0 / 398
Goodness-of-fit on F ²	0.999
Final R indices [I>2sigma(I)]	R1 = 0.0418, wR2 = 0.0858
R indices (all data)	R1 = 0.0645, wR2 = 0.0971
Largest diff. peak and hole	1.372 and -2.131 e.Å ⁻³

Table 4B.1. Atomic coordinates ($\times 10^4$) and equivalent isotropic displacement parameters ($\text{\AA}^2 \times 10^3$)

atom	x	y	z	U_{eq}^a
C(1)	8225(7)	1157(6)	-1669(5)	35(2)
C(2)	6513(7)	1012(5)	-2144(4)	31(2)
C(3)	6077(7)	505(5)	-3165(4)	27(1)
C(4)	6650(7)	1327(5)	-3746(5)	29(1)
C(5)	6012(6)	2391(5)	-3675(4)	25(1)
C(6)	6520(6)	2874(5)	-2645(4)	25(1)
C(7)	6714(6)	3271(5)	-4212(4)	27(1)
C(8)	7605(7)	3049(6)	-4763(5)	35(2)
C(9)	8195(7)	3851(6)	-5239(5)	40(2)
C(10)	7903(7)	4891(6)	-5155(5)	38(2)
C(11)	7027(7)	5147(6)	-4595(5)	38(2)
C(12)	6423(6)	4330(5)	-4134(4)	30(2)
C(13)	4255(6)	2108(5)	-4102(4)	25(1)
C(14)	3584(7)	1454(5)	-4961(4)	31(2)
C(15)	2012(7)	1170(6)	-5368(5)	35(2)
C(16)	1070(7)	1567(6)	-4912(5)	37(2)
C(17)	1710(7)	2225(6)	-4078(5)	38(2)
C(18)	3287(6)	2509(5)	-3664(5)	29(2)
C(19)	5368(6)	2417(5)	-1423(4)	25(1)
C(20)	4375(8)	2046(5)	-127(5)	38(2)
C(21)	4205(8)	1165(6)	496(5)	47(2)
C(22)	9201(6)	3989(5)	1446(4)	27(1)
C(23)	8063(7)	4288(6)	775(5)	31(2)
C(24)	7586(7)	5253(6)	973(5)	36(2)
C(25)	8215(7)	5920(6)	1801(5)	40(2)
C(26)	9344(7)	5639(6)	2471(5)	42(2)
C(27)	9832(7)	4674(6)	2294(5)	35(2)
C(28)	8947(6)	1736(5)	1887(5)	31(2)
C(29)	8204(8)	2028(6)	2508(5)	40(2)

C(30)	7606(8)	1244(6)	2988(5)	46(2)
C(31)	7773(7)	172(6)	2862(5)	43(2)
C(32)	8504(7)	-137(6)	2236(6)	47(2)
C(33)	9055(7)	625(6)	1736(5)	40(2)
C(34)	11843(6)	3056(5)	1790(4)	25(1)
C(35)	12530(7)	2617(6)	2545(5)	36(2)
C(36)	14108(7)	2952(6)	2945(5)	40(2)
C(37)	14992(7)	3718(6)	2572(5)	35(2)
C(38)	14317(7)	4152(6)	1820(5)	37(2)
C(39)	12745(7)	3817(6)	1423(5)	36(2)
N(1)	5980(5)	2050(4)	-2089(3)	23(1)
N(2)	5105(6)	1711(4)	-808(4)	31(1)
O(1)	5018(5)	3325(4)	-1385(3)	38(1)
P(1)	9775(2)	2700(1)	1215(1)	29(1)
Au(1)	9013(1)	1923(1)	-301(1)	32(1)

^a U(eq) is defined as one third of the trace of the orthogonalized Uij tensor.

Table 4B.2. Anisotropic displacement parameters ($\text{\AA}^2 \times 10^3$).

atom	U¹¹	U²²	U³³	U²³	U¹³	U¹²
C(1)	31(3)	36(4)	37(4)	-2(3)	4(3)	18(3)
C(2)	50(4)	27(4)	28(4)	7(3)	20(3)	25(3)
C(3)	38(3)	21(3)	29(4)	4(3)	15(3)	16(3)
C(4)	33(3)	29(4)	29(4)	1(3)	14(3)	15(3)
C(5)	31(3)	22(3)	25(4)	9(3)	8(3)	11(3)
C(6)	22(3)	27(4)	29(4)	11(3)	8(3)	5(2)
C(7)	21(3)	32(4)	23(4)	4(3)	1(3)	5(3)
C(8)	30(3)	44(4)	35(4)	11(3)	11(3)	13(3)
C(9)	36(4)	50(5)	33(4)	8(4)	12(3)	4(3)
C(10)	33(4)	38(4)	37(5)	10(4)	6(3)	0(3)
C(11)	37(4)	33(4)	39(5)	11(3)	3(3)	7(3)
C(12)	29(3)	31(4)	27(4)	9(3)	3(3)	9(3)
C(13)	30(3)	23(3)	25(4)	6(3)	10(3)	8(3)
C(14)	30(3)	37(4)	26(4)	6(3)	9(3)	11(3)
C(15)	35(4)	34(4)	30(4)	0(3)	4(3)	4(3)
C(16)	25(3)	37(4)	41(5)	4(4)	1(3)	5(3)
C(17)	33(3)	42(4)	47(5)	11(4)	13(3)	21(3)
C(18)	31(3)	29(4)	31(4)	4(3)	10(3)	14(3)
C(19)	27(3)	25(4)	25(4)	4(3)	8(3)	9(3)
C(20)	49(4)	32(4)	46(5)	10(4)	26(3)	19(3)
C(21)	59(5)	54(5)	41(5)	19(4)	31(4)	18(4)
C(22)	25(3)	27(4)	31(4)	5(3)	9(3)	10(3)
C(23)	28(3)	38(4)	30(4)	3(3)	8(3)	13(3)
C(24)	35(4)	44(4)	36(4)	15(4)	11(3)	23(3)
C(25)	35(4)	29(4)	59(5)	7(4)	16(3)	14(3)
C(26)	38(4)	28(4)	52(5)	-10(4)	9(3)	2(3)
C(27)	30(3)	34(4)	35(4)	0(3)	2(3)	9(3)
C(28)	19(3)	32(4)	37(4)	7(3)	-2(3)	6(3)
C(29)	49(4)	26(4)	49(5)	5(3)	19(4)	12(3)

C(30)	51(4)	43(5)	48(5)	6(4)	25(4)	7(4)
C(31)	34(4)	39(4)	57(5)	17(4)	13(3)	6(3)
C(32)	37(4)	31(4)	79(6)	20(4)	17(4)	13(3)
C(33)	33(4)	41(4)	53(5)	13(4)	15(3)	18(3)
C(34)	28(3)	25(3)	25(4)	2(3)	9(3)	11(3)
C(35)	30(3)	42(4)	38(4)	17(3)	9(3)	8(3)
C(36)	31(3)	50(5)	37(4)	18(4)	0(3)	13(3)
C(37)	25(3)	35(4)	42(5)	-3(3)	5(3)	8(3)
C(38)	37(4)	28(4)	54(5)	5(3)	28(3)	5(3)
C(39)	36(4)	40(4)	40(4)	23(4)	15(3)	11(3)
N(1)	30(3)	23(3)	20(3)	4(2)	9(2)	10(2)
N(2)	44(3)	25(3)	30(3)	7(2)	20(2)	11(2)
O(1)	54(3)	27(3)	47(3)	11(2)	26(2)	24(2)
P(1)	27(1)	31(1)	28(1)	6(1)	5(1)	12(1)
Au(1)	34(1)	37(1)	30(1)	7(1)	6(1)	18(1)

The anisotropic displacement factor exponent takes the form:

$$-2\pi^2 [h^2 a^{*2} U^{11} + \dots + 2 h k a^* b^* U^{12}]$$

Table 4B.3. Bond lengths (Å) and angles (°).

C(1)-C(2)	1.524(8)	C(5)-C(6)-H(6A)	109.3
C(1)-Au(1)	2.074(7)	N(1)-C(6)-H(6B)	109.3
C(1)-H(1A)	0.99	C(5)-C(6)-H(6B)	109.3
C(1)-H(1B)	0.99	H(6A)-C(6)-H(6B)	107.9
C(2)-N(1)	1.465(7)	C(8)-C(7)-C(12)	118.1(6)
C(2)-C(3)	1.532(9)	C(8)-C(7)-C(5)	123.0(6)
C(2)-H(2)	1	C(12)-C(7)-C(5)	118.9(5)
C(3)-C(4)	1.509(8)	C(7)-C(8)-C(9)	121.3(7)
C(3)-H(3A)	0.99	C(7)-C(8)-H(8)	119.3
C(3)-H(3B)	0.99	C(9)-C(8)-H(8)	119.3
C(4)-C(5)	1.550(8)	C(10)-C(9)-C(8)	120.0(7)
C(4)-H(4A)	0.99	C(10)-C(9)-H(9)	120
C(4)-H(4B)	0.99	C(8)-C(9)-H(9)	120
C(5)-C(6)	1.534(8)	C(9)-C(10)-C(11)	120.1(6)
C(5)-C(13)	1.538(8)	C(9)-C(10)-H(10)	120
C(5)-C(7)	1.555(8)	C(11)-C(10)-H(10)	120
C(6)-N(1)	1.472(7)	C(10)-C(11)-C(12)	119.3(7)
C(6)-H(6A)	0.99	C(10)-C(11)-H(11)	120.4
C(6)-H(6B)	0.99	C(12)-C(11)-H(11)	120.4
C(7)-C(8)	1.366(9)	C(11)-C(12)-C(7)	121.2(6)
C(7)-C(12)	1.386(8)	C(11)-C(12)-H(12)	119.4
C(8)-C(9)	1.385(9)	C(7)-C(12)-H(12)	119.4
C(8)-H(8)	0.95	C(18)-C(13)-C(14)	117.4(5)
C(9)-C(10)	1.365(10)	C(18)-C(13)-C(5)	122.2(6)
C(9)-H(9)	0.95	C(14)-C(13)-C(5)	120.3(5)
C(10)-C(11)	1.377(10)	C(15)-C(14)-C(13)	122.4(6)
C(10)-H(10)	0.95	C(15)-C(14)-H(14)	118.8
C(11)-C(12)	1.386(8)	C(13)-C(14)-H(14)	118.8
C(11)-H(11)	0.95	C(16)-C(15)-C(14)	119.1(7)
C(12)-H(12)	0.95	C(16)-C(15)-H(15)	120.5

C(13)-C(18)	1.385(8)	C(14)-C(15)-H(15)	120.5
C(13)-C(14)	1.385(9)	C(17)-C(16)-C(15)	119.3(6)
C(14)-C(15)	1.380(8)	C(17)-C(16)-H(16)	120.4
C(14)-H(14)	0.95	C(15)-C(16)-H(16)	120.4
C(15)-C(16)	1.380(9)	C(16)-C(17)-C(18)	121.9(6)
C(15)-H(15)	0.95	C(16)-C(17)-H(17)	119
C(16)-C(17)	1.356(10)	C(18)-C(17)-H(17)	119
C(16)-H(16)	0.95	C(13)-C(18)-C(17)	119.9(6)
C(17)-C(18)	1.386(8)	C(13)-C(18)-H(18)	120.1
C(17)-H(17)	0.95	C(17)-C(18)-H(18)	120.1
C(18)-H(18)	0.95	O(1)-C(19)-N(2)	120.5(6)
C(19)-O(1)	1.227(7)	O(1)-C(19)-N(1)	122.2(5)
C(19)-N(2)	1.366(7)	N(2)-C(19)-N(1)	117.3(5)
C(19)-N(1)	1.367(7)	N(2)-C(20)-C(21)	110.8(5)
C(20)-N(2)	1.448(8)	N(2)-C(20)-H(20A)	109.5
C(20)-C(21)	1.514(8)	C(21)-C(20)-H(20A)	109.5
C(20)-H(20A)	0.99	N(2)-C(20)-H(20B)	109.5
C(20)-H(20B)	0.99	C(21)-C(20)-H(20B)	109.5
C(21)-H(21A)	0.98	H(20A)-C(20)-H(20B)	108.1
C(21)-H(21B)	0.98	C(20)-C(21)-H(21A)	109.5
C(21)-H(21C)	0.98	C(20)-C(21)-H(21B)	109.5
C(22)-C(27)	1.386(9)	H(21A)-C(21)-H(21B)	109.5
C(22)-C(23)	1.394(8)	C(20)-C(21)-H(21C)	109.5
C(22)-P(1)	1.808(6)	H(21A)-C(21)-H(21C)	109.5
C(23)-C(24)	1.384(9)	H(21B)-C(21)-H(21C)	109.5
C(23)-H(23)	0.95	C(27)-C(22)-C(23)	118.8(6)
C(24)-C(25)	1.353(10)	C(27)-C(22)-P(1)	121.3(4)
C(24)-H(24)	0.95	C(23)-C(22)-P(1)	119.9(5)
C(25)-C(26)	1.376(9)	C(24)-C(23)-C(22)	119.4(6)
C(25)-H(25)	0.95	C(24)-C(23)-H(23)	120.3
C(26)-C(27)	1.383(9)	C(22)-C(23)-H(23)	120.3
C(26)-H(26)	0.95	C(25)-C(24)-C(23)	121.3(6)

C(27)-H(27)	0.95	C(25)-C(24)-H(24)	119.3
C(28)-C(29)	1.368(9)	C(23)-C(24)-H(24)	119.3
C(28)-C(33)	1.397(9)	C(24)-C(25)-C(26)	120.0(6)
C(28)-P(1)	1.818(6)	C(24)-C(25)-H(25)	120
C(29)-C(30)	1.376(9)	C(26)-C(25)-H(25)	120
C(29)-H(29)	0.95	C(25)-C(26)-C(27)	119.8(7)
C(30)-C(31)	1.363(10)	C(25)-C(26)-H(26)	120.1
C(30)-H(30)	0.95	C(27)-C(26)-H(26)	120.1
C(31)-C(32)	1.373(11)	C(26)-C(27)-C(22)	120.6(6)
C(31)-H(31)	0.95	C(26)-C(27)-H(27)	119.7
C(32)-C(33)	1.362(9)	C(22)-C(27)-H(27)	119.7
C(32)-H(32)	0.95	C(29)-C(28)-C(33)	118.6(6)
C(33)-H(33)	0.95	C(29)-C(28)-P(1)	124.1(5)
C(34)-C(35)	1.371(8)	C(33)-C(28)-P(1)	117.2(5)
C(34)-C(39)	1.383(8)	C(28)-C(29)-C(30)	120.4(7)
C(34)-P(1)	1.825(6)	C(28)-C(29)-H(29)	119.8
C(35)-C(36)	1.385(8)	C(30)-C(29)-H(29)	119.8
C(35)-H(35)	0.95	C(31)-C(30)-C(29)	120.4(7)
C(36)-C(37)	1.383(9)	C(31)-C(30)-H(30)	119.8
C(36)-H(36)	0.95	C(29)-C(30)-H(30)	119.8
C(37)-C(38)	1.360(9)	C(30)-C(31)-C(32)	119.9(7)
C(37)-H(37)	0.95	C(30)-C(31)-H(31)	120
C(38)-C(39)	1.379(8)	C(32)-C(31)-H(31)	120
C(38)-H(38)	0.95	C(33)-C(32)-C(31)	120.0(7)
C(39)-H(39)	0.95	C(33)-C(32)-H(32)	120
P(1)-Au(1)	2.2770(19)	C(31)-C(32)-H(32)	120
C(2)-C(1)-Au(1)	116.2(4)	C(32)-C(33)-C(28)	120.5(7)
C(2)-C(1)-H(1A)	108.2	C(32)-C(33)-H(33)	119.7
Au(1)-C(1)-H(1A)	108.2	C(28)-C(33)-H(33)	119.7
C(2)-C(1)-H(1B)	108.2	C(35)-C(34)-C(39)	119.3(5)
Au(1)-C(1)-H(1B)	108.2	C(35)-C(34)-P(1)	124.1(4)
H(1A)-C(1)-H(1B)	107.4	C(39)-C(34)-P(1)	116.6(4)

N(1)-C(2)-C(1)	114.0(5)	C(34)-C(35)-C(36)	120.0(6)
N(1)-C(2)-C(3)	108.1(5)	C(34)-C(35)-H(35)	120
C(1)-C(2)-C(3)	111.8(5)	C(36)-C(35)-H(35)	120
N(1)-C(2)-H(2)	107.6	C(37)-C(36)-C(35)	119.9(6)
C(1)-C(2)-H(2)	107.6	C(37)-C(36)-H(36)	120.1
C(3)-C(2)-H(2)	107.6	C(35)-C(36)-H(36)	120.1
C(4)-C(3)-C(2)	112.4(5)	C(38)-C(37)-C(36)	120.3(6)
C(4)-C(3)-H(3A)	109.1	C(38)-C(37)-H(37)	119.9
C(2)-C(3)-H(3A)	109.1	C(36)-C(37)-H(37)	119.9
C(4)-C(3)-H(3B)	109.1	C(37)-C(38)-C(39)	119.8(6)
C(2)-C(3)-H(3B)	109.1	C(37)-C(38)-H(38)	120.1
H(3A)-C(3)-H(3B)	107.9	C(39)-C(38)-H(38)	120.1
C(3)-C(4)-C(5)	111.2(5)	C(38)-C(39)-C(34)	120.7(6)
C(3)-C(4)-H(4A)	109.4	C(38)-C(39)-H(39)	119.6
C(5)-C(4)-H(4A)	109.4	C(34)-C(39)-H(39)	119.6
C(3)-C(4)-H(4B)	109.4	C(19)-N(1)-C(2)	125.3(5)
C(5)-C(4)-H(4B)	109.4	C(19)-N(1)-C(6)	117.3(5)
H(4A)-C(4)-H(4B)	108	C(2)-N(1)-C(6)	115.4(5)
C(6)-C(5)-C(13)	113.0(5)	C(19)-N(2)-C(20)	118.7(5)
C(6)-C(5)-C(4)	106.0(4)	C(22)-P(1)-C(28)	105.9(3)
C(13)-C(5)-C(4)	110.8(5)	C(22)-P(1)-C(34)	103.5(3)
C(6)-C(5)-C(7)	109.1(5)	C(28)-P(1)-C(34)	105.0(3)
C(13)-C(5)-C(7)	107.2(4)	C(22)-P(1)-Au(1)	114.8(2)
C(4)-C(5)-C(7)	110.7(5)	C(28)-P(1)-Au(1)	110.0(2)
N(1)-C(6)-C(5)	111.7(5)	C(34)-P(1)-Au(1)	116.5(2)
N(1)-C(6)-H(6A)	109.3	C(1)-Au(1)-P(1)	177.00(19)

Table 4B.4. Hydrogen coordinates (x 10⁴) and isotropic displacement parameters (Å² x 10³).

atom	x	y	z	U(eq)
H(1A)	8813	1602	-2026	42
H(1B)	8461	409	-1698	42
H(2)	5932	477	-1831	37
H(3A)	6516	-159	-3219	32
H(3B)	4943	251	-3406	32
H(4A)	6325	966	-4399	34
H(4B)	7789	1541	-3536	34
H(6A)	7658	3110	-2426	30
H(6B)	6106	3543	-2558	30
H(8)	7824	2330	-4821	42
H(9)	8804	3677	-5623	48
H(10)	8304	5440	-5484	46
H(11)	6839	5874	-4524	45
H(12)	5798	4499	-3759	35
H(14)	4230	1191	-5282	37
H(15)	1584	708	-5953	42
H(16)	-15	1382	-5181	44
H(17)	1058	2498	-3767	46
H(18)	3704	2978	-3082	35
H(20A)	3347	2158	-444	46
H(20B)	5003	2766	251	46
H(21A)	3626	444	119	70
H(21B)	3653	1385	926	70
H(21C)	5228	1096	846	70
H(23)	7619	3835	187	38
H(24)	6801	5452	517	43
H(25)	7877	6582	1921	48
H(26)	9787	6107	3053	50
H(27)	10607	4480	2758	42

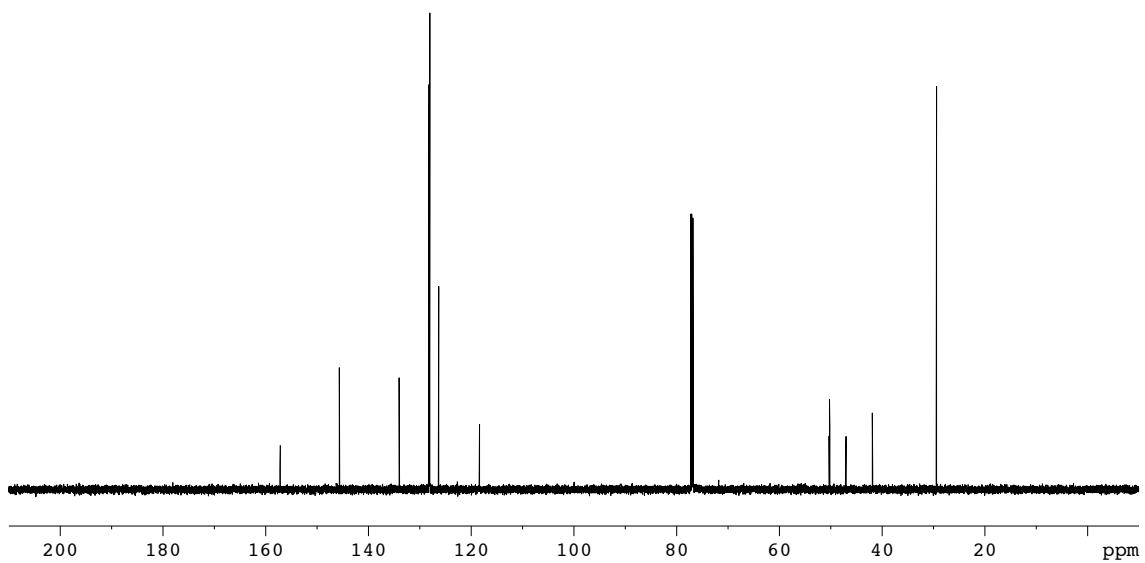
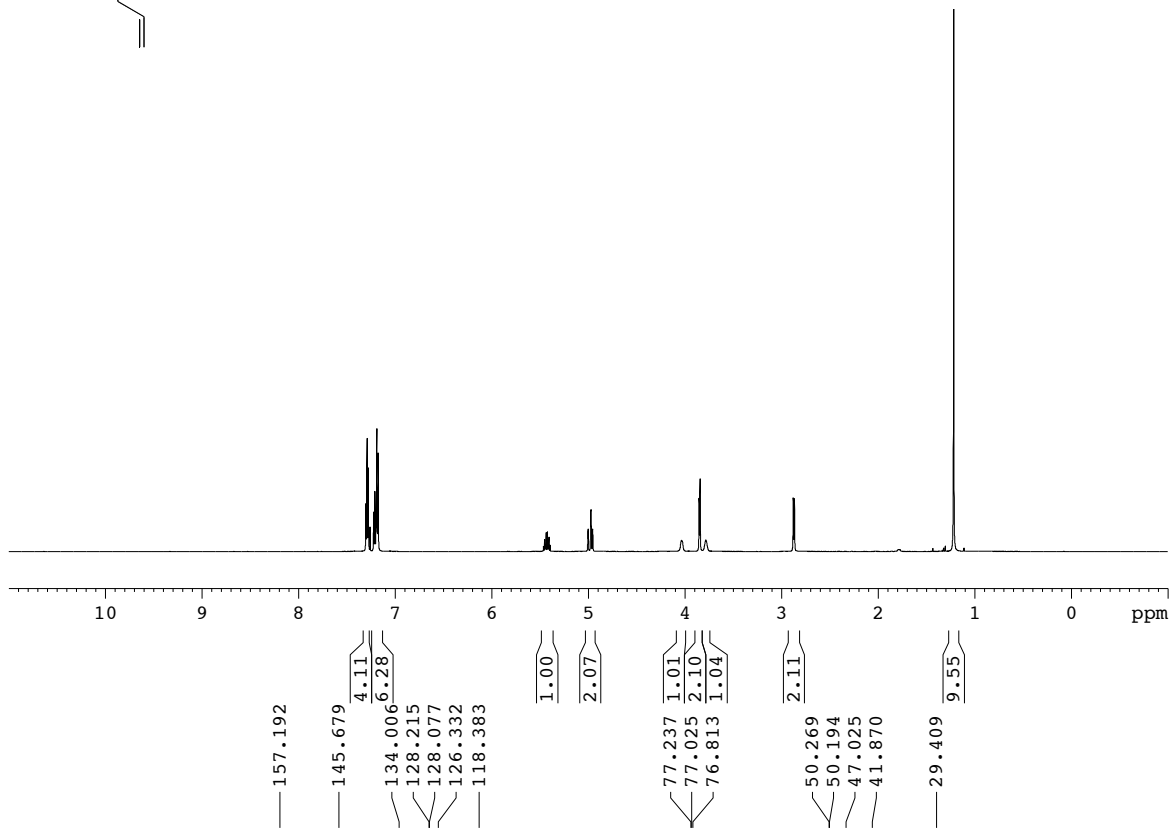
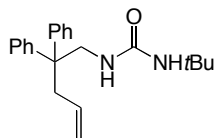
H(29)	8099	2776	2609	48
H(30)	7074	1451	3409	55
H(31)	7383	-360	3208	52
H(32)	8626	-883	2150	57
H(33)	9517	398	1283	48
H(35)	11923	2082	2795	43
H(36)	14582	2657	3475	48
H(37)	16076	3942	2842	42
H(38)	14926	4683	1569	45
H(39)	12278	4112	891	44

Appendix 4C

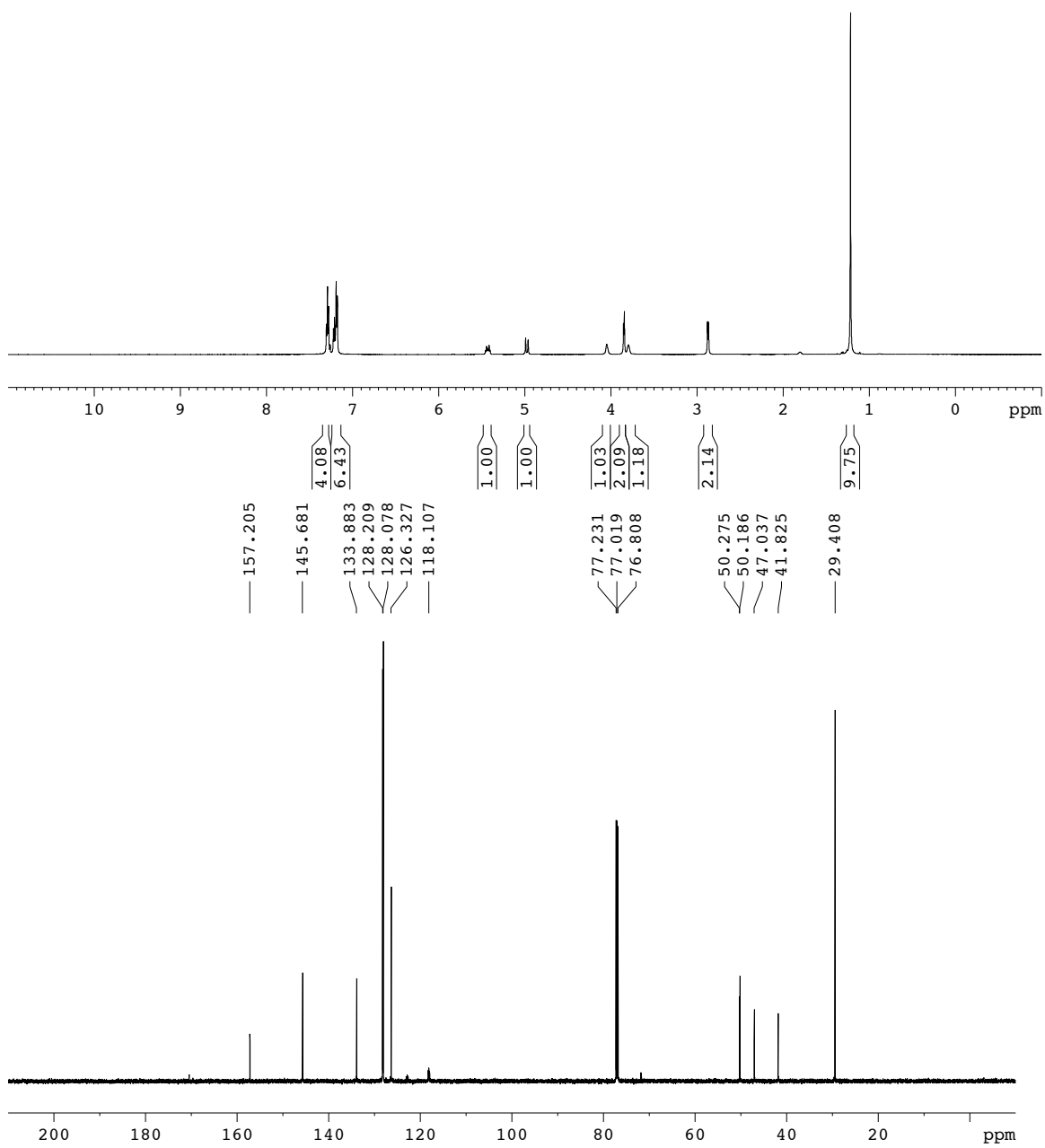
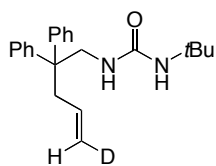
Copies of ^1H and ^{13}C NMR characterization data are included for compounds **4.31, 4.36, 4.39, 4.63, 4.64.**

Copies of ^1H , ^{31}P , and ^{13}C NMR characterization data are included for compounds **4.32, 4.43, 4.46, 4.57, 4.58.**

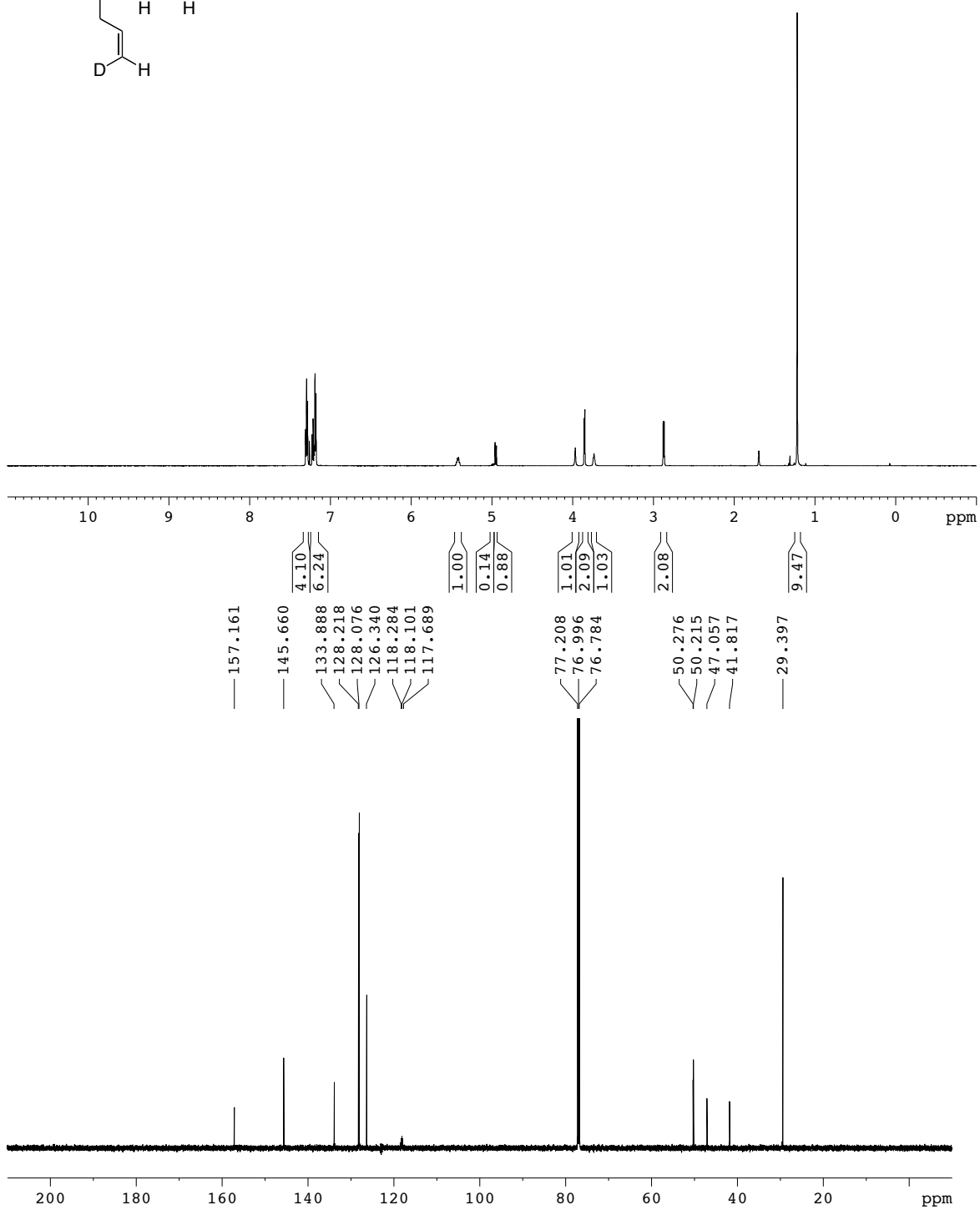
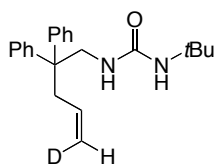
4.31



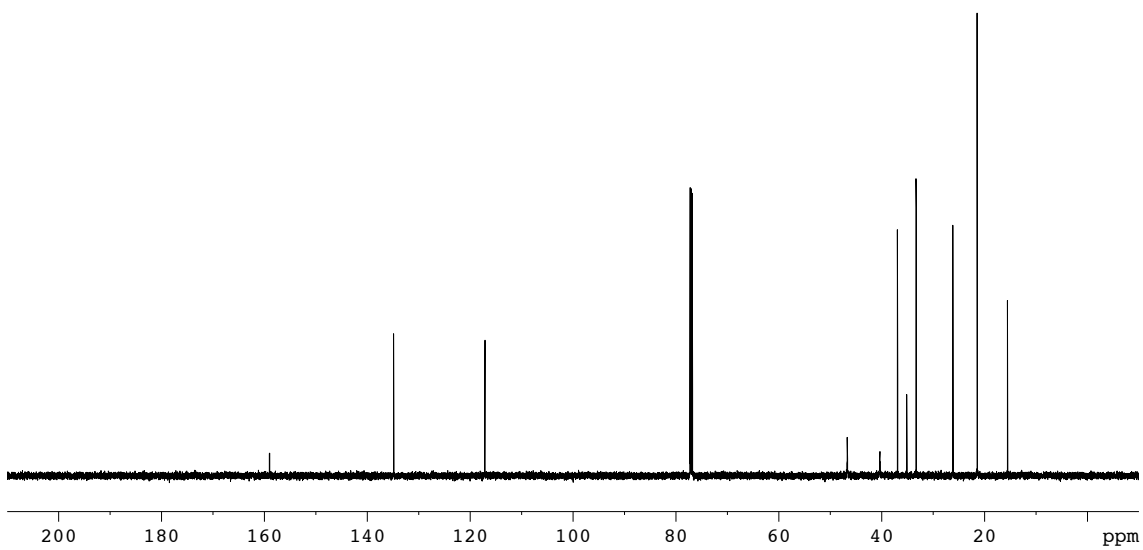
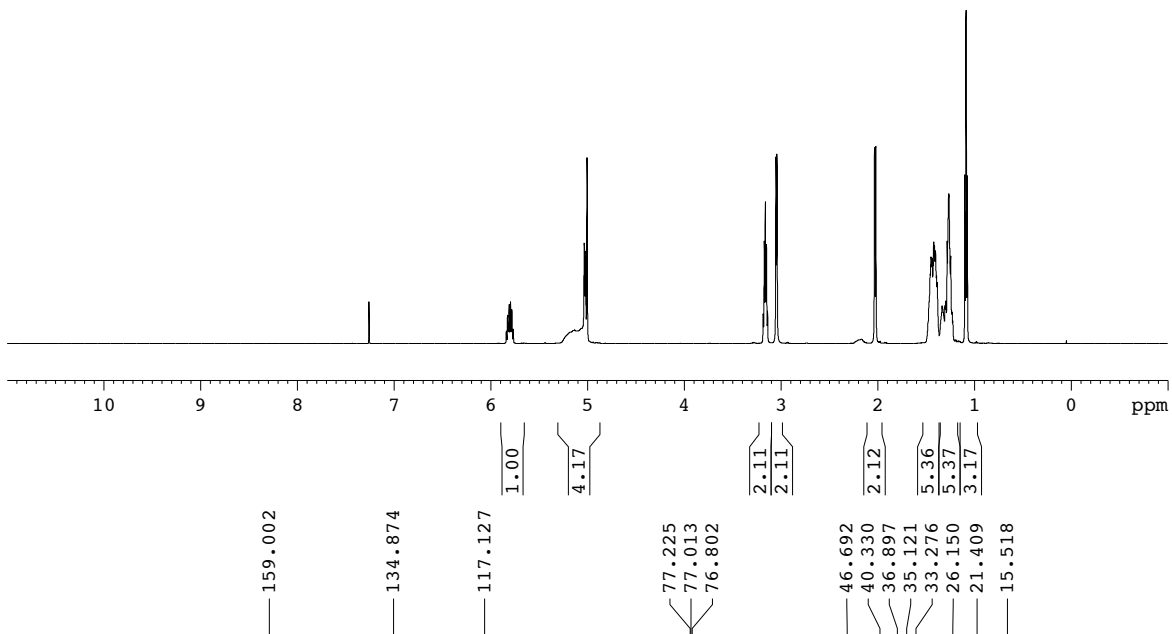
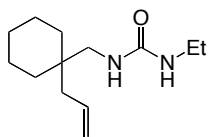
4.63



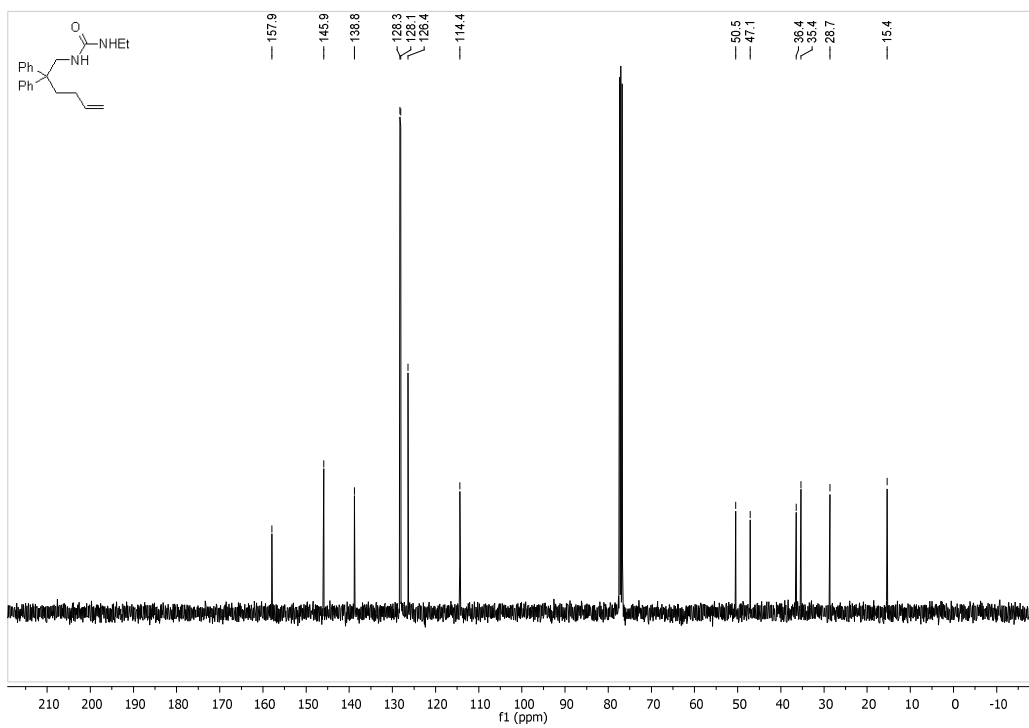
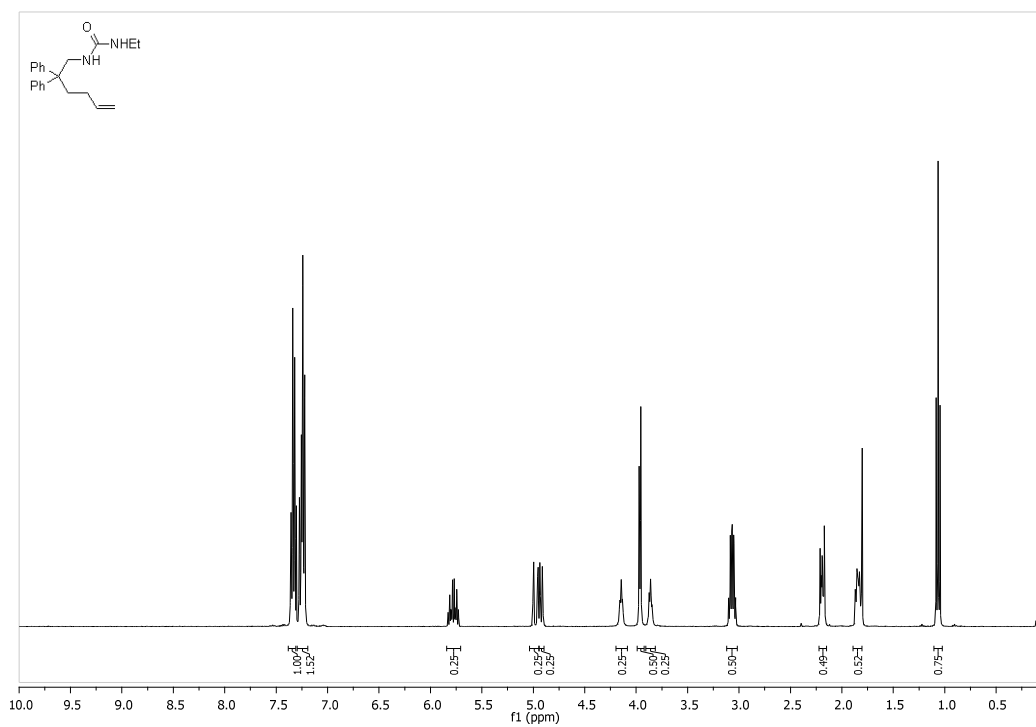
4.64



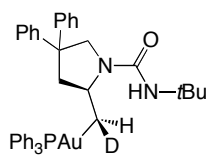
4.36



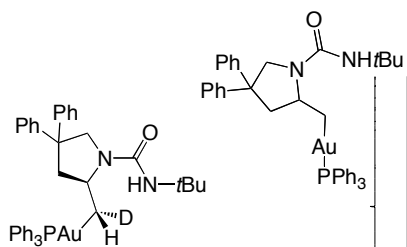
4.39



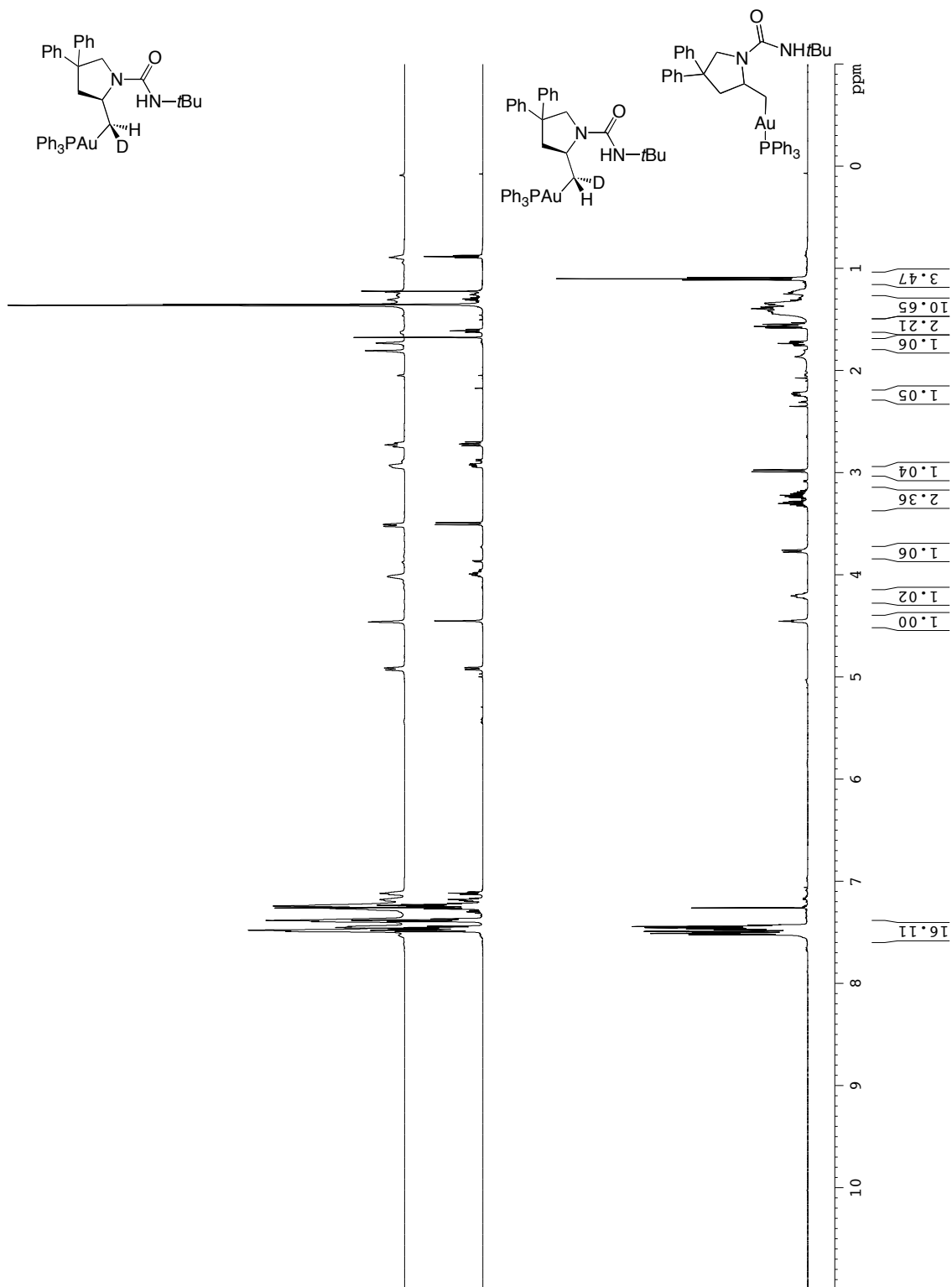
4.66



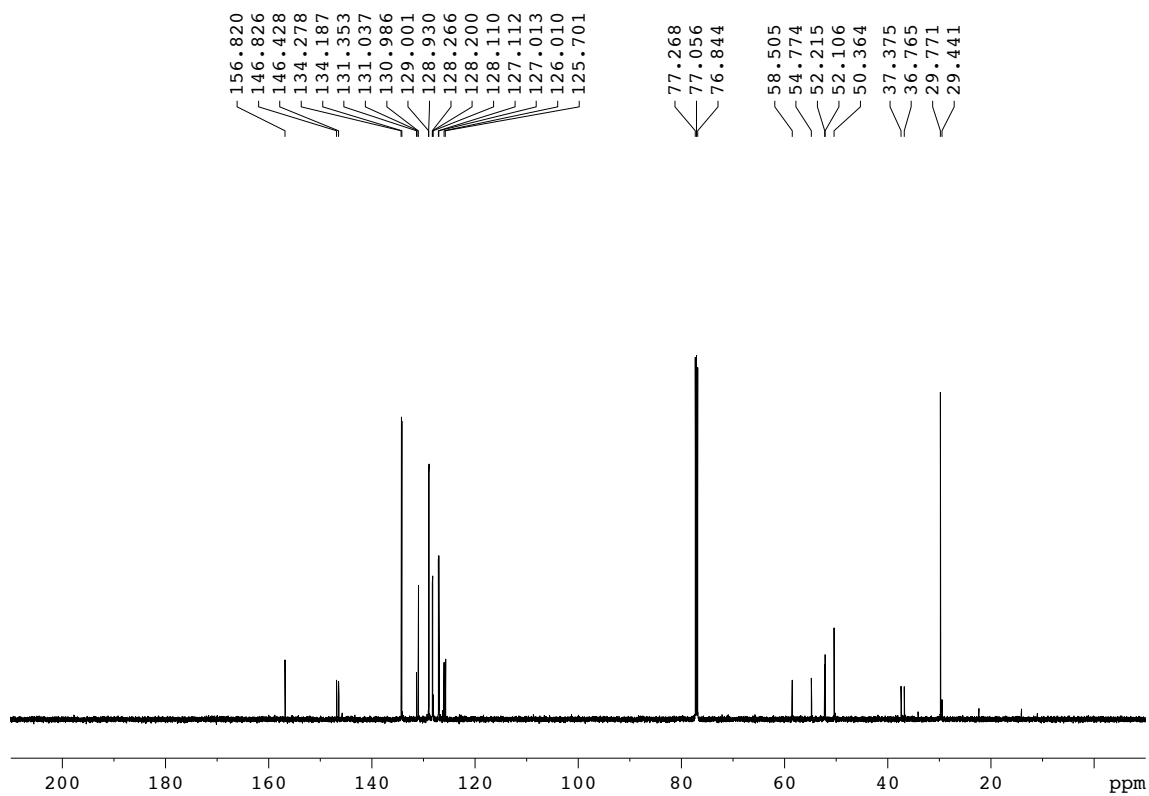
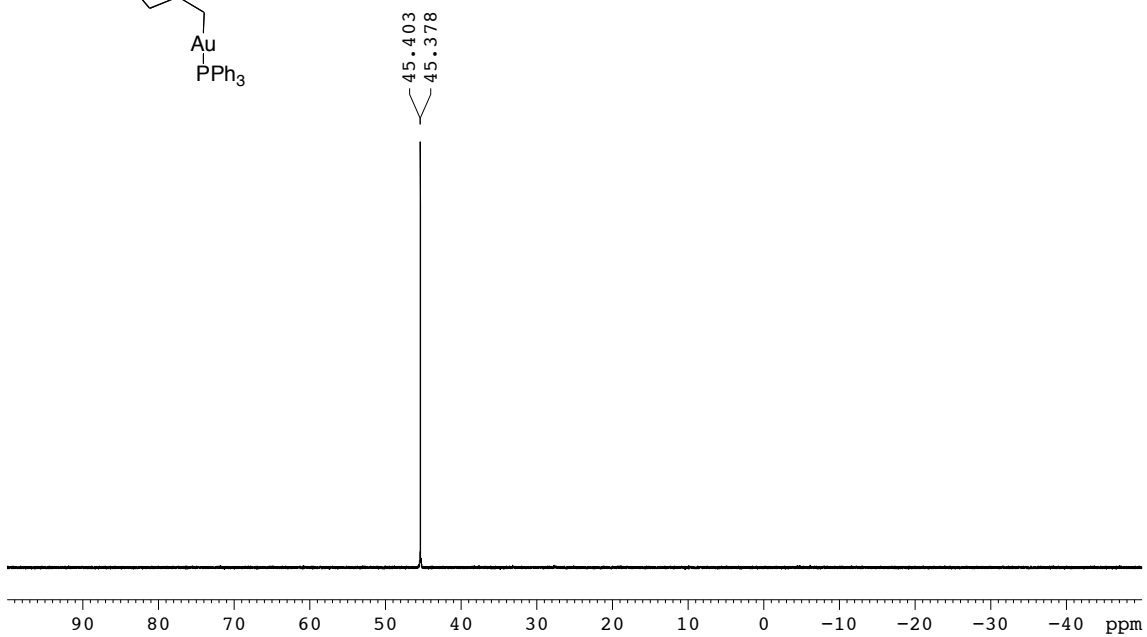
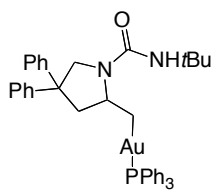
4.65



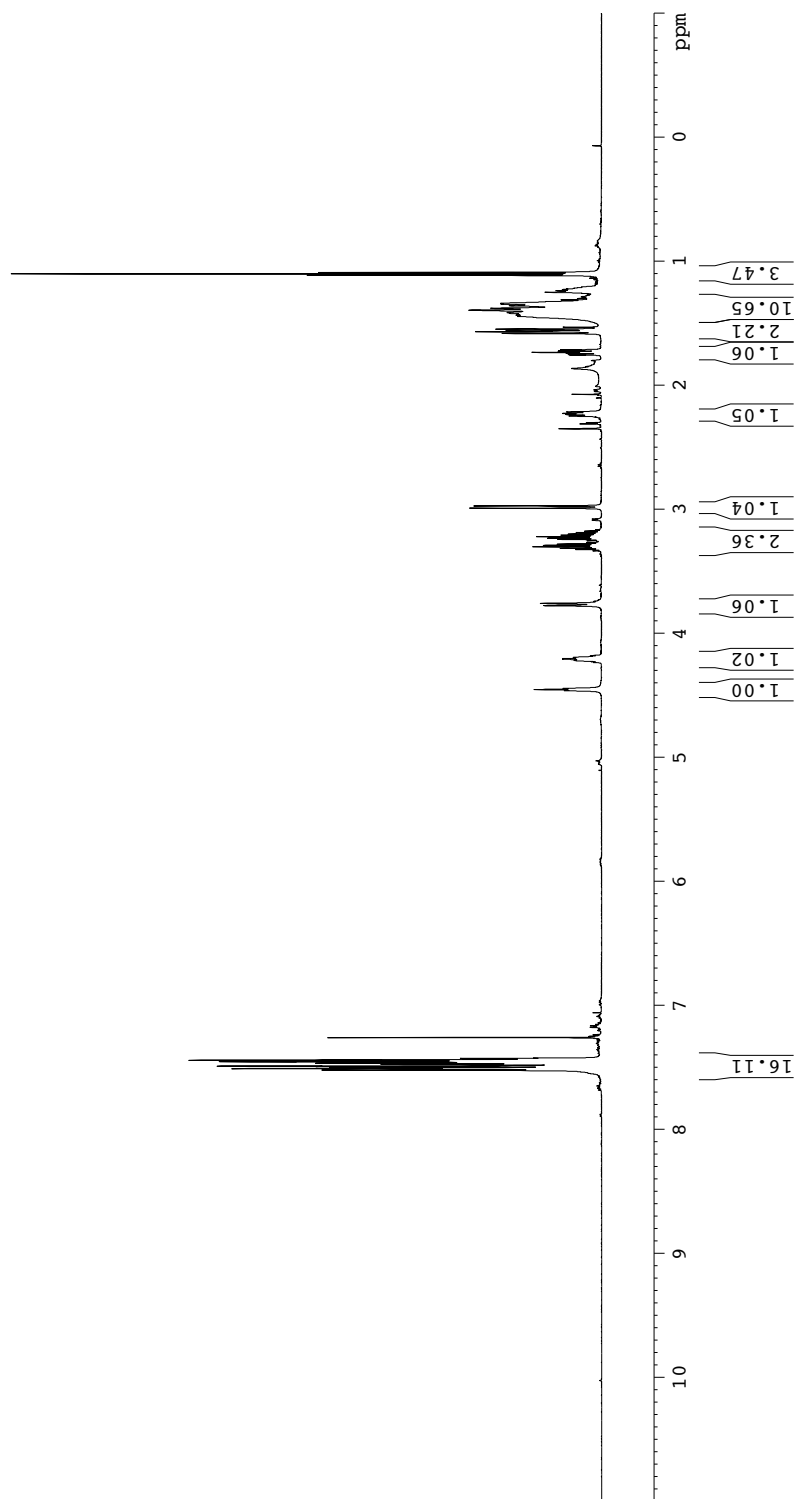
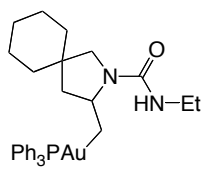
4.32



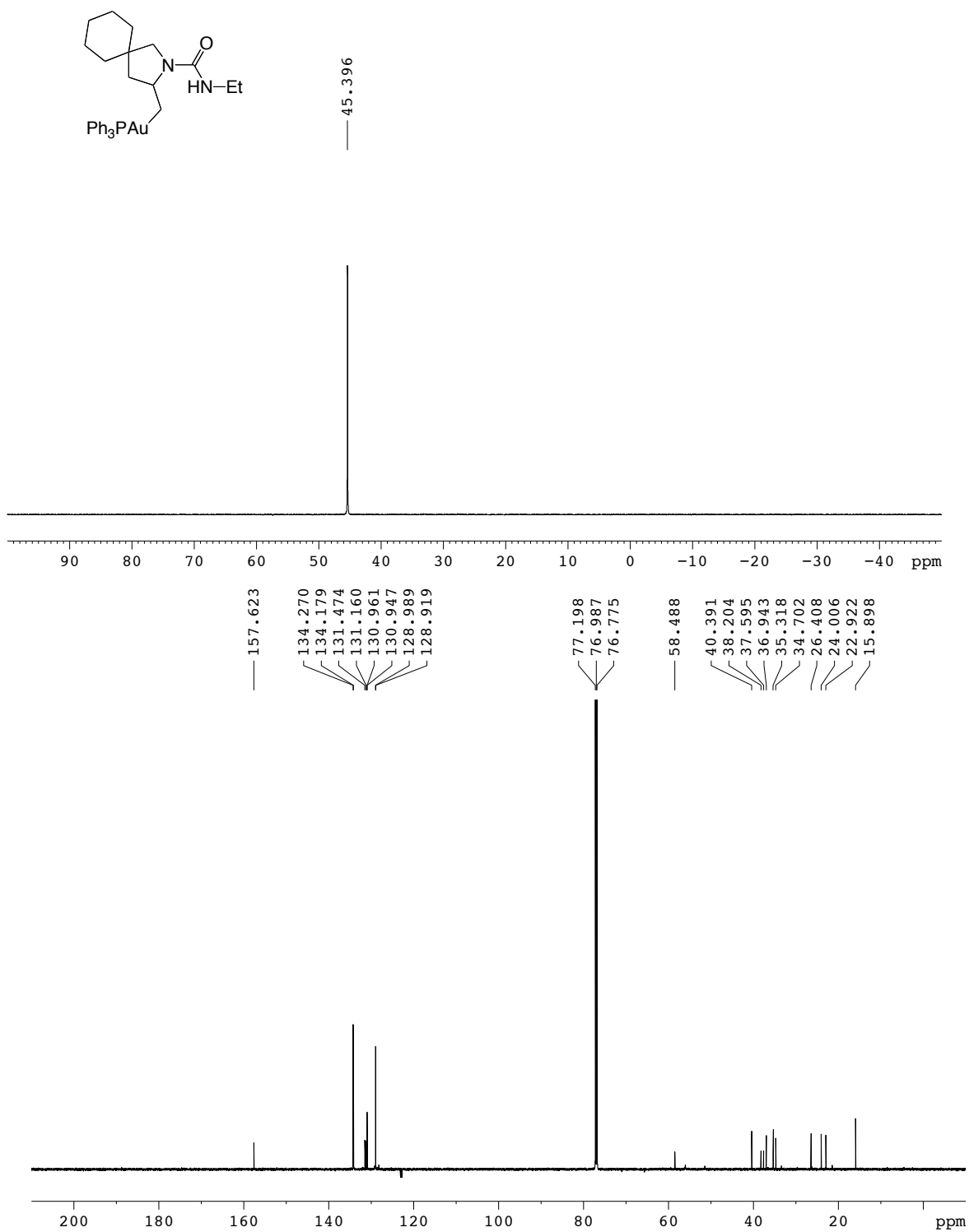
4.32



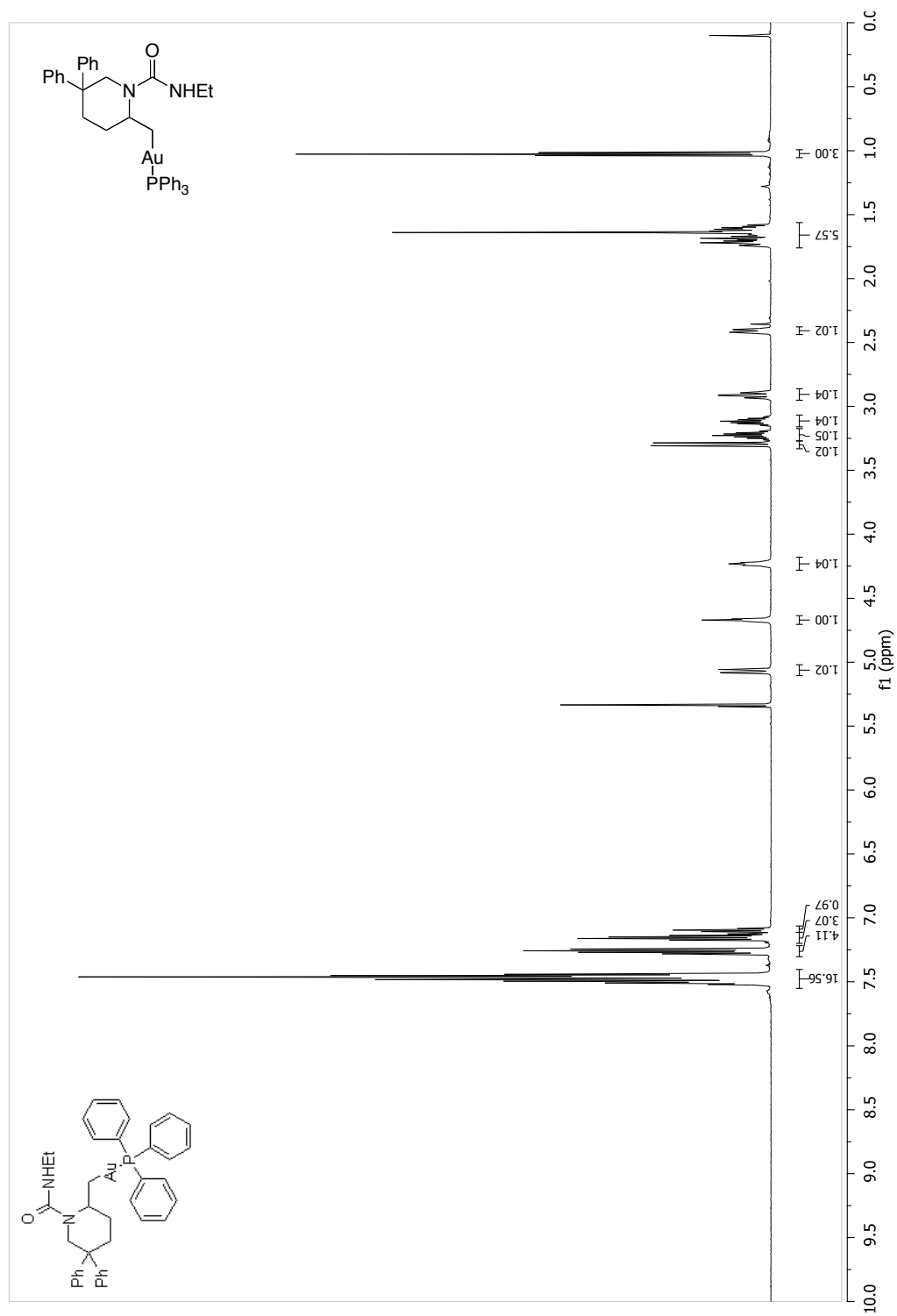
4.43



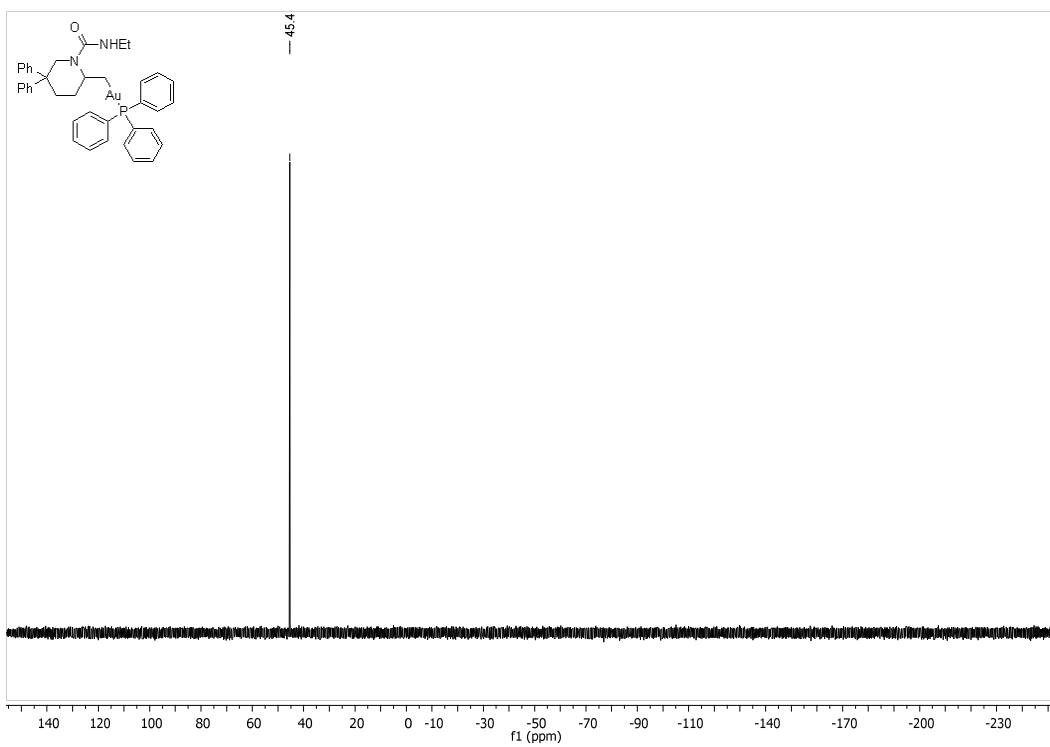
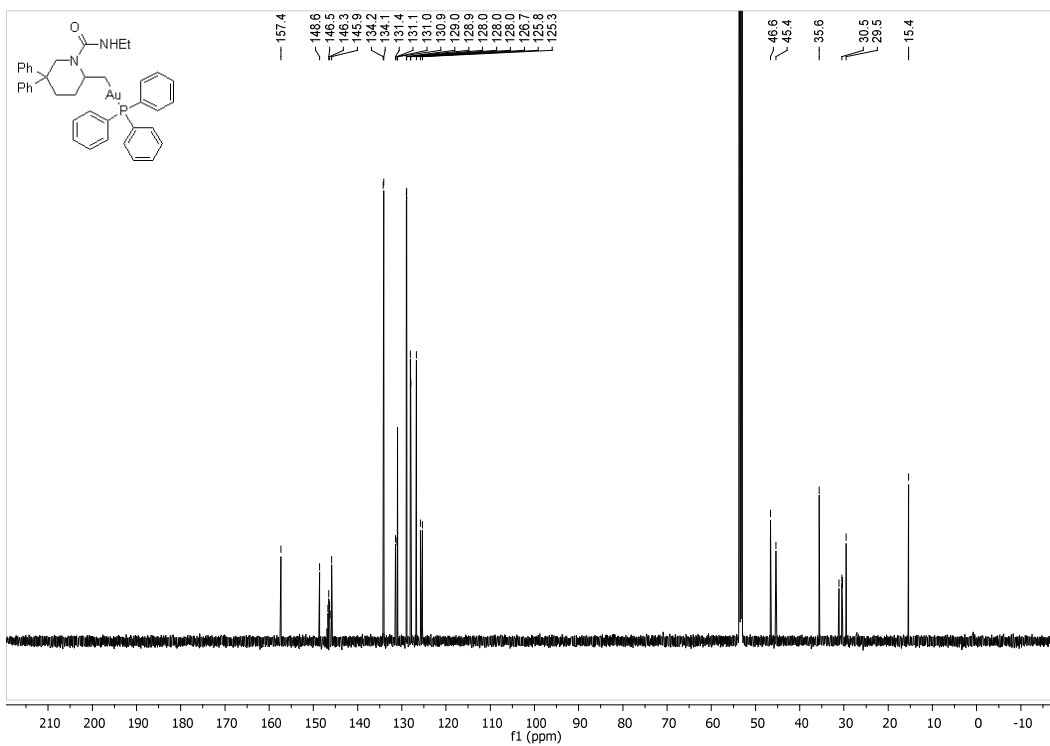
4.43



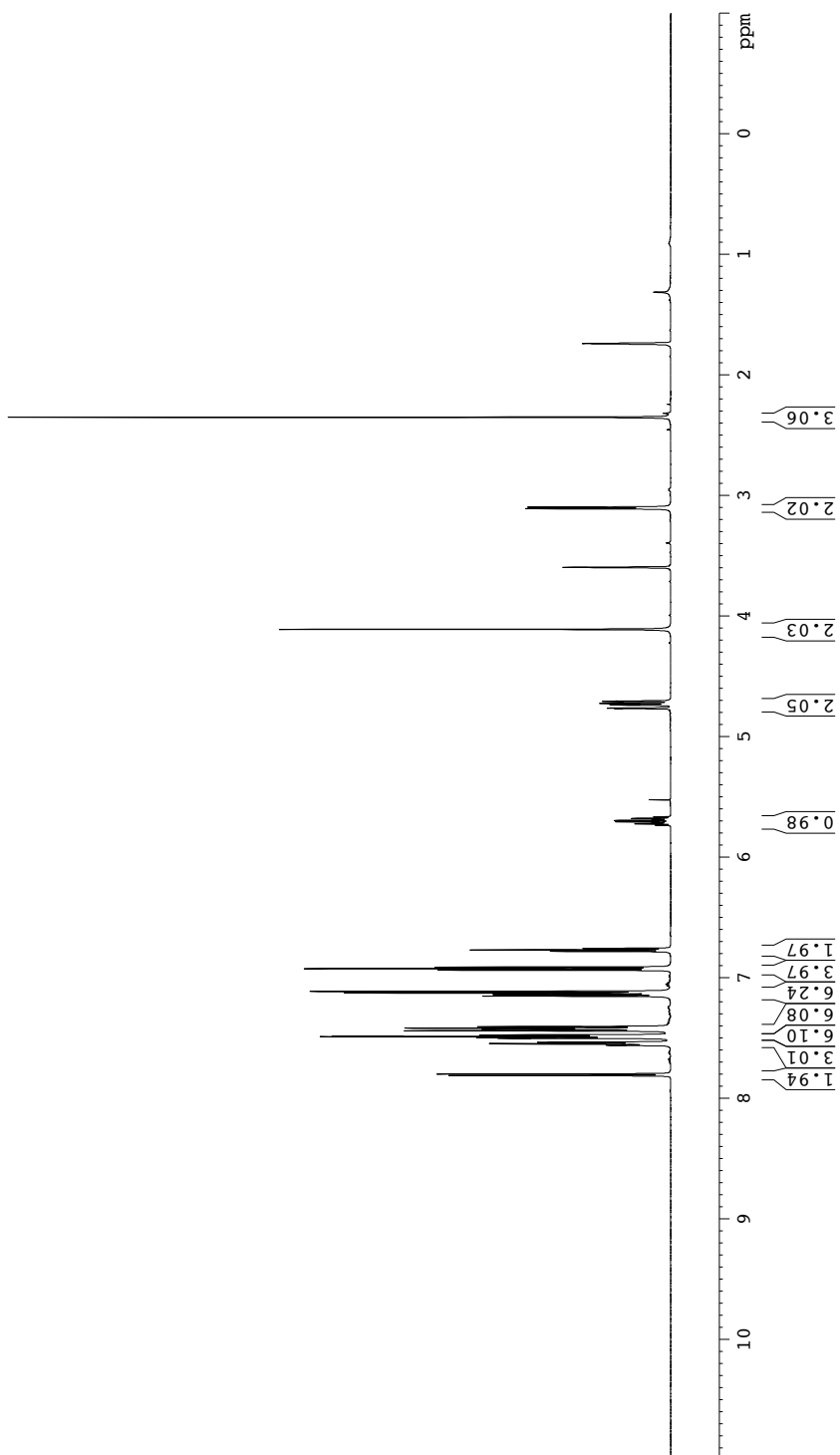
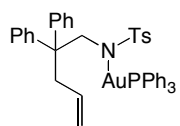
4.46



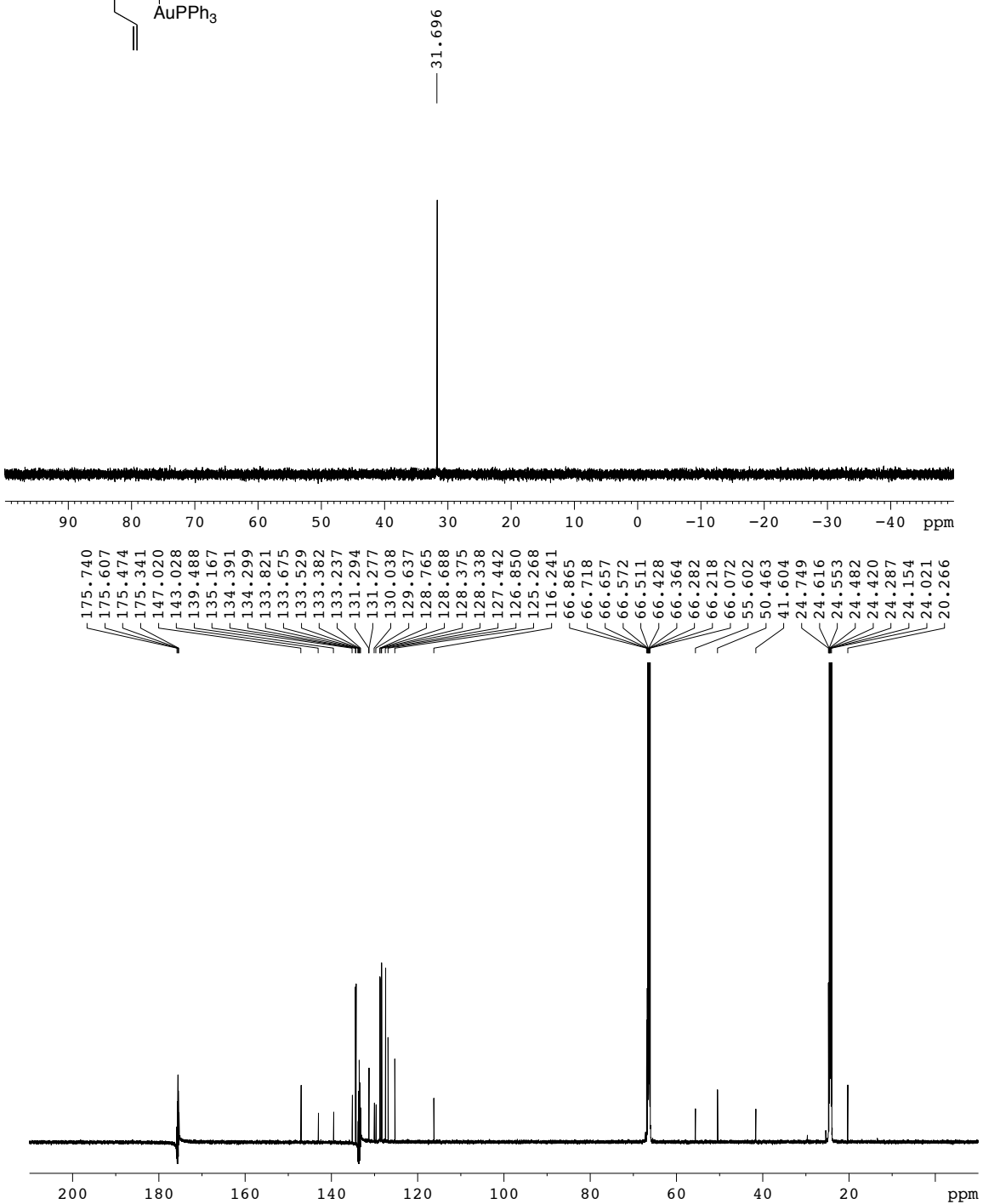
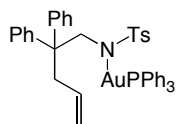
4.46



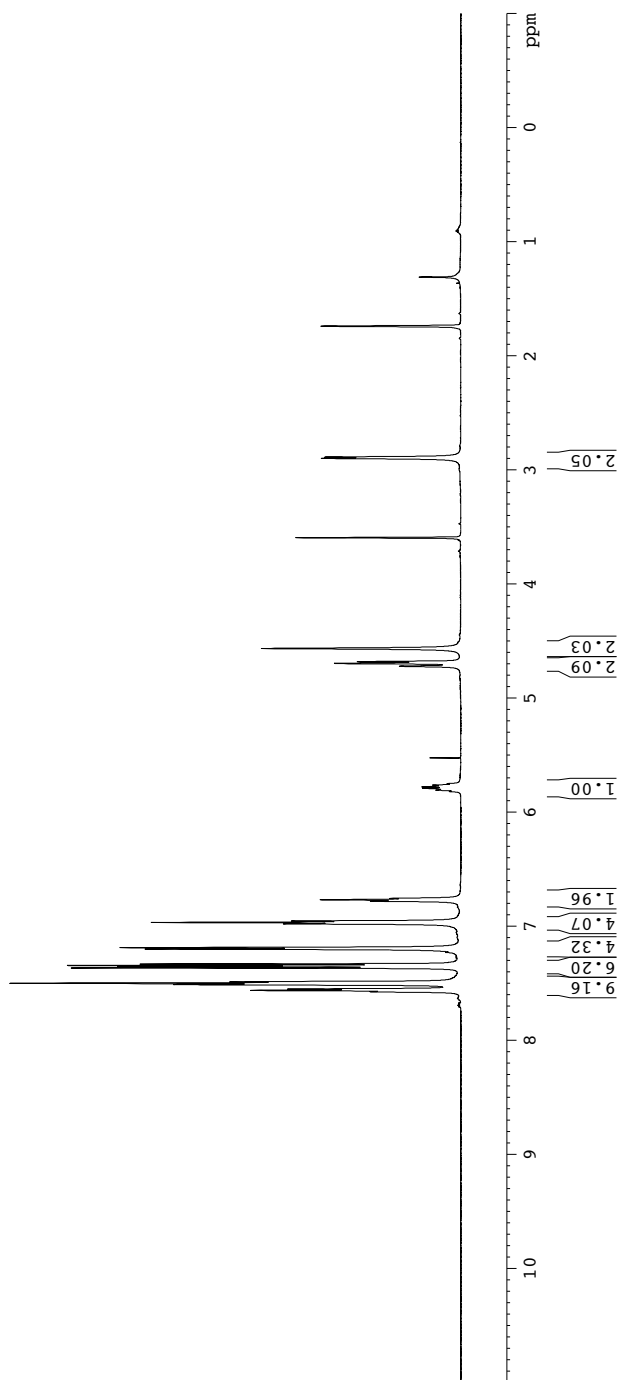
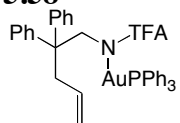
5.57



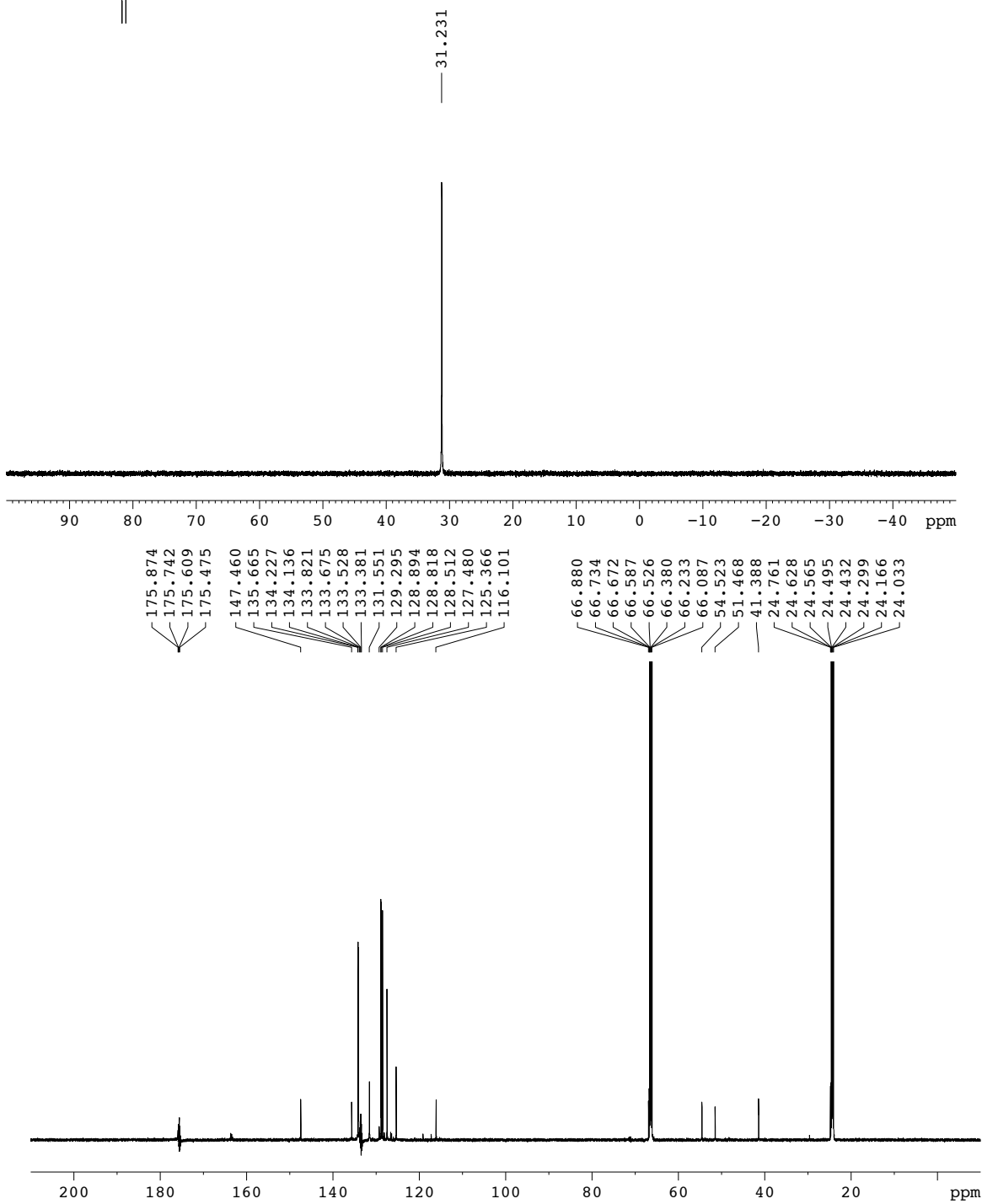
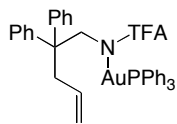
5.57



5.58



5.58



Chapter 5

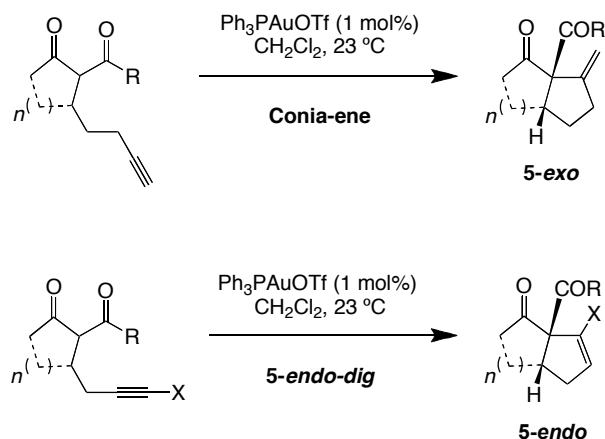
Gold(I)-Catalyzed Addition of Carbon Nucleophiles to Allenes

The nucleophilic addition of silyl enol ethers to allenes has been published (Staben, S. T.; Kennedy-Smith, J. J.; Huang, D.; Corkey, B. K.; LaLonde, R. L.; Toste, F. D. “Gold(I)-Catalyzed Cyclizations of Silyl Enol Ethers: Application to the Synthesis of (+)-Lycopladine A” *Angew. Chem., Int. Ed. Engl.* **2006**, *45*, 5991-5994), and has been described here in greater detail.¹ The remainder of the *5-endo-trig* substrates and *5-endo/exo-trig* reaction has not been previously reported.

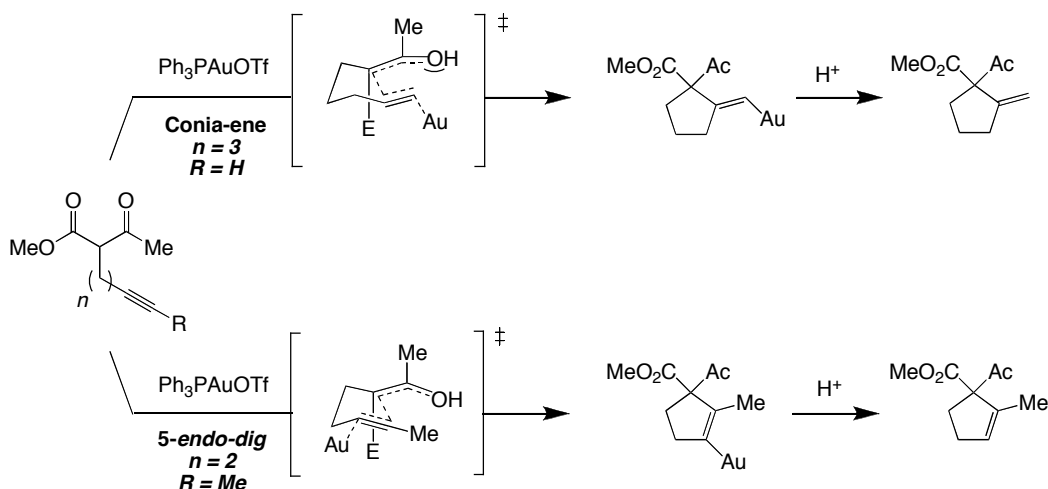
¹ Joshua Kennedy-Smith performed the initial silyl enol ether cyclization in the synthesis of sieboldine A. Steve Staben carried out the reaction of **5.24**. I was responsible for the reaction of **5.24**, including the re-optimization of conditions.

Introduction

As discussed in the previous chapters, gold(I) has been used with great success to catalyze the formation of carbon-heteroatom bonds. However, before 2005, examples of gold(I)-catalyzed carbon-carbon bond formation remained comparatively rare. Two such reactions were published by our group: gold(I)-catalyzed Conia-ene¹ and 5-*endo-dig*² cycloisomerization of acetylenic dicarbonyl compounds (Scheme 5.1). The proposed mechanism for these reactions begins by complexation of the cationic gold(I) catalyst to the alkyne (Scheme 5.2). The enol tautomer of the β -ketoester then adds to the alkyne in either a 5-*exo-dig* or a 5-*endo-dig* manner. Protonolysis of the resulting vinylgold(I) species releases the observed cyclopentenones and regenerates the gold(I)-catalyst. These transformations were some of the first demonstrations of the utility of gold(I)-catalysts to form quaternary centers under mild conditions.

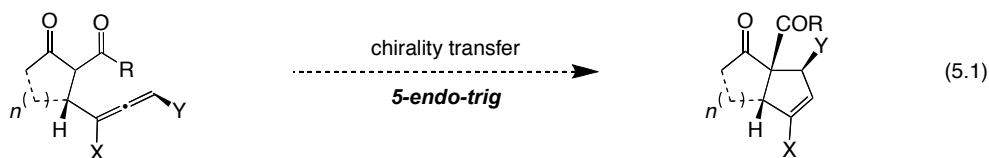


Scheme 5.1. Gold(I)-Catalyzed Conia-Ene and 5-*Endo-dig* Cyclizations.

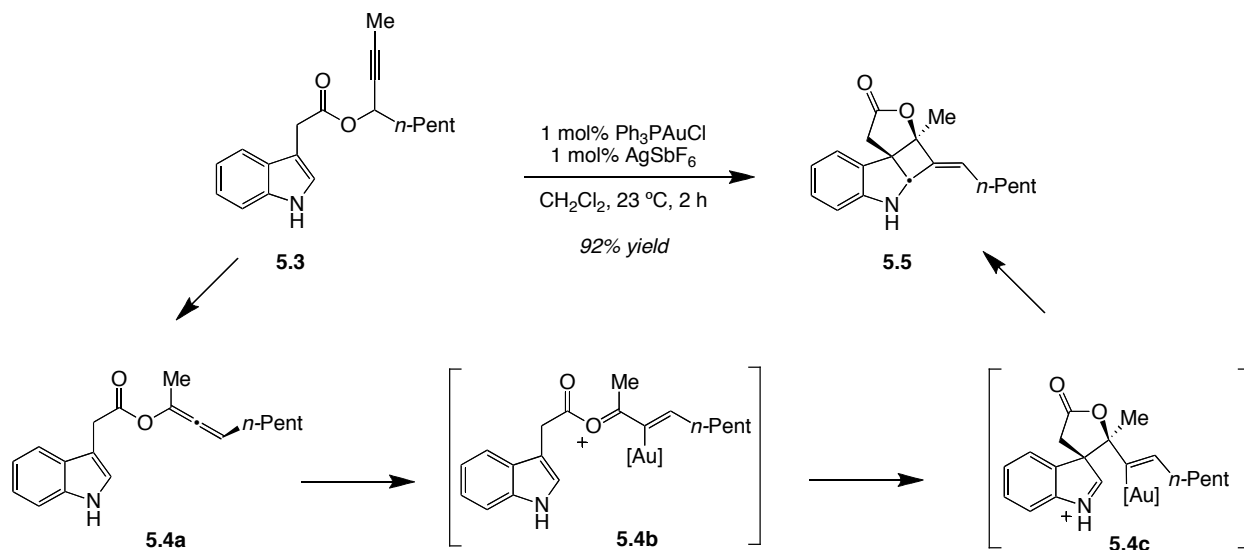
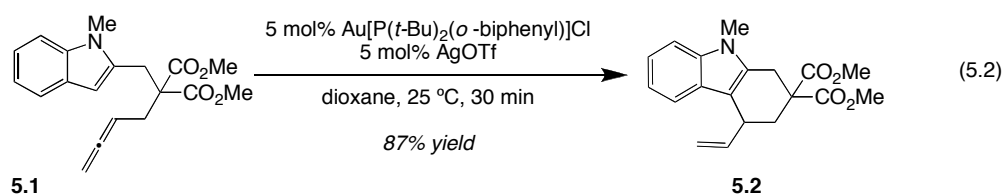


Scheme 5.2. Proposed Mechanisms of the Gold(I)-Catalyzed Conia-ene and 5-Endo-dig Cyclizations.

We were interested in expanding the scope of the addition of enolate nucleophiles to allenes. Our proposed 5-endo-trig cyclization would provide access to cyclopentene products complimentary to those formed in the Conia-ene (eq 5.1). In addition, allenes are especially attractive as electrophiles for these types of transformations; the inherent axial chirality of di- and tri-substituted allenes offers the potential for chirality transfer. Furthermore, a variety of reaction manifolds could potentially be accessed by altering the tether length to the allene. At the time, the selectivity of such a reaction remained unexplored.

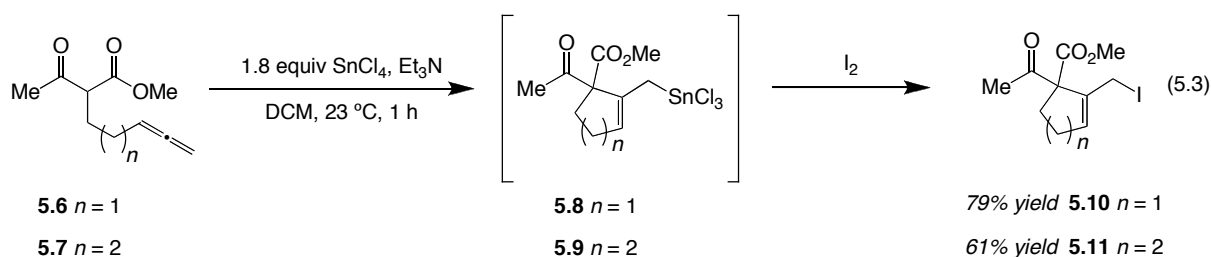


At the time of this work, a literature search revealed only two notable examples of a gold(I)-catalyzed addition of carbon nucleophiles to allenes. In 2006, Widenhoefer³ reported a 6-*exo-trig* hydroarylation of allenes (eq 5.2) catalyzed by gold(I). Zhang⁴ described a gold(I)-catalyzed 3,3-rearrangement followed by a formal [2 + 2] cycloaddition to create fused 2,3-indoline cyclobutanes (Scheme 5.3). In the proposed mechanism, the vinylgold(I) intermediate **5.4c** is intramolecularly trapped by an iminium ion. This was especially notable due to the propensity of vinylgold(I) species to undergo protonolysis. However, neither of these methods has taken advantage of chirality transfer to create stereocenters.

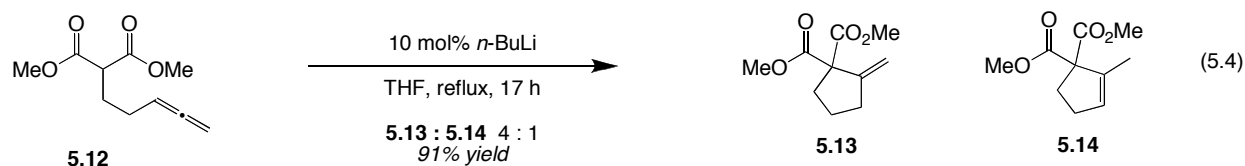


Scheme 5.3. Proposed Mechanism for a Gold(I)-Catalyzed Indole Addition to Masked Allenes.

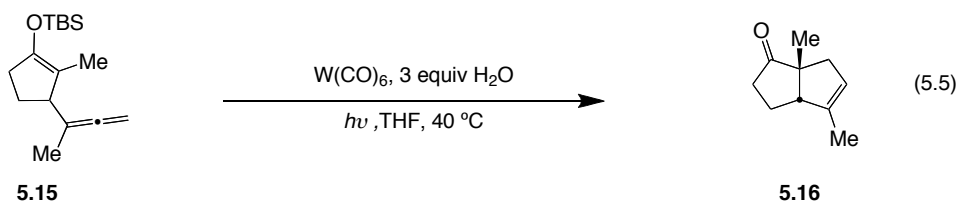
In contrast to gold, palladium, the most common metal used for the addition of stabilized nucleophiles to allenes, proceeds via either hydro- or carbopalladation.⁵ The nucleophile subsequently adds to the resultant π -allylpalladium species to produce the functionalized product. Relatively few metal mediated methods proceed via direct electrophilic activation of the allene for nucleophilic attack.⁶ One such example, shown in eq 5.3, employs tin tetrachloride to activate an allene for 5- or 6-*exo* cyclization.⁷ In the case of **5.7**, the reaction was completely selective for the 6-*exo* product (**5.11**). The 5-*endo* product was not observed at all. Also, the allyltin intermediates **5.8** and **5.9** were not isolated, but instead were reacted *in situ* with iodine. While this method was an interesting example of a cyclization under mild conditions, it required stoichiometric use of a corrosive and toxic metal salt.



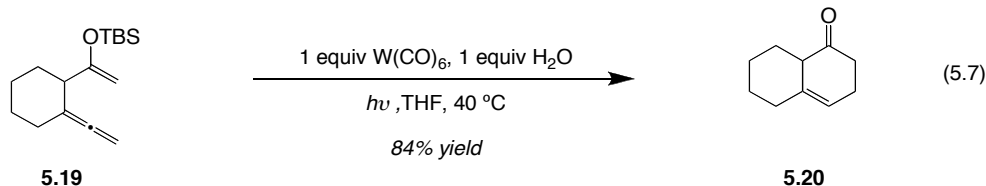
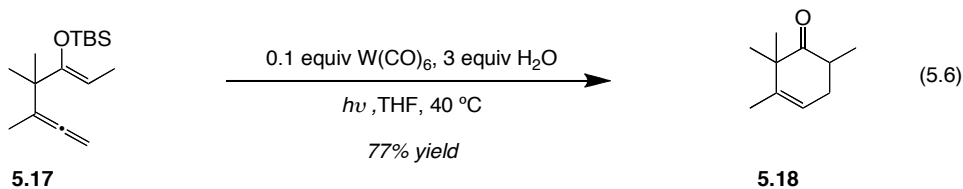
A catalytic amount of *n*-butyllithium was found to catalyze the cyclization of diester **5.12** (eq 5.4).⁸ Although this reaction proceeded with good yield (91%), the desired product was obtained as a 4:1 ratio of cyclopentenes. Because these compounds are simply alkene isomers, they were difficult to separate using normal protocols, which limits the utility of this reaction. In addition, the practical application of *n*-butyllithium as a catalyst is severely curtailed by its sensitivity to moisture.



Tungsten was also reported as a competent catalyst for the 5- and 6-*exo* addition of silyl enol ethers to allenes (eq 5.5-7).⁹ Although in most cases 10 mol% $\text{W}(\text{CO})_6$ was a sufficient amount of catalyst, certain substrates required stoichiometric quantities of metal. For instance, the yield of **5.16** was increased from 74% to 83% by using 1 equivalent of tungsten (eq 5.5). Also, methyl substituted **5.17** cyclized well with catalytic amounts of metal (eq 5.6). However, the 6-*exo* cyclization of **5.19** also needed a full equivalent of tungsten to achieve 84% yield of **5.20** (eq 5.7).



equiv $\text{W}(\text{CO})_6$	% yield
1.0	83
0.1	74

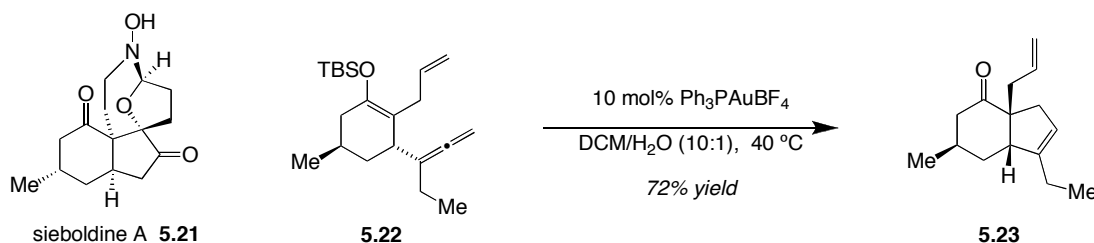


We hypothesized that gold(I) would provide complimentary reactivity to that which is achieved with other metals. In addition, the lack of methods using gold(I) for C-C bond formation provided additional motivation. The work reported herein describes our efforts using gold(I) to activate an allene for intramolecular addition of carbon nucleophiles. First, a gold(I)-catalyzed *5-endo-trig* reaction will be discussed. Second, we also discovered a gold(I)-catalyzed *5-endo/exo-trig* cyclization of substrates which contain two-carbon linkers between the pendant nucleophile and allene. Investigations into the mechanism of this cyclization are included, as well as attempts to isolate a proposed allylgold(I) intermediate.

Results

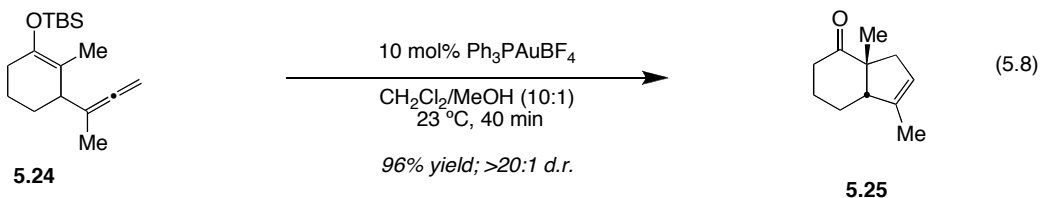
Gold(I)-Catalyzed 5-Endo-trig Cyclization

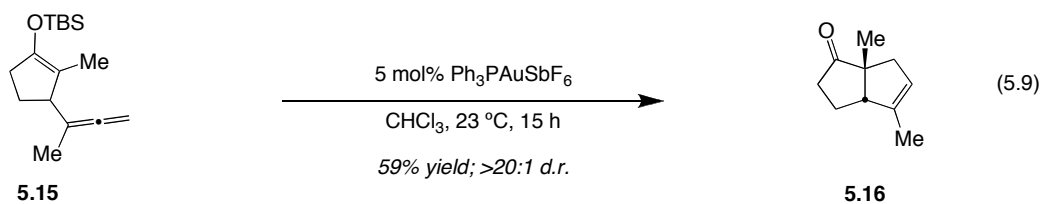
A gold(I)-catalyzed *5-endo-trig* addition to an allene was proposed by Joshua Kennedy-Smith¹⁰ as a key step in the synthesis of the natural product sieboldine A¹¹ (Scheme 5.4). This novel tetracyclic alkaloid inhibits acetylcholinesterase (IC₅₀ 2.0 μM) and has been found to be cytotoxic to murine lymphoma L1210 cells (IC₅₀ 5.1 μg/mL).¹¹ This compound was an interesting synthetic challenge due to a chiral quaternary center with two vicinal stereocenters. If a highly diastereoselective *5-endo-trig* cyclization was realized, this strategy would allow facile access to a problematic chiral quaternary center. Kennedy-Smith found that efficient cyclization occurred when silyl enol ether **5.22** was treated with Ph₃PAuBF₄ (10 mol%) in a mixture of water and dichloromethane at 40 °C (Scheme 5.4). Tetrafluoroborate was found to be the optimal counter-ion to slow competing hydrolysis, and water was a necessary co-solvent to aid deprotection after cyclization.



Scheme 5.4. Sieboldine A and the Initial Gold(I) Catalyzed *5-Endo-trig* Cyclization.

With this initial result in hand, we sought to explore the substrate scope of the allenyl cyclization. Silyl enol ether **5.24**¹² (10 mol% Ph₃PAuBF₄, 10:1 DCM:H₂O, 40 °C) yielded a single diastereomer **5.25** in excellent yield (eq 5.8). Under the same conditions, however, cyclopentene silyl enol ether **5.15** hydrolyzed rapidly to the corresponding ketone. The use of 5 mol% Ph₃PAuSbF₆ in chloroform for 15 hours minimized hydrolysis and produced 5,5-bicyclic ketone **5.16** in modest yield and excellent diastereoselectivity (eq 5.9).





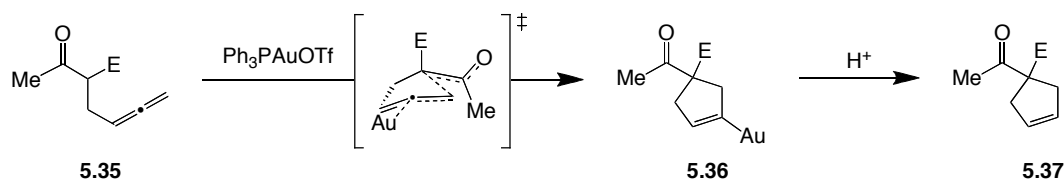
In addition to silyl enol ethers, a series of β -ketoesters were prepared and subjected to unoptimized conditions (1 mol% $Ph_3PAuOTf$, 0.2 M in CH_2Cl_2 ; Table 5.1). The 5-*endo-trig* cycloisomerization of **5.27** proceeded with good yield in 2 hours (entry 1). Bulky ester groups (entry 2) were well-tolerated, only requiring a slightly longer reaction time. Racemic 1,3-disubstituted allene **5.29** formed alkene **5.33** with modest diastereoselectivity (4:1, entry 3). Substitution of the β -keto esters with other electron withdrawing groups, such as nitriles (entry 4), needed an increased amount of gold to catalyze the cyclization. In addition to higher catalyst loading, a longer exposure to the gold(I)-catalyst (15 h) was necessary to reach 72% yield.

Table 5.1. Scope of Gold(I)-Catalyzed 5-*Endo-trig* Cyclization.^a

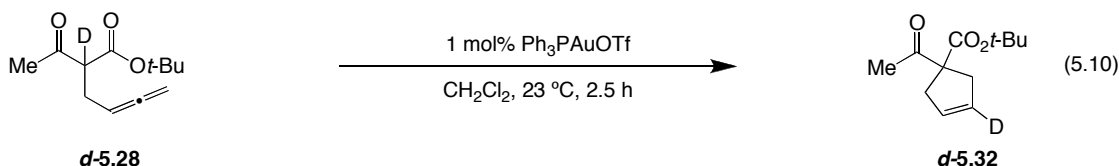
entry	substrate	time (h)	product	% yield (d.r.) ^b	
1		5.27 R = CO ₂ Me	2		5.31 85
2		5.28 R = CO ₂ <i>t</i> -Bu	2.5		5.32 86
3		5.29 R = CO ₂ <i>t</i> -Bu	2		5.33 86 (4:1)
4		5.30	15		5.34 72 ^c

^a Reaction Conditions: 1 mol% $Ph_3PAuOTf$, 0.2 M (allene) in CH_2Cl_2 , 23 °C. ^b Isolated yield after column chromatography. ^c 5 mol % $Ph_3PAuOTf$.

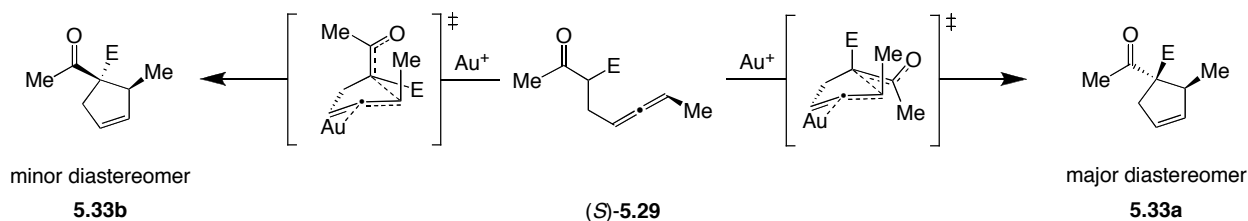
By analogy to earlier studies,¹ we hypothesized that this transformation proceeds first by the coordination of gold(I) to the terminal allenic double bond (Scheme 5.5). Then, nucleophilic addition of the enol double bond to the activated double bond in a 5-*endo-trig* fashion produces vinylgold intermediate **5.36**. Protonation of **5.36** would regenerate the cationic gold species and produce the observed products. Consistent with our proposed mechanism, deuterium labeled substrate *d*-**5.28** gave deuterated cyclopentene *d*-**5.32** (eq 5.10).



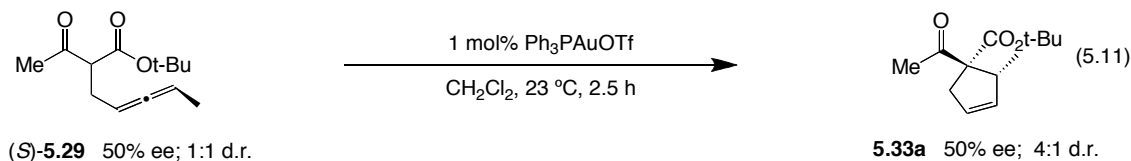
Scheme 5.5. Proposed Mechanism of Gold(I)-Catalyzed 5-Endo-trig Cyclization.



According to this mechanism, if cyclization is fast relative to isomerization, then axis to center chirality transfer should occur with 1,3-disubstituted allenes. With this thought in mind, we began examining the reactivity of a chiral 1,3-disubstituted allene. As shown earlier, treatment of **5.14** with cationic gold(I) (Table 5.1, entry 3) furnished the expected cyclopentene **5.33** in good yield with moderate diastereoselectivity. Positioning the methyl group *syn* to the *tert*-butyl ester lead to the major diastereomer.¹³ This orientation minimizes developing $A_{1,2}$ strain between the methyl ketone and terminal methyl group in the transition state (Scheme 5.6). Enantioenriched allene (*S*)-**5.29** (eq 5.11) was easily synthesized in four steps (50% ee, 1:1 d.r.)¹⁴ from commercially available (*R*)-3-butyn-2-ol according to the method of Krantz.¹⁵ Complete chirality transfer occurred upon cyclization, yielding an enantioenriched all-carbon stereocenter with a vicinal tertiary stereocenter. This reaction demonstrated the utility of our methodology, which provides mild and efficient access to challenging chiral quaternary centers.

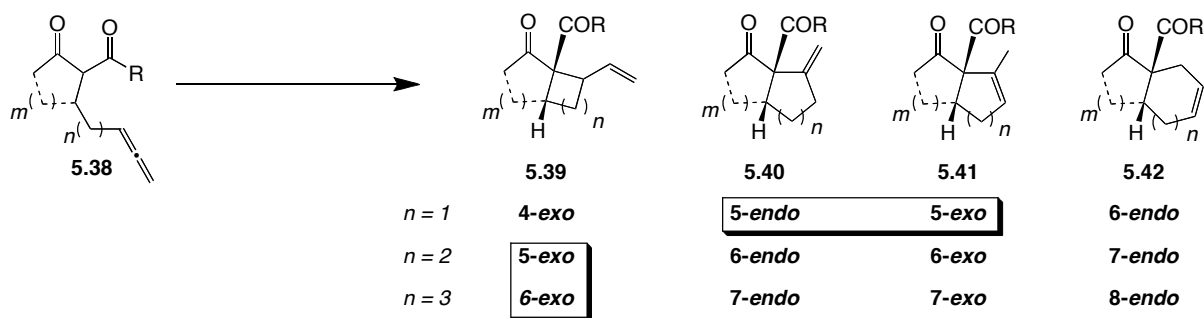


Scheme 5.6. Proposed Transition States for 1,3-Disubstituted Allene Cyclization.



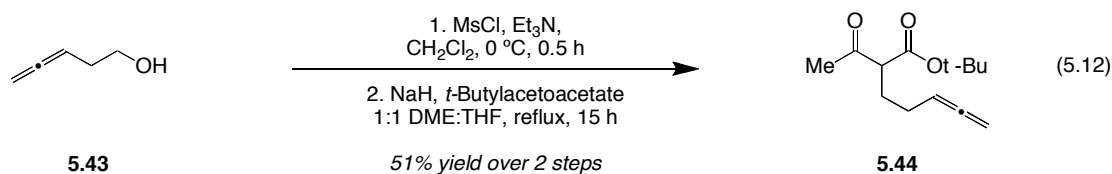
Gold(I)-Catalyzed 5-Endo/exo-trig Cyclization

When the allenyl side chain was connected via a one-carbon methylene unit, only one reaction, 5-endo-trig, was expected. Substrates with two methylene units between nucleophile and allene could plausibly produce 4-exo, 5-endo, 5-exo, or 6-endo products (Scheme 5.7).¹⁶ Even longer side chains could conceivably form medium-sized rings. Based on ring strain and relative rates of ring formation we hypothesized that for the $n = 1$ case the 6-endo and 4-exo modes would be disfavored over the 5-endo/exo mode. For the same reasons, we proposed that 5-exo and 6-exo would be favored when $n = 2$ and 3 respectively.



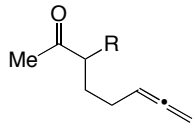
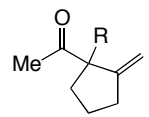
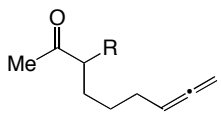
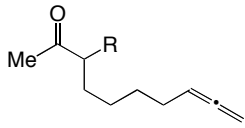
Scheme 5.7. Possible Cyclization Products.

We began our investigation into these types of cyclizations by preparing three general substrates (eq 5.12). 3,4-Pentadien-1-ol¹⁷ was treated with methanesulfonyl chloride and triethylamine to form the mesylate. Treatment with the sodium anion of *t*-butyl acetoacetate furnished compound **5.44** in 51% yield over two steps. Substrates with longer tethers (**5.45** and **5.46**) were synthesized analogously.



Remarkable selectivity for addition to the central carbon of the allene was observed. Substrate **5.44**, with a two-methylene unit tether, cyclized to form a single cyclopentene **5.47** (Table 5.2). Substrates with three and four carbon tethers (**5.45** and **5.46**) failed to react at all. Starting material was re-isolated even after extended reaction times.

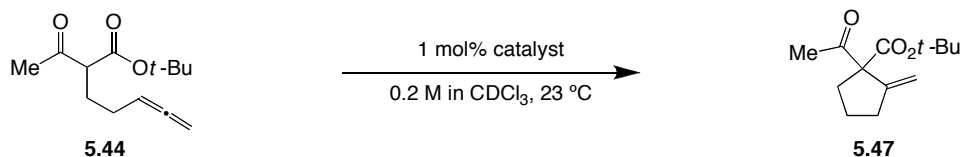
Table 5.2. Effect of Tether Length on Allene Cyclization.^a

entry	substrate	time (h)	product	% yield ^b
1		2		85%
2		18		NR ^c
3		18		NR ^c

^aReaction Conditions: 1 mol% Ph₃PAuOTf, 0.2 M (allene) in CH₂Cl₂, 23 °C. ^bIsolated yield after column chromatography. ^cOnly starting material was recovered.

With a new transformation in hand, we turned to the examination of the effect of modifying the counterion, ligand, and solvent. Substrate **5.44** was used for screening conditions. A strong counterion effect was revealed (Table 5.3, entries 1-4); trifluoromethanesulfonate was the most effective, yielding the desired product as a single cyclopentene isomer in nearly quantitative conversion (entry 1). Less basic counterions, such as tetrafluoroborate and hexafluoroantimonate (entries 2 and 3), performed comparably with much lower conversion. Neutral gold species (entries 4 and 5) failed to react with substrate **5.44**, leaving only starting material after 18 hours. Lastly, silver triflate was not a competent catalyst, cyclizing **5.44** to produce only 8% of **5.47** after 18 hours.

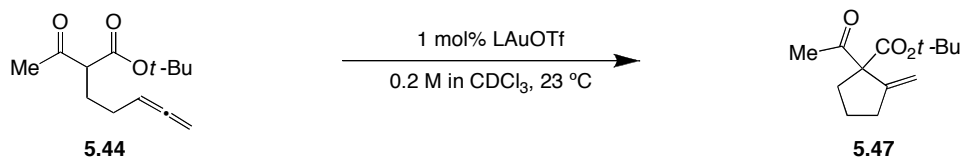
Table 5.3. Counterion Effects on Cyclization.

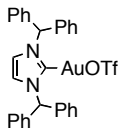


entry	catalyst	time (h)	% conv
1	Ph ₃ PAuOTf	1	92
2	Ph ₃ PAuBF ₄	3	60
3	Ph ₃ PAuSbF ₆	3	64
4	Ph ₃ PAuCl	18	0
5	[(Ph ₃ PAu)O]BF ₄	18	0
6	AgOTf	18	8

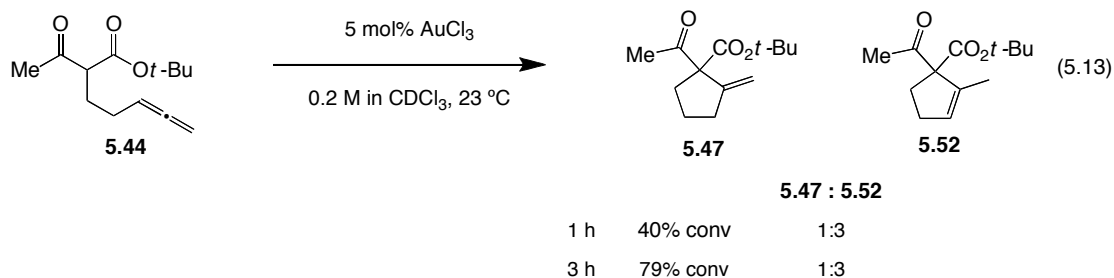
Treatment with a variety of cationic gold(I)-complexes bearing electron-deficient ligands¹⁸ (Table 5.4, entries 1-4) furnished a single cyclopentadiene **5.47** in nearly quantitative conversion. For example, phosphite **5.48** and tris(*para*-trifluoromethylphenyl)phosphine) **5.49** catalyzed the cyclization with equal conversions. However, a catalyst bearing a sigma-donating ligand (**5.51**), an N-heterocyclic carbene, was largely ineffective (entry 5). These results are consistent with the catalyst efficiencies found for the gold(I)-catalyzed Conia-ene and 5-*endo-dig* cyclizations.¹² The simplest of the complexes tested, Ph₃PAuOTf, was selected as the catalyst of choice.

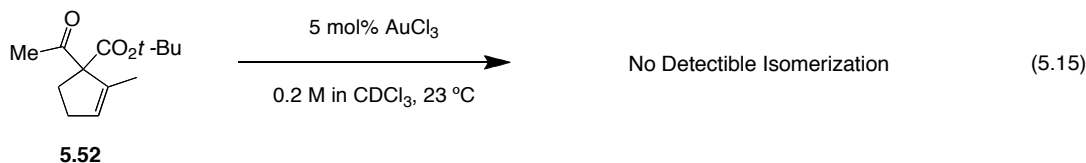
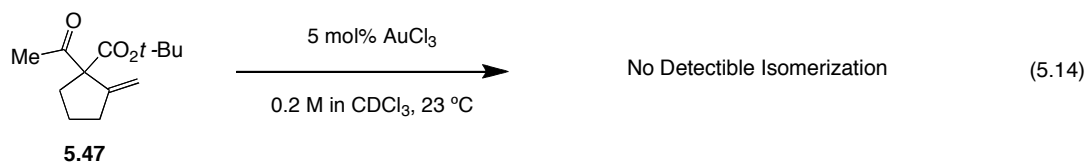
Table 5.4. Ligand Effects on Cyclization.



entry	ligand	time (h)	% conv
1	(PhO) ₃ PAuOTf (5.48)	1	90
2	(3,5-(CF ₃) ₂ C ₆ H ₃) ₃ PAuOTf (5.49)	1	92
3	(4-ClC ₆ H ₃) ₃ PAuOTf (5.50)	1	92
4	 (5.51)	3	21

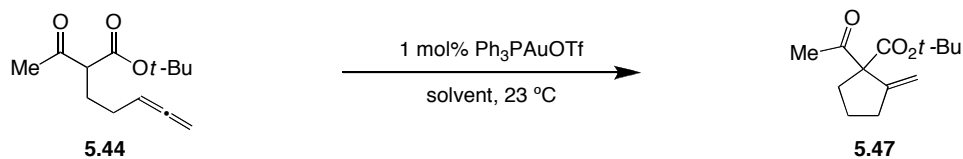
Changing the catalyst oxidation state from gold(I) to gold(III) dramatically reduced selectivity for *exo*-cyclopentene **5.47** (eq 5.13). Whereas when Ph₃PAuOTf was employed as a catalyst, only the *exo*-cyclopentene **5.47** was observed, gold(III) chloride produced a 1:3 mixture of *exo*:*endo* isomers. We theorized that this selectivity switch was caused by gold(III)-catalyzed rearrangement of the *exo*-alkene **5.47** to *endo*-**5.52** or vice versa. To test this hypothesis, two control experiments were performed. First, a sample of the *exo*-alkene **5.47** was treated with gold(III) chloride (eq 5.14). Second, a pure sample of the *endo*-alkene **5.52**¹⁹ was subjected to the reaction conditions with gold(III) chloride (eq 5.15). In both cases, however, no isomerization was detected by ¹H NMR after 18 hours.²⁰ A number of differences between gold(I) and gold(III) could account for this selectivity difference. Among other explanations, one reasonable hypothesis is that the rate of π - σ - π isomerization is faster for allylgold(III) complexes. It is also possible that the rate of S_E2 protonolysis is faster than S_E2' for gold(III). Our investigations into the mechanism of this reaction as well as the properties of allylgold(III) species will be discussed later in this chapter.





The solvent effects on the gold(I) cyclization are summarized in Table 5.5. The reaction proceeded equivalently in non-polar, non-coordinating solvents such as chloroform and benzene (entries 1 and 2). Acetone (entry 6) reduced conversion to 69%. Protic and polar media, like acetonitrile, dioxane, and methanol nearly eliminated reactivity (entries 3-5).

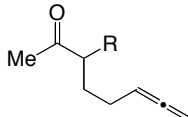
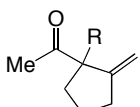
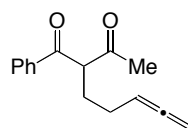
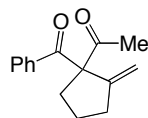
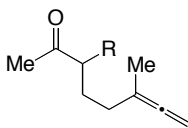
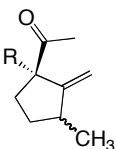
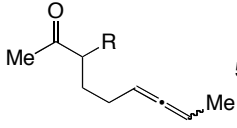
Table 5.5. Solvent Effects.



entry	solvent	time (h)	% conv
1	CDCl ₃	3	100
2	C ₆ D ₆	3	100
3	CH ₃ CN	14	0
4	d ₈ -dioxane	14	trace
5	MeOD	14	11
6	d ₆ -acetone	14	69

We next examined the scope of the cycloisomerization (Table 5.6). β -Keto-esters (entry 1) and diketones (entry 2) were well tolerated; both yielded a single cyclopentene isomer. A substrate with an internally substituted allene (entry 3) was also cyclized to form a single cyclopentene isomer, albeit with little diastereoselectivity. Unfortunately, 1,3-disubstituted allenes (entry 4) formed a complex mixture of products after extended reaction times. We theorized that the poor reactivity of this substrate was due to steric interference between the terminal methyl group and β -keto ester.

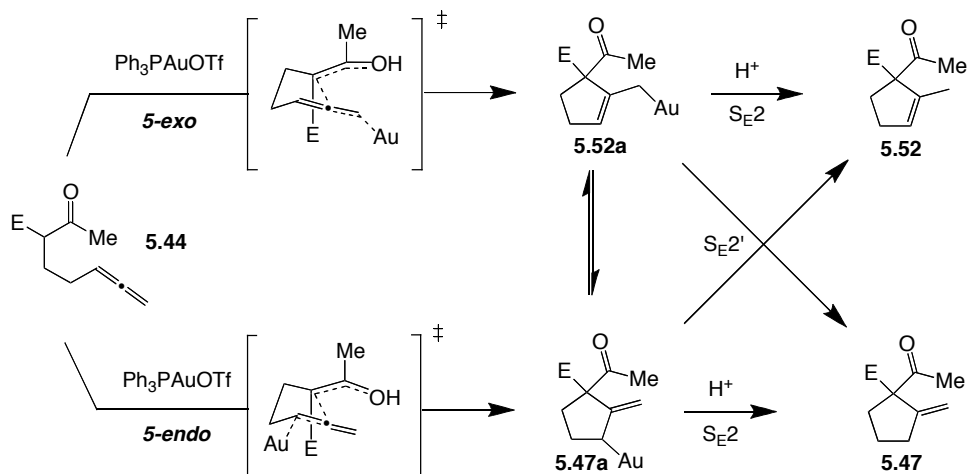
Table 5.6. Scope of Gold(I)-Catalyzed Cycloisomerization. ^a

entry	substrate	time (h)	product	% yield (d.r) ^b
1	 5.44 R = CO ₂ t-Bu	2	 5.47	85
2	 5.53	16	 5.56	>98
3	 5.54 R = CO ₂ t-Bu	2	 5.57	90 (3:2)
4	 5.55 R = CO ₂ t-Bu	18		NR ^c

^aReaction Conditions: 1 mol% Ph₃PAuOTf, 0.2 M (allene) in CH₂Cl₂, 23 °C. ^b Isolated yield after column chromatography. ^c Complex mixture of multiple products.

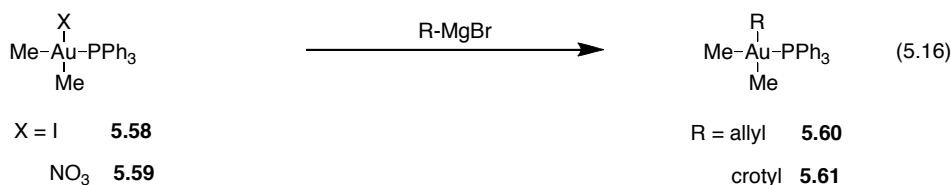
Proposed Mechanism and Allylgold(I) Species

By analogy to the Conia-ene mechanistic results,¹ we proposed that gold selectively activates the allenic double bond instead of the β-ketoester. Thus, the gold(I) cationic catalyst could coordinate either allenic double bond, activating the central carbon for nucleophilic attack in either a 5-*exo* or 5-*endo* fashion (Scheme 5.8). The resulting allylgold(I) species could subsequently react directly with an electrophile in either an S_E2 or S_E2' manner to produce the *exo*- or *endo*-cycloalkene. Alternatively, intermediates **5.52a** and **5.47a** could interconvert and then react. Because only one alkene isomer (*exo*) is observed, *endo* intermediate **5.47a** must undergo direct S_E2 protonation or *exo* intermediate **5.52a** must undergo S_E2' protonation.

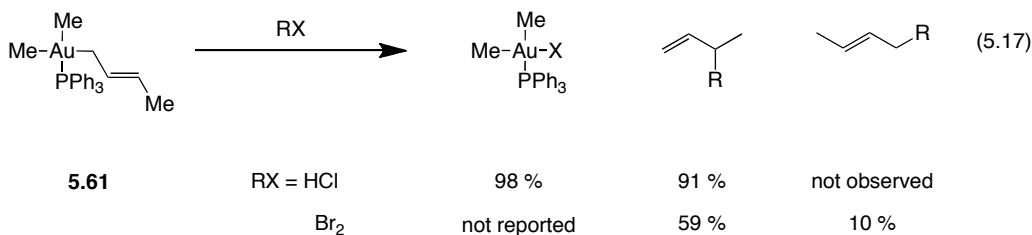


Scheme 5.8. Proposed Mechanism for the Gold(I)-Catalyzed Cycloisomerization.

The study of the mechanism of this *5-endo/exo-trig* reaction was difficult due to the interconversions of multiple intermediates (Scheme 5.8). Therefore, we turned to examine the nature of allylgold(I) species for further insight. Specifically, we wanted to address two issues: first, are allylgold(I) species configurationally stable? That is, do they isomerize readily between η^1 and η^3 configurations? Second, what is the preferential mode of reactivity with electrophiles- S_{E2} or S_{E2}' ?



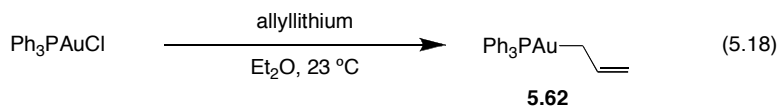
Only three reports of allylgold species were found in the literature. Two publications by Kochi and co-workers²¹ described the synthesis of allylgold(III) species **5.60** by treatment of dimethyltriphenylphosphinegold(III)iodide with allylmagnesium bromide (eq 5.16). The authors reported a crystal structure of crotyl species **5.61**, consistent with a square planar complex with the allyl anion η^1 bound to gold. The reactivity of **40** with electrophiles was also briefly investigated by Kochi (eq 5.16). When treated with aqueous acid, crotyl species **5.61** only formed 1-butene, most likely reacting in an S_{E2}' manner. However, when bromine was used as the electrophile, a 1:6 mixture of S_{E2} and S_{E2}' products was formed.



Due to the differences in selectivity between gold(I) and gold(III), we were especially interested to find a single report of an allylgold(I)-complex in the literature. Perevalova and co-workers²² described a procedure similar to that of Kochi's. Treatment of Ph₃PAuCl with allyl magnesium bromide was reported to yield triphenylphosphinegold(I)allyl species (**5.62**) in 51% yield. A specific note in this publication describes the quenching of the reaction mixture with a large quantity of water as being necessary for isolation. Since ³¹P NMR, crystal structures, and reactivity of these complexes were not reported, we undertook the synthesis and isolation of **5.62**.

Our attempts to isolate complex **5.62** via the methods described by Perevalova were not met with success. Under presumably identical conditions, Ph₃PAuCl was treated with allyl magnesium bromide. After aqueous work up, the crude material isolated showed none of the expected allyl signals in the ¹H NMR spectrum. The material isolated was identical in its ¹H NMR spectrum to that of the starting material. The ³¹P NMR was also consistent with starting material. After this disappointing result, we were forced to search for another synthetic route to **5.62**.

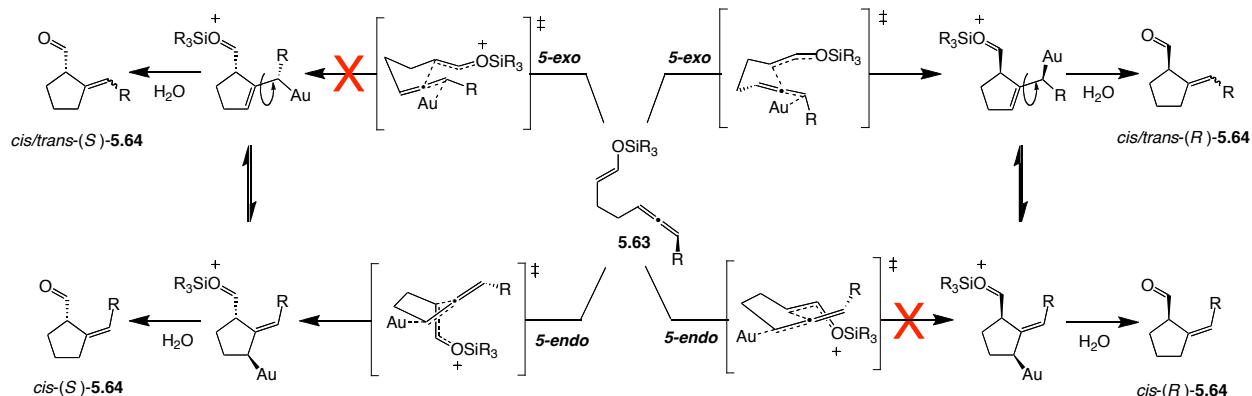
Simple alkylgold(I) complexes can be prepared easily via the treatment of Ph₃PAuCl with alkyllithium reagents.²³ By analogy, we attempted to synthesize **5.62** employing allyllithium. Due to its inherent instability, allyllithium must be prepared immediately prior to use. A number of methods exist for its synthesis, the most convenient of which involve the transmetalation of an allylmetal compound with an alkyllithium reagent.²⁴ Many attempts to prepare **5.62** were hindered by the propensity of Ph₃PAuCl to react with alkyl and aryllithium reagents used to form the corresponding alkyl- and arylgold species. The purity of allyllithium solution is of utmost importance to avoid forming these impurities. Transmetalating triphenylallytin with one equivalent of phenyllithium in ether²⁵ produced a clean allyllithium solution with no excess phenyllithium. Reacting the resulting solution of allyllithium with a suspension of Ph₃PAuCl in ether produced a remarkably clean sample of **5.62** (eq 5.18). Contrary to Perevalova's report, we found **5.62** was not stable to water. Further purification was hindered by the instability of the complex upon exposure to water, oxygen, and light.



In order to make the isolation and purification of an allylgold(I) species easier, we attempted to create a more stable complex by varying the electronic properties of the phosphine ligand. Ligands with more electron-donating character, such as tris(*para*-methoxyphenyl)phosphine and tris(*tert*-butyl)phosphine destabilized the allylgold(I) complex. These complexes were extremely light sensitive, degrading from light tan crystalline material to black tar within minutes of exposure. Ligands with electron-withdrawing character (tris(*para*-chlorophenyl)phosphine and tris(*para*-trifluoromethylphenyl)phosphine) appeared to stabilize the corresponding allylgold(I) complex. Unfortunately, due to their sensitive nature, the isolation and characterization of these complexes was never completed.

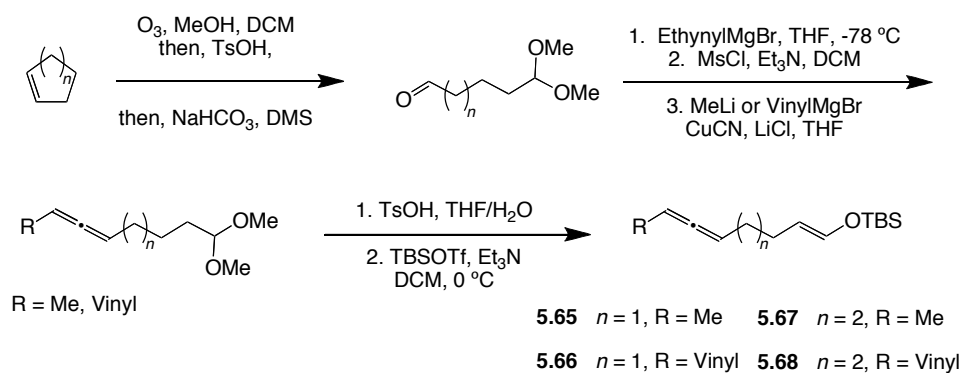
In addition to studying the nature of allylgold(I) species directly, we designed substrates that were hypothesized to provide indirect information about the nature of such species. Conformational analysis of the four proposed transition states revealed that a chiral allene should

produce a single enantiomer if reacting through a single mode of cyclization (Scheme 5.9). Thus, by examining the enantiomeric and diastereomeric ratio of the product formed, we could obtain data about the isomerization of allylgold complexes. The 5-*endo* pathway was proposed to begin with gold coordination of the internal alkene in the least sterically encumbered position - on the face opposite to the R group. Formation of (*R*)-**5.64** should be disfavored because of a large steric interaction between the R group and silyl enol ether. If 5-*endo* was the preferred pathway, and π - σ - π isomerization was slow relative to protonation, then a single enantiomer and alkene isomer - *cis*-(*S*)-**5.64** - should be observed. Similarly, a gauche butane-type interaction disfavors the formation of (*S*)-**5.64** via the 5-*exo* pathway. If 5-*exo* was the preferred pathway, then a single enantiomer - (*R*)-**5.64** - should be found. With either 5-*endo* or 5-*exo* cyclization, if π - σ - π isomerization was fast relative to protonation, either *cis*, *trans* or a mixture of alkene isomers may be observed depending on the kinetics and thermodynamics of protonolysis. In addition, the two 5-*endo* pathways may also be differentiated by distinguishing between diastereotopically deuterium labeled aldehydes (*syn* vs *anti*). A racemic product would indicate either multiple pathways or gold(I)-catalyzed racemization of the starting allene.²⁶



Scheme 5.9. Stereospecific Cyclization Pathways.

Unfortunately, previous attempts at cycloisomerization of terminally substituted allenes resulted in complex mixtures of products (Table 5.6, entry 4). We hypothesized that this was due to steric interference between the terminal substituent on the allene and β -keto ester. With this in mind, racemic silyl enol ethers derived from aldehydes were prepared from cyclopentene and cyclohexene (Scheme 5.10). With substrates in hand, initial studies were directed at finding the optimal combination of gold(I) catalyst, silver salt, and solvent. All results indicated that the gold(I)-catalyzed cyclization of these substrates (**5.65-5.68**) was complicated by competitive desilylation presumably via an α -aurated intermediate¹ and subsequent hydrolysis.



Scheme 5.10. Substrate Synthesis from Cyclopentene and Cyclohexene.

Conclusion

In summary, a mild, air and moisture tolerant gold(I)-catalyzed *5-endo-trig* cyclization of allenic dicarbonyl, silyl enol ether, and dinitrile compounds has been developed. Full axis to center chirality transfer in this reaction allows for facile access to chiral all-carbon quaternary centers with a vicinal tertiary center. In addition, a gold(I)-catalyzed *5-endo/exo-trig* cyclization has been described. Furthermore, the characterization of allylgold reactive intermediates continues to be challenging.

Experimental

General Information

Unless otherwise noted, all commercial materials were used without purification. Small scale reactions (< 3mL) were carried out in Fisher Scientific disposable scintillation vials. Dimethoxyethane (DME) was dried over 4 Å molecular sieves and stored in a schlenk flask. EMD Drisolv® (<50 ppm H₂O) N,N-dimethylformamide (DMF) was used without further purification. All other dry solvents were dried by passing through an alumina column. Silver trifluoromethanesulfonate (AgOTf) and chloro(triphenylphosphine)gold (Ph₃PAuCl) were obtained from Aldrich Chemical Company and Strem Chemicals respectively. 3,4-Pentadien-1-ol, 4,5-hexadien-1-ol, and 5,6-heptadien-1-ol were prepared according to the method of Crabbe.¹⁷ 2,3-Butadien-1-ol,²⁷ 2,3-pentadien-1-ol,¹⁵ 3,4-hexadien-1-ol,²⁸ and 4-methylhexa-4,5-dien-1-ol²⁹ were prepared according to literature procedures. Substrate **d-5.28** was prepared by exchange with D₂O and catalytic K₂CO₃ in THF. TLC analysis of reaction mixtures was performed with Merck silica gel 60 F₂₅₄ TLC plates. Flash chromatography was performed with Merck 60 silica gel (32-63 mm). ¹H and ¹³C NMR spectra were recorded with a Bruker AVB-400 spectrometer and were measured in and referenced to CDCl₃, unless otherwise noted. The enol isomers of substrates **5.27**, **5.25**, **5.44**, **5.45**, **5.46**, **5.53**, **5.54**, and **5.55** were not observed in the ¹H NMR spectra and are reported as the keto forms. IR spectra were recorded with a ThermoNicolette Avatar 370 FTIR spectrometer as thin films on a ZnSe plate. Mass spectral and analytical data were obtained via the Micro-Mass/Analytical Facility operated by the College of Chemistry, University of California, Berkeley.

Representative Procedure for the Preparation of Mesylalcohols

Methanesulfonyl chloride (930 µL, 12 mmol, 1.2 equiv) was added slowly to a cooled (0 °C) solution of 3,4-pentadien-1-ol (841 mg, 10 mmol, 1 equiv) and triethylamine (1.9 mL, 14 mmol, 1.4 equiv) in CH₂Cl₂ (10 mL). The reaction mixture was allowed to warm to room temperature and was monitored by TLC. Upon completion (30 min) the reaction mixture was quenched on a mixture of brine and sat. aq. NaHCO₃ (3:1, 50 mL), extracted with CH₂Cl₂ (3 x 50 mL), washed once with a mixture of brine and saturated aq. NaHCO₃ (3:1, 50 mL), dried (MgSO₄) and concentrated to yield 3,4-pentadienyl methanesulfonate as a crude yellow oil (1.6 g, quant). This crude oil was used without further purification.

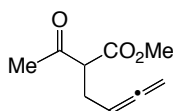
Representative Procedure A for the Alkylation of β-Ketoesters

tert-Butyl acetoacetate (2.16 mL, 13 mmol, 1.3 equiv) was added dropwise to a cooled (0 °C) suspension of sodium hydride (480 mg, 12 mmol, 1.2 equiv) in dry THF (10 mL, 1.3 M in acetoacetate). When addition was complete, the solution was stirred at rt until gas evolution

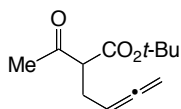
ceased (15 min). The clear solution was transferred into a solution of 3,4-pentadienylmethanesulfonate (prepared according to the general procedure; 10 mmol, or as indicated) in dry DME (10 mL, 1 M in mesylate). The mixture was heated at 80 °C for 15 h, then cooled to 23 °C. The solution was poured onto sat. aq. NH₄Cl (50 mL) in a separatory funnel, extracted with EtOAc (3 x 50 mL), dried (MgSO₄), and concentrated. The crude oil was purified by silica gel chromatography (0-5% EtOAc/Hex) to yield *tert*-butyl 2-ethanoylhepta-5,6-dienoate (**29**) as a clear, colorless oil (1.09 g, 48%). Characterization data are reported below.

Representative Procedure B for the Alkylation of β -Ketoesters

Methyl acetoacetate (450 μ L, 4.2 mmol, 1.3 equiv) was added dropwise to a cooled (0 °C) suspension of sodium hydride (144 mg, 3.6 mmol, 1.2 equiv) in dry THF (6 mL). When addition was complete, the solution was stirred at 23 °C until gas evolution ceased (15 min). The clear solution was transferred into a solution of 2,3-butadienyl methanesulfonate (prepared according to the general procedure; 3 mmol, or as indicated) in dry THF (4 mL). The mixture was stirred at 23 °C for 5 h. The solution was poured onto sat. aq. NH₄Cl (30 mL) in a separatory funnel, extracted with EtOAc (3 x 30 mL), dried (MgSO₄), and concentrated. The crude oil was purified by silica gel chromatography (0-25% EtOAc/Hex) to yield methyl 2-ethanoylhepta-4,5-dienoate (**11**) as a clear, colorless oil (340 mg, 67%). Characterization data are reported below.

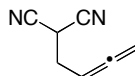


Methyl 2-ethanoylhepta-4,5-dienoate 5.27. Prepared according to procedure B with 2,3-butadienylmethanesulfonate (prepared according to the general procedure; 3 mmol) and methylacetoacetate. Purification by silica gel chromatography (0-25% EtOAc/Hex) yielded the title compound as a clear, colorless oil (340 mg, 67%). ¹H NMR (400 MHz, CDCl₃) δ 5.14 (pentet, *J* = 6.6 Hz, 1H), 4.72 (m, 2H), 3.76 (s, 3H), 3.64 (t, *J* = 7.3 Hz, 1H), 2.56 (m, 2H), 2.29 (s, 3H) ppm; ¹³C NMR (100 MHz, CDCl₃) δ 208.5, 202.4, 169.6, 87.0, 76.5, 58.6, 52.5, 29.4, 26.4 ppm; IR (thin film) ν 1956, 1742, 1716, 1149 cm⁻¹; HRMS (EI) calcd. for [C₉H₁₂O₃]⁺ 168.0786, found 169.0783; Anal. calcd.: C, 64.27; H, 7.19; found: C, 64.15; H, 7.29.

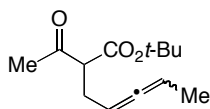


***tert*-Butyl 2-ethanoylhepta-4,5-dienoate 5.25.** Prepared according to procedure B with 2,3-butadienylmethanesulfonate (prepared according to the general procedure; 5.5 mmol) and *tert*-butylacetoacetate. Purification by silica gel chromatography (0-5% EtOAc/Hex) yielded the title compound as a clear, colorless oil (550 mg, 52%). ¹H NMR (400 MHz, CDCl₃) δ 5.14 (d, *J* =

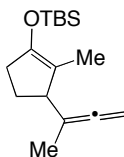
6.6 Hz, 1H), 4.73 (m, 2H), 3.52 (t, $J = 7.3$ Hz, 1H), 2.52 (m, 2H), 2.27 (s, 3H), 1.50 (s, 9H) ppm; ^{13}C NMR (100 MHz, CDCl_3) δ 208.6, 202.8, 168.2, 87.2, 82.1, 76.3, 59.9, 29.3, 27.9, 26.5 ppm; IR (thin film) ν 1957, 1732, 1713, 1141 cm^{-1} ; HRMS (EI) calcd. for $[\text{C}_{12}\text{H}_{18}\text{O}_3 + \text{H}]^+$ 211.1334, found 211.1332; Anal. calcd.: C, 68.54; H, 8.63, found: C, 68.62; H, 8.87.



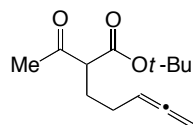
2-(Buta-2,3-dienyl)propanedinitrile 5.30. Prepared according to procedure B with 2,3-butadienylmethanesulfonate (prepared according to the general procedure; 2.6 mmol) and malononitrile. Purification by silica gel chromatography (0-10% EtOAc/Hex) yielded the title compound as a clear, colorless oil (110 mg, 36%): ^1H NMR (400 MHz) δ 5.28 (pentet, $J = 6.8$ Hz, 1H), 5.04 (m, 2H), 3.87 (t, $J = 7.1$ Hz, 1H), 2.74 (m, 2H) ppm; ^{13}C NMR (100 MHz, CDCl_3) δ 209.3, 112.4, 83.7, 78.9, 29.7, 22.6 ppm; LRMS m/z ($\text{M}+1^+$) 119. Spectral data consistent with previously reported data.³⁰



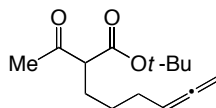
tert-Butyl 2-ethanoylhepta-4,5-dienoate 5.29. Prepared according to procedure B with 2,3-pentadienylmethanesulfonate (prepared according to the general procedure; 3.1 mmol) and *tert*-butylacetoacetate. Purification by silica gel chromatography (2.5-5% EtOAc/Hex) yielded the title compound as a clear, colorless oil (350 mg, 40%). ^1H NMR (400 MHz, CDCl_3) δ 5.11 (m, 2H), 3.53 (q, $J = 7.6$ Hz, 1H), 2.51 (m, 2H), 2.28 (s, 3H), 1.66 (m, 3H), 1.49 (s, 9H) ppm; ^{13}C NMR (100 MHz, CDCl_3) δ 205.0, 202.6, 168.3, 87.4, 87.2, 81.9, 60.0, 29.0, 27.9, 27.2, 14.2 ppm; peaks observed for the other diastereomer:³¹ ^{13}C NMR (100 MHz, CDCl_3) δ 205.1, 202.7, 168.4, 87.3, 87.2, 81.8, 60.2, 29.0, 27.9, 27.3, 14.3 ppm; IR (thin film) ν 1967, 1736, 1713, 1139 cm^{-1} ; HRMS (EI) calcd. for $[\text{C}_{13}\text{H}_{20}\text{O}_3 + \text{H}]^+$ 225.1491, found 225.1496.



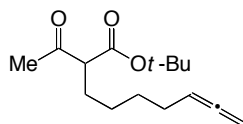
(3-(Buta-2,3-dien-2-yl)-2-methylcyclopent-1-enyloxy)(tert-butyl)dimethylsilane 5.15. Prepared according to the method of Iwasawa³². Purification by silica gel chromatography (Pretreated with 5% TEA/Hex; eluted with Hex) to yield the title compound as a clear colorless oil (178 mg, 34%): ^1H NMR (400 MHz, CDCl_3) δ 4.60 (q, $J = 3.0$ Hz, 2H), 3.13 (m, 1H), 2.32 (m, 2H), 2.11 (m, 1H), 1.73 (m, 1H), 1.62 (t, $J = 3.0$ Hz, 3H), 1.53 (br s, 3H), 0.99 (s, 9H), 0.17 (s, 6H) ppm; ^{13}C NMR (100 MHz, CDCl_3) δ 206.3, 148.3, 114.1, 101.0, 73.2, 50.0, 33.0, 25.8, 18.1, 14.9, 10.6, -2.9 ppm. Spectral data consistent with previously reported data.³²



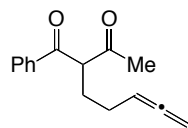
tert-Butyl 2-ethanoylhepta-5,6-dienoate 5.44. Prepared according to procedure A with 3,4-pentadienylmethanesulfonate (prepared according to the general procedure; 10 mmol). Purification by silica gel chromatography (0-5% EtOAc/Hex) yielded the title compound as a clear, colorless oil (1.09 g, 48%). $^1\text{H NMR}$ (400 MHz, CDCl_3) δ 5.07 (pentet, $J = 6.6$ Hz, 1H), 4.70 (m, 2H), 3.42 (t, $J = 7.1$ Hz, 1H), 2.23 (s, 3H), 1.98 (m, 4H), 1.47 (s, 9H) ppm; $^{13}\text{C NMR}$ (100 MHz, CDCl_3) δ 208.7, 203.4, 168.9, 88.8, 81.9, 75.4, 59.9, 29.0, 27.9, 27.3, 25.9 ppm; IR (thin film) ν 1956, 1732, 1710, 1140 cm^{-1} ; HRMS (EI) calcd. for $[\text{C}_{13}\text{H}_{20}\text{O}_3 + \text{H}]^+$ 225.1491, found 225.1496; Anal. calcd.: C, 69.61; H, 8.99, found: C, 69.30; H, 9.05.



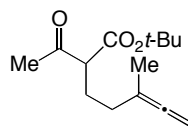
tert-Butyl 2-ethanoylocta-6,7-dienoate 5.45. Prepared according to procedure A with 4,5-hexadienylmethanesulfonate (10 mmol). Purification by silica gel chromatography (0-5% EtOAc/Hex) yielded the title compound as a clear, colorless oil (1.55 g, 65%). $^1\text{H NMR}$ (400 MHz, CDCl_3) δ 5.09 (pentet, $J = 6.6$ Hz, 1H), 4.68 (m, 2H), 3.33 (t, $J = 7.6$ Hz, 1H), 2.23 (s, 3H), 2.04 (m, 2H), 1.86 (m, 2H), 1.48 (s, 9H), 1.42 (m, 2H) ppm; $^{13}\text{C NMR}$ (100 MHz, CDCl_3) δ 208.6, 203.5, 169.1, 89.4, 81.9, 75.0, 60.8, 28.7, 27.9, 27.9, 27.5, 26.7 ppm; IR (thin film) ν 1956, 1734, 1712, 1139 cm^{-1} ; HRMS (EI) calcd. for $[\text{C}_{14}\text{H}_{22}\text{O}_3 + \text{H}]^+$ 239.1647, found 239.1649.



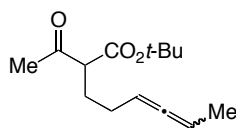
tert-Butyl 2-ethanoylnona-7,8-dienoate 5.46. Prepared according to procedure A with 5,6-heptadienylmethanesulfonate (prepared according to the general procedure; 10 mmol). Purification by silica gel chromatography (0-5% EtOAc/Hex) yielded the title compound as a clear, colorless oil (1.48 g, 59%). $^1\text{H NMR}$ (400 MHz, CDCl_3) δ 5.10 (pentet, $J = 6.8$ Hz, 1H), 4.68 (dt, $J = 6.8, 3.5$ Hz, 2H), 3.32 (t, $J = 7.3$ Hz, 1H), 2.24 (s, 3H), 2.02 (m, 2H), 1.83 (m, 2H), 1.49 (s, 9H), 1.45 (m, 2H), 1.35 (m, 2H) ppm; $^{13}\text{C NMR}$ (100 MHz, CDCl_3) δ 208.5, 169.1, 128.3, 89.7, 81.8, 74.8, 61.0, 28.8, 28.6, 28.3, 27.9, 27.9, 26.7 ppm; IR (thin film) ν 1956, 1736, 1711, 1138 cm^{-1} ; HRMS (EI) calcd. for $[\text{C}_{15}\text{H}_{24}\text{O}_3 + \text{H}]^+$ 253.1804, found 253.1805; Anal. calcd.: C, 71.39; H, 9.59, found: C, 71.03; H, 9.76.



2-(Penta-3,4-dienyl)-1-phenylbutane-1,3-dione 5.53. Prepared according to procedure A with 3,4-pentadienylmethanesulfonate (prepared according to the general procedure; 10 mmol), catalytic sodium iodide (20 mg) with dry DMF (4 mL). Purification by silica gel chromatography (0-5% EtOAc/Hex) yielded the title compound as a clear, colorless oil (150 mg, 13%). $^1\text{H NMR}$ (400 MHz, CDCl_3) δ 8.01 - 8.06 (m, 2H), 7.62 - 7.67 (m, 1H), 7.50 - 7.57 (m, 2H), 5.11 (d, $J = 6.8$ Hz, 1H), 4.66 - 4.71 (m, 2H), 4.58 (t, $J = 6.3$ Hz, 1H), 2.18 - 2.29 (m, 4H), 2.02 - 2.17 (m, 3H) ppm; $^{13}\text{C NMR}$ (100 MHz, CDCl_3) δ 208.7, 204.0, 196.4, 133.8, 128.9, 128.8, 88.9, 75.6, 62.4, 28.3, 28.1, 26.3 ppm; IR (thin film) ν 1955, 1719, 1674 cm^{-1} ; HRMS (FAB) calcd. for $[\text{C}_{15}\text{H}_{16}\text{O}_2+\text{H}]^+$ 229.1229, found 229.1235.



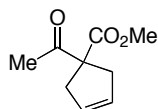
tert-Butyl 2-ethanoyl-5-methylhepta-5,6-dienoate 5.54. Prepared according to procedure A with 4-methylhexa-4,5-dienylmethanesulfonate (prepared according to the general procedure; 8 mmol). Purification by silica gel chromatography (0-6% EtOAc/Hex) yielded the title compound as a clear, colorless oil (0.90 g, 47%). $^1\text{H NMR}$ (400 MHz, CDCl_3) δ 4.65 (m, 2H), 3.41 (t, $J = 7.3$ Hz, 1H), 2.25 (s, 3H), 1.97 (m, 2H), 1.72 (m, 2H), 1.69 (t, $J = 3.3$ Hz, 3H), 1.49 (s, 9H) ppm; $^{13}\text{C NMR}$ (100 MHz, CDCl_3) δ 206.1, 169.0, 100.0, 97.3, 81.9, 74.7, 60.0, 31.0, 29.0, 27.9, 25.8, 18.6 ppm; IR (thin film) ν 1736, 1712, 1368, 1143 cm^{-1} ; HRMS (EI) calcd. for $[\text{C}_{14}\text{H}_{22}\text{O}_3]^+$ 238.1569, found 238.1566.



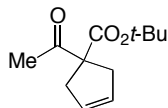
tert-Butyl 2-ethanoylocta-5,6-dienoate 5.55. Prepared according to procedure A with 3,4-hexadienylmethanesulfonate (prepared according to the general procedure; 5 mmol). Purification by silica gel chromatography (0-5% EtOAc/Hex) yielded the title compound as a clear, colorless oil (254 mg, 21%). $^1\text{H NMR}$ (400 MHz, CDCl_3) δ 4.99 - 5.16 (m, 2H), 3.45 (t, $J = 7.1$ Hz, 1H), 2.25 (s, 3H), 1.89 - 2.07 (m, 4H), 1.68 (dd, $J = 3.3$ Hz, 3H), 1.49 (s, 9H) ppm; $^{13}\text{C NMR}$ (100 MHz, CDCl_3) δ 205.0, 203.6, 169.0, 89.0, 86.3, 81.9, 59.9, 29.0, 27.9, 27.3, 26.5, 14.5 ppm; IR (thin film) ν 1965, 1736, 1713, 1138 cm^{-1} ; HRMS (EI) calcd. for $[\text{C}_{14}\text{H}_{22}\text{O}_3 + \text{H}]^+$ 239.1647, found 239.1644; Anal. calcd.: C, 70.56; H, 9.30, found: C, 70.83; H, 9.46.

General Gold(I)-Catalyzed Cycloisomerization Procedure

To a small screw-cap scintillation vial equipped with a magnetic stir bar and charged with a solution of allenyl substrate (~100 mg or as indicated; 1 equiv) in CH_2Cl_2 (0.2 M) was added Ph_3PAuCl (1 mol%, as indicated) followed by the appropriate silver salt (1 mol%, as indicated). The cloudy white reaction mixture was then stirred at room temperature and monitored periodically by TLC. Upon completion, the reaction mixture was either loaded directly on to a silica gel column and chromatographed or simply filtered thru a plug of silica gel to give the cycloisomerized products described below.



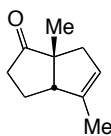
Methyl 1-ethanoylcyclopent-3-enecarboxylate 5.31. Prepared according to the general procedure with AgOTf . Purified by filtration through a silica gel plug (30% EtOAc/Hex) to yield the title compound as a clear, colorless oil (86 mg, 86%): ^1H NMR (400 MHz, CDCl_3) δ 5.61 (s, 2H), 3.75 (s, 3H), 2.95 (m, 4H), 2.20 (s, 3H) ppm; ^{13}C NMR (100 MHz, CDCl_3) δ 202.7, 173.5, 127.8, 65.3, 52.8, 39.3, 25.9 ppm. Spectral data consistent with previously reported data.³³



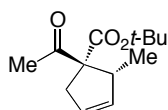
tert-Butyl 1-ethanoylcyclopent-3-enecarboxylate 5.32. Prepared according to the general procedure with *tert*-Butyl 2-ethanoylhexa-4,5-dienoate (50 mg, 0.24 mmol) and AgOTf . Purified by filtration through a silica gel plug (30% EtOAc/Hex) to yield the title compound as a clear, colorless oil (43 mg, 85%): ^1H NMR (400 MHz, CDCl_3) δ 5.60 (s, 2H), 2.93 (s, 4H), 2.22 (m, 4H), 1.49 (s, 9H) ppm; ^{13}C NMR (100 MHz, CDCl_3) δ 202.9, 172.0, 127.7, 81.9, 66.1, 39.1, 27.8, 26.0 ppm. Spectral data consistent with previously reported data.³⁴



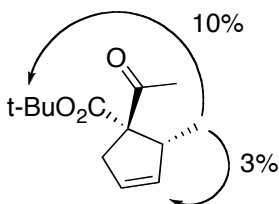
Cyclopent-3-ene-1,1-dicarbonitrile 5.34. Prepared according to the general procedure with Ph_3PAuCl (5 mol%) and AgOTf (5 mol%). Purified by filtration through a silica gel plug (30% EtOAc/Hex) to yield the title compound as a clear, colorless oil (72 mg, 72%): ^1H NMR (400 MHz) δ 5.85 (s, 2H), 3.26 (s, 4H) ppm; ^{13}C NMR (100 MHz, CDCl_3) δ 127.5, 116.9, 83.7, 45.4 ppm. Spectral data consistent with previously reported data.³⁵



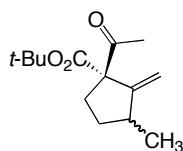
4,6-Dimethyl-3,3,6,6-tetrahydropentalen-1(2H)-one 5.16. Prepared according to the general procedure with (3-(Buta-2,3-dien-2-yl)-2-methylcyclopent-1-enyloxy)(tert-butyl)dimethylsilane (60 mg, 0.227 mmol) using chloroform as the solvent and Ph_3PAuCl (5 mol%) and AgSbF_6 (5 mol%). The crude reaction mixture was filtered through a silica gel plug (30% EtOAc/Hex), concentrated. The crude oil was purified by silica gel chromatography (0-2% EtOAc/Hex) to yield the title compound as a clear, colorless oil (20 mg, 59%): $^1\text{H NMR}$ (400 MHz, CDCl_3) δ 5.31 (br s, 1H), 2.94 (br s, 1H), 2.57 (d, $J = 16.4$ Hz, 1H), 1.93 - 2.38 (m, 5H), 1.74 (s, 3H), 1.20 (s, 3H) ppm; $^{13}\text{C NMR}$ (100 MHz, CDCl_3) δ 225.6, 140.8, 124.9, 57.3, 55.1, 43.7, 36.2, 21.9, 21.0, 14.7 ppm. Spectral data consistent with previously reported data.³²



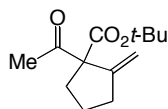
tert-Butyl 1-ethanoyl-2-methylcyclopent-3-enecarboxylate 5.33. Prepared according to the general procedure with *tert*-Butyl 2-ethanoylhepta-4,5-dienoate (50 mg, 0.223 mmol) and AgOTf . The crude reaction mixture was filtered through a silica gel plug (30% EtOAc/Hex), concentrated to yield a crude 4:1 diastereomeric mixture. The crude oil was purified by silica gel chromatography (0-2% EtOAc/Hex) to yield the major diastereomer as a clear, colorless oil (43 mg, 86%): $^1\text{H NMR}$ (400 MHz, CDCl_3) δ 5.57 - 5.62 (m, 1H), 5.49 - 5.54 (m, 1H), 3.59 (q, $J = 7.6$ Hz, 1H), 3.27 (dq, $J = 17.2, 2.3$ Hz, 1H), 2.47 - 2.55 (m, 1H), 2.22 (s, 3H), 1.51 (s, 9H), 1.04 (d, $J = 7.1$ Hz, 3H) ppm; The following NOE enhancements were observed:



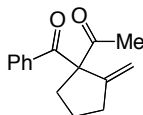
$^{13}\text{C NMR}$ (100 MHz, CDCl_3) δ 202.9, 170.2, 135.4, 125.2, 82.2, 70.1, 43.0, 38.4, 28.0, 26.4, 16.1 ppm; IR (thin film) ν 1737, 1710, 1251, 1142 cm^{-1} ; LRMS m/z ($\text{M}+1$)⁺ 225; HRMS (EI) calcd. for $[\text{C}_{13}\text{H}_{20}\text{O}_3]^+$ 224.1412, found pending; Enantiomeric excess was determined to be 50% by chiral HPLC (Whelk-O column, ethanol:hexanes = 0.5:99.5, 1 mL/min) major stereoisomer: 76%, 8.1 min; minor stereoisomer: 24%, 10.1 min.



tert-Butyl 1-ethanoyl-3-methyl-2-methylenecyclopentanecarboxylate 5.57. Prepared according to the general procedure with AgOTf. Purified directly by silica gel chromatography (1-8% EtOAc/Hex) to yield the title compound as a 3:2 inseparable mixture of diastereomers (clear, colorless oil, 90 mg, 90%): Major diastereomer: ^1H NMR (400 MHz, CDCl_3) δ 5.18-5.23 (m, 2H), 2.39-2.47 (m, 2H), 2.20 (s, 3H), 1.86-1.94 (m, 2H), 1.67 (m, 1H), 1.40 (s, 9H), 1.09 (m, 3H) ppm; ^{13}C NMR (100 MHz, CDCl_3) δ 203.5, 170.2, 153.6, 110.9, 81.8, 71.6, 39.7, 32.6, 32.4, 27.7, 26.8, 18.9 ppm; Minor diastereomer: ^1H NMR (400 MHz, CDCl_3) δ 5.18-5.23 (m, 2H), 2.54-2.58 (m, 2H), 2.19 (s, 3H), 2.01-2.04 (m, 2H), 1.70 (m, 1H), 1.46 (s, 9H), 1.10 (m, 3H) ppm; ^{13}C NMR (100 MHz, CDCl_3) δ 203.6, 170.1, 153.5, 110.5, 81.7, 71.4, 39.8, 32.9, 32.5, 27.9, 26.6, 18.2 ppm; IR (thin film) ν 2973, 1709, 1153 cm^{-1} ; LRMS m/z (M+1) $^+$ 238; HRMS (EI) calcd. for $[\text{C}_{14}\text{H}_{22}\text{O}_3 - \text{C}_2\text{H}_3\text{O}]^+$ 195.1385, found 195.1384.



tert-Butyl 1-ethanoyl-2-methylenecyclopentanecarboxylate 5.47. Prepared according to the general procedure with *tert*-Butyl 2-ethanoylhepta-5,6-dienoate (224 mg, 1 mmol) and AgOTf. Purified by filtration through a silica gel plug (30% EtOAc/Hex) to yield the title compound as a clear, colorless oil (190 mg, 85%): ^1H NMR (400 MHz, CDCl_3) δ 5.31 (t, $J = 2.0$ Hz, 1H), 5.26 (t, $J = 2.0$ Hz, 1H), 2.34 - 2.51 (m, 3H), 2.24 (s, 3H), 2.09 - 2.18 (m, 1H), 1.60 - 1.82 (m, 2H), 1.49 (s, 9H) ppm; ^{13}C NMR (100 MHz, CDCl_3) δ 203.6, 170.1, 148.9, 111.6, 81.9, 71.1, 35.0, 34.1, 27.8, 26.8, 24.0 ppm. Spectral data consistent with previously reported data.¹



1-(2-Methylene-1-(phenylcarbonyl)cyclopentyl)ethanone 5.56. Prepared according to the general procedure with 2-(Penta-3,4-dienyl)-1-phenylbutane-1,3-dione (60 mg, 0.263 mmol). Purified by silica gel chromatography (30% EtOAc/Hex) to yield the title compound as a clear, colorless oil (52 mg, 83%): ^1H NMR (400 MHz, CDCl_3) δ 7.44-7.58 (m, 5H), 5.45 (t, $J = 2$ Hz, 1H), 5.17 (t, $J = 2$ Hz, 1H), 2.78 (pentet, $J = 2.8$ Hz, 1 H), 2.54-2.61 (m, 2H), 2.23-2.31 (m, 4H), 1.77-1.89 (m, 2H) ppm; ^{13}C NMR (100 MHz, CDCl_3) 204.6, 198.0, 149.0, 135.5, 132.8, 129.3, 128.5, 113.3, 75.5, 35.9, 34.3, 27.3, 24.2 ppm. Spectral data consistent with previously reported data.³⁶

References

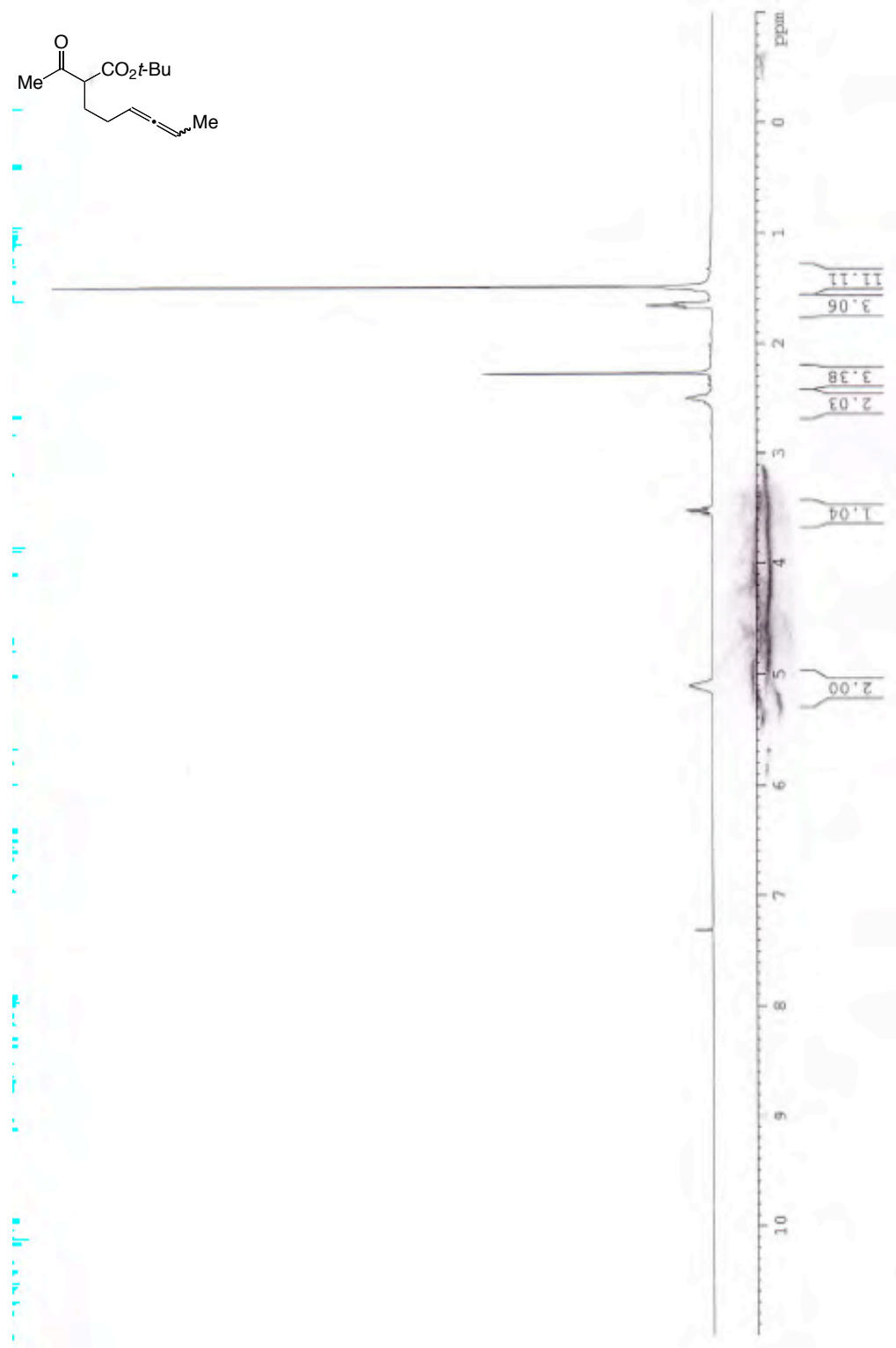
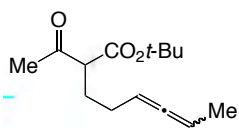
- ¹ Kennedy-Smith, J. J.; Staben, S. T.; Toste, F. D. *J. Am. Chem. Soc.* **2004**, *126*, 4526.
- ² Staben, S. T.; Kennedy-Smith, J. J.; Toste, F. D. *Angew. Chem., Int. Ed. Engl.* **2004**, *43*, 5350.
- ³ Zhang, Z.; Liu, C.; Kinder, R. E.; Han, X.; Qian, H.; Widenhoefer, R. A. *J. Am. Chem. Soc.* **2006**, *128*, 9066.
- ⁴ Zhang, L. *J. Am. Chem. Soc.* **2005**, *127*, 16804.
- ⁵ For a review of Pd-catalyzed reactions involving allenes, see: (a) Ma, S. *E. J. Org. Chem.* **2004**, 1175. For general reviews of additions to allenes, see: (b) Ma, S. *Chem. Rev.* **2005**, *105*, 2829. (c) Bates, R. W.; Satcharoen, V. *Chem. Soc. Rev.* **2002**, *31*, 12.
- ⁶ For a recent review of metal enolate additions to C-C multiple bonds, see: Dénès, F.; Péres-Luna, A.; Chemla, F. *Chem. Rev.* **2010**, *110*, 2366.
- ⁷ Kitagawa, O.; Suzuki, T.; Fujiwara, H.; Taguchi, T. *Tetrahedron Lett.* **1999**, *40*, 2549.
- ⁸ Kitagawa, O.; Suzuki, T.; Fujiwara, H.; Fujita, M.; Taguchi, T. *Tetrahedron Lett.* **1999**, *40*, 4585.
- ⁹ (a) Miura, T.; Kiyota, K.; Kusama, H.; Lee, K.; Kim, H.; Kim, S.; Lee, P. H.; Iwasawa, N. *Org. Lett.* **2003**, *5*, 1725. (b) Miura, T.; Kiyota, K.; Kusama, H.; Iwasawa, N. *J. Organomet. Chem.* **2007**, *692*, 562.
- ¹⁰ Kennedy-Smith, J. J., University of California - Berkeley, **2005**.
- ¹¹ Hirasawa, Y.; Morita, H.; Shiro, M.; Kobayashi, J. *Org. Lett.* **2003**, *5*, 3991.
- ¹² Substrate synthesized and characterized by Steve Staben.
- ¹³ Determined by NOESY.
- ¹⁴ Determined by ¹H NMR with europium *tris*-[3-(heptafluoropropylhydroxymethylene)-(-)-camphorate].
- ¹⁵ Smith, R. A.; White, R. L.; Krantz, A. *J. Med. Chem.* **1988**, *31*, 1558.
- ¹⁶ A preliminary result from a summer student, Melanie Chiu, indicated that only the 5-endo product would be formed.
- ¹⁷ Searles, S.; Li, Y.; Nassim, B.; Lopes, M.; Tran, P.; Crabbé, P. *J. Chem. Soc., Perkin Trans 1* **1984**, *4*, 747.
- ¹⁸ Cationic gold was generated *in situ* by mixing the corresponding phosphinegold(I) chloride and silver salt.
- ¹⁹ Endo-cyclopentene **5.52** was synthesized via the gold(I)-catalyzed 5-*endo-dig* cyclization.
- ²⁰ Ph₃PAuOTf also does not catalyze either of these isomerizations.
- ²¹ (a) Sone, T.; Ozaki, S.; Kasuga, N. C.; Fukuoka, A.; Komiyama, S. *Bull. Chem. Soc. Jpn.* **1995**, *6*, 1523-1533. (b) Komiyama, S.; Ozaki, S. *Chem. Lett.* **1988**, 1431.
- ²² Perevalova, E. G.; Grandberg, K. I.; Smyslova, E. I.; Dyadchenko, V. I. *Metal. Khim.* **1989**, *2*, 699.
- ²³ Tamaki, A.; Kochi, J. K. *J. Organomet. Chem.* **1973**, *61*, 441.
- ²⁴ (a) Seyferth, D.; Weiner, M. A. *J. Am. Chem. Soc.* **1961**, *83*, 3583. (b) Meyers, A. I.; Lutomski, K. A.; Laucher, D. *Tetrahedron* **1988**, *44*, 3107. (c) Hwu, J. R.; Furth, P. S. *J. Am. Chem. Soc.* **1989**, *111*, 8834. (d) Eisch, J. J. *J. Organomet. Chem.* **1981**, *2*, 91. (e) Desponds, O.; Schlosser, M. J. *J. Organomet. Chem.* **1991**, *409*, 93. (f) Clarembeau, M.; Krief, A. *Tet.* **1973**, 4155. (g) Korte, W. D.; Cripe, K.; Cooke, R. J. *J. Org. Chem.* **1974**, *39*, 1168.

-
- ²⁵ Seyferth, D.; Weiner, M. *J. Org. Chem.* **1959**, *24*, 1395.
- ²⁶ Sherry, B. D.; Toste, F. D. *J. Am. Chem. Soc.* **2004**, *126*, 15978.
- ²⁷ Molander, G. A.; Cormier, E. P. *J. Org. Chem.* **2005**, *70*, 2622.
- ²⁸ Claesson, A.; Olsson, L.-I. *J. Am. Chem. Soc.* **1979**, *101*, 7302.
- ²⁹ Jonasson, C.; Horvath, A.; Bäckvall, J. E. *J. Am. Chem. Soc.* **2000**, *122*, 9600.
- ³⁰ Meguro, M.; Yamamoto, Y. *J. Org. Chem.* **1999**, *64*, 694.
- ³¹ Diastereomers were unresolvable by ¹H NMR.
- ³² Lee, K.; Kim, H.; Miura, T.; Kiyota, K.; Kusama, H.; Kim, S.; Iwasawa, N.; Lee, P. H. *J. Am. Chem. Soc.* **2003**, *125*, 9682.
- ³³ Larionov, O. V.; Kozhushkof, S. I.; Meijere, A. D. *Synthesis* **2005**, *1*, 158.
- ³⁴ Depres, J.-P.; Greene, A. E. *J. Org. Chem.* **1984**, *49*, 928.
- ³⁵ Ahmar, M.; Cazes, B.; Gore, J. *Tetrahedron Lett.* **1985**, *26*, 3795.
- ³⁶ Gao, Q.; Zheng, B. F.; Li, J. H.; Yang, D. *Org. Lett.* **2005**, *7*, 2185.

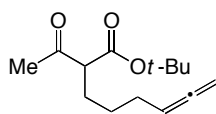
Appendix 5A

Copies of ^1H NMR characterization data are included for compounds **5.33**, **5.45**, **5.53**, **5.54**, **5.55**, **5.57**.

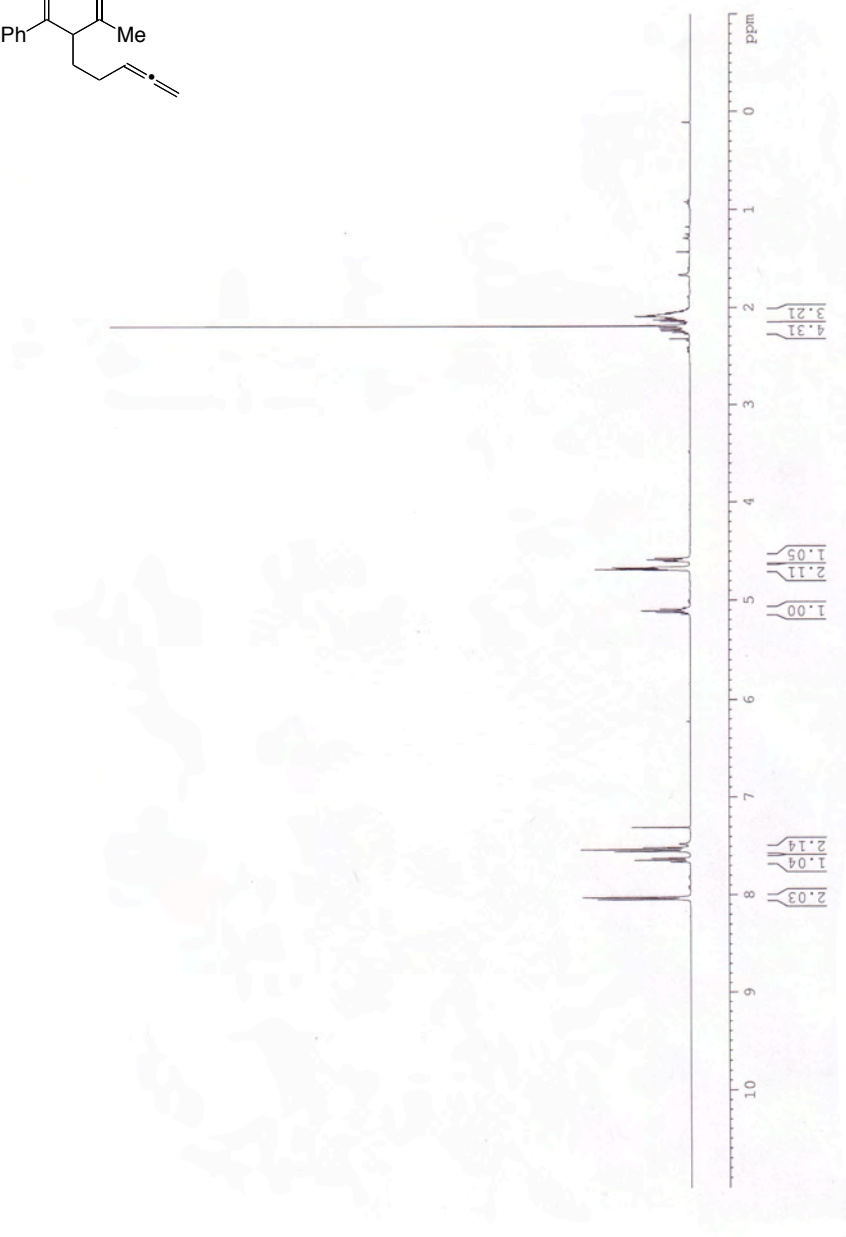
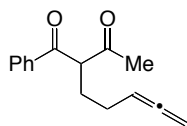
5.55



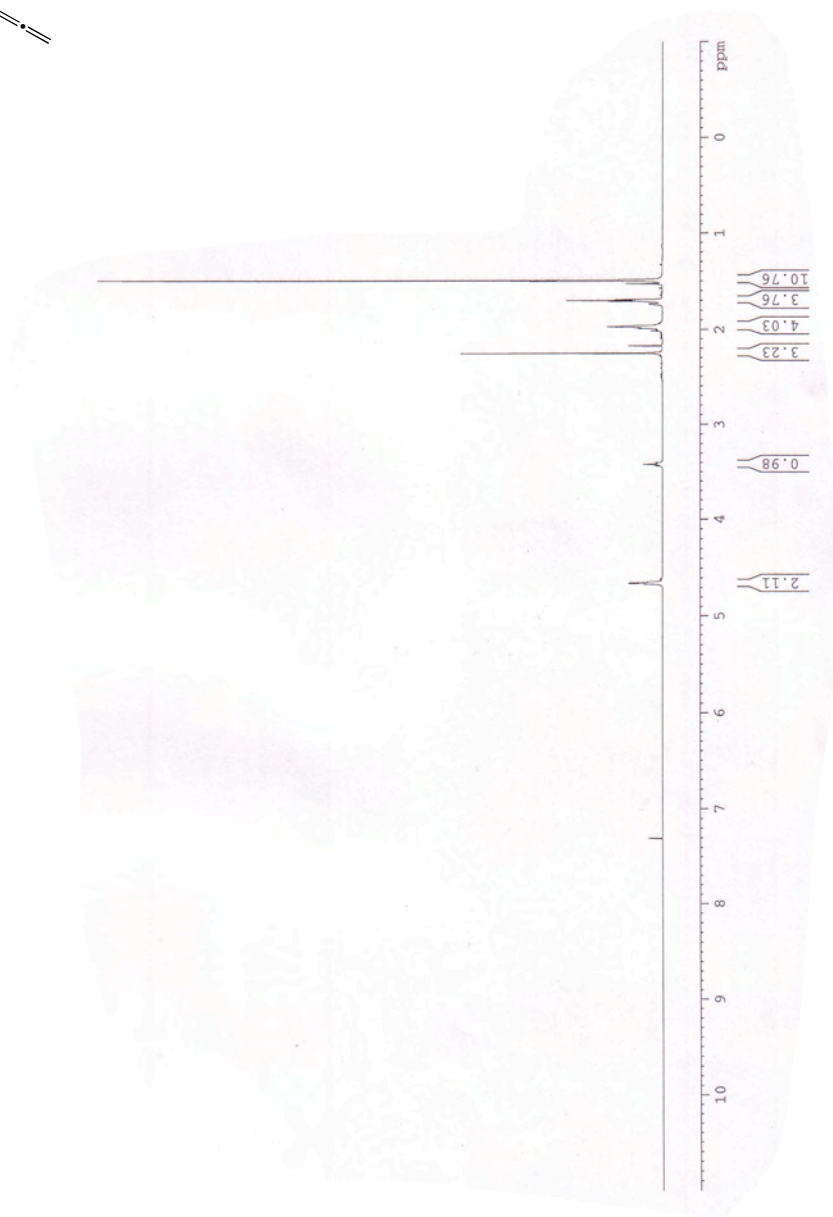
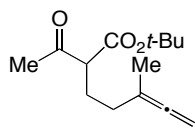
5.45



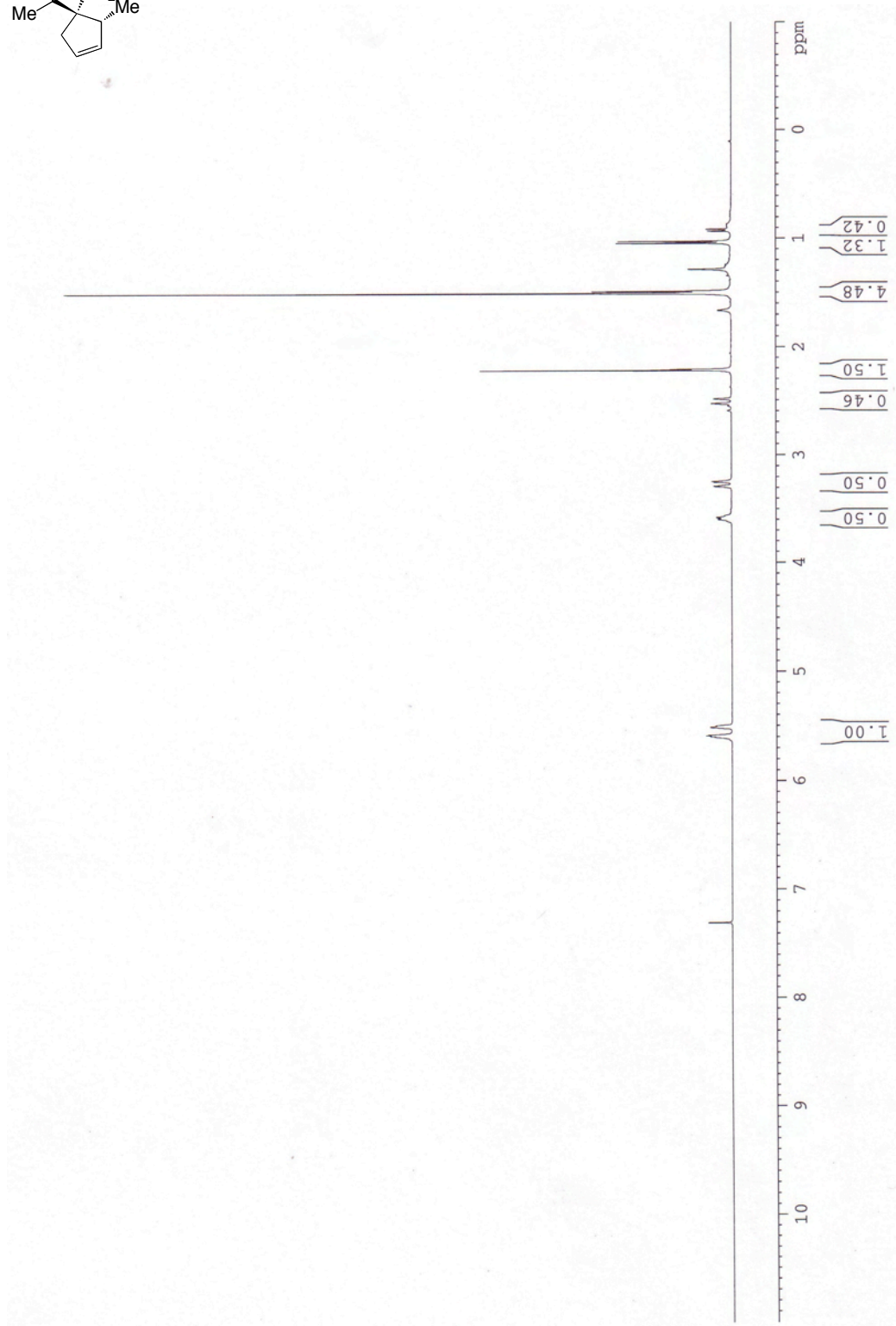
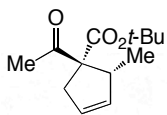
5.53



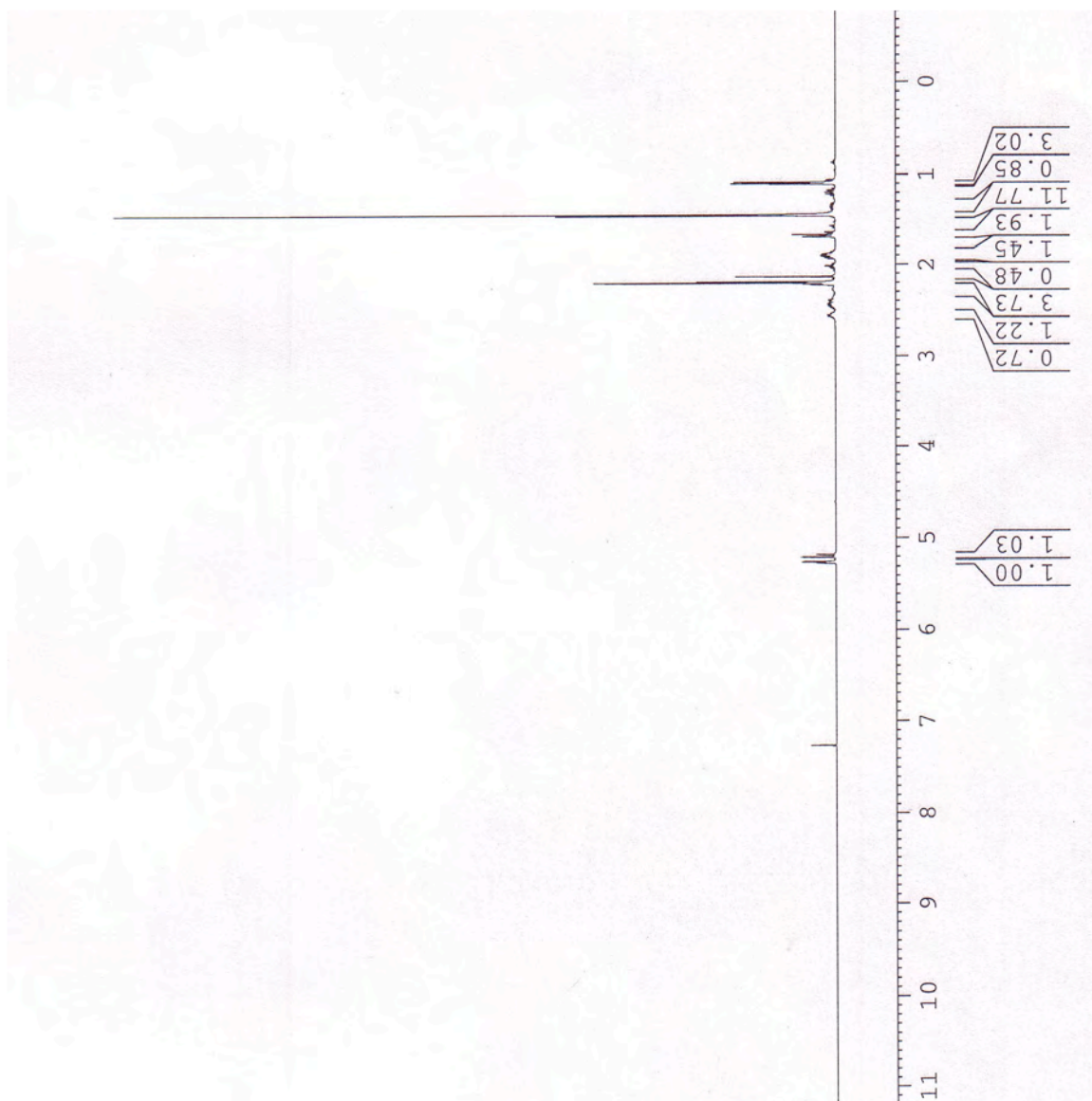
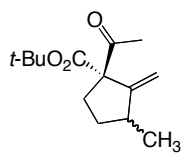
5.54



5.33



5.57

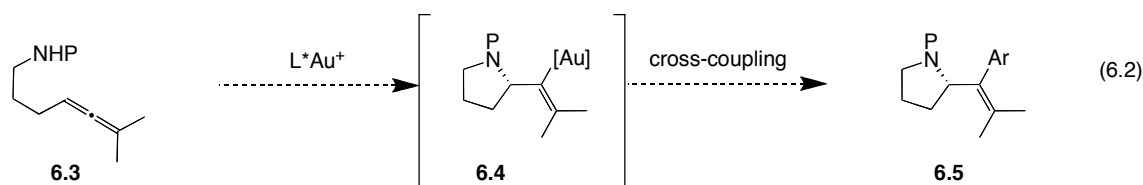
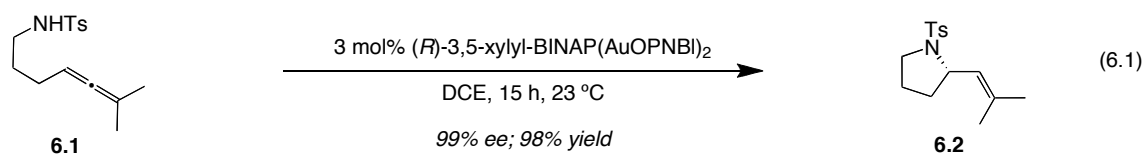


Chapter 6

Synopsis and Future Directions

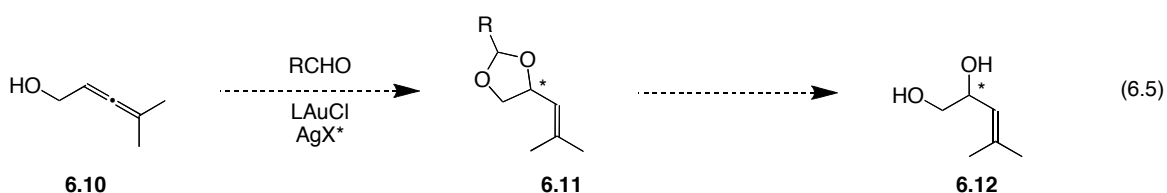
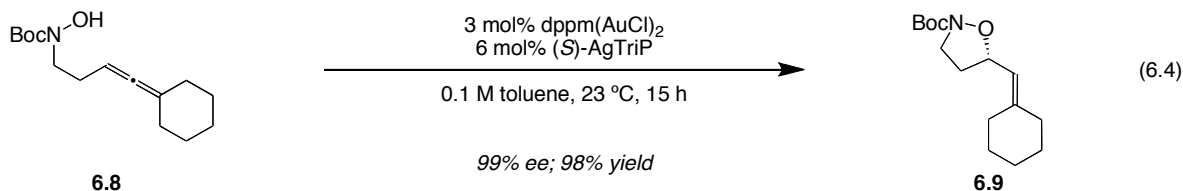
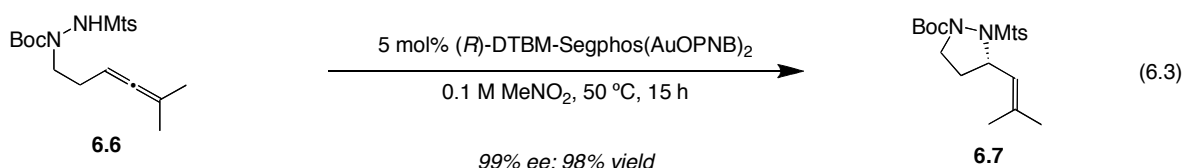
The Evolving Field of Gold(I)-Catalysis

As modern chemists we are faced with more than just providing technology to a variety of fields. We also must ensure that the reactions we create will be sustainable for the years to come. As related in chapter 1, the principle of atom economy outlines the features of an ideal reaction. While current methods are still far from this ideal reaction, the use of homogeneous gold(I)-catalysts have shown some key advantages. Simple addition reactions to carbon-carbon unsaturated bonds are easily catalyzed by gold(I). Our research has been broadly focused on expanding the scope of such gold(I)-catalyzed nucleophilic additions, specifically enantioselective additions to allenes, and the mechanism of gold(I)-alkene additions. As the field of gold(I)-catalysis matures, new investigations are proposed on the combined use of gold with other metals.



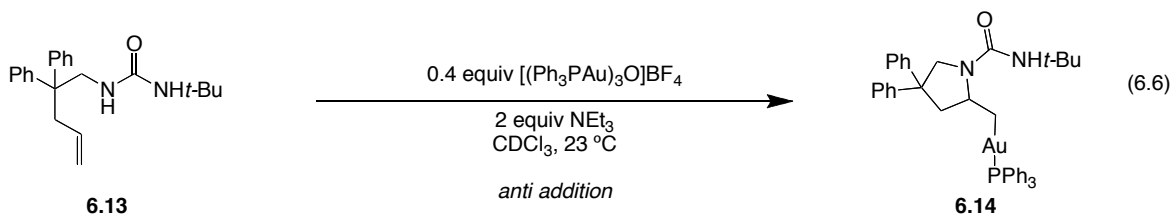
In chapter 2, we reported an enantioselective hydroamination of allenes catalyzed by phosphinegold(I)-bis-*p*-nitrobenzoate complexes (eq 6.1). Soon after our report, Widenhoefer disclosed a similar transformation using carbamate nucleophiles.¹ The catalyst (DTBM-MeOBiPHEP(AuCl)₂) employed in this reaction was also used for a dynamic kinetic enantioselective hydroamination of allenes.² To date, these gold-catalyzed reactions are the only enantioselective methods for the hydroamination of allenes. In addition, our paper described previously unknown catalytic activity of gold(I)benzoates. Researchers in our group are still exploring the special reactivity of these species. For example, our group extended the use of such complexes to a 1,3-dipolar cycloaddition.³

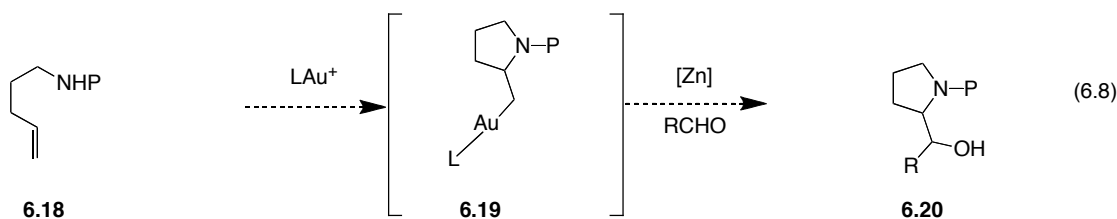
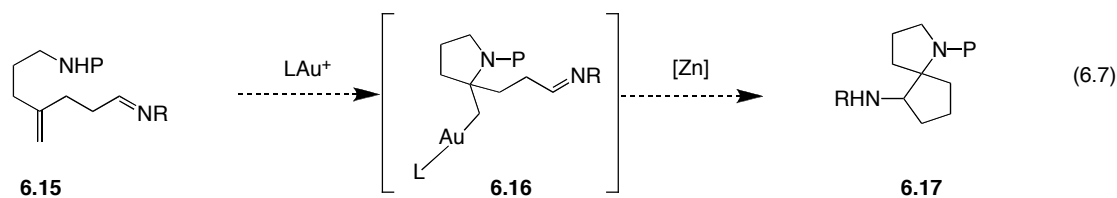
The utility of gold(I)-catalyzed hydroamination could be greatly expanded if vinylgold intermediate **6.4** could be diverted from protodemetalation. For example, this would allow access to cross-coupling products like **6.5** (eq 6.2). Although there have been a few initial reports,⁴ the combination of gold-catalysis with other transition metals remains largely unexplored. In the future, we believe dual metal-catalysis will be the basis for innovation in the field of hydroamination and gold-catalysis.



Over the course of our research into hydroamination, we noted the critical effect achiral counterions could have on the enantioselectivity of the product. A group of coworkers demonstrated the magnitude of this effect by using the counterions as the source of chirality.⁵ As we related in chapter 3, the combination of bisphosphenegold(I) complexes with a chiral counterion, (*R*)-TripAg, proved to be an effective strategy for the asymmetric synthesis of biologically relevant heterocycles (eq 6.2-6.3).

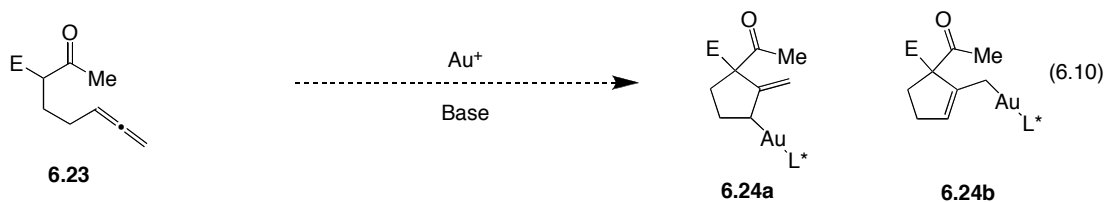
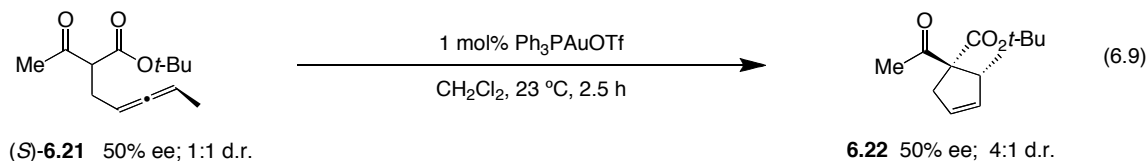
The formation of poly-oxygenated molecules is an ongoing challenge in synthesis. The gold(I)-catalyzed addition of *in situ* generated nucleophiles could provide access to such compounds (eq 6.5). For example, the nucleophilic addition of an *in situ* generated hemi-acetal could be catalyzed by gold in conjunction with a chiral counterion. However, the catalyst chosen must not catalyze intramolecular cyclization of **6.10**. The cyclic acetal **6.11** might be labile under the reaction conditions, directly yielding the desired product. Alternatively, treatment with a mild acid would release diol **6.12**.





The first direct crystallographic evidence for gold(I)-electrophilic activation of alkenes for nucleophilic addition was presented in chapter 4. In addition, we have provided the first experimental verification of an *anti*-addition mechanism for alkene amino-auration. Interestingly, a variety of protected amine nucleophiles proved competent. The implications for gold(I)-catalyzed hydroamination reactions are somewhat unclear: we were unable to complete the catalytic cycle by means of protodeauration.⁶ However, the isolation of alkylgold(I) complexes provided a platform for probing the fundamental chemistry of gold, the limits of which we are still exploring. It is somewhat ironic that our interest in gold chemistry was partially motivated by mechanisms outside of the traditional oxidative addition/reductive elimination cycles. Now we see the oxidation of gold(I) intermediates as a potential source of new reactivity.

We expect that alkylgold(I) complexes will enable the discovery of novel dual metal catalytic activity. The intra- and intermolecular trapping of imines and aldehydes are proposed examples of two such systems. In the intramolecular sense, amino-auration could be followed by transmetalation and trapping with a pendant imine (eq 6.7). This reaction would allow entry into complex spirocyclic structures. The analogous intermolecular transformation with aldehydes (eq 6.8) would generate 1,2-aminoalcohols from simple starting materials.



We also showed an example of chirality transfer in the gold(I)-catalyzed carbocyclization of allenes (6.5). This stereospecific transformation is a mild method for producing an all-carbon quaternary stereocenter with a vicinal tertiary center. Although our understanding of enantioselective gold(I) catalysis has grown, researchers in our group turned to palladium to achieve an enantioselective Conia-ene reaction.⁷ A gold-catalyzed enantioselective variant remains elusive. One of the major problems with developing the enantioselective is the lack of a stereochemical model. Such a tool is necessary to predict steric interactions and their stereochemical result. The isolation of species like **6.24a** and **6.24b** should be possible by combining the technology developed in chapter 4 and 5 (eq 6.10). These gold(I)-complexes bearing chiral ligands could be used for the basis of a stereochemical model.

Homogeneous gold(I)-catalysis continues to be an evolving field of research. As related in this dissertation, our understanding of gold(I)-reactivity has changed dramatically over the course of a mere five years. Prior to 2005, we believed that the linear two coordinate geometry of gold(I)-complexes would hinder their use in enantioselective transformations. Today, we know that this obstacle may be overcome by the use of coordinating counterions and chiral phosphine ligands. Additionally, we now have evidence of gold(I) activating alkenes for nucleophilic addition. It is our hope that these contributions will enable the continued development of gold(I)-catalysis.

References

- ¹ Zhang, Z.; Bender, C. F.; Widenhoefer, R. A. *Org. Lett.* **2007**, *9*, 2887.
- ² Zhang, Z.; Bender, C. F.; Widenhoefer, R. A. *J. Am. Chem. Soc.* **2007**, *129*, 14148.
- ³ Melhado, A. D.; Luparia, M.; Toste, F. D. *J. Am. Chem. Soc.* **2007**, *129*, 12638.
- ⁴ (a) Shi, Y.; Ramgren, S. D.; Blum, S. A. *Organometallics* **2009**, *28*, 1275. (b) Hashmi, A. S. K.; Schuster, A. M.; Rominger, F. *Angew. Chem., Int. Ed. Engl.* **2009**, *48*, 8243.
- ⁵ Hamilton, G. L.; Kang, E. J.; Mba, M.; Toste, F. D. *Science* **2007**, *317*, 496.
- ⁶ Taylor, J. G.; Adrio, L. A.; Hii, K. K. *Dalton Trans.* **2010**, *39*, 1171.
- ⁷ Corkey, B. K.; Toste, F. D. *J. Am. Chem. Soc.* **2005**, *127*, 17168.